



**US Army Corps
Engineers**

Waterways Experiment
Station

Technical Report GL-93-18
August 1993

US-CE-C PROPERTY OF THE
UNITED STATES GOVERNMENT

**LIBRARY
USE ONLY**

Geological-Seismological Evaluation of Earthquake Hazards at J. Strom Thurmond Dam

by *Ellis L. Krinitzsky, Joseph B. Dunbar*
Geotechnical Laboratory

WES

Approved For Public Release; Distribution Is Unlimited

RESEARCH LIBRARY
US ARMY ENGINEER WATERWAY
EXPERIMENT STATION
VICKSBURG, MISSISSIPPI

T A 7
W 3 4
no. G h - 93-18

28877615

Technical Report GL-93-18
August 1993

Geological-Seismological Evaluation of Earthquake Hazards at J. Strom Thurmond Dam

by Ellis L. Krinitzsky, Joseph B. Dunbar
Geotechnical Laboratory

U.S. Army Corps of Engineers
Waterways Experiment Station
3909 Halls Ferry Road
Vicksburg, MS 39180-6199

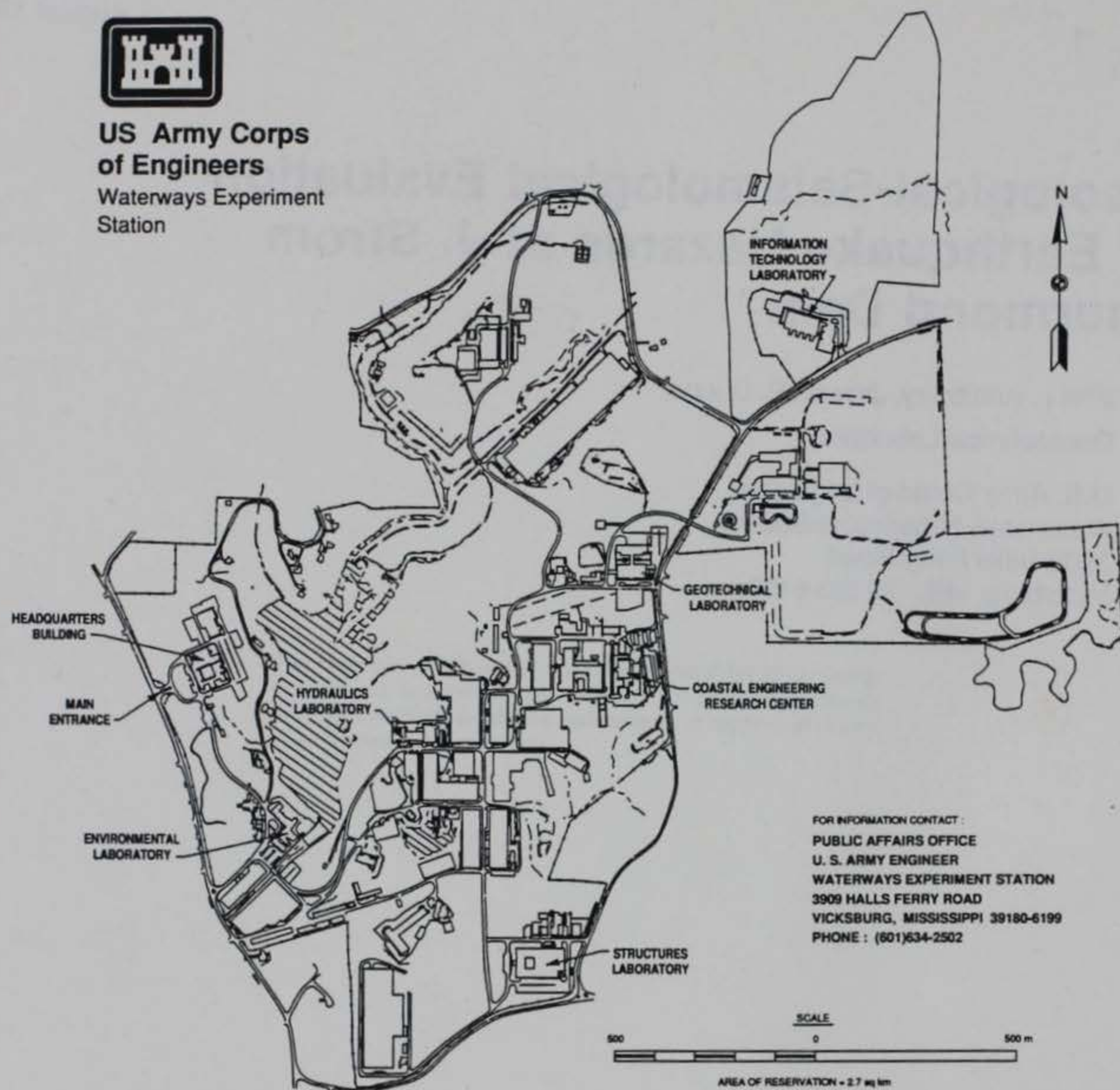
Final report

Approved for public release; distribution is unlimited

Prepared for U.S. Army Engineer District, Savannah
Savannah, GA 31402-0889



**US Army Corps
of Engineers**
Waterways Experiment
Station



FOR INFORMATION CONTACT:
PUBLIC AFFAIRS OFFICE
U. S. ARMY ENGINEER
WATERWAYS EXPERIMENT STATION
3909 HALLS FERRY ROAD
VICKSBURG, MISSISSIPPI 39180-6199
PHONE: (601)634-2502

Waterways Experiment Station Cataloging-In-Publication Data

Krinitzsky, E. L.

Geological-seismological evaluation of earthquake hazards at J. Strom Thurmond Dam / by Ellis L. Krinitzsky, Joseph B. Dunbar ; prepared for U.S. Army Engineer District, Savannah.

356 p. : ill. ; 28 cm. — (Technical report ; GL-93-18)

Includes bibliographical references.

1. Earthquake hazard analysis — South Carolina — J. Strom Thurmond Dam. 2. Dams — South Carolina — Earthquake effects. 3. J. Strom Thurmond Dam (S.C.) 4. Dams — South Carolina — Foundations. I. Dunbar, Joseph B. II. United States. Army. Corps of Engineers. Savannah District. III. U.S. Army Engineer Waterways Experiment Station. IV. Title. V. Series: Technical report (U.S. Army Engineer Waterways Experiment Station) ; GL-93-18.

TA7 W34 no.GL-93-18

PREFACE

The USAE Waterways Experiment Station (WES) was authorized to conduct this study by the US Army Engineer District, Savannah (CESAS), on 14 January 1989 by DA Form 2544, number EN-GG-89-33. A draft report, dated 30 September 1989, containing PARTS III, IV, and V, and Appendices B, C, D, E, and F was submitted to CESAS in October 1989 for review.

The project scope was later modified by MIPR number UP-H-93-22, dated 8 February 1993, for WES to complete the report and conduct the geological evaluation (PARTS I and II, and Appendix A). Originally CESAS had planned to conduct the geological evaluation in-house and WES would conduct the seismic evaluation for the dam site.

Dr. E. L. Krinitzsky, Executive Office, Geotechnical Laboratory (GL), and Mr. J. B. Dunbar, Earthquake Engineering and Geosciences Division (GG), GL, performed the investigation and wrote the report. Messrs. D. Barefoot, GG, and Bill Park, Visual Production Center (VPC), Information Technology Laboratory (ITL), assisted with the preparation of illustrations and data tabulation.

Appendices D and E of this report were prepared by Dr. P. Talwani, University of South Carolina, and Dr. L. T. Long, Georgia Institute of Technology, respectively. Drs. Talwani and Long were contracted by WES to conduct these studies.

A site visit was made to J. Strom Thurmond Dam and reservoir as part of this investigation in February 1989 by Dr. Krinitzsky (CEWES), Mr. Earl Titcomb (CESAS), Mr. Robert O'Kelly (CESAS), and Mr. Tim Pope (South Atlantic Division). The site investigation included a reconnaissance visit to the Belair, Modoc, and other faults adjacent to the dam and reservoir.

The investigation at the J. Strom Thurmond Dam was under the general direction of Dr. A. G. Franklin, Chief, GG, and Dr. William F. Marcuson III, Director, GL. During publication of this report Dr. Robert W. Whalin was the Director of WES and COL Bruce K. Howard, EN, was the Commander.

CONTENTS

	<u>Page</u>
PREFACE	1
PART I: INTRODUCTION	4
Purpose and Scope	4
Study Area	4
PART II: GEOLOGY	7
Tectonic History and Setting	7
Regional Geology	10
Introduction	10
Kiokee Belt	12
Carolina Slate Belt	13
Belair Belt	16
Tectonic Model	17
Site Geology	22
Lineaments and Faults	22
Lineaments	22
Paleozoic Faults	24
Mesozoic Faults	25
Cenozoic Faults	25
PART III: SEISMICITY	27
Relation of Seismicity and Geology	27
Distribution of Historic Earthquakes	31
Causes of Earthquakes	33
Maximum Piedmont Earthquake	36
Microearthquakes and Reservoir-Induced Seismicity	36
Introduction	36
Coastal Plain Microearthquakes	37
Piedmont Microearthquakes	39
Seismic Source Zones in the Southeastern United States	39
Earthquake Recurrence	42
Felt Earthquakes at J. Strom Thurmond Dam	46
PART IV: EARTHQUAKE GROUND MOTIONS	54
Maximum Credible Earthquake	54
Operating Basis Earthquake	54
Field Conditions	55
Recommended Peak Motions	56
Recommended Accelerograms	60
Motions for Nearby Nuclear Power Plants	60
PART V: CONCLUSIONS	64
REFERENCES	65
APPENDIX A: SITE GEOLOGY OF J. STROM THURMOND (CLARKS HILL) DAM	A1
APPENDIX B: CATALOGUE OF HISTORIC EARTHQUAKES	B1
APPENDIX C: GLOSSARY OF EARTHQUAKE TERMS	C1
APPENDIX D: SEISMIC POTENTIAL NEAR STROM THURMOND LAKE, SOUTH CAROLINA	D1

	<u>Page</u>
APPENDIX E: MAXIMUM EARTHQUAKE AT J. STROM THURMOND RESERVOIR	E1
APPENDIX F: RECOMMENDED ACCELEROGRAMS AND RESPONSE SPECTRA.	F1
SF 298	

GEOLOGICAL-SEISMOLOGICAL EVALUATION OF EARTHQUAKE
HAZARDS AT J. STROM THURMOND DAM

PART I: INTRODUCTION

Purpose and Scope

The purpose of this investigation is to define the maximum potential for earthquakes and to provide peak horizontal ground motion for earthquake shaking which might occur at J. Strom Thurmond Dam. Results of this study are for use in the engineering-seismic evaluation of J. Strom Thurmond Dam and associated structures. The dam is located on the Savannah River in the Piedmont Physiographic province of Georgia and South Carolina (see Figure 1).

This investigation includes both geological and seismological analyses and consists of the following parts: (a) a review of the regional and local geology, including an evaluation of faulting in the area, (b) a review of historical seismicity in the study area and its relationship to the geology, (c) determination of the maximum earthquake(s) that could effect the dam as well as a determination of the attenuated peak ground motions at the dam.

Study Area

The study area includes that portion of the southeastern United States in which earthquake activity may affect the structural stability of J. Strom Thurmond Dam. Portions of Georgia, South Carolina, North Carolina, and Tennessee are included in this study area. Generally the study area is limited to a 150 km radius surrounding the dam.

Also considered is an earthquake source in the vicinity of Charleston, South Carolina, where a major earthquake occurred in 1886. This earthquake is the largest historic earthquake that has occurred in the southeastern United States and caused extensive damage. Shaking from this earthquake was felt over much of the central and eastern United States. Charleston continues to be a seismic hotspot with many, small earthquakes.

J. Strom Thurmond Dam was formerly known as Clarks Hill before its name change by the Federal Government on 6 January 1988. The state of Georgia however has not officially adopted the new name change. The Georgia state

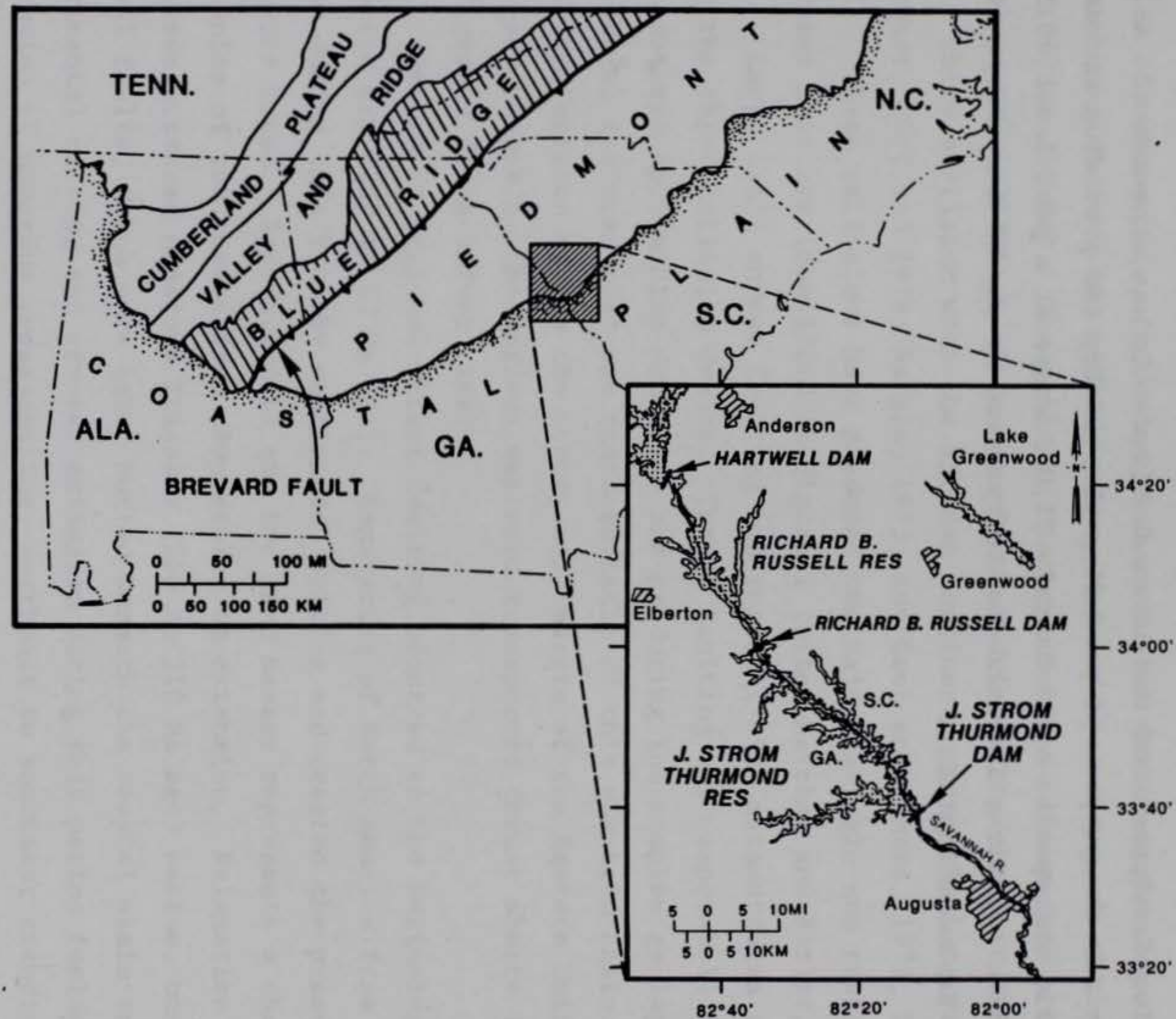


Figure 1. Physiographic subdivisions of the southeastern United States showing the location of J. Strom Thurmond (Clarks Hill) Dam and Reservoir

legislature passed a joint resolution (House Resolution No. 115, Approved 4 April 1989) that makes Clarks Hill the official state name for both the dam and reservoir.

J. Strom Thurmond Dam is a 5,680 feet (ft), 1,731 m, composite concrete-gravity and earth embankment dam located on the Savannah River. Construction of Clarks Hill or J. Strom Thurmond Dam began in 1945 and was completed in 1952. The dam was the first in a series of dams for the comprehensive development of the Savannah River. It was constructed principally for the purpose of producing electricity and providing recreation. The reservoir encompasses approximately 71,000 acres at a pool level of 330 ft (100.6 m) MSL. J. Strom Thurmond Dam is operated by the US Army Corps of Engineers, Savannah District.

PART II: GEOLOGY

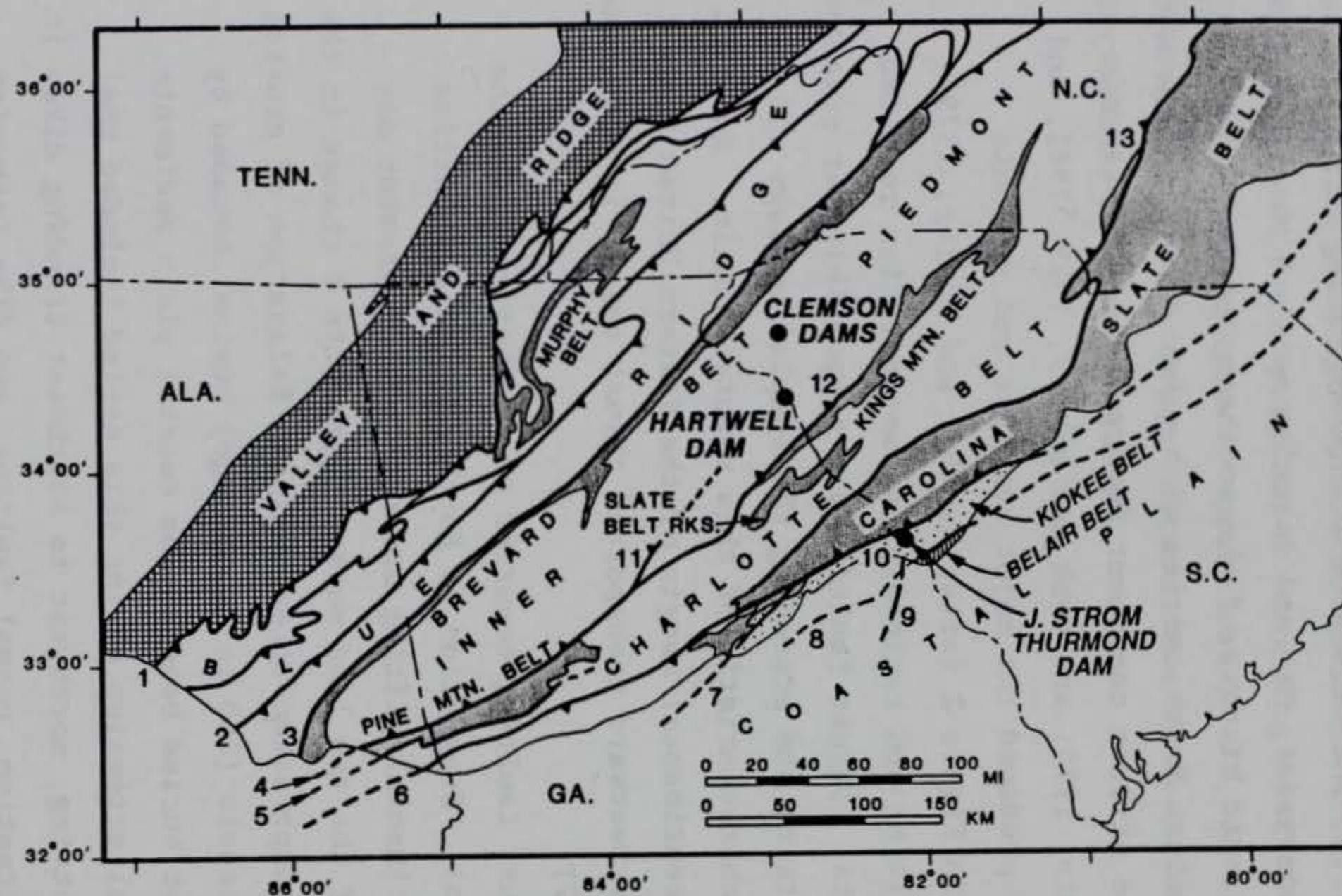
Tectonic History and Setting

The southern Appalachians are characterized by intense folding, thrust faulting, and the presence of a vast variety of sedimentary, metamorphic, and igneous rocks. The area has undergone multiple periods of deformation from a series of metamorphic, intrusive, and extrusive events beginning in the late Precambrian (before 600 million years, Ma) and spanning most of the Paleozoic Era (600 to 250 Ma). The geologic history of the southern Appalachians involves two collisions of eastern North America with other crustal fragments and a third collision with the African continent during the Late Paleozoic (Hatcher, 1972 and 1978; Rankin, 1975; and Cook and others, 1979, 1981, and 1982). These collisions have produced the major geologic and tectonic features that are identified in Figure 2 (after Hatcher and Butler, 1979).

Large scale thrust faulting and regional-wide metamorphism resulted from the three collision events. Thrust faulting was responsible for creating the southern Appalachian Mountains and producing the complex geology and structural features that are characteristic of this mountain chain. An idealized version of how the continental margin of the Eastern United States has been shaped by the various westward transported thrust sheets is presented in Figure 3 (from Oliver, 1982).

An end to regional thrust faulting occurred at the beginning of the Mesozoic Era (250 to 65 Ma ago). Separation of North America from Africa began during this time by continental rifting and created the present day Atlantic Ocean. Separation of the two land masses represents a change in the tectonism of the region from compression to extension. Relaxation of crustal stresses produced numerous Triassic (250 to 210 Ma ago) basins, bounded by normal faults, which were later buried beneath the coastal plain sediments. Continental rifting and crustal extension during this period included the intrusion of numerous cross-cutting, northwest to southeast trending dikes in the Piedmont region. Basin formation, normal faulting, and dike intrusion ended by the latter part of the Jurassic Period (210 to 145 Ma ago).

The Cenozoic (65 Ma ago to present) is, in general, a period of continental stability. During this time sediments were eroded from the



FAULTS

- | | |
|--------------------------|---------------------------------|
| 1 BLUE RIDGE THRUST | 8 AUGUSTA FAULT |
| 2 HAYESVILLE FAULT | 9 BELAIR FAULT |
| 3 BREVARD FAULT | 10 MODOC FAULT |
| 4 TOWALIGA FAULT | 11 HARTWELL FAULT |
| 5 BARTLETT'S FERRY FAULT | 12 MIDDLETON-LOWNDESVILLE FAULT |
| 6 GOAT ROCK FAULT | 13 GOLD HILL FAULT |
| 7 FLAT ROCK FAULT | |

Figure 2. Tectonic map of the southeastern United States showing subdivisions of the Piedmont Province and locations of major faults (after Hatcher and Butler, 1979; with data from Whitney, Elwood, and Stormer, 1980; and Prowell and others, 1975)

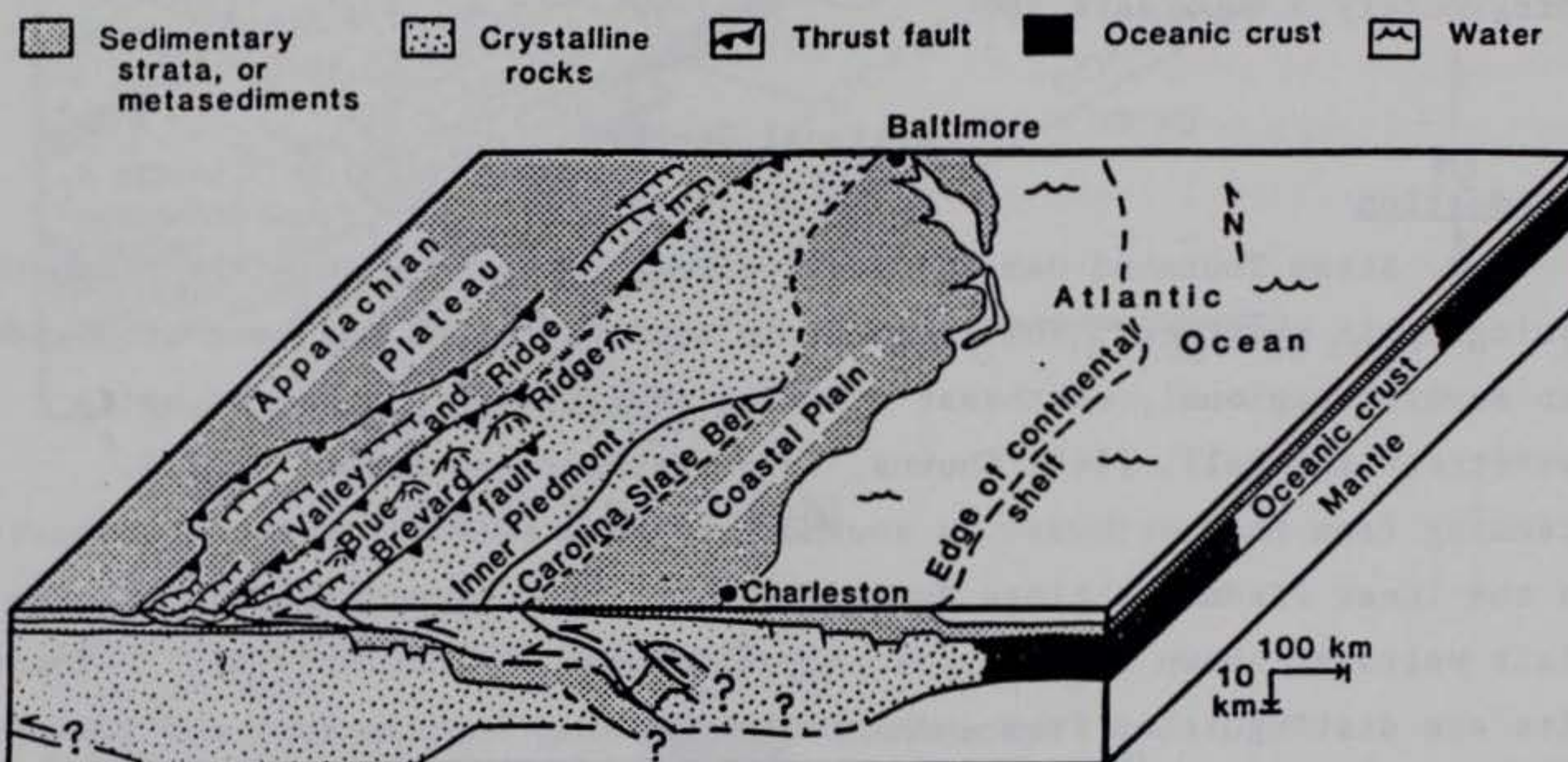


Figure 3. Generalized block diagram illustrating thrust faulting in the southeastern United States and how these thrust sheets overlie a former continental margin (from Oliver, 1982).

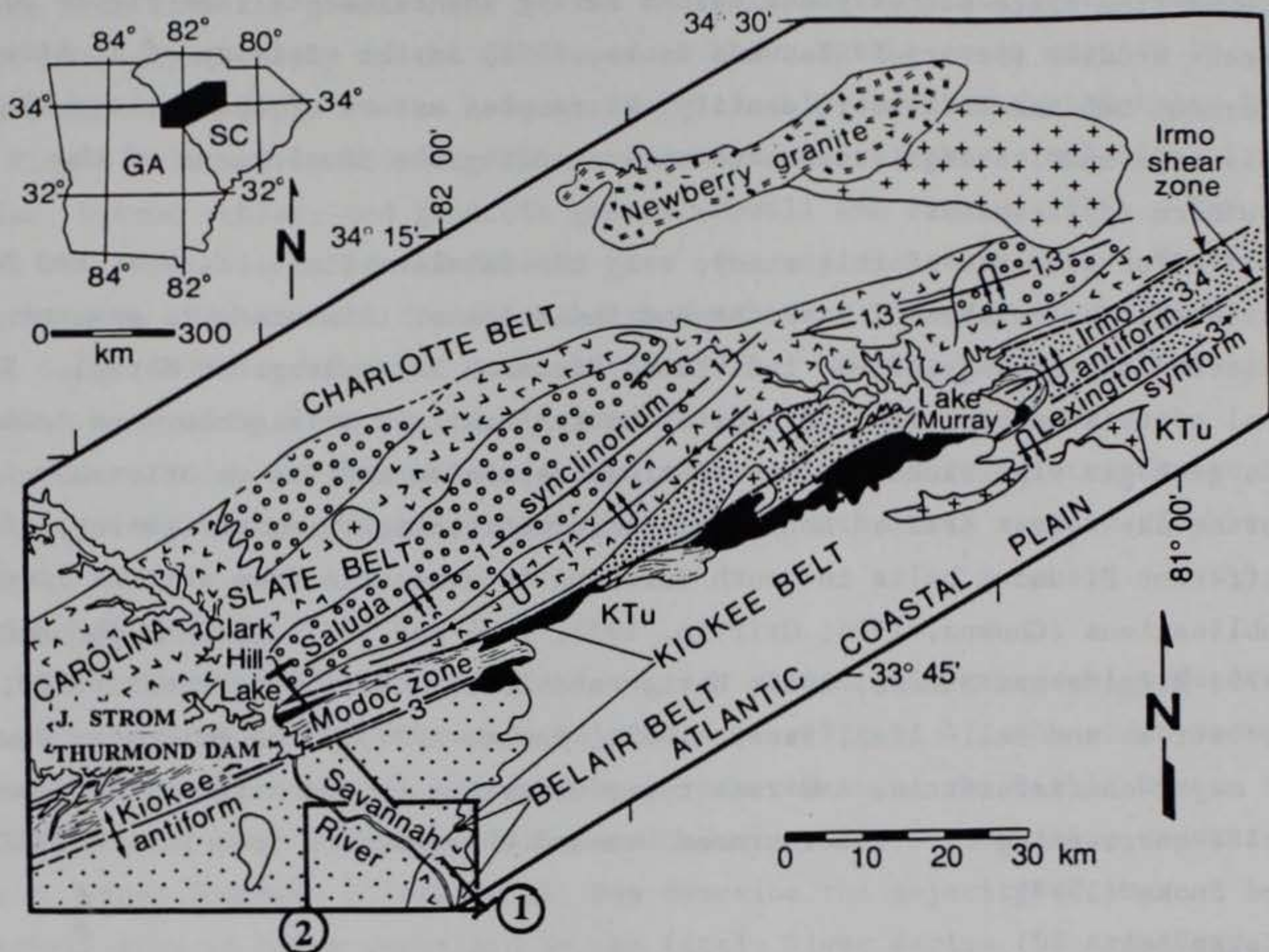
uplifted Appalachian Mountains and deposited along the continental margin to form the coastal plain. Pleistocene (2 Ma to 10,000 years) glaciation is the last major geologic disturbance to have occurred in North America. However, glaciation did not directly affect the study area as the glaciers did not advance into the Southern Appalachian region. Rather, glacial effects were indirect. Changes in climate and base level due to sea level fluctuations from advancing and melting glaciers were the major effects of Pleistocene glaciation. Fluvial systems draining the Southern Appalachians responded to these changes by aggrading or degrading their alluvial valleys. Glaciers covering much of North America during the Late Pleistocene began melting approximately 17,000 years ago; sea level reaching its present position approximately 5,000 years ago.

Regional Geology

Introduction

J. Strom Thurmond Dam and Reservoir are located within the Piedmont physiographic province. The Piedmont in South Carolina has been subdivided into several regional, northeast trending physiographic units or belts (Overstreet and Bell, 1965; Chowns, 1976; Hatcher and Butler, 1979). Extending from the northwest to southeast, these belts in order of occurrence are the Inner Piedmont, Kings Mountain, Charlotte, Carolina Slate, Kiokee, and Belair belts as shown by Figure 2 (after Hatcher and Butler, 1979). These belts are distinguished from each other according to rock type and geologic structure. In general, these belts consist of regionally metamorphosed and faulted, low to medium grade rocks (Belair, Carolina Slate, Kings Mountain, Chauga), alternating with medium to high grade metamorphic rocks (Kiokee, Charlotte, and Inner Piedmont). J. Strom Thurmond Dam is located in the Kiokee Belt. The reservoir extends across the Kiokee, Carolina Slate, and Charlotte belts as shown by the generalized geologic map in Figure 4a (from Sacks and Dennis, 1987).

Recent work by Secor (1987a) and Secor and others (1986a and 1986b) in the Piedmont shows that the belt classification of rocks in South Carolina is much too broad and general for detailed geologic interpretation and tectonic reconstruction. Secor (personal communication) suggests that the term terrains should be used in place of belts to reflect the heterogenous lithology and structure of accreted crustal fragments and thrust faulted



EXPLANATION

KTu	Cretaceous and Tertiary kaolinitic sand	shear zones	
+++	late Paleozoic granite (undeformed)	D ₂	D ₄
•••	Siluro-Devonian granite (undeformed)	late Paleozoic granite (deformed)	
•••	Cambrian Asbill Pond fmn.		
•••	Cambrian Persimmon Fork Fmn. and Lincoln-ton metadacite		
•••	Cambrian and/or late Precambrian biotite schist and paragneiss	antiform	synform
		upright	overturned
		numbers indicate fold generation	

Figure 4a. Generalized geologic map of J. Strom Thurmond (Clarks Hill) Dam and Reservoir and vicinity (from Sacks and Dennis, 1987). Note: (1) the location of geologic cross section (see Figure 4b; from Maher, 1987), and (2) location of expanded geologic map of the Belair Belt (see Figure 4d; from Maher, 1978).

blocks from plate boundary collisions during the Paleozoic (see Figure 3). Recent studies (Secor, 1987a, and Snoke, 1978) in the vicinity of J. Strom Thurmond Dam and Reservoir identify the complex nature of the geology within this area and its significance to understanding the development of the southern Appalachians.

For purposes of this study, only the Carolina Slate, Kiokee, and Belair belts will be examined. It is beyond the scope of this study to examine or describe the geology of the individual Piedmont belts in great detail. The goal of this section is to evaluate the regional and site geology to determine the geologic significance of present day tectonism and its relationship to earthquake source areas. Additional information regarding the geology of the different Piedmont belts in South Carolina is available from several excellent publications (Chowns, 1976; Griffin, 1971, 1974 and 1977; Hatcher and Butler, 1979; Higgins and others, 1988; Horton and Zullo, 1991; Overstreet, 1970; Overstreet and Bell, 1965; Secor, 1987a; Snoke, 1978). The following summary of major characteristics and rock types occurring in the different Piedmont belts surrounding J. Strom Thurmond Dam and Reservoir is from Secor (1987a) and Snoke (1978).

Kiokee Belt

The generalized geologic map in Figure 4a identifies the major lithologic and structural features within the vicinity of the dam and reservoir. Strom Thurmond Dam is situated in the Kiokee Belt, a high grade metamorphic terrain composed chiefly of fine to medium grained migmatitic (i.e., composite rock containing both metamorphic and igneous minerals) gneisses with subordinate layers of amphibolite and schist. The original character of these rocks has been intensely metamorphosed and transposed. As a result, the primary lithologic character and layering of these rocks has been nearly obliterated. The complexity of the multiple deformations that have occurred in this region are identified on the detailed geologic map in Figure A1 (see Appendix A; from Maher and Sacks, 1987), and by the structural cross section in Figure 4b (from Maher, 1987).

Included with the Kiokee Belt is the Modoc Fault zone. Strom Thurmond Dam is located a short distance down stream from this fault zone. This zone separates the low grade metamorphic rocks of the Carolina Slate Belt from higher grade rocks in the Kiokee Belt. The Modoc zone is a 3 mile (5 km) wide ductile shear zone separating the upper amphibolite facies migmatites in the

Kiokee Belt from the greenschist facies in the Carolina Slate Belt. The Modoc Fault zone dips steeply to the northwest as shown by the cross section in Figure 4b. Rock types in the zone are more closely associated with those in the Kiokee Belt and include argillite, quartz-sericite schist, mylonite gneiss, button schist, and granitic gneiss (Howell and Pirkle, 1976). The Modoc Fault zone is interpreted to be part of a major eastern United States fault system that extends from Alabama to North Carolina (Howell and Pirkle 1976; Long, 1979; and Hatcher and others, 1977). Mapping has identified repeated movements along this fault zone during the latter part of the Paleozoic as shown by Figures A1 (Appendix A) and 4b. More information on the deformational history of this zone is discussed in the next section of this report.

Carolina Slate Belt

The Carolina Slate Belt is a low grade metamorphic greenschist facies containing intrusive and extrusive volcanics (see Figure 4). On older Georgia maps and publications, this belt has been referred to as the Little River Series (Stose, 1939; Crickmay, 1952, and Chowns, 1976). Foundation reports from J. Strom Thurmond (Clarks Hill) Dam describe the majority of the reservoir area as being underlain by the Little River Series (US Army Corps, 1978). Recently, Secor (1987b) has separated the Carolina Slate Belt (or Little River Series) into the Persimmon Fork, Asbill Pond, and the Richtex Formations.

The Persimmon Fork (mv1, mv2, and gr1 on Figure A1, Appendix A) is composed predominately of coarse grained intermediate to felsic ashflow tuff and dacite lava flows or lava domes (i.e., Lincolnton Metadacite; gr1 on Figure A1, Appendix A). The thickness of this formation is unknown as post depositional deformation has intensely altered the original sedimentary character. Secor (1987b) estimates that the thickness probably exceeded several kilometers. Radiometric dating of the Lincolnton Metadacite indicates a Cambrian(?) age for this formation. Secor (1987b) suggests the original setting for these rocks may be either a subduction related volcanic arc founded on oceanic crust or perhaps a continental margin setting.

The Asbill Pond Formation is described by Secor (1987b) as a sequence of quartz-sericite schist, sericite phyllite, and biotite-amphibole gneiss that exceeds 5 km in thickness in the vicinity of Batesburg, South Carolina. Surface outcrops are present in a semi-continuous 70 km band with exposures in

Cross Section Explanation and Key

Seismic reflectors and deep faults

- I. COCORP reflector interpreted to be basal decollement by Cook and others (1983, Fig. 15b) extrapolated from line 1 some 20-25 km off section to the southwest along strike.
- IIa, b. The uppermost and lowermost reflectors, respectively, of a series of northwest-dipping reflectors seen under the Carolina slate belt (Cook and others, 1983, Fig. 15b, Line 1). This is interpreted to be the subsurface continuation of the Modoc zone; the strongly deformed orthogneiss sheets are probable good seismic reflectors.
- III. Fault splay off of major decollement postulated in order to explain the cross section geometry of the Kiokee belt as a fault-propagation fold (see text for discussion). A corresponding seismic reflection is not known to exist, but a requisite appropriate velocity contrast might not exist across the fault.
- IVa, b. Upper and lower seismic reflectors from COCORP Line 5 (Cook and others, 1983, Fig. 17b) interpreted as possible continuations of the basal decollement. Since Line 5 is offset about 70 kilometers to the SW from the cross section these lines only suggest the general depth range at which the decollement would exist.
- V. A strong SE-dipping reflector (Cook and others, 1983, Fig. 17b) that might represent a possible ramp location.
- VI. Inferred position of a seismic reflector of Petersen and others (1984) that approximately coincides with the southeastern boundary of the Belair belt identified geophysically by Daniels (1974).

Cross section construction notes

1. Zones of relatively incompetent sericitic phyllite in which D₄ dextral shear strain is concentrated.
2. Level above which cross section reconstruction is very speculative.
3. Possible sites of D₃ thrust faults on the thicker southeastern limb of the Kiokee belt foliation arch
4. Northernmost extent of Cretaceous Coastal Plain cover.
5. Four Belair belt informal stratigraphic units of mainly metavolcanic rocks with intercalated volcanic-derived metasedimentary rocks.

Figure 4c. Legend to geologic cross section in Figure 4b (from Maher, 1987)

the Kiokee Belt and the Modoc Fault zone. Relict sedimentary structures present in weakly deformed areas and not destroyed by low grade regional metamorphism, indicate a nearshore setting dominated by tidal conditions. Trilobite fossils found in a mudstone sequence in the upper part of the Asbill Pond Formation indicate the Carolina Slate Belt is an exotic terrain accreted to North America after the Middle Cambrian (Secor, 1987a).

The Richtex Formation (mm on Figure A1, Appendix A) is a widespread stratigraphic unit in the central and western Carolina Slate Belt (see Figure 4). It is a sequence of thin to massively bedded mudstone and wacke interlayered with intermediate to mafic tuffs and flows that are intruded by sheets and plugs of mafic igneous rocks (Secor, 1987b). The exact thickness of this formation is unknown as penetrative strain and extensive folding have deformed the original stratigraphy. Secor (1987b) estimates that the thickness of this formation probably exceeds a few kilometers. Stratigraphically, the Richtex is interpreted to overlie the Persimmon Fork Formation. However, it is uncertain whether the contact between the Richtex and the Persimmon is stratigraphic or tectonic. Secor (1987b) tentatively favors a tectonic boundary based on the available evidence. A tectonic boundary implies that the Richtex is part of a regional thrust faulted block which may possibly be older in age than the underlying Persimmon Fork Formation. If this latter interpretation is correct, a late Precambrian age is compatible with the unfossiliferous nature of the Richtex Formation.

Belair Belt

The Belair Belt has been correlated with the Carolina Slate Belt in the past because of similar rock types (Overstreet and Bell, 1965). The Belair Belt was first recognized by Crickmay (1952) and consists of interlayered felsic and intermediate pyroclastic rocks with subordinate sedimentary rocks that have undergone regional metamorphism to the greenschist facies (Maher, 1978). Principal rocks which constitute this belt are phyllites and slates. Maher (1978) in Figure 4d (see Figure 4a for location of map) has tentatively subdivided the Belair Belt into four major lithologic units: a) silver phyllitic metatuffs (spt), b) felsic metatuffs (lft), c) intermediate (mafic) metatuffs and associated metasediments (mts), and d) felsic metatuffs and flows (uft). A full description of the individual lithologic subdivisions is presented by Maher (1978).

Maher (1987) reports that the original bedding (S_0) is often well preserved in the rocks of the Belair Belt. Regional greenschist metamorphism has altered and imprinted a locally variable northeast foliation (S_1) upon the original rock fabric (see Figure 4d). In addition, there is another lineation that is common in the Belair Belt rocks, but no folds have been found associated with this fabric. This latter lineation trends east to west and typically plunges moderately to the east. It is uncertain what the relationship of this last lineation is to the metamorphic and deformational history for this belt. Similarities in age and stratigraphy between the Belair and Carolina Slate belts are interpreted by Maher, Sacks, and Secor (1991) to indicate the two belts are part of the same terrain (Carolina terrain).

The Augusta Fault zone separates the Kiokee and Belair belts (see Figures 2 and 4d). Maher (1987) likens the Augusta Fault zone to the Modoc zone in that both zones have a polyphase history involving both ductile and brittle components. The Augusta Fault zone is about 0.5 km (0.3 miles) wide and dips moderately to steeply (45 to 75 degrees) southward as shown by Figure 4b. The fault zone is composed of at least eight individual faults and is at least 24 km (15 miles) long (Prowell, 1978). Mylonitized, brecciated, and contorted gneisses and some phyllonites (i.e., phyllite formed by mechanical degradation) characterize this contact zone. The Augusta Fault zone is interpreted to have formed during the Paleozoic (Secor, 1978a; Maher and others, 1991).

As shown by Figure 4d, the Augusta Fault zone is displaced by a series of en echelon faults, one of which is identified as the Belair Fault (see also Figure 2). The Belair Fault is an important fault in the southeastern United States as it is one of the few documented cases of Cenozoic faulting. Further information about this fault is presented in a later section of this report.

Tectonic Model

Two general hypothesis have been proposed to explain the development of the Carolina, Kiokee, and Belair belts (Maher, 1978). According to the first hypothesis, the Kiokee Belt is the core of a regional anticlinorium with the Carolina and Belair belts on the flanks. In the second hypothesis, the Kiokee Belt is a mobile migmatitic infrastructure and the flanking Carolina Slate and

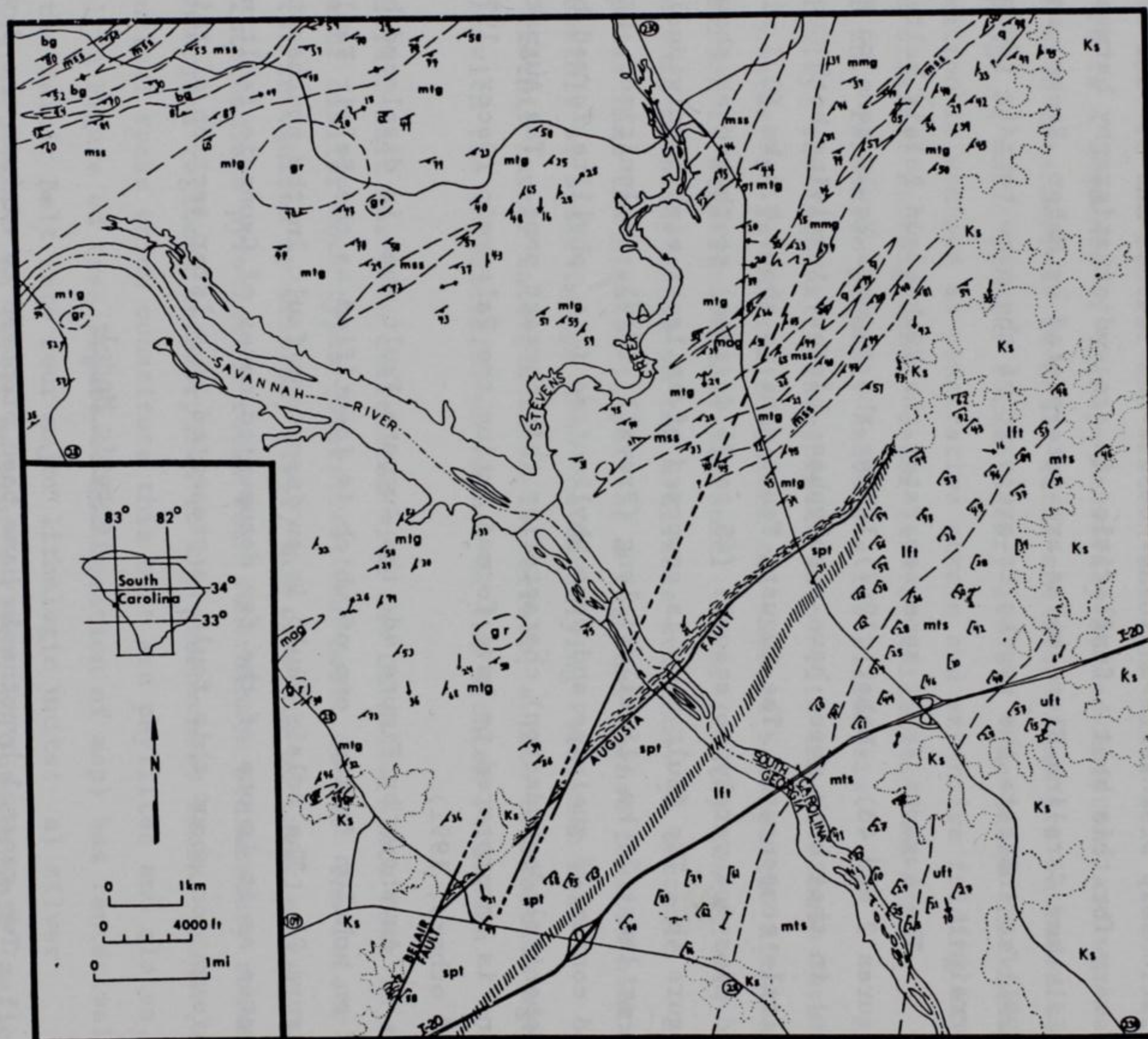

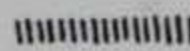


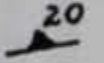
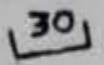
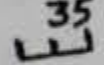
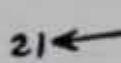
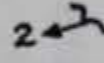


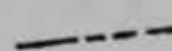


Figure 4d. Geology map of Belair and southern Kiokee belts (from Maher, 1978)

EXPLANATION

Symbols

-  Lithologic contact
-  Gradational contact
-  Fault
-  Possible fault extension
-  Strike and dip of foliation (Kiokee belt)
-  Strike and dip of cleavage (Belair belt)
-  Strike and dip of cleavage parallel to bedding
-  Trend and plunge of lineation
-  Minor fold axis
-  Road numbers
-  Roads
-  State border

Lithology

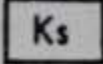
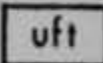
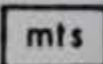
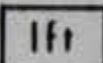
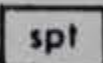
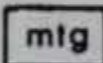
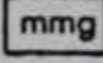
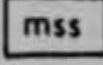
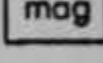
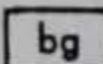
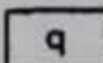
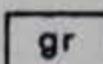
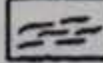
-  Coastal Plain sediments
- Belair belt
 -  Upper felsic metatuffs and flows
 -  Mafic (intermediate) metatuffs and metasedimentary rocks
 -  Lower felsic metatuffs
 -  Silver phyllitic metatuffs
- Kiokee belt (no stratigraphic order implied)
 -  Migmatitic two-mica gneiss
 -  Migmatitic muscovite gneiss
 -  Migmatitic sillimanite schist
 -  Migmatitic amphibole gneiss and/or amphibolite
 -  Biotite gneiss
 -  Metaquartzite
 -  Synkinematic granite
 -  Mylonitic rocks

Figure 4e. Legend to geologic map of the Belair Belt in Figure 4d (from Maher, 1978)

Belair belts are the suprastructure. Secor and others (1986b) favor the second model and interpret the Kiokee antiform to have developed by northwestward motion and compression of accreted terrains along a continental margin via a regional decollement (see Figure 4b, line labeled as IVa). Secor (1987) has proposed a model to explain the development of the Savannah River area at the site of the J. Strom Thurmond Dam and Reservoir as follows:

a. The Persimmon Fork and Asbill Pond formations were deposited in association with a subduction related volcanic arc during the early and middle Cambrian (570 to 525 Ma). Later, the Richtex Formation is displaced and accreted to the ancestral North American continent by the early Devonian (407 to 385 Ma); see Figure 5a (from Secor and others, 1986b).

b. The rocks in the Carolina Slate and Charlotte belts were deformed (Delmar deformation - D_1) and tightly folded sometime between 525 to 415 Ma. A subhorizontal interface developed between the infrastructure and suprastructure at mid-crustal depth. Regional metamorphism was at the greenschist facies in the suprastructure (ancestral Carolina Slate Belt) and amphibolite facies in the infrastructure (ancestral Kiokee and Charlotte belts); see Figure 5b.

c. Between 327 and 298 Ma granitic plutons were emplaced from a magmatic arc source. These plutons are strongly deformed in the northwestern part of the Kiokee Belt, Modoc Zone (see Figure 5c).

d. In addition, a second period of deformation (Lake Murray - D_2) occurs between 315 to 295 Ma with overprinting and deformation of D_2 structures and fabric. Deformation occurs along the Modoc and Augusta zones with components of normal and dextral strike slip (see Figures 5d and 5e).

e. A third period of deformation (Clarks Hill - D_3) occurs between 295 to 285 Ma as a consequence of continental collision. The collision causes infrastructure and suprastructure to be folded and displaced northwestward along a regional decollement. The D_3 Kiokee anticlinorium is formed at this time (see Figure 5f).

f. A fourth period of deformation (Irmo - D_4) occurs between 290 to 268 Ma with dextral motion in the Irmo Shear zone (see Figure 4a for location). In the J. Strom Thurmond area, the Irmo shear zone coincides with the Modoc zone and overprints the D_2 structures. Secor interprets this dextral motion to be movement between Laurentia and Gondwana in the final stages of the Alleghanian orogeny.

g. During the Mesozoic, the Paleozoic terrain is cut by northeast trending Triassic and/or Jurassic dikes and brittle faults as the supercontinent tears apart and forms the present Atlantic ocean. Between the late Mesozoic and early Cenozoic, the coastal plain forms and the Belair Fault experiences movements.

h. Present geology of the J. Strom Thurmond area as shown by Figures 5h (see also 4a, 4b, 4d, and A1, Appendix A).

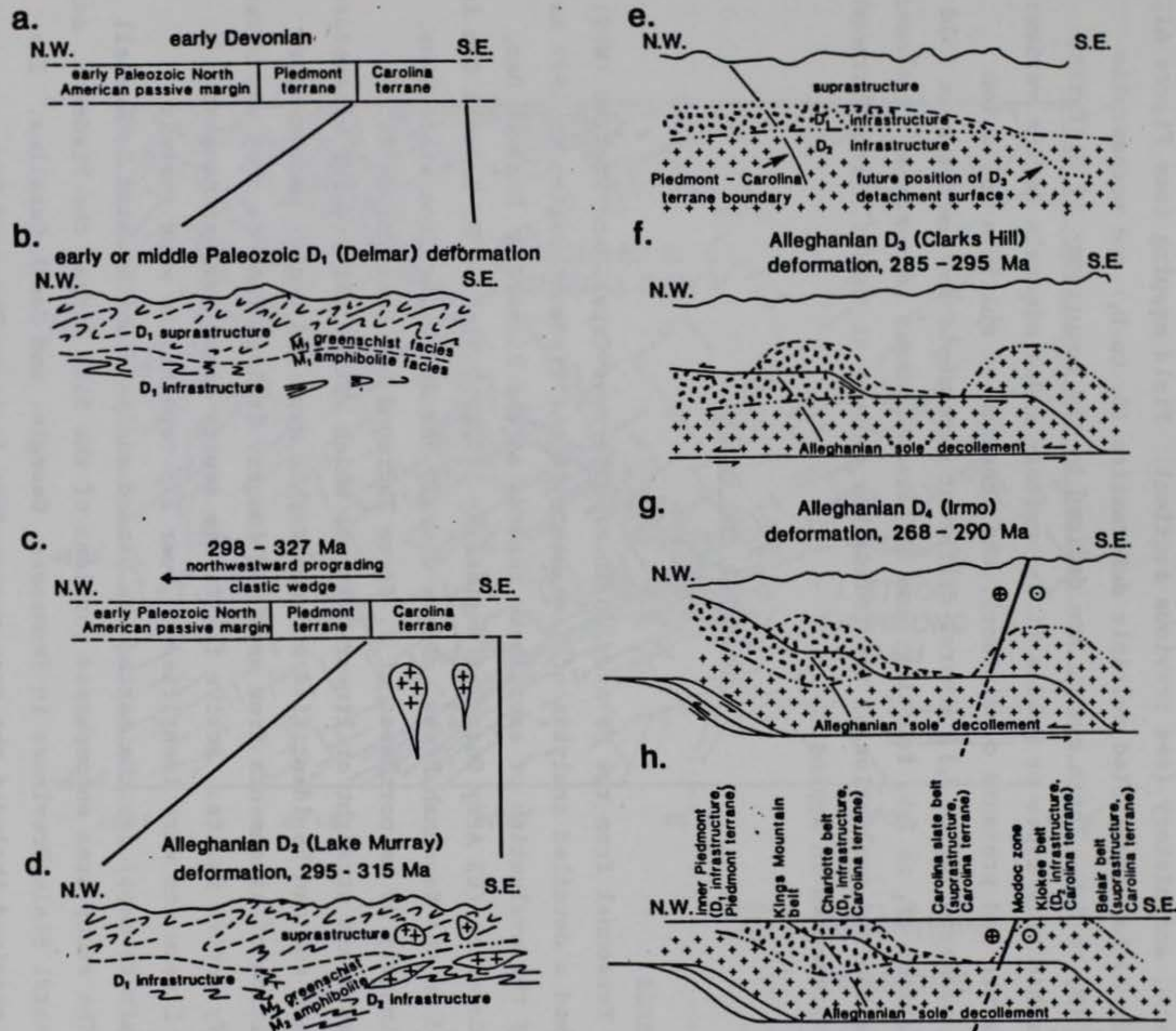


Figure 5. Tectonic model for development of the J. Strom Thurmond Dam and Reservoir area (from Secor and others, 1986b). See text for explanation of individual figures

Site Geology

Recent geologic mapping in the vicinity of J. Strom Thurmond Dam and Reservoir is presented in Figure A1, Appendix A (from Maher and Sacks, 1987). Detailed work by Maher and Sacks identifies a complex lithology, tectonic structure, and history (see previous section). Field mapping (see Figure A1, Appendix A) has identified multiple deformation (D_1 to D_4) and metamorphic events (M_1 to M_4). These events are defined by the occurrence of different metamorphic rock types or grades (i.e., certain index minerals define various temperature and pressure conditions), the presence of multiple foliation fabric elements (S_1 to S_4), several different mesoscopic and macroscopic fold orientations (F_1 to F_4), faulting, and different igneous intrusions. A closer examination and evaluation of the foundation geology at the J. Strom Thurmond Dam is presented in Appendix A.

Lineaments and Faults

Lineaments

Personnel from the US Army Engineer Waterways Experiment Station (WES), performed a detailed analysis of lineaments in the Piedmont region in 1977 as part of the evaluation of earthquake hazards at the Richard B. Russell Dam, South Carolina (US Army Corps of Engineers, 1977a). Richard B. Russell Dam is located on the Savannah River, on the Georgia and South Carolina state line, approximately 35 km northwest of J. Strom Thurmond Dam (see Figure 1). Lineaments are straight or linear features which extend for several kilometers in length and can be identified on topographic maps and aerial photographs. Recognition of lineaments from maps and imagery is important as they may often identify active faults. Active faults are source areas for earthquakes.

Lineaments were identified on over 175 topographic maps (mainly 7-1/2 minute maps) for the earthquake hazard analysis for Richard B. Russell Dam. The study area encompassed portions of the Blue Ridge, the Piedmont, and the Coastal Plain Provinces in Tennessee, Georgia, and South Carolina. The region examined included the area surrounding J. Strom Thurmond Dam. Lineaments surrounding J. Strom Thurmond Dam are presented on Figure 6 (from US Army Corps of Engineers, 1977a). The WES study concluded that two primary patterns occur in the Piedmont.

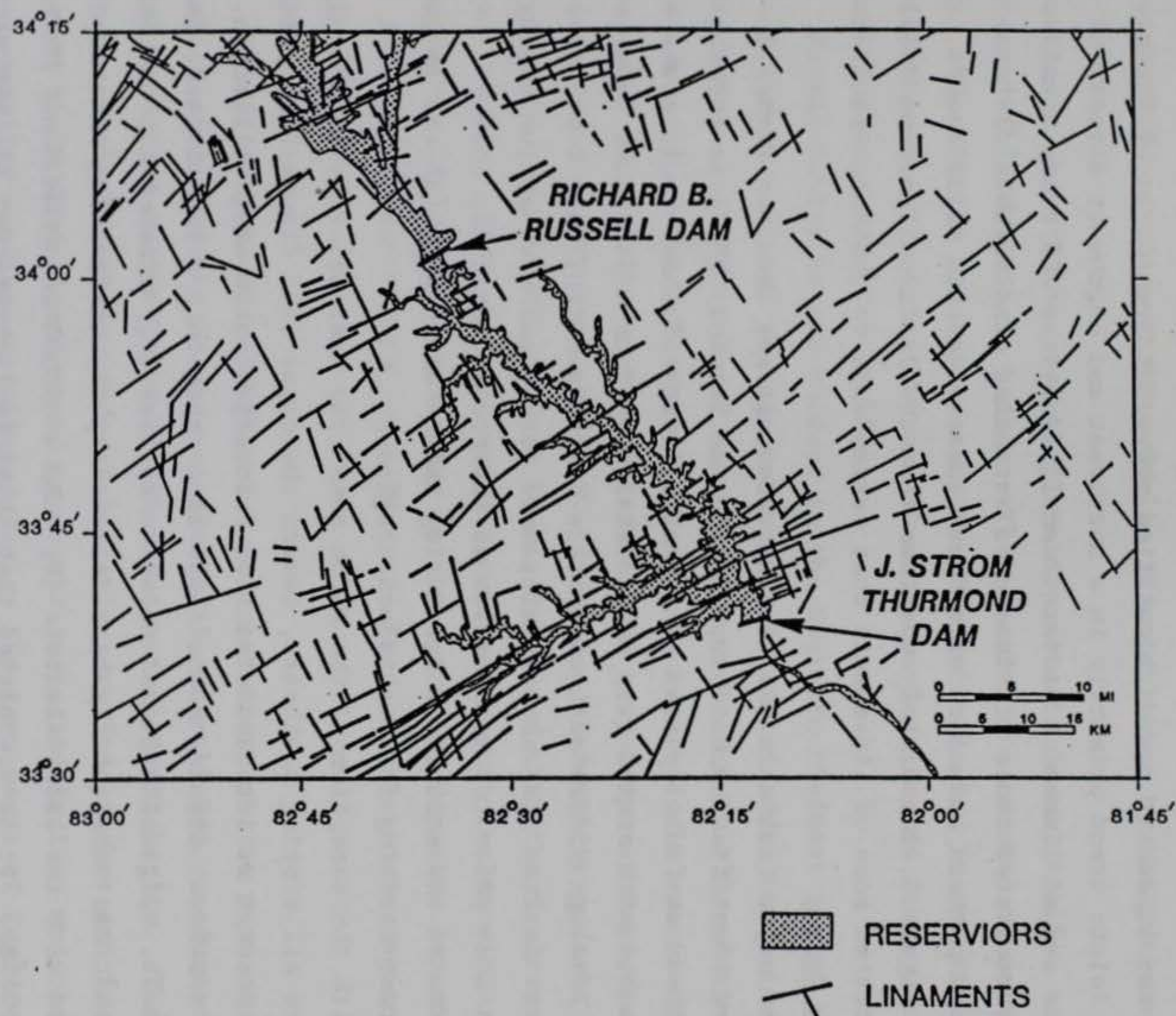


Figure 6. Lineaments surrounding J. Strom Thurmond and Richard B. Russell Dams
(from US Army Corps of Engineers, 1977a)

The first pattern is evenly dispersed and has two right angle components. This pattern generally conforms with the structural grain of the region and includes a general strike at N55°E and a right angle component striking at N35°W. These lineament patterns reflect the structure in the region and correspond to the orientation of folds, faults, major rock boundaries, dikes, or joints. Joint studies conducted in the eastern Piedmont for Richard B. Russell Dam and surrounding area indicate a close relationship with the two lineament trends identified above (US Army Corps of Engineers, 1977b). Joints trend primarily in a northeast and northwest direction.

The second lineament pattern identified by the WES study consisted of narrow concentrated zones of lineaments extending considerable distances. This second pattern coincided with known shear zones and major faults. As shown by Figure 5, immediately upstream from the J. Strom Thurmond damsite is a concentrated zone of lineaments that corresponds to the Modoc Fault Zone.

Paleozoic Faults

The major faults in the Piedmont Province are shown on Figure 2. These faults are identified by Hatcher, Howell, and Talwani (1977) as forming the Eastern Piedmont fault system. The vast majority of these fault zones are thrust faults with strike-slip components. The four major fault zones are the Brevard, Towaliga-Middleton-Lowndesville-Kings Mountain, Goat Rock-Modoc, and the Augusta faults. The above faults were formed and were active during the Paleozoic Era, prior to the creation of the present Atlantic Ocean. Development of the Atlantic Ocean during the Mesozoic marks an end to large scale thrust faulting in the Piedmont region.

With the exception of the Modoc zone, the vast majority of the mapped faults are all dipping southeast, toward the coast (see Figure 4b). These faults represent relict tectonism from Paleozoic continental collisions. The opposing northwest dipping Modoc fault zone represents a reactivated, deep seated fault, originally formed under an earlier (D_2) extensional tectonic regime, that has subsequently been deformed by thrust faulting and ramping associated with the late Paleozoic ($D_3 - D_4$) continental collisions (Secor and others, 1986b). It is speculated that these fault zones may all converge at depth into a master detachment zone as interpreted by Figure 4b, zone IVa to IV (from Maher, 1987).

Mesozoic Faults

The Mesozoic Era is characterized by extensional tectonism and the creation of large Triassic basins along the eastern edge of North America. Associated with extensional tectonism is the intrusion of numerous diabasic dikes into the crystalline rocks of the Piedmont (Ragland, 1991). These dikes generally all strike northwest to southeast and are against the regional structure. Many of the major thrust faults are cut by these dikes, and the latest movement on these thrusts faults is established by the presence of these dikes.

Buried beneath the coastal plain deposits in South Carolina are sedimentary filled Triassic basins. These basins are bounded by normal faults. The nearest Triassic basin, the Dunbarton Basin, is approximately 50 km southeast of J. Strom Thurmond Dam on the Georgia and South Carolina state line (Marine and Siple, 1974).

Normal faults at the surface in the Southern Piedmont region are numerous and are related to regional uplift and extensional tectonism during the Mesozoic. Located in the J. Strom Thurmond-Clarks Hill Reservoir area near Willington, South Carolina, the Patterson Branch Fault was identified as a terminated Triassic basin basement fault (US Army Corps of Engineers, 1977e). Trenching was conducted on Tertiary and Pleistocene gravels that were overlying the trace of the fault. It was concluded that the fault was not active. Griffin (1981) also identifies numerous normal faults with displacements of less than one meter in the saprolite deposits covering the Inner Piedmont of South Carolina. These faults are related to regional uplift during the Mesozoic.

Cenozoic Faults

The US Army Corps of Engineers, Savannah District, as part of the evaluation of earthquake hazards at Richard B. Russell Dam, performed detailed studies to detect active faults in the Southern Piedmont region. They examined aerial photography and satellite imagery for linears and faults, performed field investigations of known and suspected faults, and conducted several detailed studies on selected faults (US Army Corps of Engineers, 1977a, 1977b, 1977c, 1977d, 1977e, 1977f, and 1977g). The above studies also included an intensive field investigation in the area surrounding J. Strom Thurmond. It was determined that there are no Cenozoic faults in the Southern

Piedmont region except for the Belair Fault. Furthermore, there are no active faults in the Piedmont except for possibly the Belair Fault (see Figure 4d).

The Belair Fault is located at the Belair Clay Pits of a local brick company on the northern margin of the coastal plain near the Georgia and South Carolina state line (see Figure 2, Fault No. 9, and Figure 4d). The fault is approximately 19 km southeast of J. Strom Thurmond Dam and it is the first possible instance of Post-Tertiary fault displacement in the southeastern United States (Prowell, O'Connor, and Rubin, 1975; and O'Connor and Prowell, 1976).

Prowell, O'Connor, and Rubin (1975) trenched the fault and concluded that the Belair Fault is a 7.5 km long reverse fault which had moved approximately 2,450 years before the present. The displacement on the fault is interpreted to be approximately 1 meter. The principal basis for the age determination was made by radiocarbon dating of disseminated organic materials. The validity of the fault age has been rejected. The age was not accepted as contamination of the organic material was determined to have occurred. The US Geological Survey re-examined the age problem by conducting a follow-up study and trenched a second time across the fault zone (US Army Corps of Engineers, 1977f). They concluded that the age was not reliable as the organic material had been contaminated. The US Geological Survey concluded that the age of latest movement on the Belair Fault is unknown, but it has moved within the last 50 million years or since Eocene time.

It is concluded that there are no active faults at or near J. Strom Thurmond Dam. The basis for this determination is made from the available geologic data on the Piedmont region (see References and Appendices), from geologic site data, from studies made by the US Army Corps of Engineers (1977a, 1977b, 1977c, 1977d, 1977e, 1977f, 1977g, and 1978), from discussions with government and university geologists and seismologists knowledgeable about this area, from the seismic record for this region, and a site visit to the study area as part of this investigation.

PART III: SEISMICITY

Relation of Seismicity and Geology

Geophysical studies are useful in identifying anomalous structures deep within the subsurface. Such structures are where tectonic stresses may become concentrated and serve as potential sources for earthquakes. Gravity and magnetic studies are two principal types of geophysical studies that are used to define these geological irregularities.

Figure 7 presents the results of a gravity survey over portions of South Carolina, Georgia, and Tennessee (from Long, 1979). A gravity map identifies density variations which in turn indicate differences in rock type and thickness. The gravity map generally corroborates the major physiographic and geologic boundaries in the southeastern United States and the Piedmont Province. The Charlotte-Carolina belts (includes Kiokee Belt) are distinguished from the Inner Piedmont by the presence of a pronounced gravity high. The J. Strom Thurmond Dam is located upon the edge of the Charlotte and Carolina belts and near the southeastern edge of a gravity high.

Long (1979) interprets the gravity highs beneath the Charlotte and Carolina belts as caused by a thinner crust and/or the presence of more dense mafic to ultramafic rocks (amphibolite or basalts) in the crust. In contrast, a pronounced gravity low occurs northwest of the J. Strom Thurmond Dam, beneath the Hartwell and Clemson dams. This low is interpreted as an over-compensation (a thick upper crust) by low density continental rocks (granitic and metasedimentary rocks). Long (1979) suggests the structure and rock types present in the Piedmont in Georgia and South Carolina are the remnants of a Paleozoic rift zone. The rift zone hypothesis is compatible with the accreted terrain model in Figure 5 (Secor and others, 1986b) providing the rift zone developed during the early Paleozoic as interpreted by Hatcher and Goldberg (1991). The extent of this ancient rift zone is defined by the Towaliga Fault and the Kings Mountain Belt on its northwest edge and the Modoc Fault on the southeastern edge. He suggests that the rift would help explain the presence of the large system of faults identified by Hatcher and others (1977) in South Carolina and Georgia without requiring large strike slip or thrust movements.

The boundary separating the Charlotte-Carolina belts from the Coastal Plain is approximately represented by the 0 mgal contour. Eroded sediments

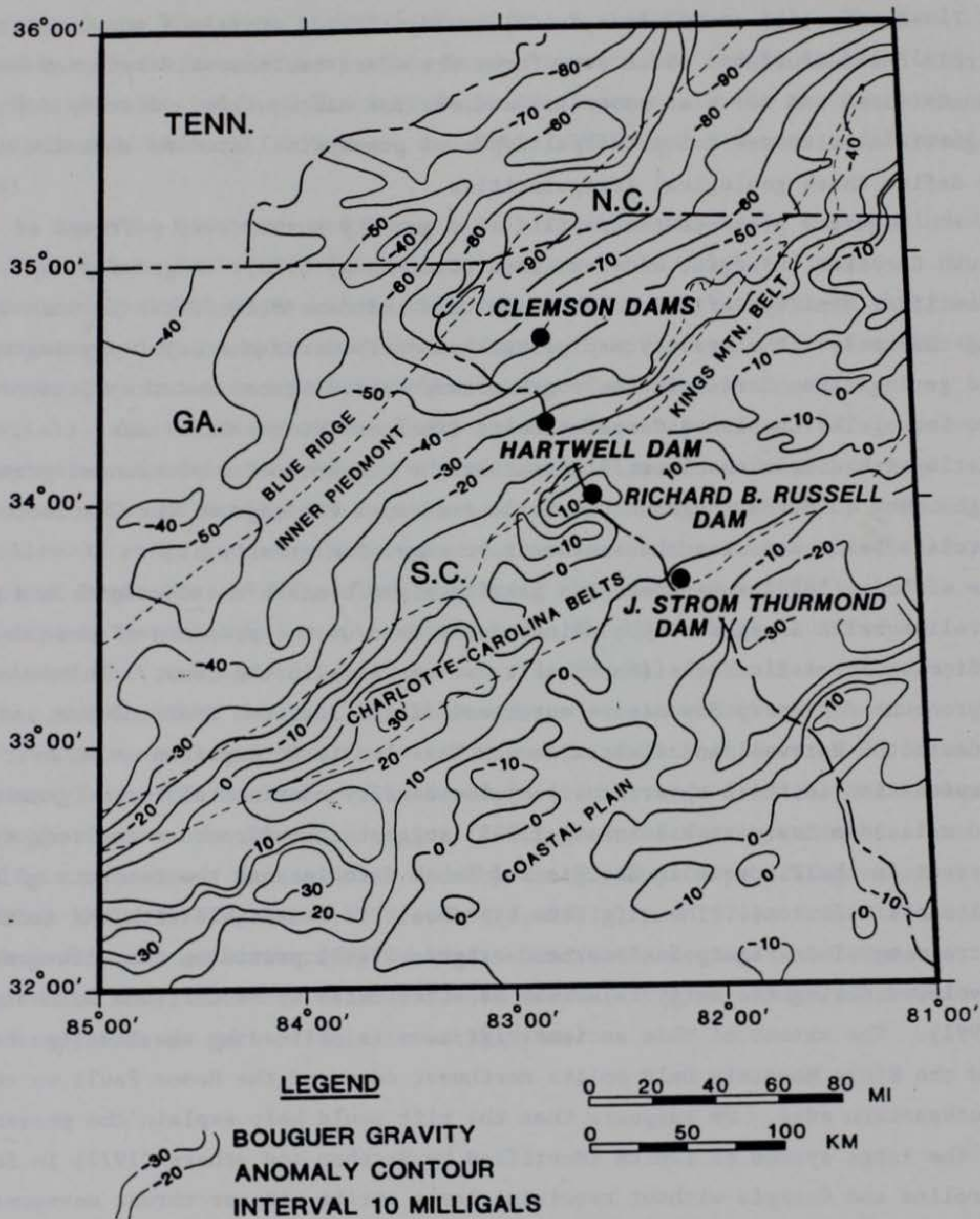


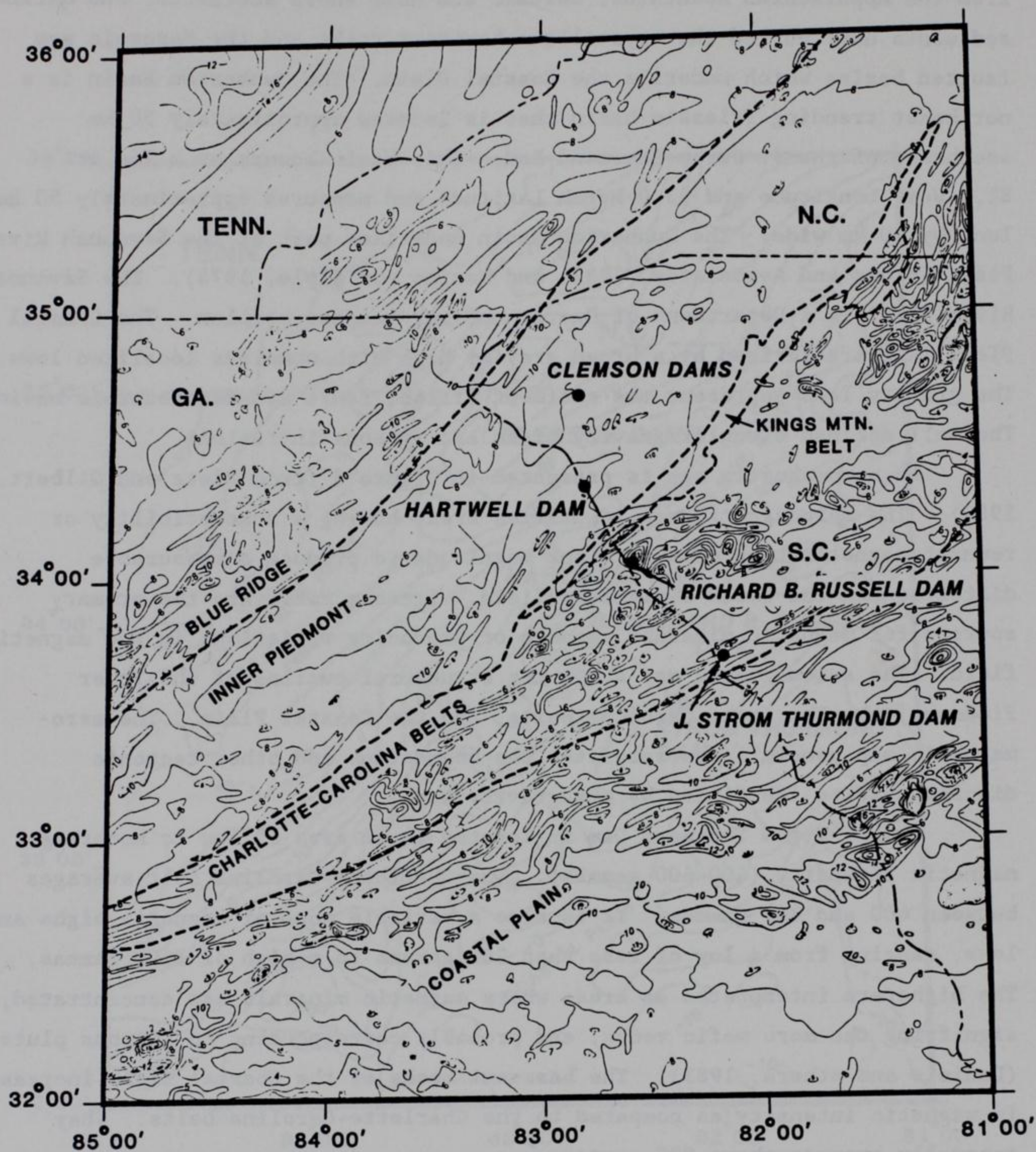
Figure 7. Gravity map of portions of Georgia and South Carolina (from Long, 1979)

from the Appalachian Mountains, deltaic and near shore sediments, and marine sediments have buried the crystalline basement rocks and the Mesozoic age faulted basins which underlie the Coastal Plain. The Dunbarton Basin is a northeast trending Triassic basin that is located approximately 50 km southeast of the J. Strom Thurmond Dam. This basin occurs as a low at 81.5 West Longitude and 33.0 North Latitude and measures approximately 50 km long by 10 km wide. The Dunbarton Basin underlies part of the Savannah River Plant (Blume and Associates, 1982; and Marine and Siple, 1974). The Savannah River Plant is a Department of Energy nuclear reactor complex. The Coastal Plain is characterized by a broad gravity high with numerous localized lows. The gravity lows represent the sediment filled, fault bounded Mesozoic basins. The well defined circular gravity highs are igneous intrusions.

An aeromagnetic map is presented in Figure 8 (from Zietz and Gilbert, 1980). The aeromagnetic map identifies areas having a susceptibility or remnant magnetization of sufficient magnitude to produce a measurable distortion in the earth's magnetic field. Igneous rocks are the primary sources for magnetic minerals capable of producing variations in the magnetic field. The aeromagnetic map shows the structural outline of the Inner Piedmont, the Charlotte-Carolina belts, and the Coastal Plain. The aeromagnetic map generally corroborates the boundaries and other tectonic discontinuities identified by the gravity map.

The J. Strom Thurmond Dam is located in an area of low to moderate magnetic intensity (400-600 gammas). The Charlotte-Carolina Belt averages between 400 and 800 gammas. It is also a variable zone of magnetic highs and lows, ranging from a low of less than 200 gammas to a high of 1600 gammas. The highs are interpreted as areas where magnetic minerals are concentrated, signifying the more mafic rocks, and probably corresponding to igneous plutons (Daniels and others, 1983). The basement rocks of the Coastal Plain increase in magnetic intensity as compared to the Charlotte-Carolina belts. They generally average above 800 gammas.

In summary, the gravity and aeromagnetic maps delineate the major structural and geologic boundaries in the Piedmont and Coastal Plain Provinces. This area contains ancient faults, plutons, Triassic basins, and a possible Paleozoic rift zone. These are all areas where tectonic stresses may be concentrated and which may produce earthquakes.



LEGEND

CONTOUR IN 100 GAMMAS,
CONTOUR INTERVAL IS 200
GAMMAS UNLESS LABELED DIFFERENTLY

0 10 20 30 40 50 MI
0 20 40 60 80 KM

Figure 8. Aeromagnetic map of portions of Georgia and South Carolina (from Zeitz and Gilbert, 1980)

Distribution of Historic Earthquakes

A catalogue of historic earthquakes from the study area (32.0° to 35.0° North Latitude and 79.5° to 84.0° West Longitude) is presented in Appendix B. The catalogue is derived from the Earthquake Data Base from the National Geophysical Data Center, National Atmospheric and Oceanic Administration (NOAA), (from Habermann, 1989). The list of historic earthquakes is arranged by date and time (Universal or Greenwich Time) and includes coordinate location of the epicenter, earthquake magnitude (m_b , M_L , and M_s), Modified Mercalli (MM) intensity, and focal depth. A glossary of terms is included in Appendix C which describes the MM intensity (MMI) scale and the different instrumental or magnitude scales that are used.

The catalogue in Appendix B contains a listing of 876 events between the years 1698 and 1988. The catalogue also identifies possible duplicate listings. Duplicate listings occur because of different interpretations of time, location, or MM intensity for an event, in which case each interpretation has been listed and the source identified. There are 147 suspected duplicate events in the catalogue in Appendix B.

The catalogue identifies a wide range of earthquakes; from events that were not felt, but instrumentally recorded, to events as large as a MM X. The vast majority of earthquakes are less than MM IV. The distribution of historic earthquakes greater than MM IV is as follows: 38 earthquakes at MM V, 20 earthquakes at MM VI, 2 earthquakes at MM VII, 1 earthquake at MM VIII, and one earthquake at MM X. The MM VIII earthquake has since been downgraded to MM VII. The reasons for downgrading this earthquake are explained fully by Krinitzsky and Dunbar (1987). This MM VII earthquake occurred on New Years day in 1913 in Union County, South Carolina. The Union County earthquake is the largest historic earthquake to have occurred in the Piedmont. This earthquake was located approximately 80 miles (125 km) northwest of J. Strom Thurmond Dam.

The distribution of historic earthquakes of MM intensity IV and greater in the study area is presented in Figure 9. Examination of Figure 9 indicates no general pattern or significant concentration of historic earthquakes surrounding the damsite. The highest concentration of earthquakes occurs southeast of the J. Strom Thurmond Dam, in the Summerville and Charleston

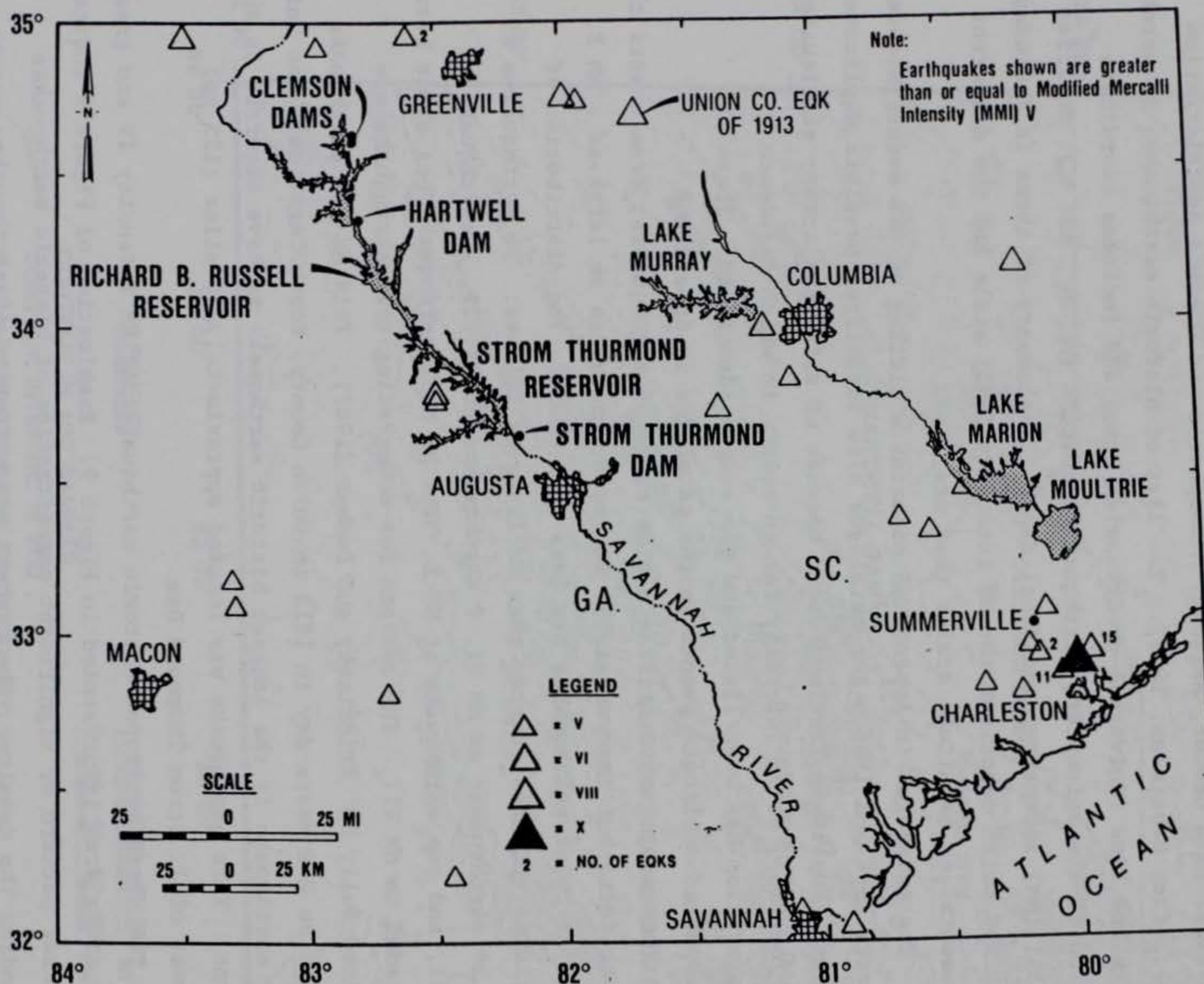


Figure 9. Distribution of historic earthquakes for region surrounding J. Strom Thurmond Dam

area. The seismic record indicates that the region surrounding the damsite is characterized by low levels of seismic activity and by small earthquakes of less than MMI VI, a level that is too low to cause damage to properly engineered structures. The historic record indicates that the Summerville and Charleston area is an active area and was the location for the largest historic earthquake in the southeastern United States. The Charleston earthquake occurred on 1 September 1886 and was an MMI X earthquake.

Causes of Earthquakes

Earthquakes are produced when strain energy is suddenly released in the form of movements along faults. Strain energy is derived from the concentration of local and regional tectonic stresses. The concentration of stress may cause sudden movements along a fault surface and results in an elastic rebound. This elastic rebound produces vibrations in the earth's crust and these vibrations are felt as an earthquake. Large earthquakes require a large stress drop, a large energy release, and usually can only be produced by fault movements originating from within the crystalline basement rocks at depths generally greater than 5 km.

The causes of earthquakes both in the study area and in the southeastern United States are not well understood since there are no active faults that have been identified. The principal theories that may explain seismicity in the study area and the southeastern United States are as follows:

- a. Focusing of regional stresses at heterogeneities, plutons or other discordant rock masses in the subsurface, and release of this stress by fault movements at depth.
- b. Introduction of magmatic materials into the lower crust, producing stresses, and generating fault movements at depth.
- c. Focusing and release of regional stresses along pre-existing zones of weakness such as ancient faults and rift zones. Stress release occurs along existing normal, strike slip, or thrust faults. Stress release is therefore dependent on the existing geologic structures and the orientation of the present stress field. The principal theories for each type of fault movement and stress condition are as follows:
 1. Regional compression causing activation and slippage along strike slip or transform faults. A major transform fault has been proposed that passes through South Carolina, extending from the Blake Fracture Zone in the Atlantic Ocean to its proposed western extension in Eastern Tennessee (Sbar, and Sykes, 1973). This zone

is based in part on the pattern of historical seismicity and is known as the Charleston-Cumberland trend.

2. Regional compression causing activation and slippage along pre-existing thrust faults.

3. Regional extension producing normal fault movements along fault bounded coastal graben structures (i.e., Triassic basins) or relaxation type movements on existing faults (Barosh, 1981; and Armbruster and Seeber, 1981).

d. Localized stress relief along joint planes or other near surface discontinuities (Talwani, 1988 and Appendix D; and Long, 1988 and Appendix E). Earthquakes are produced by fracturing in brittle rocks (primarily granitic rocks) at depths less than 2 km. These earthquakes are related to water table fluctuations and ground water movements. This mechanism has been termed "hydroseismicity" (Costain, Bollinger, and Speer, 1987).

Explanations a through c above can be interpreted as suggesting that a large earthquake can happen anywhere in the study area at a location where no historic earthquake has ever happened before. To project an earthquake into an area or a zone that has displayed no past seismicity, but is part of a major trend such as the Charleston-Cumberland trend or is near a major ancient fault, is not considered valid by the present authors unless there is evidence in the seismicity or active faults nearby. A key question that must be asked in such an evaluation as this: Is there a relation between the present tectonism and the existing geologic structures? The evidence to answer this question must be obtained from the seismicity, including very small earthquakes, or by the geologic evidence for active faults. The folding and faulting that have been mapped (see Figures 2, 4a, 4b, 4d, and A1, Appendix A) are from ancient tectonism which is no longer active today. Present day tectonism is greatly different from the tectonism which formed these ancient structures. The present seismicity is related to the stress conditions that are active today.

A detailed discussion about the distribution of regional stress in the study area is presented in Appendix D, a report by Dr. Talwani (University of South Carolina) on the "Seismic Potential Near Strom Thurmond Lake, South Carolina." Dr. Talwani identifies the existing stress conditions in South Carolina's Piedmont and at various reservoirs as determined from in-situ stress measurements and focal mechanisms. In addition, he examines the seismicity in the study area, the potential earthquake sources, and gives his interpretation for the maximum earthquake potential at the J. Strom Thurmond Dam. Dr. Talwani favors mechanism c in the above list of models for the

source for large intraplate earthquakes such as the 1886 Charleston earthquake.

Explanation b in the above list of models is favored by Dr. Long for the generation of large Charleston earthquakes. His views are presented in a report in Appendix E on the "Maximum Earthquake at Strom Thurmond Reservoir." Major intraplate earthquakes by Long's model are the result of stress amplification in the upper crust due to the injection of mobile magmatic fluids from the mantle into the lower crust. The process of fluid injection and upward migration leads to strength corrosion of the lower crust, generation of stresses in the middle crust, and the eventual failure of the weak middle and upper crust. This failure processes produces a major earthquake. Dr. Long believes that seismicity in eastern Tennessee, at Charleston, and at New Madrid, Missouri, can be explained by this mechanism. For the Charleston area, the central core of seismic activity necessary for a major earthquake to occur is lacking. Consequently, Dr. Long suggests that a major Charleston earthquake is unlikely. His model is fully explained in Appendix E.

Both Drs. Long and Talwani describe seismicity in South Carolina's Piedmont as caused by shallow stress relief along joint planes or mechanism d in the above list of models. Consequently, a major earthquake is not apt to occur by this mechanism in the Piedmont. Explanation d in the above list of models implies a very low upper bound on the maximum earthquake that can occur. The release of stress is near the surface and is unrelated to tectonic processes affecting the major geologic structures. The cause is believed to be a triggering action resulting from ground-water movements through joints. Because such earthquakes are very shallow, a damaging earthquake ($\text{MMI} \geq \text{VIII}$) is not expected to occur by this mechanism. However, if this mechanism is the primary cause of earthquakes in the southern Piedmont, then small earthquakes ($\text{MMI} \leq \text{VII}$) may occur anywhere within the study area. This type of earthquake would be especially apt to occur near reservoirs. Reservoir induced seismicity will be discussed in the next section of this report.

Dr. Long believes that the movement of ground water on joints in the shallow subsurface (less than 3 km), is the cause of the earthquakes in the Piedmont. This mechanism is in agreement with field observations and microearthquake monitoring that has been done using seismometer arrays in this region over the years. The lack of surface rupture by these very shallow earthquakes reinforces the idea that there is an apparent dissipation of

displacement at the surface by the spreading of displacements through joint sets. The effect is of a volume stress relief. The mechanism is consistent with the patterns seen in clusters of earthquakes where there have been small earthquakes induced at reservoirs in the Piedmont. Thus, these earthquakes are inferred to have no tectonic relation to major faults other than avenues for ground-water transmission.

Maximum Piedmont Earthquake

Long and Talwani both postulate that the 1913 Union County, South Carolina, earthquake of intensity MM VII may have been close to the maximum for the southern Piedmont. It does not follow, however, that the Union County maximum would occur everywhere. The historic seismicity is the only real guide for earthquake activity in the region and the seismicity shows that the Union County experience is high for the region.

It must be assumed that the largest earthquakes that can occur in the area of the J. Strom Thurmond Dam are defined by the record of historic seismicity or by the presence of earthquake-producing faults. Such faults have not been found in this region and the historic seismicity is of a very low order, $\text{MMI} \leq \text{VII}$. Also, the focal depths of these earthquakes are extremely shallow, thereby precluding potentials for larger earthquakes. Thus, earthquakes with an upper bound at MM intensity VII, matching the Union County earthquake, is assumed in this study to be a conservative maximum event for Piedmont seismicity.

Microearthquakes and Reservoir-Induced Seismicity

Introduction

Microearthquakes are earthquakes that are too small to be felt, but are recorded by seismographic instruments. Microearthquakes are useful for defining areas where tectonic stresses are concentrated. These small earthquakes are helpful in determining focal depths, fault types and their orientations, and they aid in estimating rates of earthquake recurrence. Most important, microearthquakes can determine whether there is a correlation between ancient tectonic structures (i.e., faults, plutons, etc.) and present seismicity.

Microearthquake monitoring in South Carolina began during the early 1970's and has been concentrated in the Coastal Plain, around the 1886 Charleston mesoseismal region, and at selected large reservoirs (Shedlock, 1988; Tarr and Rhea, 1983; Talwani, Appendix D; and Long, Appendix E). The monitoring program has indicated that seismicity is concentrated mainly in the Coastal Plain in three distinct zones. These three zones, located in the Charleston mesoseismal area as shown by Figure 10 (from Tarr and Rhea, 1983), consist of the Middleton Place to Charleston, Adams Run, and Bowman zones. In the Piedmont Province, microearthquake activity is diffuse, except for seismicity that has been induced by reservoirs. Microearthquake monitoring indicates that there is no association between present microearthquake activity and existing surface faults.

Coastal Plain Microearthquakes

Microseismic monitoring has shown that Coastal Plain earthquakes are concentrated at three locations (Middleton Place-Charleston, Adams Run, and Bowman, South Carolina) which are coincident with the edges of positive gravity and aeromagnetic anomalies (Tarr and Rhea, 1983). The geophysics data indicates a strong structural relationship for the seismicity. Talwani (1985) presents a broad overview of the different models proposed for Charleston seismicity. He evaluates the merits and arguments against each model, and concludes that the exact cause is still speculative, but he favors the existence of two intersecting faults that have been reactivated by the current state of stress. A more recent study by Talwani and others (1989), using stratigraphic, geophysics, and seismicity data, supports the intersecting fault model as the cause for earthquakes in the Charleston area and the probable cause for the 1886 Charleston earthquake. Furthermore, they suggest that this region has been episodically active since at least the Paleocene (67 to 58 million years before present) as indicated by displacements in the stratigraphy.

In summary, microearthquake monitoring in the Charleston area indicates that seismicity is concentrated at specific areas. Microearthquake activity is occurring from the source area of the 1886 Charleston earthquake and is occurring at generally higher levels than surrounding areas in the Coastal Plain. Monitoring indicates that these seismic source areas may be related to buried faults in the crystalline basement rock. However, further geological, geophysical, and seismological studies will be required before exact causes of

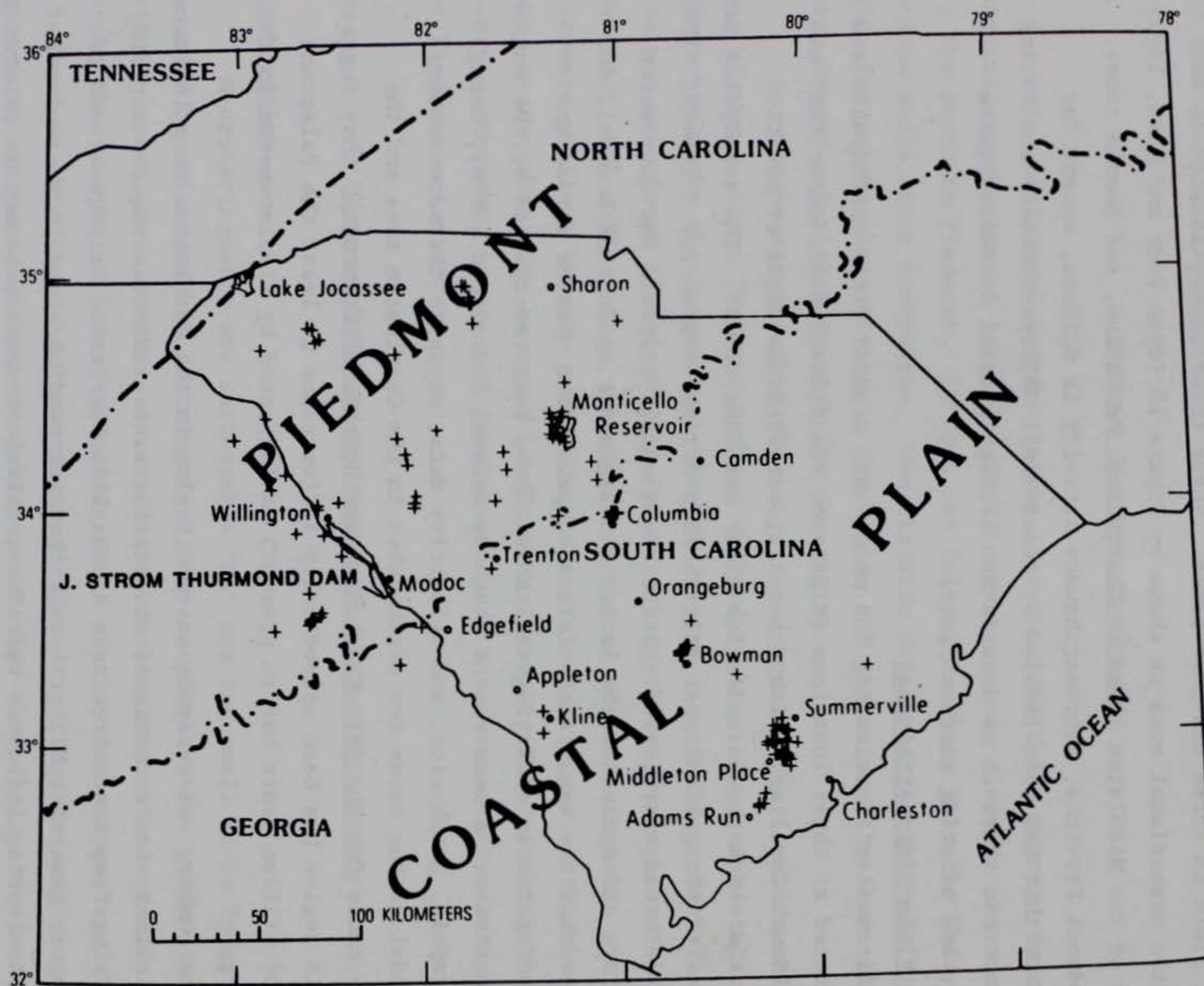


Figure 10. Distribution of earthquakes in South Carolina between 1973 and 1979 (from Tarr and Rhea, 1983) Earthquake epicenters are plotted without regard to magnitude or intensity

seismicity are determined and the nature of the geologic structures responsible are fully understood.

Piedmont Microearthquakes

Microseismic monitoring indicates that Piedmont earthquakes have unique characteristics (Long, Appendix E). These characteristics are their shallow depth (less than 2 km), swarm type of occurrence, high frequency spectral decay, correspondence between joint patterns and focal mechanisms, and seasonal variations. Consequently, a major Charleston type earthquake is not likely to occur within the Piedmont. Microearthquake monitoring has identified a relationship between several reservoirs in the Piedmont, sudden water level changes, and induced seismicity. Induced seismicity has been directly related to sudden, large changes in the reservoir levels. Reservoir-induced earthquakes have been associated with water level changes at Lake Jocassee, Lake Oconee, Lake Monticello, Lake Sinclair, and at J. Strom Thurmond Reservoir. Detailed information about reservoir-induced seismicity in the project area and its characteristics are examined and evaluated by both Drs. Talwani (see Appendix D) and Long (see Appendix E). They conclude that the maximum event possible because of ground-water influences is less than or equal to the maximum historic earthquake in the Piedmont, the MMI VII Union County earthquake in 1913.

The importance of microseismic monitoring programs has been in evaluating the characteristics of the Piedmont seismicity in determining whether a correlation exists between ancient tectonic structures and present day seismic activity. There is no correlation in the J. Strom Thurmond Dam area between present seismicity, ancient tectonic structures, and known surface faults.

Seismic Source Zones in the Southeastern United States

Earthquake source zones have been interpreted for the southeastern United States since there are no known active faults. These source zones are based on the record of historic earthquakes. The southeastern United States is in general a region of low level seismicity with areas of concentrated earthquake activity. These concentrated areas or zones are called "hotspots" and are potential sources for moderate to major earthquakes. The seismic

source zones interpreted for the southeastern United States are shown in Figure 11.

An earthquake zone as used in this report is an inclusive area over which a given maximum credible earthquake can occur. The earthquake identified for each zone in Figure 11 is the largest earthquake that can reasonably be expected to occur. It can be moved anywhere in the zone and is thus a floating earthquake.

The criteria by which the seismic zones in Figure 11 were developed are as follows:

- a. Maximum sizes of earthquakes.
- b. Density of earthquakes, using historic seismicity plus micro-seismic activity where available. A strong occurrence of both together identifies a seismic hotspot.
- c. One earthquake will adjust a boundary but cannot create a zone.
- d. Zones of greatest activity are generally as small as possible.
- e. The maximum intensity of a zone cannot be smaller but may be equal to or greater than the maximum historic earthquake.
- f. These zones are source areas. They do not necessarily represent the maximum intensity at every point since attenuations have to be taken into account.

The largest earthquake source zones in the southeastern United States are at Charleston, South Carolina, and Giles County, Virginia. The Charleston area is shown as generating an earthquake of MM X. An intensity MM X earthquake occurred at Charleston in 1886. The Giles County area is shown as possibly generating an earthquake of MM IX. An intensity MM VIII earthquake occurred at Giles County in 1897 (Bollinger and Hooper, 1971).

The J. Strom Thurmond Dam is located in the South Carolina Trend or seismic zone. The largest earthquake interpreted for the South Carolina seismic zone is intensity MM VII. The South Carolina seismic zone is a broad belt extending in a general southeast to northwest direction.

The South Carolina zone merges with the Southern Appalachian zone to the northwest. The Southern Appalachian zone is identified as a broad northeast trending belt producing earthquakes of MM VII. Two hotspot areas are contained in this zone. These hotspots are more than 100 km north of the J. Strom Thurmond Dam and are identified as producing earthquakes of MM VIII. The South Carolina zone is bordered on the southwest (Georgia) and northeast (North Carolina) by an area identified as producing earthquakes of intensity

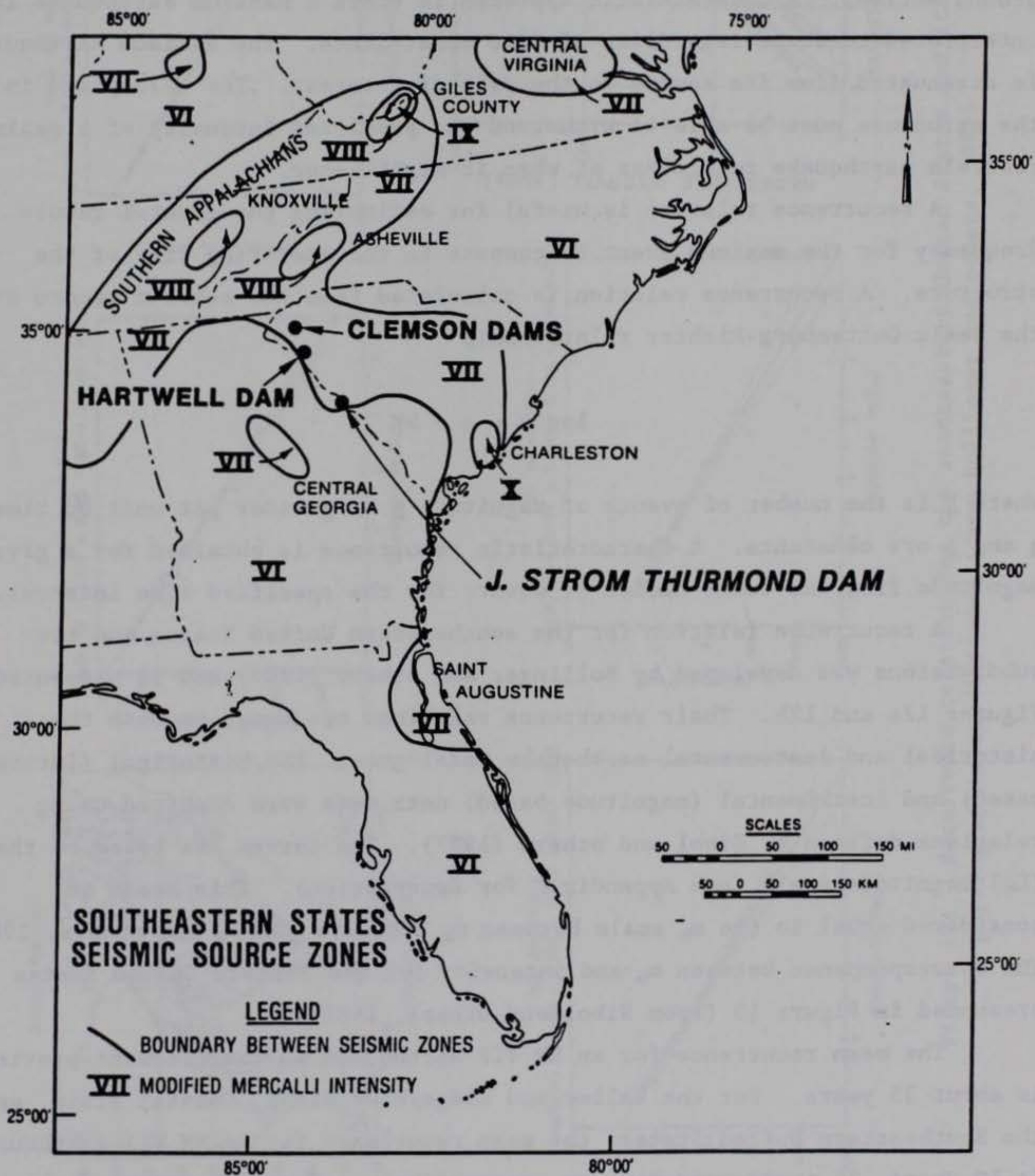


Figure 11. Seismic source zones in the southeastern United States

MM VI. This intensity level is the general background level for the southeastern United States.

Earthquake Recurrence

A deterministic approach was used in this report to specify earthquake ground motions. A deterministic approach is where a maximum earthquake is interpreted to occur regardless of time constraints. The maximum earthquake is attenuated from its source to the site of interest. The assumption is that the structure must be able to withstand the predicted intensity of a maximum credible earthquake regardless of when it might occur.

A recurrence relation is useful for estimating the general return frequency for the maximum event to compare to the operating life of the structure. A recurrence relation is calculated from the seismic record and the basic Gutenberg-Richter relationship

$$\log N = a - bM$$

where N is the number of events of magnitude M or greater per unit of time and a and b are constants. A characteristic recurrence is obtained for a given magnitude from the total number of events for the specified time interval.

A recurrence relation for the southeastern United States and its subdivisions was developed by Bollinger and others (1989) and is presented in Figures 12a and 12b. Their recurrence relations are based on both the historical and instrumental earthquake catalogues. The historical (intensity based) and instrumental (magnitude based) data sets were combined using relations defined by Sibol and others (1987). The curves are based on the m_b (Lg) magnitude scale (see Appendix C for description). This scale is considered equal to the m_b scale between m_b 2 to 6.4 (Sibol and others, 1987). The correspondence between m_b and intensity for the Eastern United States is presented in Figure 13 (from Sibol and others, 1987).

The mean recurrence for an MM VII earthquake in the Piedmont province is about 35 years. For the Valley and Ridge/Blue Ridge, Coastal Plain, and the Southeastern United States, the mean recurrence for an MM VII earthquake is 10 years, 25 years, and 8 years, respectively. The mean recurrence interval for an MM VII earthquake at Charleston is 75 years. The mean

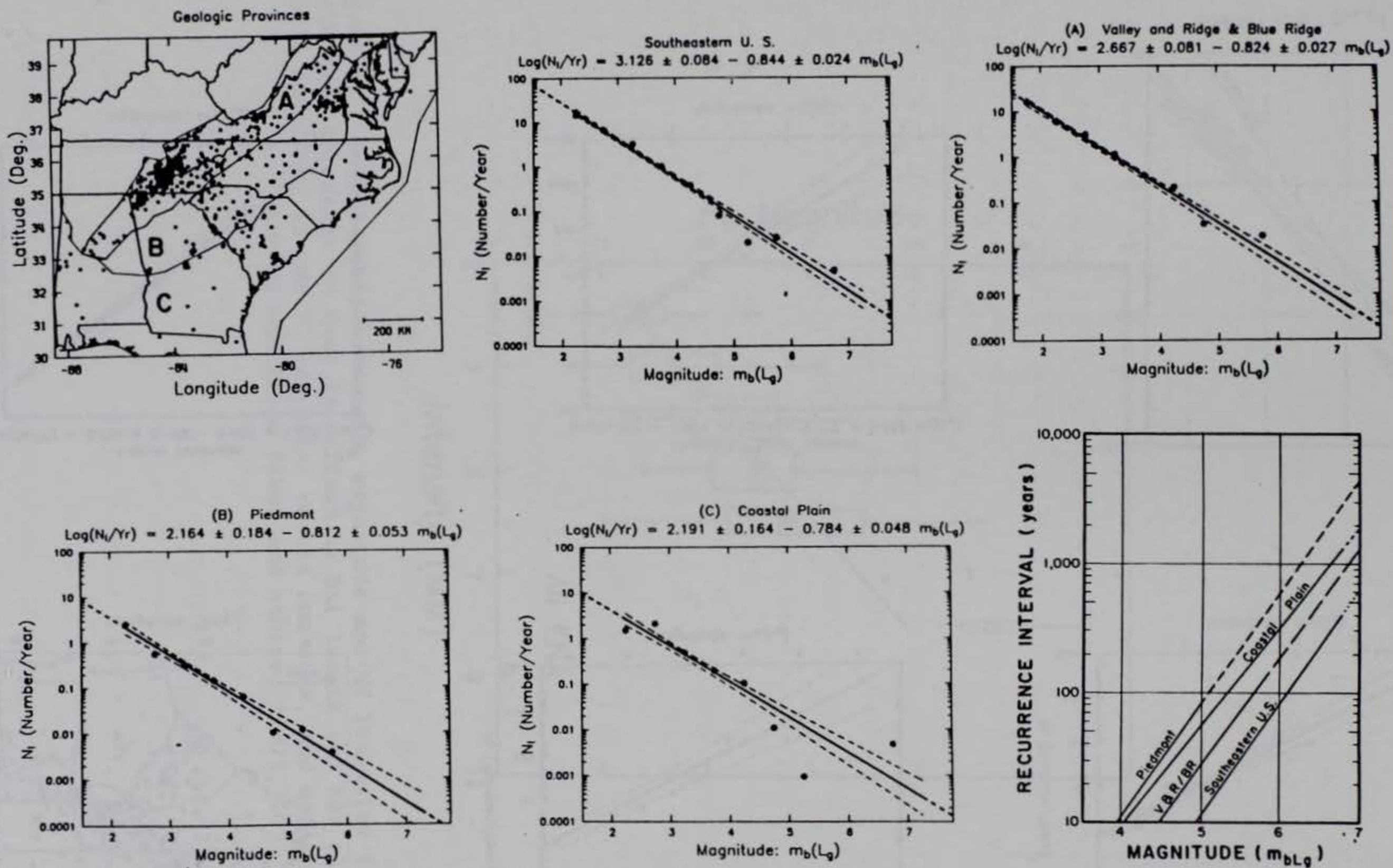


Figure 12a. Recurrence relation for the southeastern United States and its physiographic subdivisions (from Bollinger and others, 1989)

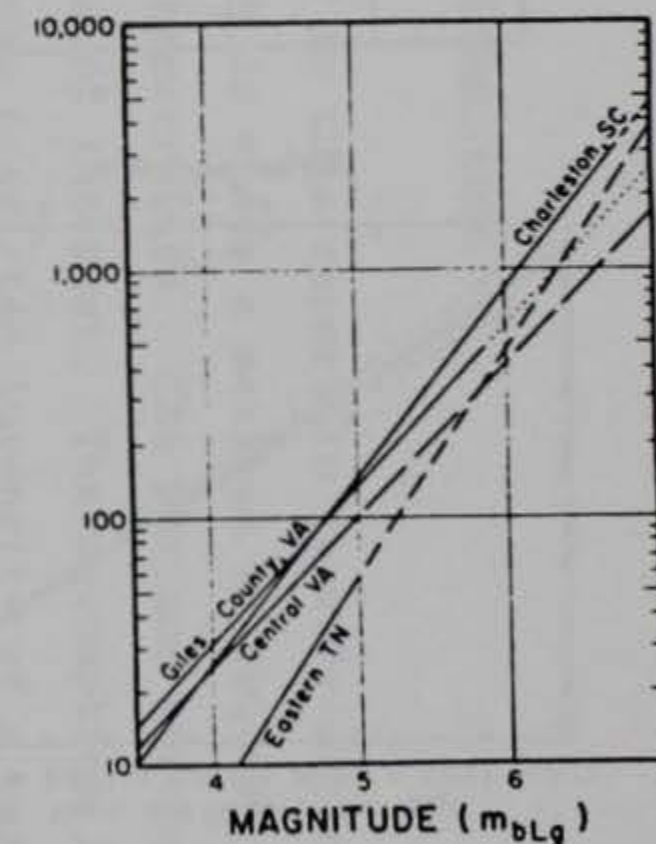
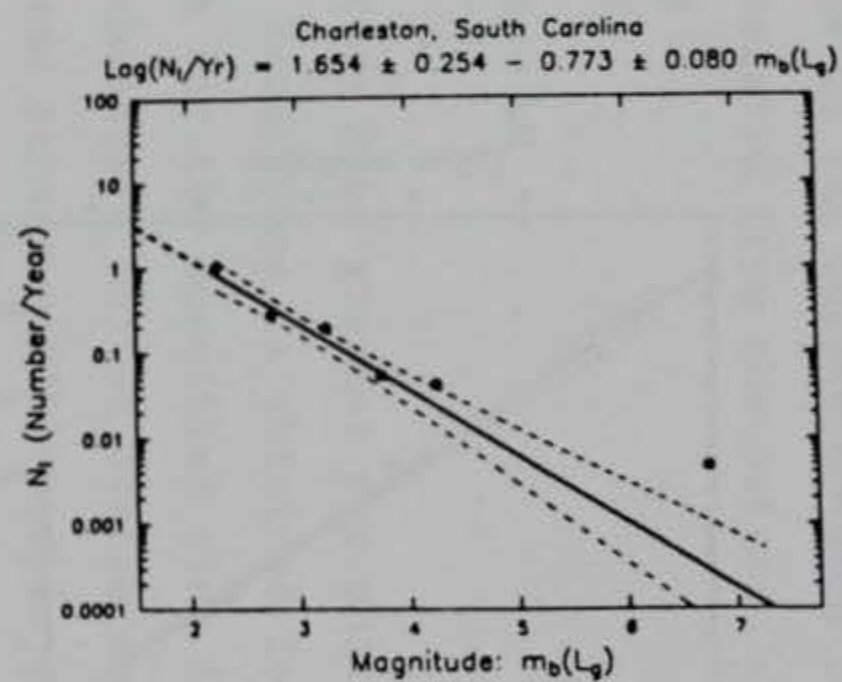
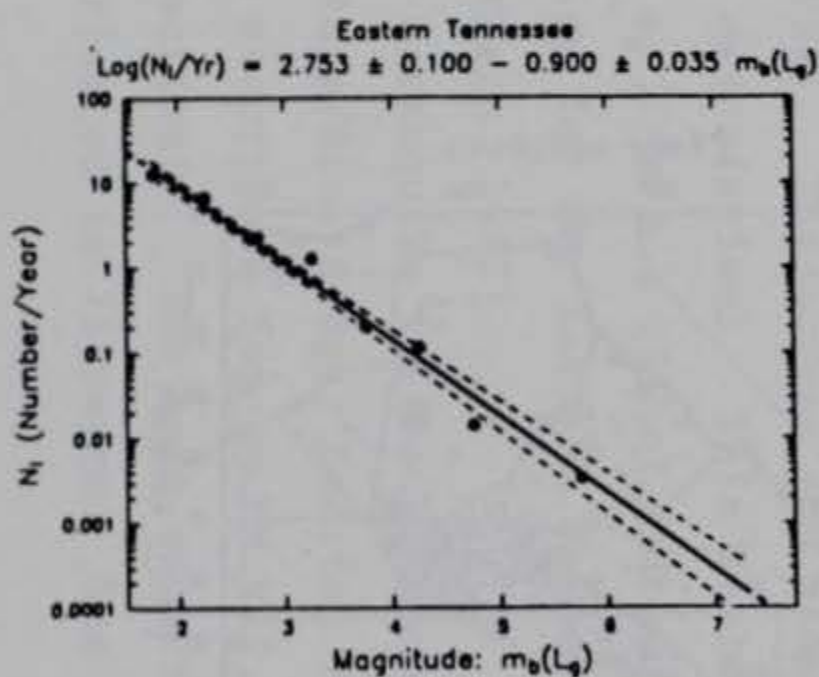
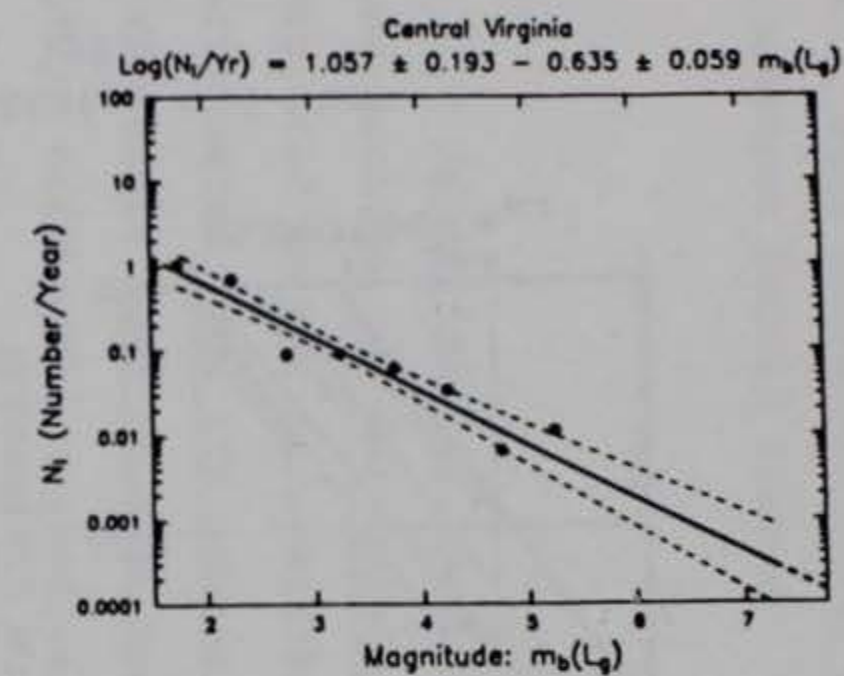
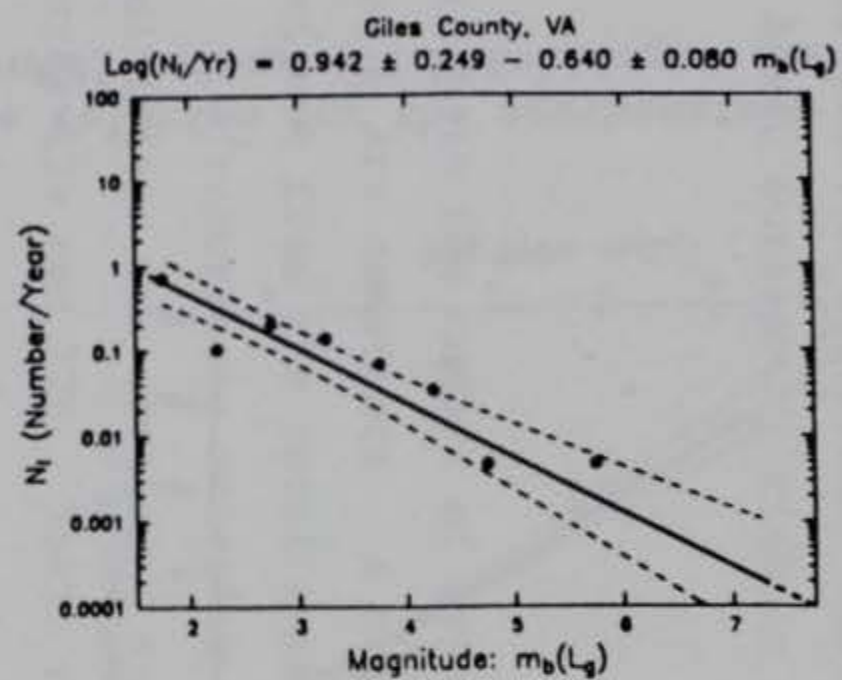
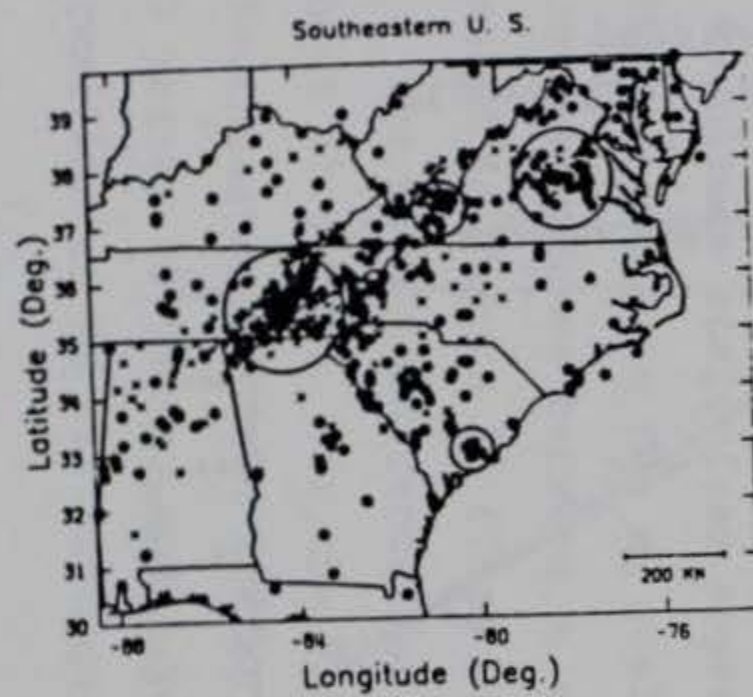


Figure 12b. Recurrence relation for selected seismic hotspots (from Bollinger and others, 1989)

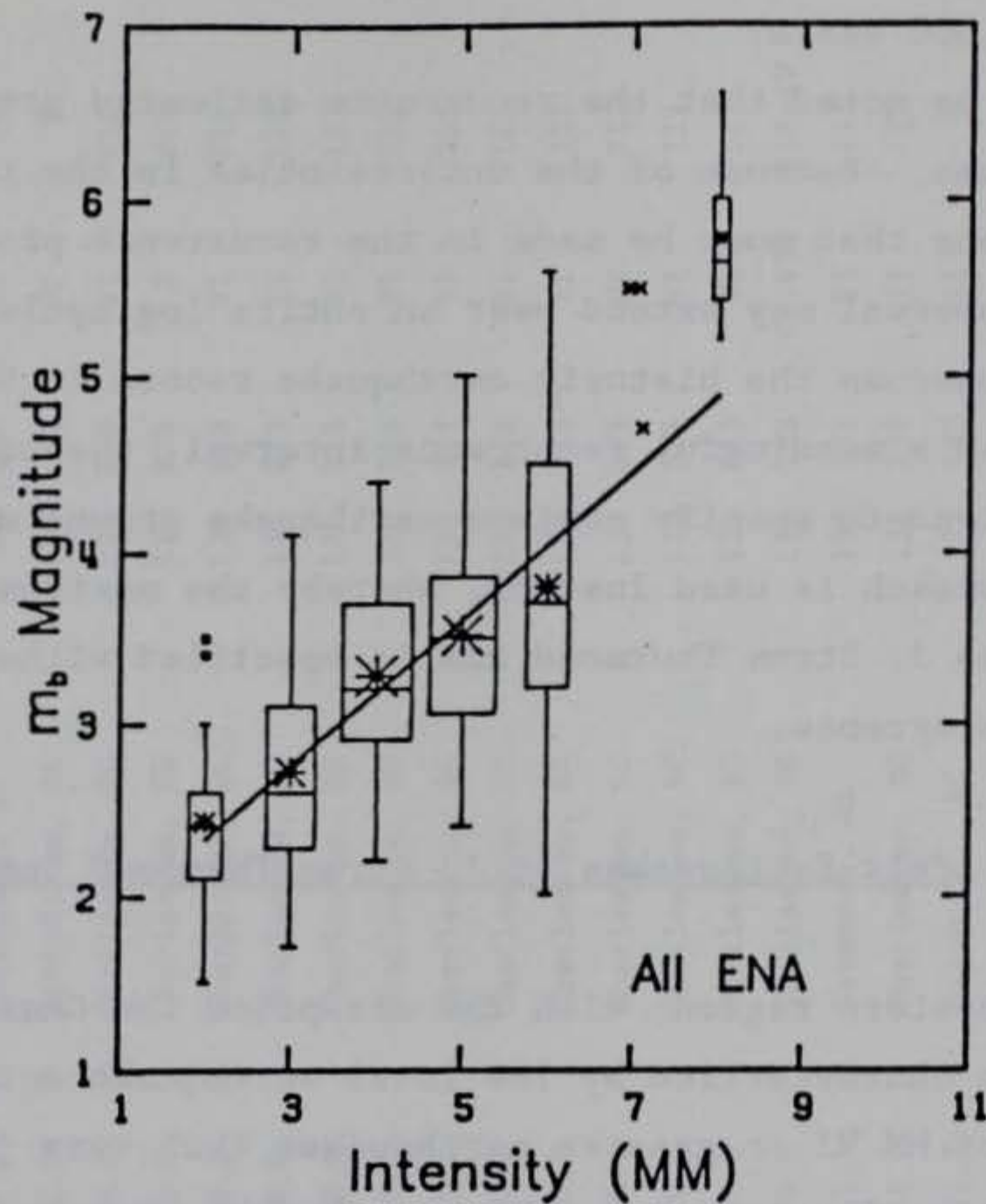


Figure 13. Relationship between m_b magnitude and MM Intensity for eastern North America; range in data is defined by bar length and box plots: mean equals asterisk, 25 and 75 quartiles equals box ends, and median equals center bar (from Sibol and others, 1987)

recurrence at Charleston for larger events (MM VIII to IX) ranges from 100 to 2,000 years. The mean recurrence at Charleston for an MM X earthquake is even greater, ranging from 1,000 to 9,000 years.

A more specific recurrence relation for the J. Strom Thurmond Dam is presented by Long in Appendix E (see Figure E11). Long calculates a recurrence estimate for the dam based on a probabilistic approach, which assumes a major event can occur during geologic time. The recurrence interval for an MM VI earthquake occurring at the J. Strom Thurmond Dam is calculated by Long to be 15,000 years.

It should be noted that the recurrence estimates presented above are for the mean values. Because of the uncertainties in the recurrence equations and the assumptions that must be made in the recurrence process, the range at each magnitude interval may extend over an entire log cycle. Because of this variability and because the historic earthquake record in this area is too short to establish a meaningful recurrence interval, the probabilistic approach is not used to specify maximum earthquake ground motions. The deterministic approach is used instead, whereby the maximum credible earthquake for the J. Strom Thurmond Dam is specified without regard to the probability of recurrence.

Felt Earthquakes at J. Strom Thurmond Dam

The southeastern region, with the exception of the Charleston, South Carolina, area is characterized by low level earthquake activity. Table 1 presents a list of MM VI or greater earthquakes that were judged to have been felt at the J. Strom Thurmond Dam. The earthquake list in Table 1 is derived mainly from the catalogue in Appendix B for earthquakes in the study boundary, and from various published sources (i.e., Bollinger, 1972, 1975, and 1977; Bollinger and Hopper, 1971; Coffman and others, 1982; Reagor and others, 1980; Stearns and Wilson, 1972; Street and Nuttli, 1984; and Visvanathan, 1980) for earthquakes which are centered outside of the study area, but which are judged to have been felt at the J. Strom Thurmond Dam. Distances from the earthquake source areas to the J. Strom Thurmond Dam are identified in Table 1 along with the attenuated intensity at the damsite.

The attenuation procedure selected for this study is based on the decrease of intensity with distance as determined from curves by Chandra

TABLE 1

FELT EARTHQUAKES AT J. STROM THURMOND DAM

Inside Study Area Boundary (See Appendix B)

Date	North Latitude	West Longitude	Location	Distance Miles KM		MMI _o *	MMI _s **	[†] Isoseismal MMI _s
02 May 1853	34.0	81.2	Lexington, SC	62	100	VI	IV	
02 Nov 1875	33.8	82.5	Lincolnton, GA	19	30	VI	V	
28 Aug 1886	32.9	80.0	Charleston, SC	138	223	VI	III	IV VIS
31 Aug 1886	32.9	80.0	Charleston, SC	138	223	X	VII	VI VIS
01 Sep 1886	32.9	80.0	Charleston, SC	138	223	VI	III	
06 Sep 1886	32.9	80.0	Charleston, SC	138	223	VI	III	
17 Sep 1886	32.9	80.0	Charleston, SC	138	223	VI	III	
21 Sep 1886	32.9	80.0	Charleston, SC	138	223	VI	III	
27 Sep 1886	32.9	80.0	Charleston, SC	138	223	VI	III	
22 Oct 1886	32.9	80.0	Charleston, SC	138	223	VI	III	
22 Oct 1886	32.9	80.0	Charleston, SC	138	223	VI	III	
05 Nov 1886	32.9	80.0	Charleston, SC	138	223	VI	III	
04 Jan 1887	32.9	80.0	Charleston, SC	138	223	VI	III	
12 Jan 1888	32.9	80.0	Charleston, SC	138	223	VI	III	
20 Jun 1893	32.9	80.0	Charleston, SC	138	223	VI-VII	III-IV	IV VIS
24 Jan 1903	32.1	81.1	Savannah, GA	125	201	VI	III	
12 Jun 1912	32.9	80.0	Charleston, SC	138	201	VII	IV	
01 Jan 1913	32.1	81.7	Union Co., SC	77	123	VII	V	II VIS
26 Jul 1945	33.75	81.38	Pelion, SC	47	76	VI	IV	V VIS

*MMI_o - Intensity at source.**MMI_s - intensity at site according to attenuation procedure in Figure 14.[†]Isoseismal MMI_s - intensity at site according to isoseismal: VIS - Visvanathan, 1980; BOL - Bollinger and Hopper, 1971; STW - Stearns and Wilson, 1972.

TABLE 1 (continued)

FELT EARTHQUAKES AT J. STROM THURMOND DAM

<u>Date</u>	<u>North Latitude</u>	<u>West Longitude</u>	<u>Location</u>	<u>Distance Miles KM</u>	<u>MMI_o*</u>	<u>MMI_s**</u>	<u>Isoseismal MMI_s</u>
24 Nov 1957	34.0	83.5	near Clayton, AL	118 189	VI	III	
03 Aug 1959	33.0	79.5	McClellanville, SC	163 260	VI	III	
27 Oct 1959	34.5	80.2	near Hartsville, SC	123 200	VI	III	
13 Jul 1971	34.76	82.98	Walhala, GA	87 140	VI	III	

Outside Study Area Boundary

16 Dec 1811	36.6	89.6	New Madrid, MO	465	XI-XII	VI-VII	VII STW
16 Dec 1811	36.6	89.6	New Madrid, MO	465	XI-XII	VI-VII	
23 Jan 1812	36.6	89.6	New Madrid, MO	465	XI-XII	VI-VII	
07 Feb 1812	36.6	89.6	New Madrid, MO	465	XI-XII	VI-VII	V-VI STW
31 May 1897	37.3	80.7	Giles Co., IA	275	VIII	IV	III BOL

(1979). His curves are shown in Figure 14 and the selected curve is that for the Eastern Province. The attenuation of MM intensity is determined by calculating the distance between the earthquake source and the damsite, selecting this distance on the horizontal axis of the attenuation curve, and then deriving the MM Intensity reduction factor. This reduction factor is subtracted from the intensity value at the source (MMI_0) to arrive at the estimated felt intensity at the site (MMI_s). Included in Table 1 are the felt intensities at the J. Strom Thurmond Dam according to published isoseismals for the significant earthquakes. The source of these isoseismals is also identified in Table 1. The comparisons between the earthquake isoseismals and the calculated site intensity are generally favorable considering the nature of the attenuation procedure. Where differences do occur, the isoseismals are preferred as they are based on actual damage reports from the earthquake.

The earthquakes in Table 1 span approximately 175 years and identify about 28 events that were large enough to have been felt. The vast majority of earthquakes in Table 1 are estimated to have been felt at intensity levels between III and IV. It is interpreted that the maximum felt earthquake at the J. Strom Thurmond Damsite was MM VII and was caused by the New Madrid, Missouri, series of earthquakes in 1811 and 1812 (see Figure 15, from Stearns and Wilson, 1972).

The Charleston earthquake of 1886 is identified by Visvanathan (1980) in Figure 16 as causing MM VI shaking at the J. Strom Thurmond Damsite. The attenuation procedure used in this study indicates that the Charleston earthquake produced MM VII damage at the damsite, one intensity unit higher than the isoseismal by Visvanathan (1980). The isoseismal map in Figure 16 shows the damsite is next to the MM VII isoseismal, near a zone where MM VIII damage was identified. There are several other locations in South Carolina where MM VIII damage was caused by the Charleston earthquake and which were at a considerable distance from the source. The attenuation of earthquake energy was not uniform as indicated by the isoseismal in Figure 16. The isoseismal indicates there were focusing effects due to the geology.

The Charleston earthquake is one of the largest historic earthquakes that has occurred in North America and the largest for the southeastern United States. This earthquake has been studied and described in detail by Bollinger (1977); Bollinger and Stover (1976); Visvanathan (1980); Armbruster and Seeber (1981); and Peters and Herrmann (1986). Specific details and information

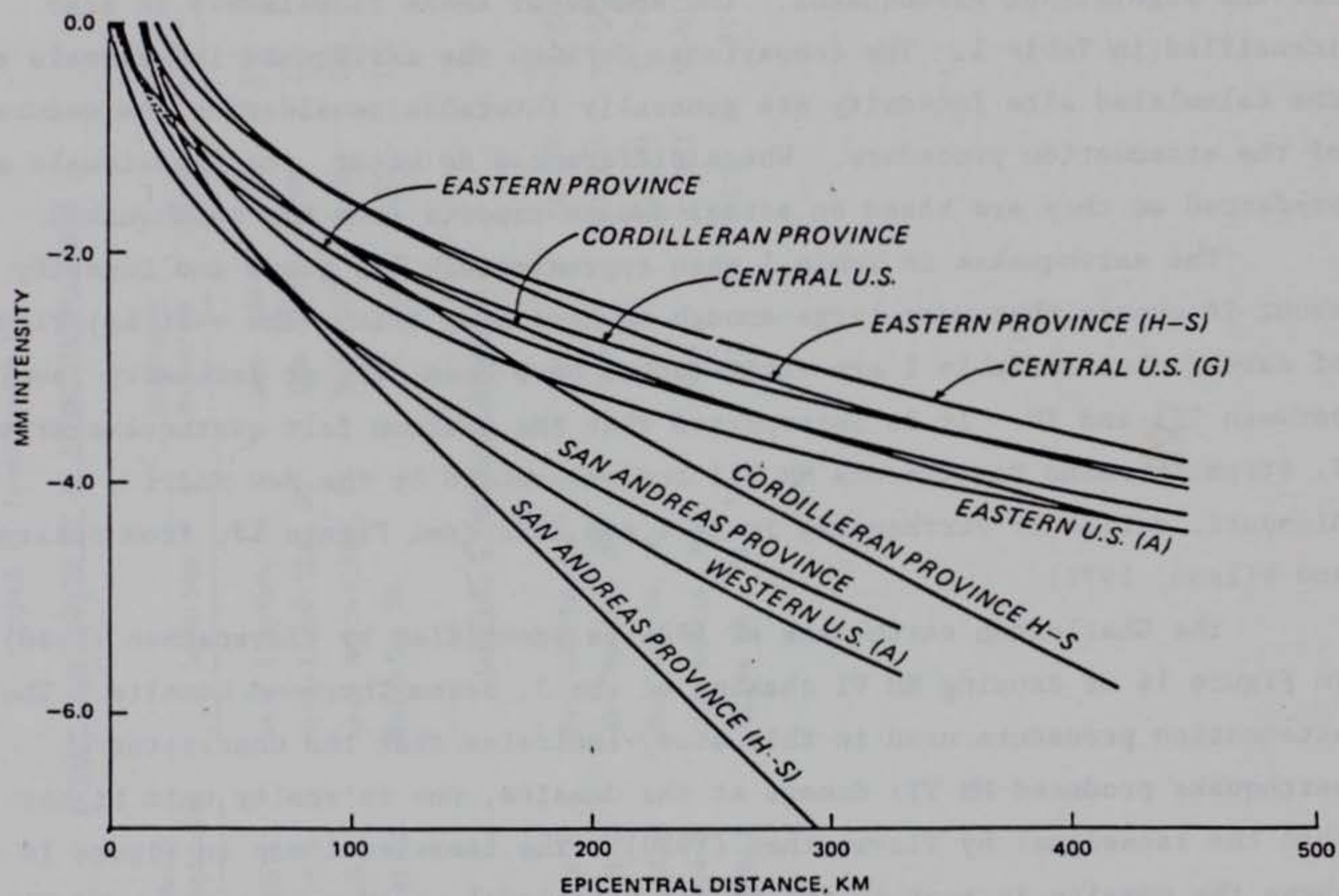


Figure 14. Attenuation of MM Intensity with distance: A - Anderson, G - Gupta, H-S - Howell and Schultz (from Chandra, 1979)

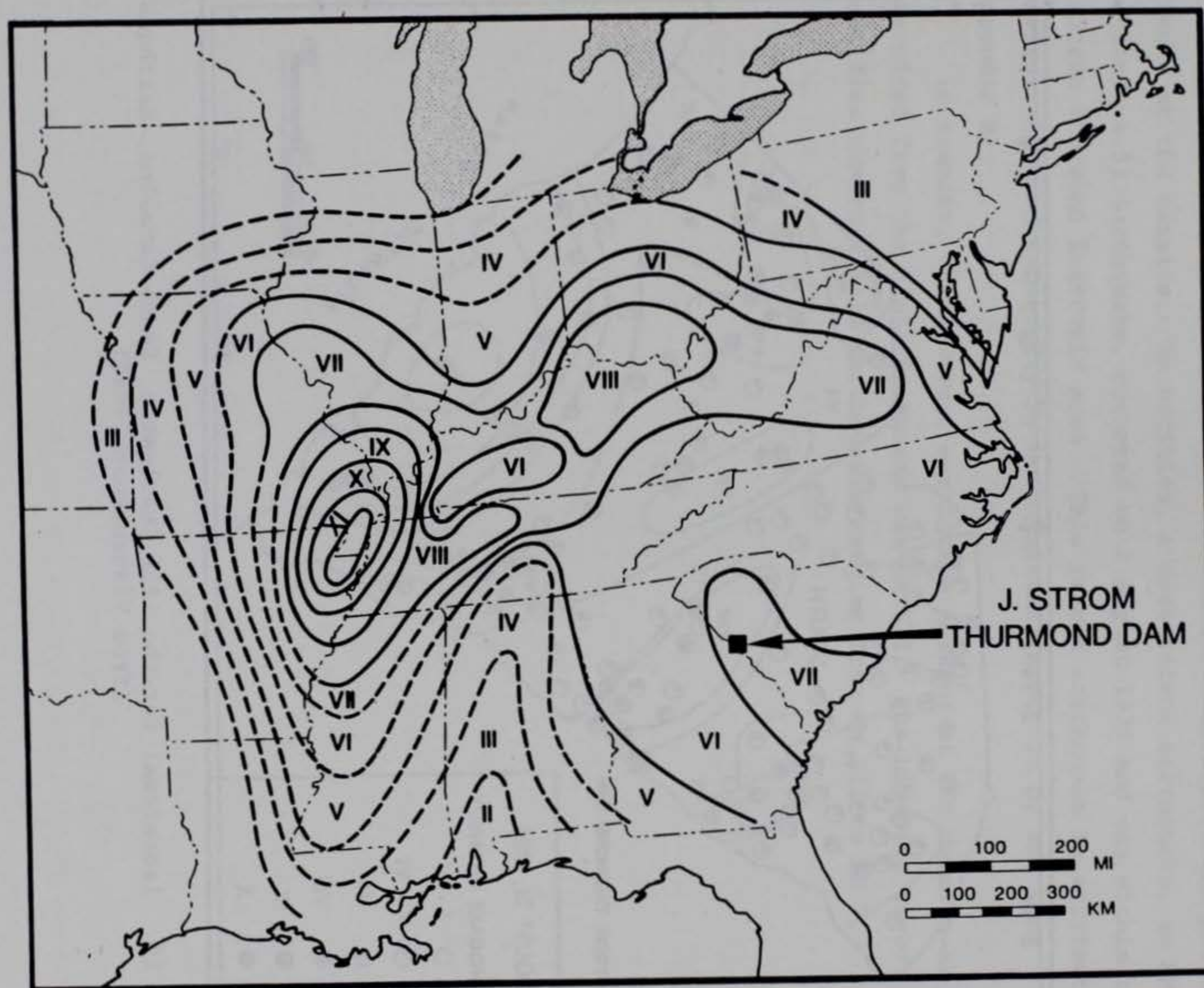


Figure 15. Composite isoseismal for the 1811 - 1812 New Madrid, Missouri, Earthquakes (from Stearns and Wilson, 1972)

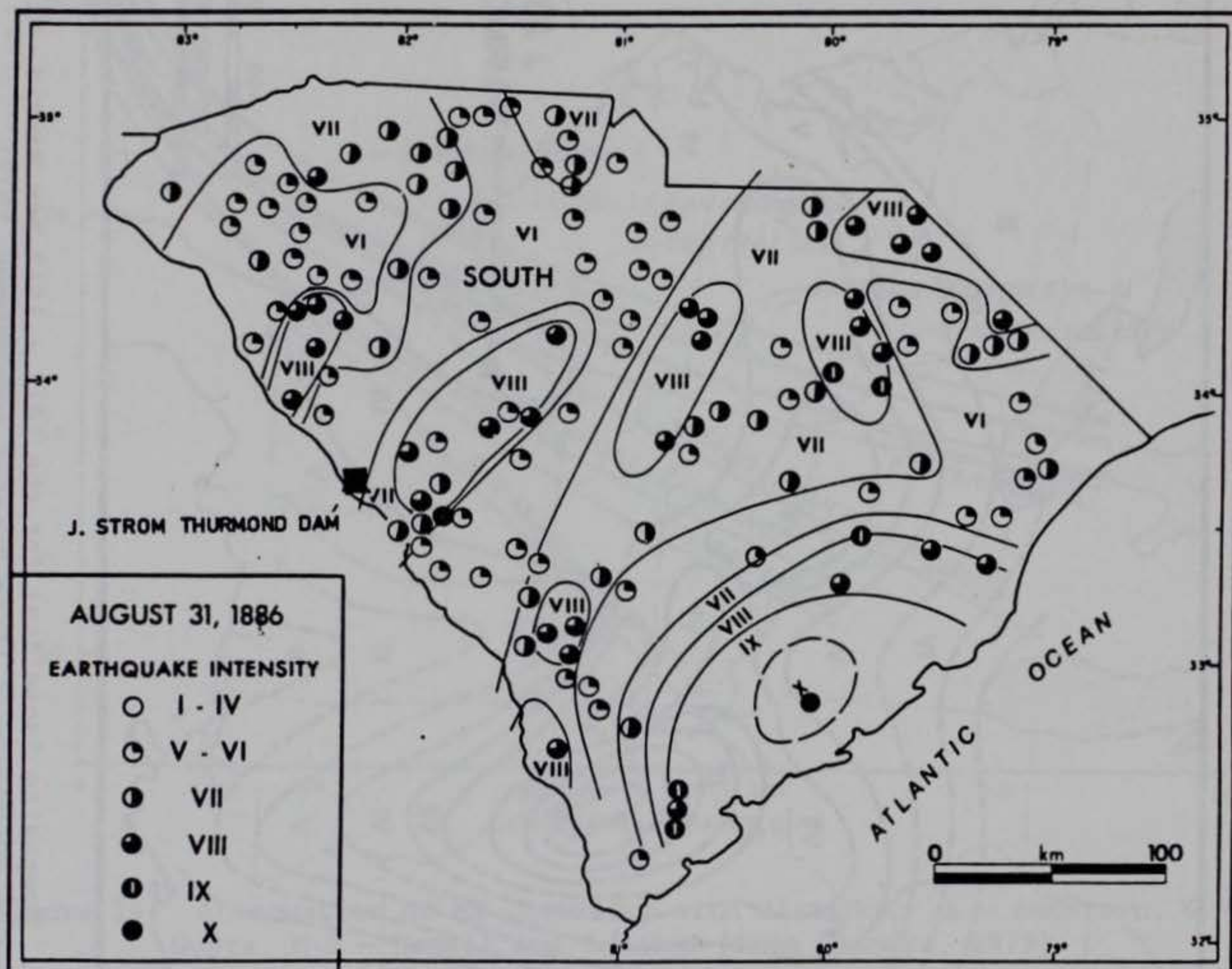


Figure 16. Isoseismal for the 1886 Charleston, South Carolina, Earthquake (from Visvanathan, 1980)

about this earthquake can be obtained from these sources. J. Strom Thurmond Dam was located approximately 140 miles (225 km) from the Charleston source area. The Charleston earthquake is interpreted to have caused the second most severe historic ground shaking at J. Strom Thurmond Dam.

The nearest moderate earthquake to the damsite occurred approximately 30 km northwest of J. Strom Thurmond Dam on 2 November 1875 and produced MM V effects at the damsite. In addition, a more recent earthquake, an MM V (local magnitude 4.3) earthquake, occurred on 2 August 1974 and was within the J. Strom Thurmond Reservoir area. This recent earthquake is attributed to reservoir induced seismicity by both Talwani (Appendix D) and Long (Appendix E).

In summary, the severest earthquake shaking at the damsite as determined from the historic record was MM VII. The historic record identifies numerous felt earthquakes ranging from MM III to MM V.

PART IV: EARTHQUAKE GROUND MOTIONS

Maximum Credible Earthquake

The maximum credible earthquake (MCE) for the J. Strom Thurmond Dam is defined as the largest earthquake that can reasonably be expected. The largest earthquake estimated for the J. Strom Thurmond Dam is intensity MM VII and is an earthquake originating from the South Carolina seismic zone.

The MCE specified for the J. Strom Thurmond Dam is a floating earthquake which can be moved anywhere within the source area of the South Carolina seismic zone. Ground motions from earthquakes originating outside of the South Carolina seismic zone would be attenuated with distance to the damsite and would be less severe than motions caused by earthquakes originating within this zone. Consequently, the severest motions from a major Charleston earthquake similar to the 1886 earthquake, attenuated to the J. Strom Thurmond Damsite, would be either comparable to or less than the maximum event interpreted for the South Carolina seismic zone. Therefore, earthquakes from source areas other than the South Carolina seismic zone are not considered to be the main hazard.

Operating Basis Earthquake

An operating basis earthquake (OBE) is an earthquake that allows minor damage to the structure, but permits the structure to remain operational with small repairs. It is an earthquake that is expected to occur during the life of the structure. The life of the structure for purposes of this report is taken at 100 years.

The MCE specified above is just below the threshold of damage for well built engineering structures (see Appendix C for description of MM VII). As such, the J. Strom Thurmond Dam should be able to sustain the maximum event with no damage or very little damage. Therefore, an OBE is not specified in this report as the MCE is within the limits of engineering design where significant damage should not occur. However, the final consideration for the OBE is an engineering decision which is based on cost-risk considerations and the potential hazard to life.

Field Conditions

Ground motions from an earthquake source are characterized as being either near field or far field. Ground motions for the same intensity level are different for each field condition. Near field motions, those originating at the earthquake source, are characterized by a large range of ground motions which are caused by complicated reflection and refraction patterns and by focusing effects of the waves which counteract the effects of geometric damping. In contrast, for far field motions the wave patterns are more orderly, they are generally more muted or dampened, and they incorporate wave spreading and attenuation effects that are characteristic for the region.

The limits of the near field are variable and are dependent on the severity of the earthquake. The relationship between earthquake magnitude (M), epicentral intensity, and the limits of the near field are given in the following set of relations (from Krinitzsky and Chang, 1987):

<u>M</u>	Maximum MM <u>Intensity - I_o</u>	Limit of Near <u>Field, km from Source</u>
5.0	VI	5
5.5	VII	15
6.0	VIII	25
6.5	IX	35
7.0	X	40
7.5	XI	45

Far field conditions are recommended for the selection of motions at the J. Strom Thurmond Dam. Near field conditions are specified only when the site of interest is within or near (15 km or less for MM VII) a seismic hotspot.

Far field motions are considered appropriate even for reservoir induced earthquakes which may occur in the near field. Far field motions are recommended because the total energy involved for shallow events such as those that may be triggered by reservoirs are not considered as great as for tectonic earthquakes. Dr. Long has indicated in Appendix E that reservoir induced earthquakes are shallow and have characteristic spectral properties that are distinguished by their high frequency components of motion. Consequently, shallow earthquakes may generate very sharp spikes (high amplitude), but they have low total energy (area under the curve for the high amplitude spikes). For earthquake damage to occur, the energy (the high

amplitude spikes) must extend beyond a single sharp spike, it must continue for several cycles.

It is uncertain what the maximum earthquake potential that can be reached for shallow hydroseismic events such as those identified for the Piedmont by Long (see Appendix E). Dr. Long suggests that reservoir induced earthquakes may trigger an event comparable to an MCE, but the probability of this happening are judged by him to be very remote. Dr. Talwani in Appendix D examines reservoir induced seismicity and concludes that the maximum earthquake that has been triggered in the Piedmont is less than magnitude 4.5. The association between reservoir induced earthquakes producing events greater than magnitude 4.5 for the Piedmont has yet to be proven. Furthermore, the world wide data for reservoir induced earthquakes does not closely correlate with a major damaging earthquake (Meade, 1982 and 1991).

The determination of the maximum earthquake from reservoir induced seismicity in the final analysis becomes one of judgment and is based on the available evidence. We concluded from the weight of all the evidence evaluated, that reservoir induced earthquakes in the Piedmont are less than magnitude 4.5. The earthquakes that determine the MCE are the deeper, tectonically activated earthquakes. Far field motions are thus specified for these events for the reasons described above.

Recommended Peak Motions

The parameters for earthquake motions specified in this report are horizontal peak values for acceleration, velocity, and duration. Duration is bracketed duration equal to or greater than 0.05 g (g = one gravity unit; 1 g = 980 cm/sec²). Values specified are for free-field motions on rock (hard sites) at the surface.

The ground motion parameters of interest are determined from the Krinitzsky-Chang (1987) intensity curves. The far field curves for acceleration, velocity, and duration are presented in Figures 17, 18, and 19. The values in these charts are derived from a large world wide data base of ground motions and represent the statistical levels of the data spread at the different intensity levels. Values in the charts are specified for the mean, mean plus one standard deviation (mean + S. D.), and mean plus two standard deviations. Recommended motions are at the mean plus one standard deviation

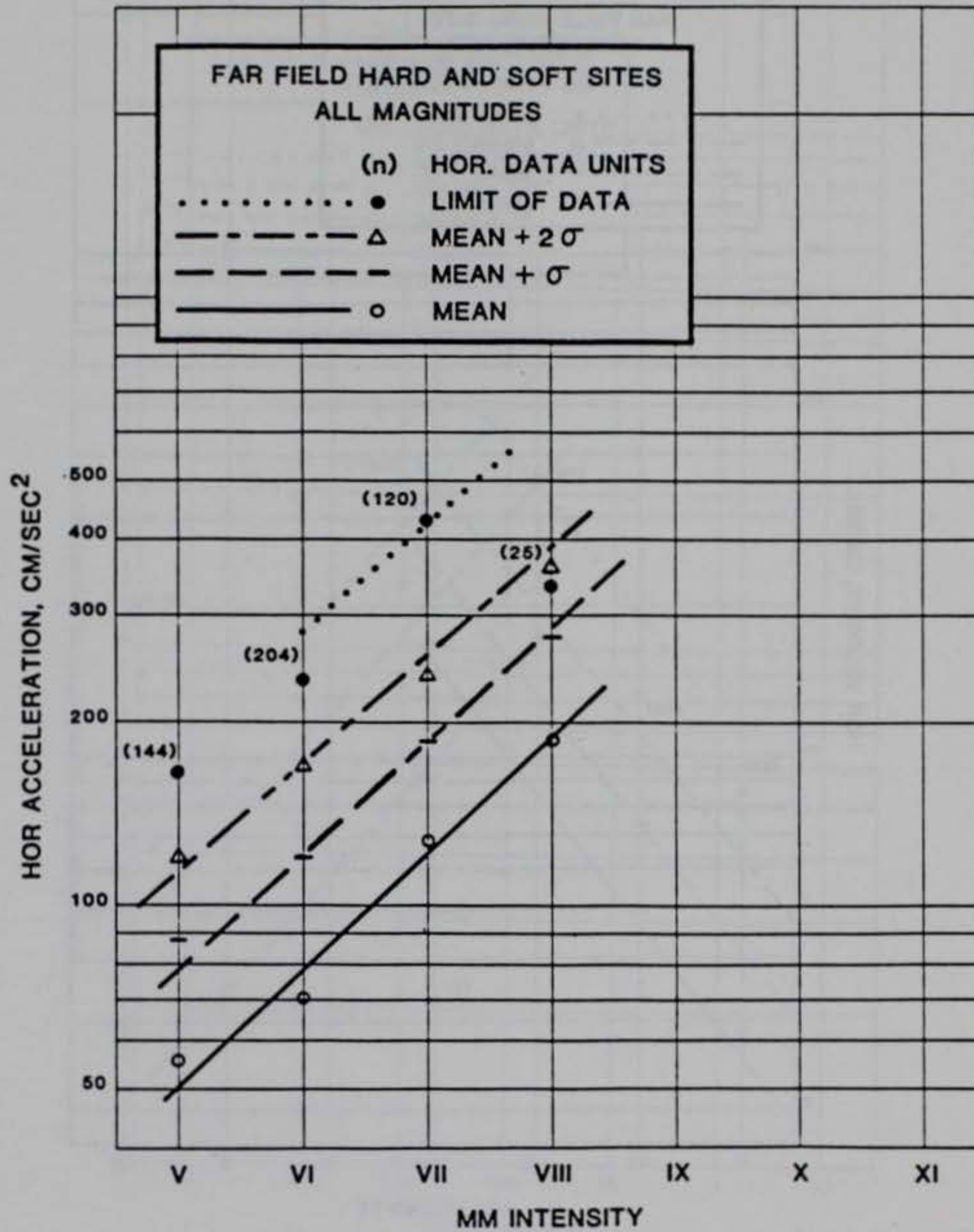


Figure 17. Chart for acceleration (from Krinitzsky and Chang, 1987)

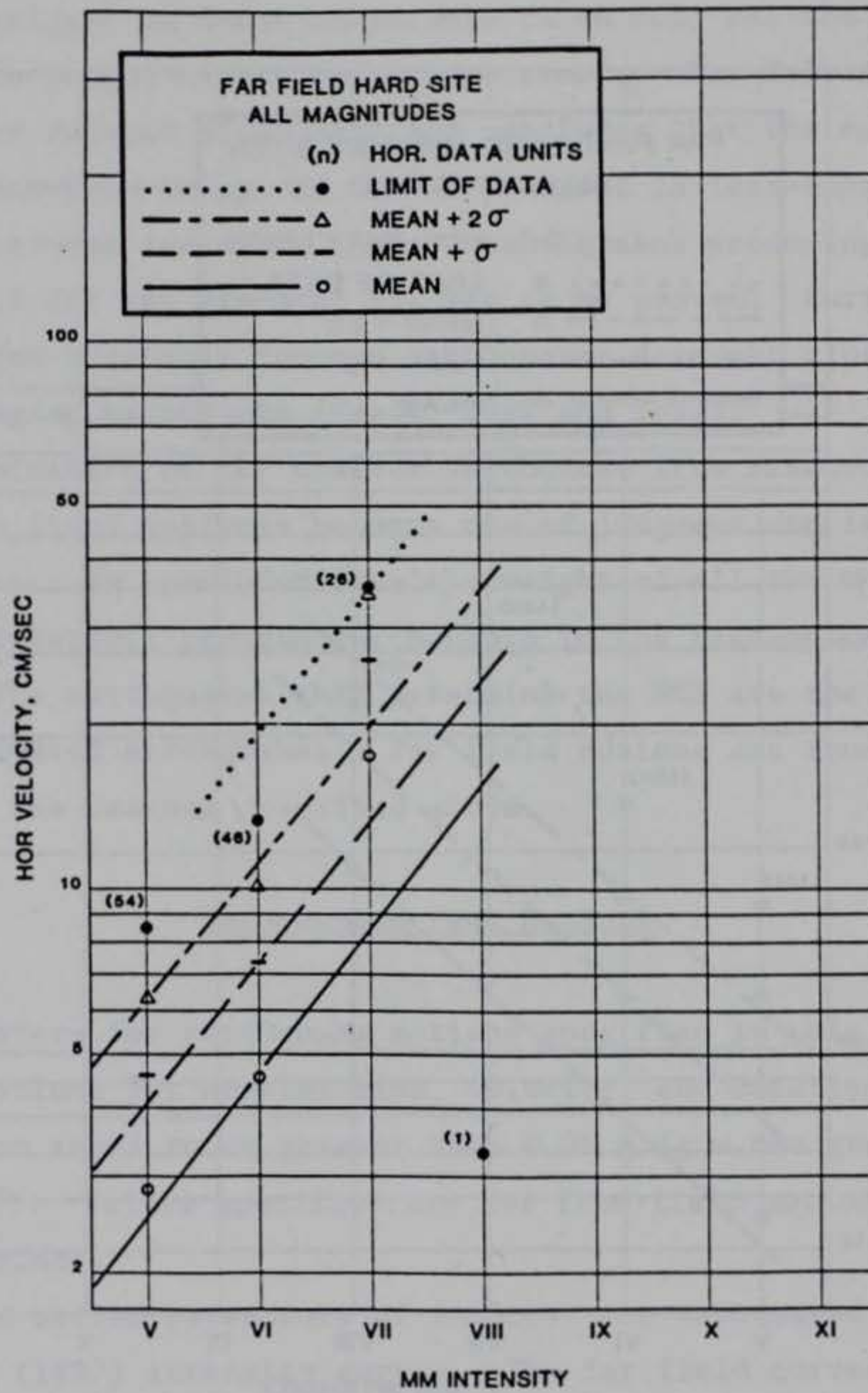


Figure 18. Chart for velocity (from Krinitzsky and Chang, 1987)

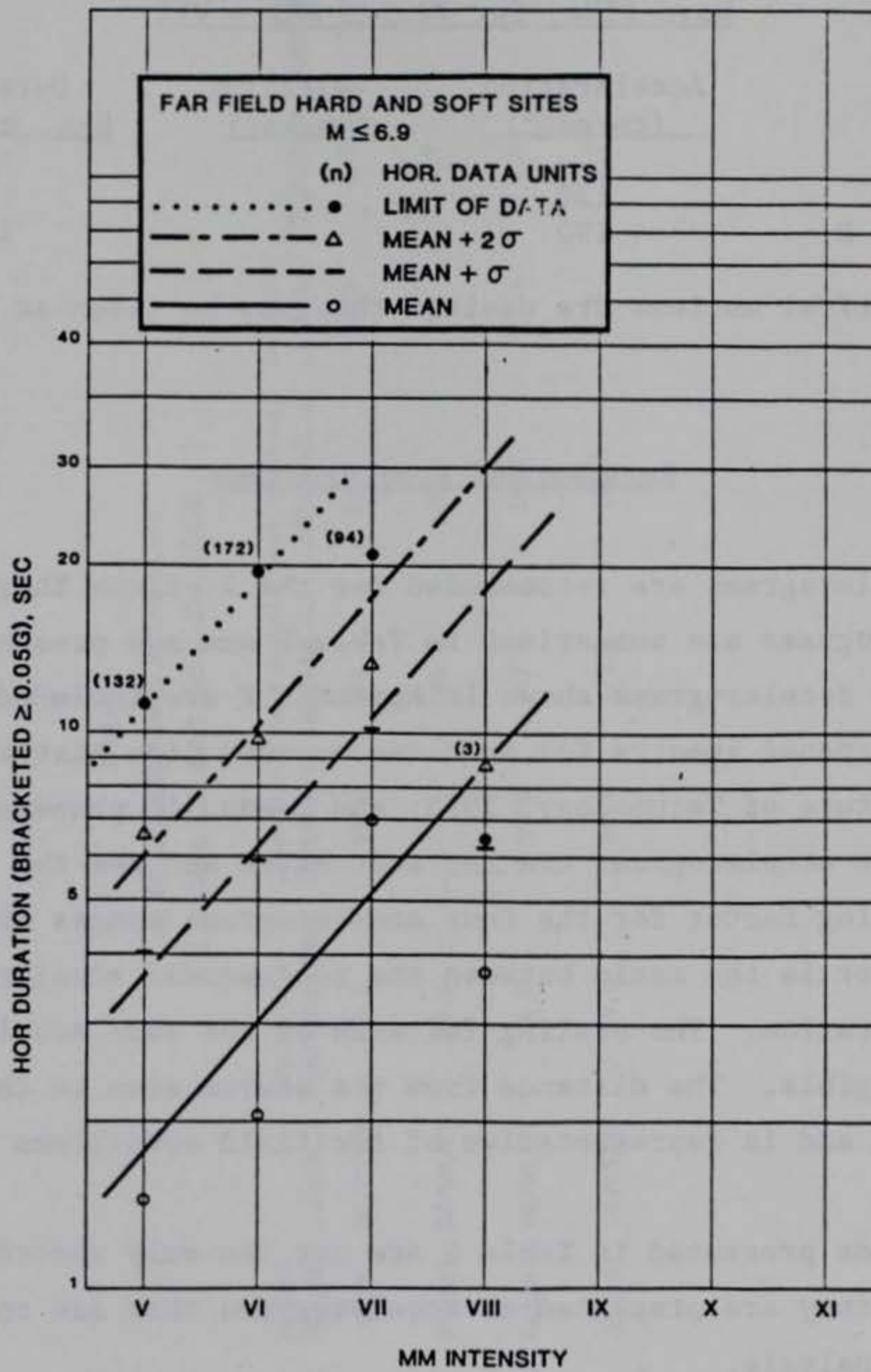


Figure 19. Chart for duration (from Krinitzsky and Chang, 1987)

or the 84 percentile where dynamic analyses requiring time histories are being considered.

The values for peak horizontal ground motions at the J. Strom Thurmond Dam are as follows:

South Carolina Seismic Zone

Hard Site, Far Field, MMI - VII

	<u>Acceleration</u> <u>(cm/sec²)</u>	<u>Velocity</u> <u>(cm/sec)</u>	<u>Duration</u> <u>Sec. \geq 0.05 g</u>
Mean	130	9	5
Mean + S. D.	190	14	11

Where vertical motions are desired they may be taken at 2/3 of the horizontal.

Recommended Accelerograms

Four accelerograms are recommended for the J. Strom Thurmond Dam. The selected accelerograms are summarized in Table 2 and are presented in Appendix F. The accelerograms shown in Appendix F are included with the quadripartite response spectra for each recommended time history (from California Institute of Technology, 1975; and Leeds, in preparation).

Two of the accelerograms are for soft sites and the two are for hard sites. The scaling factor for the four accelerograms ranges from 1.0 to 1.14. The scaling factor is the ratio between the recommended acceleration and the specified acceleration. The scaling for each of the four accelerograms is considered negligible. The distance from the source area to the site ranges from 17 to 61 km and is representative of far field conditions in the study area.

The records presented in Table 2 are not the only records that may be used. However, they are presented as accelerograms that are appropriate for an engineering analysis.

Motions for Nearby Nuclear Power Plants

Figure 20 identifies the nearby nuclear power plants, their locations, the values for safe shutdown earthquakes (SSE), and the values for the OBE

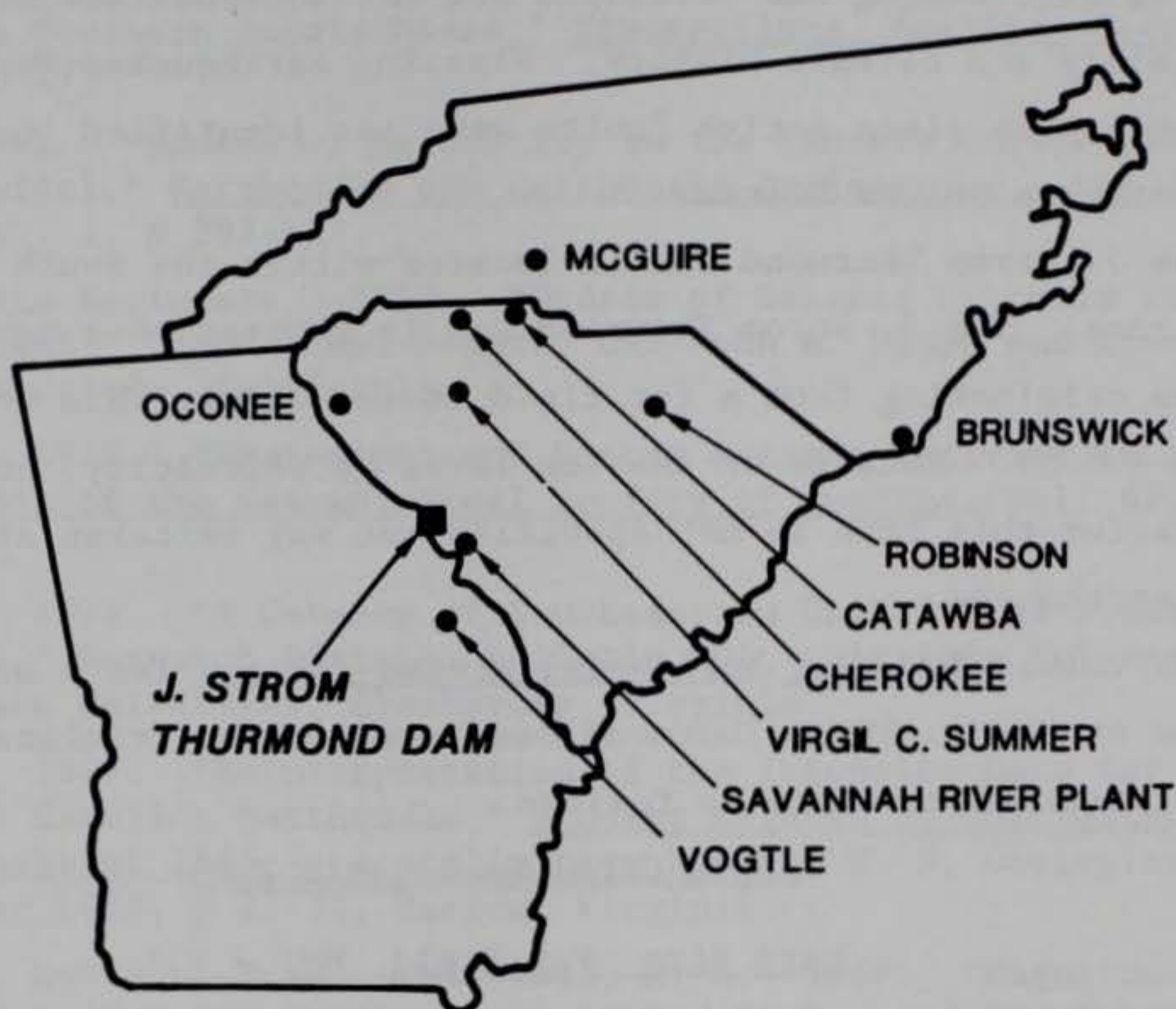
Table 2
Selected Earthquake Records for
J. Strom Thurmond Dam - Far Field

	<u>Earthquake</u>	<u>Record</u> <u>ID NO</u>	<u>Date</u>	<u>Epicentral</u> <u>Distance (km)</u>	<u>Component</u> <u>(Degrees)</u>	<u>Peak Accel</u> <u>(cm/sec²)</u>	<u>Peak Velocity</u> <u>(cm/sec)</u>	<u>Duration</u> <u>(sec)</u>	<u>Magnitude</u>	<u>Intensity</u>	<u>Site</u>	<u>Scaling</u>
61	Puget Sound, Washington Olympia Highway Test Lab	WAS5	04/29/65	61.1	S86W	194.3	12.7	9.20	6.5	VII	Soft	1.00
	Coyote Lake, California Gilroy Array 2	CAL107	06/08/79	17.0	--	186.0	10.2	7.1	5.9	VII	Soft	1.02
	San Fernando, Los Angeles Griffin Park Observatory	CAL047	02/09/71	34.0	S90W	167.4	14.6	8.34	6.6	VII	Hard	1.14
	Coalinga, California Parkfield Vineyard Canyon	CAL192	02/05/83	39.0	N00E	172.9	18.39	8.6	6.7	VI	Hard	1.10

(from Nuclear News, 1982; and Blume and Associates, 1982). The SSE is equivalent to the maximum credible earthquake. Recall that the OBE is the earthquake for which the structure is designed to resist and remain operational without major damage occurring to the structure for an earthquake that is expected to occur during the life of the structure. The OBE can be an engineering decision based on cost-risk considerations if there are no hazards to life.

The values shown for peak acceleration for the SSEs in Figure 20 need not be directly comparable to the values for the maximum credible earthquake at the J. Strom Thurmond Dam since the specification of values is dependent on the types of analyses to be performed: the SSE for a pseudostatic analysis would be a mean value; for a dynamic analysis the mean plus one S.D. would be more appropriate. In addition, the seismic zone and the site condition would introduce other variations. However, the motions for the J. Strom Thurmond Dam are very close to those presented in Figure 20, though the former were independently obtained using other methods.

NUCLEAR POWER PLANTS NEAR J. STROM THURMOND DAM



<u>PLANT NAME</u>	<u>ACCELERATION (g)[★]</u>		<u>FOUNDATION</u>
	<u>SSE (MCE)</u>	<u>OBE</u>	
VOGTLE, GA	.20	.12	SOIL
OCONEE, SC	.15	.08	ROCK
VIRGIL C. SUMMER, SC	.15	.10	SOIL
CHEROKEE, SC	.15	.08	ROCK (WEATHERED)
CATAWBA, SC	.15	.08	SOIL
ROBINSON, SC	.20	.10	SOIL
MCGUIRE, NC	.12	.08	ROCK
BRUNSWICK, NC	.16	.08	SOIL
SAVANNAH RIVER PLANT, SC	.20★★	.10	SOIL

★ SSE – SAFE SHUTDOWN EARTHQUAKE
 MCE – MAXIMUM CREDIBLE EARTHQUAKE
 OBE – OPERATING BASIS EARTHQUAKE

★★ ACCELERATION FOR DESIGN BASIS EARTHQUAKE

Figure 20. Locations of nuclear power plants and their design earthquakes
(from Nuclear News, 1983; and Blume and Associates, 1982)

PART V: CONCLUSIONS

A seismic zoning was developed for the southeastern United States based on the geology and seismic history. Floating earthquakes were assigned to each seismic zone since active faults were not identified in the study area or the southeastern United States.

The J. Strom Thurmond Dam is located within the South Carolina seismic trend or zone. The J. Strom Thurmond Dam is subject to a maximum credible earthquake originating from a far field source within this zone equal to MM VII ($M = 5.5$). Because of the low level of seismicity, an operating basis earthquake for this zone is not specified but may be taken at the maximum credible earthquake.

The values for peak horizontal ground motions for a maximum credible earthquake at the J. Strom Thurmond Dam based on the Krinitzsky and Chang (1987) intensity curves are as follows:

South Carolina Seismic Zone

Hard Site, Far Field, MMI = VII

	<u>Acceleration</u> <u>(cm/sec²)</u>	<u>Velocity</u> <u>(cm/sec)</u>	<u>Duration</u> <u>Sec. ≥ 0.05 g</u>
Mean	130	9	5
Mean + S. D.	190	14	11

Accelerograms and response spectra are included (see Appendix F) as representative of appropriate ground motions. Where vertical motions are considered, they may be taken at 2/3 of the horizontal.

REFERENCES

- Armbruster, J. C. and Seeber, L. 1981. "Seismicity and Back-slip on the Detachment of the Southern Appalachians," Transactions, American Geophysical Union, Vol. 62, p 17.
- Barosh, P. J. 1981. "Causes of Seismicity in the Eastern United States: A Preliminary Appraisal," Earthquake and Earthquake Engineering: the Eastern United States, Vol. 1, p 397-417.
- Blume and Associate Engineers. 1982. "Update of Seismic Criteria for the Savannah River Plant," Draft Final Report, URS/John A. Blume and Associate Engineers, San Francisco, California.
- Bollinger, G. A. 1972. "Historical and Recent Seismic Activity in South Carolina," Bulletin of the Seismological Society of America, Vol. 62, No. 3, p 851-864.
- Bollinger, G. A. 1975. "A Catalog of Southeastern United States Earthquakes 1754 through 1974," Research Division Bulletin 101, Virginia Polytechnic Institute and State University, Blacksburg, Virginia.
- Bollinger, G. A. 1977. "Reinterpretation of the Intensity Data for the 1886 Charleston, South Carolina Earthquake," Studies Related to Charleston, South Carolina, Earthquake of 1886 -- A preliminary Report, U. S. Geological Survey Professional Paper 1028, p 17-32, Reston, Virginia.
- Bollinger, G. A., Davison, F. C., and Sibol, M. S. 1989. "Magnitude Recurrence Relations for the Southeastern United States and Its Subdivisions," Journal of Geophysical Research, Vol. 94, No. 83, p. 2857-2873.
- Bollinger, G. A. and Hopper, M. G. 1971. "Virginia's Two Largest Earthquakes -- December 22, 1875 and May 31, 1897," Bulletin of the Seismological Society of America, Vol. 61, No. 4, p 1033-1039.
- Bollinger, G. A. and Stover, C. W. 1976. "List of Intensities for the 1886 Charleston, South Carolina Earthquake," U. S. Geological Survey, Open-File Report 76-66, Reston, Virginia.
- California Institute of Technology. 1975. "Strong Motion Earthquake Accelerograms, Corrected Accelerograms and Integrated Ground Velocities and Displacements," Vol. 2, Parts A-Y, Pasadena, California.
- Chandra, U. 1979. "Attenuation of Intensities in the United States," Bulletin Seismological Society of America, Vol. 69, No. 6, p 2003-2024.
- Chowns, T. M. 1976. "Stratigraphy, Structure, and Seismicity in the Slate Belt Rocks Along the Savannah River," Guidebook 16, Georgia Geological Society, Atlanta, Georgia.
- Coffman, J. L., von Hake, C. A., and Stover, C. W. 1982. "Earthquake History of the United States." US Department of Commerce, National Atmospheric Administration and US Department of the Interior, Geological Survey, Boulder, Colorado.
- Cook, F. A., Albaugh, D. S., Brown, L. D., Kaufman, S., and Oliver, J. E. 1979. "Thin-skinned Tectonics in the Crystalline Southern Appalachians; COCORP Seismic-reflection profiling of the Blue Ridge and Piedmont," Geology, Vol. 7, p 563-567.

- Cook, F. A., Brown, L. D., Kaufman, S., Oliver, J. E., and Petersen, T. A. 1981. "COCORP Seismic Profiling of the Appalachian Orogen beneath the Coastal Plain of Georgia," Geological Society of America Bulletin, Vol. 92, p 738-748.
- Cook, F. A., Brown, L. D., and Oliver, J. E. 1982. "The Southern Appalachians and the Growth of Continents," Scientific American, October, p 156-168.
- Costain, J. K., Bollinger, G. A., and Speer, J. A. 1987. "Hydroseismicity: A Hypothesis for the Role of Water in the Generation of Intraplate Seismicity," Seismological Research Letters, Vol. 58. No. 3, p. 41-64.
- Crickmay, G. W. 1952. "Geology of the Crystalline Rocks of Georgia," Georgia Geol. Bull., Vol. 58, Atlanta, Georgia.
- Daniels, D. L., Zietz, I., and Popenoe, P. 1983. "Distribution of Subsurface Lower Mesozoic Rocks in the Southeastern United States, as Interpreted from Regional Aeromagnetic and Gravity Maps," Studies Related to the Charleston, South Carolina, Earthquake of 1886-Tectonics and Seismicity, Geological Survey Professional Paper 1313, US Government Printing Office, Washington, D.C.
- Griffin, V. S. 1971. "The Inner Piedmont Belt of the Southern Crystalline Appalachians," Geological Society of America Bulletin, Vol. 82, p 1885-1898.
- Griffin, V. S. 1974. "Analysis of the Piedmont in Northwest South Carolina," Geological Society of America Bulletin, Vol. 85, p 1123-1138.
- Griffin, V. S. 1977. "Preliminary Geologic Map of the South Carolina Inner Piedmont Belt," Geologic Notes, South Carolina Division of Geology, Vol. 21, No. 4, p 198-204.
- Griffin, V. S. 1981. "Geology of the Anderson South, Hartwell NE, La France, and Saylor's Crossroads (7.5 Minute) Quadrangles and the Anderson (15-Minute) Quadrangle, South Carolina," South Carolina Geological Survey, Maps MS-25, Columbia, South Carolina.
- Habermann, T. 1989. "Custom Earthquake Search of the J. Strom Thurmond Dam Area (32.0 to 35.0 N, 79.5 to 84.0 W)," National Geographic Data File, National Geophysical Data Center, National Oceanic and Atmospheric Administration, Boulder, Colorado.
- Hatcher, R. D. 1972. "Developmental Model for the Southern Appalachian," Geological Society of America Bulletin, Vol. 83, p 2735-2760.
- Hatcher, R. D. 1978. "Tectonics of the Western Piedmont and Blue Ridge, Southern Appalachians: Review and Speculation," American Journal of Science, Vol. 278, p 276-304.
- Hatcher, R. D. and Butler, R. J. 1979. "Guidebook for the Southern Appalachian Field Trip in the Carolinas, Tennessee, and Northeastern Georgia," North Carolina Geological Survey, Raleigh, North Carolina.
- Hatcher, R. D., Howell, D. E., and Talwani, P. 1977. "Eastern Piedmont Fault System: Speculations on its extent," Geology, Vol. 5, p 636-640.
- Hatcher, R. D., and Goldberg, S. A. 1991. "Chapter 2: The Blue Ridge Geologic Province," In Horton, J. W. and Zullo, V. A. editors, The Geology of the Carolinas, Carolina Geological Society, Columbia, South Carolina.

- Higgins, M. W., Atkins, R. L., Crawford, T. J., Crawford, R. F., Brooks, R., and Cook, R. B. 1986. "The Structure, Stratigraphy, Tectonostratigraphy, and Evolution of the Southernmost Part of the Appalachian Orogen, Georgia and Alabama, Open-File Report 86-372, US Geological Survey, Reston, Virginia.
- Howel, D. E., and Pirkle, W. A. 1976. "Geologic Section Across the Modoc Fault Zone, Modoc, South Carolina," Stratigraphy, Structure and Seismicity in Slate Belt Rocks Along the Savannah River, Guidebook No. 16, Georgia Geological Survey, Atlanta, Georgia.
- Horton, J. W. and Zullo, V. A. 1991. The Geology of the Carolinas, Carolina Geological Society, Columbia, South Carolina.
- Krinitzsky, E. L. and Chang, F. K. 1987. "Parameters for Specifying Intensity Related Earthquake Ground Motions," State of the Art for Assessing Earthquake Hazards in the United States, Report No. 25, Miscellaneous Paper S-73-1, USAE Waterways Experiment Station, Vicksburg, Mississippi.
- Krinitzsky E. L., and Dunbar, J. B. 1988. "Geological-Seismological Evaluation of Earthquake Hazards at Hartwell and Clemson Dams," Technical Report GL-90-11, USAE Waterways Experiment Station, Vicksburg, Mississippi.
- Leeds, D. J. In preparation. "Accelerogram Database for Earthquake Ground Motions: Hard and Soft Sites," USAE Waterways Experiment Station, Vicksburg, Mississippi.
- Long, T. L. 1979. "The Carolina Slate Belt - Evidence of a Continental Rift Zone," Geology, Vol. 7, p 180-184.
- Long, L. T. 1988. "Maximum Earthquake at Hartwell Reservoir; Comparison of Probabilistic and Mechanistic Estimates," In Appendix C of report by Krinitzsky and Dunbar, 1988, Geological-Seismological Evaluation of Earthquake Hazards at Hartwell and Clemson Dams, Technical Report GL-90-11, USAE Waterways Experiment Station, Vicksburg, Mississippi.
- Long, L. T., Deman, H. E., Hsiao, H. Y., and Marion, G. E. 1976. "Gravity and Seismic Studies in the Clark Hill Reservoir Area, Stratigraphy, Structure, and Seismicity in Slate Belt Rocks along the Savannah River, Guidebook 16, Georgia Geological Society, Atlanta, Georgia.
- Maher, H. D. 1978. "Stratigraphy and Structure of the Belair and Kiokee Belts, near Augusta, Georgia," Geological Investigation of the Eastern Piedmont, Southern Appalachians, Carolina Geological Survey Field Trip Guidebook, 7-8 October, p. 47-54, Columbia, South Carolina.
- Maher, H. D. 1987. "D₃ Folding in the Eastern Piedmont Associated with Alleghanian Thrusting," Anatomy of the Alleghanian Orogeny as seen from the Piedmont of South Carolina and Georgia, Carolina Geological Society Field Trip Guidebook, p. 35-48, November 14-15, Columbia, South Carolina.
- Maher, H. D., Sacks, P. E., and Secor D. T. 1991. "Chapter 6: The Eastern Piedmont in south Carolina," In Horton, J. W. and Zullo, V. A. editors, The Geology of the Carolinas, Carolina Geological Society, Columbia, South Carolina.
- Maher, H. D. and Sacks, P. E. 1987. "Geologic Map of the Clarks Hill and Leah Quadrangles," Anatomy of the Alleghanian Orogeny as seen from the Piedmont of South Carolina and Georgia, Carolina Geological Society Field Trip Guidebook, November 14-15, Columbia, South Carolina.

Marine, W. and Siple, G. E. 1974. "Buried Triassic Basin in the Central Savannah River Area, South Carolina and Georgia," Geological Society of America Bulletin, Vol. 85, p 311-320.

Meade, R. B. 1991. "Reservoirs and Earthquakes," Engineering Geology, p. 245-262.

Meade, R. B. 1982. "The Evidence for Reservoir-Induced Macroeathquakes," State-of-the-Art for Assessing Earthquake Hazards in the United States, Miscellaneous Paper S-73-1, USAE Waterways Experiment Station, Vicksburg, Mississippi.

Nuclear News. 1982. "Map of Commercial Nuclear Power Stations in the United States-Operable, Under Construction or Ordered-August 1, 1982," LaGrange Park, Illinois.

O'Connor, B. J. and Prowell, D. C. 1976. "The Geology of the Belair Fault Zone and Basement Rocks of the Augusta, Georgia Area," Stratigraphy, Structure, and Seismicity in Slate Belt Rocks along the Savannah River, Guidebook 16, Georgia Geological Society, Atlanta, Georgia.

Oliver, J. 1982. "Probing the Structure of the Deep Continental Crust," Science, Vol. 216, No. 4547, p 689-695.

Overstreet, W. C. 1970. "Chapter 25 - The Piedmont in South Carolina," Studies of Appalachian Geology, Edited by G. W. Fisher, F. J. Pettijohn, and J. C. Reed, Interscience Publishers, John Wiley and Sons, New York.

Overstreet, W. C. and Bell, H. 1965. "The Crystalline Rocks of South Carolina," US Geological Survey Bulletin 1183, US Government Printing Office, Washington.

Prowell, D. C. 1978. "Distribution of Crystalline Rocks Around Augusta, Georgia, and their Relationship to the Belair Fault Zone," Geological Investigation of the Eastern Piedmont, Southern Appalachians, Carolina Geological Survey Field Trip Guidebook, 7-8 October, p. 55-60, Columbia, South Carolina.

Prowell, D. C., O'Connor, B. J., and Rubin, M. 1975. "Preliminary Evidence for Holocene Movement Along the Belair Fault Zone Near Augusta, Georgia," US Geological Survey, Open File Report 75-680, Reston, Virginia.

Peters, K. E. and Herrmann, R. B. 1986. "First-Hand Observations of the Charleston Earthquake of August 31, 1886, and Other Earthquake Materials," Bulletin No. 41, South Carolina Geological Survey, Columbia, South Carolina.

Ragland, P. C. 1991. "Chapter 10: Mesozoic Igneous Rocks," In Horton, J. W. and Zullo, V. A. editors, The Geology of the Carolinas, Carolina Geological Society, Columbia, South Carolina.

Rankin, D. W. 1975. "The Continental Margin of Eastern North America in the Southern Appalachians: The Opening and Closing of the Proto-Atlantic Ocean," American Journal of Science, Vol 275-A, p 298-336.

Reagor, B. G., Stover, C. W., and Algermissen, S. T. 1980. "Seismicity Map of the State of South Carolina," US Geological Survey, Map MF-1225, Reston, Virginia.

Sacks, P. E., and Dennis, A. J. 1987. "The Modoc Zone - D₂(Early Alleghanian) in the Eastern Appalachian Piedmont, South Carolina and Georgia," Anatomy of the Alleghanian Orogeny as seen from the Piedmont of South Carolina and Georgia, Carolina Geological Society Field Trip Guidebook, p. 19-34, November 14-15, Columbia, South Carolina.

Sbar, M. L. and Sykes, L. R. 1973. Contemporary Compressive Stress and Seismicity in Eastern North America: An Example of Intra-Plate Tectonics," Geological Society of America Bulletin, Vol. 84, p. 1861-1882.

Secor, D. T. 1987a. "Anatomy of the Alleghanian Orogeny as Seen from the Piedmont of South Carolina and Georgia," Carolina Geological Society Field Trip Guidebook, Edited by D. T. Secor, November 14-15, Columbia, South Carolina.

Secor, D. T. 1987b. "Regional Overview," Anatomy of the Alleghanian Orogeny as Seen from the Piedmont of South Carolina and Georgia, Carolina Geological Society Field Trip Guidebook, Edited by D. T. Secor, November 14-15, p. 1-18, Columbia, South Carolina.

Secor, D. T., Snoke, A. W., and Dallmeyer, R. D. 1986a. "Character of the Alleghanian orogeny in the Southern Appalachians: Part I. Alleghanian deformation in the eastern Piedmont of South Carolina," Geological Society of America Bulletin, v. 97, p. 1345-1353.

Secor, D. T., Snoke, A. W., and Dallmeyer, R. D. 1986b. "Character of the Alleghanian orogeny in the Southern Appalachians: Part III. Regional tectonic relations," Geological Society of America Bulletin, v. 97, p. 1345-1353.

Shedlock, K. M. 1988. "Seismicity in South Carolina," Seismological Research Letters, Vol. 59. No. 4, p. 165-171.

Sibol, M. S., Bollinger, G. A., and Birch, J. B. 1987. "Estimates of Magnitudes in Central and Eastern North America Using Intensity and Felt Area," Bulletin of the Seismological Society of America, Vol. 77, No. 5, p 1635-1654.

Snoke, A. W. 1978. "Geological Investigation of the Eastern Piedmont, Southern Appalachians," Carolina Geological Survey Field Trip Guidebook, 7-8 October, Edited by A. W. Snoke, Columbia, South Carolina.

Stearns, R. G. and Wilson, C. W. 1972. "Relationships of Earthquakes and Geology in West Tennessee and Adjacent Areas," Tennessee Valley Authority.

Stose, G. W. 1939. "Geologic Map of Georgia," Georgia Division of Mines, Mining, and Geology, Atlanta, Georgia.

Street, R. and Nuttli, O. 1984. "The Central Mississippi Valley Earthquake of 1811-1812," Proceedings of the Symposium on the "New Madrid Seismic Zone, US Geological Survey, Open File Report 84-770, p. 33-63.

Talwani, P. 1985. "Current Thoughts on the Cause of the Charleston, South Carolina Earthquakes," South Carolina Geology, Vol. 29, p. 19-38.

Talwani, P. 1988. "Seismic Potential Near Lake Hartwell, South Carolina," In Appendix D of report by Krinitzsky and Dunbar, 1988, Geological-Seismological Evaluation of Earthquake Hazards at Hartwell and Clemson Dams, Technical Report GL-90-11, USAE Waterways Experiment Station, Vicksburg, Mississippi.

- Talwani, P., Colquhoun, D. J., Acree, S. D., and Muthanna, A. 1988. "Further Neotectonic Studies of Earthquake Zones in the Eastern United States," US Nuclear Regulatory Commission Report NUREG/CR-5257, Washington, D.C.
- Tarr, A. C. and Rhea, S. 1983. "Seismicity Near Charleston, South Carolina, March 1973 to December 1979," Studies Related to the Charleston, South Carolina, Earthquake of 1886-Tectonics and Seismicity, Geological Survey Professional Paper 1313, US Government Printing Office, Washington, D.C.
- US Army Corps of Engineers. 1977a. "Design Earthquake Report, Geological and Seismological Evaluation of Earthquake Hazards at the Richard B. Russell Project," US Army Corps of Engineers, Savannah District, Savannah, Georgia.
- US Army Corps of Engineers. 1977b. "Appendix 3, Section A: Geologic Report on the Modoc Fault Zone, South Carolina and Georgia," Design Earthquake Report, Geological and Seismological Evaluation of Earthquake Hazards at the Richard B. Russell Project, US Army Corps of Engineers, Savannah District, Savannah, Georgia.
- US Army Corps of Engineers. 1977c. "Appendix 3, Section B: Geologic Report on the Area in the Western Portion of the Proposed Richard B. Russell Lake," Design Earthquake Report, Geological and Seismological Evaluation of Earthquake Hazards at the Richard B. Russell Project, US Army Corps of Engineers, Savannah District, Savannah, Georgia.
- US Army Corps of Engineers. 1977d. "Appendix 3, Section D: Diversion Channel Fault Studys," Design Earthquake Report, Geological and Seismological Evaluation of Earthquake Hazards at the Richard B. Russell Project, US Army Corps of Engineers, Savannah District, Savannah, Georgia.
- US Army Corps of Engineers. 1977e. "Appendix 3, Section E: Patterson Branch Fault - Geologic Report," Design Earthquake Report, Geological and Seismological Evaluation of Earthquake Hazards at the Richard B. Russell Project, US Army Corps of Engineers, Savannah District, Savannah, Georgia.
- US Army Corps of Engineers. 1977f. "Appendix 3, Section F: Belair Fault-Support Documentation," Design Earthquake Report, Geological and Seismological Evaluation of Earthquake Hazards at the Richard B. Russell Project, US Army Corps of Engineers, Savannah District, Savannah, Georgia.
- US Army Corps of Engineers. 1977g. "Appendix 3, Section G: Elbert and Hart Counties Georgia, and the Projection of the Towaliga Fault," Design Earthquake Report, Geological and Seismological Evaluation of Earthquake Hazards at the Richard B. Russell Project, US Army Corps of Engineers, Savannah District, Savannah, Georgia.
- US Army Corps of Engineers. 1978. "Final Foundation Report Clarks Hill Dam, Savannah River, Georgia-South Carolina," Report prepared by Ebasco Services Inc., Savannah District, Savannah, Georgia.
- Visvanathan, T. R. 1980. "Earthquakes in South Carolina 1698-1975," Bulletin 40, South Carolina Geological Survey, Columbia, South Carolina.
- Whitney, J. A., Wells, D. E., and Rozen, R. W. 1980. "Structural and Tectonic Setting of the Elberton Batholith, Eastern Georgia Piedmont," Geological, Geochemical, and Geophysical Studies of the Elberton Batholith, Eastern Georgia, Guidebook 19, 15th Annual Georgia Geological Society Field Trip, Atlanta, Georgia.

Zietz, I. and Gilbert, F. P. 1980. "Aeromagnetic Map of Part of the Southeastern United States: In Color" US Geological Survey, Geophysical Investigations Map GP-936, Reston, Virginia.

APPENDIX A: SITE GEOLOGY OF J. STROM THURMOND (CLARKS HILL) DAM

J. Strom Thurmond Dam was the first in a series of dams for the comprehensive development of the Savannah River. It was constructed principally for the purpose of producing electricity and providing recreation. The dam is a 5,680 ft (1731 m) composite concrete-gravity and earth embankment dam. Construction of Clarks Hill or J. Strom Thurmond Dam began in 1945 and was completed in 1952.

The bedrock geology of the dam and surrounding area is presented in Figure A1 (from Maher and Sacks, 1987). The dam is built on high grade metamorphic rock. Rock type identified by Figure A1 for the dam site is primarily a biotite amphibole gneiss. The initial geologic evaluation of the damsite, from boring data and excavation of the foundation, shows that the underlying rock along the centerline of the dam is variable as shown by Figure A2 (from US Army Corps of Engineers, 1967). Rock types identified by Figure A2 for the foundation centerline include various colored granites, pegmatites, and gneisses.

The concrete portion of the dam is approximately 2,282 ft (695.6 m) in length and was built on firm rock in 47 monolithic sections (see Figures A3, A4, and A5 for locations and number of monoliths). The foundation rock was hand cleaned to remove loose and weathered rock. Soft material in the foundation was excavated and removed to a depth twice its width where weathering was more than 3 to 4 in. (7.62 to 10.16 cm) wide.

The major foundation problem encountered during construction was seepage from springs and seeps by way of joints. The treatment for flowing ground water was to drill an intersecting well into the joint and syphon the water away from the foundation. These joints were then cleaned and concrete filled. Bedrock along the entire length of the dam was hand cleaned and filled with concrete to the rock surface. A grout curtain was installed by pressure grouting to a depth of 40 ft to seal the underlying foundation against seepage.

Mapping conducted during the foundation excavation and cleaning (see

Figures A6 through A14) identified two fault zones in the foundation (US Army Corps of Engineers, 1978). The first fault, identified as fault number one (US Army Corps of Engineers, 1978), strikes northeast from block 14 to block 18 (see Figure A6). The second fault, fault number 2, strikes west-northwest from block 2 to block 9 (see Figure A8). Both faults are identified as dipping to the south at about 80 degrees with the shear zone ranging from 6 in. (15.24 cm) to 8 ft (2.44 m) in width. These shear zones are composed primarily of disintegrated rock, lenses of fault gouge, and fault breccia composed of granite fragments cemented by crystalline calcite. Cross sections across the two shear zones are presented in Figure A7 (see Figures A6 and A8 for section locations). Faulting was not considered to be a structural problem from a tectonic perspective as the age of the shear zone is constrained by pegmatite veins which cross cut the fault zones at numerous locations. As noted by the detailed geologic mapping in the foundation (see Figures A6 and A8), pegmatite veins do not offset the shear zone. Radiometric dating of igneous rock from this area restrict any igneous activity to the Paleozoic and Mesozoic Periods.

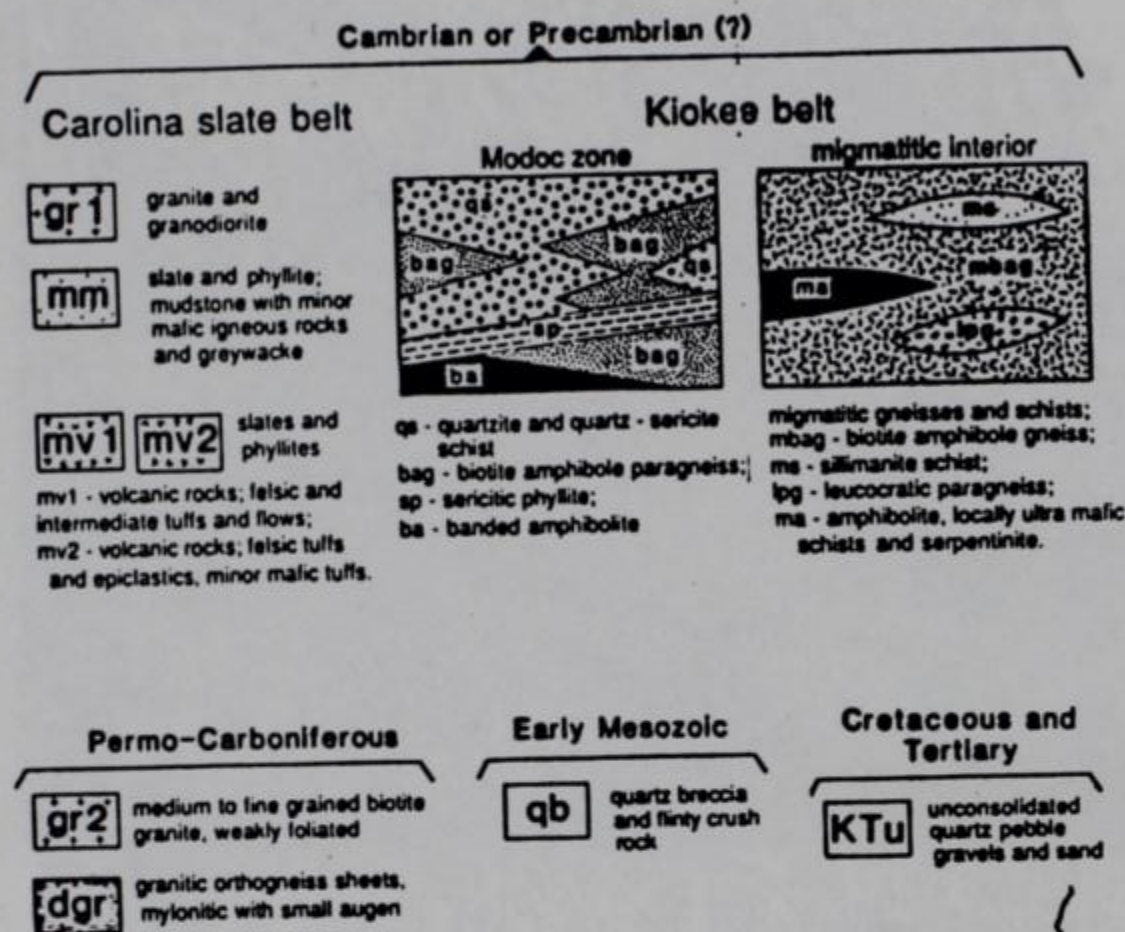
Although the two shear zones described above were not significant from a tectonic perspective, they required special treatment to seal against seepage. The first shear zone in blocks 14 and 18 was excavated to a depth twice its width, filled with concrete to rock surface, and grouted along a 4 ft spacing, rather than the usual 8 ft, to a depth of 80 ft (see Figures A4 and A5). The second shear zone in blocks 2 to 9, was treated in the same manner as the first except for treatment of block 9. Block 9 was considered a critical area and the excavation of the shear zone at this location was 3 to 4 times the width. Detailed information regarding the foundation preparation for the individual blocks is described by US Army Corps of Engineers (1978).

References

Maher, H. D. and Sacks, P. E., 1987. "Geologic Map of the Clarks Hill and Leah Quadrangles," Anatomy of the Alleghanian Orogeny as seen from the Piedmont of South Carolina and Georgia, Carolina Geological Society Field Trip Guidebook, November 14-15, Columbia, South Carolina.

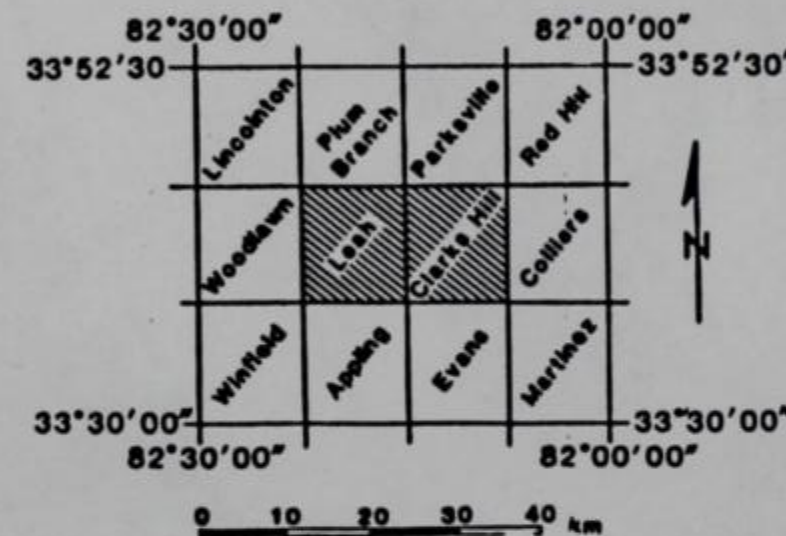
US Army Corps of Engineers, 1967. "Periodic Inspection Report No. 1," Savannah District, Savannah, Georgia.

US Army Corps of Engineers, 1978. "Final Foundation Report Clark Hill Dam, Savannah River, Georgia-South Carolina," Report prepared by Ebasco Services Inc., Savannah District, Savannah, Georgia.

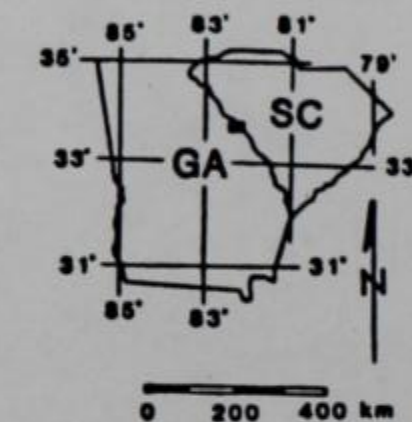


GEOLOGIC MAP OF THE CLARKS HILL AND LEAH QUADRANGLES, SC & GA

compiled by Harmon Maher and Paul Sacks



U.S. Geological Survey quadrangle maps.



Attitudes of planar and linear fabric elements

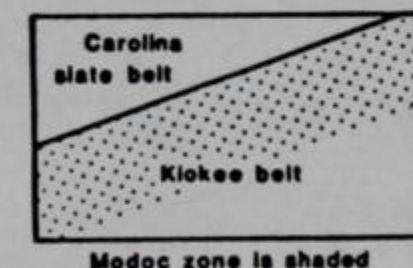
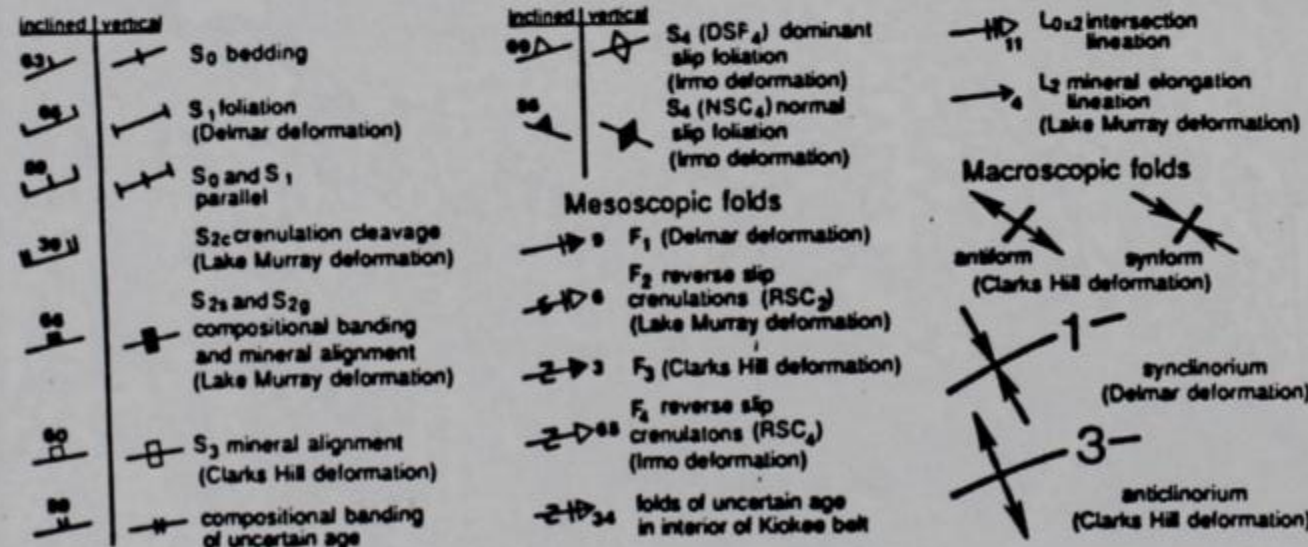
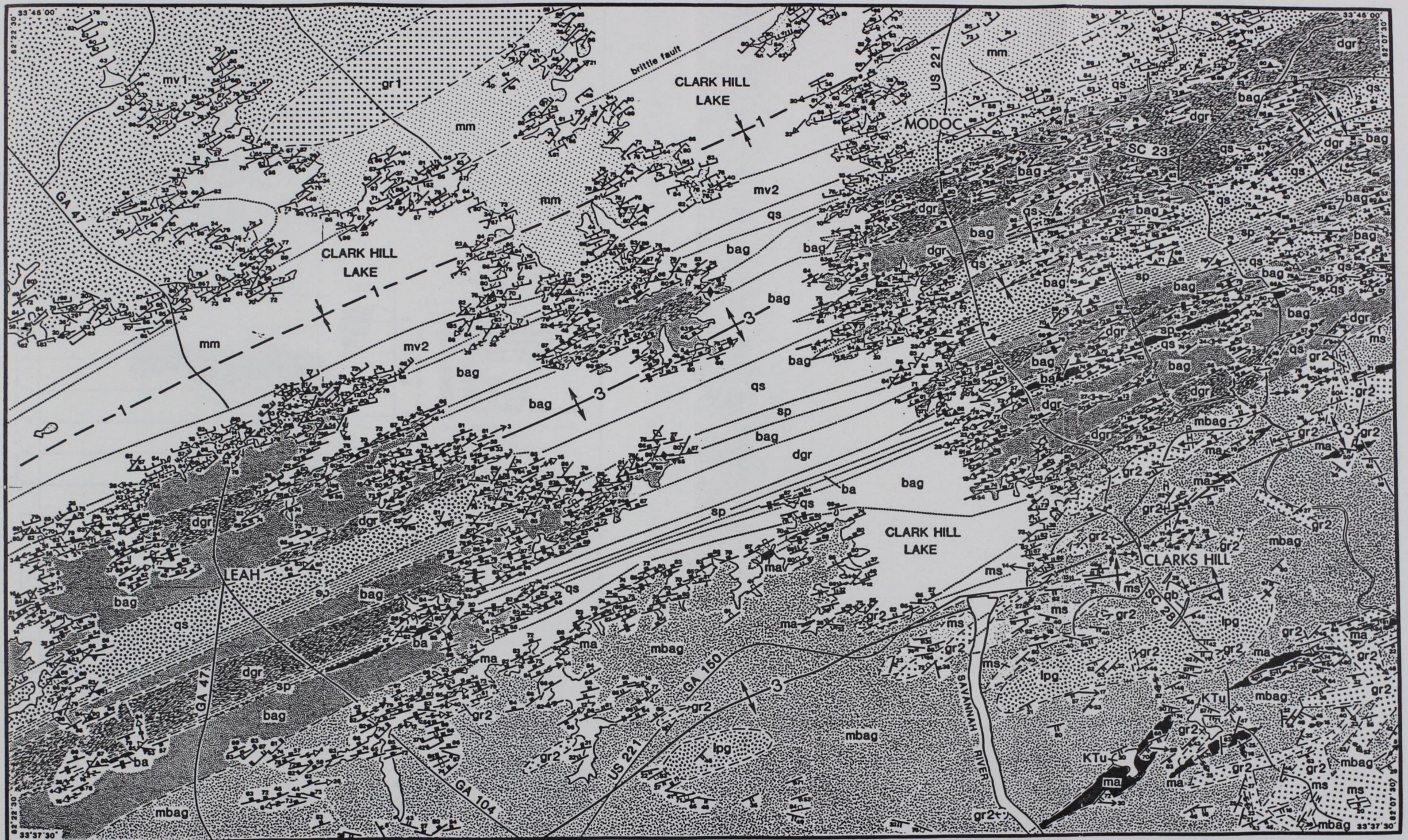


Figure Ala. Index and legend to geologic map of J. Strom Thurmond dam and reservoir area (from Maher and Sacks, 1987).



drafted by Terry Dennis

Figure Alb. Geologic map of Clarks Hill and Leah 7-1/2 minute quadrangles (from Maher and Sacks, 1987).

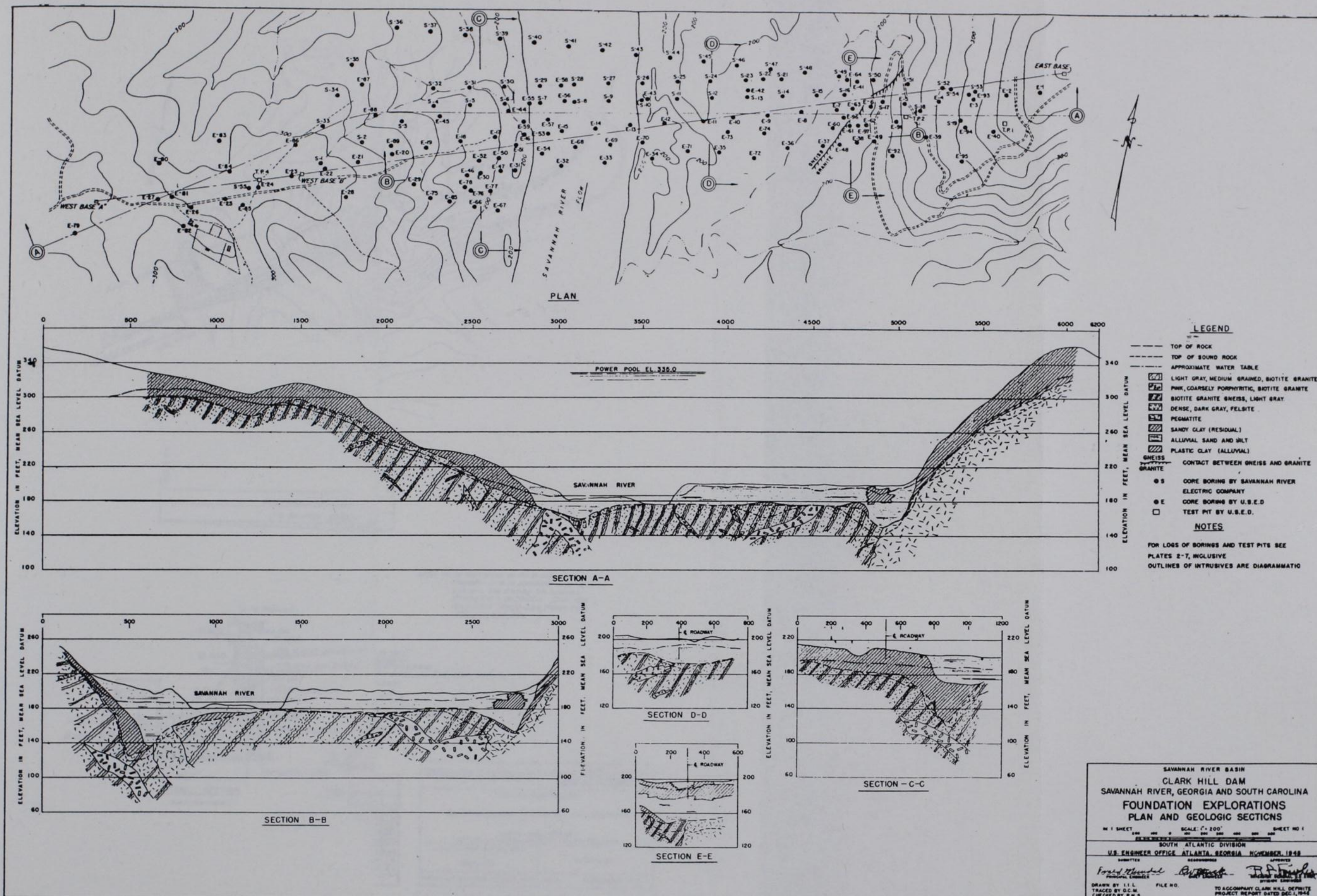


Figure A2. Boring location map and geologic cross section along centerline of J. Strom Thurmond dam (from US Army Corps of Engineers, 1967).

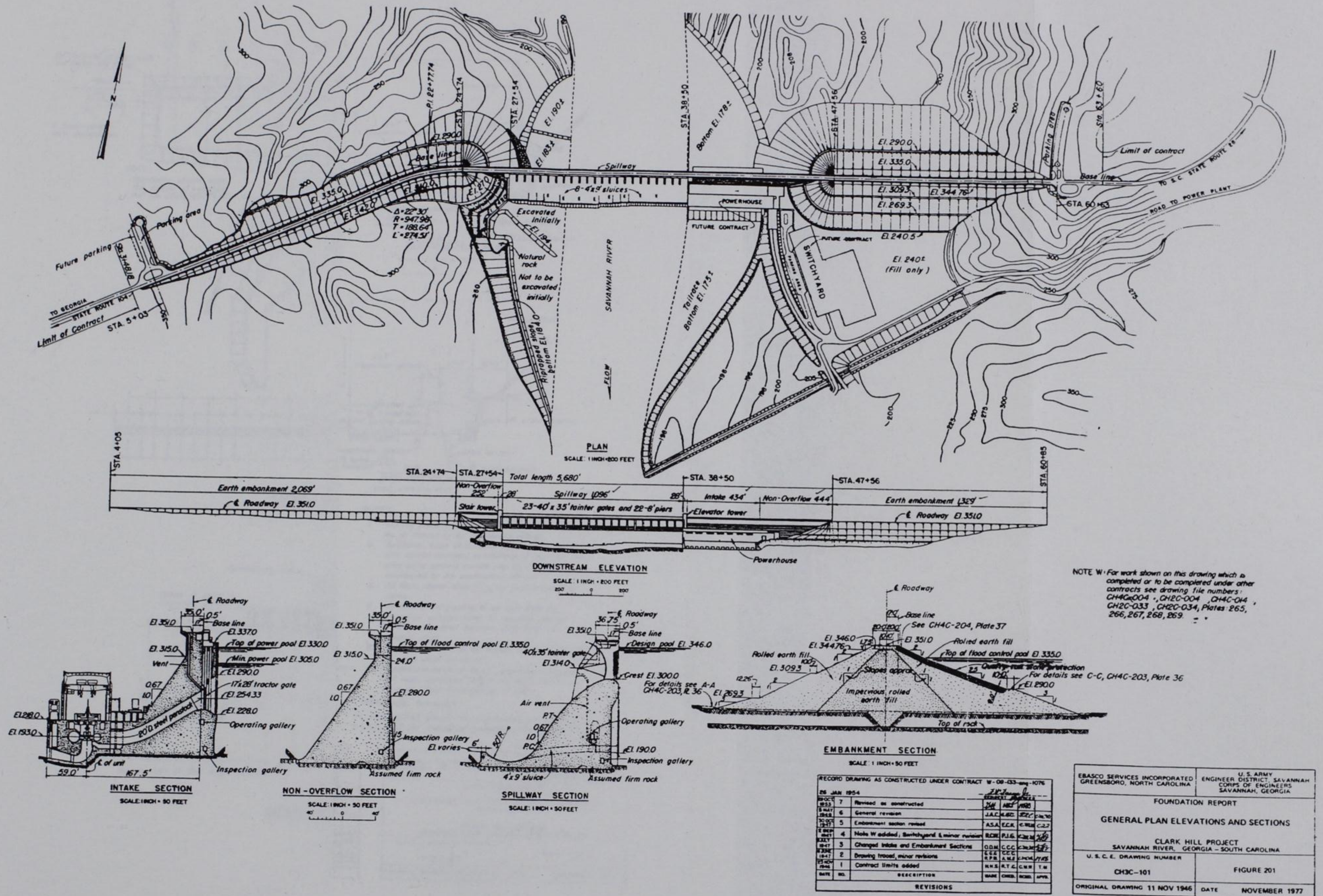


Figure A3. General plan map of J. Strom Thurmond Dam (from US Army Corps of Engineers, 1978).

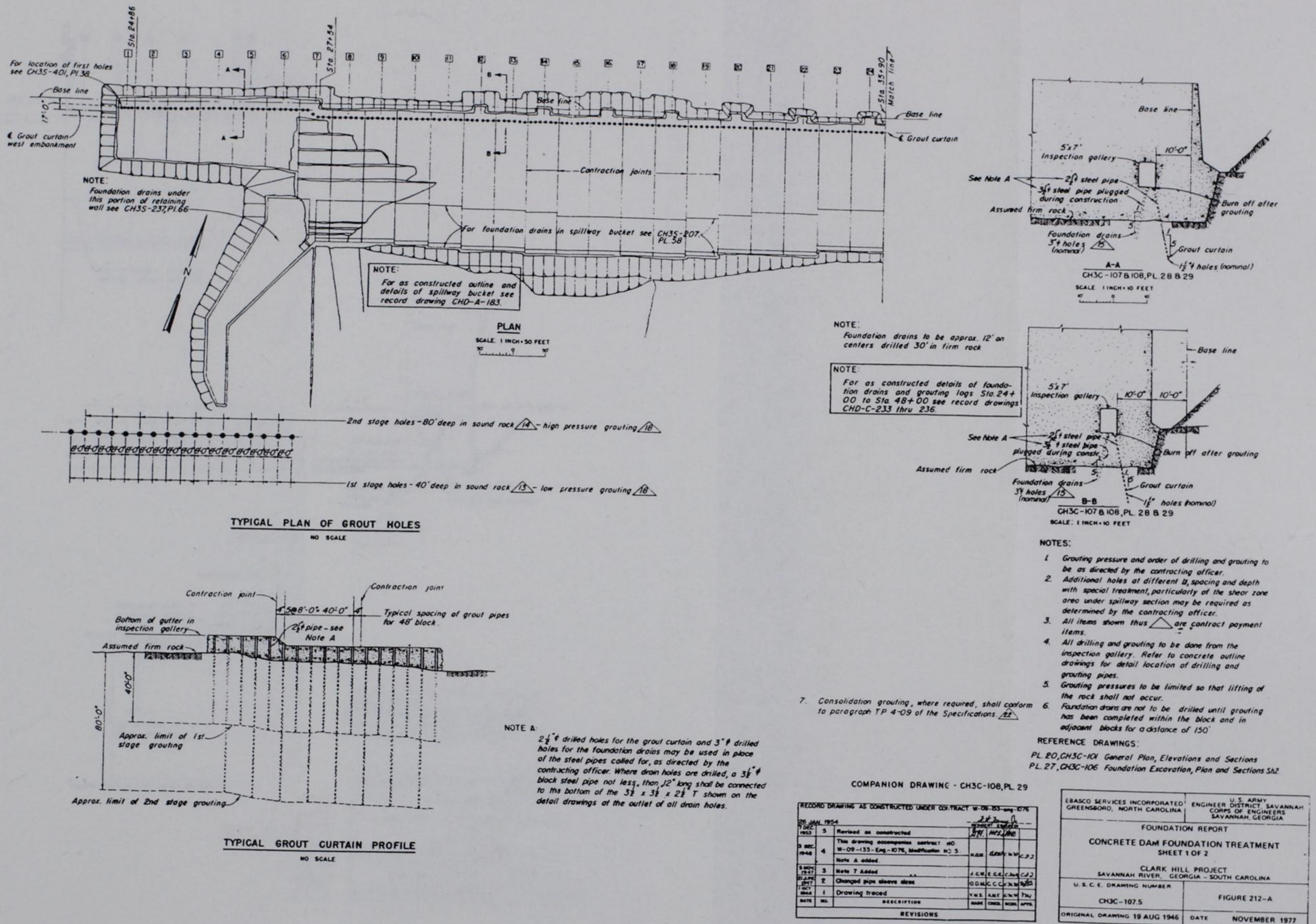
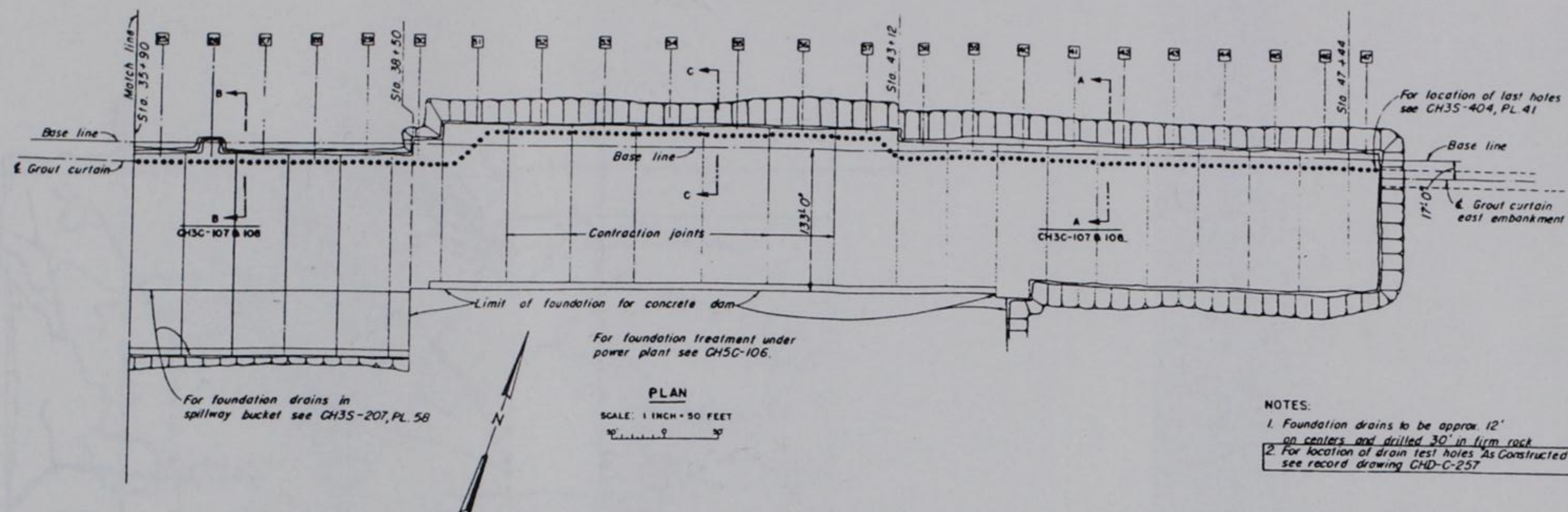


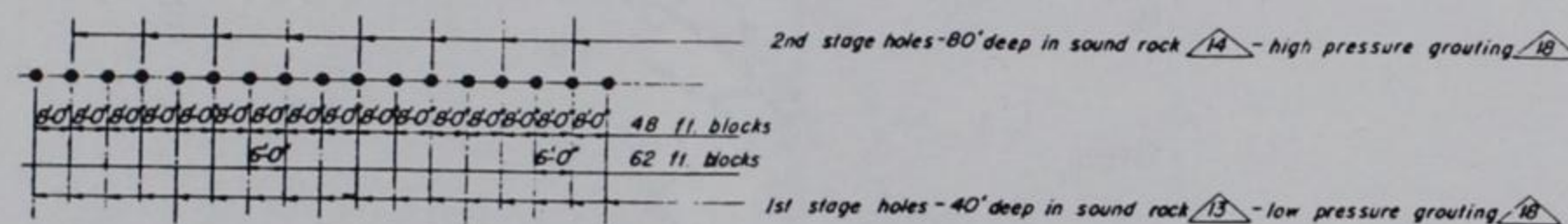
Figure A4. Index map to monoliths for western half of J. Strom Thurmond dam (US Army Corps of Engineers, 1978).



- NOTES:
1. Foundation drains to be approx. 12' on centers and drilled 30' in firm rock
 2. For location of drain test holes As Constructed see record drawing CHD-C-257

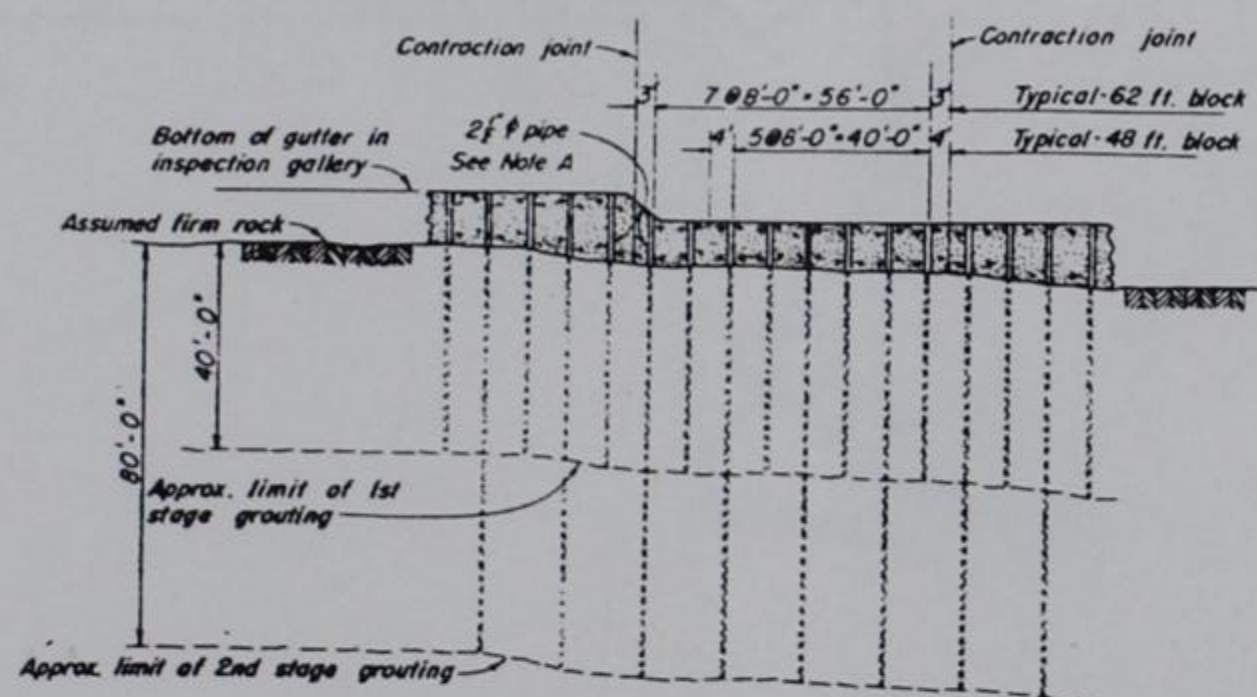
NOTE:

For as constructed details of foundation drains and grouting logs Sta. 24+00 to Sta. 48+00 see record drawings CHD-C-233 thru 236.



TYPICAL PLAN OF GROUT HOLES

NO SCALE

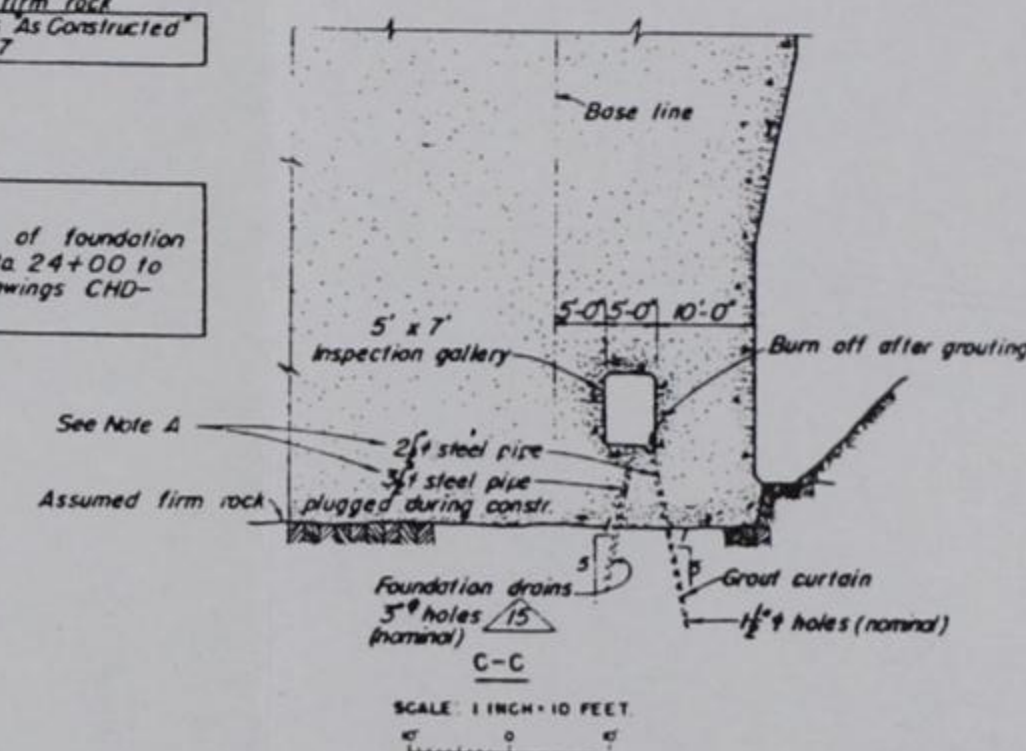


NOTE A:

2" steel pipe drilled holes for the grout curtain and 3" steel pipe drilled holes for the foundation drains may be used in place of the steel pipes called for, as directed by the contracting officer. Where drain holes are drilled, a 3" black steel pipe not less than 12' long, shall be connected to the bottom of the 3" x 3" x 2" T shown on the detail drawings at the outlet of all drain holes.

TYPICAL GROUT CURTAIN PROFILE

NO SCALE



NOTE:

For general notes and reference drawings see CH3C-107, PL 28

For work on this drawing "As Constructed" see record drawing Nos. CHD-C-233, 234, 235 & 236 for location of Foundation and Grouting.

COMPANION DRAWING - CH3C-107, PL 28

RECORD DRAWING AS CONSTRUCTED UNDER CONTRACT W-09-133-ENG-1076			
26 JAN 1954	4	Revised as constructed	24-7-0
1948	3	This drawing accompanies contract NO. W-09-133 Eng. - 1076, Modification NO. 5.	24-7-0
1947	2	Note A added.	24-7-0
1946	1	Changed pipe sleeve sizes	24-7-0
1946	1	Drawing traced	24-7-0
DATE	NO.	DESCRIPTION	NAME
			CH3C-107, PL 28

EBASCO SERVICES INCORPORATED GREENSBORO, NORTH CAROLINA	ENGINEER DISTRICT SAVANNAH CORPS OF ENGINEERS SAVANNAH, GEORGIA
FOUNDATION REPORT	
CONCRETE DAM FOUNDATION TREATMENT	
SHEET 2 OF 2	
CLARK HILL PROJECT	
SAVANNAH RIVER, GEORGIA - SOUTH CAROLINA	
U. S. C. E. DRAWING NUMBER	FIGURE 212-8
CH3C-108.3	
ORIGINAL DRAWING 19 AUG 1946	DATE NOVEMBER 1977

Figure A5. Index map to monoliths for eastern half of J. Strom Thurmond dam (US Army Corps of Engineers, 1978).



Figure A6. Detailed map of foundation geology, Blocks 1 to 9 (US Army Corps of Engineers, 1978).

EBASCO SERVICES INCORPORATED GREENSBORO, NORTH CAROLINA	U. S. ARMY ENGINEER DISTRICT, SAVANNAH CORPS OF ENGINEERS SAVANNAH, GEORGIA
FOUNDATION REPORT	
BLOCKS A-F, 1-9 FOUNDATION GEOLOGY, BUCKET DRAINS AND DOWELS	
CLARK HILL PROJECT SAVANNAH RIVER, GEORGIA - SOUTH CAROLINA	
U. S. C. E. DRAWING NUMBER	FIGURE 202-A
UNNUMBERED	
ORIGINAL DRAWING UNDATED	DATE NOVEMBER 1977

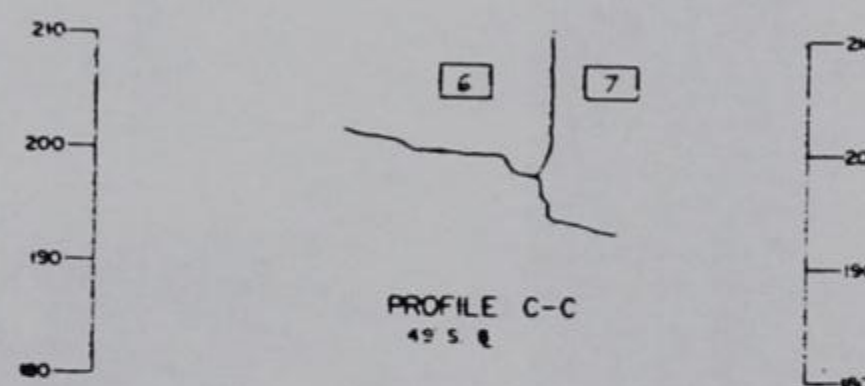
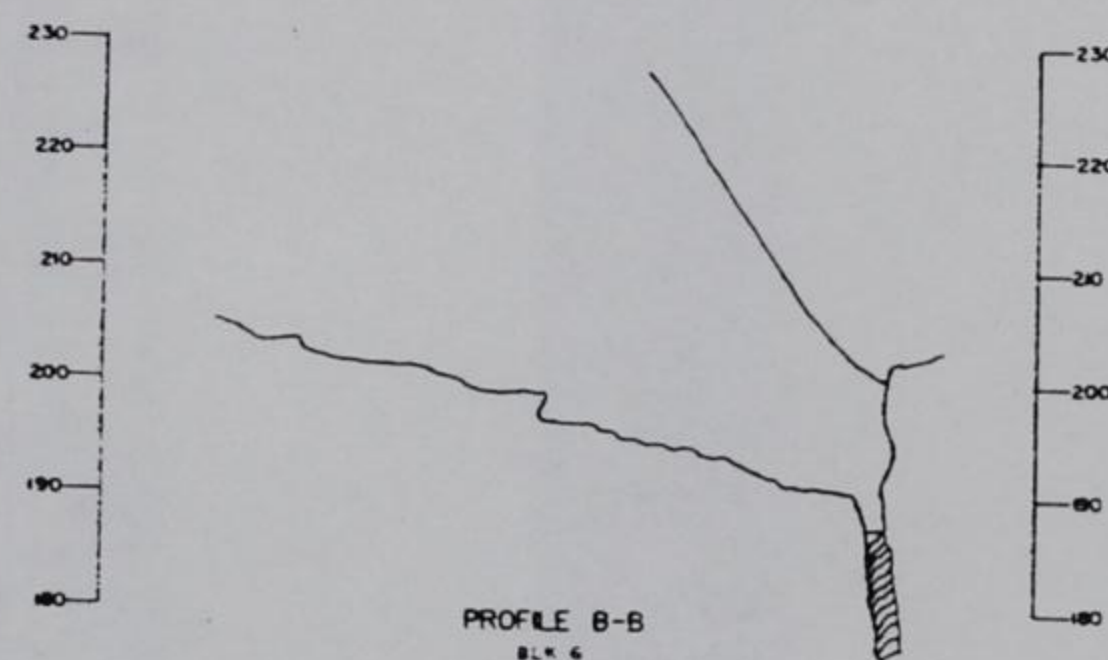
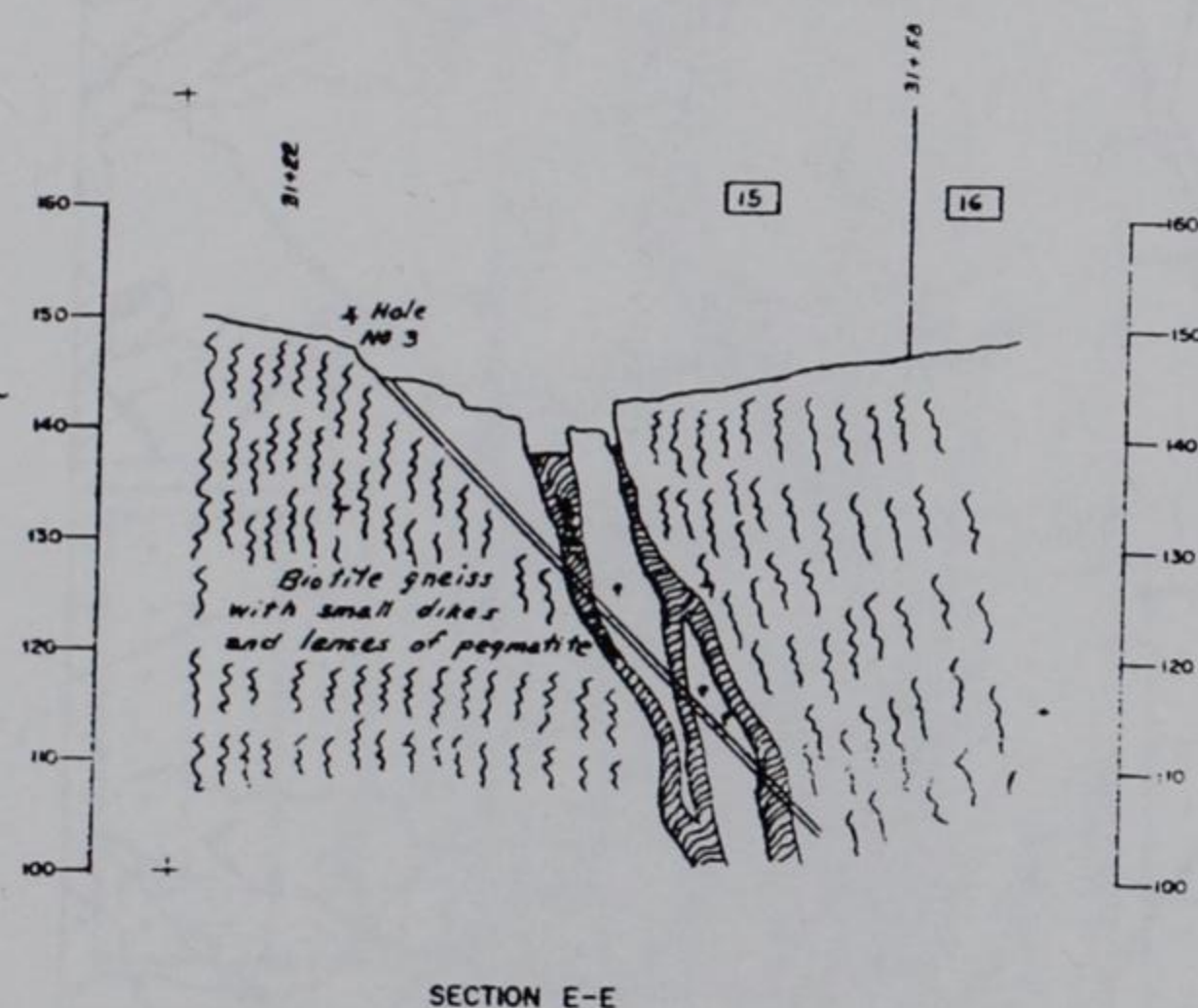
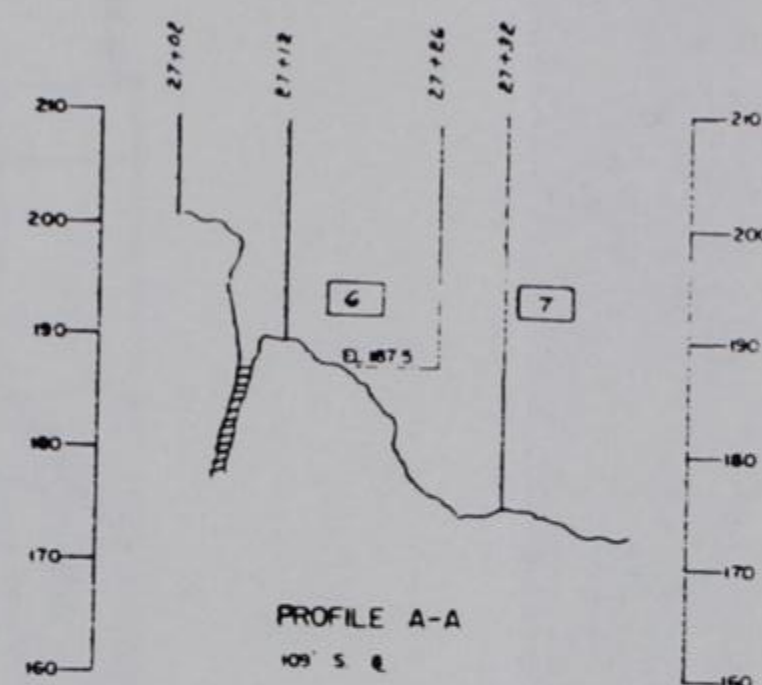
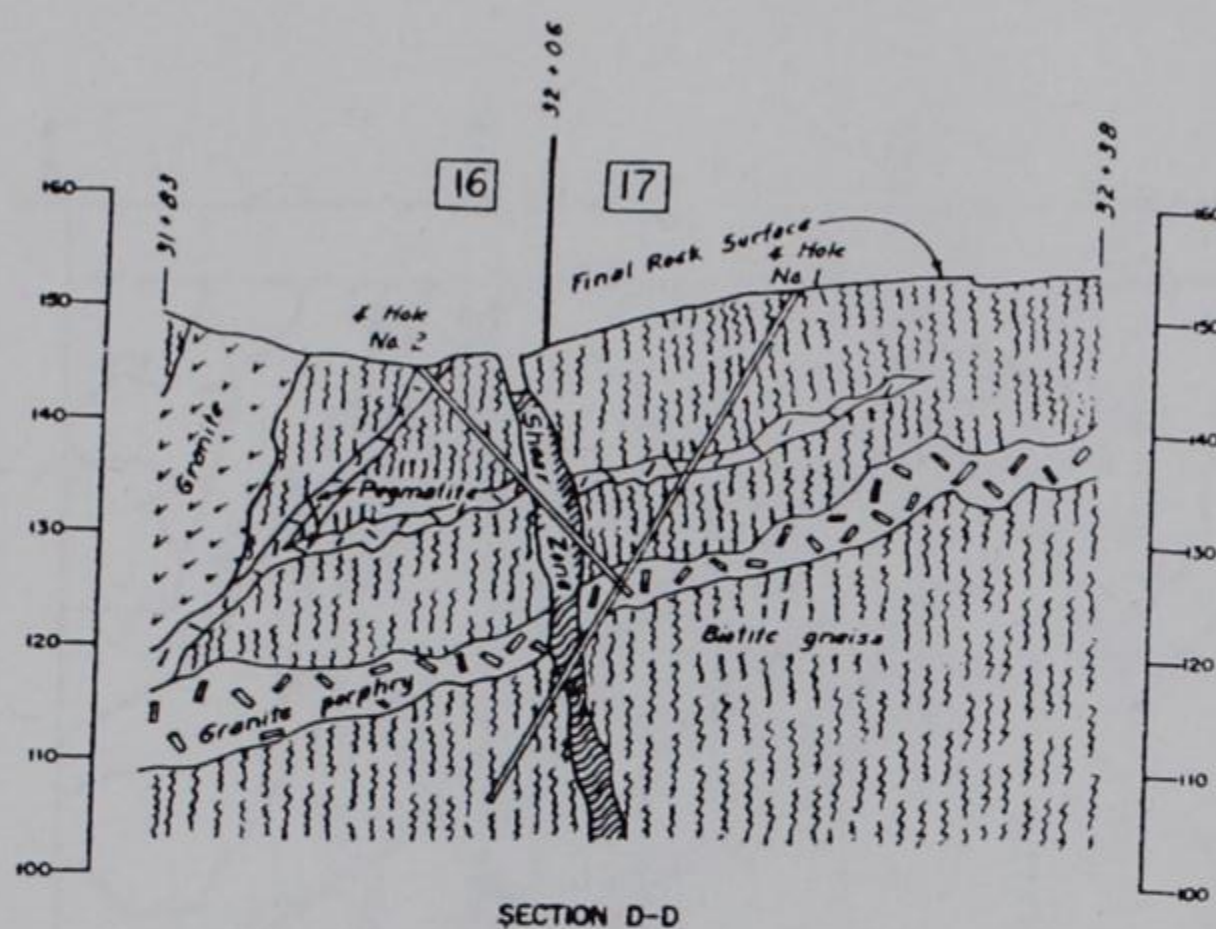


Figure A7. Geologic cross sections across shear zones (US Army Corps of Engineers, 1978).

EBASCO SERVICES INCORPORATED GREENSBORO, NORTH CAROLINA	U. S. ARMY ENGINEER DISTRICT, SAVANNAH CORPS OF ENGINEERS SAVANNAH, GEORGIA
FOUNDATION REPORT	
GEOLOGIC SECTIONS; FIRST STAGE CONSTRUCTION	
CLARK HILL PROJECT SAVANNAH RIVER, GEORGIA - SOUTH CAROLINA	
U. S. C. E. DRAWING NUMBER	FIGURE 202-B
ORIGINAL DRAWING	DATE NOVEMBER 1977

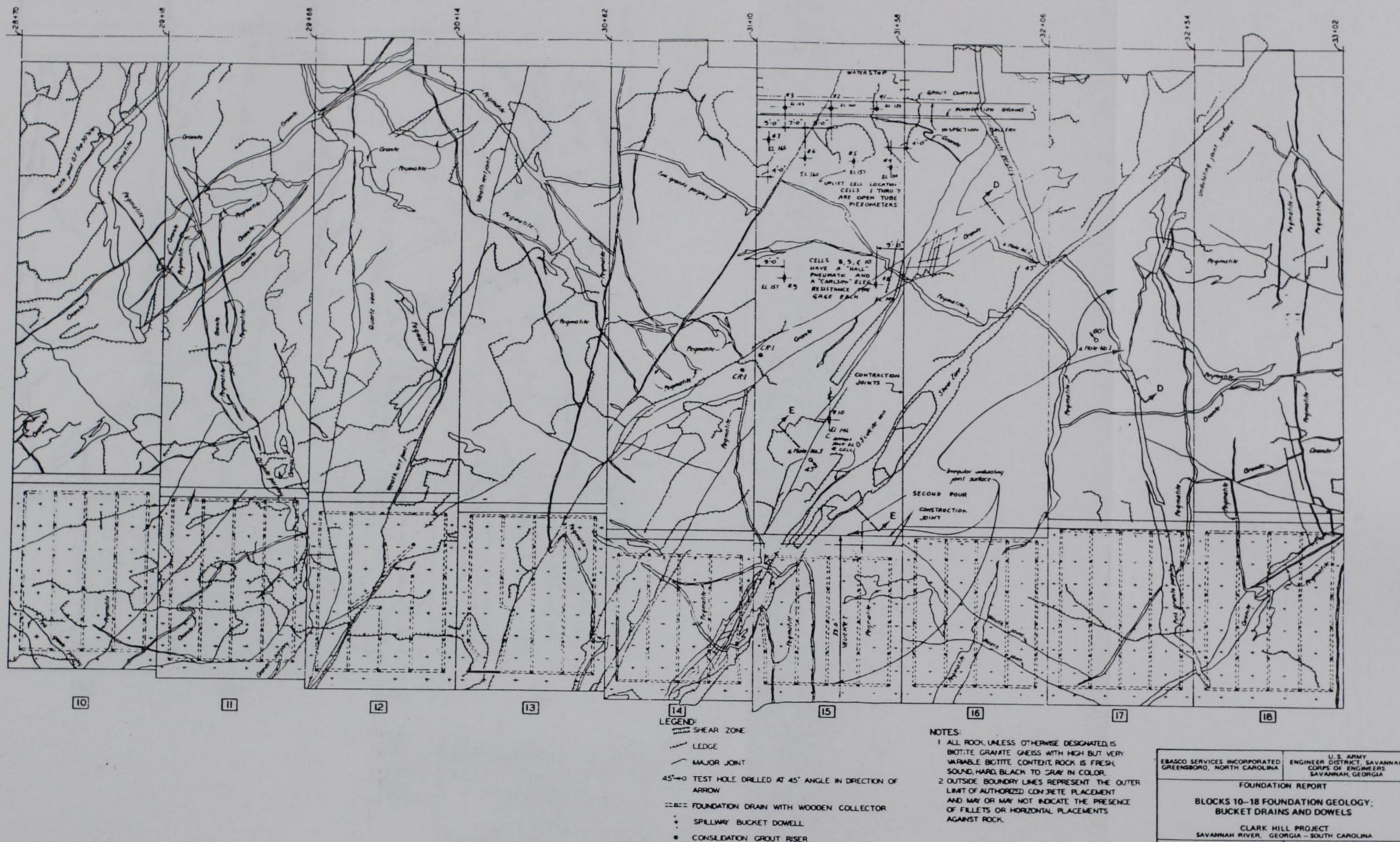


Figure A8. Detailed map of foundation geology, Blocks 10 to 18 (US Army Corps of Engineers, 1978).



NOTES:

1. ALL ROCK, UNLESS OTHERWISE DESIGNATED, IS BIOTITE GRANITE GNEISS WITH HIGH BUT VERY VARIABLE BIOTITE CONTENT. ROCK IS FRESH, SOUND, HARD, BLACK TO GRAY IN COLOR.
2. OUTSIDE BOUNDARY LINES REPRESENT THE OUTER LIMIT OF AUTHORIZED CONCRETE PLACEMENT AND MAY OR MAY NOT INDICATE THE PRESENCE OF FILLETS OR HORIZONTAL PLACEMENTS AGAINST ROCK.

BRASCO SERVICES INCORPORATED GREENSBORO, NORTH CAROLINA	U.S. ARMY ENGINEER DISTRICT, SAVANNAH CORPS OF ENGINEERS SAVANNAH, GEORGIA
FOUNDATION REPORT	
BLOCKS 19-27 FOUNDATION GEOLOGY; BUCKET DRAINS AND DOWELS	
CLARK HILL PROJECT SAVANNAH RIVER, GEORGIA - SOUTH CAROLINA	
U. S. C. E. DRAWING NUMBER	FIGURE 204
UNNUMBERED	
ORIGINAL DRAWING UNDATED	DATE NOVEMBER 1977

Figure A9. Detailed map of foundation geology, Blocks 19 to 27 (US Army Corps of Engineers, 1978).

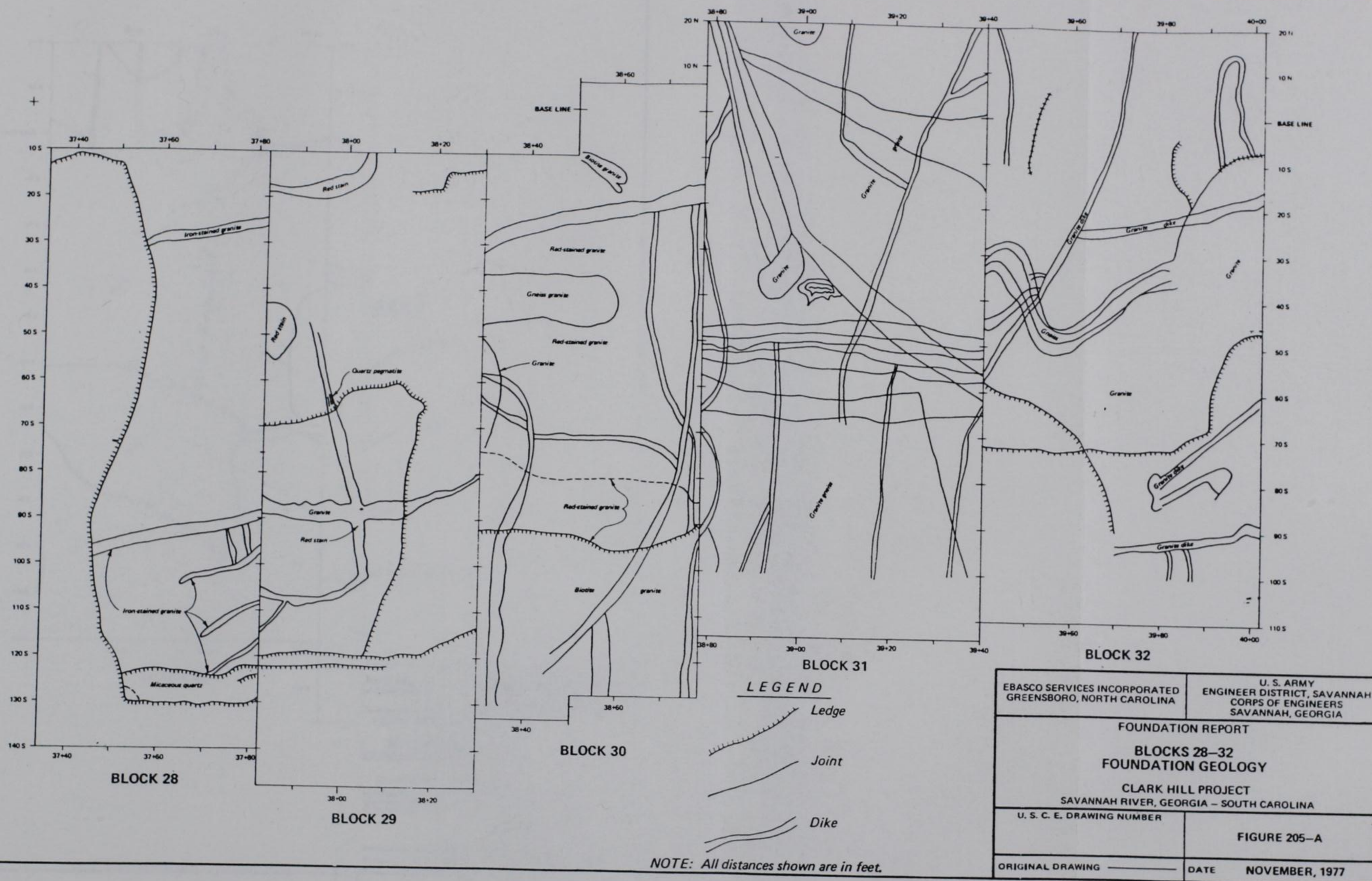
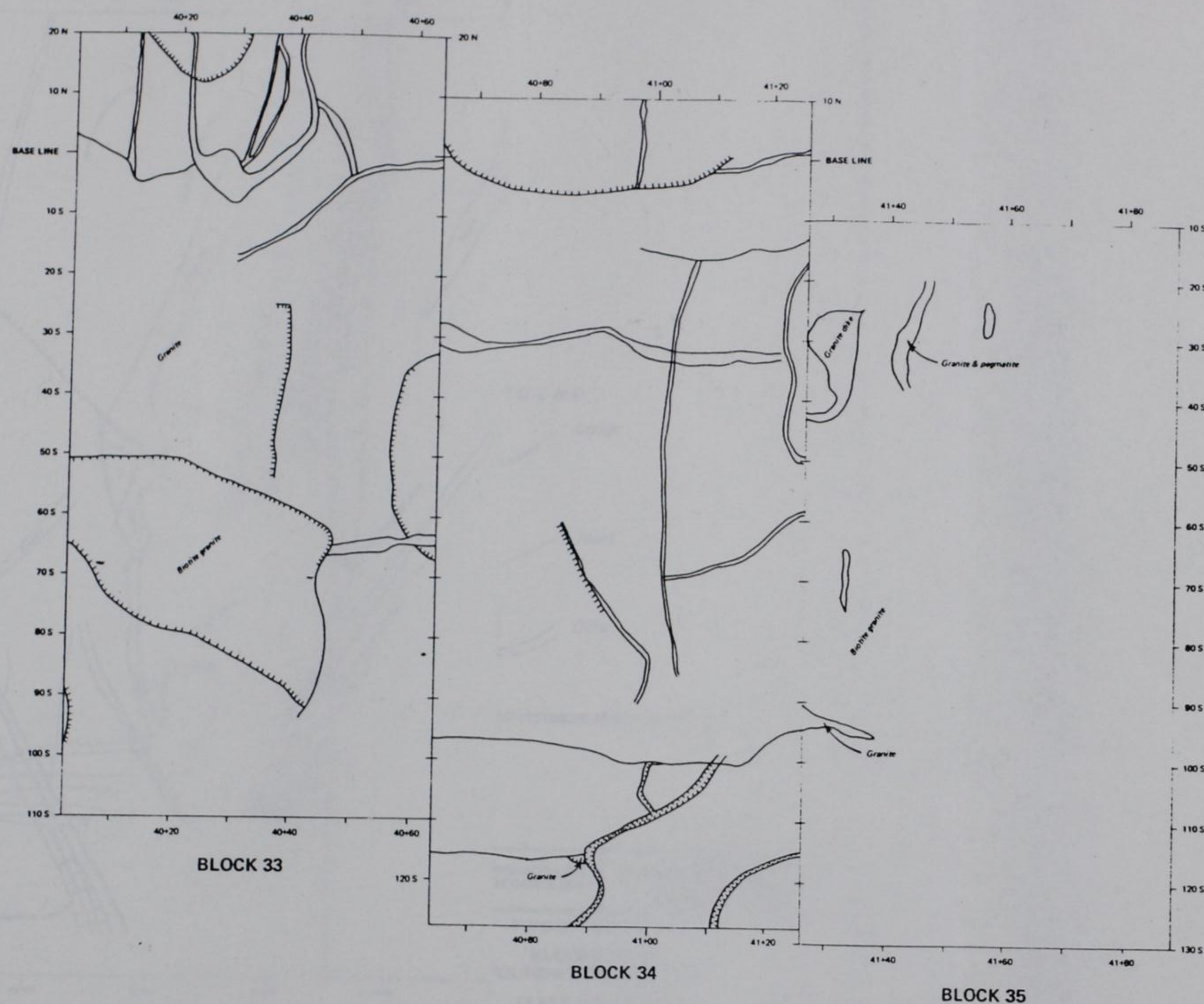
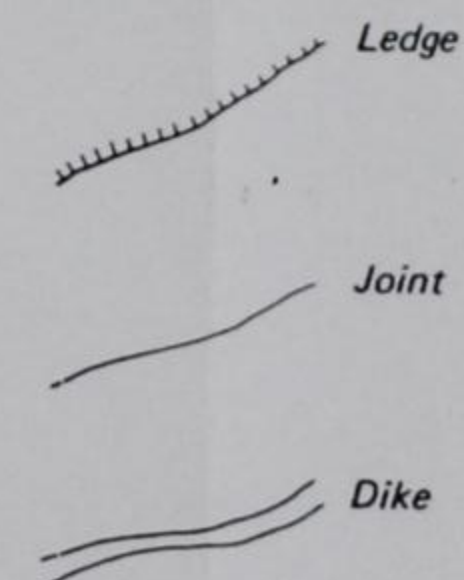


Figure A10. Detailed map of foundation geology, Blocks 28 to 32 (US Army Corps of Engineers, 1978).



LEGEND



NOTE: All distances shown are in feet.

EBASCO SERVICES INCORPORATED GREENSBORO, NORTH CAROLINA	U. S. ARMY ENGINEER DISTRICT, SAVANNAH CORPS OF ENGINEERS SAVANNAH, GEORGIA
FOUNDATION REPORT BLOCKS 33-35 FOUNDATION GEOLOGY CLARK HILL PROJECT SAVANNAH RIVER, GEORGIA - SOUTH CAROLINA	
U. S. C. E. DRAWING NUMBER	FIGURE 205-B
ORIGINAL DRAWING	DATE NOVEMBER, 1977

Figure A11. Detailed map of foundation geology, Blocks 32 to 35 (US Army Corps of Engineers, 1978).

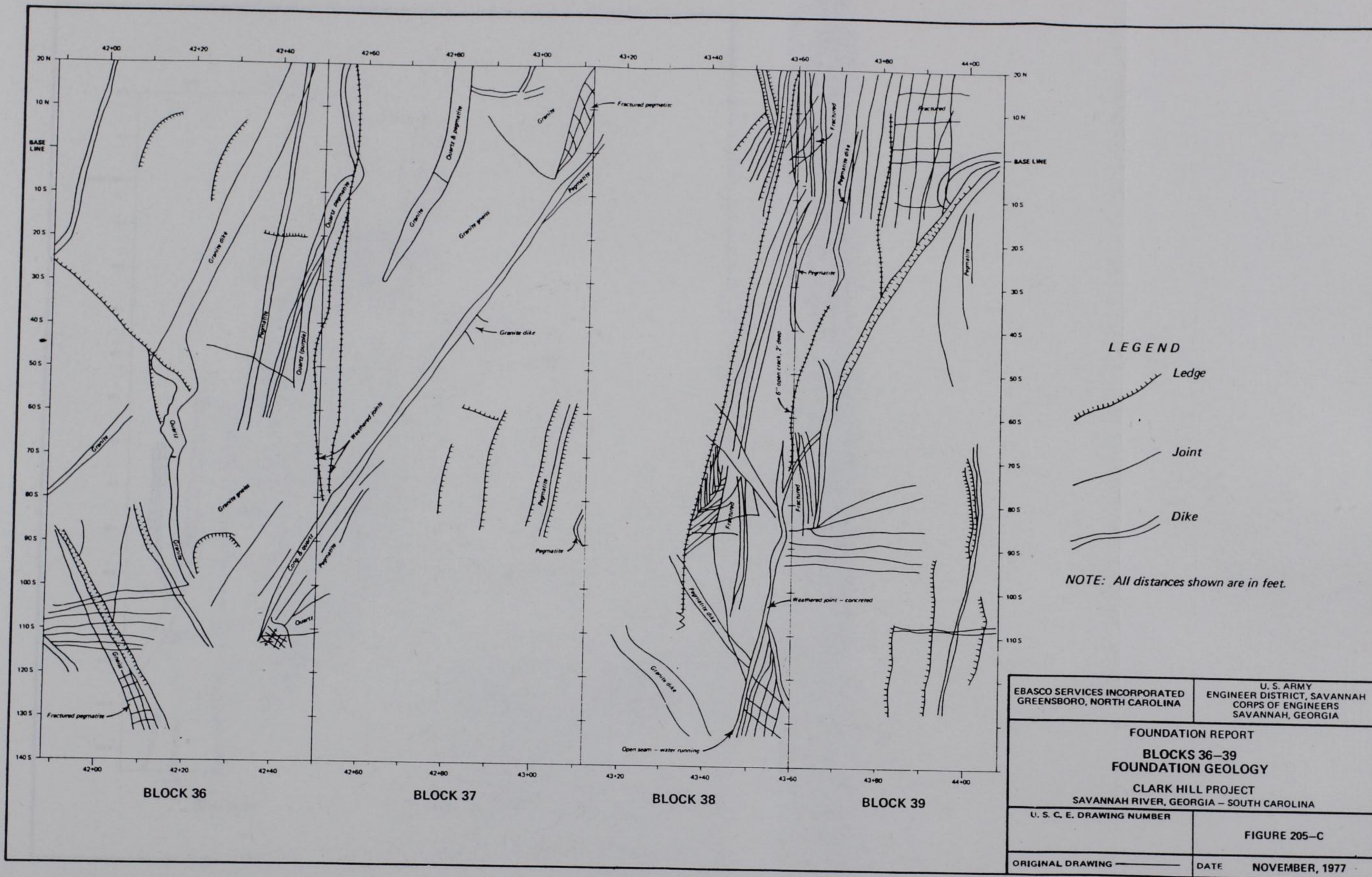


Figure A12. Detailed map of foundation geology, Blocks 36 to 39 (US Army Corps of Engineers, 1978).

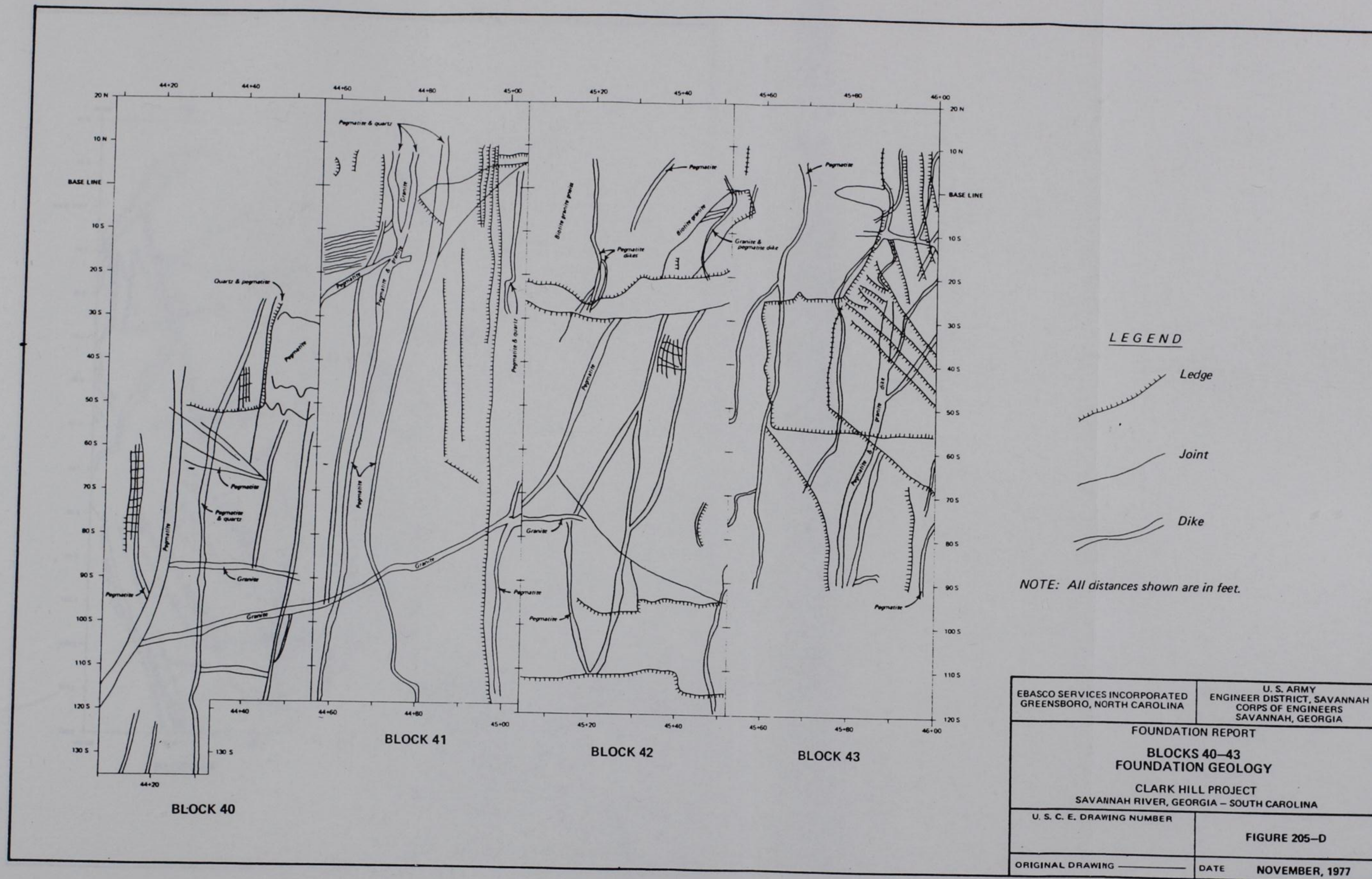
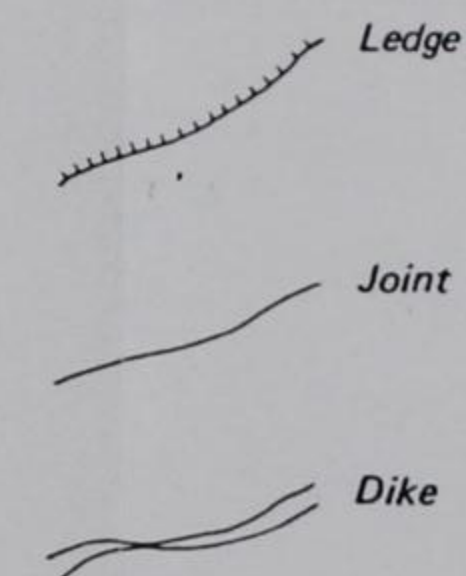


Figure A13. Detailed map of foundation geology, Blocks 40 to 43 (US Army Corps of Engineers, 1978).



LEGEND



NOTE: All distances shown are in feet.

EBASCO SERVICES INCORPORATED GREENSBORO, NORTH CAROLINA	U. S. ARMY ENGINEER DISTRICT, SAVANNAH CORPS OF ENGINEERS SAVANNAH, GEORGIA
FOUNDATION REPORT BLOCKS 44-47 FOUNDATION GEOLOGY CLARK HILL PROJECT SAVANNAH RIVER, GEORGIA - SOUTH CAROLINA	
U. S. C. E. DRAWING NUMBER	FIGURE 205-E
ORIGINAL DRAWING	DATE NOVEMBER, 1977

Figure A14. Detailed map of foundation geology, Blocks 44 to 47 (US Army Corps of Engineers, 1978).

APPENDIX B:

CATALOGUE OF HISTORIC EARTHQUAKES

(North Latitude: 32.0 to 35.0, West Longitude: 79.5 to 84.0)

From Habermann, 1989

Appendix B
J. STROM THURMOND EARTHQUAKE DATA

Source*	Date			Time			Location			Depth Km	Magnitude			Maximum Intensity
	Yr	Mo	Dy	Hr	Mn	Sec	Latitude	Longitude	Mb		Ms	Other [#]		
STO	1698	03	05				32.9	N	80.	W				III
STO	1754	05	19	16			32.9	N	80.	W				III
STO	1757	02	07				32.9	N	80.	W				III
STO	1766	11	23				32.9	N	80.	W				
STO	1799	04	04				32.9	N	80.	W				V
STO	1799	04	11	08	20		32.9	N	80.	W				V
STO	1799	04	11	19	55		32.9	N	80.	W				V
STO	1816	12	30				32.9	N	80.	W				
STO	1817	01	08	09			32.9	N	80.	W				V
USN	1826	10	15				32.	N	81.1	W				
STO	1826	10	15				32.	N	81.1	W				
STO	1843	02	07	15			32.9	N	80.	W				III
STO	1843	04	11				34.2	N	80.6	W				III
STO	1853	05	20				34.	N	81.2	W				VI
USN	1857	12	19	14	04		32.8	N	79.8	W				V
1**EQH	1857	12	19	14	04		32.9	N	80.	W				V
2**STO	1857	12	19	14	04		32.9	N	80.	W				V
STO	1860	01	19	23			32.9	N	80.	W				V
STO	1860	10					32.9	N	80.	W				III
STO	1860	10	22				34.2	N	82.	W				III
USN	1872	06	17	20			33.1	N	83.3	W				V
1**EQH	1872	06	17	20			33.1	N	83.3	W				V
2**STO	1872	06	17	20			33.1	N	83.3	W				V
USN	1875	07	28	21	05		33.1	N	83.3	W				
STO	1875	07	28	23	05		33.1	N	83.3	W				III
EQH	1875	11	02	02	55		33.8	N	82.5	W				VI
1**USN	1875	11	02	02	55		33.8	N	82.5	W				VI
2**STO	1875	11	02	02	55		33.8	N	82.5	W				VI
STO	1876	10					32.9	N	80.	W				III
STO	1876	12	12				32.9	N	80.	W				IV
STO	1877	10	09	01			35.	N	82.7	W				
STO	1879	10	27	01			34.4	N	81.1	W				III
USN	1879	12	13				35.	N	80.9	W				

(Continued)

- * See end of Appendix B for identification of sources.
 ** Indicates possible duplicate listing.
 # See end of Appendix B for magnitude type.

Source*	Date			Time			Location		Depth Km	Magnitude			Maximum Intensity
	Yr	Mo	Dy	Hr	Mn	Sec	Latitude	Longitude		Mb	Ms	Other	
USN	1879	12	13	07			35.	N 80.9	W				
USN	1884	03	31	10			33.8	N 82.5	W				II
1**STO	1884	03	31	10			33.1	N 83.3	W				III
USN	1885	10	17	22	30		33.	N 82.8	W				
1**STO	1885	10	17	22	30		33.	N 83.	W				IV
STO	1886	06					32.9	N 80.	W				III
STO	1886	08	27	06	30		32.9	N 80.	W				III
STO	1886	08	27	13	30		32.9	N 80.	W				V
STO	1886	08	28	06	30		32.9	N 80.	W				III
STO	1886	08	28	08	45		32.9	N 80.	W				VI
STO	1886	08	28	09	40		32.9	N 80.	W				IV
STO	1886	08	28	10	30		32.9	N 80.	W				II
STO	1886	08	28	18	20		32.9	N 80.	W				IV
STO	1886	08	28	19	57		32.9	N 80.	W				III
STO	1886	08	28	21	30		32.9	N 80.	W				II
STO	1886	08	29				32.9	N 80.	W				II
USN	1886	09	01	02	51		32.9	N 80.	W				X
1**STO	1886	09	01	02	51		32.9	N 80.	W				X
2**EQH	1886	09	01	02	51		32.9	N 80.	W				X
USN	1886	09	01	02	59		32.9	N 80.	W				
1**STO	1886	09	01	02	59		32.9	N 80.	W				
STO	1886	09	01	03	09		32.9	N 80.	W				
STO	1886	09	01	03	14		32.9	N 80.	W				III
STO	1886	09	01	03	30		32.9	N 80.	W				III
STO	1886	09	01	05	55		32.9	N 80.	W				III
STO	1886	09	01	06	05		32.9	N 80.	W				VI
STO	1886	09	01	07			32.9	N 80.	W				III
STO	1886	09	01	09			32.9	N 80.	W				III
STO	1886	09	01	13	25		32.9	N 80.	W				III
STO	1886	09	01	14			32.9	N 80.	W				III
STO	1886	09	01	14	59		32.9	N 80.	W				III
STO	1886	09	01	18			32.9	N 80.	W				III
STO	1886	09	01	22	15		32.9	N 80.	W				III
STO	1886	09	01	22	52		32.9	N 80.	W				II
STO	1886	09	02	01			32.9	N 80.	W				II
STO	1886	09	02	04	55		32.9	N 80.	W				V
STO	1886	09	03	04	53		32.9	N 80.	W				III
1**USN	1886	09	03	04	53		32.8	N 80.	W				
USN	1886	09	04	04	01		32.8	N 80.	W				
1**STO	1886	09	04	04	01		32.9	N 80.	W				VI

(Continued)

Source	Date			Time			Location			Depth Km	Magnitude			Maximum Intensity
	Yr	Mo	Dy	Hr	Mn	Sec	Latitude	Longitude	Mb		Ms	Other		
STO	1886	09	05	01	37		32.9	N	80.	W				
STO	1886	09	06	04	06		32.9	N	80.	W				VI
1**USN	1886	09	06	04	06		32.8	N	80.	W				
STO	1886	09	06	04	15		32.9	N	80.	W				III
STO	1886	09	06	12	30		32.9	N	80.	W				III
STO	1886	09	06	16	35		32.9	N	80.	W				IV
STO	1886	09	06	18	40		32.9	N	80.	W				II
STO	1886	09	07	04	15		32.9	N	80.	W				III
USN	1886	09	07	09	52		32.8	N	80.	W				
STO	1886	09	07	12			32.9	N	80.	W				II
STO	1886	09	07	14			32.9	N	80.	W				II
STO	1886	09	07	16	30		32.9	N	80.	W				II
STO	1886	09	07	21	52		32.9	N	80.	W				II
STO	1886	09	07	22			32.9	N	80.	W				II
USN	1886	09	08	17	55		32.8	N	80.	W				
1**STO	1886	09	08	17	55		32.9	N	80.	W				III
STO	1886	09	09	06	06		32.9	N	80.	W				III
1**USN	1886	09	09	06	06		32.8	N	80.	W				
STO	1886	09	10				32.9	N	80.	W				II
STO	1886	09	12				32.9	N	80.	W				II
STO	1886	09	13	14			32.9	N	80.	W				III
STO	1886	09	14				32.9	N	80.	W				III
STO	1886	09	15				32.9	N	80.	W				
STO	1886	09	17	06	29		32.9	N	80.	W				VI
STO	1886	09	20	05			32.9	N	80.	W				III
STO	1886	09	20	07			32.9	N	80.	W				III
STO	1886	09	21	09	25		32.9	N	80.	W				III
STO	1886	09	21	10	15		32.9	N	80.	W				VI
STO	1886	09	21	10	30		32.9	N	80.	W				V
STO	1886	09	21	21	15		32.9	N	80.	W				III
STO	1886	09	22				32.9	N	80.	W				II
USN	1886	09	27	07	02		32.8	N	80.	W				
STO	1886	09	27	19	02		32.9	N	80.	W				VI
STO	1886	09	27	22	02		32.9	N	80.	W				V
STO	1886	09	28	18			32.9	N	80.	W				III
USN	1886	09	28	18	06		32.8	N	80.	W				
STO	1886	09	30	19	20		32.9	N	80.	W				III
STO	1886	09	30	22	10		32.9	N	80.	W				III
STO	1886	10	09	03	40		32.9	N	80.	W				IV
STO	1886	10	09	05	40		32.9	N	80.	W				IV

(Continued)

Source	Date			Time			Location			Depth Km	Magnitude			Maximum Intensity
	Yr	Mo	Dy	Hr	Mn	Sec	Latitude	Longitude	Mb		Ms	Other		
STO	1886	10	09	06	48		32.9	N	80.	W				VI
STO	1886	10	09	18	46		32.9	N	80.	W				III
STO	1886	10	15	09			32.9	N	80.	W				III
STO	1886	10	15	12	40		32.9	N	80.	W				III
STO	1886	10	22	06			32.9	N	80.	W				III
STO	1886	10	22	07	20		32.9	N	80.	W				II
USN	1886	10	22	10			32.9	N	80.	W				VI
EQH	1886	10	22	10	20		32.9	N	80.	W				VI
1**STO	1886	10	22	10	20		32.9	N	80.	W				VI
STO	1886	10	22	19	45		32.9	N	80.	W				VII
1**USN	1886	10	22	19	45		32.9	N	80.	W				VII
2**EQH	1886	10	22	19	45		32.9	N	80.	W				VII
STO	1886	10	23	01	07		32.9	N	80.	W				IV
STO	1886	10	23	04	54		32.9	N	80.	W				III
STO	1886	10	30	08	40		32.9	N	80.	W				III
STO	1886	10	31	19	21		32.9	N	80.	W				III
STO	1886	10	31	21	46		32.9	N	80.	W				III
USN	1886	11	05				32.9	N	80.	W				
1**EQH	1886	11	05	17	20		32.9	N	80.	W				VI
2**STO	1886	11	05	17	20		32.9	N	80.	W				VI
STO	1886	11	07	19			32.9	N	80.	W				III
STO	1886	11	17				32.9	N	80.	W				II
STO	1886	11	28	15	10		32.9	N	80.	W				II
STO	1886	11	28	20	13		32.9	N	80.	W				IV
STO	1886	12	01				32.9	N	80.	W				III
STO	1886	12	02	06	36		32.9	N	80.	W				III
STO	1886	12	02	13			32.9	N	80.	W				III
STO	1886	12	06				32.9	N	80.	W				III
STO	1887	01	03	06	20		32.9	N	80.	W				III
STO	1887	01	04	11	44		32.9	N	80.	W				VI
STO	1887	01	04	12	40		32.9	N	80.	W				II
STO	1887	01	05	13			32.9	N	80.	W				III
STO	1887	01	11	00	57		32.9	N	80.	W				III
STO	1887	02	26	11			32.9	N	80.	W				III
STO	1887	03	04	07			32.9	N	80.	W				IV
STO	1887	03	17	14	09		32.9	N	80.	W				V
STO	1887	03	18	23	10		32.9	N	80.	W				IV
STO	1887	03	19				32.9	N	80.	W				IV
STO	1887	03	20				32.9	N	80.	W				III
STO	1887	03	22				32.9	N	80.	W				III

(Continued)

Source	Date			Time			Location		Depth Km	Magnitude			Maximum Intensity
	Yr	Mo	Dy	Hr	Mn	Sec	Latitude	Longitude		Mb	Ms	Other	
STO	1887	03	24				32.9	N 80.	W				IV
STO	1887	03	24	04	05		32.9	N 80.	W				IV
STO	1887	03	24	10			32.9	N 80.	W				II
STO	1887	03	27	18			32.9	N 80.	W				II
STO	1887	03	28				32.9	N 80.	W				IV
1**STO	1887	03	28				32.9	N 80.	W				II
STO	1887	03	30				32.9	N 80.	W				III
STO	1887	03	31				32.9	N 80.	W				III
STO	1887	04	05	11			32.9	N 80.	W				III
STO	1887	04	07	04			32.9	N 80.	W				IV
STO	1887	04	08	09			32.9	N 80.	W				IV
STO	1887	04	09	12			32.9	N 80.	W				II
STO	1887	04	10	11	30		32.9	N 80.	W				IV
STO	1887	04	14	07	25		32.9	N 80.	W				IV
STO	1887	04	14	12			32.9	N 80.	W				III
STO	1887	04	16	12			32.9	N 80.	W				III
STO	1887	04	18	05			32.9	N 80.	W				III
STO	1887	04	19				32.9	N 80.	W				II
STO	1887	04	23				32.9	N 80.	W				III
STO	1887	04	24	06			32.9	N 80.	W				III
STO	1887	04	24	07			32.9	N 80.	W				II
STO	1887	04	26	02			32.9	N 80.	W				II
STO	1887	04	26	04	30		32.9	N 80.	W				III
STO	1887	04	26	10			32.9	N 80.	W				IV
STO	1887	04	26	11	30		32.9	N 80.	W				II
STO	1887	04	28	08			32.9	N 80.	W				V
STO	1887	04	28	09			32.9	N 80.	W				III
STO	1887	04	30	03	10		32.9	N 80.	W				III
STO	1887	04	30	23	45		32.9	N 80.	W				III
STO	1887	05	06				32.9	N 80.	W				IV
STO	1887	05	12	03	30		32.9	N 80.	W				III
STO	1887	05	12	05			32.9	N 80.	W				III
STO	1887	05	14				32.9	N 80.	W				III
STO	1887	05	14	07	25		32.9	N 80.	W				
STO	1887	05	16	12			32.9	N 80.	W				III
STO	1887	05	17				32.9	N 80.	W				II
STO	1887	06	03	12			32.9	N 80.	W				IV
STO	1887	06	06				32.9	N 80.	W				III
1**STO	1887	06	06				32.9	N 80.	W				II
STO	1887	07	10	18			32.9	N 80.	W				IV

(Continued)

Source	Date			Time			Location			Depth Km	Magnitude			Maximum Intensity
	Yr	Mo	Dy	Hr	Mn	Sec	Latitude	Longitude	Mb		Ms	Other		
STO	1887	08	27	04	30		32.9	N	80.	W				V
STO	1887	08	27	09	20		32.9	N	80.	W				IV
STO	1887	08	28	03	30		32.9	N	80.	W				III
STO	1888	01	12	14	50		32.9	N	80.	W				III
STO	1888	01	12	15	54		32.9	N	80.	W				VI
STO	1888	01	15	23	40		32.9	N	80.	W				III
STO	1888	01	16	17	52		32.9	N	80.	W				IV
STO	1888	02	02				32.9	N	80.	W				II
STO	1888	02	02	03			32.9	N	80.	W				III
STO	1888	02	12				32.9	N	80.	W				III
STO	1888	02	29	11			32.9	N	80.	W				V
STO	1888	03	03				32.9	N	80.	W				IV
STO	1888	03	03	04	30		32.9	N	80.	W				IV
STO	1888	03	04				32.9	N	80.	W				IV
STO	1888	03	14	05			32.9	N	80.	W				V
STO	1888	03	20	05			32.9	N	80.	W				IV
STO	1888	03	25				32.9	N	80.	W				IV
STO	1888	04	16				32.9	N	80.	W				IV
STO	1888	04	16	16			32.9	N	80.	W				III
STO	1888	04	20				32.9	N	80.	W				III
STO	1888	04	20	03			32.9	N	80.	W				III
STO	1888	05	02				32.9	N	80.	W				IV
STO	1889	02	10	00	31		32.9	N	80.	W				IV
STO	1889	07	12	02	54		32.9	N	80.	W				IV
STO	1889	08	29	02			32.9	N	80.	W				III
STO	1890	01	15	11	42		32.9	N	80.	W				III
STO	1891	06	24	04	29		32.9	N	80.	W				II
STO	1891	10	13	05	55		32.9	N	80.	W				IV
STO	1891	12	05	22	10		32.9	N	80.	W				III
STO	1892	11	03	17	25		32.9	N	80.	W				III
STO	1892	11	04	04	45		32.9	N	80.	W				III
STO	1892	11	04	08	09		32.9	N	80.	W				III
STO	1892	11	04	11	20		32.9	N	80.	W				II
STO	1892	11	06	07	53		32.9	N	80.	W				III
STO	1892	11	08	08	03		32.9	N	80.	W				III
STO	1892	11	08	12	25		32.9	N	80.	W				III
STO	1892	11	09	21	20		32.9	N	80.	W				II
STO	1892	11	10	04	02		32.9	N	80.	W				III
STO	1892	11	10	11	58		32.9	N	80.	W				III
STO	1892	11	10	22	03		32.9	N	80.	W				II

(Continued)

Source	Date			Time			Location			Depth Km	Magnitude			Maximum Intensity
	Yr	Mo	Dy	Hr	Mn	Sec	Latitude	Longitude	Mb		Ms	Other		
STO	1892	11	11	04	47		32.9	N	80.	W				III
STO	1892	11	11	05	34		32.9	N	80.	W				II
STO	1892	11	11	07	47		32.9	N	80.	W				II
STO	1892	11	12	04	02		32.9	N	80.	W				II
STO	1892	11	23	06	20		32.9	N	80.	W				II
STO	1892	12	22	07	05		32.9	N	80.	W				II
STO	1892	12	22	11	02		32.9	N	80.	W				II
STO	1893	02	14	00	17		32.9	N	80.	W				II
STO	1893	02	14	06	14		32.9	N	80.	W				II
STO	1893	03	02	09	03		32.9	N	80.	W				II
STO	1893	03	02	16	04		32.9	N	80.	W				II
STO	1893	03	03	10	30		32.9	N	80.	W				II
STO	1893	03	03	11	27		32.9	N	80.	W				II
STO	1893	03	08	03	57		32.9	N	80.	W				II
STO	1893	06	21	04	05		32.9	N	80.	W				V
STO	1893	06	21	09	12		32.9	N	80.	W				III
STO	1893	06	21	09	48		32.9	N	80.	W				III
STO	1893	06	24	00	22		32.9	N	80.	W				III
STO	1893	06	24	06	35		32.9	N	80.	W				II
STO	1893	06	27	14	31		32.9	N	80.	W				II
STO	1893	06	29	05	24		32.9	N	80.	W				II
STO	1893	07	03	16	55		32.9	N	80.	W				II
STO	1893	07	03	19	20		32.9	N	80.	W				II
STO	1893	07	04	02	50		32.9	N	80.	W				II
STO	1893	07	04	08	45		32.9	N	80.	W				II
STO	1893	07	05	04	20		32.9	N	80.	W				II
STO	1893	07	05	08	10		32.9	N	80.	W				IV
STO	1893	07	06	03	20		32.9	N	80.	W				II
STO	1893	07	06	05	25		32.9	N	80.	W				II
STO	1893	07	06	09	05		32.9	N	80.	W				IV
STO	1893	07	07	12	15		32.9	N	80.	W				II
STO	1893	07	08	04	50		32.9	N	80.	W				II
STO	1893	07	08	07	48		32.9	N	80.	W				IV
STO	1893	07	08	15	25		32.9	N	80.	W				IV
STO	1893	07	08	15	59		32.9	N	80.	W				II
STO	1893	07	09	05	10		32.9	N	80.	W				II
STO	1893	07	09	08			32.9	N	80.	W				II
STO	1893	07	11	03	12		32.9	N	80.	W				II
STO	1893	07	12	02	10		32.9	N	80.	W				II

(Continued)

Source	Date			Time			Location			Depth Km	Magnitude			Maximum Intensity
	Yr	Mo	Dy	Hr	Mn	Sec	Latitude	Longitude	Mb		Ms	Other		
STO	1893	07	23	04	15		32.9	N	80.	W				II
STO	1893	07	25	07	54		32.9	N	80.	W				II
STO	1893	08	03	02	05		32.9	N	80.	W				II
STO	1893	08	10	04			32.9	N	80.	W				II
STO	1893	08	14	04	10		32.9	N	80.	W				II
STO	1893	08	17	06	25		32.9	N	80.	W				II
STO	1893	09	06	05	10		32.9	N	80.	W				II
STO	1893	09	19	05	25		32.9	N	80.	W				II
STO	1893	09	19	07	05		32.9	N	80.	W				IV
STO	1893	09	19	07	40		32.9	N	80.	W				IV
STO	1893	09	19	08	55		32.9	N	80.	W				IV
STO	1893	09	21	05	40		32.9	N	80.	W				III
STO	1893	09	21	07	25		32.9	N	80.	W				III
STO	1893	09	22	01	40		32.9	N	80.	W				II
STO	1893	09	25	03	20		32.9	N	80.	W				II
STO	1893	09	25	04	25		32.9	N	80.	W				II
STO	1893	09	25	09	30		32.9	N	80.	W				II
STO	1893	09	27	01	25		32.9	N	80.	W				II
STO	1893	09	30	02	10		32.9	N	80.	W				II
STO	1893	09	30	09	05		32.9	N	80.	W				III
STO	1893	10	01	01	50		32.9	N	80.	W				III
STO	1893	10	02	01	58		32.9	N	80.	W				II
STO	1893	10	02	03	15		32.9	N	80.	W				II
STO	1893	10	02	03	35		32.9	N	80.	W				II
STO	1893	10	08	04	28		32.9	N	80.	W				II
STO	1893	10	10	01	35		32.9	N	80.	W				III
STO	1893	10	17	01	40		32.9	N	80.	W				II
STO	1893	10	24	03	20		32.9	N	80.	W				III
STO	1893	10	25				32.9	N	80.	W				II
STO	1893	11	08	04	40		32.9	N	80.	W				IV
STO	1893	11	08	06	05		32.9	N	80.	W				IV
STO	1893	12	03	16	35		32.9	N	80.	W				III
STO	1893	12	27	06	51		32.9	N	80.	W				IV
STO	1893	12	27	07	17		32.9	N	80.	W				IV
STO	1893	12	27	09	09		32.9	N	80.	W				IV
STO	1893	12	27	09	56		32.9	N	80.	W				IV
STO	1893	12	28	02	20		32.9	N	80.	W				IV
STO	1893	12	29	03	46		32.9	N	80.	W				III
STO	1893	12	30				32.9	N	80.	W				II
STO	1893	12	31				32.9	N	80.	W				II

(Continued)

Source	Date			Time			Location			Depth Km	Magnitude			Maximum Intensity
	Yr	Mo	Dy	Hr	Mn	Sec	Latitude	Longitude	Mb		Ms	Other		
STO	1894	01	10				32.9	N	80.	W				II
STO	1894	01	10	08	05		32.9	N	80.	W				IV
STO	1894	01	10	08	49		32.9	N	80.	W				IV
STO	1894	01	10	09	15		32.9	N	80.	W				IV
STO	1894	01	18	06	45		32.9	N	80.	W				III
STO	1894	01	30	04	05		32.9	N	80.	W				IV
STO	1894	02	01	05	21		32.9	N	80.	W				IV
STO	1894	02	14	05	40		32.9	N	80.	W				III
STO	1894	03	05	04	15		32.9	N	80.	W				II
STO	1894	03	14	03	25		32.9	N	80.	W				II
STO	1894	03	16	19	50		32.9	N	80.	W				III
STO	1894	04	15	08	20		32.9	N	80.	W				II
STO	1894	05	26	08	15		32.9	N	80.	W				II
STO	1894	06	06	11	05		32.9	N	80.	W				III
STO	1894	06	09	10	55		32.9	N	80.	W				III
STO	1894	06	16	01	52		32.9	N	80.	W				III
STO	1894	06	16	02	16		32.9	N	80.	W				IV
STO	1894	08	11	05	10		32.9	N	80.	W				III
STO	1894	08	11	17	20		32.9	N	80.	W				III
STO	1894	08	14	03	45		32.9	N	80.	W				III
STO	1894	08	16	05	06		32.9	N	80.	W				II
STO	1894	08	19	04	23		32.9	N	80.	W				III
STO	1894	08	19	04	46		32.9	N	80.	W				III
STO	1894	08	20	07	40		32.9	N	80.	W				III
STO	1894	09	07	04	05		32.9	N	80.	W				II
STO	1894	09	10	07	33		32.9	N	80.	W				II
STO	1894	09	12	05	10		32.9	N	80.	W				II
STO	1894	09	12	05	25		32.9	N	80.	W				II
STO	1894	10	27	07	10		32.9	N	80.	W				III
STO	1894	12	11	05	27		32.9	N	80.	W				IV
STO	1894	12	20	09	40		32.9	N	80.	W				III
STO	1894	12	20	10	50		32.9	N	80.	W				III
STO	1894	12	29	07	59		32.9	N	80.	W				III
STO	1895	01	08	05	40		32.9	N	80.	W				IV
STO	1895	01	08	05	58		32.9	N	80.	W				IV
STO	1895	01	08	07	29		32.9	N	80.	W				IV
STO	1895	01	10	08	08		32.9	N	80.	W				III
STO	1895	02	07	12	53		32.9	N	80.	W				III
STO	1895	04	07				32.9	N	80.	W				III
STO	1895	04	27	07	40		32.9	N	80.	W				IV

(Continued)

<u>Source</u>	<u>Date</u>			<u>Time</u>			<u>Location</u>			<u>Depth</u> <u>Km</u>	<u>Magnitude</u>			<u>Maximum</u> <u>Intensity</u>
	<u>Yr</u>	<u>Mo</u>	<u>Dy</u>	<u>Hr</u>	<u>Mn</u>	<u>Sec</u>	<u>Latitude</u>		<u>Longitude</u>		<u>Mb</u>	<u>Ms</u>	<u>Other</u>	
STO	1895	05	06	08	50		32.9	N	80. W					III
STO	1895	07	25	04	01		32.9	N	80. W					IV
STO	1895	07	25	06	08		32.9	N	80. W					II
STO	1895	08	23	06	43		32.9	N	80. W					III
STO	1895	10	06	06	25		32.9	N	80. W					IV
STO	1895	10	20	17	08		32.9	N	80. W					IV
STO	1895	10	31	11	14		32.9	N	80. W					III
STO	1895	11	06	05	10		32.9	N	80. W					III
STO	1895	11	12	23	33		32.9	N	80. W					IV
STO	1895	11	13	03	11		32.9	N	80. W					III
STO	1895	12	03	05	26		32.9	N	80. W					III
STO	1895	12	26	06	46		32.9	N	80. W					III
STO	1896	02	10	04	18		32.9	N	80. W					II
STO	1896	03	01	07	50		32.9	N	80. W					III
STO	1896	03	03	01	45		32.9	N	80. W					II
STO	1896	03	19	08	22		32.9	N	80. W					IV
STO	1896	05	21	06	05		32.9	N	80. W					II
STO	1896	05	31	08	09		32.9	N	80. W					III
STO	1896	06	01	09	51		32.9	N	80. W					II
STO	1896	06	23	05	51		32.9	N	80. W					II
STO	1896	06	29	06	49		32.9	N	80. W					III
STO	1896	06	30	05	12		32.9	N	80. W					III
STO	1896	08	07	05	56		32.9	N	80. W					II
STO	1896	08	07	07	45		32.9	N	80. W					II
STO	1896	08	07	09	02		32.9	N	80. W					II
STO	1896	08	11	05	58		32.9	N	80. W					IV
STO	1896	08	11	06	14		32.9	N	80. W					IV
STO	1896	08	11	08	15		32.9	N	80. W					IV
STO	1896	08	11	09	24		32.9	N	80. W					IV
STO	1896	08	12	07	42		32.9	N	80. W					IV
STO	1896	08	13	03	25		32.9	N	80. W					III
STO	1896	08	14	05	43		32.9	N	80. W					IV
STO	1896	08	15	08	16		32.9	N	80. W					III
STO	1896	08	16	08	20		32.9	N	80. W					III
STO	1896	08	17	05	45		32.9	N	80. W					III
STO	1896	08	30	03	24		32.9	N	80. W					IV
STO	1896	09	08	13	31		32.9	N	80. W					III
STO	1896	09	08	18	16		32.9	N	80. W					IV
STO	1896	09	11	01	50		32.9	N	80. W					II
STO	1896	09	11	05	11		32.9	N	80. W					II

(Continued)

Source	Date			Time			Location			Depth Km	Magnitude			Maximum Intensity
	Yr	Mo	Dy	Hr	Mn	Sec	Latitude	Longitude	Mb		Ms	Other		
STO	1896	09	13	05	20		32.9	N	80.	W				III
STO	1896	11	14	08	15		32.9	N	80.	W				IV
STO	1897	02	01	12	05		32.9	N	80.	W				II
STO	1897	03	17	03	48		32.9	N	80.	W				III
STO	1897	03	30	05	20		32.9	N	80.	W				III
STO	1897	05	06	21	15		33.3	N	81.2	W				
STO	1897	05	09				33.9	N	81.6	W				III
STO	1897	05	24	21	15		33.3	N	81.2	W				
STO	1897	05	27	19			33.3	N	81.2	W				
STO	1897	06	01	05	25		32.9	N	80.	W				II
STO	1897	07	10	12	45		32.9	N	80.	W				II
							32.9	N	80.	W				III
STO	1898	09	23	14	15		32.9	N	80.	W				III
STO	1899	01	20				34.2	N	81.7	W				III
STO	1899	03	10	05	45		32.9	N	80.	W				IV
STO	1899	03	16	13	45		32.9	N	80.	W				III
STO	1899	05	05	10	43		32.9	N	80.	W				III
STO	1899	05	18	09	30		32.9	N	80.	W				II
STO	1899	11	04				34.3	N	82.8	W				III
STO	1899	12	04	12	48		32.9	N	80.	W				IV
STO	1899	12	19				34.3	N	81.4	W				III
STO	1900	01	14	10			32.9	N	80.	W				III
STO	1900	05	10	23	20		32.9	N	80.	W				III
STO	1900	08	11	00	50		32.9	N	80.	W				III
STO	1900	09	04	11	05		32.9	N	80.	W				III
STO	1900	09	24	19	36		32.9	N	80.	W				III
STO	1901	01					32.9	N	80.	W				III
STO	1901	09	05	06	38		32.9	N	80.	W				II
STO	1901	09	14	13	26		32.9	N	80.	W				II
STO	1901	09	16	17	06		32.9	N	80.	W				II
STO	1901	09	17	13	35		32.9	N	80.	W				II
STO	1901	09	29	01	25		32.9	N	80.	W				II
STO	1901	10	01	16	40		34.2	N	81.7	W				
STO	1901	12	02	00	26		32.9	N	80.	W				IV
STO	1902	01	22	15	11		32.9	N	80.	W				II
STO	1902	02	05	04	25		32.9	N	80.	W				II
STO	1902	03	18	01	45		32.9	N	80.	W				II
STO	1902	03	26	09	20		32.9	N	80.	W				II
STO	1902	05	16	03	30		32.9	N	80.	W				III
STO	1902	05	24	14	05		32.9	N	80.	W				III

(Continued)

Source	Date			Time			Location				Depth Km	Magnitude			Maximum Intensity
	Yr	Mo	Dy	Hr	Mn	Sec	Latitude	Longitude	Mb	Ms		Other			
STO	1902	06	10				34.2	N	81.7	W				III	
STO	1902	09	28	20	04		32.9	N	80.	W				II	
STO	1902	11	20				32.9	N	80.	W				II	
STO	1903	01	24	01			32.9	N	80.	W				IV	
STO	1903	01	24	01	15		32.1	N	81.1	W				VI	
1**EQH	1903	01	24	01	15		32.1	N	81.1	W				VI	
2**USN	1903	01	24	01	15		32.1	N	81.1	W				VI	
STO	1903	01	29	12	15		32.9	N	80.	W				III	
STO	1903	01	31	10	54		32.9	N	80.	W				IV	
STO	1903	02	03	10	06		32.9	N	80.	W				IV	
STO	1903	05	09	10	49		32.9	N	80.	W				III	
STO	1903	06	17	03	49		32.9	N	80.	W				II	
STO	1903	08	25	14	56		32.9	N	80.	W				III	
STO	1903	12	24	19	35		32.9	N	80.	W				II	
STO	1904	03	06	01	40		32.9	N	80.	W				II	
STO	1904	03	14	03	30		34.5	N	82.	W					
STO	1904	03	16				32.9	N	80.	W				II	
STO	1904	04	30				34.	N	81.6	W					
STO	1904	06	19	14	15		32.9	N	80.	W				II	
STO	1904	06	22	23			32.9	N	80.	W				II	
STO	1904	09	05	14	53		32.9	N	80.	W				III	
STO	1904	09	10	14	27		32.9	N	80.	W				II	
STO	1904	09	24	19	36		32.9	N	80.	W					
STO	1904	10	01	08	45		32.9	N	80.	W				II	
STO	1904	11	15	16	47		32.9	N	80.	W				II	
STO	1904	12	06	22	48		32.9	N	80.	W				II	
STO	1905	03	05	14	15		32.9	N	80.	W				III	
STO	1905	06	04				32.9	N	80.	W				III	
STO	1905	07	23	07	15		32.9	N	80.	W				II	
STO	1905	07	23	07	25		32.9	N	80.	W				II	
STO	1905	10	11	18	45		32.9	N	80.	W				III	
STO	1905	10	16	07	10		32.9	N	80.	W				II	
STO	1905	12	28	03	15		32.9	N	80.	W				II	
STO	1906	04	18				34.1	N	81.3	W					
USN	1906	08	05	06	20		33.	N	80.2	W					
1**STO	1906	08	05	06	20		32.9	N	80.	W				III	
USN	1907	04	19	08	30		32.9	N	80.	W				V	
1**STO	1907	04	19	08	30		32.9	N	80.	W				V	
2**EQH	1907	04	19	08	30		32.9	N	80.	W				V	
STO	1908	01	15	19			32.9	N	80.	W				III	

(Continued)

Source	Date			Time			Location		Depth Km	Magnitude			Maximum Intensity
	Yr	Mo	Dy	Hr	Mn	Sec	Latitude	Longitude		Mb	Ms	Other	
1**USN	1908	01	15	19			33.	N 80.2	W				III
2**STO	1908	01	15	19	01		32.9	N 80.	W				II
USN	1908	03	03	21	06		33.	N 80.2	W				III
1**STO	1908	03	03	21	06		32.9	N 80.	W				II
USN	1908	03	07	06	50		33.	N 0.2	W				III
1**STO	1908	03	07	06	50		32.9	N 80.	W				II
STO	1908	10	26	04	10		32.9	N 80.	W				III
1**USN	1908	10	26	04	10		33.	N 80.2	W				II
USN	1908	10	28	11	24		33.	N 80.2	W				III
STO	1908	12	28	11	24		32.9	N 80.	W				II
STO	1909	02	26	04			32.9	N 80.	W				III
STO	1909	08	21	13	36		32.9	N 80.	W				III
STO	1909	12	14	23			32.9	N 80.	W				III
STO	1910	05	02	09	15		32.9	N 80.	W				III
STO	1910	09	02	07	18		32.9	N 80.	W				III
STO	1910	09	12	18	29		32.9	N 80.	W				III
STO	1911	11	24	12	17		32.9	N 80.	W				II
STO	1912	03	31	20	25		32.9	N 80.	W				III
STO	1912	06	12	10	30		32.9	N 80.	W				VII
1**USN	1912	06	12	10	30		32.9	N 80.	W				VII
2**EQH	1912	06	12	10	30		33.	N 80.2	W				VII
USN	1912	06	20				32.	N 81.	W				V
1**STO	1912	06	20				32.	N 81.	W				V
STO	1912	06	29				32.9	N 80.	W				III
STO	1912	08	30	16	52		32.9	N 80.	W				II
STO	1912	09	29	08	06		32.9	N 80.	W				IV
STO	1912	10	23	01	15		32.7	N 83.5	W				IV
1**USN	1912	10	23	01	15		32.7	N 83.5	W				III
STO	1912	11	17	12	30		32.9	N 80.	W				IV
STO	1912	11	26	03	32		32.9	N 80.	W				II
USN	1912	12	07				34.7	N 81.7	W				III
STO	1912	12	07	19	10		34.7	N 81.7	W				IV
STO	1912	12	15	16	54		32.9	N 80.	W				II
USN	1913	01	01	18	28		34.7	N 81.7	W				VIII
1**EQH	1913	01	01	18	28		34.7	N 81.7	W				VII
2**STO	1913	01	01	18	28		34.7	N 81.7	W				VII
STO	1913	01	26	00	37		32.9	N 80.	W				II
STO	1913	02	05	21	06		32.9	N 80.	W				II
STO	1913	03	09	16	30		32.9	N 80.	W				III
STO	1913	06	06	18	20		32.9	N 80.	W				II

(Continued)

Source	Date			Time			Location		Depth Km	Magnitude			Maximum Intensity
	Yr	Mo	Dy	Hr	Mn	Sec	Latitude	Longitude		Mb	Ms	Other	
EQH	1914	03	05	20	05		33.5	N 83.5	W				VI
1**STO	1914	03	05	20	05		33.5	N 83.5	W				VI
2**USN	1914	03	05	20	05		33.5	N 83.5	W				VI
STO	1914	03	05	21			33.5	N 83.5	W				
STO	1914	03	06	20	30		34.7	N 81.2	W				III
STO	1914	03	07	01	20		34.2	N 79.8	W				IV
1**USN	1914	03	07	01	20		34.2	N 79.8	W				III
STO	1914	06	01	04	03		32.8	N 80.6	W				III
1**USN	1914	06	01	04	03		32.9	N 80.3	W				II
USN	1914	06	19	08	13		3.	N 80.2	W				II
1**STO	1914	06	19	08	13		32.9	N 80.	W				III
STO	1914	07	14	01	53		32.9	N 80.	W				IV
1**USN	1914	07	14	01	53		33.	N 80.2	W				II
USN	1914	07	14	08			33.	N 80.2	W				I
1**STO	1914	07	14	08			32.9	N 80.	W				II
STO	1914	09	22	07	04		32.9	N 80.	W				V
1**USN	1914	09	22	07	04		33.	N 80.3	W				V
2**EQH	1914	09	22	07	04		33.	N 80.2	W				V
STO	1914	12	23	11	55		32.9	N 80.	W				II
1**USN	1914	12	23	11	55		33.	N 80.2	W				I
STO	1915	12	13	00	55		32.9	N 80.	W				III
1**USN	1915	12	13	00	55		32.8	N 79.9	W				III
STO	1915	12	20	00	55		32.9	N 80.	W				III
STO	1916	03	02	05	02		34.5	N 82.7	W				IV
1**USN	1916	03	02	05	02		34.5	N 82.7	W				IV
STO	1916	04	16	11	56		32.9	N 80.	W				II
1**USN	1916	04	16	11	56		33.	N 80.2	W				I
USN	1916	04	30	06	45		33.	N 80.2	W				I
1**STO	1916	04	30	06	45		32.9	N 80.	W				III
STO	1916	06	25	12	05		32.9	N 80.	W				III
1**USN	1916	06	25	12	05		33.1	N 80.2	W				II
STO	1916	07	14	18	18		32.9	N 80.	W				II
1**USN	1916	07	14	18	18		33.1	N 80.2	W				
USN	1916	09	24	09	42		33.	N 80.2	W				I
1**STO	1916	09	24	09	42		32.9	N 80.	W				II
STO	1917	04	11	19	01		32.9	N 80.	W				II
1**USN	1917	04	11	19	01		33.	N 80.2	W				I
USN	1920	07	01	11	53		33.	N 80.2	W				II
STO	1920	08	01	11	53		32.9	N 80.	W				II
STO	1921	04	19	23	45		32.9	N 80.	W				III

(Continued)

Source	Date			Time			Location		Depth Km	Magnitude			Maximum Intensity
	Yr	Mo	Dy	Hr	Mn	Sec	Latitude	Longitude		Mb	Ms	Other	
USN	1921	04	23	23	48		33.	N 80.2	W				
1**STO	1921	04	23	23	48		32.9	N 80.	W				III
USN	1922	08	08	09	25		33.	N 80.2	W				II
1**STO	1922	08	08	09	25		32.9	N 80.	W				II
STO	1923	03	24	04	25		32.9	N 80.	W				III
USN	1923	05	04	10	55		34.2	N 82.5	W				II
1**STO	1923	05	04	10	55		34.3	N 82.4	W				II
STO	1924	01	01	01	06		34.8	N 82.5	W				IV
STO	1924	02	14	16	06		32.9	N 80.	W				III
STO	1924	06	03	15	43		32.9	N 80.	W				III
STO	1924	09	26	09	49		32.9	N 80.	W				
EQH	1924	10	20	08	30		35.	N 82.6	W				V
1**USN	1924	10	20	08	30		35.	N 82.6	W				V
2**STO	1924	10	20	08	30		35.	N 82.6	W				V
USN	1924	10	20	20	30		35.	N 82.6	W				V
STO	1928	12	19	22	17		32.9	N 80.	W				II
USN	1929	01	03	12	05		33.9	N 80.3	W				
1**STO	1929	01	03	12	05		33.9	N 80.3	W				IV
2**USE	1929	01	03	12	05		33.9	N 80.3	W				
USN	1929	10	28	02	15		34.3	N 82.4	W				
1**USE	1929	10	28	02	15		34.3	N 82.4	W				
2**STO	1929	10	28	02	15		34.3	N 82.4	W				IV
USN	1930	09	03	01	30		33.	N 80.2	W				
1**USE	1930	09	03	01	30		33.	N 80.2	W				
2**STO	1930	09	03	01	30		32.9	N 80.	W				II
USN	1930	12	10	00	02		34.3	N 82.4	W				
1**USE	1930	12	10	00	02		34.3	N 82.4	W				
2**STO	1930	12	10	00	02		34.3	N 82.4	W				IV
STO	1930	12	10	08			34.3	N 82.4	W				II
STO	1930	12	26	03			34.5	N 80.3	W				IV
1**USN	1930	12	26	03			34.5	N 80.3	W				IV
STO	1931	05	06	12	18		34.3	N 82.4	W				IV
USN	1932	01	06	12	35		33.	N 80.2	W				
1**STO	1932	01	06	12	35		32.9	N 80.	W				II
USN	1932	01	13	12	40		33.	N 80.2	W				
1**STO	1932	01	13	12	40		32.9	N 80.	W				II
STO	1933	06	09	11	30		33.3	N 83.5	W				IV
STO	1933	07	26	02	34		32.9	N 80.	W				III
1**USN	1933	07	26	02	34		33.	N 80.2	W				III
STO	1933	12	19	14	12		32.9	N 80.	W				IV

(Continued)

Source	Date			Time			Location		Depth Km	Magnitude			Maximum Intensity
	Yr	Mo	Dy	Hr	Mn	Sec	Latitude	Longitude		Mb	Ms	Other	
1**USN	1933	12	19	14	12		33.	N 80.2 W					IV
STO	1933	12	23	09	40		32.9	N 80. W					V
1**USN	1933	12	23	09	40		33.	N 80.2 W					
STO	1933	12	23	09	55		32.9	N 80. W					IV
STO	1934	12	09	09			32.9	N 80. W					IV
USN	1935	02	06	12	36		33.	N 80.2 W					
1**STO	1935	02	06	12	36		32.9	N 80. W					III
USN	1935	10	20	16	20		33.	N 80.2 W					
1**STO	1935	10	20	16	20		32.9	N 80. W					III
STO	1936	12	30	03	50		32.9	N 80. W					II
1**USN	1936	12	30	03	50		33.	N 80.2 W					
USN	1937	10	25	19	01		33.	N 80.2 W					
1**STO	1937	10	25	19	01		32.9	N 80. W					II
USN	1938	08	05	00	14		32.8	N 80. W					
1**STO	1938	08	05	00	14		32.9	N 80. W					II
STO	1940	01	05	08	46		32.9	N 80. W					III
STO	1940	01	05	13	45		32.9	N 80. W					III
1**USN	1940	01	05	13	45		33.	N 80.2 W					
USN	1940	10	08	01	20		33.	N 80.2 W					
STO	1940	10	08	03	20		32.9	N 80. W					II
STO	1940	12	27	09	32		32.9	N 80. W					II
1**USN	1940	12	27	09	32		33.	N 80.2 W					
USN	1942	11	01	01	20		34.4	N 81.1 W					
STO	1942	11	01	02	20		34.4	N 81.1 W					II
STO	1943	07	29	03	30		33.4	N 82. W					III
USN	1943	12	28	13	25		33.	N 80.2 W					
STO	1943	12	28	14	25		32.9	N 80. W					IV
USN	1944	01	28	16	30		33.	N 80.2 W					
STO	1944	01	28	17	30		32.9	N 80. W					IV
USN	1945	01	30	19	20		33.	N 80.2 W					
STO	1945	01	30	20	20		32.9	N 80. W					IV
USN	1945	05	18	11	20		32.8	N 80. W					
USN	1945	05	18	11	40		32.8	N 80. W					
STO	1945	05	18	12	20		32.9	N 80. W					III
STO	1945	05	18	12	40		32.9	N 80. W					III
STO	1945	06	05	12	10		32.9	N 80. W					II
USN	1945	07	26	09	32	18	34.3	N 81.4 W					IV
STO	1945	07	26	10	32	16	33.75	N 81.38 W	5	4.4		LG	VI
USN	1946	02	08	18	09		33.	N 80.2 W					
1**STO	1946	02	08	18	09		32.9	N 80. W					III

(Continued)

Source	Date			Time			Location		Depth Km	Magnitude			Maximum Intensity
	Yr	Mo	Dy	Hr	Mn	Sec	Latitude	Longitude		Mb	Ms	Other	
USN	1947	11	02	04	30		33.	N 80.2	W				
1**STO	1947	11	02	04	30		32.9	N 80.	W				IV
USN	1949	02	02	10	52		33.	N 0.2	W				
1**STO	1949	02	02	10	52		32.9	N 80.	W				IV
USN	1949	06	27	06	53		33.	N 80.2	W				
1**STO	1949	06	27	06	53		32.9	N 80.	W				IV
USN	1951	03	04	02	55		33.	N 80.2	W				
1**STO	1951	03	04	02	55		32.9	N 80.	W				IV
STO	1951	03	08	00	20		32.9	N 80.	W				II
STO	1951	03	10	08	18		32.9	N 80.	W				II
USN	1951	12	30	07	55		33.	N 80.2	W				
1**STO	1951	12	30	07	55		32.9	N 80.	W				IV
USN	1952	09	27	12	32		33.	N 80.2	W				
1**STO	1952	09	27	12	32		32.9	N 80.	W				III
USN	1952	11	19				32.8	N 80.	W				V
1**STO	1952	11	19				32.9	N 80.	W				V
USN	1956	01	05	05			34.3	N 82.4	W				
USN	1956	01	05	05	30		34.3	N 82.4	W				
STO	1956	01	05	08			34.3	N 82.4	W				IV
STO	1956	01	05	08	30		34.3	N 82.4	W				IV
USN	1956	05	19	19			34.3	N 82.4	W				
1**STO	1956	05	19	19			34.3	N 82.4	W				IV
USN	1956	05	27	23	25		34.3	N 82.4	W				
1**STO	1956	05	27	23	25		34.3	N 82.4	W				IV
USE	1957	11	24	20	06	17	35.	N 83.5	W				VI
1**USN	1957	11	24	20	06	17	35.	N 83.5	W				VI
2**STO	1957	11	24	20	06	17	35.	N 83.5	W		4.	SA	VI
USN	1958	10	20	06	16		34.5	N 82.7	W				
1**STO	1958	10	20	06	16		34.5	N 82.7	W				V
USN	1959	08	03	06	08		33.	N 79.5	W				VI
1**PDE	1959	08	03	06	08	30.	33.	N 79.5	W				VI
2**STO	1959	08	03	06	08	36.8	33.05	N 80.13	W	1	4.4	LG	VI
USN	1959	10	27	02	07	28.	34.5	N 80.2	W				VI
1**STO	1959	10	27	02	07	28.	34.5	N 80.2	W				VI
STO	1960	03	12	12	47	44.	33.07	N 80.12	W	9	4.	LG	V
STO	1960	07	24	03	37	30.	32.9	N 80.	W				V
USN	1960	07	28	03	37	30.	32.8	N 82.7	W				V
USN	1961	05	20	15	43		33.	N 80.2	W				III
1**STO	1961	05	20	15	43		32.9	N 80.	W				III

(Continued)

Source	Date			Time			Location				Depth Km	Magnitude			Maximum Intensity
	Yr	Mo	Dy	Hr	Mn	Sec	Latitude	Longitude	Mb	Ms		Other			
USN	1961	10	18	00	35		33.	N	80.2	W					
1**STO	1961	10	18	00	35		32.9	N	80.	W					III
USN	1963	04	11	17	45		34.9	N	82.4	W					IV
1**STO	1963	04	11	17	45		34.9	N	82.4	W					IV
PDE	1963	05	04	21	01	35.9	32.2	N	79.7	W	15				IV
1**USN	1963	05	04	21	01	36.	32.2	N	79.7	W	15				IV
2**STO	1963	05	04	21	01	50.3	32.97	N	80.19	W	5		3.3	SL	IV
STO	1963	10	08	06	01	43.4	33.9	N	82.5	W			3.2	SL	
STO	1964	03	07	18	02	58.6	33.72	N	82.39	W	5		3.3	SL	
STO	1964	03	13	01	20	17.5	33.19	N	83.31	W	1	4.4	3.9	SL	V
1**PDE	1964	03	13	01	20	18.1	33.2	N	83.4	W	40	4.4			V
2**USN	1964	03	13	01	20	18.1	33.2	N	83.4	W	40	4.4			V
STO	1964	04	20	19	04	44.1	33.84	N	81.1	W	3		3.5	SL	V
1**USN	1964	04	20	19	04	46.	34.	N	81.	W					V
STO	1965	04	07	07	41	10.2	33.9	N	82.5	W					
STO	1965	07	22	23	55	33.3	33.2	N	83.2	W					
USN	1965	09	09	04	37	16.	34.7	N	81.2	W					
1**STO	1965	09	09	04	37	16.	34.7	N	81.2	W					
STO	1965	09	09	14	42	20.	34.7	N	81.2	W			3.9	SL	
1**USN	1965	09	09	14	42	20.	34.7	N	81.2	W					
USN	1965	09	10	07	32		34.7	N	81.2	W					
1**STO	1965	09	10	07	32		34.7	N	81.2	W			3.	SL	
USN	1965	09	12	18	25	02.	34.7	N	81.2	W					
1**STO	1965	09	12	18	25	02.	34.7	N	81.2	W			2.9	SL	
STO	1965	11	08	12	58	01.	33.2	N	83.2	W			3.3	SL	
STO	1965	11	08	13	04	11.5	33.2	N	83.2	W					
STO	1967	10	23	09	04	02.5	32.8	N	80.22	W	19	3.8	3.4	LG	V
1**PDE	1967	10	23	09	04	10.1	33.4	N	80.7	W	33	3.8			
2**USN	1967	10	23	09	04	10.1	33.4	N	80.7	W	33	3.8			IV
STO	1968	07	10	04	24		32.9	N	80.	W					II
STO	1968	07	10	10	46		32.9	N	80.	W					II
STO	1968	07	12	01	12		32.8	N	79.7	W					IV
STO	1968	09	22	21	41	18.2	34.11	N	81.48	W	1	3.7	3.5	SL	IV
1**USE	1968	09	22	21	41	18.5	34.	N	81.5	W	22	3.7			IV
2**USN	1968	09	22	21	41	18.5	34.	N	81.5	W	22	3.7			IV
STO	1969	05	05	17	14		33.9	N	82.5	W					
STO	1969	05	09				33.95	N	82.58	W			3.3	LG	
STO	1969	05	18				33.95	N	82.58	W			3.5	LG	
STO	1969	11	04	18	58	23.	33.2	N	83.2	W					
STO	1969	11	08	01	52		33.9	N	82.5	W					

(Continued)

Source	Date			Time			Location		Depth Km	Magnitude			Maximum Intensity
	Yr	Mo	Dy	Hr	Mn	Sec	Latitude	Longitude		Mb	Ms	Other	
STO	1971	04	16	07	31		33.9	N 82.5 W					
PDE	1971	05	19	12	54	03.4	33.339	N 80.558 W	25	3.4			V
1**USN	1971	05	19	12	54	03.4	33.3	N 80.6 W	25	3.4			IV
2**STO	1971	05	19	12	54	03.6	33.36	N 80.66 W	1	3.4	3.7	LG	V
STO	1971	06	10	04	19		34.7	N 82.9 W			2.8	SL	
STO	1971	07	13	08	15		34.76	N 82.98 W					
STO	1971	07	13	09	39		34.7	N 82.9 W			2.8	SL	
STO	1971	07	13	10	54		34.7	N 82.9 W			2.9	SL	
STO	1971	07	13	11	07		34.7	N 82.9 W			2.7	SL	
STO	1971	07	13	11	42	26.	34.76	N 82.98 W			3.79	LG	VI
STO	1971	07	13	11	49		34.7	N 82.9 W			2.9	SL	
STO	1971	07	13	15	06		34.7	N 82.9 W			3.	SL	
STO	1971	07	31	20	16	55.	33.34	N 80.63 W	4		3.84	LG	III
1**PDE	1971	07	31	20	16	55.6	33.37	N 80.659 W	25				II
2**USN	1971	07	31	20	16	55.6	33.4	N 80.7 W	25				
STO	1971	08	11				33.4	N 80.7 W			3.53	LG	
PDE	1972	02	03	23	11	08.4	33.476	N 80.434 W	5G	4.5			V
1**USN	1972	02	03	23	11	08.4	33.5	N 80.4 W	5	4.5			V
2**STO	1972	02	03	23	11	09.7	33.31	N 80.58 W	2	4.5	4.5	LG	V
STO	1972	02	06				33.2	N 80.6 W					II
STO	1972	02	07	02	46		33.46	N 80.58 W			3.2	SL	III
STO	1972	02	07	02	53		33.46	N 80.58 W			3.2	SL	III
STO	1972	08	14	15	05	19.	33.2	N 81.4 W			3.	ML	III
STO	1973	03	28	11	19		34.3	N 81.4 W					
STO	1973	03	29	08	28		34.3	N 81.4 W					
STO	1973	03	29	12	19		34.3	N 81.4 W					
STO	1973	03	29	16	19		34.3	N 81.4 W					
STO	1973	10	08	13	38		33.9	N 82.5 W					
PDE	1973	12	19	10	16	08.7	32.983	N 80.26 W	8				
1**STO	1973	12	19	10	16	08.7	32.97	N 80.27 W	6		3.	SL	III
2**USN	1973	12	19	10	16	08.7	33.	N 80.3 W	8				
PDE	1974	08	02	08	52	09.8	33.872	N 82.488 W	1	4.3	4.9	LG	V
1**USN	1974	08	02	08	52	09.8	33.9	N 82.5 W	1	4.3			V
2**STO	1974	08	02	08	52	11.1	33.91	N 82.53 W	4	4.3	4.1	LG	V
STO	1974	10	08	23	22	28.	33.9	N 82.4 W	3.1				III
STO	1974	10	28	11	33		33.79	N 81.92 W			3.	ML	IV
STO	1974	11	05	03			33.73	N 82.22 W			3.7	ML	II
PDE	1974	11	22	05	25	55.5	32.9	N 80.145 W	18	4.7			VI
1**USN	1974	11	22	05	25	55.5	32.9	N 80.1 W	18	4.7			VI
2**STO	1974	11	22	05	25	56.7	32.93	N 80.16 W	6	4.7	4.3	LG	VI

(Continued)

Source	Date			Time			Location				Depth Km	Magnitude			Maximum Intensity
	Yr	Mo	Dy	Hr	Mn	Sec	Latitude		Longitude	Mb		Ms	Other		
STO	1974	11	22	06	22	44.4	32.89	N	80.14	W	10		2.7	CL	
STO	1974	12	03	08	25		33.95	N	82.5	W			3.6	ML	IV
STO	1975	04	01	21	09		33.2	N	83.2	W			3.9	SL	
STO	1975	04	28	05	46	52.6	33.	N	80.22	W	10		3.	LG	IV
STO	1975	10	18	04	31		34.9	N	83.	W					IV
PDE	1975	11	16	01	01	03.5	34.258	N	80.567	W	7				
1**STO	1975	11	16	01	01	03.5	34.26	N	80.57	W	7		2.8	LG	II
PDE	1975	11	25	15	17	33.7	34.873	N	82.958	W	5G		3.2	LG	IV
1**STO	1975	11	25	15	17	34.8	34.94	N	82.9	W	10		3.2	LG	IV
STO	1975	12	08	18	02	23.	35.	N	82.9	W					II
PDE	1976	12	27	06	57	13.9	32.223	N	82.463	W	5G		3.7	LG	V
1**STO	1976	12	27	06	57	15.2	32.06	N	82.5	W	14		3.7	LG	
PDE	1977	01	18	18	29	13.5	33.069	N	80.199	W	5		3.	MB	V
1**STO	1977	01	18	18	29	14.2	33.04	N	80.21	W	7		3.	LG	VI
STO	1977	03	30	08	27	47.8	32.95	N	80.18	W	8		2.9	CL	V
PDE	1977	05	31	23	50	13.2	32.951	N	80.244	W	8		2.3	CL	
1**STO	1977	05	31	23	50	14.	32.94	N	80.23	W	12		2.3	LG	II
STO	1977	06	05	00	42	29.7	33.05	N	81.41	W	4		2.7	CL	
PDE	1977	08	25	04	20	07.	33.392	N	80.692	W	10		3.1		V
1**STO	1977	08	25	04	20	07.5	33.369	N	80.698	W	3		3.1	LG	IV
STO	1977	09	07	14	41	32.7	34.982	N	82.927	W			2.5	CL	
PDE	1977	12	15	07	15	55.	32.996	N	80.293	W	9		2.5		
1**STO	1977	12	15	07	15	55.2	32.983	N	80.265	W	13		2.5	LG	
PDE	1977	12	15	19	16	43.1	32.923	N	80.22	W	9		3.		V
1**STO	1977	12	15	19	16	43.6	32.944	N	80.167	W	8		3.	LG	V
STO	1978	01	25	03	29	38.8	34.301	N	81.297	W	2		2.8	CL	
PDE	1978	01	25	08	29	39.	34.295	N	81.238	W	1		2.6	ML	
1**STO	1978	01	25	08	29	39.	34.301	N	81.234	W	5		2.6	LG	
STO	1978	02	04	09	14	38.5	34.304	N	81.303	W	1		2.6	CL	
STO	1978	02	08	20	35	39.6	34.06	N	82.13	W	11		2.5	CL	
STO	1978	02	09	19	19	13.8	34.617	N	81.759	W	5		2.6	CL	
STO	1978	02	10	20	23	38.7	34.343	N	81.348	W	1		2.5	CL	
STO	1978	02	11	00	19	00.7	34.343	N	81.35	W	3		2.5	CL	
STO	1978	02	11	05	19	00.2	34.346	N	81.349	W	1		2.7	CL	
STO	1978	02	11	12	00	25.8	34.336	N	81.31	W	2		2.6	CL	
STO	1978	02	14	12	45	07.2	34.342	N	81.346	W	2		2.5	CL	
STO	1978	02	14	13	09	59.5	34.351	N	81.343	W	2		2.6	CL	
STO	1978	02	14	17	06	41.1	34.79	N	81.76	W	6		2.5	CL	
STO	1978	02	15	21	14	34.2	34.349	N	81.346	W	0		2.5	CL	
STO	1978	02	16	02	14	33.4	34.332	N	81.362	W	2		2.6	CL	

(Continued)

Source	Date			Time			Location		Depth Km	Magnitude			Maximum Intensity
	Yr	Mo	Dy	Hr	Mn	Sec	Latitude	Longitude		Mb	Ms	Other	
STO	1978	02	22	07	13	25.1	34.327 N	81.35 W	1		2.6	CL	
STO	1978	02	22	12	13	24.3	34.339 N	81.35 W	1		2.8	CL	
STO	1978	02	22	13	04	59.2	34.356 N	81.352 W	0		2.5	CL	
STO	1978	02	24	07	34	10.5	34.334 N	81.348 W	1		2.7	CL	
STO	1978	02	25	04	02	42.7	34.345 N	81.351 W	1		2.5	CL	
STO	1978	02	26	06	52	35.4	34.315 N	81.297 W	1		2.6	CL	
STO	1978	02	26	11	52	33.	34.391 N	81.361 W	1		2.8	CL	
STO	1978	02	26	18	17	48.8	34.321 N	81.348 W	0		2.9	CL	
STO	1978	03	27	20	56	44.7	34.78 N	82.59 W	1		2.5	CL	
PDE	1978	04	22	06	36	22.7	34.393 N	81.316 W	0		2.6		
1**STO	1978	04	22	06	36	24.3	34.23 N	81.26 W	0		2.6	LG	
STO	1978	05	02	01	46	11.6	34.16 N	82.74 W	16		2.9	CL	
1**STO	1978	05	02	01	46	11.8	34.187 N	82.738 W	10		2.8	CL	
STO	1978	06	05	21	37	44.9	33.524 N	82.6 W	3		2.5	CL	
STO	1978	06	11	05	28	20.5	34.052 N	81.649 W	4		2.5	CL	
STO	1978	06	12	06	33	26.2	34.777 N	81.864 W	2		2.5	CL	
STO	1978	07	09	00	26	03.6	34.33 N	82.82 W	1		2.5	CL	
STO	1978	08	24	10	23	07.6	34.311 N	81.341 W	2		2.6	CL	
STO	1978	08	27	10	23	08.	34.313 N	81.337 W	2		2.7	CL	
STO	1978	08	27	10	58	16.8	34.331 N	81.312 W	7		2.5	CL	
PDE	1978	09	07	22	53	22.3	33.067 N	80.218 W	11		2.7	ML	
1**STO	1978	09	07	22	53	23.	33.063 N	80.21 W	10		2.7	LG	IV
STO	1978	10	27	16	27	18.1	34.302 N	81.326 W	2		2.9	CL	
STO	1978	11	24	11	54	40.9	34.296 N	81.347 W	1		2.6	CL	
PDE	1979	01	19	08	55	34.5	34.707 N	82.953 W	1G		2.8		IV
1**STO	1979	01	19	08	55	36.9	34.644 N	82.843 W	1		2.9	LG	IV
STO	1979	01	27	23	55	15.7	33.051 N	80.182 W	6		2.8	CL	
STO	1979	02	01	01	25	48.4	34.33 N	81.317 W	1		2.6	CL	
STO	1979	02	16	14	37	09.1	34.34 N	81.338 W	0		2.7	CL	
STO	1979	05	04	12	13	08.9	34.33 N	81.95 W	1		2.7	CL	
STO	1979	05	28	11	45	37.8	34.971 N	82.943 W	1		2.5	CL	
STO	1979	07	17	20	13	08.2	34.741 N	82.55 W	0		2.5	CL	
STO	1979	08	07	19	32	17.2	34.333 N	81.358 W	3		3.	LG	
STO	1979	08	11	02	11	56.6	32.992 N	80.223 W	10		2.5	LG	III
STO	1979	08	13	05	19	25.2	33.9 N	82.54 W	23		4.1	CL	
PDE	1979	08	26	01	31	45.	34.929 N	82.971 W	2G		3.7		V
1**STO	1979	08	26	01	31	46.6	34.945 N	82.939 W	2		3.7	LG	VI
STO	1979	09	14	00	45	31.4	34.337 N	81.324 W	2		2.7	CL	
STO	1979	10	07	08	54	36.6	34.303 N	81.342 W	1		2.8	CL	
STO	1979	10	08	07	54	09.	34.307 N	81.337 W	2		2.5	CL	

(Continued)

Source	Date			Time			Location		Depth Km	Magnitude			Maximum Intensity
	Yr	Mo	Dy	Hr	Mn	Sec	Latitude	Longitude		Mb	Ms	Other	
STO	1979	10	08	08	54	19.4	34.31 N	81.33 W	2		2.6	CL	
PDE	1979	10	08	23	20	10.1	34.314 N	81.362 W	5		2.9	ML	
1**STO	1979	10	08	23	20	11.	34.306 N	81.344 W	1		2.9	CL	III
STO	1979	10	14	08	24	57.6	34.306 N	81.338 W	2		2.9	CL	
STO	1979	10	16	07	06	26.9	34.278 N	81.329 W	1		2.8	CL	
STO	1979	10	21	15	56	10.5	34.331 N	81.34 W	2		2.6	CL	
STO	1979	11	20	15	49	02.8	34.24 N	80.695 W	0		2.5	CL	
STO	1979	12	07	05	43	34.9	33.008 N	80.163 W	5		2.8	LG	IV
1**PDE	1979	12	07	05	43	35.	33.007 N	80.168 W	15		2.9		
STO	1980	04	09	20	47	24.	34.848 N	79.941 W			2.8	CL	
STO	1980	04	24	06	16	57.2	34.329 N	81.324 W	3		3.	CL	
PDE	1980	06	22	20	33	06.2	33.012 N	80.158 W	1		2.1	ML	
1**STO	1980	06	22	20	33	06.2	33.012 N	80.158 W	1		2.1	LG	II
PDE	1980	06	22	23	35	26.5	33.015 N	80.158 W	1		1.6	ML	
1**STO	1980	06	22	23	35	26.5	33.015 N	80.158 W	1		1.6	LG	II
STO	1980	07	29	01	10	22.7	34.351 N	81.364 W	1		3.2	CL	
PDE	1980	09	01	05	44	42.3	32.968 N	80.2 W	6		2.7	LG	
1**STO	1980	09	01	05	44	42.3	32.978 N	80.186 W	6		2.7	LG	IV
STO	1980	09	10	19	49	46.4	34.122 N	82.947 W	13		2.5	CL	
STO	1980	12	16	17	40	07.8	34.786 N	82.622 W	4		2.5	CL	
STO	1980	12	27	08	40	26.7	34.346 N	81.33 W	7		2.5	CL	
STO	1981	02	21	04	48	26.5	33.604 N	81.171 W	1		2.	CL	II
PDE	1981	03	19	04	33	55.7	32.965 N	80.206 W	0G		2.5	LG	
1**STO	1981	03	19	04	33	55.7	32.96 N	80.188 W	6		2.5	LG	III
STO	1981	04	04	09	19	38.3	33.253 N	83.211 W			2.5	CL	
PDE	1982	03	01	03	33	13.6	32.936 N	80.138 W	7G		3.	LG	IV
PDE	1982	03	02	16	48	08.	34.318 N	81.376 W	5G		2.5	LG	III
PDE	1982	04	13	09	25	19.	34.291 N	81.381 W	5G		2.7	LG	III
PDE	1983	01	26	14	07	44.8	32.728 N	83.375 W	5G		3.5	LG	
PDE	1983	11	06	09	02	19.8	32.937 N	80.159 W	10G	3.3	3.1	LG	V
PDE	1983	11	06	09	04	14.6	32.929 N	80.155 W	11G		2.2	DR	
PDE	1985	06	09	00	38	42.1	33.219 N	81.661 W	5G		2.70	LG	III
PDE	1986	02	13	11	35	45.5	34.755 N	82.943 W	5G		3.50	LG	V
PDE	1986	03	09	23	49	15.3	32.968 N	80.169 W	6		2.20	MD	III
PDE	1986	03	13	02	29	31.3	33.229 N	83.226 W	5G		2.40	MD	IV
PDE	1986	05	08	15	45	46.4	33.007 N	80.178 W	5		1.40	MD	
PDE	1986	06	13	13	48	21.9	32.985 N	80.180 W	7		1.10	MD	
PDE	1986	07	22	22	49	00.5	32.931 N	80.168 W	6		1.80	MD	
PDE	1986	08	17	20	36	32.4	32.909 N	80.171 W	10		1.70	MD	
PDE	1986	09	17	09	33	49.4	32.928 N	80.152 W	8		2.60	MD	IV

(Continued)

<u>Source</u>	<u>Date</u>			<u>Time</u>			<u>Location</u>		<u>Depth</u> <u>Km</u>	<u>Magnitude</u>			<u>Maximum</u> <u>Intensity</u>
	<u>Yr</u>	<u>Mo</u>	<u>Dy</u>	<u>Hr</u>	<u>Mn</u>	<u>Sec</u>	<u>Latitude</u>	<u>Longitude</u>		<u>Mb</u>	<u>Ms</u>	<u>Other</u>	
PDE	1987	12	12	03	53	28.7	34.244 N	82.628 W	5G		3.00	LG	IV
PDE	1988	01	23	01	57	16.3	32.935 N	80.157 W	7		3.30	MD	V
PDE	1988	02	17	17	33	33.0	33.605 N	81.715 W	5G		2.50	LG	

(Concluded)

(Sheet 23 of 23)

Earthquake Source

STO Stover and others, (1984)
USN Hays and others, (1975)
EQH Coffman and others, (1982)
PDE U.S. Geological Survey
USE U.S. Department of Commerce

Magnitude Types

ML - Local magnitude
MB - Body-wave magnitude
CL - Coda-length magnitude
DR - Duration magnitude
LG - Large body-wave magnitude (Nuttli, 1973)
SL - Magnitude from Stover and others, 1984
SH - Magnitude from Stover and others, 1984
SA - Magnitude from Stover and others, 1984
MD - Duration or coda-length

REFERENCES

Coffman, Jerry L., Carl A. von Hake, and Carl W. Stover, 1982: Earthquake History of the United States, Publication 41-1, Revised Edition (Through 1970), With Supplement (1971-80), National Oceanic and Atmospheric Administration, NESDIS/NGDC, Boulder, CO, 208 pp.

Hays, Walter W., S.T. Algermissen, Alvaro F. Espinosa, David M. Perkins, and Wilbur A. Rinehard, 1975: "Catalog of Historical U.S. Earthquakes," Appendix A, Guidelines for Developing Design Earthquake Response Spectra (Technical Report M-114), Construction Engineering Research Laboratory, P.O. Box 4005, Champaign, IL, 349 pp.

Kondorskava, N.V., and N.V. Shebalin, Editors, 1982 (Russian Edition, 1975): New Catalog of Strong Earthquakes in the U.S.S.R. from Ancient Times Through 1977, Report SE-31, World Data Center-A for Solid Earth Geophysics, Boulder, CO, 608 pp.

Nuttli, Otto W., 1973: "Seismic Wave Attenuations and Magnitude Relations for Eastern North America," J. Geophys. Res., v. 78, pp.876-885.

Stover, C.W., B.G. Reagor, and S.T. Algermissen, 1984: United States Earthquake Data File, Open-File Report 84-225, United States Department of the Interior, Geological Survey, Denver, CO, 123 pp.

U.S. Department of Commerce, 1928-1981: United States Earthquakes, published annually 1928-1981 by: U.S. Coast and Geodetic Survey from 1928-1968; National Oceanic and Atmospheric Administration (NOAA) from 1969-1972; NOAA/U.S. Geological Survey, 1973-1980; and U.S. Geological Survey, 1981.

U.S. Geological Survey, monthly listings: Preliminary Determination of Epicenters, National Earthquake Information Center, Golden, CO.

APPENDIX C: GLOSSARY OF EARTHQUAKE TERMS

GLOSSARY

Accelerogram. The record from an accelerometer presenting acceleration as a function of time.

Attenuation. Characteristic decrease in amplitude of the seismic waves with distance from source. Attenuation results from geometric spreading of propagating waves, energy absorption and scattering of waves.

B-line. The slope of a straight line indicating frequency of occurrence of earthquakes versus earthquake magnitude.

Bedrock. A general term for any hard rock where it is not underlain by unconsolidated materials.

Design Spectrum. A set of curves used for design that shows acceleration velocity, or displacement (usually absolute acceleration, relative velocity, and relative displacement of the vibrating mass) as a function of period of vibration and damping.

Duration of Strong Ground Motion. The length of time during which ground motion at a site has certain characteristics. Bracketed duration is commonly the time interval between the first and last acceleration peaks that are equal to or greater than 0.05 g. Bracketing may also be done at other levels. Alternatively, duration can be a window in which cycles of shaking are summed by their individual time intervals between a specified level of acceleration that marks the beginning and end.

Earthquake. A vibration in the earth produced by rupture in the earth's crust.

1. Maximum Credible Earthquake. The largest earthquake that can be reasonably expected to occur.

2. Maximum Probable Earthquake. The worst historic earthquake.

Alternatively it is (a) the 100-year earthquake or (b) the earthquake that by

probabilistic determination of recurrence will occur during the life of the structure.

3. Floating Earthquake. An earthquake of a given size that can be moved anywhere within a specified area (seismotectonic zone).

4. Safe Shutdown Earthquake. That earthquake which is based upon an evaluation of the maximum earthquake potential considering the regional and local geology and seismology and specific characteristics of local subsurface material. It is that earthquake which produces the maximum vibratory ground motion for which certain structures, systems, and components are designed to remain functional. These structures, systems, and components are those necessary to assure: (a) the integrity of the reactor coolant pressure boundary; (b) the capability to shut down the reactor and maintain it in a safe shutdown condition; or (c) the capability to prevent or mitigate the consequences of accidents which could result in potential offsite exposures comparable to the guideline exposures of this part. (Nuclear Regulatory Commission: Title 10, Chapter 1, Part 100, 30 April 1975. Same as Maximum Credible Earthquake.)

5. Operating Basis Earthquake. The earthquakes for which the structure is designed to remain operational. Its selection is an engineering decision.

Effective Peak Acceleration. A time history after the acceleration has been filtered to take out high frequency peaks that are considered unimportant for structural response.

Epicenter. The point on the earth's surface vertically above the point where the first earthquake ground motion originates.

Fault. A fracture or fracture zone in the earth along which there has been displacement of the two sides relative to one another.

1. Active Fault. A fault, which has moved during the recent geologic past (Quaternary) and, thus, may move again. It may or may not generate earthquakes. (Corps of Engineers: ETL 1110-2-301, 23 April 1983.)

2. Capable Fault. An active fault that is judged capable of generating felt earthquakes.

Focal Depth. The vertical distance between the hypocenter or focus at which an earthquake is initiated and the ground surface.

Focus. The location in the earth where the slip responsible for an earthquake was initiated. Also, the hypocenter of an earthquake.

Free Field. A ground area in which earthquake motions are not influenced by topography, man-made structures or other local effects.

Ground Motion. Numerical values representing vibratory ground motion, such as particle acceleration, velocity, and displacement, frequency content, predominant period, spectral values, intensity, and duration.

Hard Site. A site in which shear wave velocities are greater than 400 m/sec and overlying soft layers are less than or equal to 15 m.

Hot Spot. A localized area where the seismicity is anomalously high compared with a surrounding region.

Intensity. A numerical index describing the effects of an earthquake on man, on structures built by him and on the earth's surface. The number is rated on the basis of an earthquake intensity scale. The scale in common use in the U.S. today is the modified Mercalli (MM) Intensity Scale of 1931 with grades indicated by Roman numerals from I to XII. An abridgement of the scale is as follows:

I. Not felt except by a very few under especially favorable circumstances.

II. Felt only by a few persons at rest, especially on upper floors of buildings. Delicately suspended objects may swing.

III. Felt quite noticeable indoors, especially on upper floors of buildings, but many people may not recognize it as an earthquake. Standing motor cars may rock slightly. Vibration like passing of truck. Duration can be estimated.

IV. During the day felt indoors by many, outdoors by few. At night some awakened. Dishes, windows, doors disturbed; walls make cracking sound. Sensation like heavy truck striking building. Standing motor cars rocked noticeably.

V. Felt by nearly everyone; many awakened. Some dishes, windows, etc., broken; a few instances of cracked plaster; unstable objects overturned. Disturbance of trees, poles and other tall objects sometimes noticed. Pendulum clocks may stop.

VI. Felt by all; many frightened and run outdoors. Some heavy furniture moved; a few instances of fallen plaster or damaged chimneys. Damage slight.

VII. Everybody runs outdoors. Damage negligible in buildings of good design and construction; slight to moderate in well-built ordinary structures; considerable in poorly built or badly designed structures; some chimneys broken. Noticed by persons driving motor cars.

VIII. Damage slight in specially designed structures; considerable in ordinary substantial buildings with partial collapse; great in poorly built structures. Panel walls thrown out of frame structures. Fall of chimneys, factory stacks, columns, monuments, walls. Heavy furniture overturned. Sand and mud ejected in small amounts. Changes in well water. Persons driving

motor cars disturbed.

IX. Damage considerable in specially designed structures; well designed frame structures thrown out of plumb; damage great in substantial buildings, with partial collapse. Buildings shifted off foundations. Ground cracked conspicuously. Underground pipes broken.

X. Some well-built wooden structures destroyed; most masonry and frame structures destroyed with foundations; ground badly cracked. Rails bent. Landslides considerable from river banks and steep slopes. Shifted sand and mud. Water splashed over banks.

XI. Few structures remain standing. Unreinforced masonry structures are nearly totally destroyed. Bridges destroyed. Broad fissures in ground. Underground pipe lines completely out of service. Earth slumps and land slips in soft ground. Rails bent greatly.

XII. Damage total. Waves seen on ground surfaces. Lines of sight and level distorted. Objects thrown upward into the air.

Liquefaction. The sudden, total loss of shear strength in a soil as the result of excess pore water pressure. The result is a temporary transformation of unconsolidated materials into a fluid.

Magnitude. A measure of the size of an earthquake related to the strain energy. It is based upon the displacement amplitude and period of the seismic waves and the distance from the earthquake epicenter.

1. Body Wave Magnitude (m_b). The m_b magnitude is measured as the common logarithm of the maximum displacement amplitude (microns) of the P-wave with period near one second. Developed to measure the magnitude of deep focus earthquakes, which do not ordinarily set up detectable surface waves with long periods. Magnitudes can be assigned from any suitable instrument whose

constants are known. The body waves can be measured from either the first few cycles of the compression waves (m_b) or the 1 second period shear waves (m_{b1g}).

2. Local Magnitude (M_L). The magnitude of an earthquake measured as the common logarithm of the displacement amplitude, in microns, of a standard Wood-Anderson seismograph located on firm ground 100 km from the epicenter and having a magnification of 2,800, a natural period 0.8 second, and a damping coefficient of 80 percent. Empirical charts and tables are available to correct to an epicentral distance of 100 km, for other types of seismographs and for various conditions of the ground. The correction charts are suitable up to epicentral distances of 600 km in southern California and the definition itself applies strictly only to earthquakes having focal depths smaller than about 30 km. The correction charts are suitable up to epicentral distances of about 600 km. These correction charts are site dependent and have to be developed for each recording site.

3. Surface Wave Magnitude (M_S). This magnitude is measured as the common logarithm of the resultant of the maximum mutually perpendicular horizontal displacement amplitudes, in microns, of the 20-second period surface waves. The scale was developed to measure the magnitude of shallow focus earthquakes at relatively long distances. Magnitudes can be assigned from any suitable instrument whose constants are known.

4. Richter Magnitude (M). Richter magnitude is nonspecified but is usually M_L up to 6.5 and M_S for greater than 6.5.

5. Seismic Movement (M_0). Seismic moment is an indirect measure of earthquake energy.

$$M_0 = G A D$$

where

G = rigidity modulus

A = area of fault movement

D = average static displacement

The values are in dyne centimeters.

6. Seismic Moment Scale (M_w). Expresses magnitude based on the concept of seismic moment:

$$M_w = 2/3 \log M_0 - 10.7$$

7. Comparison of Magnitude Scales. Table 7-1 presents a comparison of values for m_b , M_L , M , $\log M_0$, M_w and M_s .

Table 7-1. Comparison between m_b , M_L , M , $\log M_0$, M_w and M_s scales.

m_b	M_L	M	$\log M_0$ (dyne-cm)	M	M_s
Body-Wave	Local	Richter	Seismic Moment	Moment	Surface-Wave
5.0	5.4	5.4	24.2	5.4	5.0
5.5	5.9	5.9	25.0	6.0	5.8
6.0	6.4	6.7	26.1	6.7	6.7
6.5	6.9	7.5	27.3	7.5	7.5
7.0	7.5	8.3	28.6	8.4	8.3

Particle Acceleration. The time rate of change of particle velocity.

Particle Displacement. The difference between the initial position of a particle and any later temporary position during shaking.

Particle Velocity. The time rate of change of particle displacement.

Response Spectrum. The maximum values of acceleration, velocity, and/or displacement of an infinite series of single-degree-of-freedom systems, each characterized by its natural period, subjected to a time history of earthquake ground motion. The spectrum of maximum response values is expressed as a function of natural period for a given damping. The response spectrum

acceleration, velocity, and displacement values may be calculated from each other by assuming that the motions are harmonic. When calculated in this manner these are sometimes referred to as pseudo-acceleration, pseudo-velocity, or pseudo-displacement response spectrum values.

Saturation. Where those measures of earthquake motions (acceleration, velocity, magnitude, etc.) do not increase though the earthquakes generating them may become larger.

Scaling. An adjustment to an earthquake time history or response spectrum where the amplitude of acceleration, velocity, and/or displacement is increased or decreased, usually without change to the frequency content of the ground motion.

Seismic Hazard. The physical effects of an earthquake.

Seismic Risk. The probability that an earthquake of or exceeding a given size will occur during a given time interval in a selected area.

Seismic Zone. A geographic area characterized by a combination of geology and seismic history in which a given earthquake may occur anywhere.

Soft Site. A site in which shear wave velocities are less than 400 m/sec in a surface layer 16 or more m thick.

D1

REPORT: CONTRACT NO. DACW 3989M2647

**SEISMIC POTENTIAL NEAR
STROM THURMOND LAKE, SOUTH CAROLINA**

by

Professor Pradeep Talwani

Professor of Geophysics

Prepared for

U. S. Army Corps of Engineers

Waterways Experiment Station

P.O. Box 631

Vicksburg, MS 39180-0631

TABLE OF CONTENTS

1.	Introduction	1
2.	Regional Tectonics	4
2.1.	The Geologic Belts of the Piedmont Province	4
2.2.	Fault Zones in the Piedmont Province	9
2.3.	Regional Stress Field	13
2.4.	Conclusions.	24
3.	Seismicity	25
3.1.	Historical and Instrumental Seismicity	25
3.2.	Seismicity in the Geological Provinces	30
3.3.	Reservoir Induced Seismicity	34
3.4.	Conclusions	40
4.	Filling History and Lake Level Fluctuations	41
4.1.	Lake Size.	42
4.2.	Lake Level Fluctuations	42
4.3.	Duration of RIS.	44
4.4.	Conclusions.	45
5.	Seismicity Studies in the Strom Thurmond Lake Area.	46
5.1.	Denman's Study	46
5.2.	The August 2, 1974, Earthquake	53
5.3.	Studies Following the August 2, 1974, Earthquake	57
5.4.	Reservoir Induced Seismicity at the STLA	60
5.5.	Conclusions.	63
6.	Seismic Potential in the STLA.	65
6.1.	Distant Earthquakes Felt in the Area	66
6.2.	Prospect of an Earthquake in the Project Area.	68
6.3.	Maximum Earthquake	69
6.4.	Conclusions.	70
7.	Summary and Conclusions.	70
8.	References	73

1. INTRODUCTION

The Strom Thurmond (formerly the Clarks Hill) Lake was formed by the construction of the Strom Thurmond (formerly the Clarks Hill) Dam, located on the Savannah River, 140 miles above the mouth and 22 miles above Augusta, Georgia. The project, on the South Carolina-Georgia border, is located 67 miles downstream from Hartwell Dam. The dam was the first in a series of projects for the comprehensive development of the Savannah River for flood control, recreation, navigation and generation of hydroelectric power (Figure 1). This nearly 200 ft high and 5680 ft long dam, constructed between December, 1945 and June, 1952, lies in the Piedmont geological province.

In the preliminary geological studies that were carried out prior to the construction of the dam, potential seismic hazards were not a factor and the regional tectonics picture was not well understood. However, in recent years it has been recognized that seismic hazard is an important element that needs to be considered in the siting of critical facilities.

Approximately 32 miles upstream, the Richard B. Russell Dam was constructed in the late 1970's and early 1980's. One of the important elements that was considered prior to its construction was the potential of seismically induced ground shaking at the project site. This was because of the realization that the 1886 Charleston, the 1811-1812 New Madrid, the 1913 Union County and several smaller earthquakes had been felt at the site. Also the phenomenon of reservoir induced seismicity (RIS) had been recognized. In recent years RIS has been suggested to occur at Strom Thurmond Lake (STL) and at Richard B. Russell Reservoir and Lakes

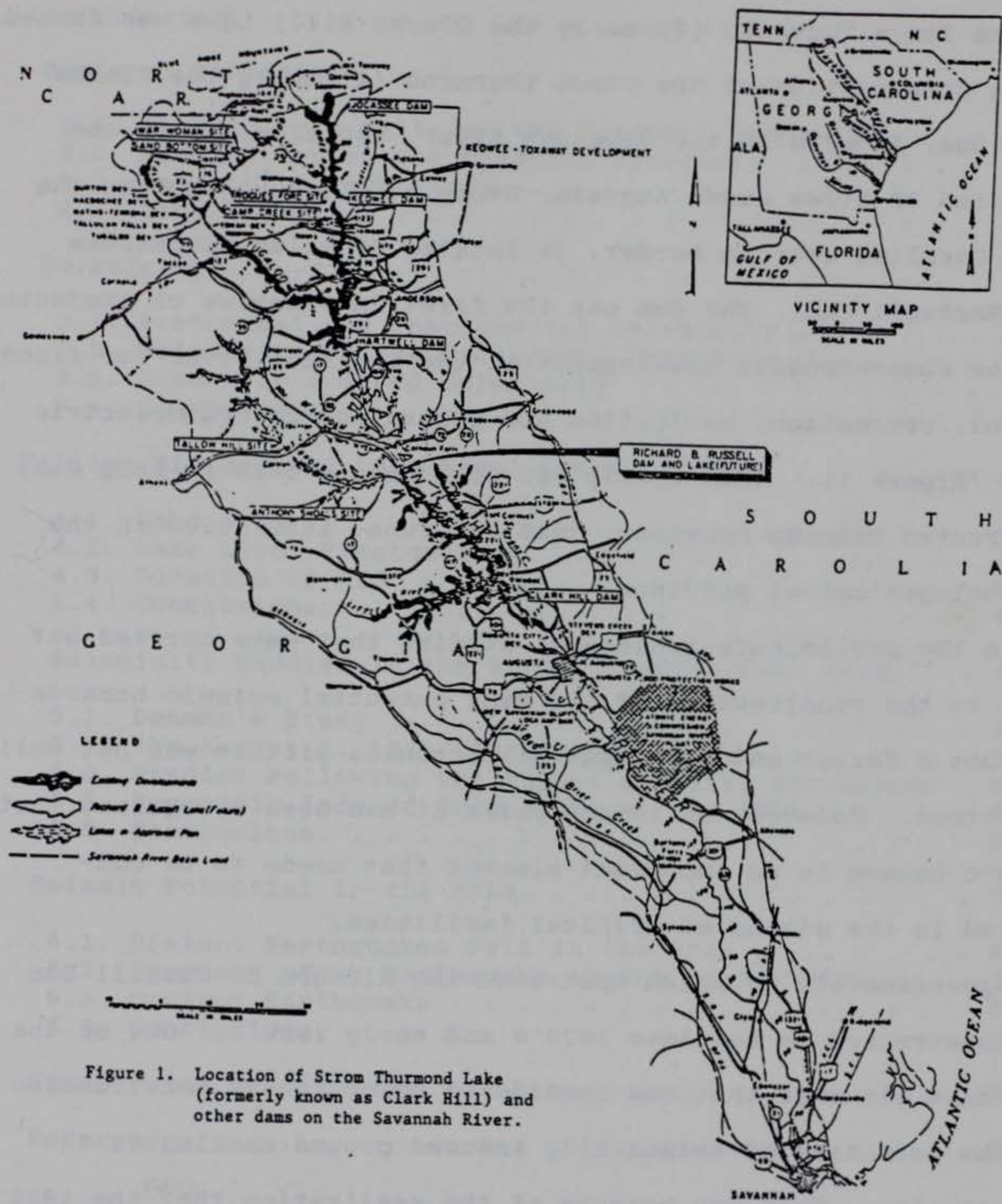


Figure 1. Location of Strom Thurmond Lake (formerly known as Clark Hill) and other dams on the Savannah River.

Jocassee and Keowee upstream. RIS has also been observed at Monticello Reservoir in central South Carolina and Lake Sinclair in Georgia. The Strom Thurmond project, as well as all of the sites of RIS, are in the Piedmont geological province.

This review, aimed at assessing the seismic potential in the Strom Thurmond Lake area (STLA), consists of the following sections. The current thinking on the tectonics of the region is reviewed in the next section. Section 3 consists of a review of the historical and current seismicity, with a special emphasis on RIS. At several locations worldwide it has been suggested that the nature of RIS is influenced by the size of the reservoir and the rates of filling and drawdown. The relevant data for the Strom Thurmond Lake area are reviewed in Section 4. The STLA was the site of some of the earliest seismological studies in the South Carolina-Georgia Piedmont province. Temporally the studies can be divided into two parts--those that preceded and those that followed the M_L 4.3 earthquake of August 2, 1974 on the South Carolina-Georgia border. These efforts are described in Section 5. The nature of seismicity in the region appears to be related to the geological belts and potential seismic zones therein. A variety of current data suggest that there is a general pattern of stationarity in the pattern of seismicity. That is, a comparison of historical and current seismic network data suggests that the same (major) sources of seismicity have been active since historical times and occurs in response to a regional stress field. Therefore in assessing the seismic potential (Section 6) these seismic sources, were kept fixed, especially at Charleston. In the Piedmont, extra conservatism in the assess-

ment of seismic hazard was built-in by allowing the Union county earthquake of 1913 to "move" to the immediate vicinity of Strom Thurmond Dam (STD). Considering all potential locations of seismicity, we conclude that the largest ground shaking at the project site can be due to an earthquake of magnitude 5.0 to 5.5 (MMI VII-VIII), the size of the Union county event, occurring in the vicinity of the site (Section 7).

2. REGIONAL TECTONICS

The Appalachian Orogen was formed along the ancient Precambrian continental margin of eastern North America by a series of compressional events that began in the Ordovician and episodically spanned much of the Paleozoic era (Hatcher, 1987). The southern and central Appalachians may best be described using subdivisions based upon the stratigraphic and lithotectonic characteristics of the rocks. These tectonostratigraphic subdivisions include the Valley and Ridge, the Blue Ridge and the Piedmont Provinces and are separated from one another by major fault zones (Figure 2).

The Blue Ridge province, bounded to the west by the Blue Ridge Thrust and to the east by the Brevard fault zone, consists primarily of metasediments and metavolcanic rocks with numerous intrusive bodies. The Blue Ridge is subdivided into the western and eastern parts by the Hayesville thrust fault (Hatcher, 1978).

2.1. The Geologic Belts of the Piedmont Province

The Piedmont Province, in which the project site is located, extends from Virginia to Alabama and consists of northeast trend-

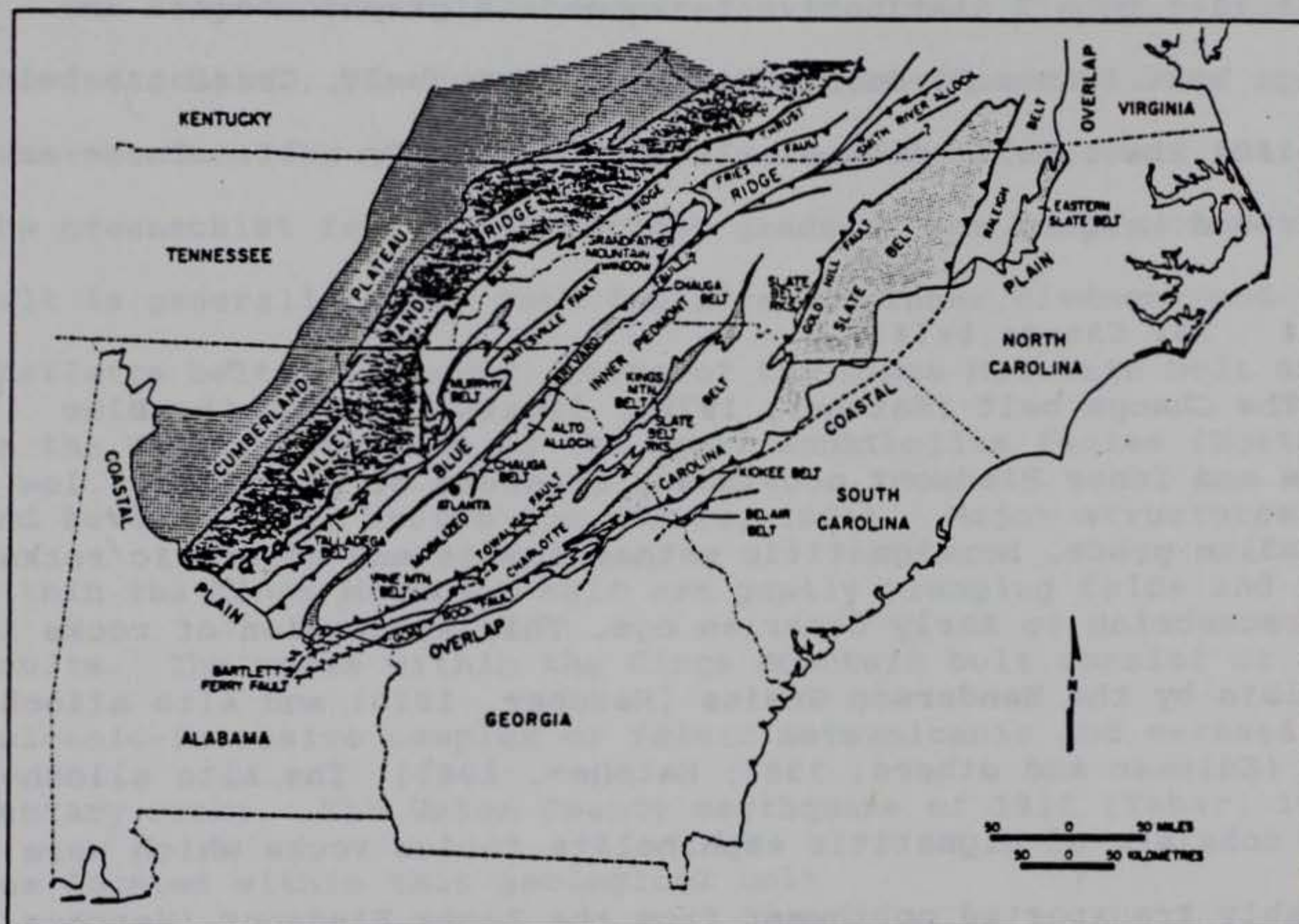


Figure 2 - Map of tectonic subdivisions of southern Appalachians.

ing belts defined on the basis of tectonic history, metamorphic grade and structural relationships. The province consists of variably deformed and metamorphosed igneous and sedimentary rocks ranging in age from Middle Proterozoic to Late Permian. The Piedmont Province in South Carolina and Georgia can be further subdivided into 7 distinctive tectonostratigraphic belts: the Chauga belt, Inner Piedmont, Kings Mountain belt, Charlotte belt, Carolina Slate belt, Kiokee belt and the Belair belt. These are described in turn.

2.1.1 *The Chauga belt*

The Chauga belt (Hatcher, 1972), located between the Blue Ridge and Inner Piedmont provinces, consists of stratified, low to medium grade, nonmigmatitic metasediments and metamafic rocks of Precambrian to Early Cambrian age. This succession of rocks is overlain by the Henderson Gneiss (Hatcher, 1970) and Alto allochthon (Edleman and others, 1987; Hatcher, 1987). The Alto allochthon consists of migmatitic amphibolite facies rocks which were probably transported northwest from the Inner Piedmont (Hatcher, 1987).

2.1.2. *The Inner Piedmont belt*

The Inner Piedmont belt contains rocks of the highest metamorphic grade found in the southern Appalachian Piedmont. These include volcanic and sedimentary rocks metamorphosed to the Almandine-Amphibolite facies. These rocks consist of amphibolite, granitic gneiss, paragneiss, metasandstone and schist. Structures generally verge towards the northwest (Hatcher, 1987). Folds are overturned to the northwest and are recumbent to re-

clined forming large thrust nappes in the northwestern Inner Piedmont (e.g. Six mile thrust nappe in South Carolina) (Griffin, 1974; Hatcher, 1987) and overlying the Chauga belt.

2.1.3. *The Kings Mountain belt*

The Kings Mountain belt separates the Inner Piedmont from the Charlotte belt. The Kings Mountain belt is separated from the Inner Piedmont by the Kings Mountain shear zone (Horton, 1981). The greenschist facies metamorphic grade of the Kings Mountain belt is generally lower than the adjacent Inner Piedmont and Charlotte belts. However, parts of the Kings Mountain belt are in the Sillimanite zone of the Upper Amphibolite facies (Horton and Butler, 1977; Horton and others, 1981). Major structures within the Kings Mountain belt are gently plunging folds and faults. The rocks within the Kings Mountain belt consist of a volcanic-intrusive complex of felsic metavolcanic and metasedimentary rocks. The Union County earthquake of 1913 (Taber, 1913) was located within this geological belt.

The Kings Mountain belt is associated with a pronounced anomaly in the potential field data. In the aeromagnetic map of Zietz and others (1982) the low frequency and low amplitude magnetic field anomalies of the Inner Piedmont change to high frequency and high amplitude anomalies at the Kings Mountain belt. In the gravity data, the location of the Kings Mountain belt is spatially associated with the change in the gravity gradient as it decreases to the northwest and is relatively flat to the east.

2.1.4. *The Charlotte belt*

The Charlotte belt is a belt of numerous intrusions and moderate to high grade metamorphism. Much of the belt has been metamorphosed to amphibolite grade. The oldest rocks are amphibolite, biotite gneiss, hornblende gneiss and schist which are thought to be derived from volcanic, volcanoclastic or sedimentary protoliths.

The rocks of the Charlotte belt were intruded by several premetamorphic and postmetamorphic plutons of diverse compositions and ages ranging from 550 to 265 Ma (Fullagar, 1971; Dallmeyer and others, 1986).

2.1.5. *The Carolina Slate belt*

The Carolina Slate belt, which extends from Virginia to Georgia, is characterized by felsic to mafic metavolcanic rocks and thick sequences of metasedimentary rocks derived from volcanic source terranes of Cambrian age (Secor and others, 1983). These rocks have been subjected to low to medium grade regional metamorphism during the period from 500 to 300 Ma and subsequently intruded by granitic and gabbroic plutons about 300 Ma (Carpenter, 1982). Based on detailed structural analysis, the Charlotte belt has been interpreted as a tectonic infrastructure of the Carolina Slate belt (Secor and others, 1986).

The gravity and aeromagnetic anomalies associated with both the Charlotte and Carolina Slate belts consists of broad highs and lows.

2.1.6. *The Kiokee belt*

The Kiokee belt is located between the Carolina Slate belt and the Atlantic Coastal Plain in central Georgia and South Carolina. The interior of the Kiokee belt is a migmatitic complex of biotite amphibole paragneiss, leucocratic paragneiss, sillimanite schist, amphibolite, ultramafic schist, serpentinite, feldspathic metaquartzites and contains granitic intrusions of Late Paleozoic age (Secor, 1987).

2.1.7. *The Belair belt*

The Belair belt located near Augusta, Georgia, is a small belt of greenschist grade metasediment and metavolcanic rocks and is separated from the Kiokee belt by the Augusta Fault zone (Hatcher and others, 1977; Maher, 1978, 1987; Prowell and O'Connor, 1978). As determined from geophysical and well data, the Belair belt extends beneath the Atlantic Coastal Plain (Daniels, 1974). The age of the main metamorphism and deformational event is uncertain but appears to be analogous to that in the Carolina Slate belt which is 530 to 580 Ma to 385 to 415 Ma (Dallmeyer and others, 1986; Secor and others, 1986).

2.2. Fault Zones in the Piedmont Province

There are essentially four major fault zones within the Piedmont Province of southeast North America: The Brevard zone, Kings Mountain shear zone, Modoc zone and the Augusta fault zone. All of these fault zones exhibit a complex history of polyphase deformation and metamorphism during the Paleozoic orogenic events. Mesozoic diabase dikes cut across the fault zones and are not offset by the faults. This implies that there has been

no movement since the emplacement of the dikes. The Modoc zone is the major fault zone which is cut by STL.

2.2.1. *The Brevard zone*

The Brevard zone extends northeast from North Carolina and into Georgia and Alabama. The Brevard zone separates the Blue Ridge Province in the northwest from the Chauga belt and Inner Piedmont in the southeast. The zone is principally located within the northwest flank of the Chauga belt.

Movement on the Brevard zone has been interpreted as having a polyphase history of movement and deformation (Hatcher, 1978; Edleman and others, 1987). Edleman and others (1987) interpret the Brevard zone as an Alleghanian dextral shear zone reactivated by a later Alleghanian thrust fault and thrust splays, the orientation of the zone being controlled by reworked pre-Alleghanian nappes.

Seismic reflection studies (Clark and others, 1978; Cook and others, 1979) indicate that the Brevard zone and Inner Piedmont are allochthonous and that the zone is a southeast dipping thrust fault that merges with a subhorizontal sole thrust at depths of about 10 miles.

2.2.2. *The Kings Mountain shear zone*

The Kings Mountain shear zone extends from North Carolina into Georgia, where it is called the Lowndesville belt (Griffin, 1970, 1981; Hatcher, 1972). The shear zone truncates rock units on both sides and appears to be a metamorphic as well as lithologic and structural discontinuity (Horton, 1981; Horton and

others, 1987). The shear zone is characterized by phyllonitic and mylonitic rocks and is steeply dipping to the southeast (Horton, 1981). The latest movement on the shear zone has been interpreted as dextral and occurring in the late Alleghanian orogeny (Horton and others, 1987).

In Georgia, the Kings Mountain shear zone is correlatable with the Middleton-Lowndesville cataclastic zone (Griffin, 1970; Hatcher, 1972; Rozen, 1981) where it is characterized by a narrow zone of intense cataclasis and is typified by quartz-sericite phyllonite and mylonitic rocks (Griffin, 1981).

2.2.3. *The Modoc zone*

The Modoc zone, located in South Carolina and Georgia, essentially separates the Carolina Slate belt to the northwest from the Kiokee belt. Recent interpretations of detailed structural investigations of the zone suggest that it is characterized as a brittle and ductile zone with a deformation and metamorphic polyphase history produced primarily during the middle-late Paleozoic Alleghanian orogeny (Secor and others, 1986; Secor, 1987). The northwest, steeply dipping zone is interpreted as originally dipping gently to the northwest with major components of normal slip and dextral strike slip.

The Irmo shear zone, near Columbia, South Carolina, is a zone of heterogeneous ductile deformation which is localized near and overprints the Modoc zone (Secor and others, 1986; Dennis and others, 1987).

Some of the best exposures of the Modoc fault zone are to be found on the shores of STL. Beaches of "button schists"--usually

associated with fault zones--are clearly exposed at Modoc when the water level is low. Geomorphically one of the more spectacular examples of the Modoc zone is the Little River, a tributary of the Savannah River in Georgia. This river lies along the Modoc fault zone and has well developed aeromagnetic and gravity anomalies associated with it.

2.2.4. *The Augusta fault*

The Augusta fault, located near Augusta, Georgia, dips approximately 45° to the southeast and has been interpreted as a dextral strike slip fault (Bobyarchick, 1981) and as a thrust fault (Maher, 1979). Maher (1978, 1987) suggests that the fault is a normal fault with dextral oblique slip movement and was active around during the Alleghanian orogeny. The tectonic and metamorphic history of the Augusta fault are very similar to that of the Modoc zone and may therefore have a common origin (Maher, 1987).

Near Augusta, Georgia, the southeast edge of the Kiokee belt and the Augusta fault are offset by the north-northeast trending Belair fault. Bramlett and others (1982) suggest that the Belair fault represents an Alleghanian age tear fault which linked two thrust segments of the Augusta fault zone. The last stages of movement on the Belair fault were interpreted as Cenozoic high angle reverse faults where it offsets the late Cretaceous and early Eocene unconformities within the Atlantic Coastal Plain sediments by approximately 30 and 12 meters, respectively (Prowell and O'Connor, 1978).

2.2.5. *The Eastern Piedmont Fault System*

Hatcher and others (1977) proposed the existence of an extensive series of faults and splays, extending from Alabama to Virginia and called it the Eastern Piedmont Fault System. In South Carolina and Georgia, this fault system includes the Modoc zone, the Irmo shear zone and the Augusta fault. Aeromagnetic, gravity and seismicity data indicate that this fault zone continues beneath the Coastal Plain sediments.

2.3. Regional Stress Field

The observed seismicity is the response of local structures to the stress field. Seismicity can result due to the action of anomalous local stress concentrations or due to the action of the tectonic stress field on pre-existing zones of weakness or both. Therefore, it is of great importance to determine the state of the ambient *in situ* stress field.

The orientation of the maximum horizontal stress (S_{Hmax}) can be determined from a variety of data. These include earthquake focal mechanisms, *in situ* stress measurements by hydrofracture and overcoring techniques and from geologic evidence of recent deformation (see e.g. McGarr and Gay, 1978; Zoback and Zoback, 1980). In recent years analysis of stress-induced wellbore elongation (or breakouts) has been increasingly used to determine the direction of S_{Hmax} (see e.g. Bell and Gough, 1979). The results of overcoring measurements on surface outcrops are not considered reliable due to a variety of local stress heterogeneities such that these results do not represent the tectonic stress field.

In the southeastern United States several studies have des-

cribed the direction of S_{Hmax} . Some of the initial results were conflicting due to inclusion of few, poor or questionable data (e.g. Sbar and Sykes, 1973; Zoback and others, 1978; Zoback and Zoback, 1980; Talwani, 1985). In the latest compilation by Zoback and others (1987) the questionable data have been weeded out and additional data incorporated (especially from wellbore breakouts). The results described a clearer picture. In the southeastern United States, these authors found that the geological, seismological and *in situ* stress data all suggest a NE to ENE compressive stress regime (characterized by strike slip or reverse faulting). This direction is consistent with plate tectonic ridge push forces for the North American plate (Zoback and others, 1987). One implication of this observation, that the observed stress regime in the region can be explained by plate tectonic sources, is that the probable cause of most of the observed seismicity is due to the action of tectonic stress on zones of locally weak structures, rather than due to inherently local stress concentrations.

2.3.1. *Stress field in the project area*

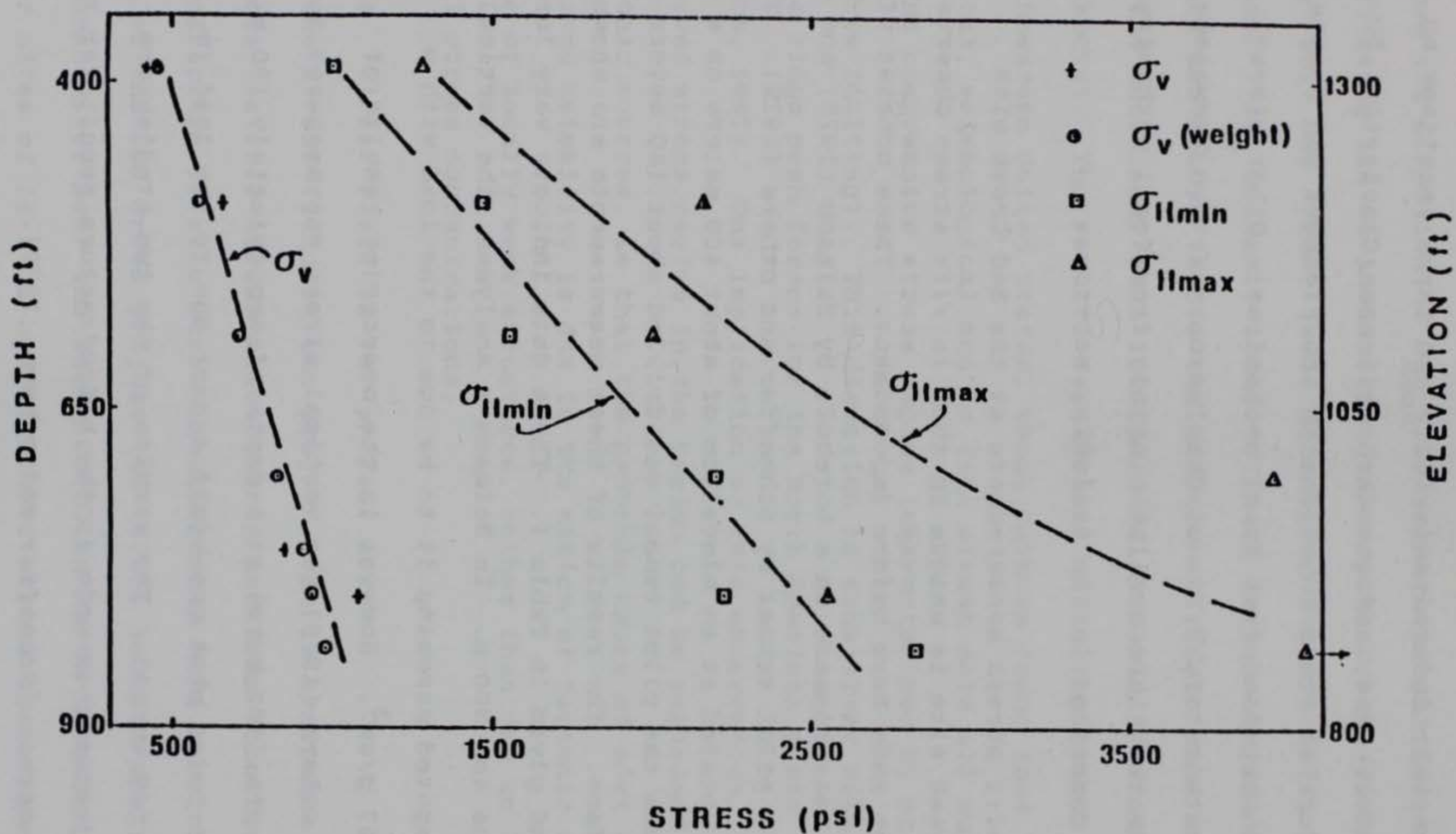
The stress field in the project area is available from two sources--*in situ* stress measurements and from focal mechanisms. Hydrofracture *in situ* stress measurements were carried out at the site of the Bad Creek project (in 1975), located upstream on the Savannah River near the South Carolina-North Carolina border. Other sites of *in situ* hydrofracture stress measurements include three locations in NW South Carolina associated with the ADCOH project, two deep holes near Monticello Reservoir associated with

a study of reservoir induced seismicity and three locations on the Savannah River Site, and one deep well near Charleston, SC. Stress directions at other locations in the Piedmont and Coastal Plain have been obtained from focal mechanisms. Other stress data in the southeastern U.S., at Charleston, eastern Tennessee, Virginia and Kentucky are available mainly from focal mechanisms. These are all described in the following sections.

2.3.1.1. *In situ* stress measurements at the Bad Creek site

The Bad Creek site is unique in that *in situ* stress observations have been made here before impoundment. These consist of hydrofracture measurements in a borehole by Haimson (1975) and overcoring in a pilot tunnel by Schaeffer and others (1979). The well head was located at an elevation of about 400 meters on a hillside whereas the pilot tunnel was drilled about 180 meters below the surface. The results of these measurements are shown in Figure 3 and given in Table 1. These data indicate very large stresses in the top 300 m. In Haimson's analyses, the vertical stress was computed assuming it to be due to the load with a density of 2.67 g/cm^3 . However in the overcoring results of Schaeffer and others (1979) the vertical stress was measured to be about 10.2 MPa (102 bars) at a depth of approximately 180 m. This is almost twice what one would expect due to the load ($\sigma_v = \rho gh = 4.9 \text{ MPa}$ (49 bars)). The results of the two studies are similar if adjustment is made in the hydrofracture result for the high vertical stress (Schaeffer and others, 1979).

Such observations are rare but not unheard of. For example, Fyfe and others (1978, p. 226) note that "... in the Snowy



From Haimson (1975)

Figure 3: Plot of the comparison of in situ stress data with the calculated stress variation with depth at Bad Creek (modified from Haimson, 1975).

Table 1

Average Principal Stress Values

Hydrofracture Data (Haimson, 1975)

Elevation a.s.l. (m)	Depth Below Surface (m)	Hmin (Mpa bars)	Direction	Hmax (MPa bars)	Direction
398	119	6.9 69	N66°W	8.8 88	N24°E
367	151	10.2 102	N84°W	14.8 148	N06°E
338	181	10.6 106	N12°W	13.8 138	N78°E
308	215	15.2 152	N22°W	27.2 272	N68°E
283	243	≥15.5 ≥155	N48°W	≥17.6 ≥176	N42°E
272	255	19.5 195	N34°W	34.0 340	N56°E
Av. at 290	236	15.9 ± 2.5 MPa 159 ± 25 bars	N20°W	22.8 ± 5.5 MPa 228 ± 55 bars	N60°E
(Site of planned powerhouse)					

Overcoring Data (Schaeffer et al., 1979)

338	181	18.4 184	N32°W	29.3 293	N57°E
-----	-----	----------	-------	----------	-------

$$\sigma_v = 10.2 \text{ MPa (102 bars)}$$

Mountain region of Australia the vertical pressure at a depth of 300 m was found to be over 120 bars, rather than 80-90 bars one would forecast using $\sigma_v = \rho gh$."

Thus, in addition to the very high horizontal stress gradients encountered at shallow depths, there are large vertical stresses also. This suggests that the rocks at shallow depths (< 500 m) are highly stressed.

2.3.1.2. Focal mechanisms at Lakes Jocassee and Keowee

Focal mechanism data were available for seismicity at Lakes Jocassee, Keowee and STL (Talwani and Rastogi, 1981; Rastogi and Talwani, 1984; Talwani and others, 1979; Talwani, 1976). Most of the solutions were for composite focal mechanisms. Those at Lakes Jocassee were from large events and their aftershocks. Two sets of solutions were available for Lake Keowee earthquakes: one for the January-February swarm (Talwani and others, 1979) and single event solutions for two felt events in February and June, 1986 (Acree and others, 1988). All these solutions yield P-axes in the NE direction in general agreement with the directions obtained from *in situ* measurements at the Bad Creek site located about 10 miles NW of Jocassee Dam.

2.3.1.3. Stress data at Monticello Reservoir, Newberry and northwest Georgia

The orientation of S_{Hmax} in the Piedmont was inferred from focal mechanisms in the Monticello Reservoir area (Talwani and Acree, 1987), for a series of earthquakes near Newberry, S.C. (Rawlins, 1986) and in NE Georgia. Figure 4 shows the average of 22 focal mechanisms for well recorded events in 1978 and 1979 at

MONTICELLO RESERVOIR

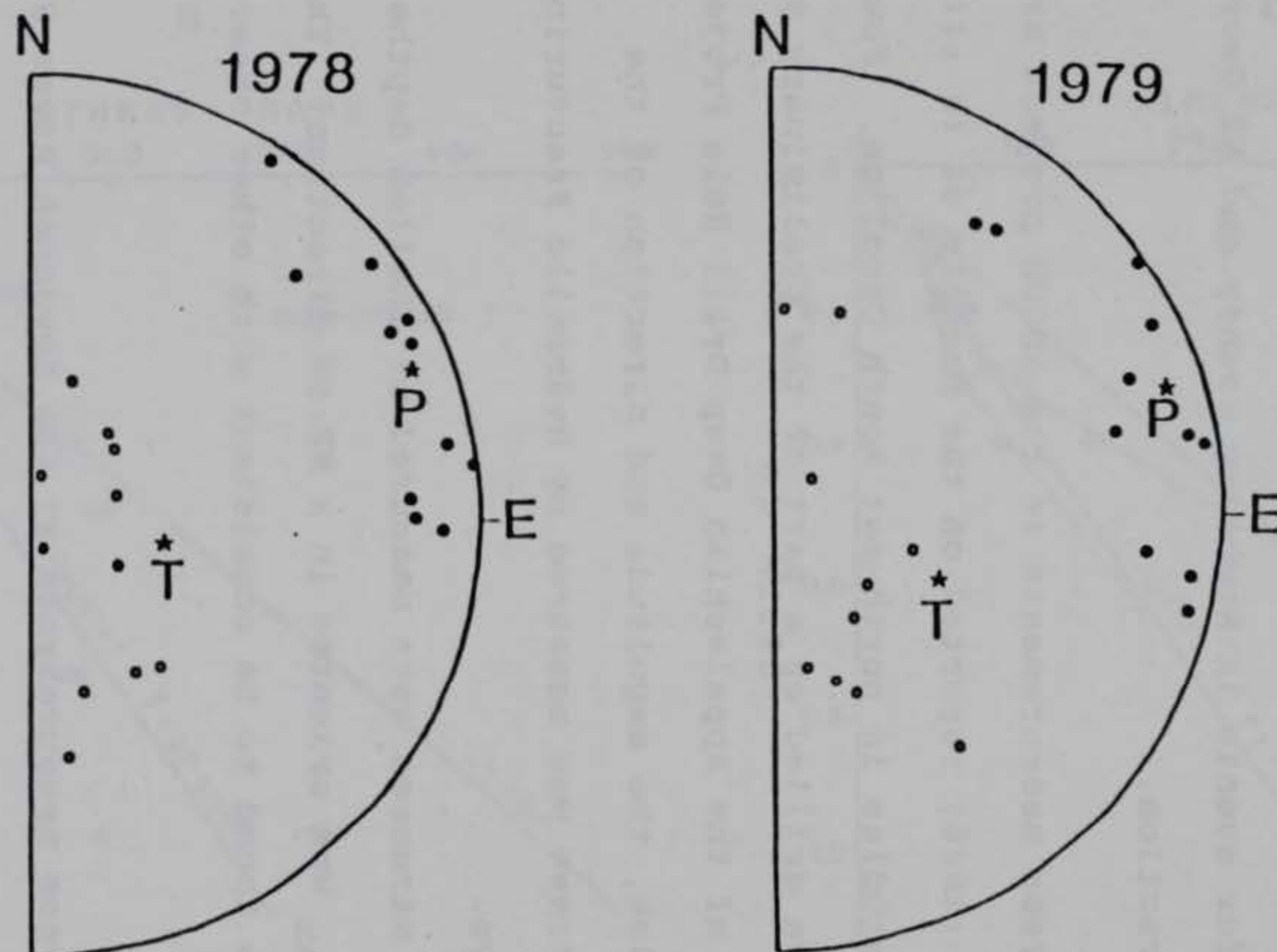


Figure 4. Plot of P & T axes obtained from composite solutions for seismicity at Monticello Reservoir. Average P and T axes are designated by stars (From Talwani & Acree, 1987).

Monticello Reservoir. The P-axes lie in the NE quadrant. A NE orientation of S_{Hmax} was also obtained from the well break out data in two 1 km deep holes at Monticello Reservoir. Hydrofracture *in situ* stress measurements in Monticello wells 1 and 2 are shown in Figure 5 and given in Table 2. The data suggest high compressional stresses that favor thrust faulting at shallow depths. The P-axes for events in Newberry county and NE Georgia all lie in the NE direction.

2.3.1.4. *In situ* stress measurements in the ADCOH project area

Coyle and others (1986) reported on the results of *in situ* stress and fracture studies in northwest South Carolina. Four shallow boreholes were drilled as a part of the preliminary site investigations phase of the Appalachian Deep Drill Hole Project. In three of these holes, the magnitude and direction of the maximum horizontal stress was measured by hydraulic fracturing and televiewer surveys.

Large horizontal stresses were measured at shallow depths and the direction of S_{Hmax} was oriented in a NE-SW direction. The stress field was thus found to be consistent with other observations in the area.

2.3.1.5. *In situ* stress measurements at the Savannah River Site

Zoback and others (1989) measured the orientation and magnitude of the principal horizontal stress within basement rocks beneath the Savannah River Site using hydraulic fracturing and borehole televiewer logging. Stress measurements were carried out in three core holes. In two holes the measurements spanned the depth interval 1000-14000 ft below surface, within the upper-

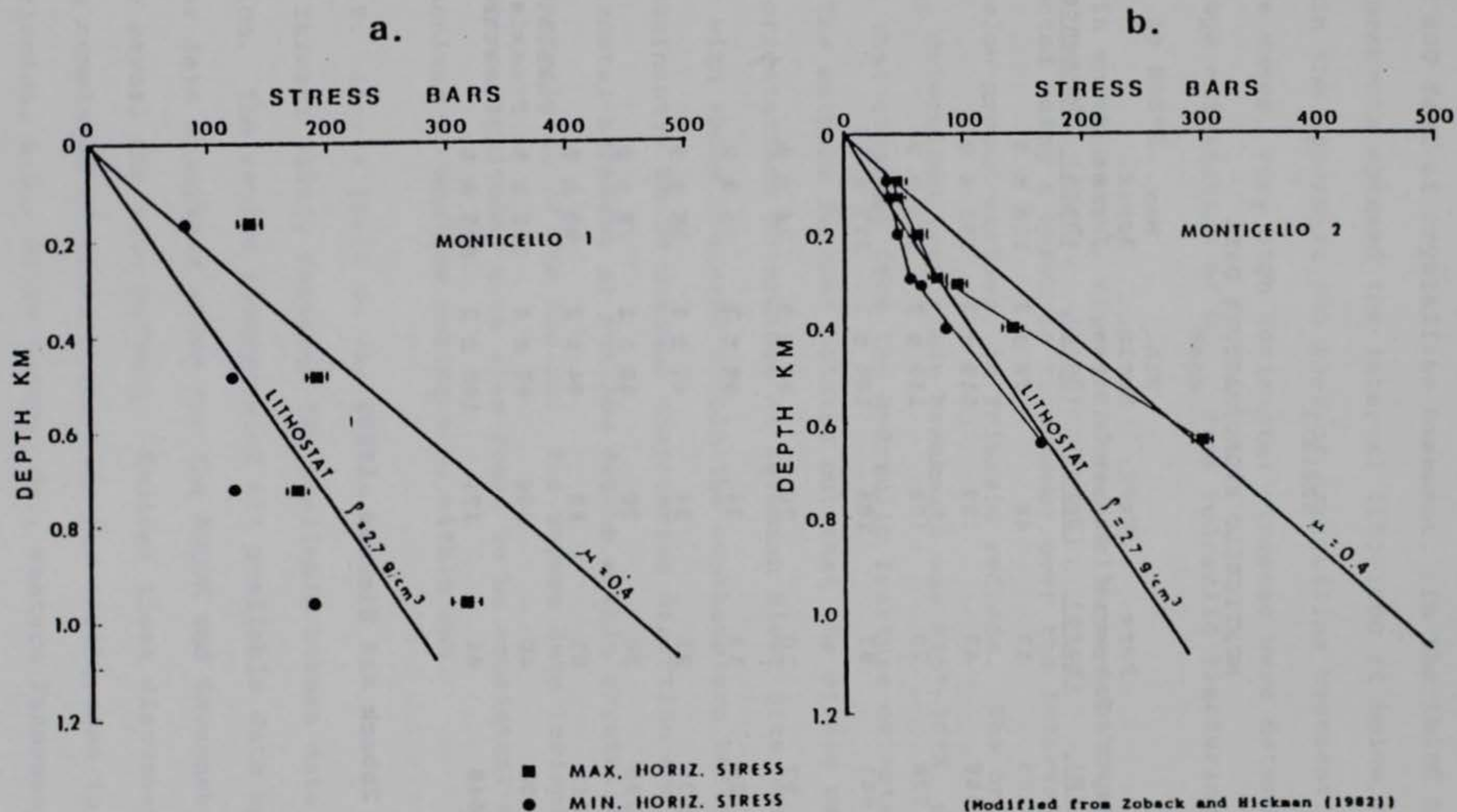


Figure 5. In-situ stress values at U.S.G.S. deep wells at Monticello Reservoir. The line labelled $\mu = 0.4$ represents the magnitude of S_{Hmax} required to initiate thrust faulting assuming a coefficient of friction of 0.4 and hydrostatic pore pressure. (From Talwani & Acree, 1987).

TABLE 2

MONTICELLO HYDROFRACTURE DATA

	<u>Depth (M)</u>	<u>Pore Pressure (Bars)</u>	<u>Vert. Stress (Bars)</u>	<u>Min. Horiz. Stress (Bars)</u>	<u>Max. Horiz. Stress (Bars)</u>	<u>Comments</u>
Mont. 1	165	17	44	79 \pm 2	135 \pm 9	
	486	49	129	119 \pm 2	193 \pm 9	
	728	73	193	119 \pm 2	173 \pm 9	
	961	97	255	186 \pm 2	317 \pm 13	
Mont. 2	97	10	26	34 \pm 2	44 \pm 9	
	128	13	34	36 \pm 2	45 \pm 9	
	205	21	54	47 \pm 2	58 \pm 9	
	298	30	79	56 \pm 2	75 \pm 9	
	312	31	83	64 \pm 2	95 \pm 9	
	400	40	106	87 \pm 2	142 \pm 9	Possible Preexisting Fracture
	646	64	171	166 \pm 2	305 \pm 9	

(Data from Zoback and Hickman, 1982)

most 400 feet of crystalline basement. In the third hole, measurements spanned the interval 1150-1800 ft below surface, within the uppermost 900 feet of crystalline basement. In all three cases, very high horizontal stresses were determined. The average orientation of S_{Hmax} from hydraulic fracturing measurement is N65°E.

In another well, stress-induced wellbore breakouts were detected using a borehole televiewer over the interval 1225-1325 ft below ground surface, in Triassic redbeds. The orientation of S_{Hmax} determined from these breakouts was N55°-70°E, consistent with that obtained from the hydraulic fracture orientations.

The authors further pointed out that the stress magnitudes and orientations determined at Savannah River Site were consistent with those measured within the southeastern United States--a predominantly NE-SW maximum compression direction and very high horizontal stresses at shallow depths within crystalline rock are characteristic of the region. The stress data (orientations and relative magnitude) were also found to be consistent with focal mechanisms of shallow earthquakes within SRS.

2.3.2. Stress field in the region

Talwani (1985) reviewed the available stress data in the region. The review incorporated all available data up to 1984. Newer data discussed above for the ADCOH and Savannah River Site also reveal the same pattern. Besides those discussed above, the data consisted of focal mechanisms for earthquakes in the Charleston, S.C., Giles County, Va., eastern Tennessee and Kentucky regions. All of the data suggest that the orientation of

S_{Hmax} in the region is oriented in the ENE-WSW to NE-SW directions.

2.3.3. *Conclusions*

Detailed data at reservoirs in the Piedmont and for other earthquakes in the region all suggest that the orientation of S_{Hmax} in the southeastern U.S. is oriented in a NE-SW to ENE-WSW direction. Where the magnitude of the stresses are available (e.g. Bad Creek, Monticello Reservoir, ADCOH site and Savannah River Site), the shallow stresses are very high and the data support the regional picture, i.e. the project lies in a compressional stress regime and that any seismicity will be a result of the interaction of this regional stress field on local zones of weakness. The observations of very high stresses in boreholes to depths of <1 km and relatively shallow seismicity in the Piedmont (<5 km) suggest an intriguing possibility. These observations suggest that the top portions of the crust associated with very high stresses is decoupled from a lower stress midcrust. If this is the case the shallow depth (with smaller fractures) limits the size of the largest earthquake in the area.

2.4. Conclusions

The STLA lies in the Piedmont physiographic province. A review of the geology and tectonics of the region shows that it consists of alternating belts of differing lithologies and metamorphic grades. No active faults are known to exist. Any seismicity that might result, would therefore be due to the interaction of high compressional stresses observed in the Piedmont on

pre-existing zones of weakness. The predominant zones of weakness in the Piedmont are networks of joints, thus limiting the size of the largest earthquake. We do not anticipate any earthquakes larger than the Union County event of 1913, i.e. 5.0 to 5.5 corresponding to MM intensity VII to VIII.

3. SEISMICITY

In this section we describe the historical and instrumental seismicity within each physiographic province in the region surrounding STL. Large felt earthquakes have occurred in the historical past. The most notable and the largest event (Modified Mercalli intensity (MMI) = X, magnitude (m_b) = 6.7) is the 1886 Charleston, South Carolina earthquake.

3.1 Historical and Instrumental Seismicity

The historical activity was studied by Bollinger (1973) who divided the felt activity from 1754 to 1970 into distinct seismic zones, with the southern Appalachian parallel and the central Virginia and South Carolina-Georgia seismic zones transverse to the Appalachian trend. Later Bollinger and Visvanathan (1977) extended the historical seismicity back to 1698 without a change in the pattern.

Recently Talwani (1989) reviewed the seismotectonics of the southeastern U.S. In a more comprehensive review, Bollinger and others (1988) have reviewed the seismicity of the southeastern U.S. from 1698-1986 for a forthcoming Decade of North American Geology (DNAG) volume. In the section below we present some of the important results relative to the tectonics of the region taken from that review.

Bollinger and others (1988) note that their catalog lists 1088 events (483 with $M > 3$) for the pre-network period, 1698-1977 (Figure 6). The most recent issue of the SEUSSN bulletin (Sibol and others, 1988) lists 806 events with $M > 0.0$ (Figure 7) (59 with $M > 3$, Figure 8) for the network period, July 1977 through June 1988. Bollinger and others (1988) further note that the historical seismicity was characterized by ". . . the decidedly non-random spatial distribution of epicenters with patterns that are parallel as well as oblique to the northeasterly tectonic fabric of the host region . . .". Seismicity was observed throughout the extent of the Appalachian highlands (south of 40° north), while the seismicity was observed in the Piedmont province only in Virginia, South Carolina and Georgia. Only the Coastal Plain of South Carolina was seismically active.

The instrumentally recorded seismicity lowered the detection threshold and allowed for more accurate locations. A comparison of the epicenters located by network monitoring (Figure 7) and the non-instrumental historical epicenters (Figure 6) shows that they both display the same general spatial patterns--some local clusters in the Piedmont and Coastal Plain, and an elongated trend along the Appalachian highlands. However, temporally we note some distinctions. To quote Bollinger and others (1988), ". . . modern seismic activity decreases are seen in the northern Virginia Appalachians and the South Carolina Piedmont while relative increases of seismicity have occurred recently in the northeastern Kentucky Plateau and on the southeastern Tennessee Appalachians . . .". Thus, in a time frame of a few hundred years,

Southeastern U. S. Seismicity: 1698 - 1977

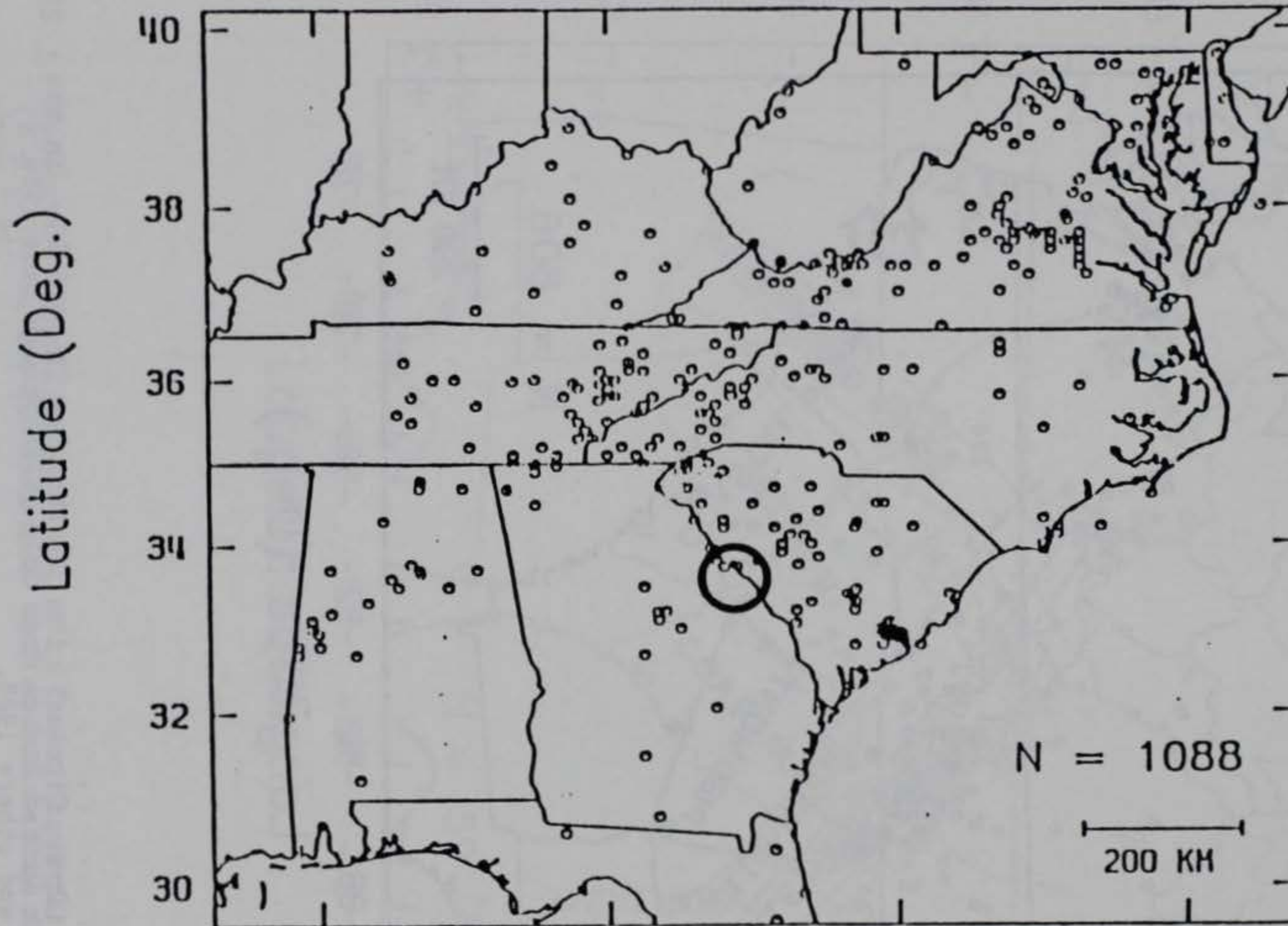


Figure 6. Historical seismicity of the southeastern U.S. (1698-1977). The open circles are the locations of the felt events. Solid circle is with 50 mile radius centered at STD (From Bollinger & others, (1988).

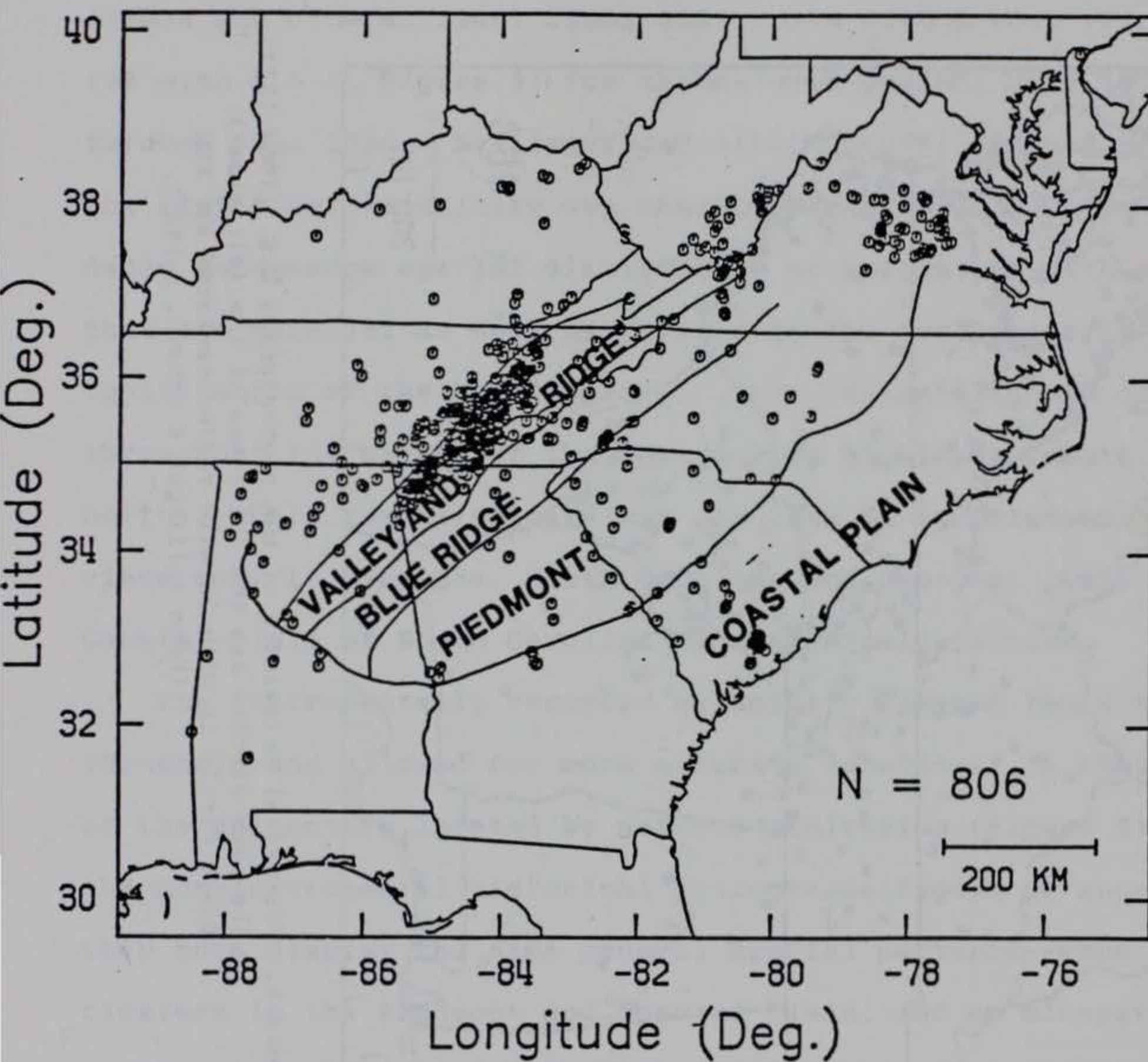


Figure 7 Epicenters (Open Circles) for Earthquakes ($M \geq 0.0$) in the Southeastern United States from July 1977 through June 1988. From Sibol and others 1988.

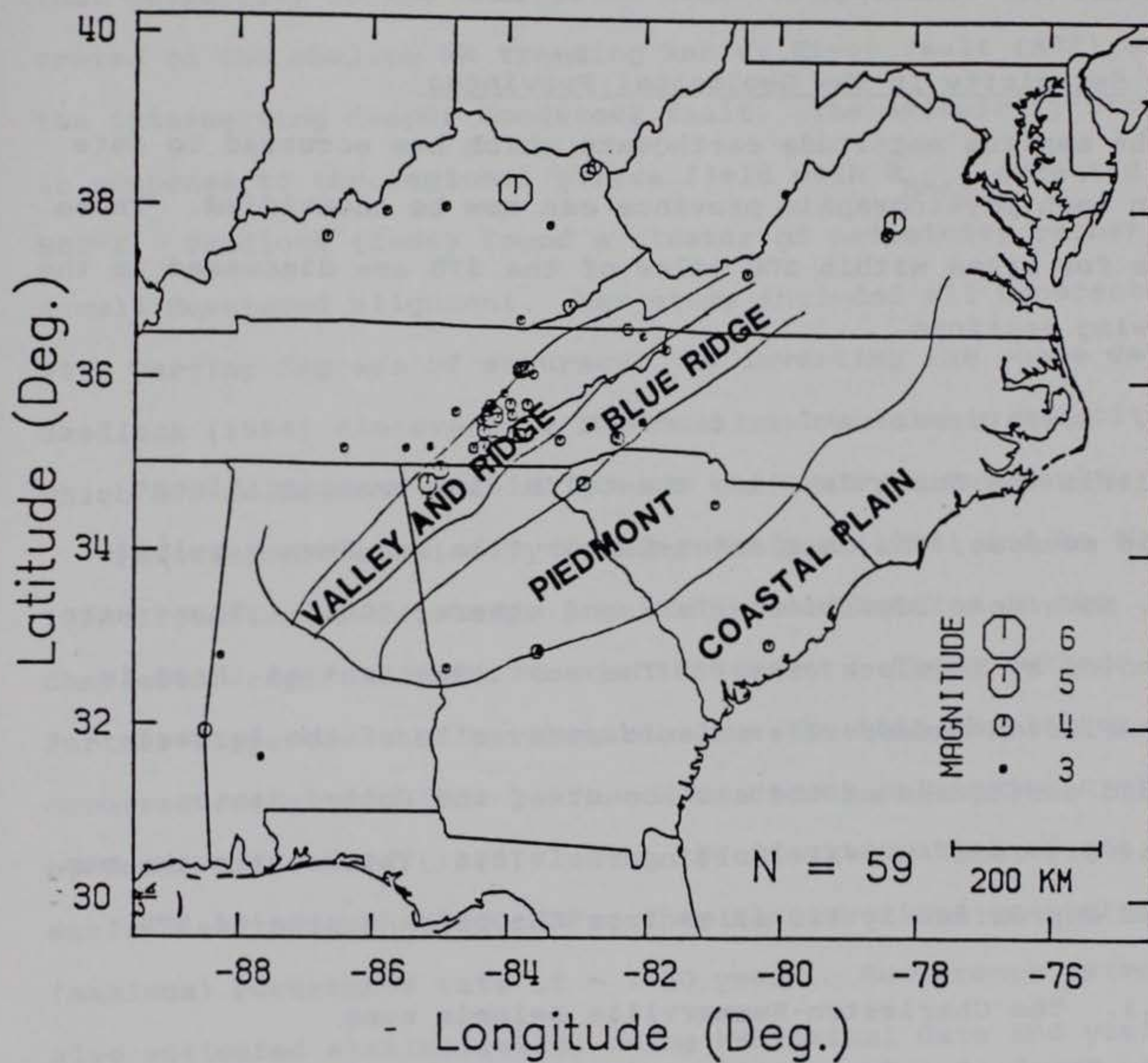


FIGURE 8 Epicenters (Open Circles - Scaled to Event Magnitude) for Earthquakes ($M \geq 3.0$) in the Southeastern United States from July 1977 through June 1988.
From Sibel and others 1988.

the seismicity is spatially stationary. For purposes of consideration of seismic hazard within the lifetime of critical facilities, the seismicity sources can be considered regionally fixed and not floating.

3.2. Seismicity in the Geological Provinces

The maximum magnitude earthquake which has occurred to date within each physiographic province can now be identified. These events for areas within 300 miles of the STD are discussed in the following sections.

3.2.1. *South Carolina Coastal Plain*

Within the South Carolina Coastal Plain, two significant seismic sources, the Charleston-Summerville and Bowman seismic zones, have been identified (Tarr and others, 1981). These were also noted by Shedlock (1988). The most important of these is the Charleston-Summerville seismic zone, site of the largest recorded earthquake on the east coast of the United States (August 31, 1886--MMI=X) (Bollinger, 1975). This earthquake was located approximately 120 miles from the present site of STD.

3.2.1.1. The Charleston-Summerville seismic zone

The Charleston-Summerville seismic zone has been the subject of multidisciplinary studies by the U.S. Geological Survey (Rankin, 1977; Gohn, 1983) and by the University of South Carolina. Talwani (1985) reviewed the various data and postulated models. Dewey (1985) reviewed the various hypotheses. Both authors described a general absence of consensus on the cause.

However, recent studies (Talwani, 1986; Lennon, 1985; Muthana and others, 1987; Poley and Talwani, 1986; Talwani and Cox, 1985) have supported the earlier suggestions by Talwani (1982) that seismicity in the Charleston-Summerville region was concentrated on the shallow NW trending Ashley River fault (ARF) and the intersecting deeper Woodstock fault. The seismicity occurs in response to the regional stress field with S_{Hmax} oriented $\sim N60^{\circ}E$. Shedlock (1988) found a cluster of seismicity rather than a well developed alignment. Her study included all hypocenters with varying degrees of accuracy. By inverting the phase data, Shedlock (1988) discovered a NW trend of low seismic velocities, which are coincident spatially with the Ashley River fault.

Paleoseismic studies by Talwani and Cox (1985) led to the identification of two large prehistoric earthquakes in the Charleston region similar to the 1886 event. These authors further suggested that earthquakes like the 1886 Charleston event occurred every 1500-1800 years. More recent paleoseismic studies by Weems and others (1986) led to the identification of one earlier earthquake ~ 7200 YBP. They also obtained an average (maximum) recurrence rate of ~ 1800 years. Recurrence rates were also estimated statistically, using historical data and yielded a return period of about 1600 years (Amick and Talwani, 1986).

Talwani (1986) reconciled all these observations in a seismotectonic model wherein the seismicity in the Charleston-Summerville area occurs at the intersection of the ARF and Woodstock faults, in response to a compressional stress regime with S_{Hmax} oriented ENE, where large events occur every ~ 1500 years.

3.2.1.2. The Bowman seismic zone

In a recently completed seismotectonic study of the Bowman seismic zone, located about 31 miles NW of the Charleston-Summerville seismic zone, Smith and others (1987) concluded that the low level of seismicity was occurring at the intersection of an unidentified NW trending feature with the ENE to EW trending border fault of a buried Triassic basin. None of the earthquakes, which began in the early 1970's, has exceeded magnitude 4.5.

3.2.1.3. Coastal Plain seismicity outside the Charleston-Summerville and Bowman seismic zones

The largest events in the Coastal Plain province outside the Charleston-Summerville and Bowman seismic zones occurred near Wilmington, N.C., in 1884 and 1958. They were assigned a MM intensity of V. The largest magnitude estimated for this zone is 5.0.

For estimating the seismically induced shaking at the project site, for events occurring in the Coastal Plain province, we therefore consider a MM intensity X in the Charleston-Summerville zone as the largest possible earthquake.

3.2.2. *Piedmont Province*

The largest recorded earthquake within the Piedmont physiographic province, in which the STLA lies, occurred in Union County, South Carolina, on January 1, 1913 (MMI=VII-VIII) (Bollinger, 1975). This event was assigned an epicentral intensity VIII on the Rossi Forrel scale by Taber (1913). It was located approximately 80 miles NNE of STD.

The Union County earthquake is the largest event to have occurred in the South Carolina Piedmont province. Its magnitude has been variously estimated as being 5.0 to 5.5. Geologically the estimated epicenter lies on the Kings Mountain shear zone.

Closer to the dam site, an earthquake (MMI=VI) occurred near Lincolnton, Ga., near the Georgia-South Carolina border on November 1, 1875, about 20 miles NW of STD. An earthquake with a maximum intensity of V was attributed in 1958 to Anderson, South Carolina, approximately 65 miles from the dam site.

A swarm of shallow microearthquakes, many of which were felt, occurred in the vicinity of Newberry, SC, located about 60 miles from STD. Two earthquake swarms that occurred there in 1982 and 1983 were studied by Rawlins (1985) who found that seismicity was possibly associated with the eastern flank of the buried Newberry granite pluton. The nature of the shallow seismicity--swarms, very shallow and low magnitude--is similar to reservoir induced seismicity and it is possible that a local stress concentration in the pluton may account for the observed activity.

3.2.3. *Blue Ridge and Valley and Ridge Provinces*

Currently, the most seismically active region in the southeastern United States is the southern Appalachian seismic zone (or the eastern Tennessee seismic zone) within the Blue Ridge and Valley and Ridge physiographic provinces (Figure 6). The largest event within this zone occurred in Giles County, Virginia, (maximum MMI=VIII) (Bollinger, 1975) on May 31, 1897. This event was located approximately 280 miles from STD. The greatest concen-

tration of recent seismicity (Figure 7) is located less than approximately 180 miles from the dam.

3.3. Reservoir Induced Seismicity

Reservoir induced seismicity has been well documented in at least four sites and strongly suggested to occur at two sites in the Piedmont province surrounding the STLA (Figure 9). The largest event at any of these sites has been less than magnitude 4.5 and the microearthquake activity has been characterized by the shallow depths and the swarm-like temporal character of the observed seismicity. The best studied cases of RIS occurred at Lakes Keowee and Jocassee upstream of the project site and at Monticello Reservoir in SC and Lake Sinclair in GA, east and west of the project site. A strong case has been made for RIS at the STLA (Section 5) and a possible case has been made for the current activity being observed at the Richard B. Russell Reservoir area. The latter site is upstream of the STLA. Thus the project site is one of the six locations of RIS in the Piedmont province of South Carolina and Georgia. The seismicity at these sites is discussed below.

3.3.1. *RIS in the Strom Thurmond Lake area*

The earliest suggestion of RIS in the STLA was made by Denman (1974). Continuous seismicity was observed in the vicinity of the STLA following a magnitude 4.3 earthquake in August 1974 (Talwani, 1976). Swarms of earthquakes lasting for several months were observed within about 2 miles from the reservoir. Excellent correlation was observed between the water level fluctuations and the ensuing activity. The observation that the

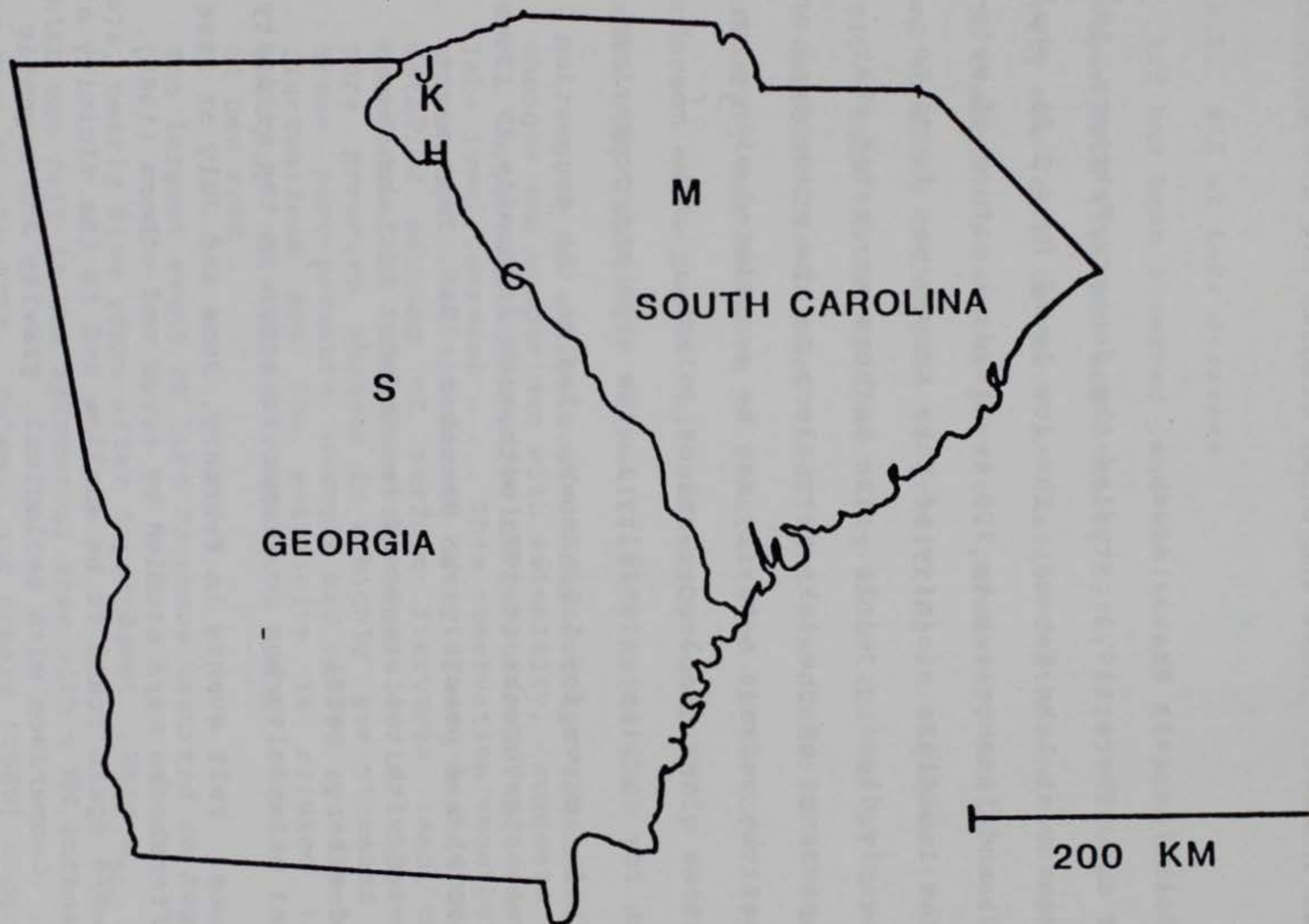


Figure 9. Locations of seismically active reservoirs in the region surrounding Lake Hartwell. The reservoirs are located with letters: J - Lake Jocassee, K - Lake Keowee, H - Lake Hartwell, M - Monticello Reservoir, C - Clark Hill Reservoir, and S - Lake Sinclair.

seismicity occurred 26 miles upstream of STD and 22 years after its impoundment led to the questioning of the suggestion that the activity was induced. These and other studies are discussed in Section 5.

3.3.2. *RIS in the Lake Keowee area*

Talwani and others (1979) studied the January-February, 1978, earthquake swarm at Lake Keowee. The low level ($M < 2.2$), shallow (< 3 km) and intense (up to 200 events/day) nature of seismicity in the immediate vicinity of Lake Keowee was found to occur on steeply dipping joints. The authors suggested that, ". . . The presence of the lake very close to the epicentral area suggests that the seismic activity may be associated with pore fluid migration along the larger set of joints . . .".

A search for earlier seismicity in the area and comparison with the filling curve for Lake Keowee, led to the suggestion that the Seneca earthquake of 1971 with a MM intensity IV (Sowers and Fogle, 1979) and possibly the December, 1969, felt event, were associated with two stages of impoundment of Lake Keowee (Talwani and others, 1979).

Low level seismicity has continued to occur in the vicinity of Lake Keowee. Felt events in February, June and July of 1986 and their aftershocks were studied by Acree and others (1988). The events were again found to be shallow and in the vicinity of Lake Keowee. Comparison with geological, gravity and magnetic data suggested that the seismicity was associated with a local shallow body rather than throughgoing faults. No correlation was evident between the lake level changes and the February 1986

events. However rapid fluctuations in water level did precede the event in June and July 1986 providing a possible triggering mechanism.

3.3.3. *RIS at Lake Jocassee*

RIS has been observed (and monitored) at Lake Jocassee since October 1975 (Talwani and others, 1976, 1978, 1980). The seismicity was found to occur at shallow depths and was associated with changes in various physical parameters and as such it was used to study techniques of predicting earthquakes (Talwani, 1981). Some of the salient facts about the RIS at Lake Jocassee are described in Talwani (1981) and are summarized here. The seismicity was found to be concentrated in the heavily fractured Henderson augen gneiss unit and was predominantly associated with strike slip faulting. Talwani (1981) noted that

" . . . An analysis of 10-day average lake levels and changes and comparison with seismicity, suggests that . . . larger earthquakes follow periods of rapid sustained lake level increase . . . This observation together with an analysis of the stress data, focal mechanisms and detailed mapping of surface fractures lead us to conclude that the observed seismicity is triggered by pore pressure changes in a highly pre-stressed rock. These pore-pressure changes are caused by lake level fluctuations and the seismicity is related to an existing network of fractures, rather than to breaking of new rock . . .".

The largest event at Lake Jocassee occurred on August 25, 1979, nearly five years after impoundment. This m_{bLg} 3.7 event, which was felt in the epicentral area with a MM intensity VI, was not felt in the STLA. Talwani and others (1980) suggested that the occurrence of this event was possibly associated with a rapid, sustained period of lake level changes.

3.3.4. *RIS at Monticello Reservoir*

Detailed studies of RIS at Monticello Reservoir commenced soon after its impoundment in December 1977. After intense seismicity following the impoundment, shallow ($< 2-3$ km) and low activity ($M \leq 2.8$) has gradually decreased. Even in 1989, an occasional $M 2+$ event is recorded, but the general pattern of activity is one of slow decrease (Figure 10). The seismicity is associated with shallow fractures in the vicinity of several plutons that have intruded into the country rock. (See Talwani and Acree (1987) for a detailed study of the RIS at Monticello Reservoir).

3.3.5. *RIS at Lake Sinclair, GA, and Richard B. Russell project sites*

Reservoir induced seismicity at Lake Sinclair, Ga., has been studied by Prof. L.T. Long and his students at the Georgia Institute of Technology. The seismicity was found to be shallow and occurred in swarms. No information is available as to possible association with lake level fluctuations.

After its initial impoundment of the Richard B. Russell Dam in late 1983, initially no seismicity was observed (L.T. Long, personal communication). Long (1986) located three events each in 1985 and 1986 which he suspected might have been induced. However recently we have located some events there, the magnitude 3.1 event in May 1987 being the largest. The studies of possible RIS at the Richard B. Russell site that have been carried out to date are lacking in detail and are basically inconclusive.

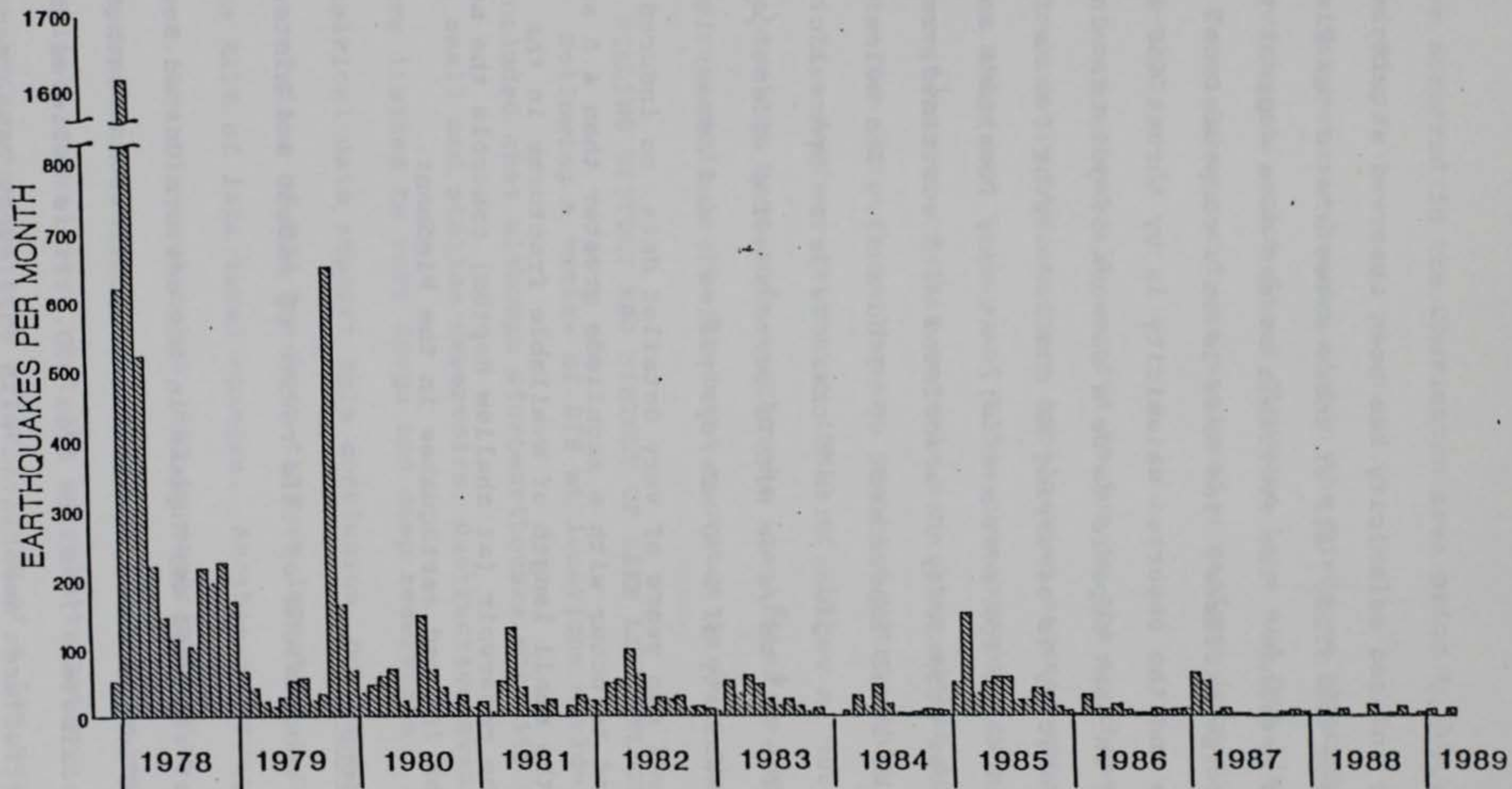


Figure 10. Earthquakes per month since impoundment of Monticello Reservoir in December 1977- March 1989.

3.3.6. *Conclusions*

Reservoir induced seismicity has been observed at six reservoirs including the STLA. All of these sites lie in the Piedmont physiographic province. The available stress data suggest the presence of large stresses. The area is in a compressional stress regime and the observed seismicity is by thrust and strike slip faulting on what appears to be a network of joints. In all cases the seismicity is occurring at shallow depths (<5 km for all events and <3 km for most events). At many locations and for many events, the seismicity is associated with sustained, rapid periods of lake level impoundment or withdrawal. The seismicity appears to occur in regions with a characteristic hydraulic diffusivity of $\sim 10^4 \text{ cm}^2/\text{s}$ or with a corresponding effective fracture permeability of 1-10 mDarcys (Talwani and Acree, 1985).

With several man years of very detailed data, no induced event was found to occur with a magnitude greater than 4.5 suggesting that the small length of available fractures in the vicinity of the reservoir (at shallow depths) controls the maximum size of the induced earthquakes in the Piedmont.

3.4. Conclusions

The major conclusions of this review of recent and historical seismicity are:

1. The largest recorded earthquake in the eastern United States (maximum MMI=X) occurred in 1886 near Charleston, South Carolina, approximately 75 miles from STD. It is believed that tectonic structures associated with this event have been identified and that possibly three other events of this

have occurred in the Charleston area prior to historical recording.

2. The largest earthquake within the Piedmont physiographic province, in which Strom Thurmond Lake and Dam lie, occurred at Union County and was assigned a maximum intensity (MMI) of VII-VIII.
3. The most seismically active region in the southeastern U.S. is currently the southern Appalachian seismic zone within the Blue Ridge and Valley and Ridge physiographic provinces. The closest extent of this seismic zone lies within 100 miles of STD. The largest earthquake recorded within this zone resulted in a maximum intensity (MMI) of VIII.
4. The maximum magnitude earthquake identified as triggered by any reservoir in the Piedmont province is less than 4.5.

4. FILLING HISTORY AND HISTORY OF LAKE LEVEL FLUCTUATIONS

Following a review of RIS at locations worldwide it was concluded that although microearthquake activity was observed at small and shallow reservoirs, destructive events ($M > 5.0$) were limited to very large and deep reservoirs. Although empirical data support this conclusion, our experiences in the studies of RIS has been that an important parameter is the RATE of lake level changes. Another observation has been, that in most cases, RIS is associated with the initial impoundment and is associated with a perturbation of the region's seismicity. But the seismicity pattern returns to the background pattern after a lapse of a few years, which may vary from about 5 to 20 years. A possible and important

exception to this has been the observed seismicity at the STLA, nearly 22 years after impoundment.

In this section we compare the size and lake level fluctuations at STL with Lakes Jocassee and Keowee and Monticello Reservoir, other locations of RIS, where these parameters have been monitored for over 10 years and also with Lake Hartwell (See also Table 3).

4.1. Lake Size

STL was filled during the years 1952-1954. Details of the initial filling history are not available. At a water elevation of 330 feet above sea level (a.s.l.) (top of the flood control gates) the lake covers approximately 70,000 acres with a capacity of approximately 2.0×10^6 acre-feet. The maximum height of the dam above the lowest foundation is about 200 ft (Corps of Engineers, 1978).

STL (70,000 acres) covers a significantly larger surface area than Lake Jocassee (7500 acres) or the Monticello Reservoir (6800 acres), two reservoirs with well documented histories of RIS. The reservoir capacity at STL ($2.0-2.5 \times 10^6$ acre-ft) is more than twice that of the deeper Lake Jocassee (1.16×10^6 acre-ft) and significantly greater than that of Monticello Reservoir (0.4×10^6 acre-ft) (Figure 9). These data are compared in Table 3.

4.2. Lake Level Fluctuations

Strom Thurmond Lake experiences seasonal water level fluctuations. The highest levels are generally recorded during the spring with levels decreasing during the summer and fall. The facility is designed for a maximum variation of 34 ft. However,

TABLE 3

Relative size of Reservoirs in the Piedmont

Lake	Surface Area X 10 ³ acres	Capacity X 10 ⁶ acre-ft	Maximum depth ft.
Hartwell	61.9	2.86	1390
Jocassee	7.5	1.16	3660
Monticello	6.8	0.4	1360
Strom Thurmond	70-78.5	2.0-2.5	2000*
Keowee	18.3	0.96	1440

* Near the epicentral region the maximum depth was less than 50 ft.

the maximum seasonal variation has been usually within 10 ft. In comparison, Lake Jocassee, a pumped storage facility, experiences normal water level variations of up to 10 ft, with a maximum drawdown of 15 ft during repairs to the dam. Lake levels at Monticello Reservoir, also a pumped storage facility, vary within a 5 ft range. Thus, seasonal variations at STL are in the same range, though slightly higher than variations at Lake Jocassee and Monticello Reservoir.

4.3. The Duration of RIS

Seismicity triggered by reservoir impoundment is currently believed to result from adjustments of the *in situ* stress field to increases in stresses (due to the water load) and pore pressures (predominantly due to diffusion from the reservoir) at hypocentral depths (Talwani and Acree, 1985). In time the stress field adjusts to the new conditions imposed by the reservoir and induced seismicity declines.

STL was impounded over 35 years ago, and the earliest seismograph were deployed in the area only in the early 1970's. Thus, no data exist concerning possible triggering of microearthquake activity associated with the initial reservoir impoundment. Based on experience at Lake Jocassee and Monticello Reservoir, it is expected that any seismic activity associated with the initial impoundment of STL would have declined toward the preimpoundment background level by this time.

Water level variations also perturb the stress field and can trigger seismicity (Talwani and Acree, 1985). As discussed in Section 3, the region around the lake exhibits a low level of

seismicity. Initially, the area was not sufficiently instrumented to detect any microearthquake activity that may have been triggered by lake level fluctuations (see also Section 5).

4.4. Conclusions

1. STL covers a larger surface area and reservoir capacity than other seismically active lakes (Jocassee and Monticello) in the region. The maximum depth at STL is within the range of depths of these other impoundments.
2. Water level fluctuations at STL are comparable to those experienced at impoundments which have triggered seismicity. Such fluctuations perturb the *in situ* stress field and can trigger seismicity in the immediate vicinity of the lake.
3. Due to the lack of instrumentation, the existence or extent of any microearthquake activity associated with impoundment of STL is unknown. However, studies in the last 15 years indicated that microearthquake activity was observed in the vicinity of the lake after deployment of suitable sensitive seismographs.
4. Induced seismicity triggered by the initial filling of STL is expected to have declined toward the background (natural) level of activity by now. Thus barring sudden large lake level changes (which exceed changes in the past) we would not expect any significant new RIS at STL. The occurrence of a magnitude 4.3 earthquake over 20 years after impoundment and over 40 miles from the dam suggests that the occurrence of similar earthquakes in the future cannot be ruled out.

5. SEISMICITY STUDIES IN THE STROM THURMOND LAKE AREA

The Strom Thurmond Lake area (STLA) has been a site of seismological studies for at least a decade and a half. Temporally, these studies can be divided into three parts: studies associated with the August 2, 1974, magnitude 4.3 earthquake (Section 5.2) and those that preceded it (Section 5.1.) and those that followed it (Section 5.3). The earliest studies were by Denman (1974). He was able to document the occurrence of microearthquake activity in the STLA at least since 1963 and noted that one of the largest earthquakes to occur in Georgia in historical times occurred near Lincolnton in 1875, located only 7 miles from the STLA. Immediately following the 1974 earthquake, aftershocks studies were carried out in the area. These were followed by detailed geological and geophysical investigations. In an attempt to understand the cause of the earthquakes, the very long sequence of aftershocks and the water level in the lake were monitored and correlations with the levels and the seismicity led to the suggestion that the seismicity was induced (Section 5.4). These aspects are described in some detail in the following sections.

5.1. Denman's Study

The earliest study of seismicity in the STLA was by Denman (1974). This section is taken from that study.

5.1.1. *The November 1, 1875, Lincolnton, Georgia, earthquake*

Historically (up to the time of Denman's study), Georgia had experienced only four events with Modified Mercalli intensity V or greater for which the epicenters were located within the state.

Of the two with MMI VI, one occurred on November 1, 1875 at 21:55 UTC. Based on sparse intensity data the epicenter was located in the Washington-Lincolnton area in eastcentral Georgia, about 6 to 8 miles West of the Savannah River and 18 miles NW of STD. The shock was reported to have been felt over an area of 25,000 square miles, and lasted approximately thirty seconds in the epicentral area. The earthquake was felt in Atlanta, Gainesville, Madison, Augusta, Macon and Savannah in Georgia, and at Spartanburg and Columbia in South Carolina (Figure 11). The shock was reported to have been followed by two or three felt aftershocks. As Bridges (1975) observed,

" . . . Prior to the installation of the Worldwide Standard Seismograph Station at ATL in 1963, events smaller than local magnitude 3.5 probably would not have been reported. Low level activity may possibly have been occurring in this area for many years. In this sparsely populated area such activity would likely have gone unnoticed, or have been passed off as large blasts from one of the numerous Elberton granite quarries. . . ."

5.1.2. *Other events in the STLA (1963-1974)*

Denman (1974) developed a technique to identify events in the STLA recorded at ATL. The minimum detection threshold was estimated at about local magnitude 1.8 ± 0.3 . On reviewing seismograph records at ATL, he discovered at least 15 events with local magnitudes ranging from 2.6 to 3.4 that occurred in the STLA between July, 1963, and July, 1974 (Table 4). Long (1974) also reported on about 40 events in the magnitude range 1.8 to 3.4 that occurred between April and August, 1969. This swarm included four of the 15 events mentioned earlier.

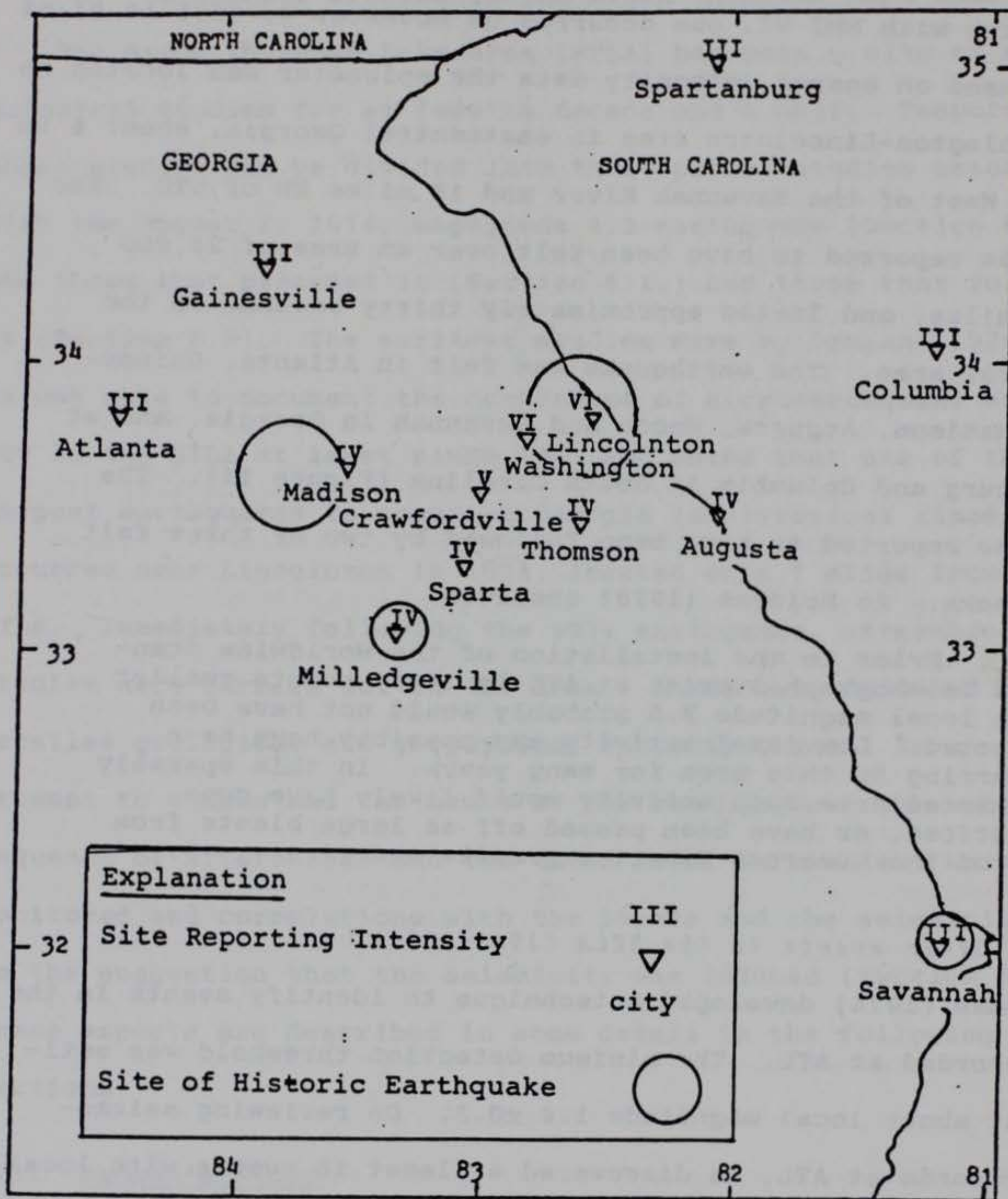


Figure 11. Intensities of November 1, 1875 earthquake and epicenters of earthquakes of intensities V or greater in Georgia.
From Denman, 1974.

Table 4. Catalog of Clark Hill Events,

July, 1963 Through July, 1974

Date	Time (GMT) P at ATL ⁺	S-P Seconds	Distance Kilometers ⁺⁺	M _{BLG}
7/04/74	02:18	21.60	192.4 ± 10	2.6
2/13/74	06:56	21.50	191.5 ± 10	2.7
10/08/73	13:38	21.30	189.7 ± 10	3.3
4/26/71	09:04	21.44	190.9 ± 10	2.7
4/16/71	07:31	21.22	188.9 ± 10	3.3
5/18/69	10:56	21.66	192.9 ± 10	3.2
5/18/69	10:54	21.65	192.8 ± 10	3.4
5/09/69	12:14	21.47	191.2 ± 10	3.2
5/05/69	22:39	21.60	192.4 ± 10	2.7
4/07/65	07:41	21.10	187.9 ± 10	3.5
4/06/65	21:19	19.36	172.4 ± 10	2.6
12/29/64	07:16	21.69	193.2 ± 10	3.2
12/28/64	17:33	21.83	194.4 ± 10	2.9
3/07/64	18:03	19.31	172.0 ± 10	3.6
10/07/63	06:02	21.04	187.4 ± 10	3.4

⁺P wave arrival at ATL to the nearest minute.⁺⁺Accuracy is ± 10 km based on a ± 0.1 sec error in the measured

S-P times.

(From Denman, 1974)

A review of Table 4 (after Denman, 1974, updated by Bridges, 1975) suggests that all of these events are not from the same epicentral area. The difference in arrival time of S and P waves (S-P times) recorded at ATL vary by as much as 2.52 s, or about 14 miles radially. However, these S-P times are clustered around 19.34 ± 0.02 s and 21.45 ± 0.4 s, suggesting two possible sources. The best located events in this period occurred on May 9, 1969 and on February 13, 1974 and were located at 33.79°N , 82.58°W and 33.62°N , 82.48°W respectively, with an accuracy of ± 6 miles (Denman, 1974). The 1969 event was located near Lincolnton, GA, whereas the 1974 event was located on the Little River, close to its junction with the Savannah River. That was also the location of two events on May 18, 1969, and one each on April 16, 1971, and April 4, 1965 (Figure 12).

5.1.3. *Microearthquake surveys (September, 1973-April, 1974)*

In order to better locate these earthquakes, Denman (1974) monitored the area with portable seismographs during the period September, 1973 to April, 1974. The instruments were moved around, but concentrated around two possible source zones (Figure 13). A total of 85 instrument days worth of data were collected, and 11 events were identified. According to Denman (1974), "Since single stations were used for most of the monitoring, these events can not be uniquely located. . .". The author suggested ". . . a possible common epicentral zone in southern Lincoln County. . .". A three station array was then set up to cover the Little River area. (In Figure 13, Little River is the boundary between Lincoln and Columbia counties.)

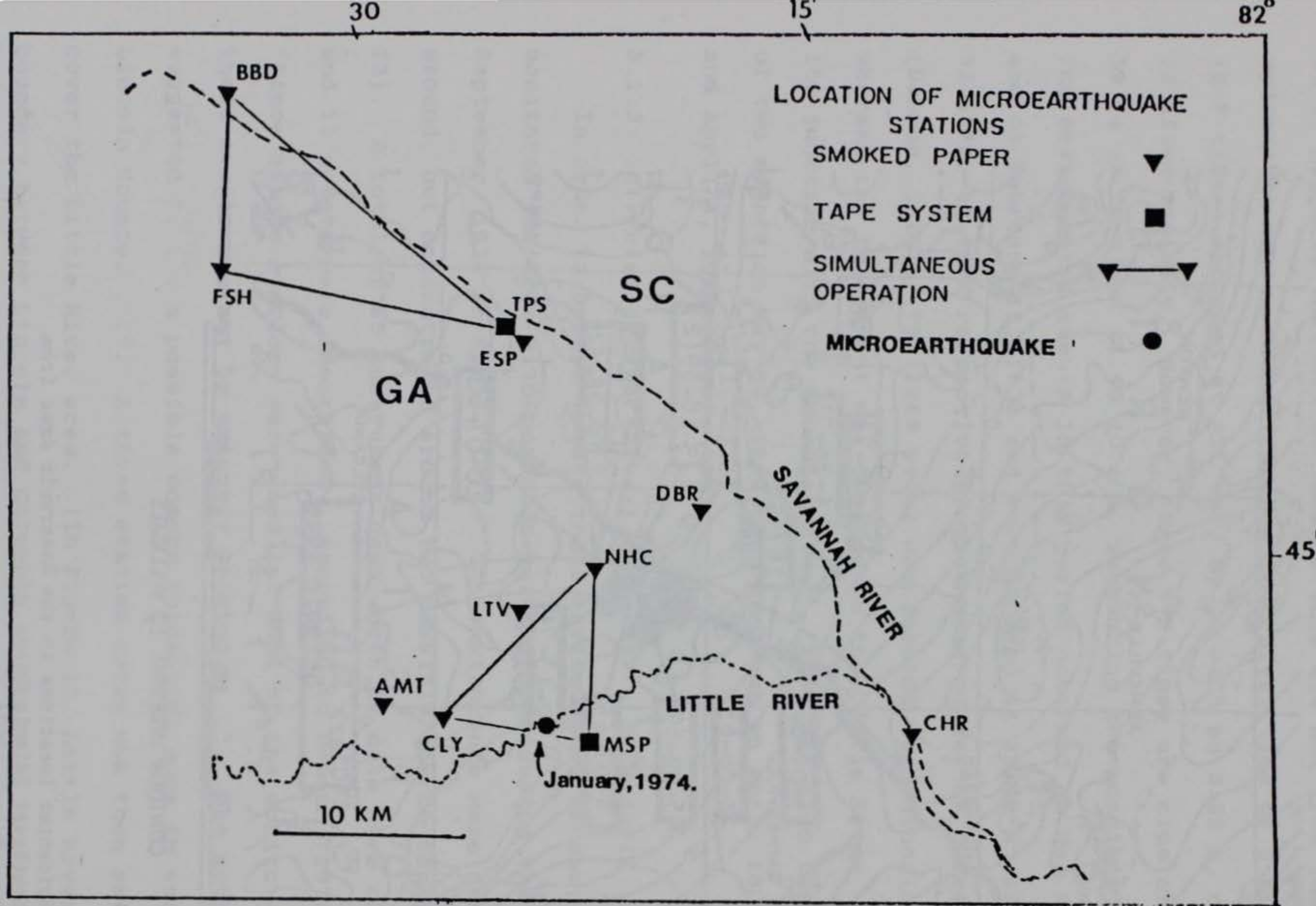


Figure 13. Locations of microearthquake stations occupied . Adapted from Denman 1974

5.1.3.1. The January 4, 1974, event

During the operation of the Little River array, one micro-earthquake was recorded on three stations on January 4, 1974. The epicenter was computed as $33^{\circ}39.63'N$ and $82^{\circ}24.12'W$ with ". . . a maximum probable error of ± 0.1 km . . .". This location falls over the Little River arm of the STLA (Figure 13). No depth was given, although Denman (1974) suggested a near surface focus of the event.

Interestingly, this location is to the ENE of poorly located events in southern Lincoln County (Section 5.1.2., above). These are the April 4, 1965, May 18, 1969, April 16, 1971 and February 13, 1974, events. Given the poor location accuracy of these events, Denman (1974) claims ± 10 km, it is possible that they also occurred in the epicentral area of the January 4, 1974, event.

5.2. The August 2, 1974, Earthquake

A Modified Mercalli intensity V earthquake hit the South Carolina-Georgia border in the STLA at 4:52am (EDST) on August 2, 1974. The epicenter (based on the location of aftershocks) was within about 1 mile of $33^{\circ}56.8'N$, $82^{\circ}29.75'W$ (Talwani and others, 1975). The location supplied by the National Earthquake Information Center (NEIC) $33^{\circ}52.32'N$, $82^{\circ}29.28'W$ placed the event in Georgia (Figure 14). NEIC assigned it a fixed depth of 1 km. The University of South Carolina epicenter is about 10 miles north of Lincolnton--the location of the 1875 MMI VI event.

This local magnitude 4.3 earthquake was felt over an area of nearly 15,000 square miles (Figure 15a, b). This early morning

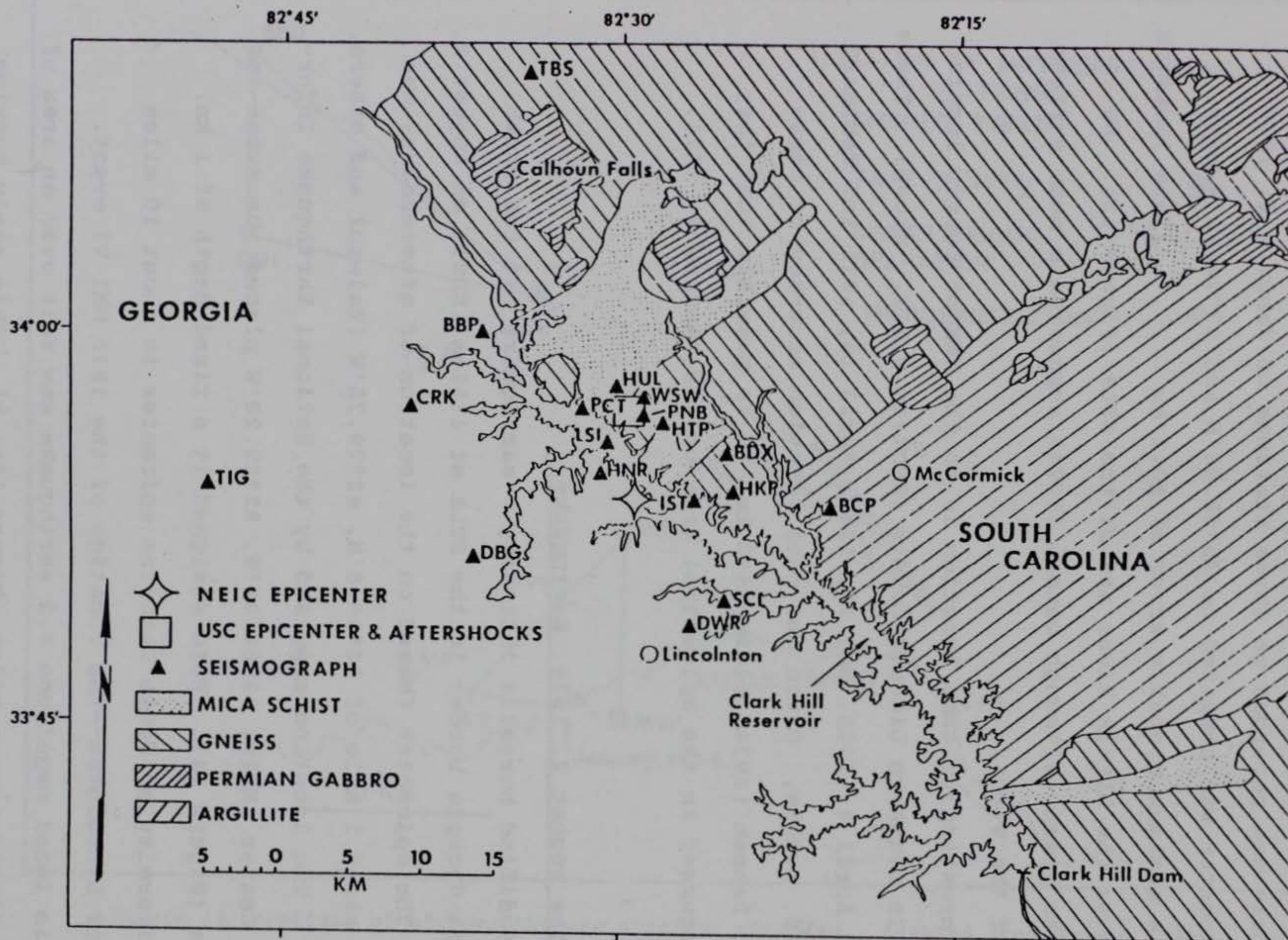


Figure 14. Simplified Geologic map of the epicentral region. Triangles indicate sites occupied by portable seismographs in August 1974 and March 1975. Water level data were obtained at Clark Hill Dam. Our epicentral location, based on aftershocks is shown by an open square.

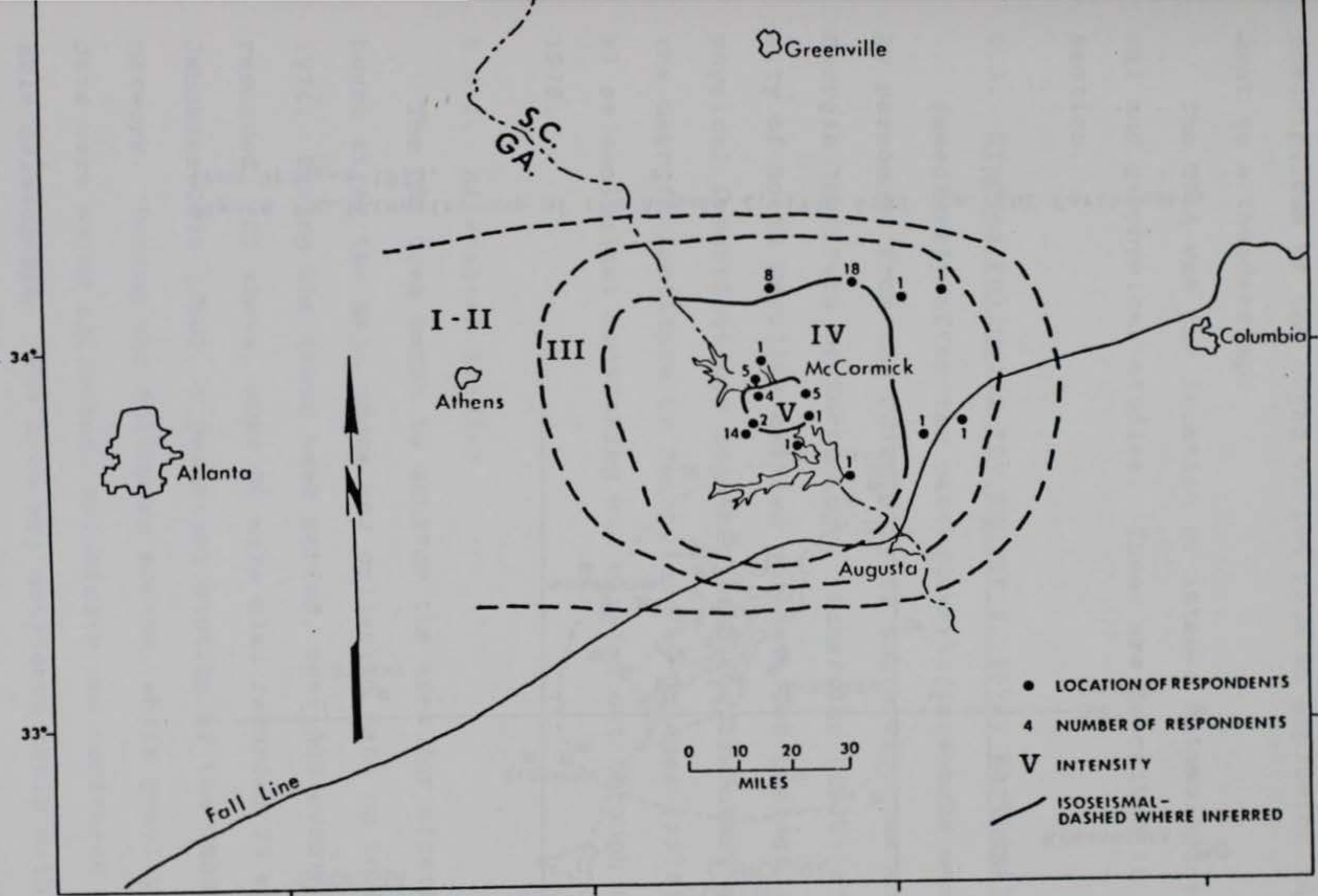


Figure 15a. Isoseismal map of August 2, 1974 earthquake. From Scheffler 1976

Figure 15b. Intensity Map of the August 2, 1974 4:52 a.m. EDT Earthquake.
From Bridges 1975.

earthquake was heard over a large area and the sound was most commonly described as that due to a passing freight train. Other descriptions of the sound varied from an explosion in the basement to a thunderclap.

The STLA was the location of intense seismological, geological and geophysical studies. These are described in the next section.

5.3. Studies Following the August 2, 1974, Earthquakes

Immediately after the earthquake, aftershocks were monitored by personnel from the University of South Carolina and the Georgia Institute of Technology. Scheffler (1976) at the University of South Carolina carried out detailed geological and geophysical investigations together with complementary studies at the Georgia Institute of Technology by Bridges (1975). Additional seismological monitoring was carried out through the summer of 1975.

5.3.1. *Aftershock studies*

The USC team began to monitor the area for aftershocks a few hours after the main shock and collected data up to August 21, 1974. During the three week period, over 500 events were recorded. Of these, over 20 were also recorded 75 miles away at Jenkinsville (JSC), a permanent station of the USGS-USC seismic network. During the following months, while gravity and magnetic data were being collected, seismicity was monitored on one portable seismograph. The area was monitored again with three to five portable seismographs for just over a week in March, 1975 and for about seven weeks in the summer of 1975. Over 1,000

events were recorded. Monitoring continued for another year using one portable seismograph.

Initially, the three station portable network which was supplemented by three stations from the Georgia Tech portable array was widely spaced. After detecting the initial seismicity, the stations were redeployed forming a tight network (Figure 14) in order to obtain more accurate hypocentral locations. The aftershocks occurred in a tight cluster near the station HUL, and their locations were taken to be the location of the main shock of August 2, 1974. The main shock had been located by NEIC using data from ATL and other permanent stations of the SC seismic network. The USC location was found to be about 4 miles to the north of the NEIC location (Figure 14). Both these locations were North of the two clusters identified by Denman (1974), and lay within the region of highest intensity (Figure 15a, b).

Bridges (1975) monitored the STLA with one or more (up to three) instruments intermittently for about 10 months. Continuous seismicity was recorded--hundreds of events were recorded, although relatively few were located.

The depths of the earthquakes recorded by Talwani and others, (1975), Talwani (1976) and Bridges (1975) were all shallow--usually in the top 2 km.

Bridges (1975) obtained estimates of the stress drop associated with the main event using various empirical relationships and typically got stress drops between 1 and 7 bars with one outlier at 12 bars. For a microearthquake with magnitude between 0 and 1, he obtained stress drops between 30 and 100 bars.

5.3.2 *Identification of the STLA earthquakes at JSC for the period January, 1974, to September, 1975*

As noted in the previous section, of the 500 events recorded in the epicentral area, over 200 were also identified at JSC--75 miles away. The clear S and P arrivals, characteristic S-P times and relationship between the duration and zero to peak shear wave amplitude at JSC (normalized at 60 db) was used to identify and ascribe magnitudes to the STLA event recorded at JSC. The threshold magnitude for an STLA event to be recorded at JSC was found to be about 1.5. In this period over 150 events with magnitudes greater than 1.5 were identified with the largest event, other than the August 2, 1974, event, having a magnitude 3.6. The seismic energy was calculated for each day and compared with lake levels (next section).

5.3.3 *Geological, geophysical and seismological studies*

The results of detailed geological studies in the area were compared with detailed gravity and magnetic data (Scheffler, 1976). These in turn were compared with hypocentral locations and focal mechanisms (Talwani, 1976).

The results of detailed geologic mapping in the immediate epicentral area led to the discovery of a shallow NE trending feature (Talwani, 1976). The seismicity was found to be concentrated in a small volume with an areal extent of $2 \times 3 \text{ km}^2$ and to a depth extent of 2 km (see the above mentioned reference for details). Composite focal mechanisms suggested normal and strike slip faulting on NE and NW trending nodal planes. No major faults were found, and it was concluded that the seismicity was

associated with NE and NW sets of joints in the affected volume-- located about 2 miles from STL. Using surface waves, Herrmann (1986) obtained a northwest striking almost vertical dip-slip fault solution.

5.4. Reservoir Induced Seismicity at the STLA

The earliest suggestion of RIS in the STLA came from Denman (1974) who compared the reservoir water levels for the years 1968 through 1974 with recorded seismicity (Figure 16). He noted two occasions where a change in water level of over 6 ft was followed within three to four weeks by microearthquakes. Peak reservoir levels in 1969 and 1971 were followed by a swarm of earthquakes during the summer of 1969 and by two microearthquakes in April, 1971. There were many other changes in the water level: however, if any microearthquakes followed, they were too small to be detected by ATL, about 120 miles away.

Figure 17, taken from Talwani (1975) is for the time period January, 1974, to September, 1975, and shows the daily water level at STD, average rainfall, and the number of seismic events at the STLA ($M_L \geq 1.5$) recorded at JSC (Section 5.3.2.) and the logarithm of the daily energy release associated with these events. We notice that low level seismic activity is present throughout this period, and appears to decrease slightly after the main shock (August 2, 1974) and its aftershocks. Except for the main shock and the period immediately following it, there are other times when the energy release exceeded the ambient level. These appear to be associated with rapid changes in water levels or rainfall exceeding one inch per day.

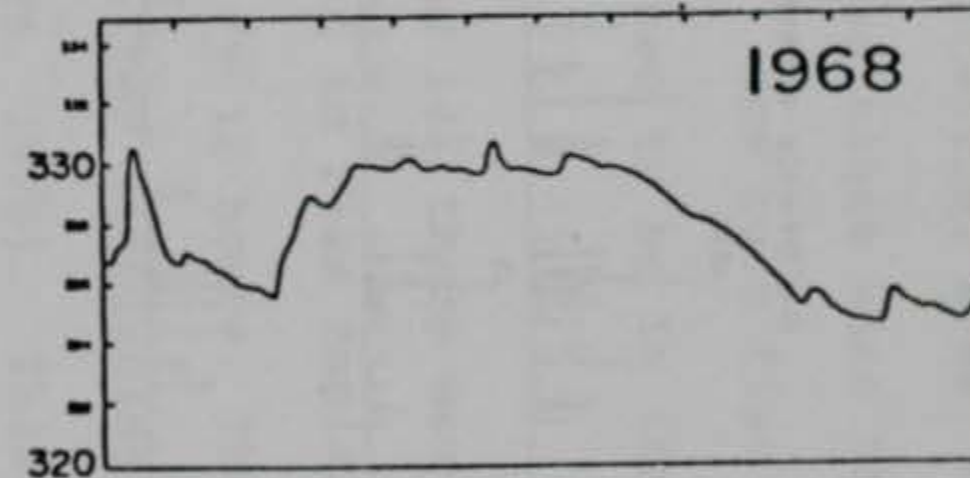
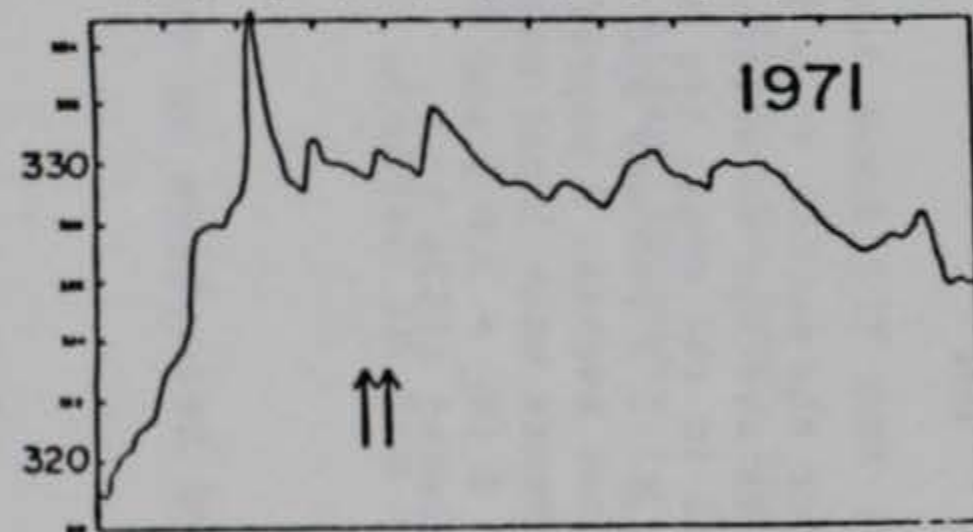
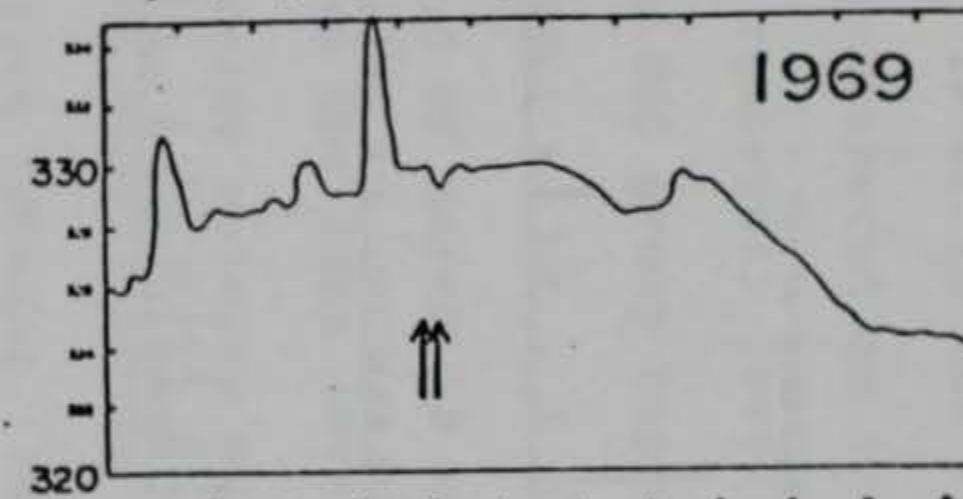
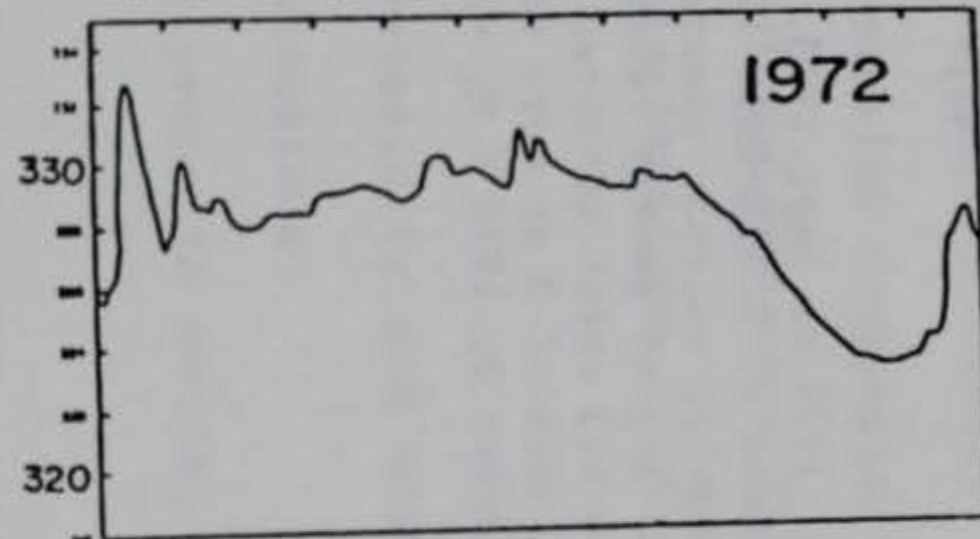
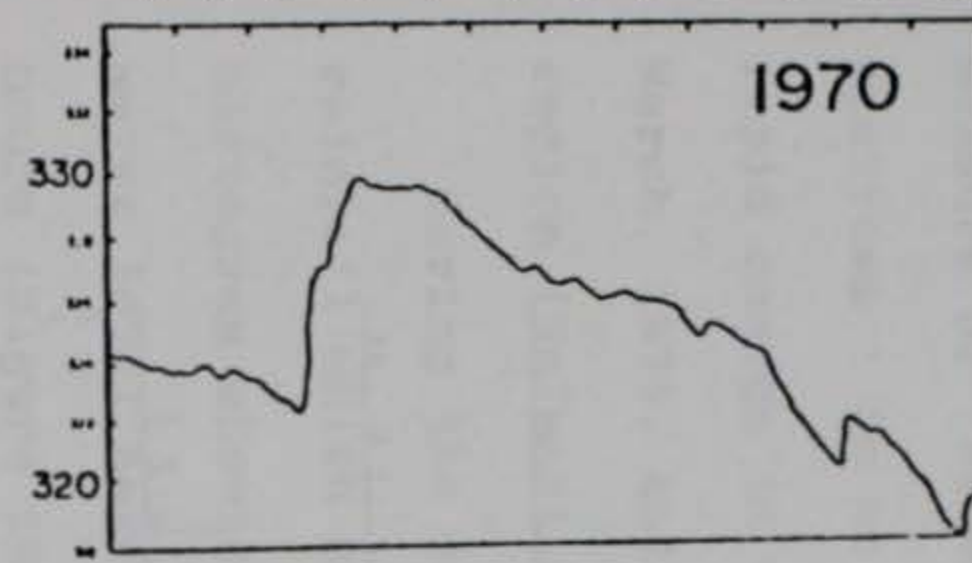
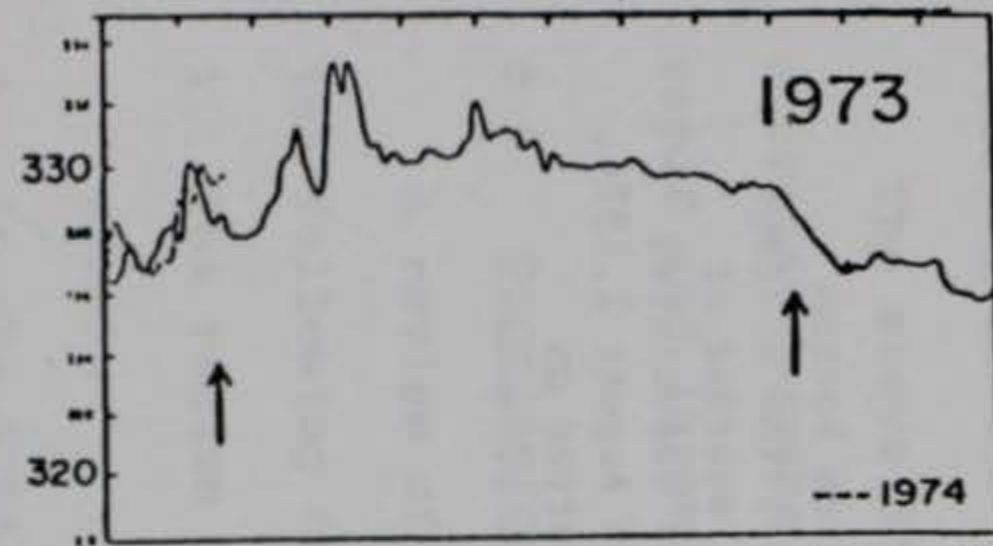


Figure 16. Clark Hill Reservoir Lake levels for 1968- 1974. Arrows represent times of earthquake occurrences. From Denman, 1974.

McCORMICK EVENTS RECORDED AT JSC

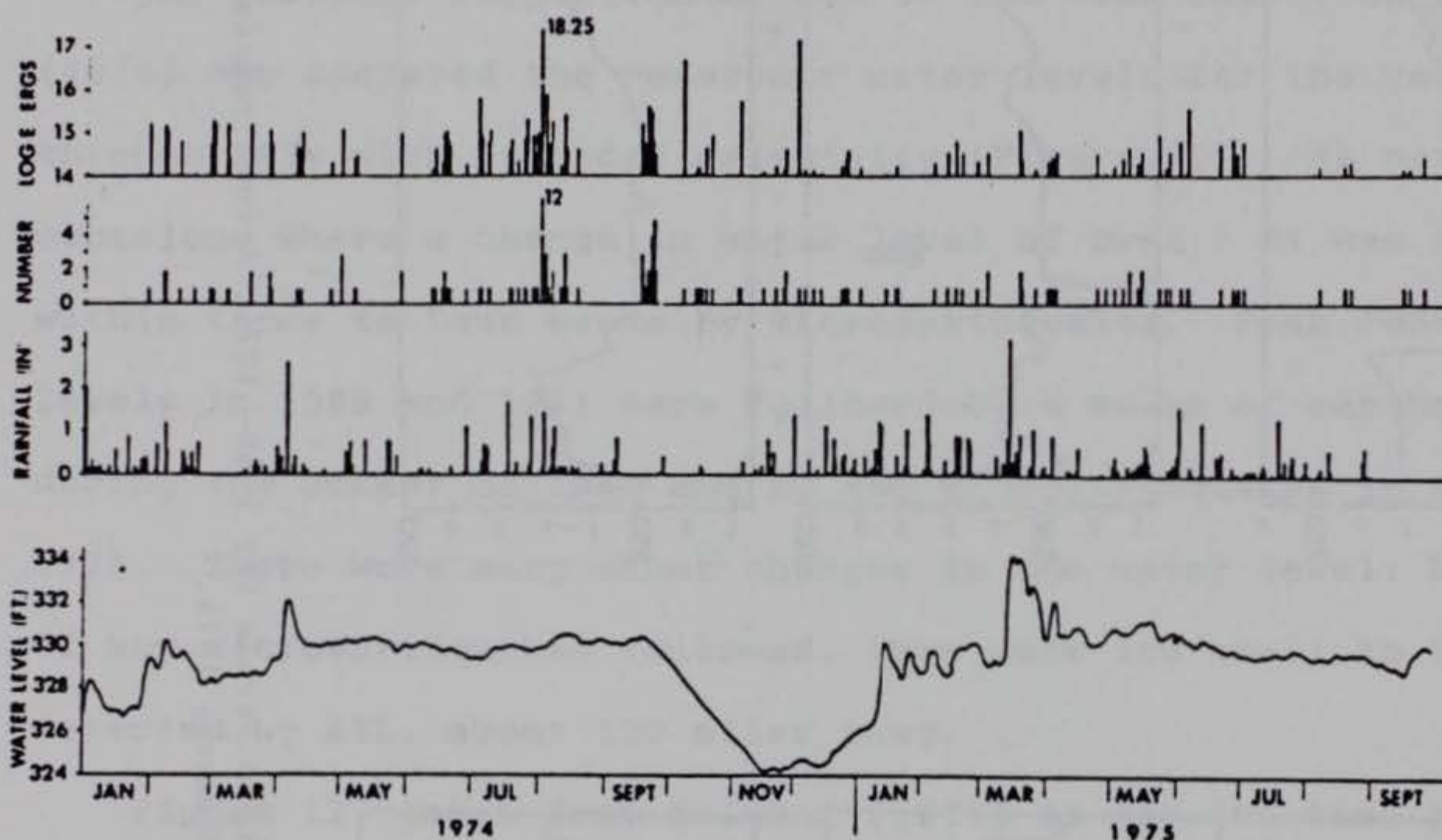


Figure 17. Data for the period from Jan. 1974 to Sept. 1975. From bottom up, shows average waterlevel data at Clark Hill Dam, the average rainfall in the area, the number of seismic events recorded at JSC ($M_L \geq 1.5$) per day and the log of energy release associated with those events. A magnitude 4.3 event occurred on August 2, 1974. Other events with local magnitudes of 3 or more occurred on October 8 ($M_L = 3.0$) and December 3, 1974 ($M_L = 3.6$). From Talwani (1976)

Two shocks with $M_L \geq 3.0$ occurred on October 8 and December 3, 1974. These events appear to follow sudden changes in the water level (Figure 17). Water levels at STD were not very good measure of the water level in the epicentral area, over 20 miles upstream. So we concentrated on those times when there was a rapid change in the reservoir level. One such time occurred in March, 1975, and the USC group happened to be in the epicentral region (Talwani, 1975).

During the period of March 13 and 14, there was very heavy rainfall which caused the lake levels to rise rapidly. On a histogram showing energy release every 12 hours, the curve for water level have been superimposed after displacing it by 46 hours (Figure 18), from Talwani, 1975, 1976). This figure indicates that the shallow seismicity followed the water level rise by about two days, and the energy released in the earthquake was related to the load (water level).

The above discussion suggests that some (if not most) of the microearthquake seismicity near the STLA has been induced by rapid and large fluctuations of the water levels.

5.5. Conclusions

A review of seismicity and other studies in the STLA leads to the following conclusions:

1. The region is prone to seismicity as evidenced by the 1875 event.
2. In the STLA there are two sources of seismicity--the northern cluster near the epicenter of the August 2, 1974, and Novem-

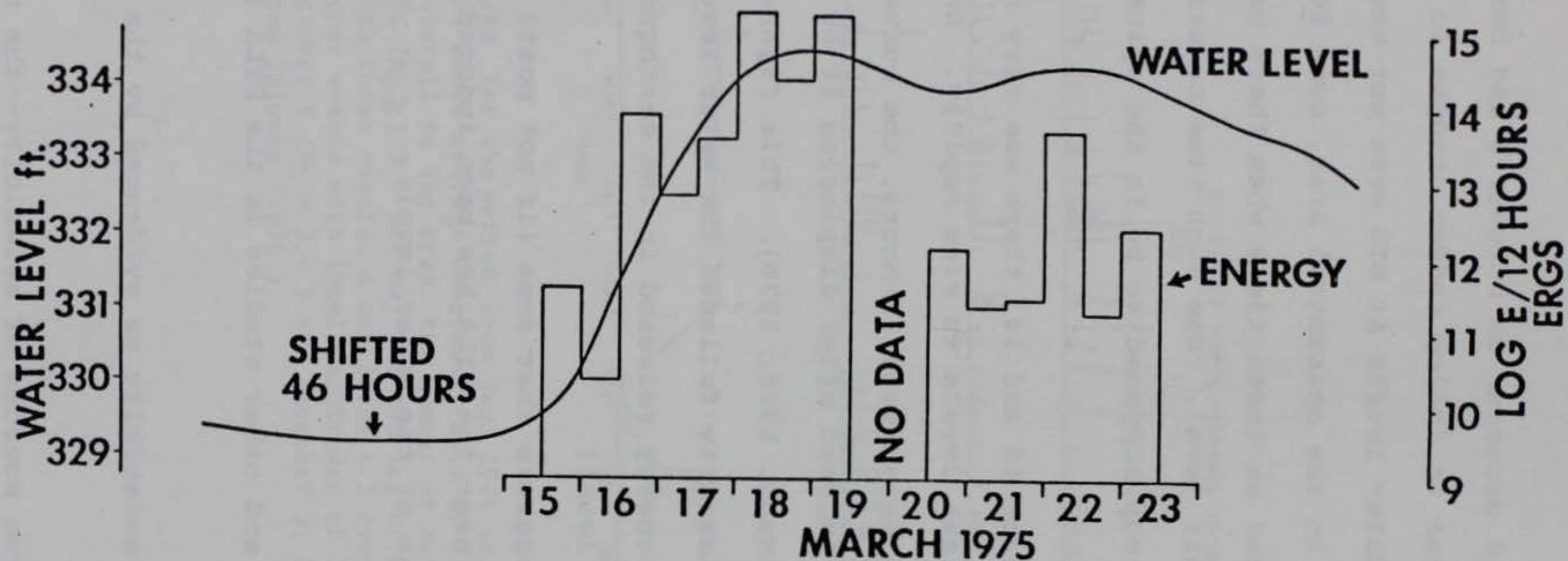


Figure 18. The water level data have been shifted 46 hours and superposed on a histogram showing the energy release every 12 hours. An excellent correlation is seen indicating that the energy release is related to the water level at an earlier time. From Talwani (1976).

ber 1875, events, and the southern cluster where the branch of the Little River meets the Savannah River.

3. Geophysical and geological data led to identification of the southern source zone as a part of the Modoc fault zone.
4. The best located events are shallow and lie in the top 3 km.
5. Several microearthquakes, both before and after the August 2, 1974, event appear to be induced and show temporal associates with large (and rapid) fluctuation of lake level.
6. The magnitude of these events are small. The largest event (M_L 4.3) is less than the largest event recorded for the Piedmont.
7. The shallow hypocentral depths, large horizontal stresses and the presence of historical seismicity leads to the possible conclusion that the induced seismicity is only a "hastening" process of natural seismicity that would have occurred at a later time.

6. SEISMIC POTENTIAL IN THE STLA

Although earthquakes have occurred in the STLA in the past one hundred years, we do not have a complete and uniform record of monitoring. Therefore, we cannot estimate accurately the nature of the seismicity by statistical techniques (from b-values). No active faults are known and therefore the technique of using fault dimensions or slip rates cannot be used. So we have to rely almost exclusively on historical and current instrumental data to estimate the seismic hazard. In this section we first discuss the earthquake potential in the project area and

then estimate the maximum intensity of seismically induced ground shaking that can be expected at the project site.

6.1. Distant Earthquakes Felt in the Area

Not only were the large events at Charleston in 1886, New Madrid in 1811-1812 and Giles County, Virginia in 1897 felt in the STLA, several lesser well known events were also felt. These include the Union County earthquake of 1913, with an epicentral MM intensity of VII-VIII, the Columbia, SC, event of July 1945, with an epicentral MM intensity of VI, and some events with MM intensities of VII-VIII in Charleston. The various earthquakes described above occurred in different tectonic provinces and their causes are not well understood. Besides these, the Lincoln, GA, MM intensity VI event on November 1, 1875, and the local magnitude 4.3 event of August 2, 1974, event occurred in the immediate vicinity of the STLA.

The studies described in Section 5 led to the conclusion that there were two possible seismic sources in the STLA--to the north where the November, 1875, and the August, 1974, events occurred and to the south. The southern zone of activity was identified by Talwani (1975) as being a part of the Modoc fault zone (Figure 19). (At that time the fault had been named the Goat Rock fault.) The seismicity along this very ancient and effectively "dead" fault zone is of a very low level--with all known events having magnitudes of 3 or less.

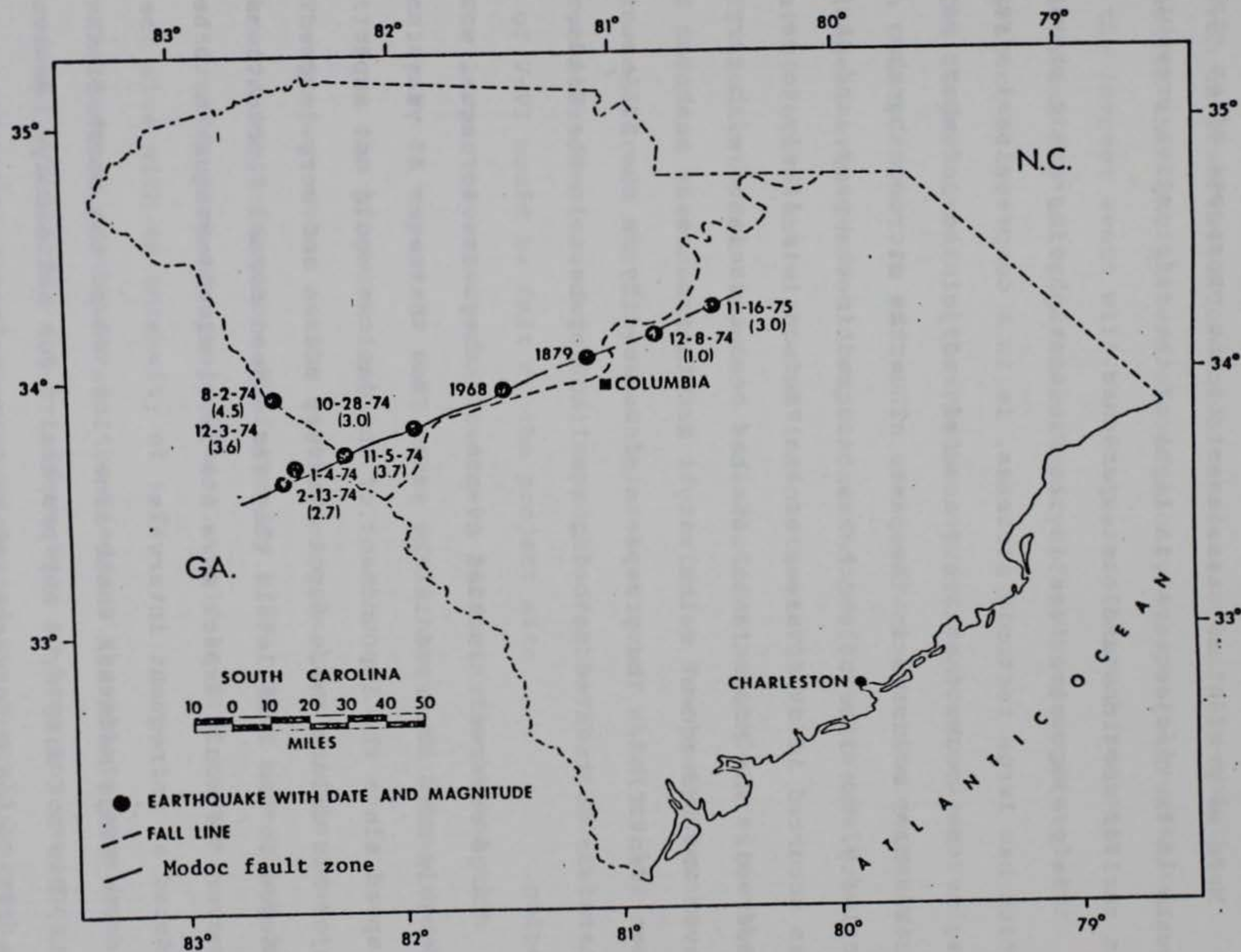


Figure 19. Modoc fault zone and associated earthquakes. Adapted from Talwani (1975)

6.2. Prospect of an Earthquake in the Project Area

Here we present our assessment of the prospects of an earthquake in the project area in light of the information presented in earlier sections and our experience.

The project site lies in the Piedmont physiographic province, which has large tectonic stresses, is in a compressional stress regime, has rocks that are fractured and jointed and where earthquakes have occurred in the past. Thus the microearthquake activity, the like of which has occurred in the past, and that has occurred in other areas of the Piedmont, is likely to be observed. The Modoc fault zone has been associated with very low level and infrequent seismicity. No other zones of weakness have been identified. The prospects of seismicity in the STLA must therefore be treated as being equal to anywhere in the Piedmont region.

Large reservoir induced events, if they were to occur, would probably have occurred in the past. Now that over 35 years have elapsed since the impoundment of the dam, we would not expect any major RIS unless there was to be very sudden and very large changes in the lake levels that far exceed normal fluctuations. However, we would expect more low level microearthquakes to be induced at infrequent intervals.

The Kings Mountain shear zone, located to the north of the STLA, has not displayed any propensity for seismicity. However, the 1913 Union County earthquake is suspected to have been associated with it. Therefore future activity on the Kings Mountain shear zone cannot be ruled out.

6.3. Maximum Earthquake

From an observation of the historical seismicity and the suggestion that the pattern of seismicity is spatially stationary, the largest event will be considered for each tectonic province and the anticipated intensity of shaking suggested for the project site.

The largest event in the Piedmont province occurred near Union County, S.C., in 1913. In our most conservative scenario, the largest event we would expect at the project site would be a repeat of this event with a MM intensity of VII-VIII.

In the next scenario would be a Piedmont event located on the Kings Mountain shear zone. Thus if the Union County earthquake was to reoccur on the Kings Mountain shear zone, which at its closest location is about 30 miles north of the STD, a MM intensity of V-VI would be felt at the project site.

The largest event at Charleston in 1886 was associated with intensity X. A repeat of that event would have a MM intensity of about VI at the project site.

The largest event in the southern Appalachian seismic zone has been associated with a MM intensity VIII. This zone which is over 150 miles from the project site, would be felt at the project site with an intensity of < VI.

The largest earthquake in the Piedmont thought to have been induced had a magnitude < 4.5. If we were to have any resurgence of RIS at the STLA, the largest anticipated event would be with a magnitude of 4.5 or less.

6.4. Conclusions

Although distant events have been felt in the STLA in the past, the prospect of a future large earthquake at the project site is comparable to any other location in the Piedmont, i.e. low. The most conservative estimate of the size of the maximum earthquake at the project site is an event equal in size to the Union County event, which is about a magnitude 5.0 to 5.5 with an epicentral intensity of VII-VIII.

7. SUMMARY AND CONCLUSIONS

In this report we presented a review of available data on the tectonics and seismicity data that could be used to assess the seismic potential in the STLA. The following conclusions were reached:

1. The project site lies in the Piedmont physiographic province, which consists of alternating belts of differing lithologies and metamorphic grades. In the absence of any active faults and a high compressional stress regime any seismicity would be due to the interaction of an ambient stress field on pre-existing zones of weakness. The predominant zones of weakness in the Piedmont are networks of joints, thus limiting the size of the largest earthquake.
2. The largest recorded earthquake in the eastern United States (maximum MMI=X) occurred in 1886 near Charleston, South Carolina, approximately 120 miles from the present dam at STL. It is believed that tectonic structures associated with this event have been identified and that possibly three other events of this magnitude have occurred in the Charleston area

prior to historical recording.

3. The largest earthquake within the Piedmont physiographic province, in which the STLA lies, occurred at Union County and was assigned a maximum intensity (MMI) of VII-VIII.
4. The most seismically active region in the southeastern U.S. is currently the southern Appalachian seismic zone within the Blue Ridge and Valley and Ridge physiographic provinces. The closest extent of this seismic zone lies within 120 miles of STD. The largest earthquake recorded within this zone resulted in a maximum intensity (MMI) of VIII.
5. The maximum magnitude earthquake identified as triggered by any reservoir in the Piedmont province is less than 4.5.
6. STL covers a larger surface area and reservoir capacity than other seismically active lakes (Jocassee and Monticello) in the region. The maximum depth at STL is within the range of depths of these other impoundments.
7. Water level fluctuations at STL are comparable to those experienced at impoundments which have triggered seismicity. Such fluctuations perturb the *in situ* stress field and can trigger seismicity in the immediate vicinity of the lake.
8. Earlier seismicity studies have identified two seismic sources in the STLA.
9. Induced seismicity triggered by the initial filling of STL is expected to have declined toward the background (natural) level of activity by now. Thus barring sudden large lake level changes (which exceed changes in the past) we would not expect any *significant* new RIS in the STLA, although we could get infrequent sequences of low level seismicity.

10. Although distant events have been felt at STL in the past, the prospect of a future large earthquake at the project site is comparable to any other location in the Piedmont, i.e. low. The most conservative estimate of the size of the maximum earthquake at the project site is an event equal in size to the Union County event, which is about a magnitude 5.0 to 5.5 with an epicentral intensity of VII-VIII.

8. REFERENCES

- Acree, S.D., Acree, J.R. and Talwani, P., 1988. The Lake Keowee, South Carolina, earthquakes of February through July 1986, *Seismological Research Letters*, 59, 63-70.
- Amick, D. and Talwani, P., 1986. Earthquake recurrence rates and probability estimates for the occurrence of significant seismic activity in the Charleston area: The next 100 years, *Proceedings of the Third U.S. National Conference on Earthquake Engineering*, 1, Earthquake Engineering Research Institute, pp. 55-64.
- Bell, J.S. and Gough, D.I., 1979. Northeast-southwest compressive stress in Alberta: Evidence from oil wells, *Earth and Planetary Science Letters*, 45, 475-482.
- Bobyarchick, A.R., 1981. The Eastern Piedmont Fault System and its relationship to Alleghanian tectonics in the Southern Appalachians, *Journal of Geology*, 89, 335-347.
- Bollinger, G.A., 1973. Seismicity of the southeastern United States, *Bulletin of the Seismological Society of America*, 63, 1785-1808.
- Bollinger, G.A., 1975. A Catalog of Southeastern United States Earthquakes, *Research Division Bulletin 101*, Dept. of Geological Sciences, Virginia Polytechnic Institute, Blacksburg, VA, 68 p.
- Bollinger, G.A. and Visvanathan, T.R., 1977. The seismicity of South Carolina prior to 1886, in Rankin, D.W., ed., *Studies Related to the Charleston, South Carolina, Earthquake of 1886 -- A preliminary report*, U.S. Geological Survey Professional Paper 1028, pp. 33-42.
- Bollinger, G.A., Johnston, A.C., Talwani, P., Long, L.T., Shedlock, K.M., Sibol, M.S. and Chapman, M.C., 1988. Seismicity of the southeastern U.S.--1698 to 1986: DNAG volume, in press.
- Bollinger, G.A., Sibol, M.S. and Mathena, E., 1984. Seismicity of the Southeastern United States, July 1, 1983-December 31, 1983, *Bulletin 13*, Seismological Observatory, Virginia Polytechnic Institute, Blacksburg, VA, 98 p.
- Bramlett, K.W., Secor, D.T., Jr. and Prowell, D.C., 1982. The Belair Fault: A Cenozoic reactivation structure in the Eastern Piedmont, *Geological Society of America Bulletin* 93, 1109-1117.
- Bridges, S.R., 1978. Evaluation of stress drop of the August 2, 1974, Georgia-South Carolina earthquake and aftershock sequence, Masters Thesis, Georgia Institute of Technology, 103 p.

- Carpenter, R.H., 1982. Slate belt of Georgia and the Carolinas: Geology, stratigraphy, structure and exploration potential, in Allard, G.O., and Carpenter, R.H., eds., *Exploration for Metallic Resources*, University of Georgia, Department of Geology, Center for Continuing Education, pp. 14-18.
- Clark, H.B., Costain, J.K. and Glover, L., III, 1978. Structural and seismic reflection studies of the Brevard ductile deformation zone near Rosman, North Carolina, *American Journal of Science*, 278, 419-441.
- Corps of Engineers, 1978. Final foundation report, Clarks Hill Dam, Savannah River, Georgia-South Carolina: Corps of Engineers, Savannah, GA, 28 p.
- Cook, F.A., Albaugh, D.S., Brown, L.D., Kaufman, S. and Oliver, J.E., 1979. Thin-skinned tectonics in the crystalline Southern Appalachians: COCORP seismic reflection profiling of the Blue Ridge and Piedmont, *Geology*, 7, 563-567.
- Coyle, B.J., Zoback, M.D. and Moos, D., 1986. *In situ* stress and fracture studies in the three ADCOH site survey core holes, *EOS Transactions, American Geophysical Union*, 67, 1242.
- Dallmeyer, R.D., Wright, J.E., Secor, D.T., Jr. and Snoke, A.W., 1986. Character of the Alleghanian orogeny in the southern Appalachians: Part II. Geochronological constraints on the tectonothermal evolutions of the eastern Piedmont in South Carolina, *Geological Society of America Bulletin*, 97, 1329-1344.
- Daniels, D.L., 1974. Geologic interpretation of geophysical maps, central Savannah River area, South Carolina and Georgia: U.S. Geological Survey, Geophysical Investigation Map GP-893, 1:250,000, 3 sheets.
- Denman, H.E., 1974. Implications of seismic activity at the Clarks Hill Reservoir, Masters Thesis, Georgia Institute of Technology, 103 p.
- Dennis, A.J., Sacks, P.E. and Maher, H.D., 1987. Nature of the Late Alleghanian strike-slip deformation in the eastern South Carolina Piedmont: The Irmo shear zone, in Secor, D.T., Jr., ed., *Anatomy of the Alleghanian orogeny as seen from the Piedmont of South Carolina and Georgia: Carolina Geological Society fieldtrip guidebook for 1987*, South Carolina Geological Survey, pp. 49-66.
- Dewey, J.W., 1985. A review of recent research on the seismotectonics of the southeastern seaboard and an evaluation of hypotheses on the source of the 1886 Charleston, South Carolina, earthquake: U.S. Nuclear Regulatory Report, NUREG/CR-4339, 45 p.

- Department of Energy, 1984. Southeastern regional geologic characterization report: Volume 1: U.S. Department of Energy, DOE/CH-6(1), 474 p.
- Edleman, S.H., Liu, A. and Hatcher, R.D., Jr., 1987. The Brevard zone in South Carolina and adjacent areas: An Alleghanian orogen scale dextral shear zone reactivated as a thrust fault, *Journal of Geology*, 95, 793-806.
- Fullagar, P.D., 1971. Age and origin of plutonic intrusions in the Piedmont of the southeastern Appalachians, *Geological Society of America Bulletin*, 82, 2845-2862.
- Fyfe, W.S., Price, N.J. and Thompson, A.B., 1978. *Fluids in the Earth's Crust*, Elsevier, Amsterdam, 383 p.
- Gohn, G.S., ed., 1983. Studies related to the Charleston, South Carolina, earthquake of 1886--Tectonics and seismicity: U.S. Geological Survey Professional Paper 1313, 375 p.
- Griffin, V.S., Jr., 1970. Position of the Kings Mountain belt in Abbeville County, South Carolina, *Southeastern Geology*, 12, 105-113.
- Griffin, V.S., Jr., 1974. Analysis of the Piedmont in northwest South Carolina, *Geological Society of America Bulletin*, 85, 1123-1131.
- Griffin, V.S., Jr., 1981. The Lowndesville belt north of the South Carolina-Georgia border in Horton, J.W., Jr., Butler, J.R., and Milton, D.J., eds., *Geological Investigations of the Kings Mountain Belt and Adjacent Areas in the Carolinas*, *Carolina Geological Society Field Trip Guidebook for 1981*, South Carolina Geological Survey, pp. 166-173.
- Haimson, B.D., 1975. Hydrofracturing stress measurements, Bad Creek Pumped Storage project: Report for Duke Power Company, 19 p.
- Hatcher, R.D., Jr., 1970. Stratigraphy of the Brevard zone and Poor Mountain area, northwestern South Carolina, *Geological Society of America Bulletin*, 81, 933-940.
- Hatcher, R.D., Jr., 1972. Developmental model for the southern Appalachians, *Geological Society of America Bulletin*, 83, 2735-2760.
- Hatcher, R.D. Jr., 1978. Tectonics of the western Piedmont and Blue Ridge, southern Appalachians: Review and speculation, *American Journal of Science*, 278, 276-304.
- Hatcher, R.D., Jr., 1987. Tectonics of the southern and central Appalachian internides, *Annual Reviews of Earth and Planetary Science*, 15, 337-362.

- Hatcher, R.D., Jr., Howell, D., and Talwani, P., 1977. Eastern Piedmont Fault System: Speculation on its extent, *Geology*, 5, 636-640.
- Herrmann, R.B., 1986. Surface-wave studies of some South Carolina earthquakes, *Bulletin of the Seismological Society of America*, 76, 111-122.
- Horton, J.W., Jr., 1981. Geologic Map of the Kings Mountain Belt between Gaffney, South Carolina, and Lincolnton, North Carolina, *in* Horton, J.W., Jr., Butler, J.R., and Milton, D.J., eds., *Geological Investigations of the Kings Mountain Belt and Adjacent Areas in the Carolinas*, Carolina Geological Society Field Trip Guidebook for 1981, South Carolina Geological Survey, pp. 6-18.
- Horton, J.W., Jr. and Butler, J.R., 1977. Guide to the geology of the Kings Mountain belt in the Kings Mountain area, North Carolina and South Carolina, *in* Burt, E.R., ed., *Field Guide for Geological Society of America*, Southeastern Section Meeting, Winston-Salem, North Carolina: North Carolina Dept. Natural and Economic Resources, Geology and Mineral Resources Section, pp. 76-143.
- Horton, J.W., Jr., Butler, J.R., Schaeffer, M.F., Murphy, C.F., Connor, J.M., Milton, D.J. and Sharp, W.E., 1981. Field guide to the geology of the Kings Mountain belt between Gaffney, South Carolina and Lincolnton, North Carolina, *in* Horton, J.W., Jr., Butler, J.R., and Milton, D.J., eds., *Geological Investigations of the Kings Mountain Belt and Adjacent Areas in the Carolinas*, Carolina Geological Society Field Trip Guidebook for 1981, South Carolina, Geological Survey, pp. 213-247.
- Horton, J.W., Jr., Sutter, J.F., Stern, T.W. and Milton, D.J., 1987. Alleghanian deformation, metamorphism and granite emplacement in the central Piedmont of the Southern Appalachians, *American Journal of Science*, 287, 635-660.
- Lennon, G., 1985. Identification of a northwest trending seismogenic graben near Charleston, South Carolina, Masters Thesis, Columbia, University of South Carolina, 92 p.
- Long, L.T., 1974. Earthquake sequence and b values in the southeast United States, *Bulletin of the Seismological Society of America*, 64, 267-273.
- Long, L.T., 1986. Georgia/Alabama regional seismographic network, annual report August, 1985-June 1986, prepared for the U.S. Nuclear Regulatory Commission, pp. 33 p.

- Maher, H., 1978. Stratigraphy and structure of the Belair and Kiokee belts near Augusta, Georgia, *in* Snoke, A.W., ed., *Geological Investigations of the Eastern Piedmont, Southern Appalachians*, South Carolina Geological Survey, Carolina Geological Society Guidebook for 1978, pp. 47-54.
- Maher, H., 1979. The Belair belt of South Carolina and Georgia: Stratigraphy and depositional regime as compared to the Carolina Slate belt, *Geological Society of America Abstracts with Programs*, 11, 187.
- Maher, H.D., Jr., 1987. Kinematic history of mylonitic rocks from the Augusta fault zone, South Carolina and Georgia, *American Journal of Science*, 287, 795-816.
- Muthanna, A., Talwani, P. and Colquhoun, D.J., 1987. Preliminary results from integration of stratigraphic and geophysical observations in the central South Carolina Coastal Plain, *Seismological Research Letters*, 58, 102.
- McGarr, A. and Gay, N.C., 1978. State of stress in the Earth's crust, *Annual Review of Earth and Planetary Science*, 6, 405-436.
- Poley, C.M. and Talwani, P., 1986. Recent vertical crustal movements near Charleston, South Carolina, *Journal of Geophysical Research*, 91, 9056-9066.
- Prowell, D.C. and O'Connor, B.J., 1978. Belair fault zone: Evidence of Tertiary fault displacement in eastern Georgia, *Geology*, 6, 681-684.
- Rankin, D.W., ed., 1977. Studies related to the Charleston, South Carolina, earthquake of 1886--A preliminary report: U.S. Geological Survey Professional Paper 1028, 204 p.
- Rastogi, B. K. and Talwani, P., 1984. Reservoir-induced seismicity at Lake Jocassee in South Carolina, USA, *in* Gowd, T. N., ed., *Proceedings of Indo-German Workshop on Rock Mechanics*, N.G.R.I., Hyderabad, India, pp. 225-232.
- Rawlins, J., 1986. Seismotectonics of the Newberry, South Carolina earthquakes, Masters Thesis, Columbia, University of South Carolina, 68 p.
- Rozen, R.W., 1981. The Middleton-Lowndesville cataclastic zone in the Elberton East quadrangle, Georgia, *in* Horton, J.W., Jr., Butler, J.R. and Milton, D.J., eds., *Geological Investigations of the Kings Mountain Belt and Adjacent Areas in the Carolinas*, Carolina Geological Society Fieldtrip Guidebook for 1981, South Carolina Geological Survey, pp. 174-180.

- Sbar, M.L. and Sykes, L.R., 1973. Contemporary compressive stress and seismicity in eastern North America: An example of intraplate tectonics, *Geological Society of America Bulletin*, 84, 1861-1881.
- Schaeffer, M.F., Steffans, R.E. and Hatcher, R.D., Jr., 1979. *In situ* stress and its relationship to joint formation in the Toxaway gneiss, northwestern South Carolina, *Southeastern Geology*, 20, 129-143.
- Scheffler, P.K., 1976. The McKormick County, South Carolina, earthquake of 2 August, 1974: Geological and Geophysical investigations, Masters Thesis, Columbia, University of South Carolina, 65 p.
- Secor, D.T., Jr., 1987. Regional Overview, *in* Secor, D.T., Jr., ed., *Anatomy of the Alleghanian Orogeny as Seen from the Piedmont of South Carolina and Georgia*, Carolina Geological Society Fieldtrip Guidebook for 1987, South Carolina Geological Survey, pp. 1-18.
- Secor, D.T., Jr., Samson, S.R., Snoke, A.W. and Palmer, A.R., 1983. Confirmation of Carolina Slate belt as an exotic terrane, *Science*, 221, 649-651.
- Secor, D.T., Snoke, A.W., Bramlett, K.W., Costello, O.P. and Kimbrell, O.P., 1986. Character of the Alleghanian orogeny in the Southern Appalachians: Part I. Alleghanian deformation in the eastern Piedmont of South Carolina, *Geological Society of America Bulletin*, 97, 1319-1328.
- Shedlock, K.M., 1988. Seismicity in South Carolina, *Seismological Research Letters*, 59, 165-172.
- Sibol, M.S., Bollinger, G.A. and Mathena, E., 1987. Seismicity of the Southeastern United States, January 1, 1987-July 31, 1987: Bulletin 20, Seismological Observatory, Virginia Polytechnic Institute, Blacksburg, VA, 84 p.
- Sibol, M.S., Bollinger, G.A. and Mathena, E.C., 1988. Seismicity of the southeastern United States, January 1, 1988-June 30, 1988, *Southeastern U.S. Seismic Network Bulletin*, 22, 92 p.
- Smith, W.A., Talwani, P. and Colquhoun, D.J., 1987. The seismotectonics of the Bowman Seismic Zone, South Carolina, submitted to the *Geological Society of America Bulletin*.
- Sowers, G.F. and Fogle, G.H., 1979. Seneca, South Carolina, earthquake, July 13, 1971, *Earthquake Notes*, 50, 25-36.
- Taber, S., 1913. The South Carolina earthquake of January 1, 1913, *Bulletin of Seismological Society of America*, 3, 6-13.

- Talwani, P., 1975. Crustal structure of South Carolina. second technical report, U.S. Geological Survey, Contract Nno. 14-08-0-001-14553, 79 p.
- Talwani, P., 1976. Earthquakes associated with the Clarrks Hill Reservoir, South Carolina--A case of induced seismicity *Engineering Geology*, 10, 239-253.
- Talwani, P., 1981. Earthquake Prediction Studies in South Carolina, in Simpson, D. W., and Richards, P. G., eds., *Earthquake Prediction: An International Review*, M. Ewing Series, 4, American Geophysical Union, pp. 381-393.
- Talwani, P., 1982. An internally consistent pattern of seismicity near Charleston, South Carolina, *Geology*, 10, 654-658.
- Talwani, P., 1985. Current thoughts on the cause of the Charleston, South Carolina earthquakes, *South Carolina Geology*, 29, 19-38.
- Talwani, P., 1986. Seismotectonics of the Charleston region: Proceedings of the Third U.S. National Conference on earthquake engineering, Earthquake Engineering Research Institute, v. 1, pp. 15-24.
- Talwani, P., 1989. Seismotectonics in the southeastern United States, in Gregersen, S. and Basham, P.W., eds., *Earthquakes at North-Atlantic Passive Margins: Neotectonics and Post-glacial Rebound*, pp371-392.
- Talwani, P., Secor, D.T. and Scheffler, P., 1975. Preliminary results of aftershock studies following the 2 August 1974, South Carolina earthquake, *Earthquake Notes*, 46, 21--28.
- Talwani, P., Stevenson, D., Chiang, J. and Amick, D., 1976. The Jocassee earthquakes: A preliminary report: Third Technical Report to the U.S. Geological Survey, Contract No. 14-08-001-14553, 92 p.
- Talwani, P., Stevenson, D., Sauber, J., Rastogi, B.K., Drew, A., Chiang, J. and Amick, D., 1978. Seismicity studies at Lake Jocassee, Lake Keowee and Monticello Reservoir, South Carolina (October 1977-March 1978), Seventh Technical Report to the U.S. Geological Survey, Contract No. 14-08-001--14553, 190 p.
- Talwani, P., Stevenson, D., Amick, D. and Chiang, J., 1979. An earthquake swarm at Lake Keowee, South Carolina, *Bulletin of the Seismological Society of America*, 69, 825-841.
- Talwani, P., Rastogi, B.K. and Stevenson, D., 1980. Induced seismicity and earthquake prediction studies in South Carolina: Tenth Technical Report, Contract 14-08-001-176570, U. S. Geological Survey, Reston, VA, 213 pp.

- Talwani, P. and Rastogi, B.K., 1981. Search for precursory changes in amplitude ratio of P and S waves for Jocassee, South Carolina earthquakes, Final Technical Report, NSF, Contract No. EAR7818126, 119 p.
- Talwani, P. and Acree, S., 1985. Pore pressure diffusion and the mechanism of reservoir induced seismicity, *Pure and Applied Geophysics*, 122, 947-965.
- Talwani, P. and Cox, J., 1985. Paleoseismic evidence for recurrence of earthquakes near Charleston, South Carolina: *Science*, 229, 379-381.
- Talwani, P. and Acree, S., 1987. Induced seismicity at Monticello Reservoir: A case study, Final Technical Report, Contracts 14-08-0001-21229 and 14-08-0001-22010, U.S. Geological Survey, Reston, VA, 351 p.
- Tarr, A.C., Talwani, P., Rhea, S., Carver, D. and Amick, D., 1981. Results of recent South Carolina seismological studies, *Bulletin of the Seismological Society of America*, 71, 1883-1902.
- Weems, R.E., Obermeier, S.F., Pavich, M.J., Gohn, G.S., Rubin, M., Phipps, R.L. and Jacobson, R.B., 1986. Evidence for three moderate to large prehistoric Holocene earthquakes near Charleston, S.C., *in Proceedings of the Third U.S. National Conference on Earthquake Engineering, Charleston, South Carolina*, Earthquake Engineering Research Institute, pp. 3-13.
- Zietz, I., Riggle, F.E. and Daniels, D.L., 1982. Aeromagnetic map of South Carolina: In color, U.S. Geological Survey Geophysical Investigations, Map GP-951, 1:1000000.
- Zoback, M.D., Healy, J.H., Roller, J.C., Gohn, G.S., and Higgins, B.B., 1978. Normal faulting and in situ stress in the South Carolina Coastal Plain near Charleston, *Geology*, 6, 147-152.
- Zoback, M.L. and Zoback, M.D., 1980. State of stress in the conterminous United States, *Journal of Geophysical Research*, 85, 6113-6156.
- Zoback, M.D. and Hickman, S., 1982. *In situ* study of the physical mechanisms controlling induced seismicity at Monticello Reservoir, South Carolina, *Journal of Geophysical Research*, 87, 6959-6974.
- Zoback, M.L., Nishenko, S.P., Richardson, R.M., Hasegawa, H.S. and Zoback, M.D., 1987. Mid-plate stress, deformation and seismicity, *in* Vogt, P.R., and Tucholke, B.E., eds., *The Geology of North America, Volume M, The Western North Atlantic Region*, Geological Society of America, pp. 297-312.

Zoback, M.D., Moos, D. and Stevenson, D. 1989. The state of stress and the relation to tectonics in the central Savannah River area of South Carolina, in Khair, A.W., ed., *Rock Mechanics as a Guide for Efficient Utilization of Natural Resources, Proceedings of the 30th U.S. Symposium*, A.A. Balkeme, Rotterdam, 553-562.

APPENDIX E: MAXIMUM EARTHQUAKE AT STROM THURMOND RESERVOIR

MAXIMUM EARTHQUAKE AT STROM THURMOND RESERVOIR

by

Leland Timothy Long

Professional Geologist
State of Georgia #445

and

Professor of Geophysics
School of Geophysical Sciences
Georgia Institute of Technology
Atlanta, Georgia 30332

1 JULY 1989

Prepared for U. S. Army Engineer
Waterways Experiment Station
P. O. Box 631
Vicksburg, MS 39180-0631

MAXIMUM EARTHQUAKE AT STROM THURMOND RESERVOIR

Preface

The Piedmont Province, the host geologic province for the Strom Thurmond Reservoir (previously Clark (or Clarks) Hill Reservoir) has experienced earthquakes of magnitude 4.5 and may experience earthquakes as large as magnitude 5.8. The existence of a maximum earthquake on the order of magnitude 5.8 can be argued from the mechanism for earthquakes in the Piedmont Province and from the developing understanding of stress and rock strength in the near-surface crystalline rocks. A probabilistic approach can be used to determine the expected level of seismicity, although the usual assumption of a linear recursion relation would not be appropriate at magnitudes near the maximum earthquake. Also, the seismicity recorded in the 2.0 to 4.5 magnitude range includes both natural and reservoir induced earthquake swarms which would influence estimates of the recursion relation. Because the fundamental mechanism for reservoir induced and natural events is the same, the induced and natural events are indistinguishable except in their spatial and temporal clustering.

The essence of the request for this analysis is to apply the arguments and data pertaining to a maximum earthquake in the Piedmont Geologic Province near the Strom Thurmond Reservoir to the determination of a maximum earthquake and to provide estimates of the expected rate of occurrence of smaller earthquakes. Although many hypotheses have been put forward to explain intraplate seismicity and a consensus in opinions is not yet a reality, the explanations utilized in this report will be limited to mechanisms accepted or developed by the author for the Piedmont and author's new mechanism for possible major intraplate earthquakes. These models in some respects differ significantly from conventional explanations for seismicity. For example, the Piedmont seismicity and major intraplate earthquakes are treated as very different phenomenon and the existence of Piedmont type seismicity does not imply a potential for major intraplate seismicity. I do not know of any geologic or seismic evidence that would suggest that a major intraplate earthquake could occur in the Piedmont, but the possibility exists that one could occur in a few surrounding areas.

This manuscript will summarize and interpret the results of nearly 20 years of research projects, directed studies and student thesis at Georgia Tech and other institutions. I appreciate the opportunity to pull this material together in the context of these developing models. The dedication and hard work of many students have created an extensive body of knowledge. I express appreciation for the efforts of each, and apologize for any omissions.

Leland Timothy Long

CONTENTS

	Page
PREFACE.....	i
TABLE OF CONTENTS.....	ii
INTRODUCTION.....	1
DESCRIPTION OF MECHANISM FOR MAJOR EARTHQUAKES.....	3
The Model for Major Earthquakes.....	3
Sites for Possible Major Earthquakes.....	5
Restrictions on Sites for Major Earthquakes.....	6
Uncertainty in the Model.....	6
DESCRIPTION OF PIEDMONT SEISMICITY.....	7
Introduction.....	7
Geologic Setting.....	7
Reservoir Induced Versus Natural Seismicity.....	8
Depth of Focus.....	8
Swarm Activity.....	9
Focal Mechanisms.....	9
Spectral Properties.....	10
HISTORICAL SEISMICITY.....	11
STATISTICAL DETERMINATION OF RISK.....	13
Introduction.....	13
Definition of Area.....	13
Catalog of Significant Events.....	13
Minor Lists from Reservoir Areas.....	14
Analysis of Time Dependence.....	14
Discussion of Confidence in Statistics.....	17
Statistical Consideration of a Maximum Earthquake....	18
Maximum Intensity from a Major Earthquake.....	19
DIRECT IDENTIFICATION OF ACTIVE SEISMIC ZONES.....	20
Introduction.....	20
Relation of Seismicity to Joint Intensities.....	20
Role of Stress in Piedmont Seismicity.....	21
Stresses in the Strom Thurmond Reservoir Area.....	22
MECHANISM PROPOSAL FOR A MAXIMUM PIEDMONT EARTHQUAKE.....	24

CONTENTS (cont.)

	<u>Page</u>
SUMMARY AND CONCLUSIONS.....	25
BIBLIOGRAPHY.....	26
FIGURES.....	47
APPENDIX I, A local weakening of the brittle-ductile transition can explain some intraplate seismic zones.	
APPENDIX II, Studies of Piedmont Earthquakes, Aftershocks, and swarms	
APPENDIX III, Preliminary Report on the Seismicity at the Richard B. Russell Reservoir	
APPENDIX IV, Fracture intensity and reservoir induced seismicity	
APPENDIX V. List of Piedmont Earthquakes	

MAXIMUM EARTHQUAKE AT STROM THURMOND RESERVOIR

INTRODUCTION

The Strom Thurmond Reservoir (previously referred to as the Clark Hill Reservoir or Clarks Hill Reservoir) is situated entirely within the Piedmont Physiographic province and impounds the Savannah River on the border between Georgia and South Carolina. The Southern Piedmont province extends from eastern Alabama to Virginia. Its northwest boundary is defined by the Brevard shear zone in Georgia, South Carolina and North Carolina. Its southeast boundary is marked by the onlap of Coastal Plane sediments. Piedmont type rocks have been traced under the Coastal Plane sediments to the edges of Triassic/Jurassic rift basins; which mark the most recent evidence of major tectonic activity in the southeastern United States. The Piedmont province is part of the continental crust of the North American continent which lies on the North American Plate. The closest plate boundary seismic activity associated with the North American Plate is in the Caribbean and at the Atlantic Ridge. These boundaries are too distant for their earthquakes to be experienced in the area of the Strom Thurmond Reservoir. Hence, this analysis will be limited to the problems of intraplate seismicity and, in particular, the mechanisms of shallow Piedmont seismicity (considered herein to be equivalent to reservoir induced seismicity) and a few sites of potential major intraplate earthquakes.

The unfortunate emergence and perseverance of the concepts of brittle failure or slip along existing fractures in the crust for major earthquakes has inhibited development of models that could be useful in defining potential sites and times for major earthquakes. Although slip along existing fractures is the most widely accepted explanation for intraplate earthquakes, the mechanism is incomplete and fails to explain the accumulation of stress or the timing of the event. Also, slip along existing fractures becomes harder to accept for earthquakes at depth in the crust where stress relaxation is dominated by viscous flow.

The improved understanding of the mechanism for deformation in the deep crust and the identification of the brittle-ductile transition at mid-crustal depths (Chen and Molnar, 1983; Meissner and Strenhlau, 1982) has added a new dimension to discussions of stress distributions and strength in the crust. The mechanisms of earthquakes can no longer be assumed independent of depth. The depth dependence of an earthquake mechanism is supported by the correlation of the maximum depth of earthquakes in continental interiors with the depth to the brittle-ductile transition. From the surface to about 15 km, the maximum strength of the crust is determined by the shear stress required to cause frictional slip on fractures. The failure stress, according to Byerlee's Law, is proportional to depth. Below 20 km, applied stresses are relaxed through viscous flow. Whereas at shallow depths the maximum stress is controlled by frictional resistance, an increasing function with depth, at greater depths the maximum stress is controlled by viscosity, a decreasing function with temperature and hence depth. The combined effects of these two strength limitations create a mid-crustal zone that

is considerably stronger than crustal material shallower than 10 km or deeper than 25 km.

The zone of high strength is the primary vehicle for transmitting plate boundary stresses to the interior of the plates. Stresses related to plate boundary mechanisms and transmitted by the high strength portion of the crust are regional stresses. Local stresses which are superimposed on the regional stresses can be derived from density anomalies and topographic loading (Kuang et al., 1989). The local stresses and regional stresses in the crust are estimated to be of the same magnitude, about 50 MPa. Secondary stresses may exist that are related to modification of regional or local stresses by variations in elastic constants; however, under normal conditions these perturbations will be limited to about 30 percent of the applied stresses. The high-strength portion of the crust can sustain stresses significantly greater than the stress levels implied by stress drops computed for earthquakes. Hence, any mechanism for earthquakes must include an explanation for failure at low stress. Once such a mechanism is defined, it can provide a basis for estimating the potential occurrence of earthquakes and their hazards.

Two mechanisms, which satisfy the above constraints on crustal stress and strength, exist for intraplate earthquakes. The first proposed by Long (1988) applies to major earthquakes. A major intraplate earthquake represents a rupture of the high-strength portion of the crust. The mechanism of Long (1988) proposes that a zone of decreased strength at depth in the crust is required to concentrate stress and cause sudden failure. The second mechanism applies to smaller earthquakes on shallow joints or faults. This mechanism applies to the shallow crust where the failure mechanism of frictional slip can operate at low stress levels. This mechanism is generally accepted for reservoir induced earthquakes, but in this analysis it is extended to all Piedmont earthquakes. Costain et al. (1988) refer to this mechanism as hydroseismicity and apply it to most continental earthquakes.

The two mechanisms are distinct and will be considered separately in an analysis for the maximum earthquake at Strom Thurmond Reservoir. The mechanism for major earthquakes require a disturbance in crustal strength at depth and earthquakes of magnitude 7.0 or more would be limited to areas where such disturbances are in operation. Currently, in the southeastern United States such areas are limited and none are in the Piedmont. The closest identified zone is in southeastern Tennessee. The mechanism for shallow Piedmont earthquakes limits the magnitude of Piedmont type earthquakes to less than magnitude 5.8. Furthermore, the location of these events is limited by rock type at the surface and the ability of the near-surface rocks to sustain stress.

DESCRIPTION OF MECHANISM FOR MAJOR EARTHQUAKES

The Model for Major Earthquakes

The high-strength portion of the crust can sustain stresses that are significantly greater than those estimated to exist during earthquakes. Consequently, rupture in a major earthquake requires a mechanism to weaken the crust. Traditional models for seismicity invoke existing fault planes in appropriate orientation for the zone of weakness; however, such models have difficulty explaining the initiation of shear failure at depth in the crust. In a non-traditional model, Long (1988) used the concept of a distortion of the brittle-ductile transition in the crust as a basis for intraplate continental earthquakes. Long's new model treats the occurrence of a major intraplate continental earthquake as a transient phenomenon which can be described as a sequence of five phases (figure 1). Each phase is characterized by its own set of physical properties and seismicity. Observations of the seismicity can be used to interpret the phase of the sequence and evaluate the potential for a major earthquake.

Phase 1, Initiation: The sequence of events leading to a major intraplate earthquake may be initiated with a disturbance in the hydraulic or thermal properties of a small portion of the crust at or below the brittle-ductile transition. Such a disturbance could be induced by the intrusion of a sill or by partial melting. At the time of the initial disturbance, the brittle-ductile transition would not be penetrated by fluids from below. A horizontal zone of partial melt is formed and becomes a source for fluid and thermal perturbation of the overlying crust. The growing evidence for thin reflectors in deep seismic reflection data and the observation that a sharp Moho is characteristic of recent tectonic events supports the wide-spread development of zones of disturbance in the lower crust.

Phase 2, Strength Corrosion: A corrosion in the strength of the lower crust could be caused by an upward migration of fluids or heat from the recently implanted sill or partial melting of the lower crust. The fluids may be driven by the higher temperatures of the sill or they may follow vertical tension cracks related to regional plate stress. Fluid pressures could vary between hydrostatic and lithostatic in sealed compartments controlled by a complex feedback among fluid flow, temperature, chemistry and strength. The evidence for strength corrosion comes primarily from studies of rock strength that confirm that fluids and increased temperature decrease the strength of rocks. During phase 2, small earthquakes would begin to occur in the perturbed zone in the lower crust. This central zone or core of weakness would be a continuing zone of anomalous seismicity through phase 3. The dominant focal mechanism would be strike slip because the distortion of the weakened central zone, which would be analogous to the distortion surrounding a hole in a plate, will keep the vertical axis the neutral axis. The corrosion of strength would imply preference over existing fault planes for new fault planes closely aligned with the direction of maximum shear stress. The migration of fluids or heat in this and later phases would

be expected to exhibit anomalous Q, such as observed by Jin and Aki, 1988. The presence of fluids in cracks and microcracks at depth in the crust explains (Al-Shukri and Mitchell, 1988) the association of enhanced earthquake activity with low velocity in the crust near the New Madrid seismicity.

Phase 3, Stress Concentration: The area of developing weakness must also be under regional tectonic plate stress if energy is to be available for a large event. As a weakened central zone relaxes, regional tectonic stress is transferred to the surrounding more rigid crust where it is concentrated the greatest at the boundary of the core of the weakness. In this phase, earthquake activity is greatest in the central zone, but surrounding the central zone earthquakes may occur with fault planes too small to rupture the strongest portion of the crust. These could represent stress adjustments on shallow planes of weakness, where the source of stress could be a reaction of the shallow crust to flexure about the deforming core of weakness. Because a major earthquake is not known to have occurred in historic times in southeastern Tennessee, that area is suspected to be in phase 3.

Phase 4, Major Failure: A major earthquake occurs when the stress surrounding the central disturbed zone exceeds the strength of the crust, perhaps, because the dispersing crustal fluids have spread beyond the central disturbed zone and weakened the crust or because the stress load has shifted to the outside of the core of weakness. Two distinct patterns of faulting are possible when a major earthquake occurs. The first pattern would consist of near-vertical faults striking parallel to the planes of maximum shear stress of the regional field and extending away from diagonally opposite edges of the central core. These faults could be connected in the central zone by a fault or a series of faults in the complimentary direction. The first pattern is exhibited by the New Madrid seismicity. The second pattern would develop when deformation is resisted by a thinned strong portion of the crust above the deforming core. In this case the major earthquake will occur on a reverse fault with some strike slip components and dimensions comparable to the size of the core of weakness. With these dimensions, a typical magnitude could be in the 6.0 to 7.0 range and possibly smaller than earthquakes exhibiting the first pattern. The second pattern was exhibited by the Marryat Creek, Australia, earthquake (McCue et al., 1987).

Phase 5, Decay: The final phase in the occurrence of a major intraplate earthquake is an extended aftershock sequence. The fluids, no longer replenished by the hydraulic or thermal disturbance of the lower crust, dissipate from the core. The dissipation of the fluids allows the strength of the crust to return to its original condition. Additional earthquakes are inhibited except along the weakened fractures with residual fluid content. Aftershock activity concentrates on the fault plane of the main event(s) and associated faults instead of in the core. The New Madrid area would be in phase 5.

Sites for Possible Major Earthquakes

Only two sites of past or potential major intraplate earthquakes are currently known to exist within 300 km of the Strom Thurmond Reservoir area. These are the southeastern Tennessee seismic zone and the epicentral zone of the Charleston 1886 earthquake.

The effects of the Charleston 1886 earthquake have been studied extensively with no definitive agreement on the mechanism. If the mechanism of Long (1988) applies, the Charleston earthquake is in the later stages of an aftershock sequence of phase 5. The current seismicity in the aftershock zone is sparse and is limited to relatively shallow (less than 15 km) events and there is no suggestion of a central core of deeper seismicity (15 to 20 km for the Coastal Plain) with uniform strike slip focal mechanisms. Until the activity in a central zone develops in response to a disturbance in the lower crust, a major earthquake from the Charleston vicinity is unlikely.

In contrast to the Charleston aftershock zone, the seismicity in southeastern Tennessee exhibits many of the attributes of phase 3 in the process leading to a major earthquake. The southeastern Tennessee activity is, like the New Madrid seismicity, beginning to reveal evidence of anomalous properties of the crust, particularly in the area of greatest seismicity. Epicenters in southeastern Tennessee for earthquakes occurring in the last 10 years have been carefully relocated using a revised velocity model. The pattern resulting from the relocation is remarkably similar to the distribution of epicenters in the New Madrid seismic zone (figure 2). However, the alignment along suspected faults is not as distinct in southeastern Tennessee, suggesting either that the precision of location needs improvement or that a fracture zone has not yet developed as would be expected by a major earthquake. Velocity anomalies in southeastern Tennessee are suggested by travel time residuals from the relocated earthquakes. The distribution of anomalous velocity would be similar to the velocity anomaly discovered by Al-Shukri and Mitchell (1988) for the New Madrid seismicity. The decay of coda from earthquakes in the central zone is anomalous suggesting that the central zone has low Q . A simple inversion for Q structure suggests that azimuthal variations of coda decay can be explained by a zone of anomalously low coda Q (less than 100) in the area of southeastern Tennessee which contains the largest and most numerous events (Long et al., 1987). The low coda Q suggests a perturbation in the fluid or fracture properties of the crust and the correspondence with a zone of more intense seismicity is consistent with the reaction of a central zone of weakness to regional plate stress. Of particular interest is the distribution of focal mechanisms. These have been examined in detail by Long and Zelt (preliminary draft Appendix I). The focal mechanisms of southeastern Tennessee are in agreement with the hypotheses that the earthquakes are caused by deformation around a zone of weakness in the crust.

Restrictions on Locations of Major Earthquakes

The proximity of seismic zones to rift basins (Dewey, 1988) as well as observations of Long (1976), Kane (1977) and McKeown (1978) suggest that there is an association between structures typical of the lower crust in continental rifts and a susceptibility to hydraulic or thermal perturbations in the lower crust. The Charleston, S.C. earthquake occurred near a Jurassic-Triassic rift basin and the New Madrid events are associated with the Reelfoot rift. The southeastern Tennessee seismicity is at the southern end of the East Coast Gravity High, a significant Precambrian rift. Since most of the Piedmont is underlain by stable continental crust with no evidence of rifting. The observation of an association between continental rifts and seismicity does not suggest that a major earthquake is likely to develop in the Piedmont. Although the Charlotte and Carolina Slate Belts exhibit some properties of rift structures (Long, 1979), they are instead the results of the overthrusting of the shelf edge of the North American Continent during the Paleozoic closing of the Atlantic Ocean. The positive anomalies which are found in the Charlotte and Carolina Slate Belts and are typical of rift structures can be interpreted as fragments of oceanic crust. Hence, the crustal structures most conducive to major events are not present in the Piedmont physiographic province and the seismicity should be limited to near-surface Piedmont type earthquakes.

Uncertainty in Model

The transition from phase 3 activity to a major earthquake may not be certain. The observations in southeastern Tennessee may only represent a minor transient perturbation of the lower crust with insufficient intensity to develop the stress amplification or crustal weakness needed to generate a major earthquake. Also, the existing volume of weakened crust may lack the geometry or strength to fail in a major earthquake.

Another uncertainty in the model for major earthquakes is the time between the onset of the perturbation in the lower crust and the major earthquake. Evidence on the rate of movement of magma suggest this time could be on the order of a few years. A critical factor in detecting the onset of the sequence leading to a major event is the detection and location of the small deep focus earthquakes which should accompany the perturbation in the lower crust. While the seismicity in southeastern Tennessee suggests that detection is possible, large events on other continents (Denham, 1988) have not been preceded by an obvious sequence of foreshocks.

DESCRIPTION OF PIEDMONT SEISMICITY

Introduction

Earthquakes in the Piedmont Province of Georgia and South Carolina have unique properties that distinguish them from events in many other seismic areas of the continental interior. These properties are their near surface to 2.0 km depth of focus (Dunbar, 1977; Fogle et al., 1976; Talwani, 1977), their swarm-type occurrence and associated high *b* values (Long, 1974; Talwani et al., 1979; Johnson, 1984), their cubic high-frequency spectral decay (Marion and Long, 1980), their association with reservoirs and water loading (Talwani, 1976; Costain et al. 1987; Jones et al., 1986), and the similarity between joint directions and focal mechanism solutions (Guinn, 1980). In addition, areas of induced seismicity contain numerous diversely oriented small fractures and lithological inhomogeneities that could control the diffuse induced seismicity (Secor, et al., 1982). The studies of Piedmont earthquakes, aftershocks and swarms are reviewed in Appendix II. Taken singly or in concert, these properties of Piedmont earthquakes support an association between Piedmont seismicity and shallow joints or fractures. In addition to the association between Piedmont seismicity and shallow joints the intensity of jointing correlates with seismicity. In areas of induced seismicity the epicenters are more likely to occur in areas adjacent to rocks of high rock quality.

Geologic Setting

A significant factor in the mechanism for Piedmont earthquakes is the common geologic setting of the near-surface rocks. Igneous and metamorphic rocks dominate surface exposures in the Piedmont. Most geological studies before 1980 emphasized the division of the Piedmont into Belts. Because the rock assemblages exhibit considerable heterogeneity, the belts were erroneously large, lumping together too many terrains to be useful tools in structural interpretation. The belts were more closely related to late stages in the development of the geologic structures and were not always internally consistent features. As such, the boundaries would not necessarily represent significant contrasts in seismogenic properties of the crust. Recently, Higgins (1987) has abandoned the "belt" concept in favor of an accretionary wedge-terrain paradigm. The Piedmont may best be divided into components of an accretionary wedge complex consisting largely of accreted terrains now arranged in a series of imbricate thrust slices. Following thrusting, the Piedmont accretionary complex was highly metamorphosed, migmatized, and intruded by granites. This history has generated a complex surface distribution of rock types, including metadacites, granites, granite gneisses, and schists. It will be argued below that the schistosity and fractures of the different rock types influence the susceptibility to seismicity. In particular, earthquakes tend to occur in granite gneisses with low fracture density and weak schistosity. As a result of the complex history and inhomogeneity, the surface properties of the Piedmont

rocks vary from friable schists to massive granites, although below the depth of weathering (0 to 200 m depending on rock type) the crystalline rocks exhibit an average compressional velocity of 6.05 km/s.

Reservoir Induced Versus Natural Seismicity

The question of reservoir induced seismicity versus natural seismicity as an origin for Piedmont events must be considered because many recent events are clearly associated with reservoir impoundment. These include earthquakes at Lake Jocassee, Lake Oconee, Monticello Reservoir, and Richard B. Russell Reservoir. Other seismic areas are close to reservoirs but the timing and spatial associations are not as clear cut. These include Lake Keowee, Lake Sinclair, and Strom Thurmond Lake. Those few examples of seismic activity that appear removed from reservoirs can usually be associated with other types of ground water perturbation. The Columbus, Georgia, events of 1984 (Jones et al., 1986) were located near quarries that had recently been flooded. The Macon, Georgia, events were in the immediate vicinity of an area of kaolin mining that had recent ceased water removal operations and had thus allowed the ground water table to recharge. In general, recent studies lend greater support to the role of fluids in shallow crustal rocks in the triggering of earthquakes (Costain et al., 1988).

The Richard B. Russell Lake seismicity (Appendix III) and the Lake Oconee Seismicity, appears to deviate from the diffuse pattern exhibited by the Jocassee and Monticello Reservoir seismicity. The Richard B. Russell seismicity and Oconee seismicity are located on extensions of the Middleton-Lowndesville fault trace. This fault exhibits a brittle phase of deformation in its development that may have facilitated fluid penetration and the triggering of earthquakes in rocks in or adjacent to the shear zone.

Depth of Focus

Because the Piedmont earthquakes are shallow and in high-velocity near-surface rocks, the accurate determination of depth requires stations at less than 1.0 km spacing and timing precision of .02 seconds if a depth precision of 0.1 km in the 0.3 to 2.0 km depth range is desired. In the Strom Thurmond Lake (Clarks Hill Reservoir) area, Dunbar (1977) relocated eighty one microearthquakes recorded on smoked paper and magnetic tape recorders. The velocity model for the study area was determined from local travel time data obtained by Dunbar (1977) and by Leary et al. (1974). The Dunbar model, which included a velocity gradient, was used in the relocation. The hypocenters located with a gradient velocity model were an average of 10 percent shallower than those located using a constant velocity model. The depths ranged from 0.1 to 1.8 km with a mean depth of 0.6 km \pm 0.3 km. Only 5 of the eighty events were deeper than 1.5 km.

A significant implication of the use of a gradient model is that a depth solution that does not include two or more stations within a distance of twice the depth will be unreliable (possibly non-unique). Because the seismic station distribution is sparse in the Piedmont, reliable depths above 8 km are limited. Estimates of depth that are not constrained by a station within one focal depth should be considered suspect. Reliable depths of focus have been computed for Jocassee Lake earthquakes by Talwani (1977) and Fogle et al., (1976). The analysis of Fogle et al. (1976) used the technique proposed by Dunbar (1977) while the analysis of Talwani (1977) used the traditional constant velocity layered model of program HYP074. The range in focal depths in both independent studies vary from the surface to 3.0 km. A few events located as deep as 4 km, but these were usually low-quality hypocenters. The average station separation was 3 to 7 km, thus severely limiting depth computation for events shallower than 1.3 km in the center of the reservoir and shallower than 3 km for most of the active area. The hypocenters were scattered above the Brevard shear zone in the Henderson Gneiss. In a field study of microearthquakes in a swarm at Lake Keowee, South Carolina, Talwani et al., (1979) and Acree et al., (1988) similarly found a distribution of hypocenters from the surface to 2 km depth.

The depths of focus for Monticello earthquakes are difficult to assess, again because the station spacing was at best 2 km. The subsequent uncertainty in depth computation has yielded a depth range of near-surface to 4 km. The design of the original net with its 7 km spacing was of marginal use in depth computation and some early reports suggested deeper, but poorly constrained, hypocenters. In a short field monitoring study using five portable recorders spaced at less than 0.5 km apart, Smith (1980) obtained depths of focus that were typically 0.5 km deep.

Swarm Activity

An earthquake swarm is characterized by events of similar magnitude occurring over a short period of time. A b value which is high would be typical of swarm type occurrences and high b values have been documented by Long (1974) for the Seneca (or Keowee) earthquake sequence. Talwani et al., (1979) also obtained a high b value for the Keowee swarm. Johnson (1984) documented a swarm of earthquakes in Twiggs County, Georgia, which occurred from December, 1982, through May, 1983. The b value for all events was 0.73 ± 0.03 , but the recursion relation was not linear and the b value increases to greater than 1.0 for the larger events.

Focal Mechanisms

Focal mechanisms for the Strom Thurmond Lake (Clarks Hill Reservoir) area and Lake Jocassee were reviewed by Guinn (1980). Focal mechanisms for other areas and other studies in these areas show similar

results. The focal mechanisms tend to cluster in groups that are consistent with surface joint systems. Acree et al., (1988) also noted an association with joint systems in the Lake Keowee area. The focal mechanism which dominates a cluster often changes with time.

Spectral Properties

The theory of seismic spectra and the observed spectra for the Lake Sinclair area, Strom Thurmond Reservoir area and the Monticello Reservoir area were evaluated by Johnston, (1980), with the objective of identifying a spectral discriminant for reservoir induced seismicity. The source theory suggests that a discontinuous rupture front speed will generate high-frequency energy which dominates the spectrum for frequencies higher than the corner frequency. These spectra (which decay as the square of the frequency) decay more slowly than spectra dominated by a gradual change of rupture velocity. Hence, the velocity and smoothness of faulting control the high-frequency spectral content. Earthquakes on lubricated or smooth-slipping shallow faults, which are hypothesized to be typical of reservoir induced earthquakes, would generate less high-frequency seismic energy. The displacement spectra of these types of earthquakes would consequently decay as the cube of frequency at frequencies above the corner frequency. Spectra from Strom Thurmond Lake, Jocassee, and Monticello Reservoir areas generally exhibit a cubic decay with frequency above the corner frequency expected for reservoir induced seismicity. Marion and Long (1980) showed a distinct difference in spectral properties between Piedmont earthquakes and earthquakes in Southeastern Tennessee, with those in southeastern Tennessee having a significantly lower slope (1.5 to 2.0).

The potential influence of depth of focus on the spectral slope was studied by Wilson (1983). He evaluated the hypothesis that the increased normal stress with increased depth would increase the frictional resistance on the fault surface and increase the high-frequency spectral content. Relations among depth, spectral slope, and corner frequency were examined for 70 digitally recorded events at Monticello Reservoir, South Carolina, and 35 events at Mammoth Lakes, California. At Monticello Reservoir, the range of depth was not sufficient to show a variation in spectral slope with depth. However, the high-frequency slope does vary with depth for the Mammoth Lakes events. At Mammoth Lakes, the average slope of -3.0 at 4.0 km depth changes to 2.5 at 11 km depth confirming that normal stress is important in the properties of reservoir induced earthquakes and the lack of normal stress may differentiate these shallow events from deeper tectonic events.

HISTORICAL SEISMICITY

The pre-network seismicity (Figure 3) shows the wide-spread occurrence of earthquakes in the southeastern United States. Reliable depths of focus were not available for earthquakes before 1970, but are expected to be consistent with depths determined more recently with network data. The pattern of seismicity is dominated by a zone of activity along the southern Appalachians, the Charleston aftershock zone and scattered events in the intervening areas, particularly in a band connecting the Charleston and southeastern Tennessee seismic areas. The epicenters computed during the last eight years of more dense station coverage (Figure 4) have reproduced the same general pattern of seismicity, but the rates of activity in some areas are significantly different. For example, current seismicity is sparse in western North Carolina and northern Alabama, and is much less than would be predicted by the historical data. In contrast, the activity in southeastern Tennessee has exceeded estimates based on historical seismicity.

Seismic zones are areas in which the probability of occurrence of earthquakes is defined for use in statistical studies. Most classical seismic zones are areas where the historical seismicity is greater than surrounding areas. Some recent studies have extended the concept of a seismic zone to include areas of uniform crustal structure, areas in which an hypothesis for major event applies, and areas defined for no reason except expert opinion. This extension mixes observational data with speculative causal mechanisms and imagination, thus creating patterns of risk that may appear incompatible with existing data. In either the classical or extended definitions, seismic zones remain the basis for probabilistic estimates of seismic risk using techniques proposed by Cornell (1968).

The classical seismic zones which cover portions of the Southern Piedmont are evident in the historical seismicity as presented by Hadley and Devine, (1974) (figure 5). Two of these zones, the Central Virginia Zone and the Georgia-South Carolina Transverse Seismic Zone were defined by Bollinger (1973) (figure 6). The Georgia-South Carolina Transverse Seismic Zone was created largely to connect the Charleston, South Carolina, seismicity and the seismicity in the Southern Appalachian Seismic Zone (Bollinger, 1973), and to explain the greater number of events in the Piedmont of South Carolina than in western Georgia or North Carolina. This zone is transverse because its longer dimension is transverse to the northeast trend of the geologic structures of the Southern Appalachians. The Central Georgia Seismic Zone (Allison, 1980) is very similar to the Central Virginia Seismic Zone in its diffuse pattern of epicenters. Bollinger (1973) included this seismicity in the Georgia-South Carolina Transverse Seismic Zone.

When examined in detail, not one of these seismic zones has a uniform distribution of seismicity and all the zones that include the Piedmont province are strongly influenced by reservoir induced seismicity. The seismicity is so sparse and transient that more detailed zones are not practical except in southeastern Tennessee. The Piedmont

seismicity through 1988 (figure 7) does reveal an interesting pattern. Two northeast trending zones of greater activity are apparent. One begins at Columbus, Georgia, and extends northeast through the Lake Sinclair, Strom Thurmond Reservoir, and Monticello Reservoir, South Carolina. The second extends northeast from Jocassee Reservoir through North Carolina. The southwest end may extend into Georgia, based on the occurrence of a few small events near Gainesville which were felt in an area of one km radius and recorded on a portable seismograph in June, 1982. These two trends might describe the seismicity of the Piedmont better than existing seismic zones. A more appropriate explanation might be that the seismicity correlates with geologic or lithologic units which may just be more prevalent in the suggested zones. In this analysis, the objective is to define the maximum earthquake that could be experienced at Strom Thurmond Reservoir. An estimate of seismic activity based on uniform distribution of seismicity and a restriction of seismicity to these two trends will be generated for comparison with the historical seismicity.

In all of the southeastern United States surrounding the Strom Thurmond reservoir, only two areas exhibit a concentration of deeper focus earthquakes. These two areas are the southeastern Tennessee area and the Charleston area. The Giles Co. Virginia, seismic zone also exhibits deep focus earthquakes but it is outside the range of influence for the Strom Thurmond Reservoir. All the other concentrations of epicenters are shallow Piedmont type earthquakes or isolated single events of unknown depth.

STATISTICAL DETERMINATION OF RISK

Introduction

The statistical determination of risk requires a definition of the area and the level of seismicity. The basis for determination of seismicity rates is ultimately dependent on lists of earthquakes. In this section the seismic catalogs are examined and used to provide a statistical estimate of the susceptibility of the Strom Thurmond Reservoir area to large earthquakes.

Definition of the Area

The Southern Piedmont physiographic province serves as the definition of the area of seismicity in this analysis. The Southern Piedmont province extends from eastern Alabama to Virginia. Its northwest boundary is defined by the Brevard shear zone in Georgia, South Carolina and North Carolina. Its southeast boundary is marked by the onlap of Coastal Plain sediments. In Georgia and South Carolina, Piedmont type rocks extend under the Coastal Plain sediments to where the crust is disrupted by Triassic/Jurassic rift basins. Also, similar crystalline rocks are found at the surface northwest of the Brevard shear zone in the Blue Ridge province. For seismicity analysis, a definition of seismic zones in terms of crustal structure and rock type would be more appropriate than physiographic features. Since the Piedmont type seismicity applies to areas of stable, thick crust with crystalline rocks at the surface, an extension of the seismogenic properties to some adjacent areas would be appropriate. However, the boundary in some adjacent areas would be ambiguous because the surface geology is hidden. For this reason and the fact that few events occur in the region just outside the Piedmont physiographic province, the choice between the physiographic province boundary and the boundary of the seismic zone is irrelevant.

Catalog of Significant Events

The seismicity for the Piedmont has been collected in a single list of magnitude 2.0 and larger or significant events (Appendix V). The earthquake documentation is derived from the LLL and EPRI seismicity lists with modifications and additions suggested by recent publications and studies. The recently relocated earthquakes of the Charleston area (Seeber and Armbruster, 1987) were not included in the list because the detection and location methods are questionable. The list has been updated with data from quarterly earthquake lists from Georgia Tech and the SEUSSN Bulletin.

The epicenters of the Piedmont earthquakes are plotted in figure 7. The intensities used in this study are the maximum modified Mercalli intensity reported in the literature or other lists. For some events in

the 1800's, an intensity was not given and these were arbitrarily assigned intensity III. The magnitudes are assumed to be equivalent to mb, but rarely are they true mb. Most instrumental magnitudes are mbLg (or mN) proposed by Nuttli to relate the Lg phase amplitude to mb. The net data from the late 1970's and 1980's are largely based on a duration magnitude MD (Teague and Sibol, 1984) which is scaled to mbLg for large events. This scale is often extended from its calibrated range of above magnitude 2.0 to as small as magnitude 0.0; however, the character of seismograms vary significantly at short durations and this extension is questionable. Johnson (1984) in a study of events near Macon, Georgia, obtained relations to correct for a significant deviation in linearity in the duration magnitude scales. The estimated magnitude is either the measured magnitude or a magnitude based on the relation $mb = 1.2 + 0.6I$, which was used in the LLL study and is very similar to the generally accepted relation $M = 1.0 + (2/3)I$. The LLL relation was used in statistical relations for the entire data set except in studies involving only intensity.

Minor Lists from Reservoir Areas

The monitoring of reservoir induced earthquakes has yielded many precisely located microearthquakes. In the typical Piedmont reservoir area, the crystalline rocks which are close to the surface are efficient transmitters of seismic energy and background noise levels are low. These conditions are favorable for the detection of events as small as $m = -3.0$ for stations within 2.0 km of the hypocenter. For example, one days record during the aftershock monitoring of the August 2, 1974, McCormick, S.C. earthquake showed over 500 small events. Unfortunately, such close monitoring of the seismicity is field work intensive and the data coverage is typically uneven. Reservoirs where seismic monitoring has been concentrated include Jocassee, Strom Thurmond, Sinclair, Keowee, and Monticello. The transient and long term behavior of the reservoir induced Seismicity is evident in the Strom Thurmond and Sinclair Reservoir seismicity. Two trends in the rate of activity can be observed. The first is that following a normal aftershock sequence, the activity decays in an extended aftershock sequence that lasts three to six months. The second is that the spring and summer months usually exhibit greater levels of seismicity, typically following by one month a sharp increase in water level in the spring. These variations, however, are short term and would not influence statistics for larger events.

Analysis of Time Dependence

Either the consistency in the documentation or the rate of occurrence of Piedmont earthquakes has been non-stationary. The completeness of the record in the 1800's is understandably less than after the installation of the WSSN stations BLA and ATL in the early 1960's. Never-the-less, differences in the rate of occurrence exist that are not easily explained by detection threshold alone. Some possible explanations for these variations and their effect on the statistical treatment

of the seismicity will be discussed below.

Aftershock Removal: The usual procedure in statistical studies of seismicity is to remove suspected aftershocks. The rate of decay in the numbers of events per day in an aftershock sequence clearly violates the stationarity and random distribution assumptions invoked in most statistical treatments of seismicity. In the Piedmont, aftershock sequences are of normal length and with few exceptions aftershocks do not appear in the list of events. Hence, the removal of normal aftershocks would not significantly change any derived statistical parameters. On the other hand, most active areas in the Piedmont are identified by swarms of significant events, each event with its own aftershock sequence. If the swarm is short, usually only one significant event is listed; however, if the swarm extends over a period of months, many of the events may be listed.

The swarms could be treated either as single events or as multiple events, depending on the physical basis assumed for the statistical model. Under the assumption that the seismicity is used to identify areas of potential seismicity and not the level of activity, the swarms should be treated as single events. Such a treatment would be appropriate for models used to compute the risk when the historical seismicity is considered insufficient to define the rate of seismicity or when other factors, such as reservoir impoundment, might change the rate of seismicity. If the seismicity is used to define the rate of energy release, then the individual events in the swarm should be used. The latter treatment would be appropriate for models in areas where the seismicity has been shown to be stationary and the level of activity is expected to be constant.

The treatment of swarms as single events is the more appropriate assumption for the Piedmont. This treatment is consistent with the mechanism for Piedmont events described herein and the non-stationarity apparent in detection and occurrence. The distribution of active areas near Strom Thurmond Reservoir will be used to evaluate the maximum event. The rate of activity based on all events will be used to compute the risk at Strom Thurmond Reservoir for comparison with the maximum earthquake.

Seasonal Variations: At all magnitude levels, the earthquakes in the Piedmont occur more often in the winter months (see figure 8). The magnitude 4 (intensity V) and larger follows the same pattern as the magnitude 3 (intensity III) and larger events. The seven peak months registered 10 to 15 events and the four low-seismicity months registered only about five events each. An explanation for this may be found in the average monthly rain fall recorded in Charlotte, North Carolina; chosen as a typical central location in the Piedmont. The averages are for 1951 through 1980 and are assumed to be typical of the last 200 years. The March peak in rain fall is followed by a peak in seismicity in May. On the other hand, the spring and summer high levels are 6 months out of phase with the fall and winter high-level seismicity. Hence, the relation to water level increases noted in the Strom Thurmond Hill Reservoir

seismicity may carry over to a general relation between rain fall and Piedmont seismicity, but the relation may not be direct. If possible, average annual rain fall should be extended back for direct comparison. Costain et al. (1988) discuss a possible correlation between stream flow and strain energy release in central Virginia for the period 1925 to 1987.

Premonitory Variations: The large numbers of small events that have occurred in the Strom Thurmond Reservoir area and near Jocassee Reservoir have made these areas appealing as laboratories for the study of earthquake prediction. Talwani et al. (1978) and Fogle et al., (1976) have monitored the seismicity at Lake Jocassee for variations in seismicity parameters such as the changes in the ratio of P-wave to S-wave velocity first observed as precursors of large events at Blue Mountain Lake, New York. Significant variations with time were observed in the b and a values. The data suggested that some of the magnitude 2+ events might have been predicted, but overall a satisfactory criteria for prediction was not developed. The perturbations in activity level and b values were only observed in the smallest events and such variations would not affect the statistics for larger events considered in this study.

Relations to Cultural Activity: The correlation of Piedmont seismicity with rain noted above is only one factor in the connection between rain fall, ground water and induced seismicity. In addition to having the water available through rain fall, the water must gain access to seismic depths through ground water recharge. This process may have been influenced by industrial development and a change in forest cover in the Piedmont.

The relation between seismicity and large reservoirs filled in the last 30 years has been well documented. The possible relation between smaller reservoirs that predate these major reservoirs and seismicity has not been considered in detail. In general, many of the smaller mill ponds were probably built during the population expansion and industrialization that evolved in the Piedmont following the Civil War. A notable decrease in Piedmont activity exists in the depression years of the 1930's (see figure 9). The amount of ground surface covered by forest versus the area cleared for agriculture could be a factor also in the facility and rate in which surface waters gain access to ground water systems.

The industrialization and agricultural development in the Piedmont in the late 1800's and the building of large reservoirs after the 1940's, if responsible for the increased seismicity during those times, would suggest that the Piedmont seismicity may in part be transient. The transient character of reservoir induced seismicity is well known, with activity typically increasing to a peak usually within a few years of filling. This peak is then followed by sporadic swarms of activity that decrease in frequency and intensity with time. The possibility then

exists that Piedmont seismicity will continue to decline, except near new reservoirs, and will stabilize at a significantly lower level than apparent today. This assumption would hold provided that the reservoirs are triggering existing stresses and provided that the reservoirs or other mechanisms are not in some way creating stress in the rocks.

Discussion of confidence in statistics

The recursion relation,

$$\text{Log}(N_c) = a - bM,$$

where a is the Logarithm of the number of magnitude $M = 0$ events per unit time and b is the rate of decrease in activity with increased magnitude is a prime objective of statistical evaluations of lists of earthquakes. It is the usual basis for computation of expected number of events of a particular size at a site. Complex statistical and probabilistic techniques have been developed for evaluation of a and b from large data sets. Traditionally, the completeness of the data set is evaluated for a given magnitude range by Stepp's (1972) method and the uncertainties in the determination of a and b are computed using maximum likelihood estimators (Aki, 1965). For the Piedmont events with measures of maximum intensity in Appendix V, the recursion relation is shown in figure 10. The number of events (about 50 of intensity V and larger) is marginally sufficient for the use of maximum likelihood estimators. Furthermore, as will be seen below, the distribution of intensities with magnitude varies with time.

The value of b for the total Piedmont data set for intensity V or greater is 0.5 ± 0.15 . The b value is for intensity and should be divided by 0.6 to convert to magnitude. The resulting value of 0.8 for magnitude is consistent with other observed b values for tectonic earthquakes. The value for a is dependent on the length of time assumed for complete coverage. The earliest reported event was 1776 and the cumulative magnitude per year versus year suggests a reasonably steady rate of activity from 1875 to present. The historical data cover 110 to 210 years. For this analysis a time of 150 years is assumed with the understanding that the uncertainty is ± 30 years. The corresponding a value is 2.0 ± 0.2 , or 100 intensity 0 events per year in the Piedmont. The area defined for the Piedmont seismicity consists of 17 one degree quadrangles or 170000 km² assuming an average of 10000 km² for each degree quadrangle. The a value for quarter degree quadrangles, the units assumed in risk computation below, is then 0.2 ± 0.2 for each year in each quarter degree. The resulting recursion relation for the Piedmont seismicity is,

$$\text{Log}(N_c) = 0.2 \pm 0.2 - (0.5 \pm 0.15) I$$

where N_c is the cumulative number of events per year per 2500 km² of intensity greater than or equal to I (MM).

An examination of the recursion relation for three separate time periods reveals the uneven distribution of observed intensities as a function of time. The data before 1928 contain all the intensity VII earthquakes in the Southern Piedmont. Otherwise, the b value is within the uncertainty for the all earthquakes and the a value is also the same after corrections for the reduced time period. Hence, the seismicity before 1928 and the seismicity through the present are consistent. After 1948 the recursion relation is more normal except for a b value ($b = 0.7$) which is higher than the average value. The period between 1928 and 1948 represents 20 years when the overall level of seismicity was low and only intensity IV events were reported. This type of distribution is not consistent with a normal statistical distribution. Either these 20 years are anomalous or seismic documentation during this time period was inconsistent. For these reasons, the uncertainties of the values of a and b are probably greater than suggested by the maximum likelihood method.

Statistical Consideration of a Maximum Earthquake

The recursion relation implies no bounds at higher magnitudes, indicating only a reduced probability for the occurrence of the larger events. The recursion relation implies that two intensity VIII events should have been reported; however, none were reported. The probability that this would happen is 0.15 and is within the uncertainty of the data, particularly considering that one or more of the intensity VII events could have been in sparsely populated areas where intensity VIII reports would not be available.

A maximum intensity (i.e. maximum magnitude) event would be suggested by a significant under reporting of events, or equivalently, an increase in b value. Long (1974) noted a change in b value with magnitude but the observed change in value with increased magnitude was toward a lower b value. Although this relation indicates abnormally large numbers of small events, the low b values at higher magnitudes suggests a normal tectonic distribution without a maximum magnitude. As noted above, the lack of intensity VIII events would indicate an increase in b value but the observed data are still within the statistical uncertainty of the data. Hence, the data are suggestive, but inconclusive, for a maximum intensity at intensity VIII.

An alternate technique is to consider, arbitrarily, that the maximum intensity would correspond to an event that would occur in a given (long) time period. A justification for this approach could be found in a consideration of the length of time that stresses could be retained in the shallow crust, given the processes of chemical weathering that would be accelerated by high stress levels. If a 10000 year period is chosen, then the maximum intensity (or magnitude) event can be found by calculating the effect of uniform seismicity in the surrounding area. Figure 15 shows the expected rate of occurrence for the Strom Thurmond area for two models of seismicity. The first is uniform seismicity for the entire Piedmont. The second is a concentration of activity into two

sub-parallel bands, one extending through the Hartwell area and the other along the fall line. These two distributions of seismicity give return periods for the Strom Thurmond area of 15,000 years to 15,000 years for intensity VI.

The return periods were computed in terms of particle velocity in order to utilize the attenuation relation from Long (1974). The relations from Nuttli (1973) were used to convert intensity at the source to particle velocity prior to attenuation to the site. Standard methods for numerical integration of seismicity were used to obtain the probability of occurrence.

Maximum Intensity from a Major Earthquake

The maximum intensity expected for a major earthquake is based on observed intensity versus distance relations. For the Charleston epicenter, which is not considered active, the maximum intensity experienced at the Strom Thurmond reservoir was VIII. For a New Madrid size earthquake from southeastern Tennessee, the attenuation relations of Street (1982) give an intensity VIII also. No estimate of repeat time is assigned because major earthquakes following the model presented in this report would be transient phenomenon of duration less than 100 years. The separated in time of major earthquakes, if more than one occurs would be an unknown long time period.

DIRECT IDENTIFICATION OF POTENTIAL EARTHQUAKE SITES IN THE PIEDMONT

Introduction

The distribution of earthquakes in the Piedmont along two parallel trends suggests a possible correlation with rock type or crustal structure. The rock type, as characterized by the division of the Piedmont into belts of similar properties, is parallel to the major crustal structures. Because reservoir induced seismic activity correlates with jointing and rock type, the existence of the two parallel trends is perhaps best explained by the occurrences of appropriate granite gneiss geologic units at the surface.

Relation of Seismicity to Joint Intensity

A geologic field study of the area of induced seismic activity at Monticello Reservoir, South Carolina, Secor, et al. (1982) identified the source rock for the seismicity as the Winnsboro plutonic complex, a heterogeneous quartz monzonite. According to Secor et al. (1982)

"the Winnsboro complex contains numerous diversely oriented small fractures and lithological inhomogeneities having a maximum length of the order of 1-2 km. These local inhomogeneities, together with an irregular stress field, are interpreted to control the diffuse seismic activity that is occurring around Monticello Reservoir."

The possible relation of joints and small fractures to seismicity has been studied further at Georgia Tech in a field survey (Sorlien, 1987) in the Strom Thurmond Reservoir area near the McCormick S. C. epicenters. The results of that study suggest that the seismicity correlates with the edges of zones of granite gneiss with low measures of the trimean joint intensity (figure 12). The trimean joint intensity was devised as a means of standardizing estimates of rock quality. The low values correspond to zones of strong rock, rock able to accumulate significant stress and release that stress along existing joints or small fractures as microearthquakes. The surrounding areas which consist of more highly fractured rock, rock with significant schistosity, or weathered mafic rock, are unable to store the stresses required for significant induced seismicity. The Keowee seismic zone was studied in a similar way by Malcolm Schaefer, (Personal Communication) with similar results. This technique may prove to be the best method to predict susceptibility to induced seismicity, or equivalently, Piedmont seismicity. The details of the field study are presented in Appendix IV.

Role of Stress in Piedmont Seismicity

In order for a weakening of a joint or fracture surface to lead to a shallow Piedmont earthquake, a shear stress must exist on the fracture. The shear stress can be from stresses remaining after previous tectonic activity or can be recently introduced.

Residual stresses would include the stresses from flexure of the crust by the loading of the Coastal Plane sediments and regional stresses related to uplift and erosion. They could also include stresses from the compression or extension of the crust by changes in plate boundary forces that would change the direction or magnitude of the dominant regional stress.

The local or recently induced stresses include stresses induced by reservoir impoundment. The load of the water has been noted to contribute to induced seismicity. The contribution is significant for reservoirs greater than 100 m deep. However, in the Piedmont the reservoirs are less than 100 m deep and significantly shallower near the sites of induced seismicity. Instead the mechanisms for induced and natural Piedmont earthquakes depend on penetration of the crystalline rock by fluids and eventual weakening of fracture surfaces at shallow depths. The penetration of fluids can influence stress in three ways:

First, the fluids can change the fluid pressure in the rock and an increase in hydrostatic pressure in the fluids can decrease the shear strength. Events triggered by this mechanism can occur almost immediately, and the delay is limited only by the time required to propagate a pressure pulse to depth, typically less than one month in the Piedmont.

Second, given a time period of a few months, variations in temperature of fluids moving through fractures can induce thermal stresses by cooling or heating the rock adjacent to the fracture. Although a thermal stress mechanism is acknowledged for areas of anomalously high temperatures, its role in Piedmont seismicity has not been examined in detail. Preliminary estimates of seasonal changes in temperature of reservoir water suggest that magnitude 2.0 earthquakes could easily be caused by thermal perturbations of the ground water. The observed increase in Piedmont events in the winter months supports the thermal mechanism in that the colder water temperature would cause contraction of the rock which would ease penetration of fluids into the rock and decrease frictional resistance.

Third, irregular weathering patterns near the surface would cause an uneven release of stress in an irregular geometry of resistant rock which could create zones in which the remaining unweathered rock would be capable of amplifying stress or failing in an earthquake.

Stresses in the Strom Thurmond Reservoir Area

During the study of joint spacing reported in Appendix IV, data were gathered on relative timing of joint formation and movement. Observations include joint terminations, microstructures such as riedel shears, striations, and extension jointing. These observations can be used in an interpretation of the stress history of the area. On selected outcrops, where most joint surfaces were exposed, attitudes of all joints were measured. Where striated fractures were present, the attitude of the fracture and pitch and sense of the striation were determined and the striation or slickenside were described. Stress field solutions were obtained by the method of right dihedral angles (Angelier, 1977, 1979). The sense of motion of striations on black manganese dioxide or pyroclastic slickenside surfaces was more difficult to determine, and normal slip on these surfaces may have been related to gravitational failure decoupled from a tectonic stress field. North of the study area in the Richard B. Russell Reservoir area unusually reliable striation indicators were observed for 4 microfaults. Using sense of movement indicators after Angelier (1985), reverse motion was interpreted and was consistent with reverse offsets of a few centimeters on joints.

The SE joint set is offset by ENE striking fractures, implying that the SE joints are the oldest fractures. The SE striking set is easily recognized because the joints that make up the set are very continuous, planar, and parallel. In the Strom Thurmond Reservoir area the SE set has a 5 mm mineral coating, implying that they were under more tension than other orientations at the time of mineralization. In some cases sub-horizontal microfractures offset vertical joints, while in others the sub-horizontal surfaces of joints terminate against other joints. In both cases the sub-horizontal surfaces are more recent, and may be related to unloading.

Variability existed in the orientation and type of microfault, as well as in the direction of paleostress field that caused the slip. In the Strom Thurmond Reservoir area clear sinistral and dextral striations were observed on the same SE striking joint surface, with the dextral motion in both cases being older. The two generations of motion are mixed among nearby outcrops in the Strom Thurmond Reservoir area. Stress solutions can not be made without separating these apparently anomalous movements.

Focal mechanisms of the aftershocks of the McCormick earthquake were not consistent, with individual aftershocks often showing focal mechanisms that differed from previous events (Guinn, 1977). These include a low angle thrust for the main quake; EW striking sinistral faults, SE striking normal and dextral faults, and low angle thrusts for various sets of aftershocks. A mixture of focal mechanism solutions and stress directions have been observed at other reservoirs in the S. Carolina Piedmont (Zoback and Hickman, 1982; Hainson and Zoback, 1974). Talwani (1977) reports that focal mechanism solutions favor a maximum horizontal compressive stress axis oriented NW at Lake Jocassee, while

nearby hydraulic fracturing show it to be NE.

The striation data of this study suggest that the older stress field involved a NNW-SSE compression, while the younger suggests an E-W to ENE compression. Relative dating is inferred by overprinting of striations on two outcrops, and the freshness of the striation. Locally, in the Richard B. Russell Reservoir area, reverse dip slip shows a uniaxial stress field, with the least principal stress vertical, perhaps, related to unloading. It was assumed that even hard rock striations are eventually destroyed in a fluid filled crack, since soluble minerals will eventually be dissolved from the striations or deposited onto the striations. The motion that caused the striations occurred after the last major plate tectonic event in the Mesozoic, and perhaps recently, since older striations would be destroyed and overprinted during tectonism.

The changes in the principle direction of stress from NNW-SSE to ENE suggests that the area has experienced a variety of stress directions and magnitudes. The observation that the most recent stress release was due to vertical unloading and that focal mechanisms are highly variable suggests that the local stresses dominate the near-surface rocks in the Strom Thurmond Reservoir area. This decreases the likelihood that regional stresses exist and could lead to larger (magnitude 4.5 to 5.5) events in the Piedmont.

MECHANISM PROPOSAL FOR A MAXIMUM PIEDMONT EARTHQUAKE

The 1982 New Brunswick earthquakes have all the properties of a Piedmont earthquake, except an association with a reservoir. Hence, these earthquakes will be used as a model for a maximum Piedmont earthquake. The magnitude range of 5.6 to 5.8 for the larger event is considered appropriate for the maximum Piedmont earthquake. The largest event would suggest a maximum magnitude of 5.8.

The maximum depth for the New Brunswick earthquakes was about 7 km. The maximum Piedmont earthquake is constrained to shallow depths by hydrostatic pressure, which increases the strength of joints or minor fractures with increased depth. For tensional stress conditions, the average regional plate stress is below the stress needed for failure at depths below about 10 km; however, this relation, from Meissner and Strehlau (1982), is highly dependent on properties of the joint surface. The depth of rupture for the New Brunswick earthquakes may be considered a reasonable limit to the depth of Piedmont earthquakes. Its stress drop of 35 to 70 Bar is high compared to other earthquakes and consistent with its occurrence in a zone of high crustal strength. The combination of stress drop and maximum fault size are consistent with a maximum magnitude 5.8 event as computed from the relations of Randal (1973).

The New Brunswick earthquakes were located in a large undeformed granite. The granite is more rigid than the surrounding rocks, consistent with the location of events in rocks of high measured rock quality in the Strom Thurmond Reservoir area. The primary association of geology with seismicity is the correspondence between the joint directions and inferred faulting and in the rock quality as measured by joint intensity. The concentration of activity in the granite is consistent with the lack of evidence for activity on nearby faults and shear zones. The existence of inactive shear zones and other inactive surface geology features imply that the many faults and shear zones in the Southern Piedmont should not pose a seismic risk.

The lack of surface rupture and the apparent dissipation of displacement at the surface by joints is characteristic of a release of volume stress. The volume stress release mechanism is consistent with the observation of clusters of earthquakes in Lake Sinclair area and other reservoir induced seismicity areas. The source of stress for these events is not known. A proposed mechanism for the New Brunswick earthquakes was glacial rebound and the resulting bending of the crust. Because this mechanism is not operative in the Southern Piedmont, the maximum Piedmont earthquake might actually be less than those observed in the New Brunswick events. A second mechanism would be the triggered release of stored tectonic plate stress which has been proposed for the reservoir induced activity in the Southern Piedmont.

SUMMARY AND CONCLUSION

In this study, the mechanism for an intraplate earthquake occurring in the southeastern United States is assumed to fit one of two distinct models. For major earthquakes, the mechanism is dependent on deformation of the lower crust and the resulting amplification of stress in the strong central portion of the crust. The second model is for the Piedmont type earthquake, which in the Piedmont province is the same model developed for reservoir induced seismicity.

If a major earthquake were to occur in southeastern Tennessee, the only currently suspect area for a major event, the intensity at the Strom Thurmond Reservoir would be about VIII (MM). No estimate can be placed on the probability of such an event occurring because it may be a short term process (less than 100 yr) and because the triggering mechanism depends on a perturbation of fluids in the lower crust, a phenomenon not well understood.

A statistical analysis of Piedmont earthquakes indicated that an intensity VII event would be experienced once every 10,000 to 30,000 years in the Strom Thurmond Reservoir area. The statistics are uncertain not only because of expected gaps in historical record, but also because the rate of activity may have been influenced by reservoir impoundment, related industrial activities and rain fall.

Measurements of stress directions from studies of joints and from earthquake focal mechanisms suggest that the directions are highly inhomogeneous. This suggests that local sources of stress dominate and that the level of regional stress is low.

The development of the Piedmont earthquake mechanism allows interpretation of a maximum earthquake. The maximum earthquake for a Piedmont type event is 5.8 under conditions of high horizontal stress; however, in this low-stress environment of the southern Piedmont near the Strom Thurmond Reservoir the maximum event is probably less.

The near surface stresses in the Strom Thurmond Reservoir area are varied in direction and are likely low in magnitude.

MAXIMUM EARTHQUAKE AT STROM THURMONT RESERVOIR

BIBLIOGRAPHY OF CITED AND SUPPLEMENTAL REFERENCES CONCERNING PIEDMONT GEOLOGY AND SEISMOLOGY

- Acharya, Hemendra, 1980. Spatial correlation of large historic earthquakes and moderate shocks >10 km deep in eastern North America, Geophysical Research Letters, v. 7, No. 12, 1061-1064.
- Acree, S. D., J. R. Acree, and Pradeep Talwani, 1988. The Lake Keowee, S.C. earthquakes of February through July, 1986, Seismological Research Letters, Vol. 59, pp 63-70.
- Aki, K., 1965. Maximum likelihood estimate of b in the formula $\log N = a - bM$ and its confidence limits, Bull. Earthquake Res. Inst. Tokyo Univ., v. 43, 237-239.
- Allison, J. D., 1980. Seismicity of the Central Georgia Seismic Zone, Master Thesis, Georgia Institute of Technology, Atlanta, GA, pp.
- Amick, D. and P. Talwani, 1986. Earthquake recurrence rates and probability estimates for the occurrence of significant seismic activity in the Charleston area, the next 100 years, in Proc. on 3rd Nat. Conf. on Earthquake Engineering, v. 1, 55-64.
- Angelier, J. and P. Mechler, 1977. Sur une methode graphique de recherche des contraintes principales egalement utilisable en tectonique et en seismologie: la methode des diedres droits. Bull. Soc. Geol. France, no. 6, 1309-1318.
- Angelier, J., 1979. Determination of the mean principal stresses for a given fault population. Tectonophysics, 56, T17-T26.
- Angelier, J., Colleta, B. and R.E. Anderson, 1985. Neogene paleostress changes in the Basin and Range, A case study at Hoover Dam, Nevada-Arizona, G.S.A. Bull., v. 96, p. 347-361.
- Angevine, C.L., Turcotte, D.L., and M.D. Furnish, 1982. Pressure solution lithification as a mechanism for the stick slip behavior of faults, Tectonics, v. 1 no.2, p. 151-160.
- Barosh, P.J., 1986. Neotectonic movement, earthquakes and stress state in the eastern United States, Tectonophysics, 132, p. 117-152.
- Barton, N., Lien, R., and J. Lunde, 1974. Engineering classification of rock masses for the design of tunnel support, Rock Mechanics, 6, p. 189-236.
- Bell, H., III, 1973. Some results of geochemical sampling in McCormick county, South Carolina, Geological Survey Bulletin 1376.

Bell, M. L. and A. Nur, 1978. Strength changes due to reservoir-induced pore pressure and stresses and application to Lake Oroville, J. Geophys. Res., 83, 4469-4483.

Benson, A. F. and Fogle, G. H., 1974. Intensity survey of Lincoln County, Georgia, McCormick County, South Carolina, earthquake of August 2, 1974, Earthquake Notes, 45, 27-29.

Bevis, M., and L. Gilbert, 1984. The fracture fabric of the southeast USA, EOS, v. 65, no. 16.

Billings, M.P., 1972. Structural Geology, Third Edition, Prentice-Hall, Englewood Cliffs, New Jersey, 588 p.

Bishop, A. W., 1974. The strength of crustal materials, Engineering Geology, 8, 139-153.

Bles, J.L., and B. Feuga, 1986. The Fracture of Rocks, Elsevier, 127 p.

Bles, J.-L., and Y. Gros, 1986. Genese des failles dans les granites: posteriorite des grandes failles par rapport a la petite fracturation, C.R. Acad. Sc. Paris, t.303, serie II, no. 15.

Bollinger, G. A., and M. G. Hopper, 1972. The earthquake history of Virginia 1900 - 1970, Dept. of Geological Sciences, VPI & SU, Blacksburg, VA.

Bollinger, G. A., 1972. Historical and recent seismic activity in South Carolina, Bull. Seism. Soc. Am. 62, 851-864.

Bollinger, G. A., 1973. Seismicity and crustal uplift in the southeastern United States, Am. J. Sci., Cooper 273-A, 396-408.

Bollinger, G. A., 1973. Seismicity of the southeastern U. S., Bull. Seism. Soc. Am. 63, 1785-1808.

Bollinger, G. A., 1975. A catalog of Southeastern United States earthquakes 1754 through 1974, in Research Division Bulletin 101, Dept. of Geological Sciences, Virginia Polytechnic Institute and State University, Blacksburg, VA.

Bollinger, G. A., 1975. A microearthquake survey of the central Virginia seismic zone, Earthquake Notes, 46, 3-13.

Bollinger, G. A., 1986. Network results for Virginia's intraplate seismicity -spatial and mechanical variability, Earthquake Notes, 57, 6.

Bollinger, G. A., M. C. Chapman, and M. S. Sibol, 1984. Virginia regional Seismic Network, 77-134-27, p. 14.

- Bollinger, G. A., M. C. Chapman, M. S. Sibol, and J. K. Costain, 1985. An analysis of earthquake focal depths in the southeastern U. W., Geophys. Res. Lett., 12, 785-788.
- Bollinger, G. A., and M. S. Sibol, 1985. Seismicity, seismic reflection studies, geology and gravity in the central Virginia seismic zone: Part 1. Seismicity, Bull. Geol. Soc. Am., (in Press)
- Bollinger, G. A., A. G. Teague, J. W. Munsey, and A. C. Johnston, 1985. Focal mechanism analyses for Virginia and Eastern Tennessee earthquakes (1978-1984), Report NUREG/CR-4288 RA, 83p, U.S. Nuclear Regulatory Commission, 1717 H Street, Washington D.C. 20555, 57 pp.
- Bollinger, G. A., and R. I. Wheeler, 1982. The Giles County, Virginia, seismogenic zone-- Seismological results and geologic interpretations, U.S. Geological Survey Open File Report, 82-585, 136p.
- Bott, M.H.P., and N.J. Kusmir, 1984. The origin of tectonic stress in the lithosphere. in: S.M. Naqvi, K. Gupta and Balakrishna (Editors), Lithosphere: Structure, Dynamics and Evolution, Tectonophysics, 105, 1-13.
- Bridges, S. R., 1975. Evaluation of stress drop of the August 2, 1974, Georgia-South Carolina earthquake and aftershock sequence, Master Thesis, Georgia Institute of Technology, Atlanta, GA, 103 p.
- Bufone, E. and A. Udias, 1979. A note on induced seismicity in dams and reservoirs in Spain, Bull. Seism. Soc. Am., 69, 1629-1632.
- Burger, H., Shala, W. and V. Weber, 1985. Geostatistical methods for the analysis and prediction of fractures. In: P.S. Glaeser (Editor), The Role of Data in Scientific Progress, Elsevier, CODATA.
- Carder, D. S., 1945. Seismic investigations in the Boulder Dam area, 1940-1944, and the influence of reservoir loading on earthquake activity, Bull. Seism. Soc. Am., 35, 175-192.
- Castle, R. O., M. M. Clark, A. Grantz, and J. C. Savage, 1980. Tectonic state: its significance and characterization in the assessment of seismic effects associated with reservoir impounding, Eng. Geol., 15, 53-99.
- Cornell, A., 1968. Engineering Seismic Risk Analysis, Bull. Seism. Soc. Am. 58, 1583-1606.
- Costain, J. K., G. A. Bollinger, and J. A. Speer, 1986. Hydro-seismicity: A hypothesis for intraplate seismicity near passive rifted margins, Earthquake Notes 57, 13.
- Costain, J. K., G. A. Bollinger, and J. A. Speer, 1987. Hydro-seismicity: a hypothesis for the role of water in the generation of intraplate seismicity, Seism. Res. Lett., 58, 41-64.

- Costain, J. K., G. A. Bollinger, and J. A. Speer, 1987. Hydro-seismicity: a hypothesis for the role of water in the generation of intraplate seismicity, Geology, 15, 618-621.
- Crough, S.T., 1983. Rifts and swells: geophysical constraints on causality, Tectonophysics, 94, 23-37.
- Davis, G.H., 1984. Structural Geology of Rocks and Regions, John Wiley and Sons, New York, 447 p.
- Davison, F. C., and M. J. Bode', 1987. A note on the December 1986 - January 1987 Richmond, Virginia, felt earthquake sequence, Seism. Res. Letters, 58, No. 3, 73-80.
- Davison, F. C., M.C. Chapman, J.W. Munsey, and G.A. Bollinger, 1984. A note on the Cunningham, Virginia earthquake of August 17, 1984, in the Central Virginia Seismic Zone, Earthquake Notes 55, 26-33.
- Denman, H. E., Jr., 1974. Implications of seismic activity at the Clark Hill Reservoir, unpublished thesis, Georgia Institute of Technology, Atlanta, Georgia, 103p.
- Dorman, LeRoy M., 1972. Seismic crustal anisotropy in northern Georgia, Bull. Seism. Soc. Am., 62, 39-45.
- Duc, A. C., 1980. Source properties of induced earthquakes at Monticello Reservoir, South Carolina, Master Thesis, University of South Carolina, Columbia, SC, 151 pp.
- Dunbar, D. M., 1977. A seismic velocity model of the Clarks Hill Reservoir area, Master Thesis, Georgia Institute of Technology, Atlanta, GA, 59 pp.
- Engelder, T., 1982. Is there a genetic relationship between selected regional joints and contemporary stress within the lithosphere of North America?, Tectonics, v. 1, no. 2, 161-177.
- Engelder, T., 1985. Loading paths to joint propagation during a tectonic cycle: an example from the Appalachian Plateau, U.S.A., Journal of Structural Geology, v. 7, nos. 3/4, 459-476.
- Fabbri, L.A. (1986). Geophysical interpretation of a portion of the Southern Appalachian Blue Ridge and Inner Piedmont, Master's Thesis, Univ. of South Carolina, 68 pp.
- Fletcher, J. B., 1979. Spectra from high-dynamic range digital recordings of Oroville, California, aftershocks and their source parameters (preprint)????

- Fletcher, J. B., 1982. A comparison between the tectonic stress measured in situ and stress parameters from induced seismicity at Monticello Reservoir, South Carolina, J. Geophys. Res., 87, 6931-6944.
- Fogle, G. H., R. M. White, A. F. Benson, L. T. Long, and G. F. Sowers, 1976. Reservoir induced seismicity at Lake Jocassee, northwestern South Carolina, Law Engineering Testing Co., Marietta, Georgia.
- Fyfe, W. S., N. J. Price and A. B. Thompson, 1978. Fluids in the Earth's Crust, Elsevier, Amsterdam, 383pp.
- Gauthier, B. and J. Angelier, 1986. Distribution et signification geodynamique des systemes de joints en contexte distensif: un exemple dans le rift de Suez, C.R. Acad. Sc. Paris, t. 303, Serie II, no. 12.
- Gough, D.I., and W.I. Gough, 1976. Time dependence and trigger mechanism for the Kariba (Rhodesia earthquakes, Engineering Geology, 10, 211-217.
- Guinn, S. A., 1977. Earthquake focal mechanisms in the southeastern United States, Masters Thesis, Georgia Institute of Technology, Atlanta, GA, 150 pp.
- Guinn, S.A., 1980. Earthquake focal mechanisms in the southeastern United States, Nureg/Cr-1503, 150 p.
- Griffin, V. S., Jr., 1973. Geology of the Old Pickens Gaudrangle, South Carolina, Publication MS-18, Div. of Geology, S.C., State Development Board, Columbia, S.C., 54 pp.
- Gupta, H. K., 1983. Induced Seismicity hazard mitigation through water level manipulation at Koyna, India: A suggestion, Bull Seis. Soc Am., 73, 679-682.
- Gupta, H. K. and B. K. Rastogi, 1976. Dams and Earthquakes, Developments in Geotechnical Engineering 11, Elsevier Scientific Publishing Co., Amsterdam, 229 pp.
- Gupta, H. K., B. K. Rastogi, and H. Narain, 1972a. Common features of the reservoir-associated seismic activities, Bull. Seism. Soc. Am. 62, 481-492.
- Gupta, H. K., B. K. Rastogi, and H. Narain, 1972b. Some discriminatory characteristics of earthquakes near the Kariba, Kremasta, and Koyna artificial lakes, Bull. Seism. Soc. Am. 62, 493-507.
- Hadley, J. B., and J. F. Devine, 1974. Seismotectonic map of the eastern United States: Miscellaneous Field Studies Map MR-620, U. S. Geol. Survey, Reston, VA, 8 p. and 3 maps.
- Haimson, B. D., 1975. Hydrofracturing stress measurements, Bad Creek Pumped Storage project, Report for Duke Power Company, 19pp.

- Haimson, B. C., and M. D. Zoback, 1978. A new look at the hydrofracturing stress measurements near the Monticello Reservoir, S. Carolina, EOS (Am. Geophys. Union Trans.), 65, No. 16, 278.
- Hancock, P.L., 1985. Brittle microtectonics: principles and practice, Journal of Structural Geology, v. 7, nos. 3/4, 437-457.
- Hasegawa, H.W., J. Adams, and K. Yamazaki, 1985. Upper crustal stresses and vertical stress migration in eastern Canada, Journal of Geophysical Research, v. 90, no. B5, 3637-3648.
- Hatcher, R. D., Jr., 1977. Macroscopic polyphase folding illustrated by the Toxaway dome, eastern Blue Ridge, South Carolina-North Carolina, Geol. Soc. Am. Bull., 88, 1678-1688.
- Hatcher, R. D., Jr., 1987. Tectonics of the southern and central Appalachian internides, Annual Reviews of Earth and Planetary Sciences, v. 15, p. 337-362.
- Hatcher, R. D., and I. Zietz, 1980. Tectonic implications of regional aeromagnetic and gravity data from the Southern Appalachians: International Geological Correlation Program-Caledonide Orogen Project Symposium, edited by Wones, D., 235-244.
- Higgins, M. W., R. L. Atkins, T. J. Crawford, R. F. Crawford, III, Regekah Brooks, R. B. Cook, 1986. The structure, stratigraphy, tectonostratigraphy, and evolution of the southern most part of the Appalachian Orogen, Georgia, and Alabama. U. S. Geological Survey, Open File Report 86-372.
- Hooper, M.G., and G. A. Bollinger, 1971. The earthquake history of Virginia 1774 to 1900, Dept. of Geological Sciences, VPI & SU, Blacksburg, VA.
- Hubbert, M. K. and W. W. Rubey, 1959. The role of fluid pressure in mechanics of overthrust faulting, Bull. Geol. Soc. Am., 70, 115-160.
- Hutchenson, K., and P. Talwani, 1982. Gravity survey of the Irmo Quadrangle, South Carolina, South Carolina Geology, 26 (1), 25-38.
- Jacob, K. H., W. D. Pennington, J. Armbruster, L. Seeber, and S. Farhattulla, 1979. Tarbela Reservoir, Pakistan: A region of compressional tectonics with reduced seismicity upon initial reservoir filling, Bull. Seism. Soc. Am., 69, 1175-1192.
- Johnson, A. P., 1984. The Twiggs County earthquake swarm, Master Thesis, Georgia Institute of Technology, Atlanta, GA 125 pp.
- Johnston, A.C., D.J. Reinbold and S.I. Brewer, 1985. Seismotectonics of the southern Appalachians, Bull. Seism. Soc. Am. 75, 291-312.

- Johnston, G. L., 1980. A seismic spectral discriminant for reservoir induced earthquakes in the southeastern United States, Master Thesis, Georgia Institute of Technology, Atlanta, GA, 115 pp.
- Jones, Frank B., L. T. Long, M. C. Chapman, and K.-H. Zelt, 1985. Columbus, Georgia, earthquakes of October 31, 1982, Earthquake Notes, 56, No. 2, 55-61.
- Kean, A. E., and L. T. Long, 1980. A seismic refraction line along the axis of the Southern Piedmont and crustal thicknesses in the southeastern United States, Earthquake Notes, 51,4, 1-13.
- Keith, C.M., D.W. Simpson and O.V. Soboleva, 1982. Induced seismicity and style of deformation at Nurek reservoir, Tadjik SSR., Journal of Geophysical Research, v. 87, no. B6, 4609-4624.
- Kuang, Jian, 1988. Intraplate stress and seismicity in the southeastern United States, Ph.D. Thesis, Georgia Institute of Technology, Atlanta, GA. 119 pp.
- Latynina, L.A., 1981. Hydrogeological effects in deformations of the Earth's surface, Izvestiya, Earth Physics, v. 17, no. 11, 812-816.
- Leary, P., P. Malin, R. A. Phinney and R. Voncolln, 1975. Seismic travel time experiment with air gun source, Clarks Hill Reservoir, South Carolina, March 1975, Field Report, Princeton University,
- Lee, C. K., 1980. A study of the crustal structure of north central Georgia and South Carolina by analysis of synthetic seismograms, Master Thesis, Georgia Institute of Technology, Atlanta, GA, 121pp.
- Long, L. T., 1974. Earthquake sequences and b values in the southeast United States, Bull. Seism. Soc. Am. 64, 267-273.
- Long, L. T., 1976. Short-period surface wave attenuation and intensities in the Georgia-South Carolina Piedmont Province, Earthquake Notes, 47, 3-11.
- Long, L. T., 1979. The Carolina Slate Belt-Evidence of a continental rift zone, Geology, 7, 180-184.
- Long, L. T., 1982. Seismicity of Georgia, in Arden, D. D., Beck, B. F., and Morrow, E., eds., Proceedings of the second symposium on the geology of the southeastern Coastal Plain, Americus, Georgia, March 5-6, 1979: Atlanta, Georgia Geologic Survey Information Circular 53, 202-210.
- Long, L. T., H. E. Denman, H. Hsiao, and G. E. Marion, 1976. Gravity and seismic studies in the Clarks Hill Reservoir Area, Georgia Geological Society, Guidebook 16, 33-41.
- MacCarthy, G. R., 1964. A descriptive list of Virginia earthquakes through 1960, J. of the Elisha Mitchell Scientific Society 80, 95-114.

- McDonald, K.C., D.A. Castillo, S.P. Miller, P.J. Fox, K.A. Kastens, and Bonatti, 1986. Deep-tow studies of the Vema Fracture Zone: Tectonics of a major slow slipping transform fault and its intersection with the Mid-Atlantic Ridge. J. Geophys. Res., v. 91, No. B3, 3334-3354.
- Marion, G. E., and L. T. Long, 1980. Microearthquake spectra in the southeastern United States, Bull. Seism. Soc. Am. 79, 1037-1054.
- Marion, G. E., 1977. The spectral analysis of microearthquakes that occur in the southeastern United States, Masters Thesis, Georgia Institute of Technology, Atlanta, Georgia, 154p. (see Marion and Long, 1980)
- Meissner, R., and Strehlau, 1982. Limits of stresses in continental crusts and their relation to the depth-frequency distribution of shallow earthquakes, Tectonics, 1, 73-78.
- Merkler, G., G. Bock, and K. Fuchs, 1981. Correlation between seismic microactivity, temperature and subsidence of water level at reservoirs, J. Geophysics, 49, p. 198-206.
- Moos, D., and Zoback, M. D., 1983. In situ studies of velocity in fractured crystalline rocks, J. Geophys. Res., 88, B3, 2345-2358.
- Munsey, J. W., and G. A. Bollinger, 1985. Focal mechanism analyses for Virginia earthquakes, 1978 - 1984, Bull. Seism. Soc. Am. 75, 1613-1636.
- Narasimhan, T.N., W.N. Houston and A.M. Nur, 1980. The role of pure pressure in deformation in geologic processes. Prepared for the U.S. Dept. of Energy, contract W-7405-ENG-48, submitted to Geology.
- Nava, S. J., and A. C. Johnston, 1984. Rivers and earthquakes: A correlation for New Madrid and the Mississippi River, Earthquake Notes, 55, 15.
- Nielson, R.A., 1979. Natural fracture systems: Description and classification. Geologic Notes, v. 63, No. 12, 2214-2232.
- Nicolas, A., 1984. Principes de tectonique, Masson, Paris, 190 p.
- Nur, A., 1973. Role of pore fluids in faulting. Phil. Trans. R. Soc. Lond. A. 274, 297-304.
- Nur, A. and J.D. Byerlee, 1971. An exact effective stress law for elastic deformation of rocks and fluids. J. Geophys. Res. v.?, 6414-6419.
- Nur, A., Bell, M.L., and P. Talwani, 1973. Fluid flow and faulting, 1: A detailed study of the dilatancy mechanism and premonitory velocity changes, Proc. Conf. on Tectonic Problems of the San Andreas Fault System, ed. R.L. Kovach and A. Nur, Stanford, 391-404.

- Nuttli, O. W., 1973. Seismic wave attenuation and magnitude relations for Eastern North America. Jour. Geophys. Res. 78, 876-885.
- Nuttli, O. W., G. A. Bollinger, and D. W. Griffiths, 1979. On the relation between Modified Mercalli intensity and body wave magnitude, Bull. Seism. Soc. Am., 69, 893-909.
- Overstreet, W. C. and H. Bell, III, 1965. The crystalline rocks of South Carolina: U. S. Geol. Survey Bull. 1186, 126 pp.
- Poley, C.M. and P. Talwani, 1986. Vertical tectonics in the Charleston, South Carolina area, J. Geophys. Res., 91, 9056-0966.
- Price, N.J., 1966. Fault and Joint Development, Pergamon Press, London.
- Prowell, D. C., 1983. Index of Cretaceous and Cenozoic faults in the eastern United States, U. S. Geological Survey Miscellaneous Field Studies Map MR-1269, Scale 1:2,500,000.
- Prowell, D. C. and B. J. O'Connor, 1978. Belair fault zone: Evidence of Tertiary fault displacement in eastern Georgia, Geology, 6, 681-684.
- Radford, E., 1988. A relocation of earthquakes in the Lake Sinclair area, Master Thesis, Georgia Institute of Technology, Atlanta, Georgia.
- Randal, M. J., 1973. The spectral theory of seismic sources, Bull. seism. Soc. Am., 63, 1133-1144.
- Rastogi, B.K. and Talwani, P., 1980. Relocation of Koyna earthquakes, Bull. Seism. Soc. Am., 70, 1849-1868.
- Rastogi, B., and Talwani, P., 1980. Spatial and temporal variations in t_s/t_p at Monticello Reservoir, South Carolina, Geophys. Res. Let., 7, 781-784.
- Rastogi, B.K. and P. Talwani, 1983. Reservoir-induced seismicity at Lake Jocassee in South Carolina, USA, in Proceedings of Indo-German Workshop on Rock Mechanics (12 & 13 Oct 1981), edited by T.N. Gowd and R. Rummel, National Geophysical Research Institute, Hyderabad, India, 225-232.
- Reagor, B. G., C. W. Stover, and S. T. Algermissen, 1980. Seismicity map of the state of Virginia, U. S. Geol. Survey Map MF-1257, Reston, VA.
- Reinbold, D. J., and A. C. Johnston, 1986. Historical seismicity in the Southern Appalachian Seismic Zone, USGS Final Technical Report, Contract No. 14-08-0001-21902, 40 pp.

Reinhardt, J., D. C. Prowell, and R. A. Christopher, 1984. Evidence for Cenozoic tectonism in the southwest Georgia Piedmont, Geological Society of America Bulletin, 95, 1176-1187.

Rice, J. R. and M. P. Cleary, 1976. Some basic stress diffusion solutions for fluid-saturated elastic porous media with compressible constituents, Rev. Geophys. Space Phy., 14, 227-241.

Rispoli, R. and G. Vasseur, 1983. Variation with depth of the stress tensor anisotropy inferred from microfault analyses. Tectonophysics, 93, 169-184.

Robinson, A. and P. Talwani, 1983. Building damage at Charleston, South Carolina, associated with the 1886 earthquake Bull. Seism. Soc. Am., 73, (2), 633-652.

Roeloffs, E.A., 1986. Stress and pore pressure changes due to annual water level cycles in seismic reservoirs, (Abs.) EOS Trans. Am. Geophys. Un., 66, 314.

Roeloffs, E.A., T.F. Cho, and B.C. Haimson, 1986. Stress and pore pressure changes due to annual water level cycles in seismic reservoirs, National Earthquake Hazards Reduction Program, Summaries of Technical Reports, Volume XXII, Open File Report 86-383, 473-474.

Ross, C.P., 1987. The origin of vertical fractures and their effects on seismic velocity, Comprehensive exam, Georgia Tech.

Rudnicki, J.W., 1984. Coupled deformation-diffusion effects. Final Technical Report, Contract 14-08=0001-21818, U.S.G.S., Reston, VA, 16pp.

Rundle, T.A., M.M. Singh and C.H. Baker, 1985. In situ stress measurements in the earth's crust in the eastern United States, final report, Engineers International, Inc., prepared for U.S. Nuclear Regulatory Commission, 75 pp.

Sauber, Jeanne and P. Talwani, 1980. Application of Kellis-Borok and McNally prediction algorithms to earthquakes in the Lake Jocassee area. South Carolina, Phys. Earth and Planetary Interiors, 21, 167-281.

Sbar, M. L. and L. R. Sykes, 1973. Contemporary compressive stress and seismicity in eastern North America: An example of intraplate tectonics, Geol. Soc. Amer. Bull. Vol. 84, 1861-1882.

Schaeffer, M.F., 1987. Geology of the Keowee-Toxaway complex, northwestern South Carolina, Field Trip Guidebook, Assoc. of Eng. Geol., 30th Annual Meeting, Atlanta, Ga., 15-93.

Schaeffer, M.F., R.E. Steffans and R.D. Hatcher, Jr., 1979. In-situ stress and its relationship to joint formation in the Toxaway gneiss, northwestern South Carolina, Southeastern Geology, 20, 129-143.

Scheffler, P. K., 1976. The McCormick county, South Carolina Earthquake of 2 August, 1974, Master Thesis, University of South Carolina, Columbia, SC.

Scholtz, C. H., 1968. The frequency-magnitude relation of micro-fracturing in rock and its relation to earthquakes, Bull. Seism. Soc. Am. 58, 399-415.

Scholz, C. H., and C. A. Aviles, 1986. The fractal geometry of faults and faulting, in Earthquake Source Mechanics, (eds. S. Das, J. Boatwright, and C. H. Scholz) Geophysical Monograph 37, American Geophysical Union, Washington, D.C. 147-155.

Scholz, C. H., L. R. Sykes, and Y. P. Aggarwal, 1973. Earthquake prediction: a physical basis, Science, 181, 803-810.

Schultz, S., R.O. Burford, and B. Mauko, 1983. Influence of seismicity and rainfall on episodic creep on the San Andreas fault system in central California, J. Geophys. Res. 88, no. B9, 7475-7484.

Secor Jr., D. T., L. S. Peck, D. Pitcher, D. Powell, D. Simpson, W. Smith, and A. Snoke, 1982. Geology of the area of induced seismic activity at Monticello Reservoir, South Carolina, J. Geophys. Res., 87, B8, 6945-6957.

Secor, D.T., Jr., 1965. Role of fluid pressure in jointing, American Journal of Science, v. 263, 633-646.

Seeber, L., and J. G. Armbruster, 1987. The 1886-1889 aftershocks of the Charleston, South Carolina, earthquake: a widespread burst of seismicity, Jour. Geophys. Res., 92, No. B3, 2663-2696.

Seeberger, D.A., and Zoback, M.D., 1982. The distribution of natural fractures and joints at depth in crystalline rock, J. Geophys. Res. 87, 5517-5534.

Setterquist, S., and M. Sibol, 1987. Energy release cyclicity in Seismological Research Letters, 58, 104.

Severy, N. I., G. A. Bollinger and H. W. Bohannon, Jr., 1975. A seismic comparison of Lake Anna and other Piedmont Province reservoirs in the eastern U.S.A., Preprint, 1st Int'l Symposium on Induced Seismicity, Banff, Alberta, 24 pp.

Sibol, M. S., and G. A. Bollinger, 1981. A note on the recent seismicity in the Scottsville, Virginia, area, Earthquake Notes, 52, No. 4, 11-22.

Sibol, M. S., and G. A. Bollinger, 1984. Hypocenter listing from Southeastern U. S. Seismic Bulletins No. 1-12 (July 1977-July 1983), Southeastern U. S. Seismic Bulletin No. 12A, 44 pp., Va. Polytechnic Institute, Blacksburg, VA. 24061.

Sibol, M. S., G. A. Bollinger, and J. B. Birch, 1987. Estimation of magnitudes in the central and eastern North America using intensity and felt area, Bull. Seism. Soc. Am. 77, (in press).

Simpson, D.W., 1976. Seismicity changes associated with reservoir loading, Engineering Geology, 10, 123-150.

Simpson, D.W. and O.B. Soboleva, 1977. Water level variations and reservoir-induced seismicity at Nurek, U.S.S.R., (Abs.) EOS Trans. AGU, 58, 1196.

Simpson, D.W. and S.K. Negmatullaev, 1978. Induced Seismicity studies in Soviet Central Asia, Earthquake Info. Bull., 10, 209-213.

Simpson, D.W. and S.K. Negmatullaev, 1981. Induced Seismicity at Nurek Reservoir, Tadjikistan, USSR, Bull. Seis. Soc. Am., 71, 1561-1586.

Simpson, D.W. and T.N. Narashimhan, 1986. Reservoir-induced earthquakes and the hydraulic properties of the shallow crust, (Abs.) EOS, Trans. Am. Geophys. Un., 67, 242.

Smith, G. E., 1980. A focal mechanism study using both P-wave first motions and S-wave polarization angles. Master Thesis, Georgia Institute of Technology, Atlanta, GA, pp.

Smith, W.A. and P. Talwani, 1987. Results of a refraction survey in the Bowman Seismogenic Zone, South Carolina, South Carolina Geology, in print.

Smith, W.A. and P. Talwani, 1987. A gravity and magnetic study across the Dutchmans Creek gabbro pluton, Fairfield Co., South Carolina, South Carolina Geology, in print.

Snow, D.T., 1972. Geodynamics of seismic reservoirs, in Proc. Sym. Percolation Through Fissured Rock, Int. Soc. Rock Mech., T2-J, 1-19, Stuttgart.

Snow, D.T., 1977. Induced seismicity at Richard B. Russell reservoir, In: Geologic and Seismological Evaluation of Earthquake Hazards at the Richard B. Russell Project, Army Corps of Engineers, Savannah, Georgia.

Soboleva, O.V., 1980. Change in the focal mechanisms of weak earthquakes under the influence of the Nurek water-reservoir Isvestia, Earth Physics, v. 16, no. 1, 21-27.

Sorlien, C. C., L. T. Long, and T. J. Schmitt, 1987. Zones of induced seismicity defined by rock quality, (abs.) Association of Engineering Geologists, Annual Meeting, October 1987. Atlanta, Georgia.

- Sowers, G. F., and G. H. Fogle, 1975. Seneca, South Carolina earthquake, July 13, 1971, Law Engineering Testing Company, Marietta, Georgia.
- Stevenson, D.A. and P. Talwani, 1987. Anomalous changes in ts/tp ratios and two successful earthquake predictions at Lake Jocassee, South Carolina, USA, In Proc. of Symposium on Earthquake Prediction, Prune, India, in print.
- Stihler, S., 1985. Seismic refraction, anisotropy and seismicity in South Carolina, Master's Thesis, University of South Carolina, Columbia, 102 pp.
- Stihler, S.D. and P. Talwani, 1987. Depth to Moho in the Lake Jocassee and Summerville areas of South Carolina, submitted to Seis. Res. Lett.
- Stover, C. W., B. G. Reagor, S. T. Algermisses, and L. T. Long, 1979. Seismicity map of the state of Georgia, Miscellaneous Field Studies, Map MR-1060, U.S. Geological Survey.
- Talwani, P., 1987. The use of geophysical lineaments in the search of locations of intraplate seismicity, Geol. Soc. India. Bull., Special Volume on the US/India Workshop on "Regional Geophysical Lineaments and their Tectonic and Economic Significance," in print.
- Talwani, P., 1986. Seismotectonics of the Charleston region, in Proc. of 3rd Nat. Conf. on Earthquake Engineering, v. 1, 15-24.
- Talwani, P., 1981. Earthquake prediction studies in South Carolina, An International Review, Maurice Ewing Series 4, ed. D.W. Simpson and P.G. Richards, Am. Geophys. Un., Washington, D.C., 381-393.
- Talwani, P., 1976. Earthquakes associated with the Clark Hill reservoir, South Carolina - A case of induced seismicity, Engineering Geology, 10, 239-253.
- Talwani, P., 1979. An empirical earthquake prediction model. Phys. Earth and Planetary Interiors, 18, 288-302.
- Talwani, P., 1977. Stress distribution near Lake Jocassee, South Carolina, Pageoph 115, 275-281.
- Talwani, P., 1982. Internally consistent pattern of seismicity near Charleston, South Carolina, Geology, 10 (12), 654-658.
- Talwani, P., 1983. Tectonic models - old and new, in Hays, W.W. and Gori, P.L., eds., A workshop on 'The 1886 Charleston, South Carolina earthquake and its implications for today' - Proceedings of Conference XX, U.S. Geological Survey Open File Report 83-843, p. 88-99.
- Talwani, P., 1985/86. Current thoughts on the cause of the Charleston, South Carolina Earthquakes, South Carolina Geology, 29, 19-38.

Talwani, P., and S. Acree, 1985. Pore pressure diffusion and the mechanism of reservoir-induced seismicity, J. Pure and Applied Geophysics., 122, 947-965.

Talwani, P., and S. Acree, 1987. Induced seismicity at Monticello Reservoir: A case study. Final Technical Report, Contracts 14-08-0001-21229 and 14-08-0001-22010, U.S.G.S., Reston, VA., 351 pp.

Talwani, P., and J. Cox, 1985. Paleoseismic evidence for recurrence of earthquakes near Charleston, South Carolina, Science, 229, 379-381.

Talwani, P., W.S. Moore, and J. Chiang, 1980. Radon anomalies and microearthquakes at Lake Jocassee, South Carolina, J. Geophys. Research, 85, No. B6, 3079-3088.

Talwani, P. and B.K. Rastogi, 1980. Search for precursory changes in amplitude ratio of P and S waves for Jocassee, South Carolina earthquakes, Final Technical Report, NSF, Contract No. EAR7818126, 119 pp.

Talwani, P., B.K. Rastogi, and D. Stevenson, 1980. Induced seismicity and earthquake prediction studies in South Carolina, Tenth Technical Report, Contract 14-08-001-17670, U.S.G.S., Reston, VA, 213 pp.

Talwani, P., J. Rawlins, and D.E. Stephenson, 1985/86. The Savannah River Plant, South Carolina, Earthquake of June 8, 1985, Earthquake Notes, 56, 2, in press.

Talwani, P., D. T. Secor and P. Scheffler, 1975. Preliminary results of aftershock studies following the 2 August 1974 South Carolina earthquake, Earthquake Notes, 46, No. 4, 21-28.

Talwani, P., D. Stevenson, J. Chiang, J. Sauber, and D. Amick, 1977. The Jocassee earthquakes (March-May '77) a progress report, Fifth Technical Report, Contract 14-08-0001-14553, U.S.G.S., Reston, VA, 49 pp.

Talwani, P., D. Stevenson, D. Amick and J. Chiang, 1979. An earthquake swarm at Lake Keowee, South Carolina, Bull. Seism. Soc. Am. 69, 825-841.

Talwani, P., D. Stevenson, J. Sauber, B. K. Rostogi, A. Drew, J. Chiang, and D. Amick, 1978. Seismicity studies at Lake Jocassee, Lake Keowee, and Monticello Reservoir, South Carolina (October 1977-March 1978). U. S. Geol. Survey Report, No. 14-08-0001-14553, 151 pp.

Teague, A. G., and M. S. Sibol, 1984. 1984 revision of the duration magnitude formula for the Virginia Tech Seismic Network; Appendix 2 in Virginia Regional Seismic Network Quarterly Report 88-134-27, June 15, 1984, by G. A. Bollinger, M. C. Chapman, and M. S. Sibol, submitted to Nuclear Regulatory Research, Washington DC, 18 pp.

- U.S. Geological Survey, 1978. Aeromagnetic survey of N.W.-South Carolina, Sheet 3, 1:62500, U.S. Geol. Surv. Open File Report 78-847.
- Van Nieuwenhuise, R.E., 1980. Well level fluctuations related to the occurrence of earthquakes at Lake Jocassee, South Carolina, M.S. thesis, Univ. of South Carolina, Columbia, SC, 119 pp.
- Van Nieuwenhuise, R.E. and P. Talwani, 1977. Evidence for spatial correlations between ground water flow and seismicity at Lake Jocassee, South Carolina, Earthquake Notes, 48, No. 3, 30.
- Vergely, P., W. Sassi and E. Carey-Gailhardis, 1987. Analyse graphique des failles a l'aide des focalisations de stries, Bull. Soc. Geol. France, 8, no. 2, 395-402.
- Wentworth, C. M., and Mergner-Keefer, M., 1981. Regenerate faults of small Cenozoic offset: Probable earthquake sources in the southeastern United States, U.S. Geological Survey Open-File Report 81-356, 37 pp.
- Wheeler, R.L., and J.M. Dixon, 1980. Intensity of systematic joints: Methods and application, Geology, v. 8, 230-233.
- Wilson, J. K., 1983. Influence of focal depth on the displacement spectra of earthquakes, Master Thesis, Georgia Institute of Technology, Atlanta, GA, 78 pp.
- Wong, Po-zen, 1988. The statistical physics of sedimentary rock, Physics Today, v 41, no. 12, 24-32.
- York, J. E., and Oliver, J. E., 1976. Cretaceous and Cenozoic faulting in eastern North America, Geological Society of America Bulletin, 87, 1105-1114.
- Zoback, M.D., R.N. Anderson and D. Moos, 1985. ADCOH site study: Shallow borehole in-situ stress and geophysical logging program, in First Year Summary Report to the National Science Foundation-Appalachian Ultradeep Core Hole Project: Phase 1 Preliminary Site Investigation and Selection, 33-41.
- Zoback, M. D., and S. Hickman, 1982. In situ study of the physical mechanisms controlling induced seismicity at Monticello Reservoir, South Carolina, J. Geophys. Res., 87, B8, 6959-6974.
- Zoback, M. D., and M. L. Zoback, 1981. State of stress and intraplate earthquakes in the United States, Science, 213, 96-104.
- Zoback, M. L., and M. D. Zoback, 1985. Uniform NE to ENE maximum horizontal compressive stress throughout mid-plate North America, EOS (Am. Geophys. Union Trans.), 66, 1056.

MAXIMUM EARTHQUAKE AT STROM THURMOND RESERVOIR

BIBLIOGRAPHY OF CITED AND SUPPLEMENTAL REFERENCES ON STRESS IN THE CRUST AND A MODEL FOR A MAJOR EARTHQUAKE

Aggarwal, Y.P. and L.R. Sykes, 1978. Earthquakes, faults and nuclear power plants in southern New York, *Science*, 200, pp. 425-429.

Al-Shurri, H. J., and B. J. Mitchell (1988). Reduced seismic velocities in the source zone of New Madrid earthquakes, *Bull. Seism. Soc. Am.* 78, 1491-1509.

Al-Shukri, H. J., and B.J. Mitchell, and H.A.A. Ghalib (1988). Attenuation of seismic waves in the New Madrid seismic zone, *Seismological Research Letters* 59, 133-140.

Alterman, Z. and F.C. Karal, 1968. Propagation of elastic waves in layered media by finite difference methods, *BSSA*, Vol. 58, pp. 367-398.

Artyushkov, E.V., 1973. Stresses in the lithosphere caused by crustal thickness inhomogeneities, *J. Geophys. Res.*, 78, pp. 7675-7708.

Barosh, P.J., 1986. Neotectonic movement, earthquakes and stress state in the eastern United States, *Tectonophysics*, 132, pp. 117-152.

Bollinger, G.A., C.J. Langer and S.T. Harding, 1976. The Eastern Tennessee Earthquake Sequence of October through December, 1976, *BSSA*, Vol. 66, No. 2, pp. 525-547.

Boore, O.M., 1972. Finite difference solution to the equations of elastic wave propagation, with application to Love waves over dipping interfaces, Ph. D. Thesis, Massachusetts Institute of Technology, Cambridge, Massachusetts.

Bott, M.H.P. and N.J. Kusznir, 1984. The origin of tectonic stress in the lithosphere, *Tectonophysics*, Vol. 105, pp. 1-13.

Byerlee, J., 1978. Friction of rocks, *Pure and Applied Geophysics*, 116, pp. 615-626.

Campbell, D.L., 1978. Investigation of the stress concentration mechanism for intraplate earthquakes, *Geophysical Research Letters*, Vol. 5, No. 6, pp. 477-479.

Chen, W. P., and P. Molnar (1983). Focal depth of intracvontinental and intraplate earthquakes and their implications for the thermal and mechanical properties of the lithosphere, *J. Geophys. Res.* Vol. 88, pp 4183-4214.

Clark, P.J and F.C. Evans, 1954. Distance to Nearest Neighbor as a measure of spatial relationships in populations, *Ecology*, Vol. 35, No. 4, pp. 445- 453.

- Denham, D. (1988). Australian seismicity - the puzzle of the not so stable continent, *Seismological Research Letters* 59, 235-240.
- Desai, C.S. and J.F. Abel, 1972. *Introduction to the finite element method*, Van Nostrand Reinhold Co., New York.
- Dewey, J.W., 1985. A review of recent research on the seismotectonics of the southeastern seaboard and an evaluation of hypotheses on the source of the 1886 Charleston, South Carolina, earthquakes, *NUREG/ CR-4339*.
- Dewey, J.W. (1988). Midplate seismicity exterior to former rift-basins, *Seismological Research Letters* 59, 213-218.
- Dice, L.R., 1952. Measure of the spacing between individuals within a population, *Contrib. Lab. Vert. Biol. Univ. Mich.*, 55, p. 1-23.
- Fleitout, L. and C. Froidevaux, 1982. Tectonics and topography for a lithosphere containing density heterogeneities, *Tectonics*, Vol. 1, pp. 21-56.
- Fleitout, L. and C. Froidevaux, 1983. Tectonic stress in the lithosphere, *Tectonics*, 2, pp. 315-324.
- Fox, F.L., 1970. Seismic geology of the eastern United States, *Assoc. Eng. Geologists Bull.* 7, pp. 21-43.
- Geiger, L., 1910. Herdbestimmung bei Erdbeben aus den Ankunftszeiten, *K. Gesell. Wiss. Goettingen*, 4, pp. 331-349.
- Gettings, M.E., 1988. Variation of depth to the brittle ductile transition due to cooling of a mid-crustal intrusion, *Geophysical Research Letters*, Vol. 15, No. 3, pp. 213-216.
- Guinn, S.A. and L.T. Long, 1977. A computer method for determination of valid focal mechanism solutions using P-wave first motions applied to southeastern United States earthquakes, *Abstract, Earthquake Notes*, Vol. 48, No. 3, p. 16.
- Guinn, S.A., 1980. *Earthquake Focal Mechanisms in the Southeastern United States*, *NUREG/CR-1503*.
- Herrmann, R.B., 1975. A Student's Guide to the use of P and S wave data for focal mechanism determination, *Earthquake Notes*, Vol. 46, No. 4, pp. 29-39.
- Herrmann, R.B., 1979. Surface wave focal mechanisms for Eastern North American Earthquakes with Tectonic Implications, *Journal of Geophysical Research*, Vol. 84, No. B7, pp. 3543-3552.
- Huebner, K.H. and G.A. Thornton, 1982. *The Finite Element Method for*

Engineers, John Wiley and Sons, New York.

Isacks, B.J. Oliver and L.R. Sykes, 1968. Seismology and the new global tectonics, *J. Geophys. Res.*, 73, pp. 5855-5899.

Jin, Anshu, and K. Aki (1986). Spatial and temporal correlation between coda Q and seismicity in China, *Bull. Seism. Soc. Am.* 78, 741-769.

Johnston, A.C., D.J. Reinbold, and S.I. Brewer, 1985. Seismotectonics of the Southern Appalachians, *BSSA*, Vol. 75, pp. 291-312.

Kane, M.F., 1977. Correlation of major eastern earthquake centers with mafic/ultramafic basement masses, *U.S. Geol. Survey Prof. Paper* 1028-O.

Keller, G.R., A.E. Bland and J.K. Greenberg, 1982. Evidence for a major late Precambrian tectonic event (rifting?) in the eastern midcontinent region, United States, *Tectonics*, Vol. 1, No. 2, pp. 213-223.

Kelly, R., R.W. Ward, S. Treitel and R.M. Alford, 1976. Synthetic seismograms: A finite difference approach, *Geophysics*, Vol. 41, pp. 2-27.

Kuang, J., L. T. Long, and J.-C. Mareschal, 1989. Intraplate seismicity and stress in the southeastern United States, *Tectonophysics*, (in press)

Liow, J.-S., Tie An and L.T. Long, 1985. Earthquake Location: A Consideration of independent computation of origin time, epicenter and depth, *Abstract, Earthquake Notes*, Vol. 56, No. 3, p. 77.

Liow, J.-S. and L.T. Long, 1985. Analysis of reflections from the base of the crust in southeastern Tennessee, in *Summary Report for contract GSA-80-3053, Geological Survey of Alabama; A Study of Seismicity and Earthquake hazard in northern Alabama and adjacent parts of Tennessee and Georgia*, Georgia Institute of Technology, School of Geophysical Sciences, Atlanta, GA 30332, 16 pp.

Long, L.T. and J.H. McKee, 1973. A microearthquake survey near Bowman, South Carolina, *abstract, Earthquake Notes*, 44, p. 65.

Long, L.T., 1976. Speculations concerning Southeastern Earthquakes, mafic intrusions, gravity anomalies, and stress amplification, *Earthquake Notes*, Vol. 47, No. 3, pp. 29-35.

Long, L.T. and J.W. Champion, Jr., 1977. Bouguer Gravity Map of the Summerville-Charleston, South Carolina, Epicentral Zone and Tectonic Implications, *Geol. Survey Prof. Paper* 1028-K.

Long, L.T. and J.-S. Liow, 1986a. Crustal Thickness, velocity structure, and the isostatic response function in the southern Appalachians, in *Reflection Seismology: The Continental Crust*, *Geodynamics Series*, Vol. 14, AGU, pp. 215-222.

Long, L.T., J.-S. Liow and F.B. Jones (1987). A technique for the

- inversion of coda Q, (abs.) Seism. Res. Letters 58, 101.
- Long, L.T., J.S. Liow, An Tie and K.-H. Zelt, 1986b. Seismicity and Crustal Structure in southeastern Tennessee, Abstracts, EOS Transactions, AGU, Vol. 67, No. 16, p. 314.
- Long, L.T., K.-H. Zelt, J.-S. Liow, R.P. Propes, J. Shand, D. Reinbold and B. Schechter, 1986c. The North Georgia Earthquake of October 9, 1984, Earthquake Notes, Vol. 57, No. 3, pp. 77-82.
- Long, L.T., 1988a. A Mechanism for Major Intraplate Earthquakes, Abstract, EOS, Transactions, AGU, Vol. 69, No. 16, p. 402.
- Long, L.T., 1988. A model for major intraplate continental earthquakes, Seismological Research Letters, Vol 59, pp 273-278.
- Mareschal, J.C. and Jian Kuang, 1987. Intraplate Stresses and Seismicity: The role of topography and density heterogeneities, Tectonophysics, Vol. 132, pp. 153-162.
- McCue, K., B. C. Barlow, D. Denham, T. Jones, G. Gibson and M. Michael-Leiba (1987). Another chip off the old Australian Block, EOS, Trans., Am Geophys. Union 68, 609.
- McKenzie, D.P., 1969. The relationship between fault plane solution for earthquakes and the directions of principal stresses, BSSA, Vol. 59, pp. 591-601.
- McKeown, F.A., 1978. Hypothesis: Many earthquakes in the central and southeastern United States are causally related to mafic intrusive bodies, Jour. Research U.S. Geol. Survey, Vol. 6, No. 1, pp. 41-50.
- Meissner, R. and J. Strehlau, 1982. Limits of stresses in continental crusts and their relation to the depth-frequency distribution of shallow earthquakes, Tectonics, Vol. 1, No. 1, pp. 73-89.
- Oudenhoven, M.S., C.O. Babcock, and W. Blake, 1972. A method for the prediction of stresses in an isotropic inclusion or orebody of irregular shape, U.S. Bureau of Mines, Report of Investigations 7645, 36 pp.
- Propes, R.L., 1985. Crustal Velocity variation in the Southern Appalachians, Thesis, Master of Science, School of Geophysical Sciences, Georgia Institute of Technology, Atlanta, GA 30332.
- Rankin, D.W., 1976. Appalachian salients and recesses: Late Precambrian continental breakup and the opening of the Iapetus Ocean, J. Geophys. Res., 81, pp. 5605-5616.
- Reddy, J.N., 1984. An Introduction to the Finite Element Method, McGraw Hill Company.

- Reinbold, D. and J. Cornwell, 1983. The Greenback, Tennessee Earthquakes of 24 September 1982 and their tectonic associations, TEIC Special Report No. 9, Tennessee Earthquake Information Center, Memphis State University.
- Richardson, R.M., S.C. Solomon and N.H. Sleep, 1979. Tectonic stress in the plates, *Rev. Geophys. Space Physics*, 17, pp. 981-1019.
- Sachs, L., 1982. *Applied Statistics, A Handbook of Techniques*, Springer Verlag, pp. 139-141.
- Snoke, J.A., J.W. Munsey, A.G. Teague and G.A. Bollinger, 1984. A Program for Focal Mechanism Determination by combined use of Polarity and SV/P Amplitude Ratio Data, Abstract, *Earthquake Notes*, Vol. 55, No. 3, p. 15.
- Solomon, S.C., R.M. Richardson, E.A. Bergman, 1980. Tectonic Stress Models and Magnitudes, *J. Geophys. Res.*, 85, pp. 6086-6092.
- Sorlien, C. C., Long, L. T., and Schmitt, T. J., 1987. Zones of induced seismicity defined by rock quality, (abs.) Association of Engineering Geologists, 30th Annual Meeting, Atlanta, Georgia, October 8-13.
- Strang, G. and G.J. Fix, 1973. *An analysis of the finite element method*, Prentice-Hall, Englewood Cliffs, New Jersey.
- Street, R.L. (1982). A contribution to the Documentation of the 1811-1812 Mississippi Valley earthquake Sequence, *Earthquake Notes* 53, 2, 39-52.
- Street, R.L., R.B. Herrmann, and O.W. Nuttli, 1974. Earthquake Mechanics in the Central United States, *Science*, V. 184, No. 4143, pp. 1285-1287.
- Sykes, L.R., 1978. Intraplate seismicity, reactivation of preexisting zones of weakness, alkaline magmatism, and other tectonism postdating continental fragmentation, *Rev. Geophys. Space Phys.*, 16, pp. 621-688.
- Teague, A.G., 1984. Focal Mechanisms for Eastern Tennessee earthquakes, 1981-1983, Master's Thesis, Virginia Polytechnic Institute and State University, Dept. of Geological Sciences, pp. 161.
- Teague, A.G., G.A. Bollinger, and A.C. Johnston, 1986. Focal Mechanism analyses for eastern Tennessee earthquakes (1981- 1983), *BSSA*, Vol. 76, No. 1, pp. 95- 109.
- Tie An, J.-S. Liow and L.T. Long, 1986. Study of traveltime residuals at seismic stations in the southeastern Tennessee area, *SEUSSN Report* No. 18, pp. 73-77.
- Tzeng, W.S., 1982. Investigation of SV to P Wave Amplitude Ratio for determining focal mechanism, Thesis, Master of Science, School of Geophysical Sciences, Georgia Institute of Technology, Atlanta, GA

30332.

Winester, Daniel, 1984. Basement features under the southern Appalachians from gravity and magnetics, Master's Thesis, Georgia Institute of Technology, Atlanta, Georgia, 104 pp.

Zienkiewicz, O.C., 1983. The Finite Element Method, McGraw-Hill, London.

Zoback, M.L. and M.D. Zoback, 1980. State of stress in the conterminous United States, J. Geophys. Res., 85, pp. 6113- 6156.

Zoback, M.D., 1983. Intraplate earthquakes, crustal deformation and in situ stress, U.S. Geol. Survey, Open file Report 83-843, pp. 169- 178.

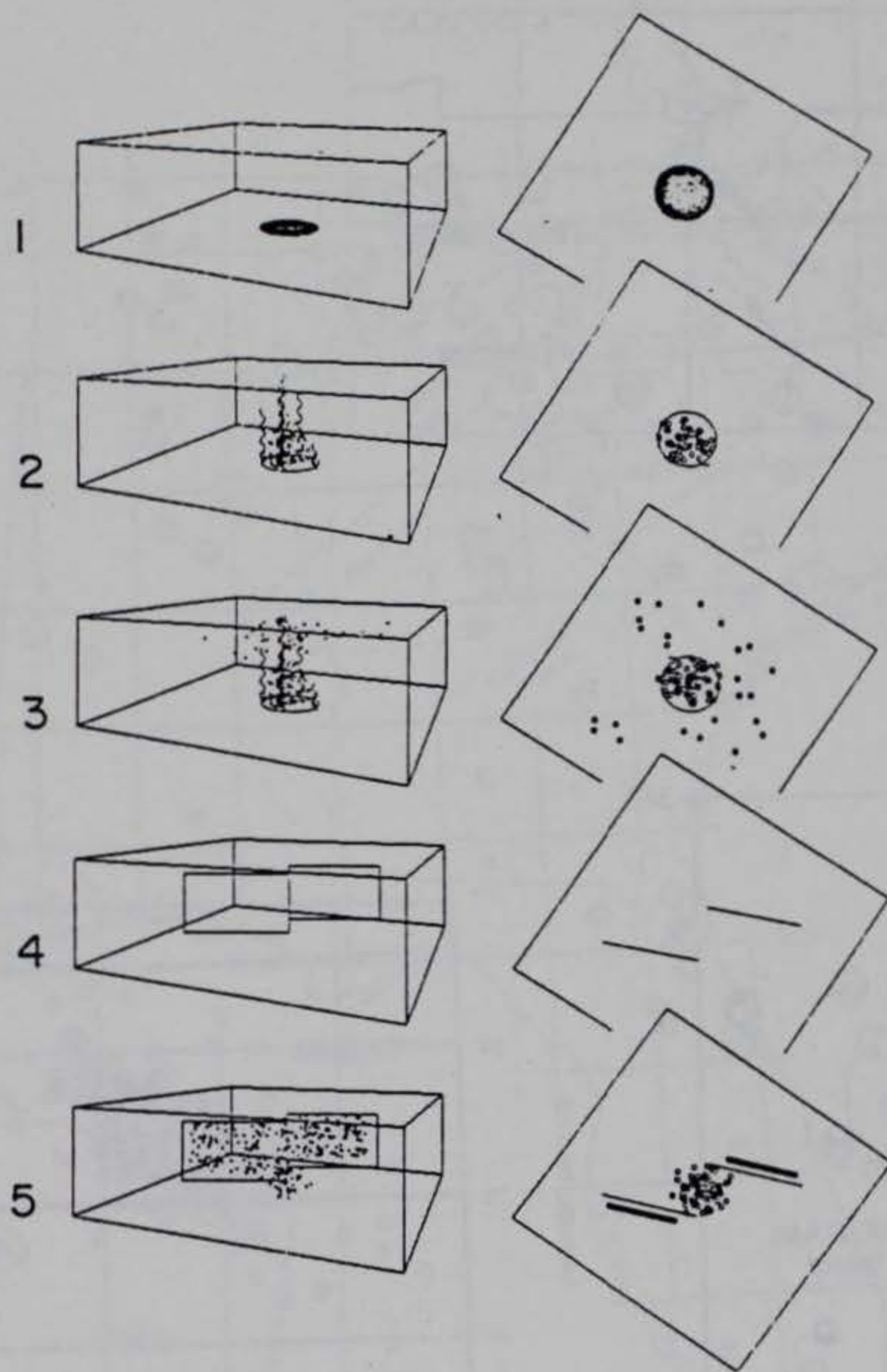
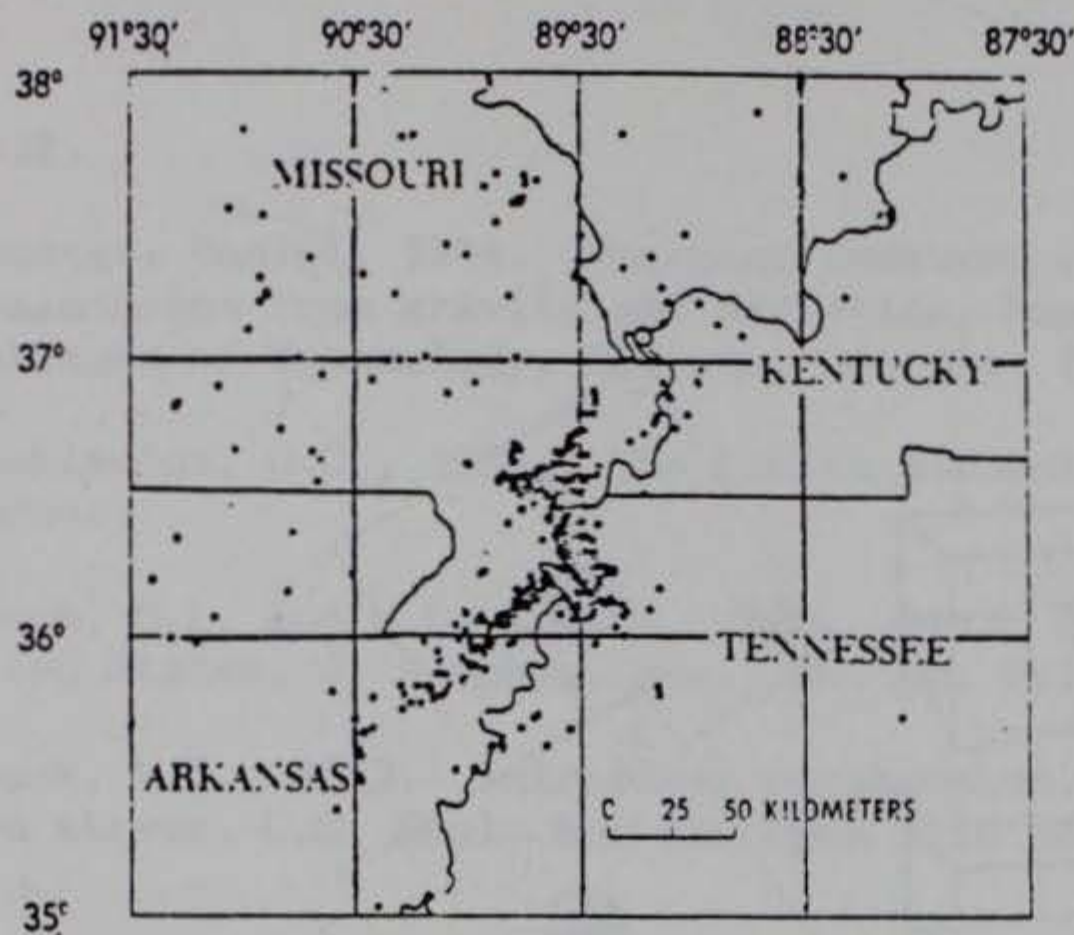


Figure 1. Illustration of the five phases of a major intraplate earthquake. 1) Initiation by underplating. 2) Strength corrosion by fluid and thermal diffusion. 3) Stress concentration as indicated by increased shallow seismicity (epicenters are small dots). 4) Failure along major faults (outlined by rectangles). 5) Crustal healing during an extended aftershock sequence.



DEPTH
 ○ <15 KM
 ○ >15 KM

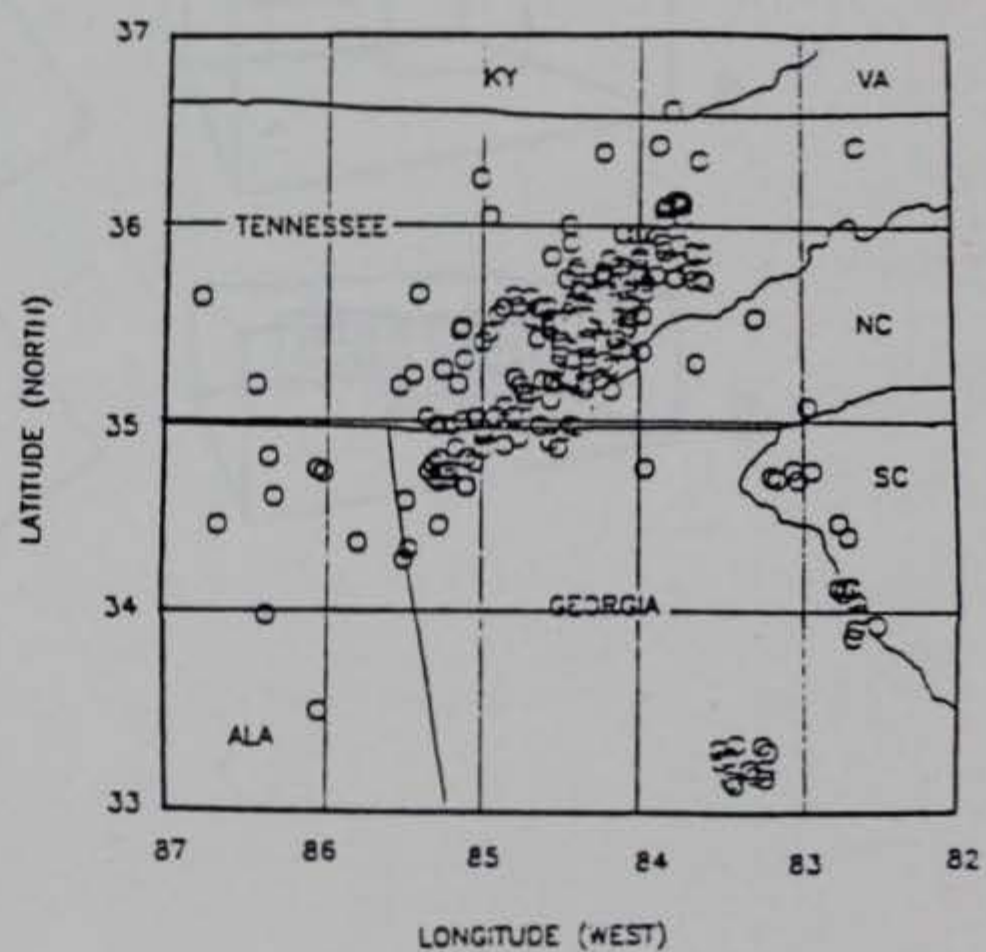
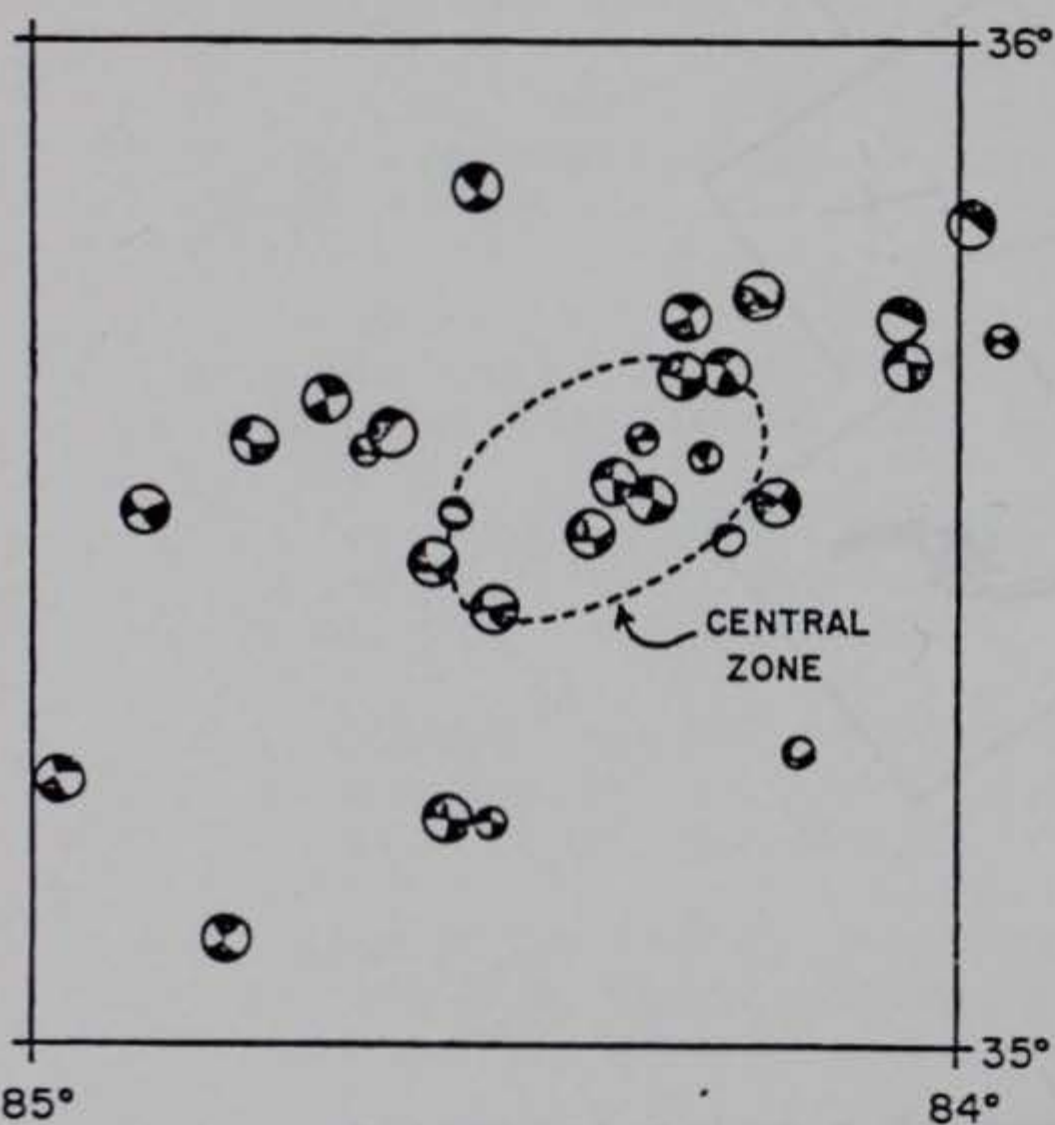


Figure 2. Pattern of seismicity (lower right) and focal mechanisms (lower left) for southeastern Tennessee; a possible example of phase 3. Pattern of seismicity for New Madrid (top); a possible example for phase 5.

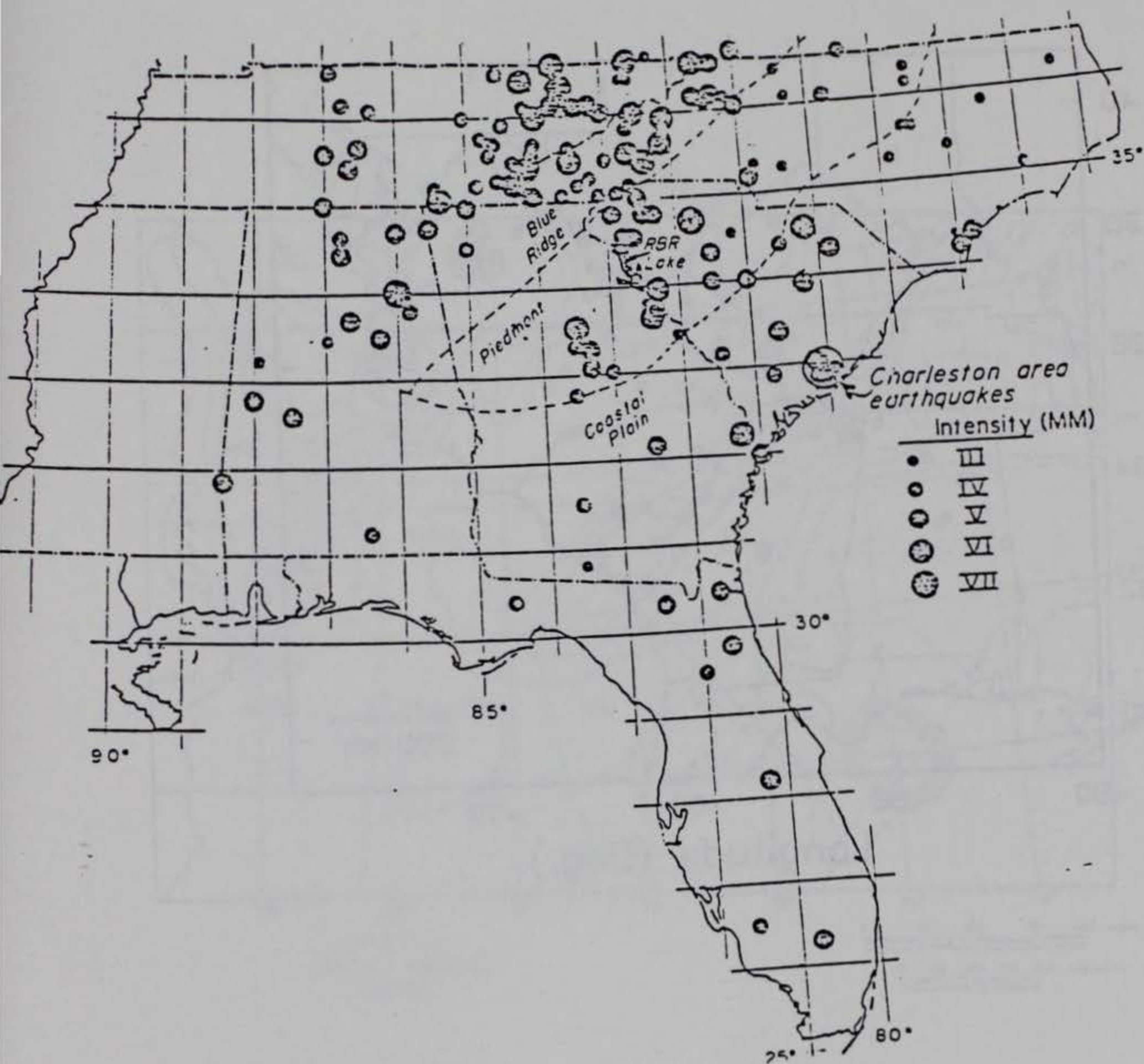


Figure 3. Distribution of earthquakes in the southeastern United States relative to the Piedmont Province. The Stom Thurmond Reservoir is at the foot of RBR Lake. Epicenters from Bollinger (1975) with updates and corrections through 1980.

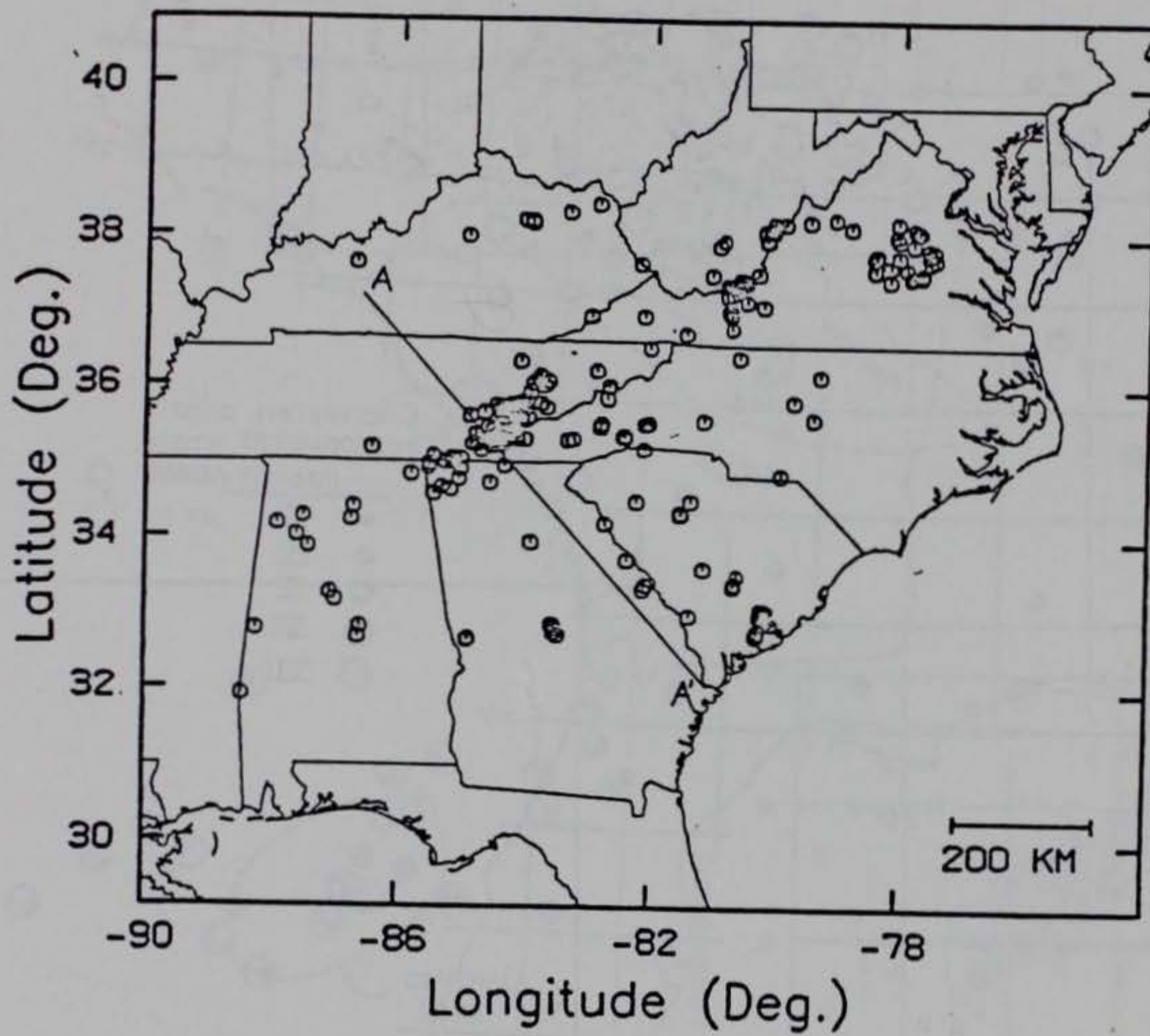


Figure 4. Seismic data after 1980 based on data from the SEUSSN bulletin.

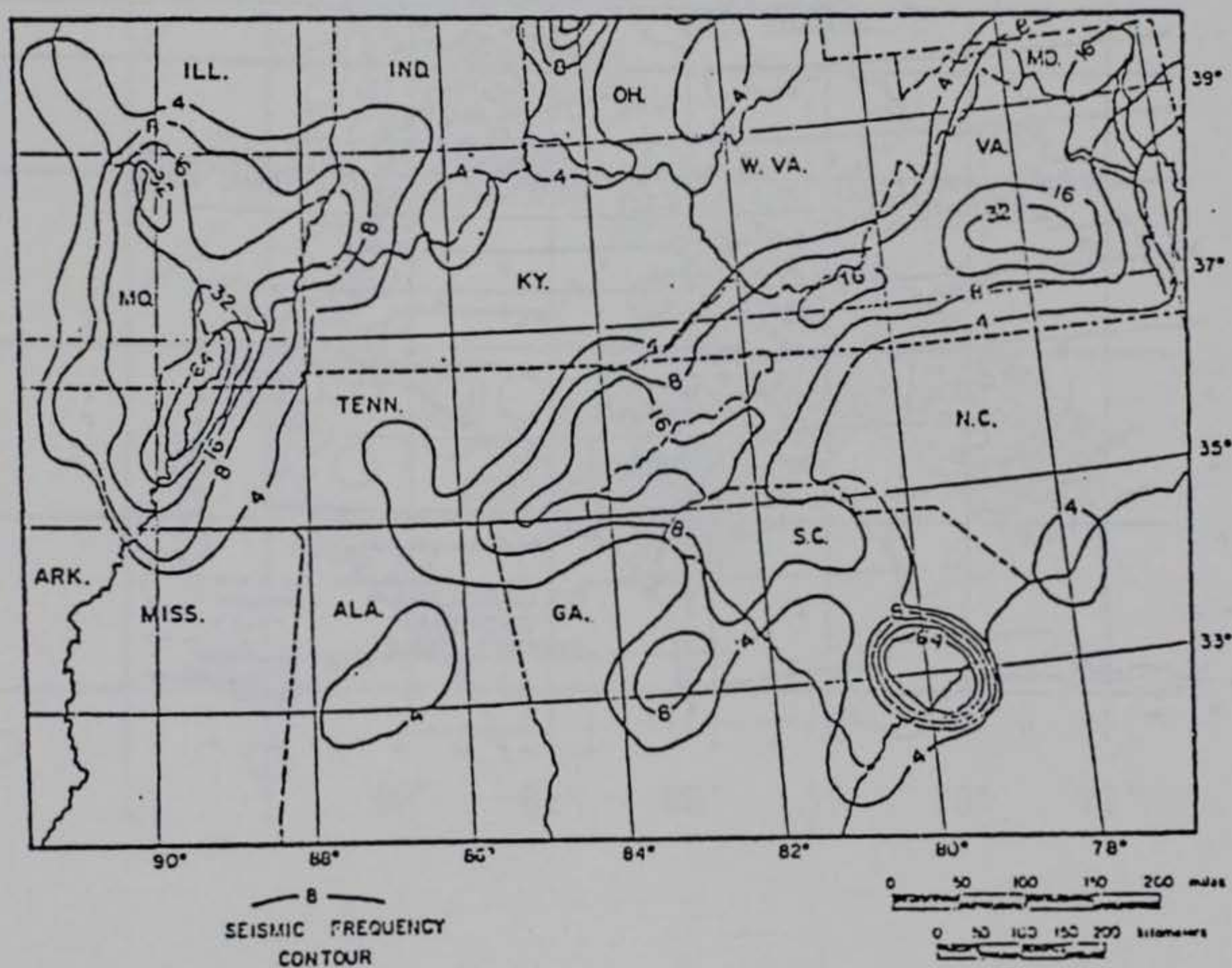


Figure 5. Seismic Intensity Occurrence Contour Map of the Eastern United States. Each contour encloses areas experiencing equal numbers of earthquakes ($I > III$) for the period 1800 - 1942 (from Hadley and Devine, 1974).

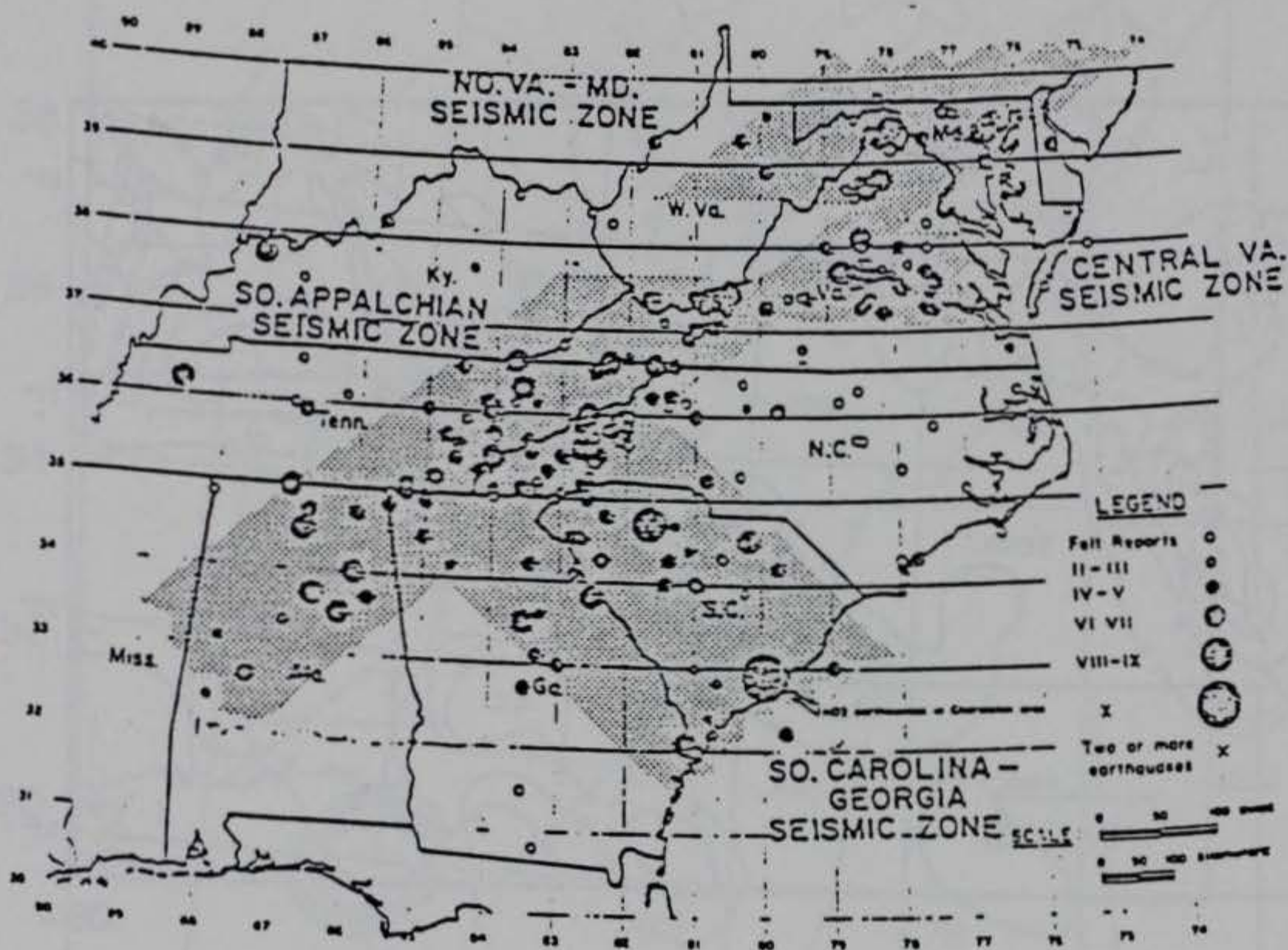


Figure 6. Historical seismicity (1754 - 1970) and definition of seismic zones in the southeastern United States (from Bollinger, 1973).

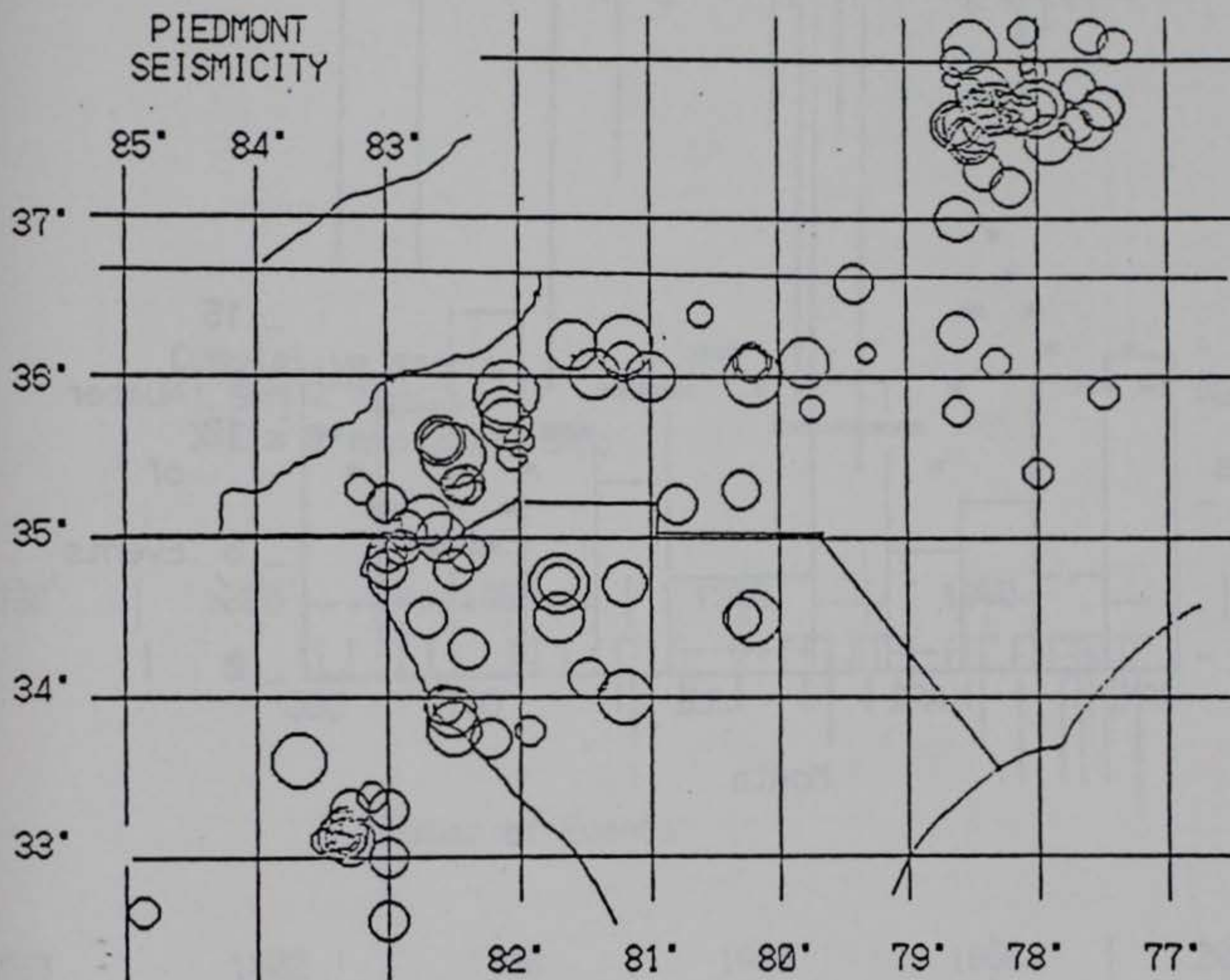


Figure 7. Seismicity of the Piedmont. Data are from Appendix I and events outside the Piedmont are not plotted.

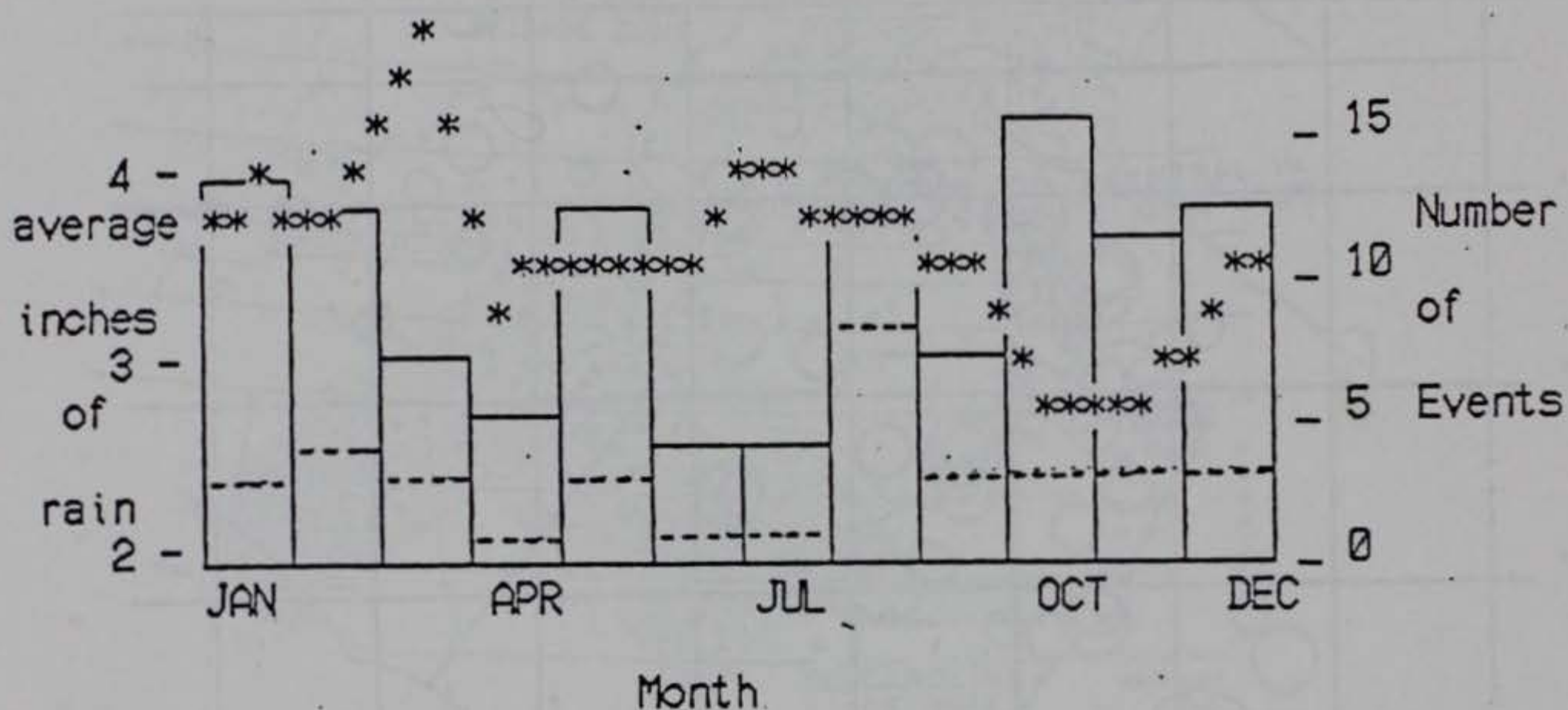


Figure 8. Number of earthquakes per month in the Piedmont. Solid line for magnitude > 3.0 and dashed line for magnitude > 4. The stars are average inches of rain each month from 1955 to present.

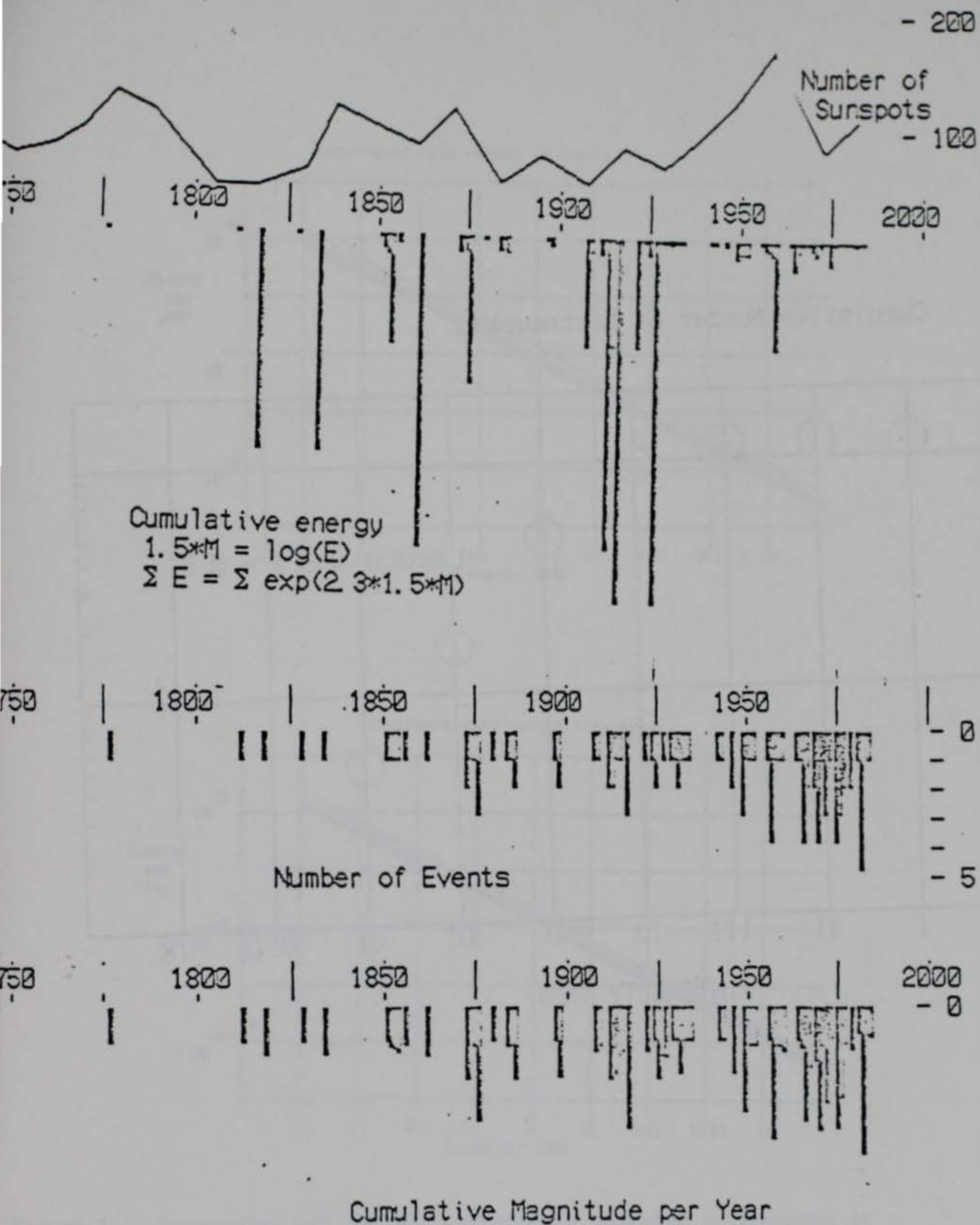


Figure 9. Annual occurrence of earthquakes verses year. Earthquakes rates are compared by energy, total magnitude and number of events per year. Peaks in sun spot cycles are shown for comparison.

Cumulative Number of Earthquakes

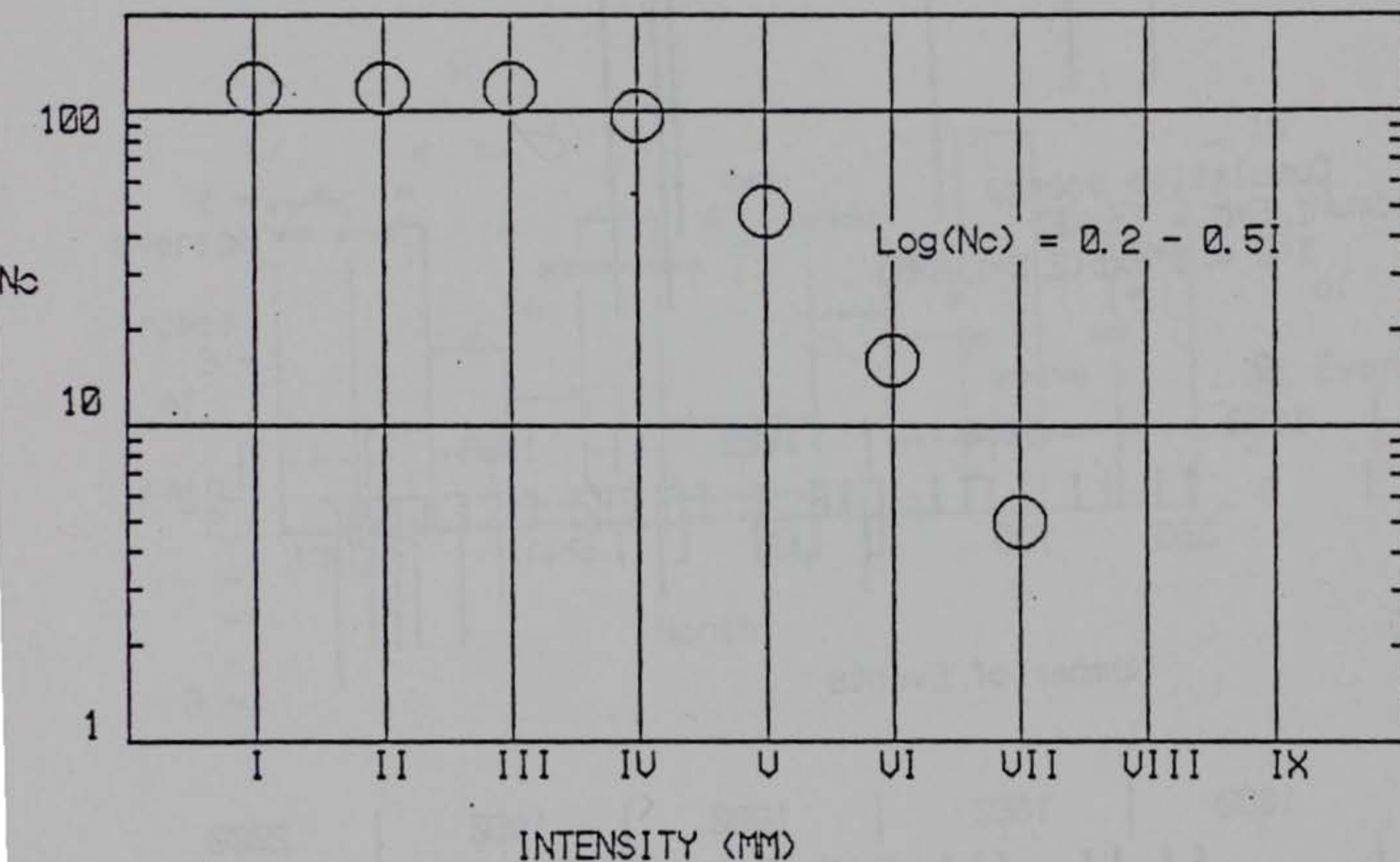


Figure 10. Recursion relation for southern Piedmont. N_c is number of events of intensity I and greater per year per 2500 km².

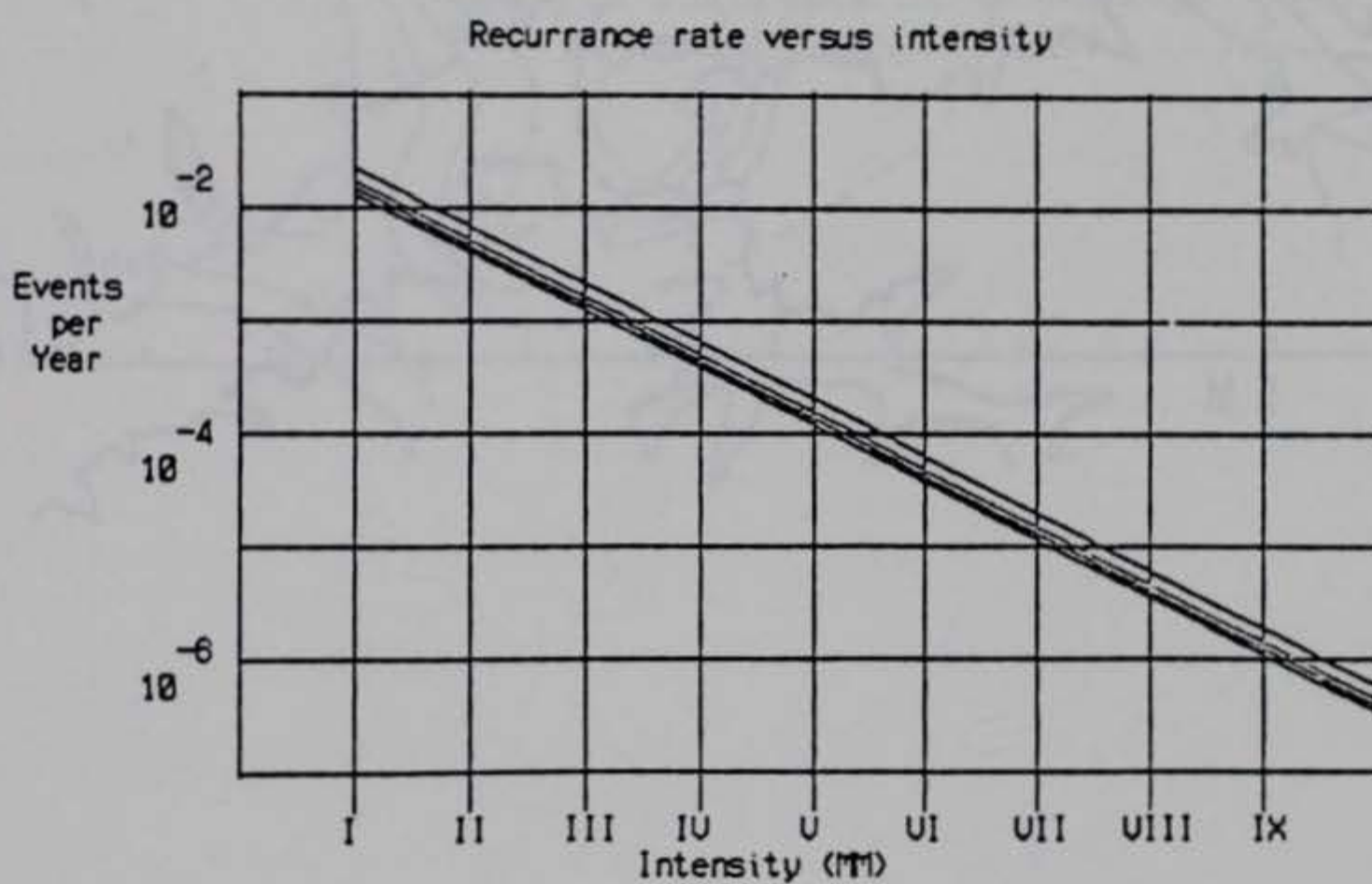
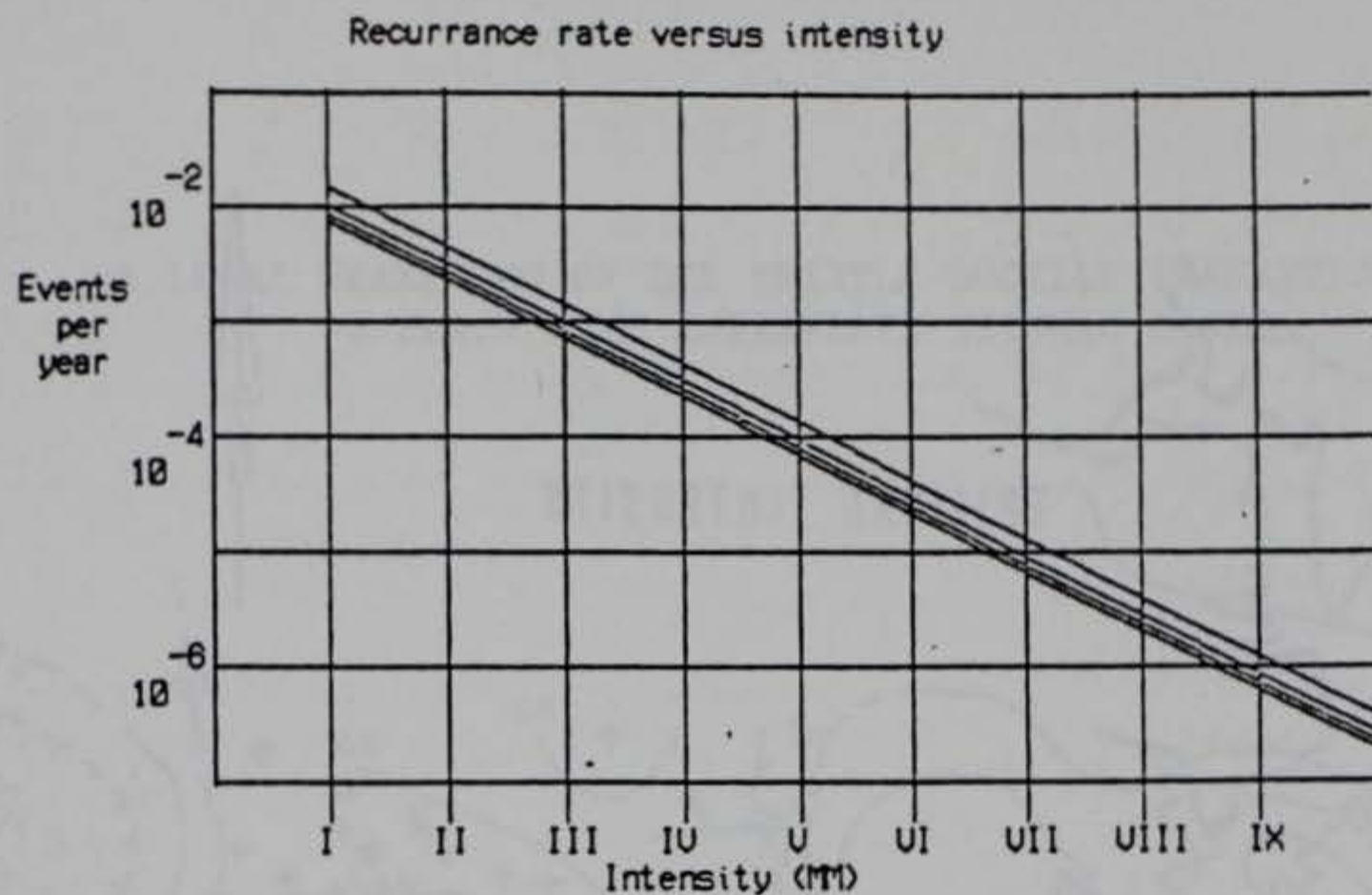


Figure 11. Recurrence rate versus intensity of expected earthquakes at Strom Thurmond Reservoir. The four lines are for the four corners of the quarter degree square surrounding the reservoir area. The top plot is for two parallel bands of Piedmont seismicity. The bottom plot is for a uniform distribution of Piedmont seismicity.

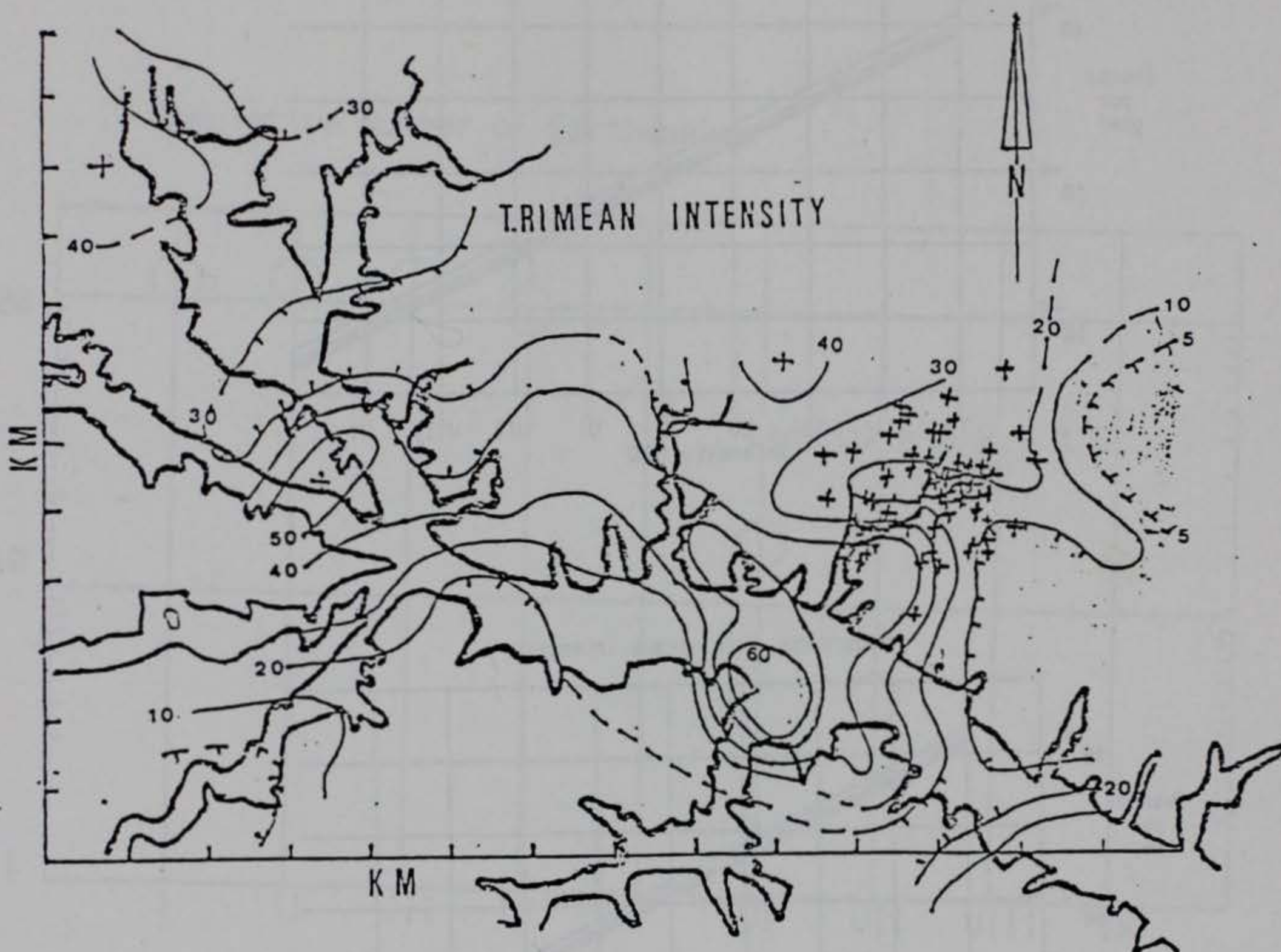


Figure 12. Trimean joint intensity measures for the Strom Thurmond Reservoir Area and their relation to reservoir induced earthquakes (from Sorlien, 1987).

A LOCAL WEAKENING OF THE BRITTLE-DUCTILE TRANSITION CAN
EXPLAIN SOME INTRAPLATE SEISMIC ZONES

by

Leland Timothy Long and Karl-Heinz Zelt⁺
School of Geophysical Sciences
Georgia Institute of Technology
Atlanta, Georgia 30332

⁺Now with Shell International, Den Haag, Netherlands.

A LOCAL WEAKENING OF THE BRITTLE-DUCTILE TRANSITION
CAN EXPLAIN SOME INTRAPLATE SEISMIC ZONES

ABSTRACT

A transient decrease in the strength of the lower crust which would accompany a localized shallowing of the brittle-ductile transition can concentrate crustal deformation. Within the zone of weakened lower crust, stress relaxation would occur through viscous or dislocation creep in response to regional plate stress. Stresses would concentrate in the stronger elastic crust around and above the zone of decreased strength. Two-dimensional finite-element models of zones of weakness subjected to a regional plate stress, predict stress amplification of 10 to 100 percent surrounding the local decrease in strength. An analysis of the displacements and stresses in the model suggests that strike slip faulting should dominate in the central local area of decrease in crustal strength. Above this zone the strike slip faulting should exhibit a strong thrust component. The compression and extension of the crust surrounding the weakened zone in the vicinity of the brittle-ductile transition predicts that the dominant strike slip faulting should exhibit components of normal faulting on the edges of the weak zone which are in line with the regional stress and reverse faulting on the edges which are along a line through the weak zone transverse to the regional stress.

The focal mechanisms and seismicity of southeastern Tennessee fit the stress directions and relative magnitudes predicted by models for a zone of weakness in the lower crust. The seismicity is diffused over a narrow elliptical zone trending northeast with the greatest concentration of activity

near the center. The central zone is characterized by deep-focus strike slip events with predominantly north or east striking nodal planes. These events are responding directly to compression in the direction of the regional compressive stress and extension perpendicular to the regional compressive stress within the weak zone. The uniformity of the focal mechanism solutions suggest that these earthquakes form new faults. The area surrounding the central zone is characterized by focal mechanisms with components of reverse or normal fault movements. Events with normal components are dominant on the edges in line with the regional stress as predicted by the stress model for a weak central zone under stress. The agreement between observed earthquake focal mechanisms in southeastern Tennessee and models of crustal stress surrounding a zone of weakness suggests that these events may be caused by a transient perturbation in the hydraulic or thermal properties of the lower crust.

INTRODUCTION

Many hypotheses have been offered for major intraplate earthquakes, such as the 1886 Charleston, South Carolina, earthquake, and intraplate seismic zones such as in southeastern Tennessee (Dewey, 1985; Long, et al., 1986). A pervading paradigm underlying most hypotheses is that the stresses generated at plate boundaries and, possibly, by topographic or density loads reactivate pre-existing faults or other zones of weakness. In southeastern Tennessee focal mechanism solutions enabled by seismic networks installed in the early 1980's are now sufficient to consider whether they fit these pervading hypotheses.

The dominance of compressional stress in the interiors of crustal plates has long been recognized (McKenzie, 1969; Sbar and Sykes, 1973). Stresses in plate interiors are induced at mid-ocean ridges (Turcotte and Schubert, 1982) and can be transmitted over a large distance by the elastic lithosphere. Other sources of stress associated with plate boundaries are stresses related to slab-pull forces near subduction zones (Bott and Kusznir, 1984), stresses related to transform faults (Byerlee, 1978) and related to viscous shear of asthenospheric convective flow (Richardson et al., 1979; Solomon et al., 1980; Fleitout and Froidevaux, 1982, 1983). Mareschal and Kuang (1987), and Kuang, et al. (1989) investigated the role of stresses from topographic and density loading and concluded that the local variations in the stress field are comparable in magnitude to the plate tectonic stresses. Zones of increased magnitude of stress were consistent with the seismicity in southeastern Tennessee, but the observed strike slip focal mechanisms could not be predicted with the same pattern of zones of high stress. The maximum stresses associated with these sources are on the order of tens of MPa. In comparison,

stresses required to cause brittle failure of the upper crust can range from 8 MPa at shallow depths to 9000 MPa in the lower crust (Meissner and Strehlau, 1982). Consequently, tectonic stresses alone cannot cause brittle failure unless the strength of the crust is low at the earthquake focus, usually assumed to be on an old fault.

The southeastern United States is situated within the North American Plate, where earthquakes of magnitude greater than 5.0 are rare and where the last major tectonic activity occurred in the Jurassic Period, during the opening of the Atlantic. In-situ stress measurements and earthquake focal mechanisms (Sbar and Sykes, 1973; Zoback and Zoback, 1980; Zoback, 1983) show that the greatest principal (compressive) stress in North America is horizontal and trends along the direction of plate motion, consistent with the regional stress originating from ridge push forces near the mid-Atlantic ridge. For southeastern Tennessee Zoback and Zoback (1980) predict northeast-southwest compression, consistent with 14 previously available focal mechanism solutions (Johnston et al., 1985; Teague et al., 1986).

Sykes (1978) proposed that intraplate earthquakes reactivate and follow pre-existing zones of weakness, such as sutures developed in the Appalachian orogenic belt during the closing of the Proto Atlantic Ocean. Other cited zones of weakness which exhibit seismicity are the Ottawa-Bonnechere rift graben (Rankin, 1976) and the late Precambrian-early Paleozoic continental rift in the New Madrid area. Talwani (1988) argued that major earthquakes prefer the intersection of zones of weakness. Other authors have stressed high-angle reverse motion on reactivated normal faults bordering Triassic basins along the eastern seaboard (Prowell and O'Connor, 1978; Reinhardt et al., 1984; Aggarwal and Sykes, 1978). Bollinger and Wheeler (1988) argued that the Giles county, Virginia, seismicity was best explained by Iapetan normal faults.

These hypotheses do not explain the temporal and spatial clustering of earthquake epicenters in southeastern Tennessee and western North Carolina (Bollinger, 1973) or in the Charleston area. Estimates of recurrence rates from contemporary seismicity imply cumulative Quaternary displacements that are much larger than geological data can justify without invoking temporal clustering (Coppersmith, 1988). To explain the spatial clusters of seismicity in the eastern United States, attempts have been made to correlate earthquakes with mafic crustal units. These correlations are largely attempts to associate seismicity with concentrations of stress in the crust induced by inhomogeneous distributions of material properties. Fox (1970) was one of the first to speculate on the possible significance of the association of epicenters with mafic Paleozoic rocks in the Blue Ridge province. In studies of the Bowman and Charleston, South Carolina, seismicity, Long (1976) proposed a stress amplification mechanism that may explain seismicity near mafic intrusives interpreted from gravity data and noted that the stress concentrations around or in an inclusion are a function of the ratio of the Young's modulus of the inclusion to that of the host, the shape of the inclusion and the applied stress. Kane (1977) extended the correlation of mafic intrusions with seismicity to other areas in the eastern United States. Long and Champion (1977) argued that earthquakes in the Charleston, South Carolina, area were better explained by stress amplification in or near a large mafic crustal intrusion than by reactivation of the known faults. McKeown (1978) correlated the orientation of mafic intrusives with fault orientations and existing focal mechanism solutions for the New Madrid seismic zone and the southern Appalachian seismic zone. McKeown (1978) then used the stress calculations of Oudenhoven et al. (1972) to explain anomalous stress around solid inclusions of various shapes. Whereas the above mentioned

authors assumed intrusions stiffer than the surrounding plate, Campbell (1978) determined theoretical stress values associated with weakened intrusions. He suggested that mafic intrusions weakened possibly by serpentinization may concentrate stresses more than 200 percent above the regional values. The highest differential stress factor was found in the plate just outside the inclusion, implying that most or all brittle-failure earthquakes near a weak inclusion will occur in the plate nearby, not in the inclusion itself. The lack of a definitive association with seismicity has characterized all the mafic intrusion and stress concentration hypotheses. While they demonstrate the capability of variations in crustal rigidity to generate anomalous stress, many significant crustal units which should be anomalously rigid do not exhibit seismicity and the predicted stress distributions have not been confirmed with focal mechanisms.

The discovery and improved understanding of the brittle-ductile transition at mid-crustal depths (Chen and Molnar, 1983; Meissner and Strehlau, 1982) has added a new dimension to discussions of stress distributions in the crust. The depth to the brittle-ductile transition correlates with the maximum depth of earthquakes in continental interiors. A perturbation in the depth to the brittle-ductile transition due to the thermal effects of the cooling of a mid-crustal intrusion was investigated by Gettings (1988). He speculated that the residual thermal effects of an intrusives of late Miocene age or younger could cause shallowing of the brittle-ductile transition of 3 kilometers or more at the present and thus provide an area of possible stress amplification or concentration to explain the 1886 Charleston seismicity.

Long (1988) used the concept of a distortion of the brittle-ductile transition in the crust to hypothesize a new model for major intraplate

continental earthquakes. In Long's model the perturbation is caused primarily by the more rapid movements of fluids instead of the slower mechanism of thermal conduction. Long's (1988) model is based on a sequence of five phases. In the first phase of a major intraplate earthquake, the hydraulic or thermal properties of a portion of the continental crust at Moho depths is disturbed. Such a disturbance could be induced by the intrusion of a sill or by partial melting. In the second phase the upward migration of fluids or heat from the area of recent disturbance corrodes the strength of the crust at the brittle-ductile transition. As a weakened central zone deforms in response to tectonic plate stress during the third phase, stresses are concentrated in the surrounding rigid crust. The fourth phase is the possible occurrence of a major earthquake when the stress surrounding the weakened central zone exceeds the crustal strength, either because the concentrated stresses are anomalously high or because the dispersing fluids have spread and weakened the crust outside the central zone. The final and fifth phase in the occurrence of a major intraplate earthquake is an extended aftershock sequence which is concentrated on the fault plane of the main event.

The hypotheses of Long (1988) and Gettings (1988) are new and their use of a perturbed brittle-ductile transition and have not previously been confirmed by seismic data. Long's (1988) hypothesis is based on recent seismic data and other geophysical data and relates a crustal stress model to a new mechanism for large intraplate earthquakes. In this study Long's (1988) model is tested by examining the stresses surrounding various shapes and sizes of a zone of crustal weakness within a compressed elastic crust. The magnitudes and directions of the principal stresses, which are computed using the finite element technique, are used to ascertain regions of likely seismicity and the relative location of strike-slip, normal and reverse focal

mechanism solutions. In this study an attempt will be made to correlate the observed focal mechanism solution distribution for southeastern Tennessee with these computed crustal stresses.

SEISMICITY OF SOUTHEASTERN TENNESSEE

Over 296 well located earthquakes from southeastern Tennessee revealed a dominant cluster in the approximate center (84.3°W , 35.7°N) of the southeastern Tennessee seismicity (Fig 1). Smaller and less active clusters are found to the northeast near Maryville (84°W , 35.8°N) Tennessee (see Bollinger et al., 1976) and to the southwest in northwest Georgia (Long et al., 1986). Nearly continuous zones of seismicity extend from the central cluster to the southwestern cluster in Georgia.

The directions of first motion and SV/P amplitude ratios were used to determine 41 single-event and two composite focal mechanism solutions for earthquakes in southeastern Tennessee and northern Georgia. The pertinent data for each event are listed in Table 1. The statistical estimate of confidence was developed by (Zelt, 1988) as an extension to the method of focal mechanism determination proposed by Guinn and Long, 1977.

Over half of the focal mechanism solutions are strike slip and consistent with the 14 focal mechanisms reported by Johnston et al., 1985, and Teague et al., 1986. Of the remaining, eight are strike slip with a normal or reverse component, six are normal and five are reverse with a strike slip component. The measure of confidence of the focal mechanism solutions verify that for southeastern Tennessee and northwestern Georgia, solutions with large normal and reverse components exist with the same confidence level as the dominant strike-slip focal mechanism solutions. The depths of focus range from the

base of the Paleozoic sediments at approximately 3 km to 30 km and their average depth is 15 km. Figure 1 shows the distribution of these events with depth in a northeast-southwest profile. The average focal depth for strike-slip earthquakes is below the average at 17.3 ± 4.6 km. The average depth of earthquakes with normal or reverse focal mechanism solutions occurred near the average depth.

The central seismic zone between 84.2W and 84.5W and 35.5N and 35.8N is sampled by 20 focal mechanism solutions (Fig. 2). Fifteen of these 20 events are either dominantly strike-slip or have a large strike-slip component. The central seismic zone is surrounded by areas where focal mechanisms with normal or reverse components are prominent. Three of the 5 normal or reverse events and three events with a large strike-slip component are on the edge of the central seismic zone. The level of seismicity on the edge is less than in the central zone. The epicenters near the southwestern edge of the central zone suggest a north-northwest alignment. Some of the strike slip events with either anomalous P-axes directions or reverse or normal components are located along this alignment.

The dip of the B axis can be used as a measure of the deviation of the focal mechanism from pure strike slip. The dips of the null-axes (Fig 3), indicate that the most prominent zone of near-vertical dip, corresponding to pure strike-slip regimes, is the central cluster of epicenters centered about 35.55N and 84.35W. This central region is surrounded by three regions of low B-axis dips, thus regions of normal or reverse components. The two events that appear anomalous in the central zone are shallow. Events further to the west and to the south-southwest are also nearly pure strike slip, but there are insufficient events to define anomalous focal mechanisms surrounding these events.

In order to determine which of the low B-axis dip regions corresponds to normal or reverse faulting, the dip of the tension axis was subtracted from the dip of the pressure axis for each solution (Fig. 4). This difference ranges from -90 to +90, where -90 corresponds to a pure reverse fault and +90 to a pure normal fault. Values close to zero correspond to strike-slip mechanisms or near-vertical movement on vertical faults. The central cluster is dominated by strike slip faulting with reverse faulting. The northeast and southwest edges of the central zone are dominated by strike slip faulting with components of normal faulting. In southeastern Tennessee earthquakes with normal and reverse components fit a pattern of reverse faulting in a central zone of high-level of activity surrounded by a zone of horizontal extension.

FINITE ELEMENT MODELS

Stress modeling in this study is based on the second order, multivariate finite element equations, outlined in Chapter 4.5 of Reddy (1984), with special emphasis on the plane elastic deformation of a linear elastic solid. The finite element technique divides the model space into a mesh of area elements which are approximations of the physical media. The horizontal crustal plates under investigation in this study are modeled using plane stress formalism in which the longitudinal dimension is small compared to the x and y dimensions. Stresses in the z-direction are neglected or studied separately in vertical profiles.

The compression of zones of weak crustal rock within a more rigid elastic crust is modeled by assigning a lower Young's modulus to the weak zone. The weak zones are given circular and ellipsoidal shapes because these shapes are expected to be similar to the shapes of sills and other intrusive bodies.

Smooth shapes are considered appropriate for modeling the dispersion of fluids from intrusive bodies, a possible mechanism for weakening of the crust. Two zones of weak material are used to simulate the geometry suggested by the focal mechanisms in the crustal volume of southeastern Tennessee. The material types used are all isotropic. No body forces are applied and the model solutions are for elastic material properties. All stress magnitudes are based on a regional lithospheric stress of 5 MPA. Other values of stress can be obtained by scaling the computed stresses.

The boundary conditions are designed to simulate a horizontal plate under horizontal compression. The left boundary is held at zero displacement and a stress is applied to the right boundary. The side boundaries are constrained to zero normal displacement but are free to move tangential to the boundary.

The average hydrostatic pressure of the entire grid is used to simulate crustal equilibrium under compression without zones of weakness. When this average hydrostatic pressure is subtracted from the hydrostatic pressure value of each individual point, changes in the form of extension and compression initiated by crustal weakening can be estimated in the more rigid plate. In evaluating stresses available for earthquakes occurring above the plate, changes in compressive stress in the plate may be more important than absolute values in establishing patterns of normal or reverse components in the faulting.

Single Large Circle

A single large circular zone was chosen for its simplicity and appropriateness for models of the weak zone created by a sill or other intrusive within the lower crust (Fig 5). The universally compressive stress

in both principal stress axis directions (Fig 6) is consistent with the boundary conditions and applied regional stress. The applied stress creates compression of the crust parallel to the stress and the boundary conditions leave the displacement perpendicular to the stress unchanged. The principal stresses indicate stress concentrations near the boundary of the weak zone. Stresses are 50 percent higher near the boundary than in the rest of the rigid crustal material and 240 percent higher than in the material used to model the weak zone. The stresses can be divided into their deviatoric and hydrostatic components. The deviatoric stresses (Fig. 7) describe the stress available for shear failure in earthquakes. The regional compression and boundary conditions force all deviatoric stresses to be extensional perpendicular to the applied stress and compressional parallel to the applied stress. Fig. 7 also shows little change in the state of stress within the weak zone. The magnitude of deviatoric stress within the weak zone is only about 40 percent of the deviatoric stress on the boundary of the weak zone and is determined by the arbitrary choice of reduced values of the elastic constants used to simulate the weakened rock.

The hydrostatic stresses provide a measure of the extension and compression of the plate. All hydrostatic stresses are negative (or of compressive character) for the same reason that all stresses were dominantly compressive. Fig. 8 represents the hydrostatic stresses of each point with the hydrostatic stress of the entire grid subtracted. This display is appropriate for illustrating changes induced by the transient introduction of a weak zone. The geologic analogy would be the weakening of a portion of the crust, which is in an equilibrium state and a measure in change in compression or extension of the plate induced by the weak zone. The stresses indicate two zones of compression which are situated on the sides of the weak zone normal

to the applied stress. The magnitude of the change is approximately 10 percent. The decreased stress of the weak zone should not be construed as extension because the change in material properties controls the stress. Instead, above the deformed weak zone compression and hence thrust faulting would be expected. The extension relative to a plate of uniform stress exists outside the weak zone on the sides in line with the applied stress. The extensional zones above the plate would be zones of possible normal fault earthquakes and the compressional zones would be zones of possible reverse fault earthquakes induced by the transient introduction of the weak zone.

In the weak zone, the stress levels must decrease and are controlled by the distortion of the surrounding plate. Normally, compression is in line with the applied stress and extension is normal to the applied stress. Consequently, any earthquakes occurring within the weak zone, would have their null axis vertical. These strike slip mechanisms would represent a direct response to the regional stress.

Two Adjacent Circles

The stress model for two adjacent circles was chosen to be able to interpret the interaction of a system of sills or other types of weak zones within the crust and to model possible weak zones delineated by focal mechanisms in southeastern Tennessee. The general properties of the stress concentrations are similar to those of the single large circle. These similar properties include the compression perpendicular to the applied stress and the relative extension on the edges of the weak zone parallel to the applied stress. The primary difference relates to increases in stress contrast that are proportional to the fraction of the total width of the model that contains

the weaker material. For two circles aligned parallel to the applied stress (Fig 9), 10 km wide separation zone between the two circles is not a zone of stress concentration. The small separation allows a continuous weak zone of low stress from one circle to the other. Two circles, therefore, behave like a single weak body which is peanut-shaped, when they are aligned parallel to the applied stress.

For two circles aligned perpendicular to the applied stress, the finite element stresses are similar to those for circles in line with the stress, except that the stress zone separating the two circular zones shows stress concentrations about 300 percent larger than in the surrounding elastic plate. In the deviatoric stress (Fig. 10) the elastic material separating the circles amplifies the applied stress instead of being absorbed in the weak zone as it is in the case of the circles aligned with the regional stress. The increased stress within the separation is explained by the direct application of the applied stress to the separation of the two circles. Fig. 10 shows a distinct central zones for each weak zone surrounded by zones of higher stress. The patterns of stress are thus distinctly different in the vicinity of the weak zones and depend on the orientation of the complex weak zone in the applied stress.

Two circles located along a diagonal (45 degrees) relative to the applied stress show zones of deviatoric stress concentrations at the boundary of the circles including the zone separating the two circles. The stresses are of the same magnitude found for the other two-circle models. The deviatoric stresses (Fig. 11) show that two circular weak zones oriented diagonally to the applied stress remain independent zones of weakness and do not merge into a continuous weak zone. However, the deviatoric stresses on the connecting bridge are on the order of 100 percent greater than the average stress. This

increase is significant in that it suggests that irregularities within the central weak zone can generate significantly anomalous deviatoric stresses. Also, the diagonal orientation creates large intermediate zones of neither compressive nor extensional character immediately next to the circular weak zones. This can be seen to the right of the top circular weak zone and to the left of the bottom circular weak zone in Fig. 11. The diagonally aligned circles concentrate stresses between the two weak zones and provides a complex pattern of extensional and compressional zones.

Also, an ellipsoidal zone in various orientations was examined to simulate a continuous linear weak zone in an applied stress. The results are similar to those of the two adjacent circles with the exception that stress concentrations on the edges could be 50 percent greater. An ellipsoidal zone could represent perturbation of the strength of a fault zone by fluids. The deviatoric stresses for an ellipsoidal zone with its major axis parallel to the applied stress show negligible contrast with the surrounding stronger crust beside the weak zone. Stress concentrations appear only along the boundaries, particularly at the ends, of the ellipsoidal weak zone with its major axis perpendicular to the direction of applied stress with magnitudes similar to those of the two adjacent circles.

Crustal Perturbation in Vertical Profile

A perturbation of the strength of the lower crust leading to elastic or viscous deformation also affects the stresses in the shallow crust. In order to examine the influence on stresses above the weak zone, a vertical profile was examined. The surface sedimentary layers were added to assess the effects of sediments on stress in this shallow crust (Fig. 12). The model for the

vertical profile differs from the model for crustal inclusions examined previously in that the top of the sediments is a free surface. The deviatoric stress (Fig. 13) shows a concentration of shear stress above the zone of perturbation. The model is analogous to a shallowing of the brittle-ductile transition zone. The deviatoric stresses are about 200 percent higher over a weakened crust than in the surrounding crust. The 200 percent increase is comparable to the largest shear stress observed in the analysis of stress amplification in a horizontal plate; the two weak zones at a diagonal to the applied stress. The direction and magnitude of the principal stress axes favor earthquakes on reverse faults above the weak zone. The low stress levels in the sediments show that low-velocity sedimentary basins are largely insulated from the stresses in the crust. The deeper sedimentary basins could contribute to the amplification of crustal stress by constricting the thickness of the stress channel. A large abrupt change in crustal structure can thus concentrate stress in one area, which in this case is the zone between the sediments and the top of the weak zone.

CONCLUSIONS AND DISCUSSION

In southeastern Tennessee a pattern of earthquake focal mechanisms is observed that can be modeled by two mid-crustal weak zones oriented at 45 degrees to the regional compressional stress. The factors that support this conclusion are as follows:

- 1) The shape of the pattern is defined by the concentration of seismic activity in a central zone surrounded by lower levels of seismicity with extensions to the northeast and southwest.

2) In the central zone the earthquakes below 15 km uniformly have strike slip focal mechanisms with northeast-southwest trending compressional axes. The stress model suggests that the stress directions in the weak zone should deviate only slightly from the regional stress field and that the null axis should be vertical.

3) The shallow events above the weak zone show large thrust components. The stress model for a vertical section predicts that above the weak zone the stress is amplified and is characterized by a thrust component.

4) All of the earthquakes in the central zone show some thrust component in agreement with the models showing compression in and above the weak zone.

5) The focal mechanisms for events surrounding the central zone depend on their position relative to the applied regional stress.

Events on the axis parallel to the regional stress show a normal component in the predominantly strike slip focal mechanisms. The few events on the axis perpendicular to the the regional stress show a thrust component. The horizontal stress models indicate that the change in the stress induced by a transient weakening of the crust is compressional on the edges of the central zone perpendicular to direction of the regional stress and extensional on the edges in line with the regional stress.

The model and the observed seismicity in southeastern Tennessee correspond to phase 3 of Long's (1988) five-phase hypothesis for major intraplate earthquakes. In phase 3 the weakened central zone is being deformed by regional compressive stress and the surrounding elastic crust is bearing the load no longer supported by the central zone. The regional compressive stress is required since without a regional stress the deformation of the central zone would not create the deviatoric stresses for the earthquakes. A local weakening of the crust by a perturbation of its

hydraulic or thermal properties is required in order to trigger the events in zones where the crust is normally stronger and to allow concentration of the seismicity in limited seismic zones such as in southeastern Tennessee. Also, the transient appearance of the perturbation should be relatively short in duration, otherwise the dispersion of fluids in the zone of perturbation would smooth the zone of weakness and decrease the concentration of stress, as well as provide time for relaxation of the stresses. The transient character of this model suggests, further, that zones of weakness associated with intraplate seismicity are created in time periods of a few years and are not necessarily those that have existed over hundreds of years.

Variations in the P-axis orientation has sometimes been ascribed to the preferential failure of pre-existing planes of weakness in a uniform stress field. The uniformity we observe for focal mechanisms in the central zone argues for a direct response to the direction of regional stress. The variations in focal mechanisms for shallow events and those in the surrounding elastic plate fit a pattern. Although existing faults may contribute to the determination of focal mechanisms in these zones, the general pattern is that predicted by stress models for a weakness in a plate subjected to regional stress. Hence, in southeastern Tennessee stress inhomogeneity, rather than preferential failure of pre-existing planes of weakness, is our preferred explanation for diversity in the focal mechanisms.

The zone of weakness can be generated by perturbations in the hydraulic properties and/or thermal properties of the lower crust. Figure 14a is a simplified conceptual diagram showing the strength of the crust in tensional and compressive tectonic environments. A temperature increase (Fig. 14b) predicts a shallowing of the brittle-ductile transition. An increase in fluid content in the lower crust would create a localized decrease in the frictional

strength. The change is more pronounced than that caused by a thermal perturbation and is also more pronounced in zones of crustal extension. In the southeastern Tennessee seismicity, the zones of predicted extension are those exhibiting the greater level of seismicity suggesting that a hydraulic perturbation is the more likely explanation for the seismicity. Also, the greater time and energy required to effect a thermal perturbation favor an explanation based on fluid movement.

The important conclusions from this analysis are as follows:

- 1) The focal mechanisms of earthquakes in southeastern Tennessee fit a pattern predicted by stress modeling of a zone of weakness in the lower crust.
- 2) The different orientations of focal mechanisms can be explained by inhomogeneity in stress.
- 3) The seismicity can be explained by a transient perturbation in the fluid properties of the lower crust.

ACKNOWLEDGMENTS

This research was supported primarily by the Nuclear Regulatory Commission, Office of Nuclear Regulatory Research. Supplemental support was provided by the Corps of Engineers, Savannah District, and the Tennessee Valley Authority. Computer time was provided by the School of Geophysical Sciences and the Advanced Computational Methods Center at the University of Georgia through the Supercomputing Support Group of the Office of Computing Services at the Georgia Institute of Technology.

List of Figures

- Figure 1. Seismicity of southeastern Tennessee. The events shown have been relocated with station corrections applied and represent a select subset of the observed data in southeastern Tennessee.
- Figure 2. Focal mechanism solutions and epicenters in the central zone. The bar indicates the horizontal projection of the P-axis. Events with confidence levels below 0.75 have been left open.
- Figure 3. Dip of the B axis of the focal mechanism solution for the central zone. The dip of the B axis indicates deviation from pure strike slip motion.
- Figure 4. Difference between the dip of the tension axis and the dip of the pressure axis. Negative values suggest reverse faulting and positive values suggest normal faulting components in the predominant strike slip focal mechanisms.
- Figure 5. Model for a single circular zone of weakening in a horizontal crustal plate.
- Figure 6. Stress surrounding a weak circular zone in a horizontal crustal plate. Arrows indicate principal stress directions and magnitudes.
- Figure 7. Deviatoric stresses surrounding a weak zone in a horizontal crustal plate.
- Figure 8. Hydrostatic stresses surrounding a weak zone in a horizontal crustal plate.
- Figure 9. Deviatoric stress for two circular zones of weakened crust aligned parallel to the applied stress.
- Figure 10. Deviatoric stress for two circular zones of weakened crust aligned perpendicular to the applied stress.
- Figure 11. Deviatoric stress for two circular zones of weakened crust aligned at 45 degrees to the direction of applied stress.
- Figure 12. Geologic model for a vertical profile across a zone of weakness in the crust.
- Figure 13. Deviatoric stress in a vertical section across a zone of weakness in the crust.
- Figure 14. Simplified conceptual diagram showing (a) changes in the strength of the crust induced by (b) thermal and (c) fluid disturbances in the lower crust.

REFERENCES

- Aggarwal, Y.P. and L.R. Sykes, 1978. Earthquakes, faults and nuclear power plants in southern New York, Science, 200, pp. 425-429.
- Bollinger, G.A., 1973. Seismicity of the southeastern United States, Bull. Seism. Soc. Am., 63, pp. 1785-1808.
- Bollinger, G.A., C.J. Langer and S.T. Harding, 1976. The Eastern Tennessee Earthquake Sequence of October through December, 1976, Bull. Seism. Soc. Am., Vol. 66, No. 2, pp. 525-547.
- Bollinger, G.A. and R.L. Wheeler, 1988. The Giles County, Virginia, seismic zone--Seismological results and geological interpretations, U.S. Geological Survey Professional Paper, 1355, U.S. Government Printing Office, Washington, D.C., 85pp.
- Bott, M.H.P. and N.J. Kusznir, 1984. The origin of tectonic stress in the lithosphere, Tectonophysics, Vol. 105, pp. 1-13.
- Byerlee, J., 1978. Friction of rocks, Pure and Applied Geophysics, 116, pp. 615-626.
- Campbell, D.L., 1978. Investigation of the stress concentration mechanism for intraplate earthquakes, Geophysical Research Letters, Vol. 5, No. 6, pp. 477-479.
- Chen, W.-P. and P. Molnar, 1983. Focal depths of intracontinental and intraplate earthquakes and their implications for the thermal and mechanical properties of the lithosphere, J. Geophys. Res., Vol. 88, pp. 4183-4214.
- Coppersmith, K. J., 1988. Temporal and spatial clustering of earthquake activity in the central and eastern United States, Seismological Research Letters, Vol. 59, No. 4, pp. 299-304.
- Dewey, J.W., 1985. A review of recent research on the seismotectonics of the southeastern seaboard and an evaluation of hypotheses on the source of the 1886 Charleston, South Carolina, earthquakes, NUREG/CR-4339.
- Fleitout, L. and C. Froidevaux, 1982. Tectonics and topography for a lithosphere containing density heterogeneities, Tectonics, Vol. 1, pp. 21-56.
- Fleitout, L. and C. Froidevaux, 1983. Tectonic stress in the lithosphere, Tectonics, 2, pp. 315-324.
- Fox, F.L., 1970. Seismic geology of the eastern United States, Assoc. Eng. Geologists Bull., 7, pp. 21-43.
- Gettings, M.E., 1988. Variation of depth to the brittle ductile transition due to cooling of a mid-crustal intrusion, Geophysical Research Letters, Vol. 15, No. 3, pp. 213-216.

- Guinn, S.A. and L.T. Long, 1977. A computer method for determination of valid focal mechanism solutions using P-wave first motions, Earthquake Notes, Vol. 48, No. 4 pp 21-33.
- Guinn, S.A., 1980. Earthquake Focal Mechanisms in the Southeastern United States, NUREG/CR-1503.
- Johnston, A.C., D.J. Reinbold, and S.I. Brewer, 1985. Seismotectonics of the Southern Appalachians, Bull. Seism. Soc. Am., Vol. 75, pp. 291-312.
- Kane, M.F., 1977. Correlation of major eastern earthquake centers with mafic/ultramafic basement masses, U.S. Geol. Survey Prof. Paper 1028-O.
- Kuang, Jian, L.T. Long, and J.C. Mareschal, 1989. Intraplate seismicity and stress in the southeastern United States, Tectonophysics (in press).
- Long, L.T., 1976. Speculations concerning Southeastern Earthquakes, mafic intrusions, gravity anomalies, and stress amplification, Earthquake Notes, Vol. 47, No. 3, pp. 29-35.
- Long, L.T. and J.W. Champion, Jr., 1977. Bouguer Gravity Map of the Summerville-Charleston, South Carolina, Epicentral Zone and Tectonic Implications, Geol. Survey Prof. Paper 1028-K.
- Long, L.T., 1988. A model for major intraplate continental earthquakes, Seismological Research Letters, Vol 59, NO. 4, pp 273-278.
- Long, L.T., R.E. White, and J. Dwyer, 1986. The Charleston earthquake Hypotheses - A classification by fundamental tectonic processes, Proceedings of the Third U. S. National Conference on Earthquake Engineering, August, 24-25, 1986, Charleston, South Carolina, pg 25-32.
- Mareschal, J.C. and Jian Kuang, 1987. Intraplate Stresses and Seismicity: The role of topography and density heterogeneities, Tectonophysics, Vol. 132, pp. 153-162.
- McKenzie, D.P., 1969. The relationship between fault plane solution for earthquakes and the directions of principal stresses, Bull. Seism. Soc. Am., Vol. 59, pp. 591-601.
- McKeown, F.A., 1978. Hypothesis: Many earthquakes in the central and southeastern United States are causally related to mafic intrusive bodies, Jour. Research U.S. Geol. Survey, Vol. 6, No. 1, pp. 41-50.
- Meissner, R. and J. Strehlau, 1982. Limits of stresses in continental crusts and their relation to the depth-frequency distribution of shallow earthquakes, Tectonics, Vol. 1, No. 1, pp. 73-89.
- Oudenhoven, M.S., C.O. Babcock, and W. Blake, 1972. A method for the prediction of stresses in an isotropic inclusion or orebody of irregular shape, U.S. Bureau of Mines, Report of Investigations 7645, 36 pp.

- Prowell, D.C. and B.J. O'Connor, 1978. Belair fault zone: Evidence of tertiary fault displacement in eastern Georgia, Geology, Vol. 6, pp. 681-684.
- Rankin, D.W., 1976. Appalachian salients and recesses: Late Precambrian continental breakup and the opening of the Iapetus Ocean, J. Geophys. Res., 81, pp. 5605-5616.
- Reddy, J.N., 1984. An Introduction to the Finite Element Method, McGraw Hill Company.
- Reinhardt, J., D.C. Prowell and R.A. Christopher, 1984. Evidence for Cenozoic tectonism in the southwest Georgia Piedmont, Geol. Soc. Am. Bull., Vol. 95, pp. 1176-1187.
- Richardson, R.M., S.C. Solomon and N.H. Sleep, 1979. Tectonic stress in the plates, Rev. Geophys. Space Physics, 17, pp. 981-1019.
- Sbar, M.L. and L.R. Sykes, 1973. Contemporary compressive stress and seismicity in eastern North America: an example of intraplate tectonics, Bull. Geol. Soc. Am., 84, pp. 1861-1882.
- Solomon, S.C., R.M., Richardson, E.A., Bergman, 1980. Tectonic Stress Models and Magnitudes, J. Geophys. Res., 85, pp. 6086-6092.
- Sykes, L.R., 1978. Intraplate seismicity, reactivation of pre-existing zones of weakness, alkaline magmatism, and other tectonism postdating continental fragmentation, Rev. Geophys. Space Phys., 16, pp. 621-688.
- Talwani, P., 1988. The intersection model for intraplate earthquakes, Seismological Research Letters, Vol. 59, No. 4, pp 305-310.
- Teague, A.G., G.A. Bollinger, and A.C. Johnston, 1986. Focal Mechanism analyses for eastern Tennessee earthquakes (1981- 1983), Bull. Seism. Soc. Am., Vol. 76, No. 1, pp. 95- 109.
- Zelt, Karl-Heinz, 1988. Investigation of the cause of earthquakes in southeastern Tennessee and northern Georgia using focal mechanisms and models of crustal stress, Ph.D. Thesis, Georgia Institute of Technology, Atlanta, Georgia, 231 pp.
- Zoback, M.L. and M.D. Zoback, 1980. State of stress in the conterminous United States, J. Geophys. Res., 85, pp. 6113- 6156.
- Zoback, M.D., 1983. Intraplate earthquakes, crustal deformation and in situ stress, U.S. Geol. Survey, Open file Report 83-843, pp. 169-178.

TABLE I Earthquake locations and focal mechanisms.

Date	Origin Lat.	Long.	Dur.	Depth	# of Sig.	Tension	Pressure	Null	P-T
YrMoDa	Time	North West	Mag.	km	pts.	az.	dip az.	dip az.	dip
820130	12:39	35.80 83.94	2.8	18.8	9	0.76	38 47 221	43 130	1 -4
820224	12:10	35.72 84.29	1.3	20.4	8	0.69	189 7 283	27 86	62 20
820905	10:11	35.21 84.51	3.2	8.4	12	0.86	138 2 229	24 44	66 22
820924	21:57	35.68 84.24	3.2	14.0	12	0.78	161 25 257	14 14	61 -11
821214	06:35	35.29 84.17	2.4	9.1	11	0.81	312 8 51	47 215	42 39
821215	02:27	35.75 84.22	2.1	19.2	9	0.65	252 57 13	18 112	26 -39
830118	05:09	35.58 84.27	2.3	11.2	11	0.71	335 49 71	6 166	40 -43
830129	18:08	36.12 83.74	2.1	20.7	10	0.91	322 31 220	20 102	52 -11
830304	14:03	35.60 84.34	2.3	8.0	7	0.71	53 20 150	17 277	63 -3
830316	09:13	35.22 84.55	2.6	16.9	6	0.71	327 8 234	16 83	72 8
830405	03:17	35.54 84.19	2.1	18.8	7	0.96	176 16 266	3 6	74 -13
830526	12:30	35.67 84.27	2.5	14.6	12	0.88	146 4 54	19 247	71 15
831016	22:02	35.86 84.55	2.5	19.8	12	0.84	348 24 82	9 191	64 -15
840207	06:32	35.65 84.64	1.8	20.4	7	0.71	19 2 289	1 172	88 -1
840525	10:15	35.60 84.62	2.0	24.1	11	0.87	319 34 110	53 219	14 19
840830	16:26	35.55 84.35	3.1	21.1	16	0.96	142 12 59	3 315	78 -9
840830	16:41	35.55 84.35	2.4	18.0	7	0.99	331 7 239	16 84	72 9
841009	11:54	34.77 85.19	3.5	15.0	22	0.78	298 6 29	7 168	81 1
841107	09:31	35.59 84.64	2.0	18.7	14	0.71	308 40 199	21 88	43 -19
850309	14:29	35.03 85.03	2.5	9.7	12	0.68	8 6 277	8 134	80 2
850312	13:04	35.87 83.57	2.0	25.6	12	0.82	311 7 218	16 64	72 9
850410	10:53	35.72 84.06	2.3	22.0	11	0.53	14 24 226	62 110	13 38
850420	04:21	35.48 84.56	2.5	9.4	13	0.78	20 1 151	89 290	1 88
850712	18:20	35.20 85.15	3.0	19.6	10	0.60	123 17 216	9 333	71 -8
850815	17:31	35.67 83.95	1.8	12.5	8	0.78	100 3 190	2 314	86 -1
850924	00:01	35.68 84.05	1.7	19.1	9	0.88	140 10 233	16 19	71 6
851220	15:15	34.93 84.76	2.9	9.3	7	0.68	329 0 236	81 59	9 81
860107	01:26	35.60 84.76	3.1	17.5	24	0.95	107 11 198	4 308	78 -7
860127	06:44	35.88 83.65	2.6	15.0	11	0.83	289 8 21	17 175	71 9
860419	07:40	35.19 85.51	3.0	21.0	27	0.91	183 9 280	35 81	53 26
860423	07:18	34.79 85.30	1.8	19.1	8	0.60	120 2 24	70 211	20 68
860519	23:46	35.53 84.54	2.6	9.7	14	0.67	284 11 16	15 159	71 4
860602	07:46	35.43 84.50	2.5	18.6	14	0.87	132 32 31	17 277	53 -15
860624	19:22	35.98 83.94	2.8	28.8	14	0.67	131 1 40	41 222	49 40
860711	14:26	34.93 84.99	3.8	20.7	30	0.98	329 18 60	3 159	72 -15
860719	12:31	34.94 84.97	1.9	10.6	10	0.66	349 40 226	32 112	33 -8
860807	12:36	35.49 84.54	2.5	14.9	11	0.49	285 15 25	32 174	54 17
860819	20:51	36.26 85.01	2.9	20.0	13	0.73	112 20 244	62 15	19 42
861115	12:08	35.88 83.82	2.0	16.4	9	0.70	172 2 81	7 278	83 5
870112	18:56	35.50 84.25	2.1	14.8	9	0.85	320 23 121	65 227	7 42
870222	10:35	36.39 84.21	2.8	19.0	14	0.81	314 2 44	1 161	88 -1
870327	01:26	35.60 84.76	3.9	17.5	35	0.99	323 4 53	6 199	83 2
870901	23:02	35.51 84.40	3.2	16.9	17	0.99	304 20 41	18 170	63 -2

The significance measure is based on the number of points, the distribution of data points, quality of first motions and SV/P ratios, and a Chi-square estimate of goodness-of-fit.

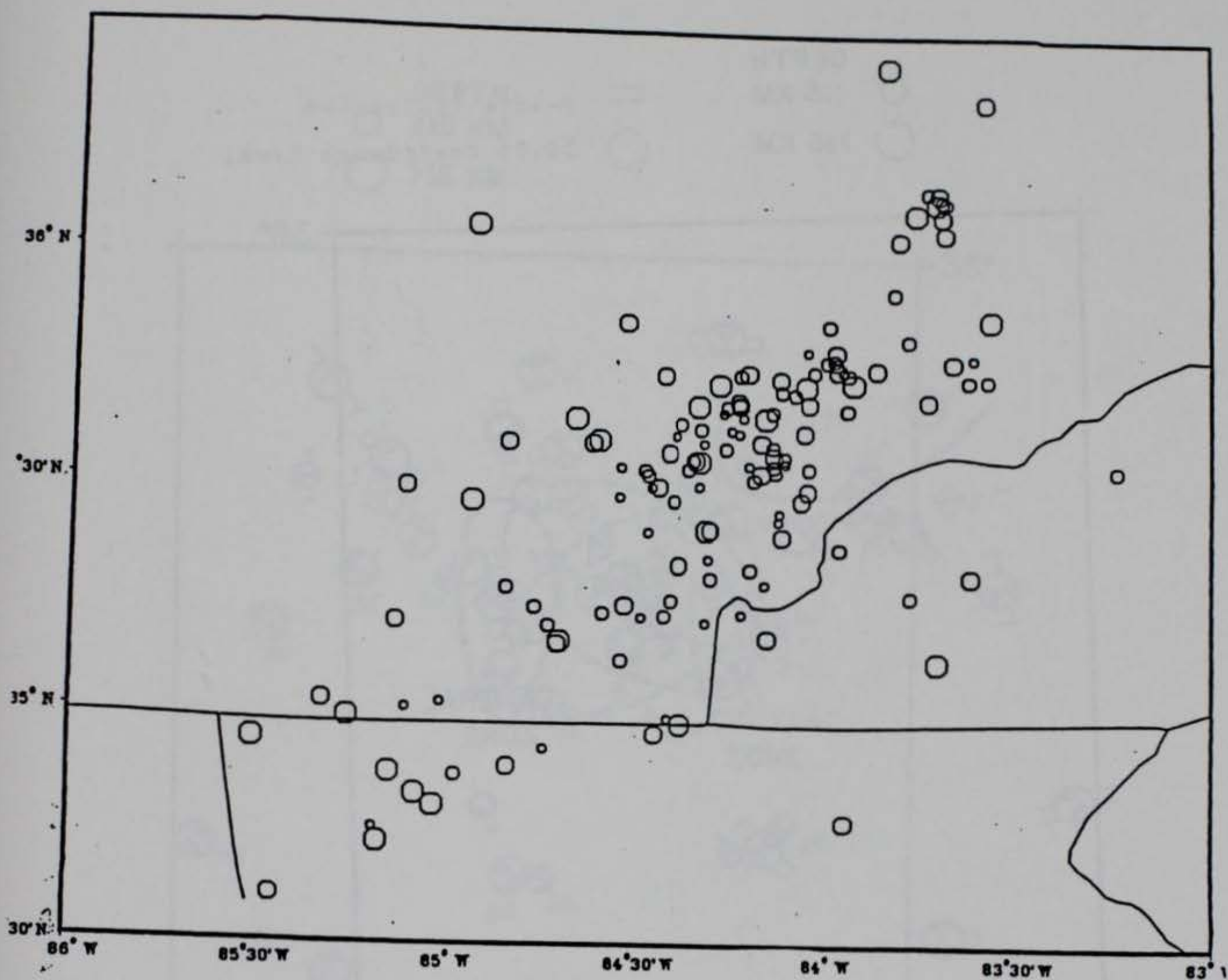


Figure 1. Seismicity of southeastern Tennessee. The events shown have all been carefully relocated and represent a subset of the observed data in southeastern Tennessee.

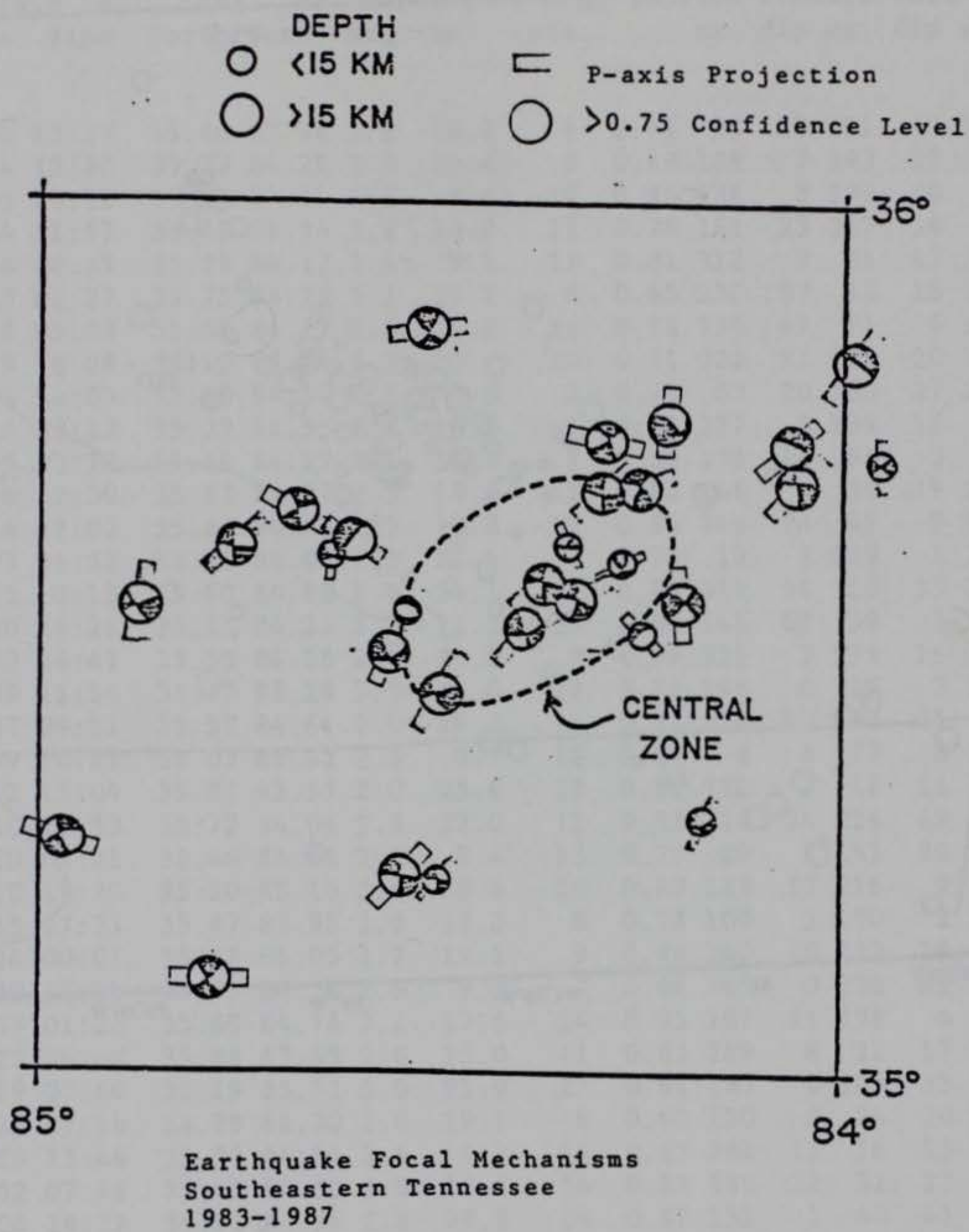


Figure 2. Focal mechanism solutions and epicenters in the central zone.

Dip of B axis
 90° = strike slip

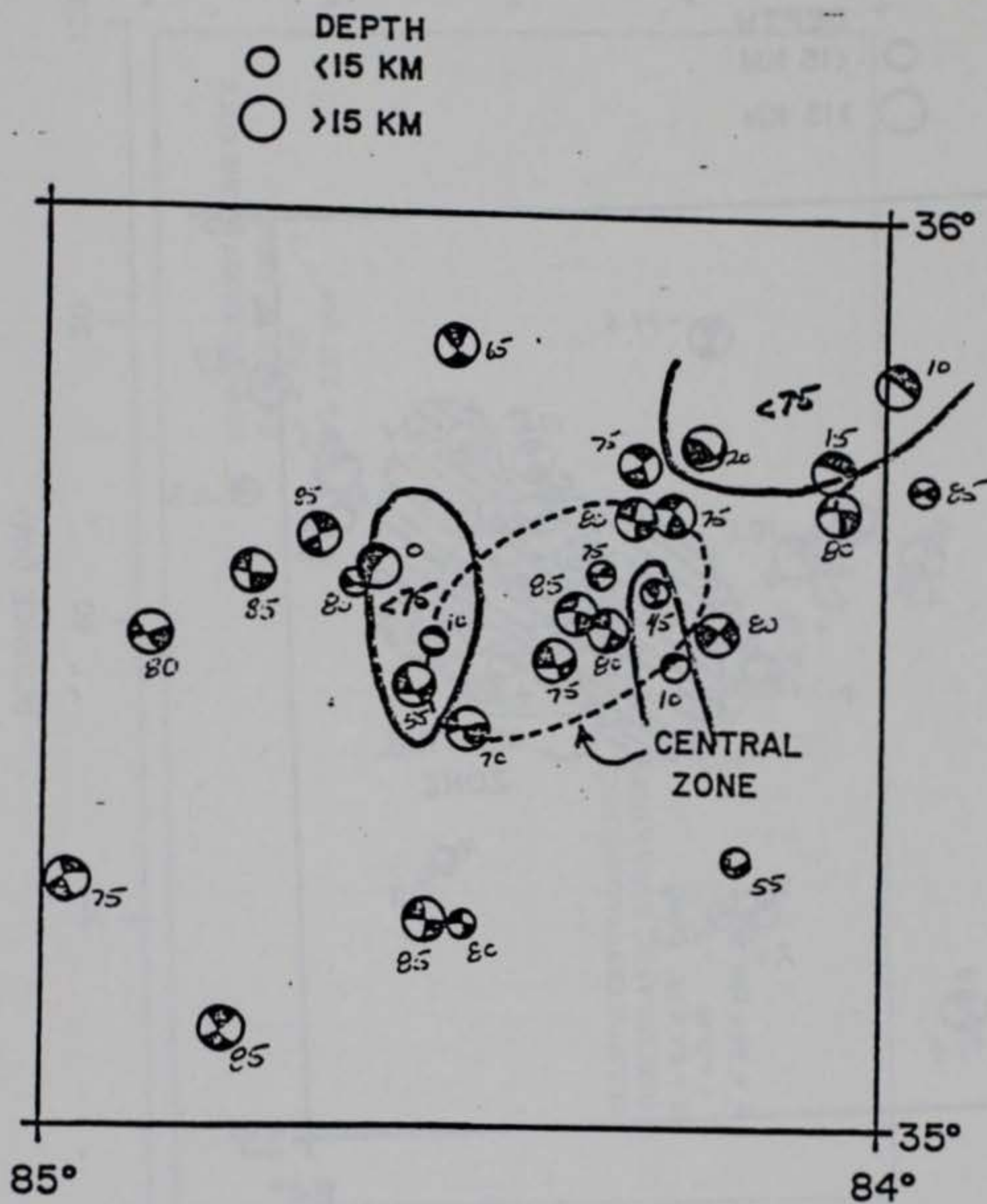

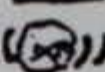


Figure 3. Dip of the B axis of the focal mechanism solution for the central zone. The dip of the B axis indicates deviation from pure strike slip motion.

Difference between dip of P axis
and dip of T axis.

P-T { - Reverse 
+ Normal 

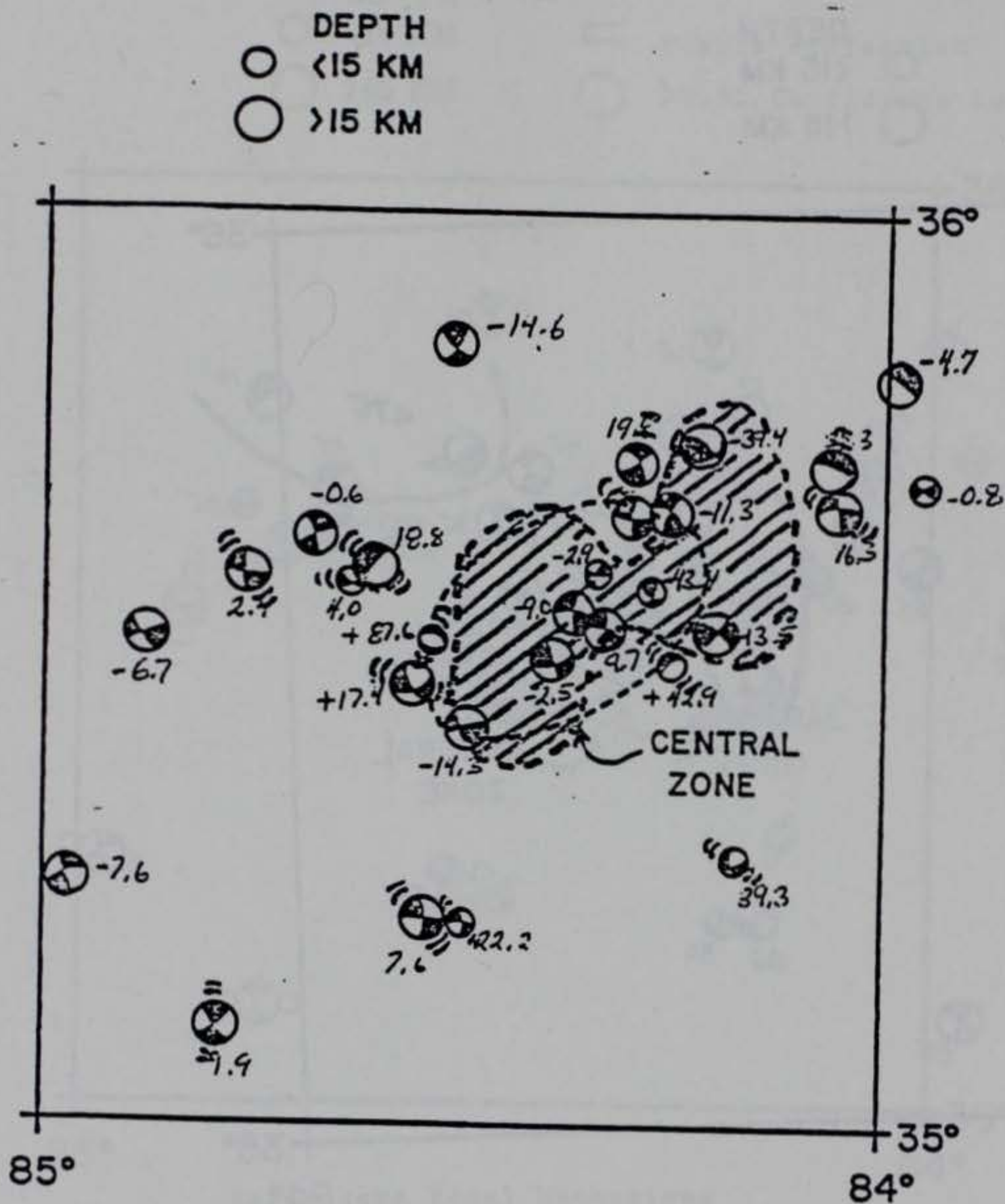
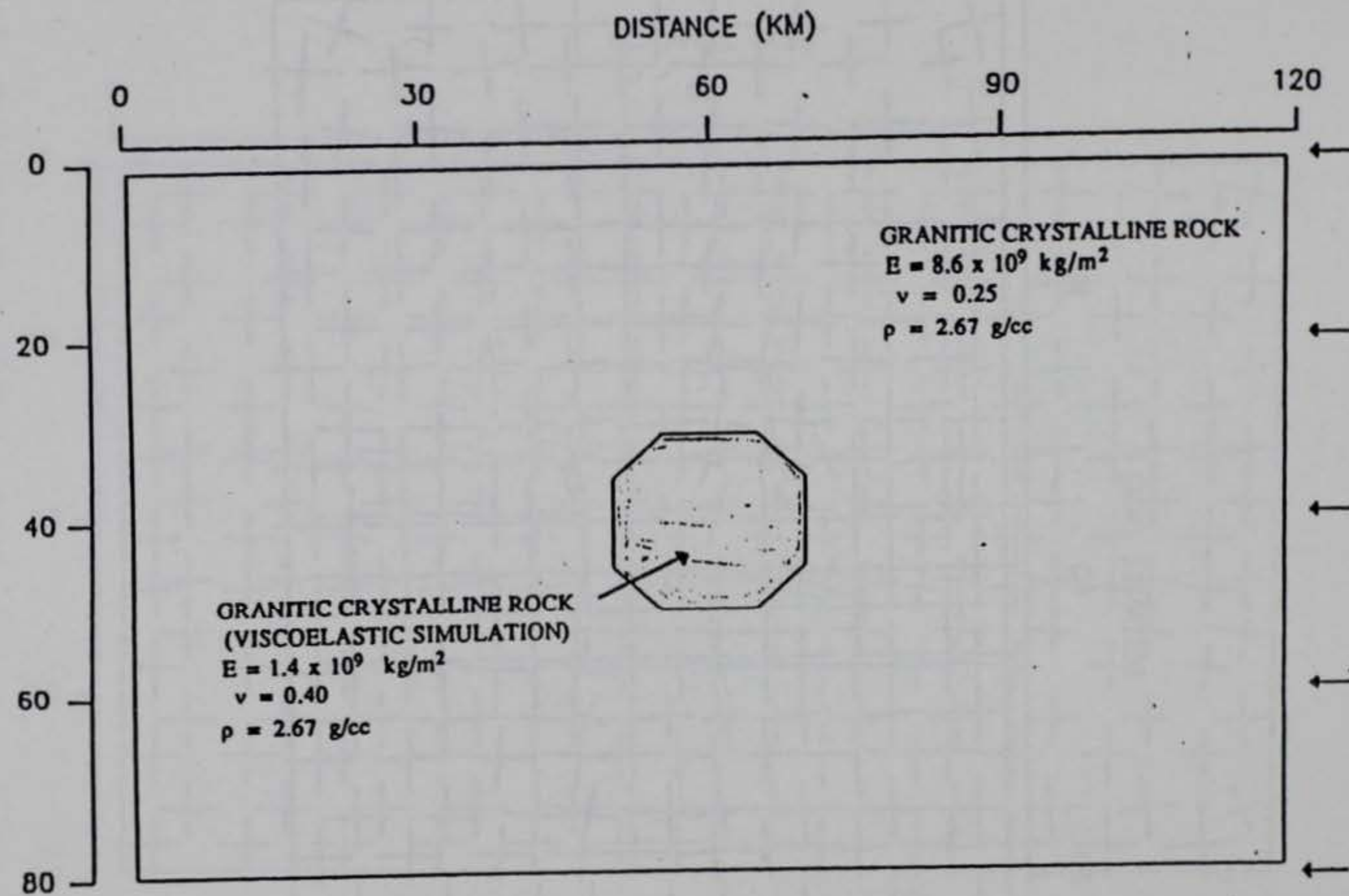


Figure 4. Contour plot of the difference between the dip of the tension axis and the dip of the pressure axis. Negative values are reverse faulting and positive values are normal faulting.

Figure 5. Model for a single circular zone of weakening in a horizontal crustal plate.



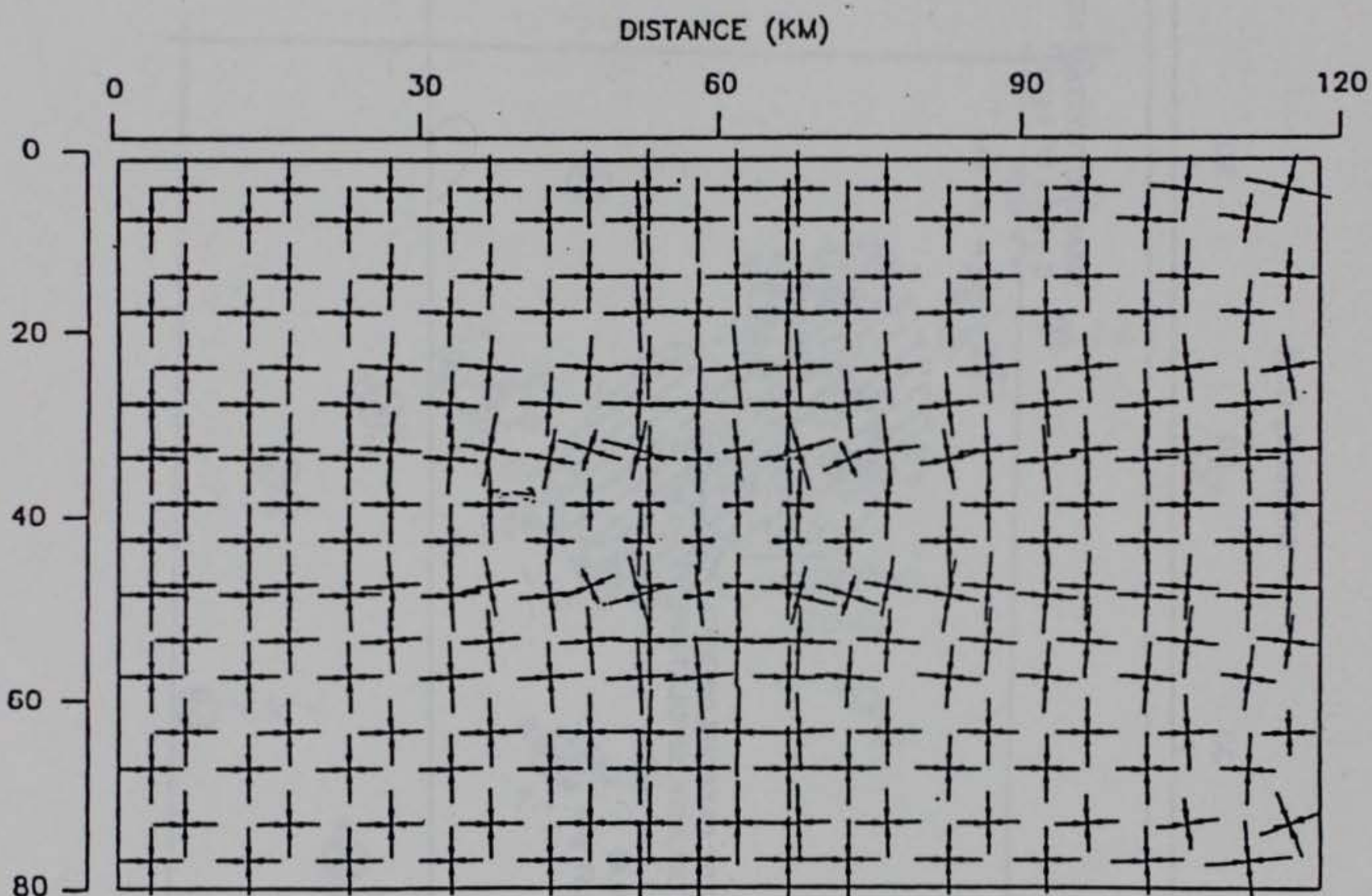


Figure 6. Stress surrounding a weak circular zone in a horizontal crustal plate.

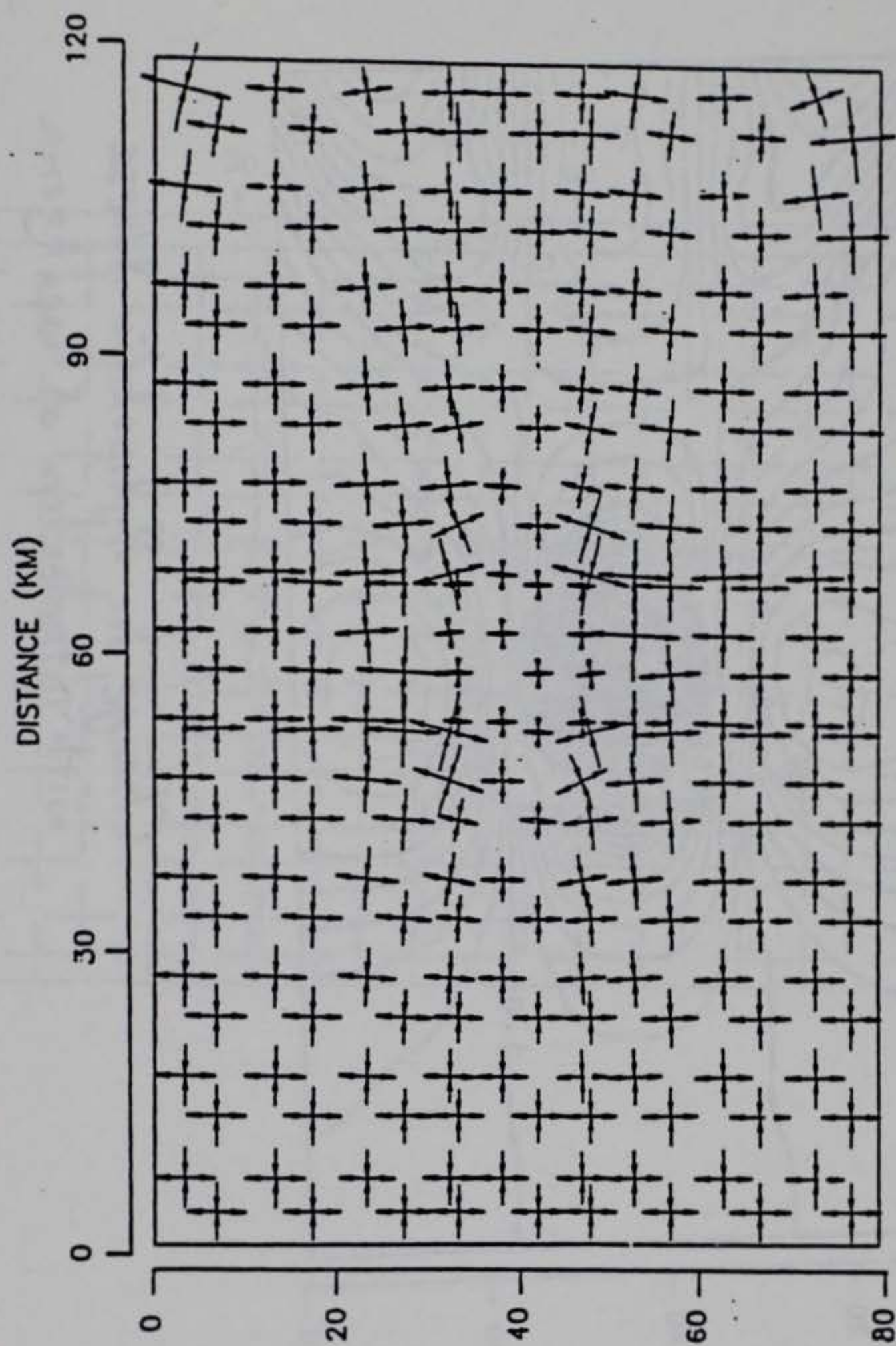
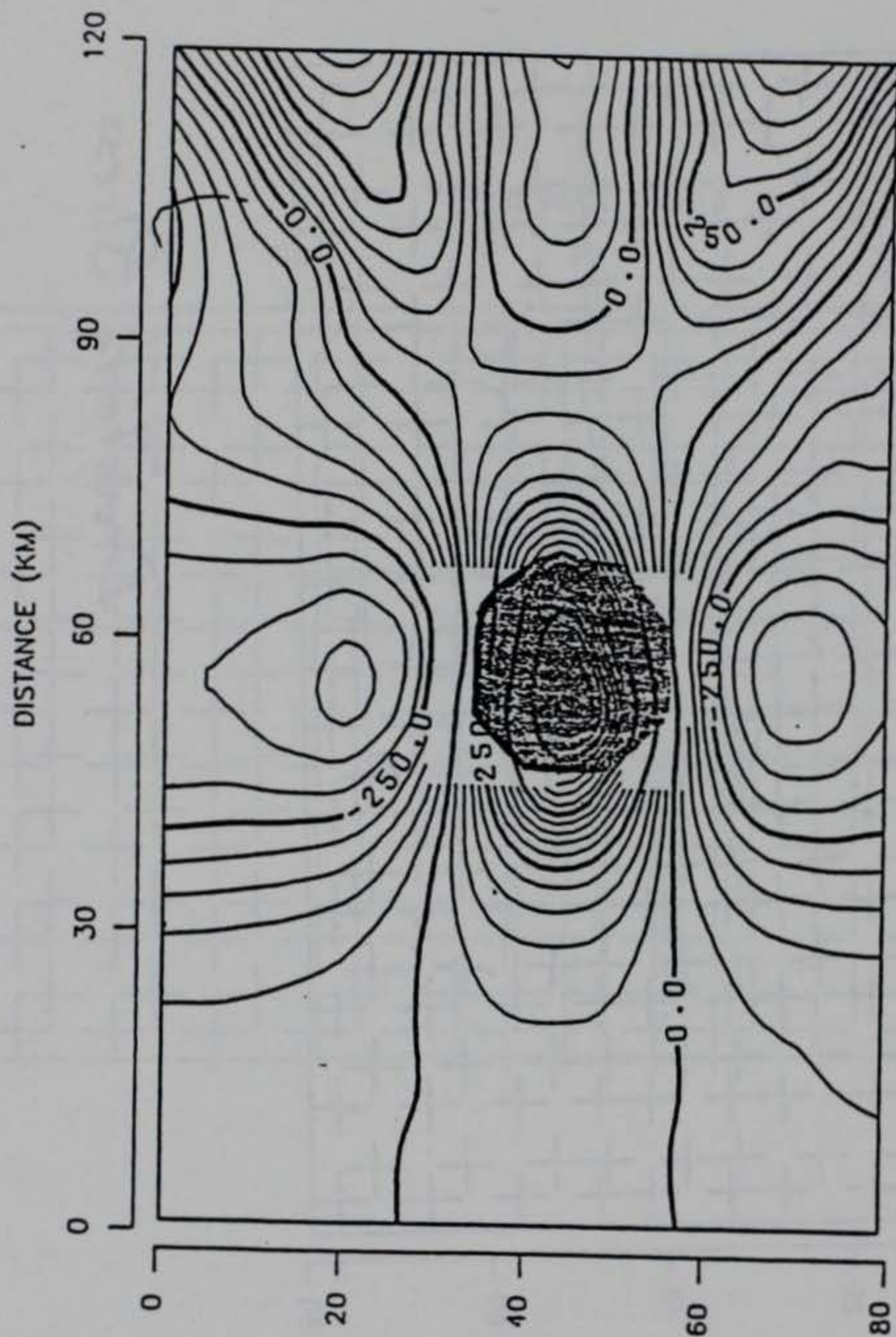


Figure 7. Deviatoric stresses surrounding a weak zone in a horizontal crustal plate.

Deviatoric Stress



*Change in Hydrostatic Stress
with introduction of weak zone*

Figure 8. Hydrostatic stresses surrounding a weak zone in a horizontal crustal plate.

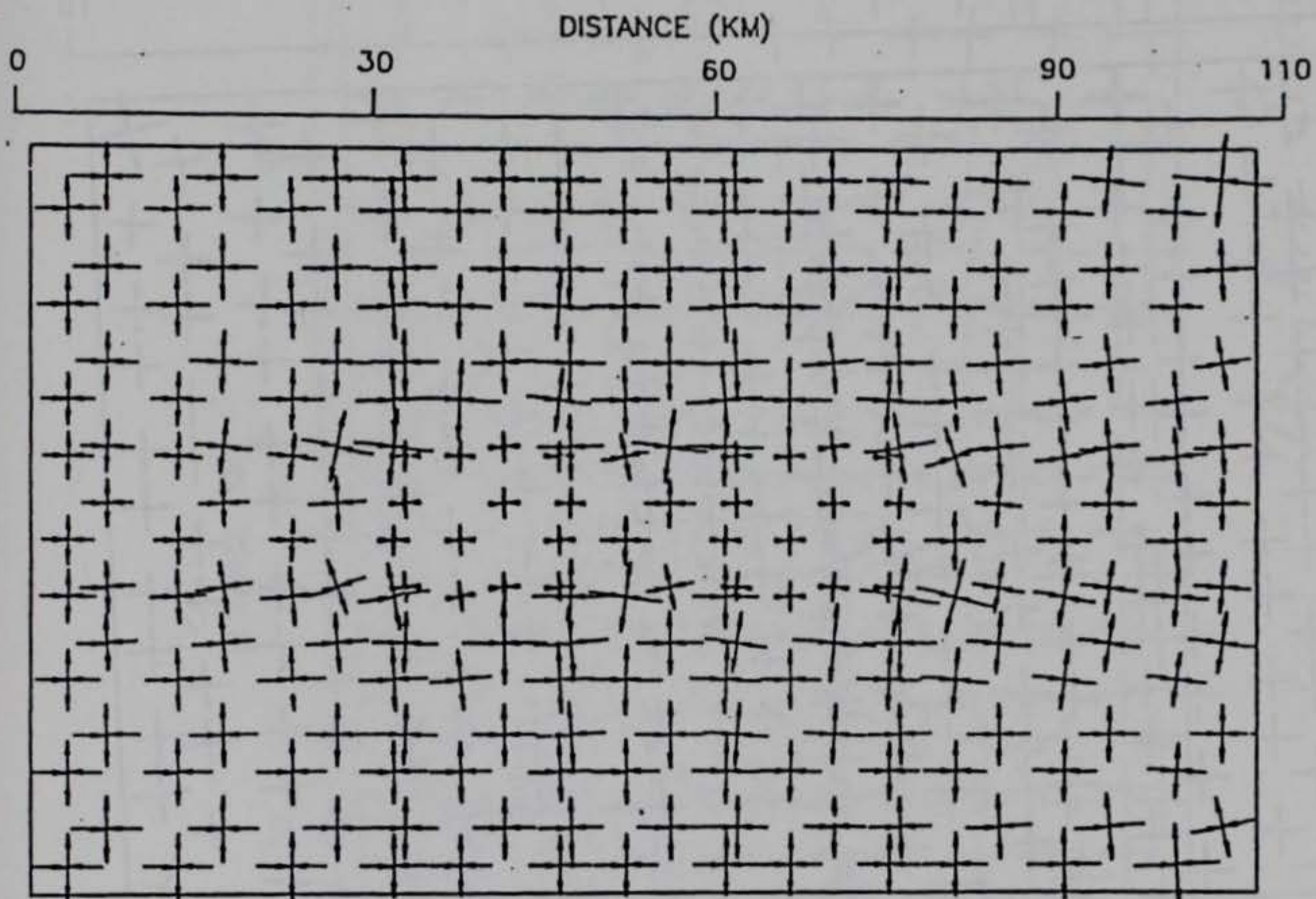


Figure 9. Two circular zones of weakened crust aligned parallel to the applied stress.

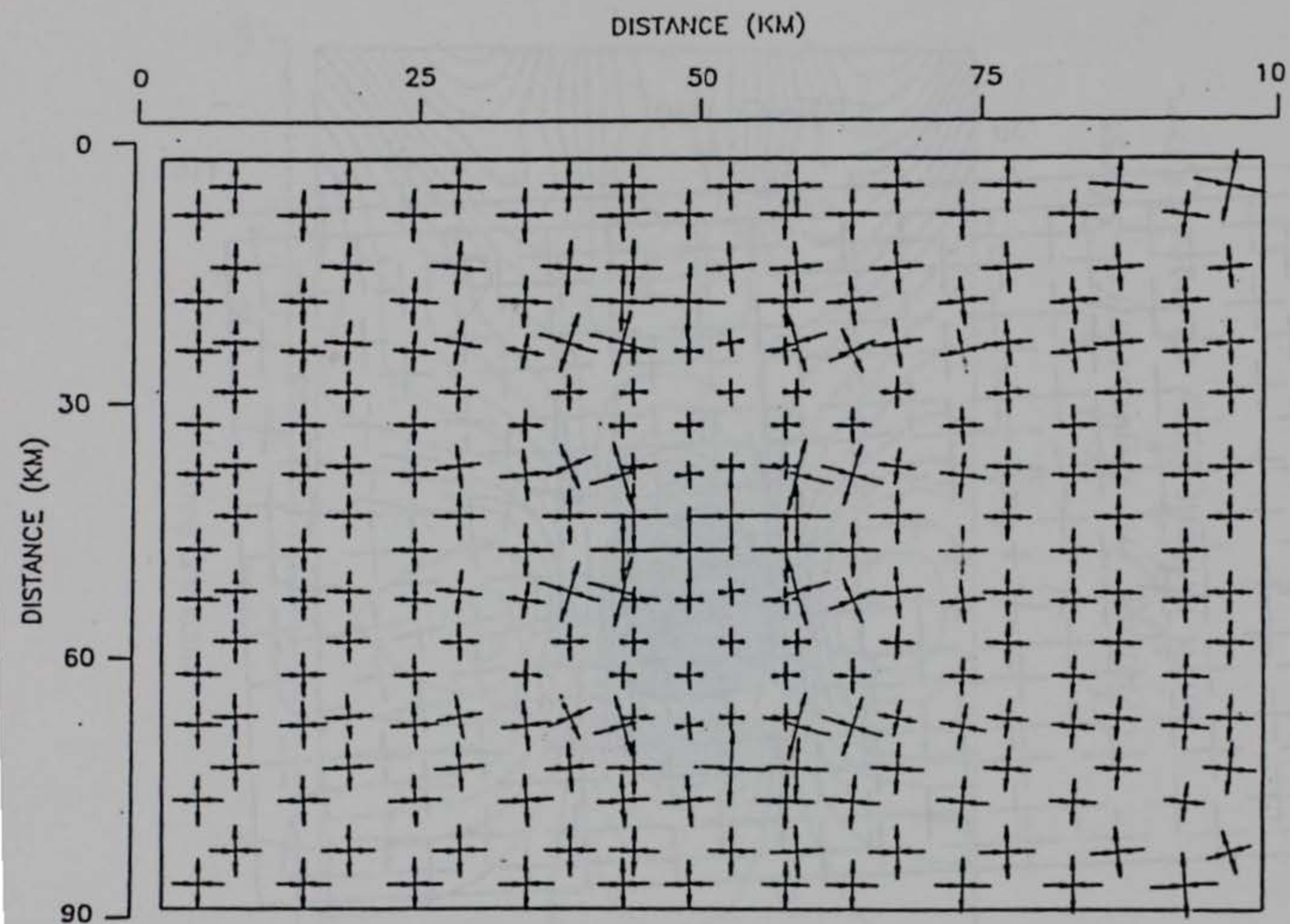
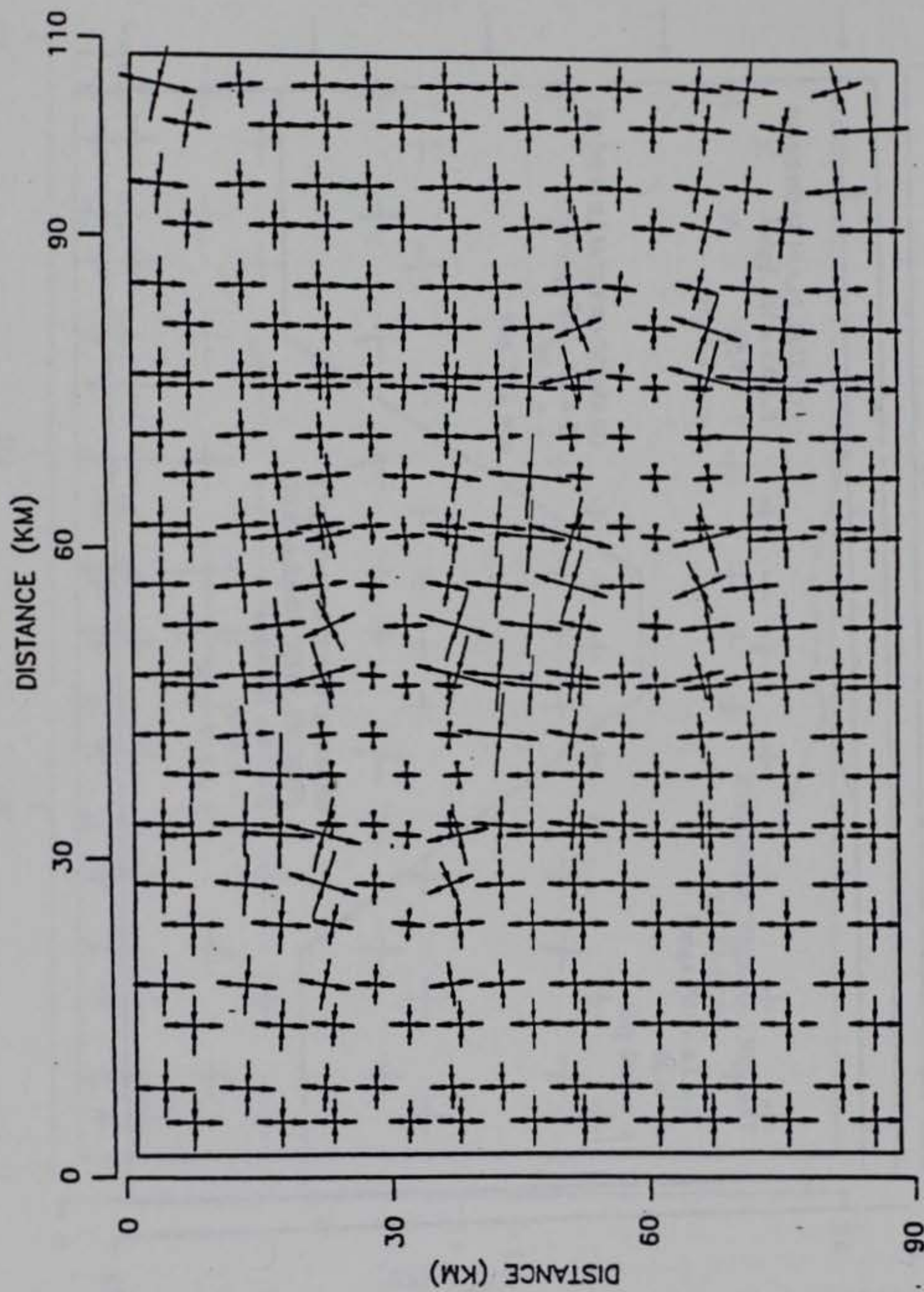


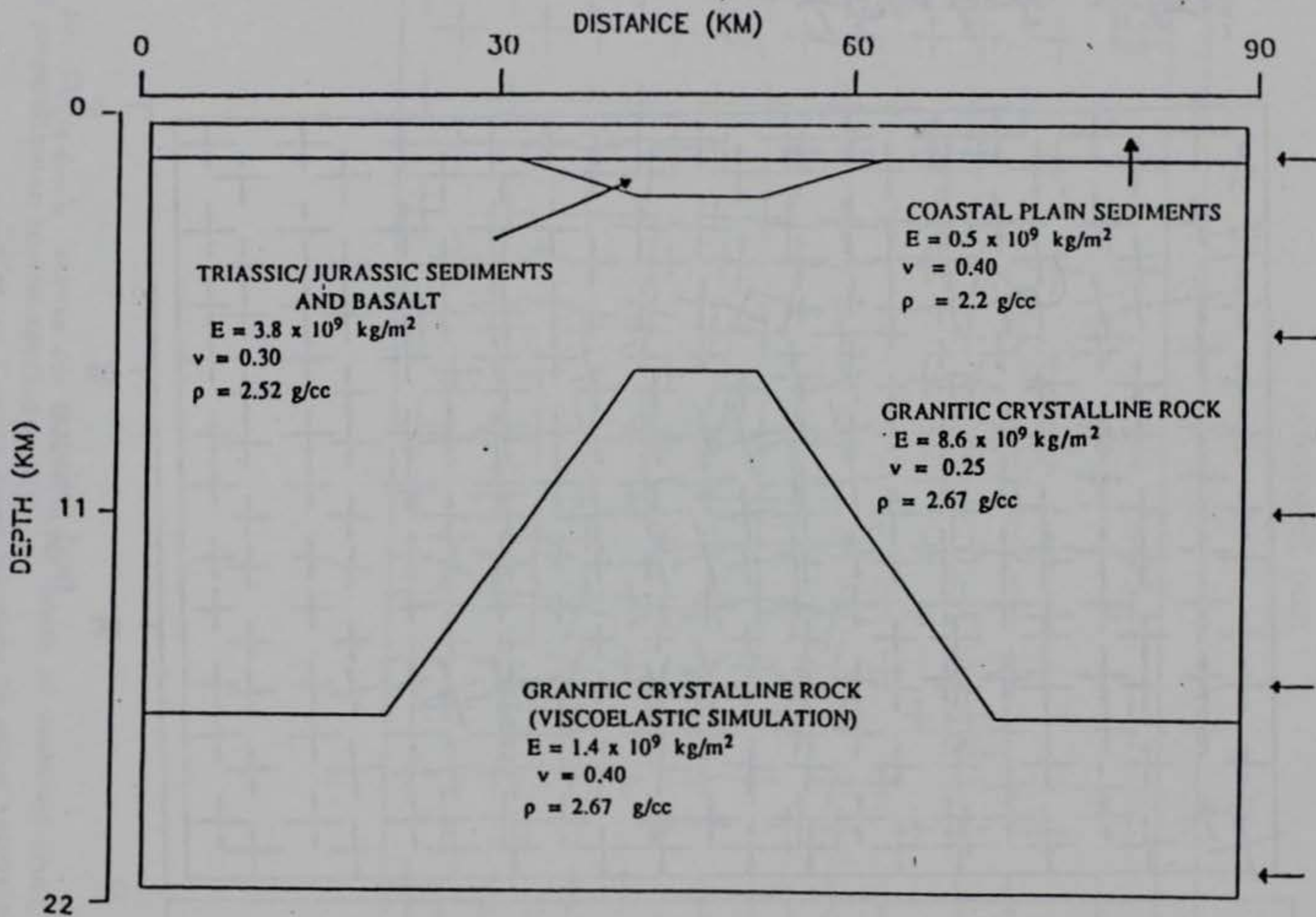
Figure 10. *Isostatic* stress for two circular zones of weakened crust, aligned perpendicular to the applied stress.

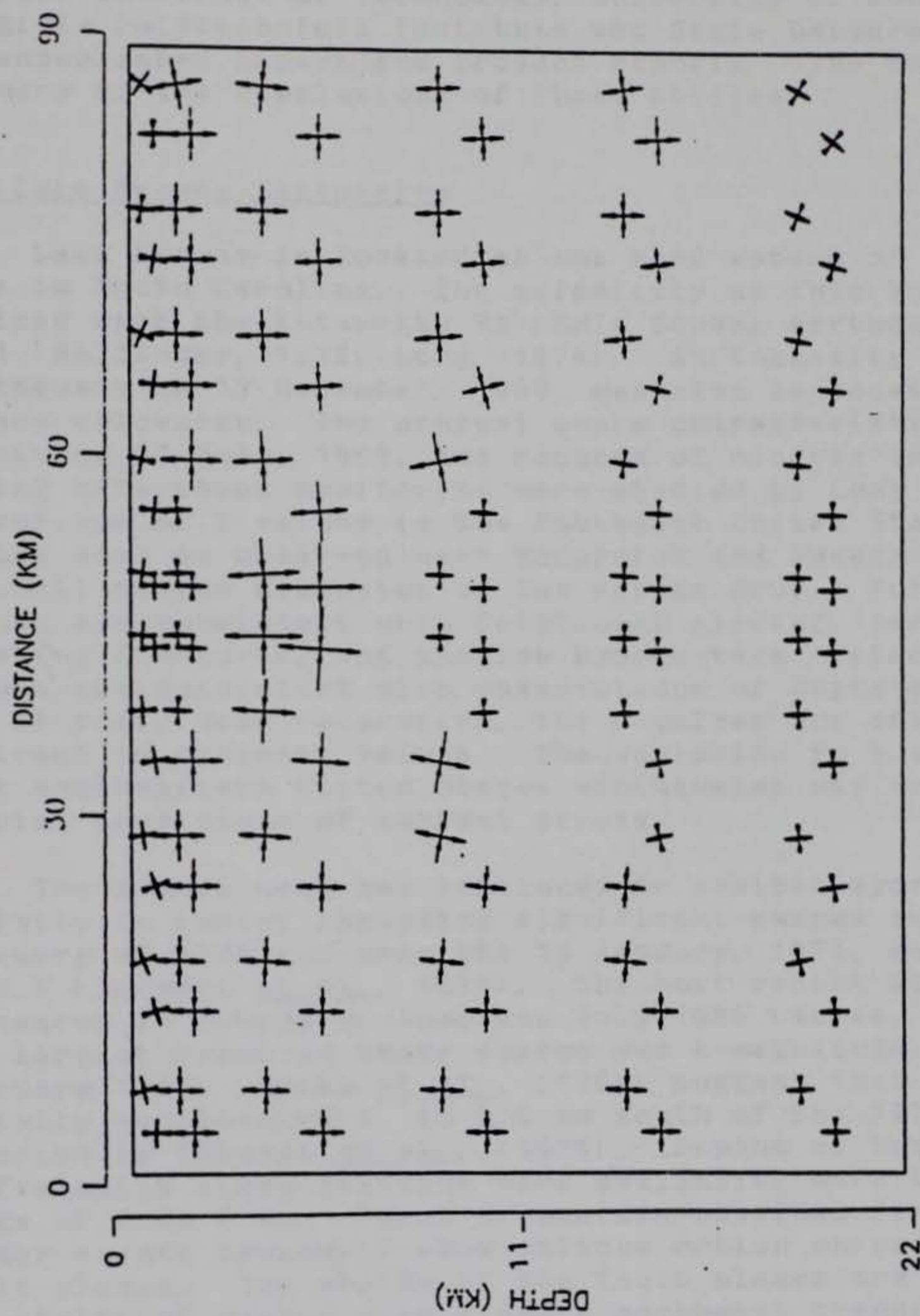


Deviatoric Stress

Figure 11. Two circular zones of weakened crust aligned at 45 degrees to the direction of applied stress.

Figure 12. Geologic model for a vertical profile across a zone of weakness in the crust.





Deviatoric Stress

Figure 13. Stress in a vertical section across a zone of weakness in the crust.

Appendix II. Studies of Piedmont Earthquakes, Aftershocks and Swarms

The studies of Piedmont earthquakes, aftershocks and swarms are extensive. Many of the studies are found in Masters Theses at Georgia Institute of Technology, University of South Carolina and Virginia Polytechnical Institute and State University, as well as in unpublished papers and project reports. The following is a summary of the conclusions of these studies.

The Lake Keowee Seismicity

Lake Keowee is located at the head waters of Hartwell reservoir in South Carolina. The seismicity at this location was first noticed with the intensity VI (MMI) Seneca earthquake of 13 July, 1971 (Bollinger, 1972; Long, 1974). An intensity V (MMI) earthquake on 13 December, 1969, may also be located near the Seneca epicenter. The unusual swarm characteristics of the Seneca events on 13 July, 1971, and records of microearthquakes recorded during aftershock monitoring were studied by Long (1974) in a comparison of b values in the Southeast United States. High b values such as observed near McCormick and Seneca are attributed to small source dimension or low stress drop. Furthermore, high b values are consistent with frictional sliding, perhaps along existing fractures, and shallow hypocenters. Also, the high b values are consistent with observations of Gupta *et al.* (1972 a and b) that, near reservoirs, the b values are often high in contrast to regional values. The variation in b values suggests that southeastern United States earthquakes may originate from varying conditions of ambient stress.

The Seneca area has continued to exhibit sporadic bursts of activity in swarms including significant swarms in January and February of 1978 and near the 19 January, 1979, event of magnitude MD 3.4 (Talwani *et al.*, 1979). The most recent activity consisted of swarms in February, June and July 1986 (Acree, *et al.*, 1988). The largest event in these swarms was a magnitude 3.2 event on 13 February 1986. Acree *et al.*, (1988) suggest that the 1986 activity was located 1. to 2.0 km south of the 1978 activity reported by Talwani *et al.*, (1979). Depths of focus, where sufficiently close stations were available, were typically in the range of 0 to 2 km. Focal mechanisms obtained for some of the larger events typically show oblique motion on nearly vertical fault planes. The strike of the fault planes are consistent with the strike of mapped joints and a northeast trending compressive crustal stress.

The Jocassee Seismicity

The spectra of earthquakes in the Jocassee Reservoir vicinity were studied by Marion and Long (1980), in a comparison with spectra from events in McCormick, S.C., and Maryville, Tennessee. The spectra of the Piedmont events are best modeled by an equidimensional fault which nucleates rupture at a point and has a

rupture velocity approaching the P-wave velocity. The high-frequency content and stress drop of a typical Piedmont micro-earthquake can be explained by brittle fracture of an irregularity or rigid portion of the fault plane. The transonic slip can be explained by pre-existing surfaces with low frictional resistance such as shallow joints. In these areas, the earthquakes occur at depths typically less than 2.0 km. Variations in the high-frequency trends can be explained by variations in the orientation of the fault plane. The most prominent distinction between the Piedmont events and the southeastern Tennessee earthquakes interpreted from spectra is the difference in rupture velocity and the implied non-existence of frictional resistance exceeding 5.357 times the driving shear stress on the fault plane. The frictional resistance is determined by confining pressure as well as the existence of compressional or tensional deviatoric stresses. Therefore, movements on shallow-joint planes with minimal resistance are compatible with the low-stress shallow earthquake mechanisms such as the strike slip and normal mechanisms found in the Jocassee Reservoir area (Fogle et al., 1976; Talwani, 1977) or the normal faulting mechanism found in the Clark Hill Reservoir area (Guinn, 1977; Long et al., 1978).

The Richard B. Russell Seismicity

The Richard B. Russell Lake, directly below Hartwell Reservoir on the Savannah River, was filled in December, 1983. Only about three magnitude less than 1.0 events were detected each year since filling until December, 1987. On December 12, 1987, a M_D 2.3 event occurred close to station LDV (Loudsville, South Carolina) on the Savannah River in the Richard B. Russell Lake. A normal aftershock sequence of 30 detected events occurred during the eight days following the main event. A M_D 2.5 earthquake occurred on December 24, 1987, at 22:46 UT, a M_D 2.0 on January 26, 1988, at 01:46, and a M_D 2.0 on January 27, 1988, at 22:06 UT. The last three $M_D > 2$ events did not exhibit measurable aftershock sequences. Although four years have passed since filling of this reservoir, the activity is typical of reservoir induced sequences. A large portion of the Richard B. Russell Lake is underlain by mafic geologic rocks; however, in the area of the recent activity the geologic units are a granite gneiss. An association of reservoir induced seismicity with granite gneiss has been noted in Clarks Hill, Jocassee, and Monticello reservoirs. A significant factor in the Richard B Russell Lake induced events is the association of the events with mapped faults. The two major events locate on the Loudsville-Towaliga fault zone. The details of this study are given in Appendix III.

The Strom Thurmond Reservoir (McCormick, S. C.) Seismicity

The Strom Thurmond Reservoir area was intermittently monitored prior to the August 2, 1974, earthquake and nearly continuously monitored following the earthquake to the present. The detection threshold for uniform coverage is about 1.5, but during many time periods a threshold of less than 0.0 was possible. Two trends in the rate of activity can be observed.

The first is that following a normal aftershock sequence, the activity decays in an extended aftershock sequence that lasts three to six months. The second is that the spring and summer months usually exhibit greater levels of seismicity, typically following by one month a sharp increase in water level in the spring.

A. Aftershock sequence

Bridges (1975) listed the major aftershocks of the August 2, 1974, earthquake and showed that the activity decayed to significantly less than one magnitude 1.8 event per day within 10 days. A normal decay rate of time to the first power for Omari's law was observed (see figure 6) suggesting that the sequence should have been completed in essentially 10 days. However, late in August and in September two swarms occurred that contained more magnitude 2.0 events than appeared in the aftershock sequence (see Figure 7). This extended or delayed "aftershock" sequence has proven typical of the Clarks Hill Reservoir seismicity, as well as the seismicity in other reservoirs.

B. Seasonal variations

Seismicity in the Strom Thurmond Reservoir area for the years 1978 through 1980 show two swarms initiating in the spring and extending through the summer. Both swarms followed by about one month a rise in the water level. A general observation of the rate of this seismicity is that there may be a tendency to increase the activity level in the spring and summer; however, these were the only two years with an apparent triggering by a change in water level.

The spectra of the Strom Thurmond Reservoir microearthquakes (also known as the Clark(s) Hill or McCormick, S. C., seismicity) were studied by Marion and Long, (1980), and compared with events from the Jocassee Reservoir area. The spectral properties of these microearthquakes were identical to those of the Jocassee microearthquakes described with the Jocassee seismicity. The hypocentral depths, which are in the 0 to 1.2 km range, were discussed under depths of focus above. Studies on the stress conditions and association of rock quality and type with induced seismicity are discussed in Appendix IV.

The Monticello Reservoir Seismicity

The induced seismicity of the Monticello Reservoir has been extensively studied. An insitu study of the physical mechanisms controlling induced seismicity (Zoback and Hickman, 1982) suggested that the earthquakes were caused by an increase in pore pressure large enough to trigger reverse-type fault motion on pre-existing fault planes. The activity occurs in a zone of relatively large shear stresses at a depth of less than 300 meters. Zoback and Hickman speculate that the increase in pore pressure reduces the normal stress on the fault, and Fletcher (1982) states that fault friction then causes the sudden failure. the pore

pressure also allows larger displacements and a lower final stress than where the effective stress is high. Zoback and Hickman's (1982) model of the seismicity at Monticello suggests that future earthquakes will occur infrequently and will be a result of eventual pore fluid diffusion into isolated zones of low permeability. In addition, they state that these earthquakes are expected to be limited in magnitude by the small dimensions of the seismogenic zones. Stress drops for the Monticello Reservoir earthquakes ranged from 0.2 to 4.0 bars (Fletcher, 1982) for events in the 0 to 1.0 Magnitude range. Four events of Magnitude 2.8 to 3.0 showed stress drops of 13 to 92 bars. These are consistent with shear stresses measured by Zoback and Hickman (1982) at depths of 0.2 to 1.0 km in a drill site north of the reservoir.

The Central Georgia Seismicity

The seismicity of central Georgia is contained within a circle of radius 75 km, centered on Milledgeville, Georgia, and includes Lake Sinclair and Lake Oconee. The seismicity is moderate and includes historic events as large as 4.9 m_{bLg} . The larger historical earthquakes are documented by Allison (1980). Central Georgia continues to experience sporadic activity. Lake Sinclair was impounded in the 1950's, and a Magnitude 4.0 event occurred in 1964. Since that time, the vicinity of the reservoir has shown a steady rate of seismicity, typically occurring in swarms of a few weeks to months in duration (See figure 9 for earthquake occurrences versus time). A reasonable measure of the activity has required local monitoring, since the larger events in many of the swarms are about magnitude 2.0 and the threshold for detection by station ATL (WSSN) was also about 2.0 for the Lake Sinclair area. The continued seismicity along with near-by reservoir induced seismicity raised the possibility that the Lake Sinclair seismicity is reservoir induced and increased concern that the new reservoir, Lake Oconee, would induce significant activity. Because of this concern, the seismicity was closely monitored during the impoundment of Lake Oconee by Wallace Dam in 1977.

The impoundment of Lake Oconee by Wallace Dam was followed by only a few small events and significant reservoir induced seismicity was not triggered. A post-filling swarm with M_D between -0.3 and 0.8 that occurred in May, 1980, showed little variation in magnitude and did not precede a M_D 1.5 or larger event as in the usual case of earthquake swarms near Lake Sinclair. The events in the Lake Oconee swarm occurred in a very tight cluster on an lineament marking the location of a fault zone.

The majority of the seismicity in central Georgia occurs in the Lake Sinclair area. The spatial distribution of the epicenters with respect to Lake Sinclair and the characteristics of the swarms suggests possible reservoir induced seismicity. A study of the high-frequency decay of displacement spectra, however, suggested a natural cause for the Lake Sinclair events (Johnston, 1980).

The epicenters of Lake Sinclair events occur in clusters

APPENDIX III

Preliminary Report on the Seismicity at the Richard B. Russell Reservoir

by Lisa Hillhouse⁺ and L.T. Long

School of Geophysical Sciences
Georgia Institute of Technology
Atlanta, Georgia 30332

ABSTRACT: On December 12, 1987, at 03:53 UTC (10:53 p.m. EST, December 11, 1987, local time), an earthquake of magnitude 2.3 was felt in Elbert and Hart Counties, Georgia. This and subsequent events marked the first significant reservoir-induced seismicity at the Richard B. Russell Lake. Earthquakes were recorded from December, 1987, to February, 1988. Three of the 33 events were felt. Before impoundment in December, 1983 no natural seismic activity had been observed. Between December, 1983, and December, 1987, 21 earthquakes of magnitude less than one were identified.

Prepared July, 1988.

Acknowledgments. The seismic net in the Richard B. Russell Reservoir area was installed by Georgia Tech for the U.S. Army Corps of Engineers, Savannah District. The support for maintenance of the net was provided by the Savannah District, U.S. Army Corps of Engineers from 1979 through 1985 under Contract DACW21-83-C-0014. After 1985, the net was combined with the Clarks Hill seismic monitoring stations and supported by the Nuclear Regulatory Commission under Contract NRC-04-85-122. Support to study data from the Richard B. Russell seismic net was provided by the U.S. Geological Survey under Contract 14-08-0001-21241 during the initial impoundment period.

⁺ Now at the University of Washington, Seattle, Washington.

Introduction

The Richard B. Russell Lake lies in an area of the Georgia and South Carolina Piedmont which is underlain by complex units of mafic rocks, granite gneiss, and mica schist. The lake now covers a 130 km² area of this region of highly deformed and metamorphosed rocks. The Richard B. Russell Lake had been conspicuous in the Southern Piedmont in its lack of seismic activity immediately after impoundment. Several other man-made lakes covering similar geologic terrain in the Southern Piedmont, such as the Clarks Hill Reservoir, Lake Oconee, Lake Jocassee, Lake Sinclair, and Monticello Reservoir, all experienced reservoir-induced seismicity.

Only isolated small events were detected in the four years between filling in December, 1983, and the December, 1987, swarm (Figure 1). These suspected natural events occurred on the average of three per year, although during the period of January to April, 1986, six events were recorded. The rate of activity (Figure 1) increased over the past four years, with the exception of the quiet period from July, 1986, to July, 1987.

The Seismic Network

During the December 1987 swarm, the Richard B. Russell Seismic Network consisted of three vertical-component, short-period seismic systems (see Figure 2 for locations). The stations operating during December, 1987, were: BEV, near the former town of Beverly, Georgia; LDV, 8 km south-southeast of Lowndesville, South Carolina; CHF, located south of Calhoun Falls, Georgia; and

THE SEISMICITY OF RICHARD B. RUSSELL RESERVOIR 1 DEC 87 - 31 JAN 88

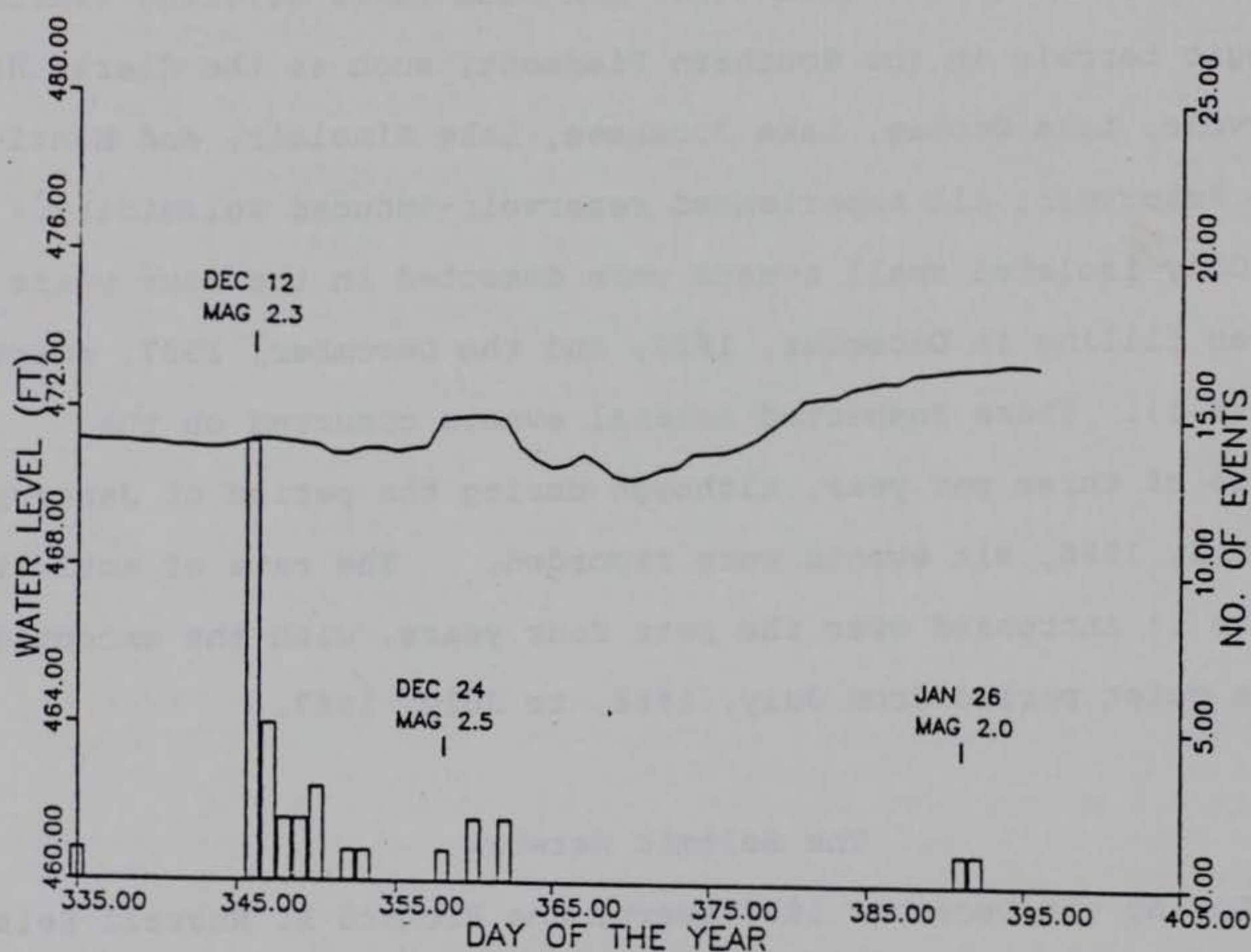


Figure 1. A comparison of water level changes with magnitude and occurrence time of earthquakes in the vicinity of Lake Richard B. Russell.

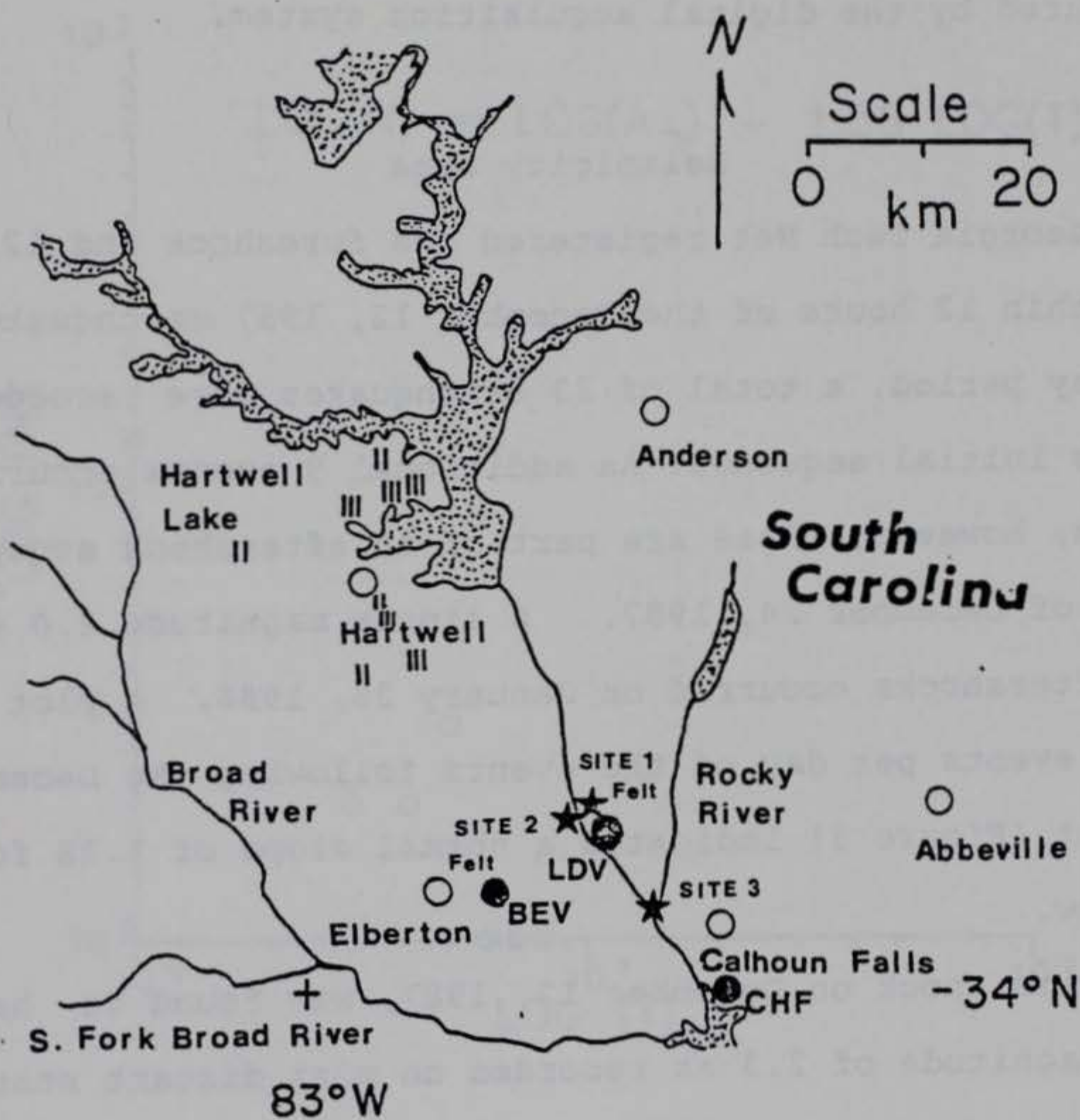


Figure 2. Location of seismic stations, epicenters of located events and the distribution of Modified Mercalli intensities.

CH6 in the Clarks Hill Reservoir area. The stations were installed in 1980 by Georgia Tech with the support of the Army Corps of Engineers. The seismic data have been continuously recorded with ink pen on paper helical records and intermittently as digital data with LDV serving as a trigger station. Nine events were captured by the digital acquisition system.

Seismicity Data

The Georgia Tech Net registered one foreshock and 12 aftershocks within 12 hours of the December 12, 1987 earthquake. Within an 8 day period, a total of 23 earthquakes were recorded (Table I) in this initial sequence. An additional 9 events occurred within 3 weeks; however, these are part of an aftershock sequence for the event of December 24, 1987. A single magnitude 2.0 event without aftershocks occurred on January 26, 1988. A plot of the number of events per day of the events following the December 12, 1987, event (Figure 3) indicates a normal slope of 1.38 for Omari's law.

The main shock on December 12, 1987, was found to have a duration magnitude of 2.3 as recorded on most distant stations in the Georgia Tech Network (see Table II for durations at all stations). The duration magnitude at station LDV (Table I) is significantly smaller than the duration magnitude of 3.1 determined at distant stations. In general, durations at more distant stations were interpreted to be significantly longer than those of the Georgia Tech net. The explanation for the discrepancy lies in the occurrence of an aftershock immediately following the earth-

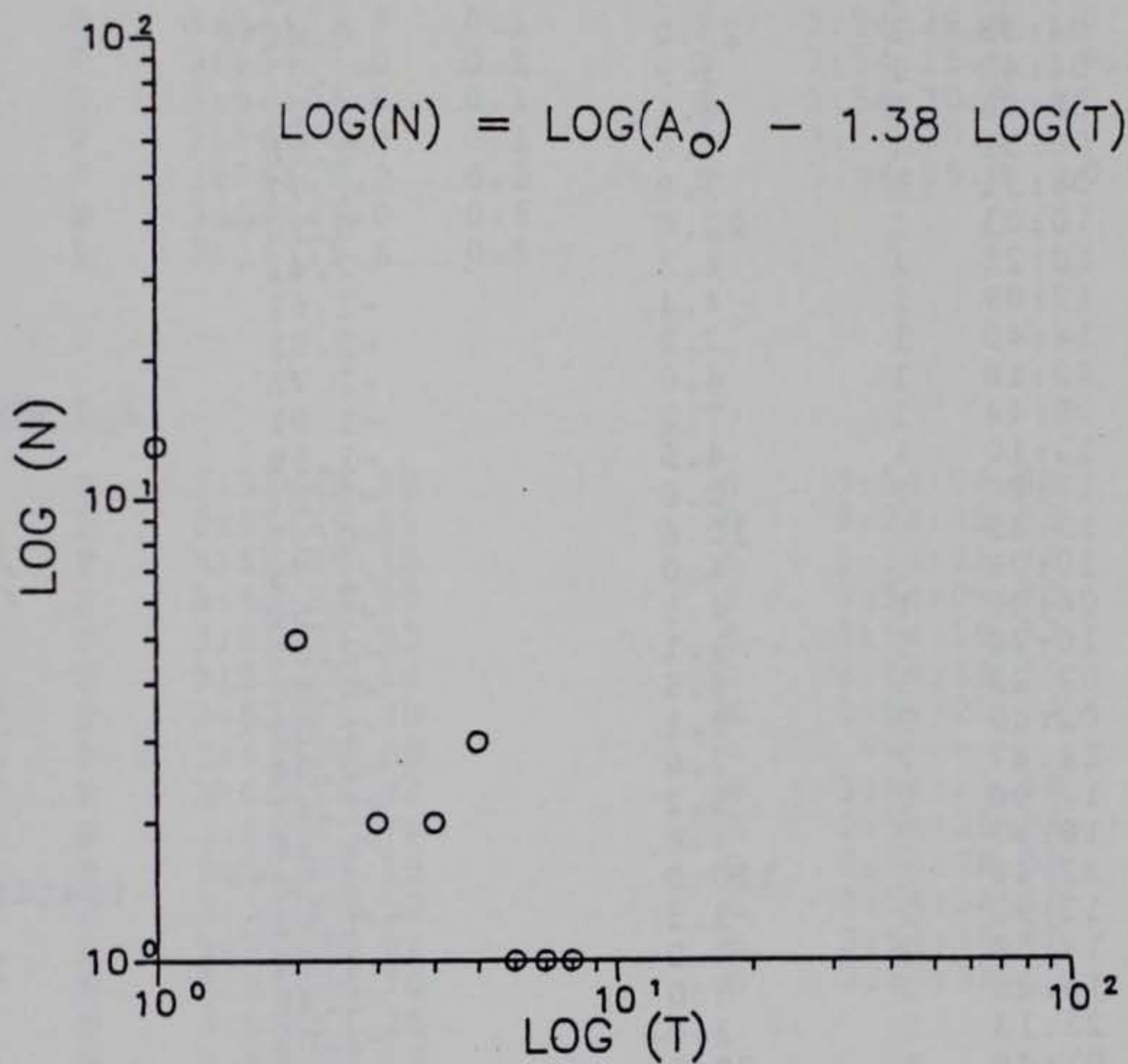


Figure 3. Decay rate of aftershock sequence (number of events per day).

TABLE 1. Earthquakes Recorded at Seismic Station LDV.

<u>MO:DAY</u>	<u>TIME</u> (UTC)	<u>TYPE</u> LDV	<u>DURATION</u> (SECONDS)	<u>MAGNITUDE</u> (DURATION)*	<u>AMPLITUDE</u> ⁺ (mm)
12:12	03:29	1	4.3	-1.64	5.7
	03:53	1	166.0	2.30**	(saturated)
	03:54	1	34.0	0.30**	39.2
	03:56	1	4.0	-1.73	7.0
	04:16	1	7.5	-0.96	10.7
	04:38	1	23.0	0.40**	43.0
	04:42	1	3.9	-1.77	4.8
	08:08	1	6.1	-1.21	10.0
	08:31	1	3.6	-1.86	6.2
	08:31	1	3.9	-1.77	7.2
	10:03	1	22.0	0.30**	38.8
	10:29	1	2.3	-2.42	2.5
	12:09	1	4.4	-1.62	5.9
	14:40	1	3.2	-2.01	4.0
12:13	00:18	1	4.0	-1.73	6.6
	08:44	1	7.2	-1.01	13.2
	13:10	1	4.5	-1.59	7.6
	13:26	1	2.6	-2.27	5.6
	13:39	1	10.6	-0.53	25.5
12:14	10:21	1	4.0	-1.75	6.5
12:15	06:31	1	4.5	-1.59	6.8
	16:26	1	3.1	-2.05	6.6
12:16	02:23	3	8.5	-0.80	10.2
	02:49	3	7.1	-1.02	4.0
	14:47	2	7.6	-0.94	12.8
12:18	17:04	2	5.2	-1.41	4.9
12:19	16:37	2	4.6	-1.56	6.5
12:24	22:46	2	110.0	2.50**	(saturated)
12:26	12:32	2	3.5	-1.90	4.5
	14:58	2	7.0	-1.04	17.0
12:28	18:25	2	5.0	-1.46	4.7
	23:13	2	3.0	-2.09	2.0
1:26	01:46	1	70.0	2.00**	***
1:27	22:06	2	50.0	1.39	36.8
3:06	17:10	3	10.0	-0.60	4.5

Type	S-P at LDV	Longitude	Latitude	error(km)
1	0.43 s	82° 42.0'	34° 9.7'	±1
2	0.55 s	82° 42.6'	34° 9.6'	±2
3	0.95 s	82° 38.6'	34° 5.0'	±1

- * $M_D = -3.45 + 2.85 \log_{10}(D)$
D = duration in seconds of signal above background noise level
- + Recorded at station LDV, saturation level is 53 mm.
- ** Determined using LDV and at least 2 additional stations.
- *** Could not be determined from record.

TABLE 2. Arrival Times and Location Parameter of December 12, 1987 Earthquake.

Station	Phase	Time	Error	Phase	Time	Error	Duration
DCT	P	3:53:58.9	0.1	S	3:54:23.7	0.2	170.
CDG	P	3:53:59.0	0.1	S	3:54:31.4	0.2	130.
RHT	P	3:54:04.9	0.1	S	3:54:31.2	0.2	140.
ETG	P	3:53:47.2	0.1	S	3:54:02.1	0.2	200.
OCA(Z)	P	3:54:22.8	0.5	S	3:55:03.5	0.5	120.
CBT	P	3:54:03.9	0.1	S	3:54:29.8	0.2	110.
ATL	P	3:53:57.0	0.1	S	3:54:16.1	0.2	170.
RCT	P	3:54:04.8	0.1	S	3:54:30.9	0.2	200.
DALG	P	3:54:04.4	0.1	S	3:54:30.3	0.2	100.
TDA	P	3:54:18.2	0.2	S	3:54:55.9	0.5	140.
BKA	p	3:54:47.0	0.5				140.
TSA	P	3:54:35.6	0.5				160.

Magnitude 3.1

BBG	P	3:53:49.32	S	3:54:04.48	265.
TRYN	P	3:53:49.62	S	3:54:05.22	262.
RBNC	P	3:53:50.38	S	3:54:05.74	239.
WSSR	P	3:53:52.70	S	3:54:09.80	
BRBC	P	3:53:57.52	S	3:54:18.32	
BENN	P	3:53:58.14	S	3:54:19.58	
TKL	P	3:53:59.40	S	3:54:20.74	244.
RICH	P	3:53:59.98		-----	
GMG	P	3:53:59.92	S	3:54:23.38	
ETT	P	3:54:01.76	S	3:54:25.26	278.
GBTN	P	3:54:03.18	S	3:54:28.58	271.
SMTN	P	3:54:08.30	S	3:54:38.18	
PKNC	P	3:54:08.64	S	3:54:36.08	
RCG	P	3:54:09.70	S	3:54:38.82	
BHT	P	3:54:12.36			
CCVA	P	3:54:12.02			

quake, which may have caused the tail of the coda to appear excessively long. Because the Georgia Tech station LDV is located only 3.3 km from the epicenter and because the influence of the aftershock could be minimized, the duration magnitude of 2.3 was estimated from only the three closest stations.

The three largest aftershocks of the December 12, 1987, earthquake were approximately equal in magnitude, about 0.3. Out of the nine events following this aftershock sequence, two additional magnitude 2.0 earthquakes were recorded. The first was a duration magnitude 2.5 earthquake on December 24, 1987, at 22:46, and the second was a duration magnitude 2.0 earthquake on January 26, 1988, at 01:46. The first had 4 aftershocks and the second had none.

Intensity Data

The maximum Modified Mercalli intensity of the December 12, 1987, earthquake was estimated to be III. Because of the distance between the earthquake and the city of Hartwell, the small magnitude and the limited sampling of felt reports, a contour of intensities was not possible. Also, the epicentral zone is sparsely populated. Most of the intensity reports came from a questionnaire in the Hartwell Sun published one week after the mainshock. The event was reported felt in Elberton and Lowndesville, but there were too few reports to assign an intensity. The observed intensities are shown in Figure 2 and suggest a general north-south trend and approximate area of 1500 square kilometers. Data are not available for the second two magnitude 2.0 events.

Location of Events

The 33 events that occurred in the Richard B. Russell area in December, 1987, and January, 1988, were separated into three types based on distance from LDV and character of the trace. Accurate locations of these three types were possible by use of S-P times from digitally recorded events. The S-P times and locations are given in Table I. Although sufficient data were available from regional seismic stations to locate the three magnitude >2.0 earthquakes, travel times to regional distances are not sufficiently uniform to allow a location to better than 10 km. The locations from the stations within 35 km were found using a local velocity model based on travel times from quarry blasts. The P-wave velocity is 6.05 km/s and the S-wave velocity is 3.54 km/s (Propes, 1986) for the Richard B. Russell region of the Charlotte and Carolina Slate belt of the Piedmont Province. In addition, a local velocity of 6.15 was used for arrivals at station LDV to compensate for the mafic rocks under that station. The epicenters were computed with an assumed focal depth of 1 km, based on similar shallow focal depth for the reservoir induced events in the Piedmont. This assumption is further supported by the character of the waveform of these events, in which the surface waves dominate, and are of high amplitude (see Figure 4 for examples). The locations are shown in Figure 2. Event type 1 and 2 are close together and about 4 km northwest of station LDV. Event type 3 is located about 8 km southeast of station LDV. Both locations are under the main channel of the impounded Savannah River. The locations for event types 1 and 2 are within 2 km of each other

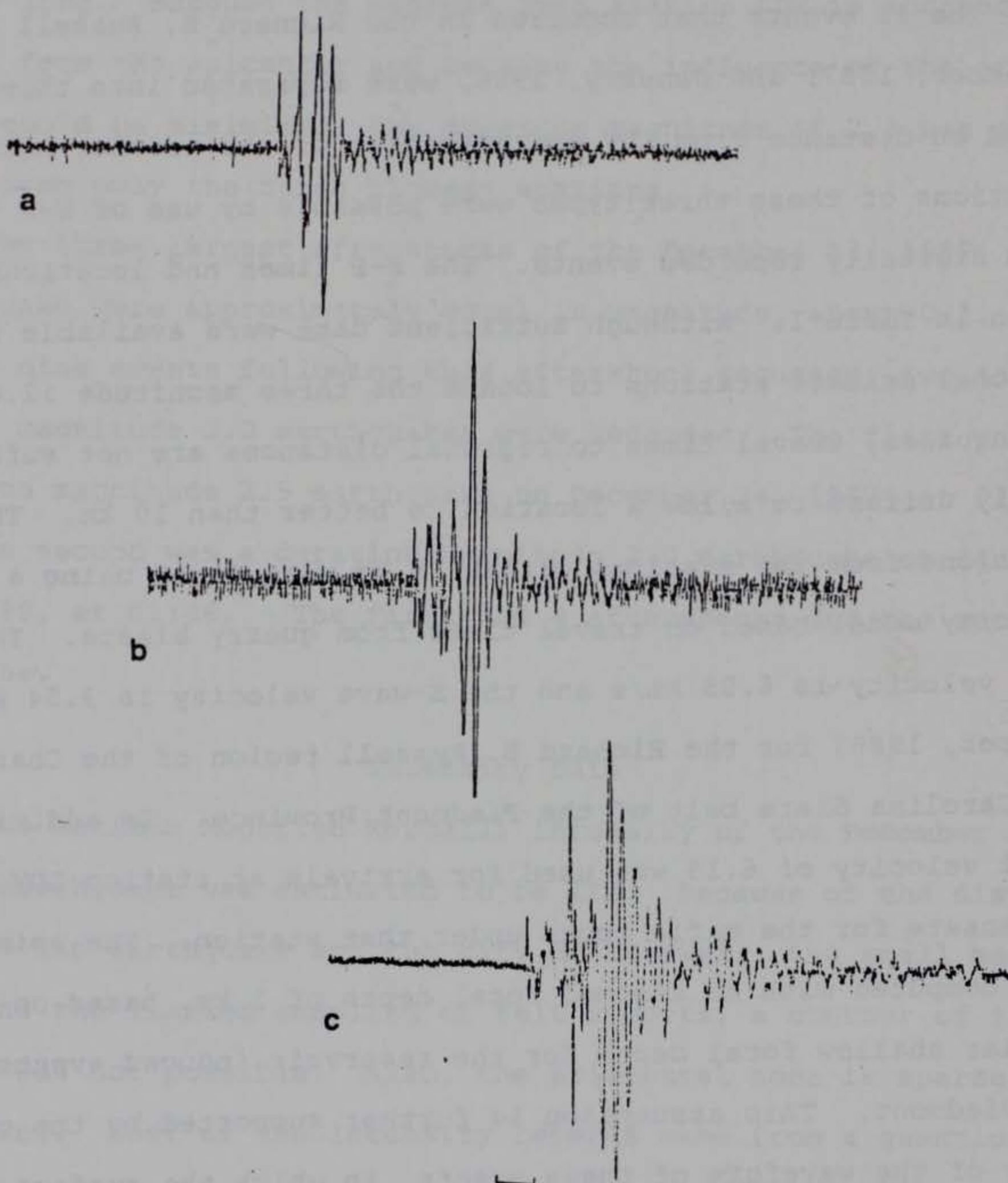


Figure 4. Digital records of the three types of earthquakes. a) Type one aftershock on December 13, 1987. b) Type two aftershock at 18:26 on December 28, 1987. c) type three event at 02:23 on December 16, 1987.

and may be contiguous. The locations for event types 1 and 2 are on the northern edge of the higher velocity amphibolite schist under station LDV and event type 3 is on its southern edge.

Recursion Relations and b-Value

The cumulative number of events N_C greater than a given magnitude M_D may be expressed by the traditional Gutenberg-Richter recursion relation, in which the seismicity rate "a" and slope "b" may be found from a plot of $\log N_C$ versus M_D . However, the b value implied by the duration magnitude is anomalously low, suggesting that the M_D values are inappropriate at magnitudes below 2.0. Earthquakes of duration less than 20 seconds exhibit locally unique variations in the characteristics of the waveform.

Typically, the amplitude increases at a slower rate than the duration at these low magnitudes, as compared to events of more than 20 seconds duration (Johnson, 1984). Instead, b values were calculated from the relative amplitudes of the traces. A more precise amplitude reading was possible when measuring the maximum deflection of the S-wave amplitude. The graph of the cumulative number of events of amplitude A and greater, N_C , versus amplitude, A, (Figure 5) resulted in:

$$\log (N_C) = 2.28 - 0.82 \log (A)$$

Since LDV was down 40 percent of the eight day period and was often noisy when operating, many small events may have been missed or obscured by noise on the records. Because the small magnitudes may have been under reported, the b-value calculated could be smaller than the true value for this swarm.

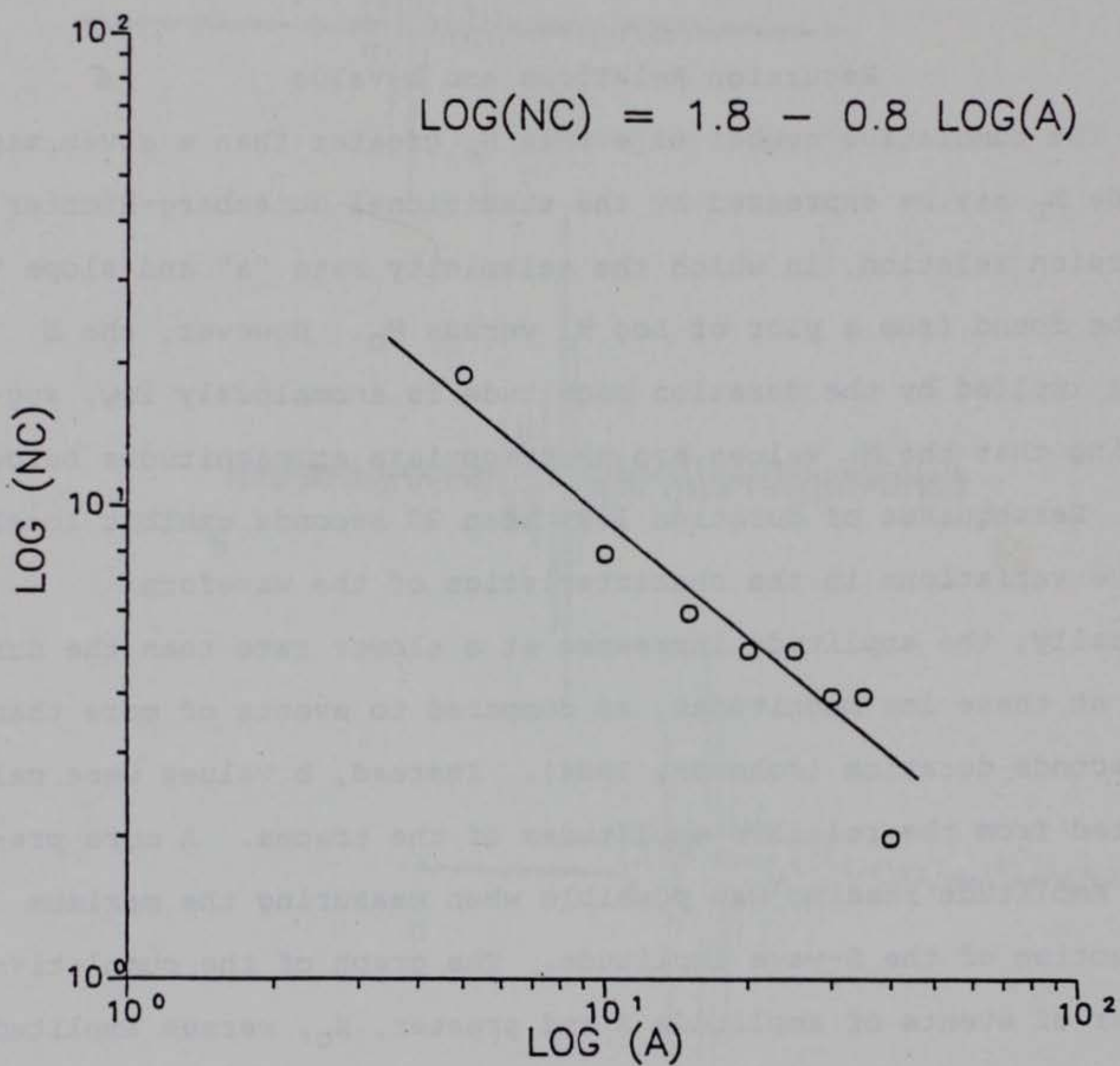
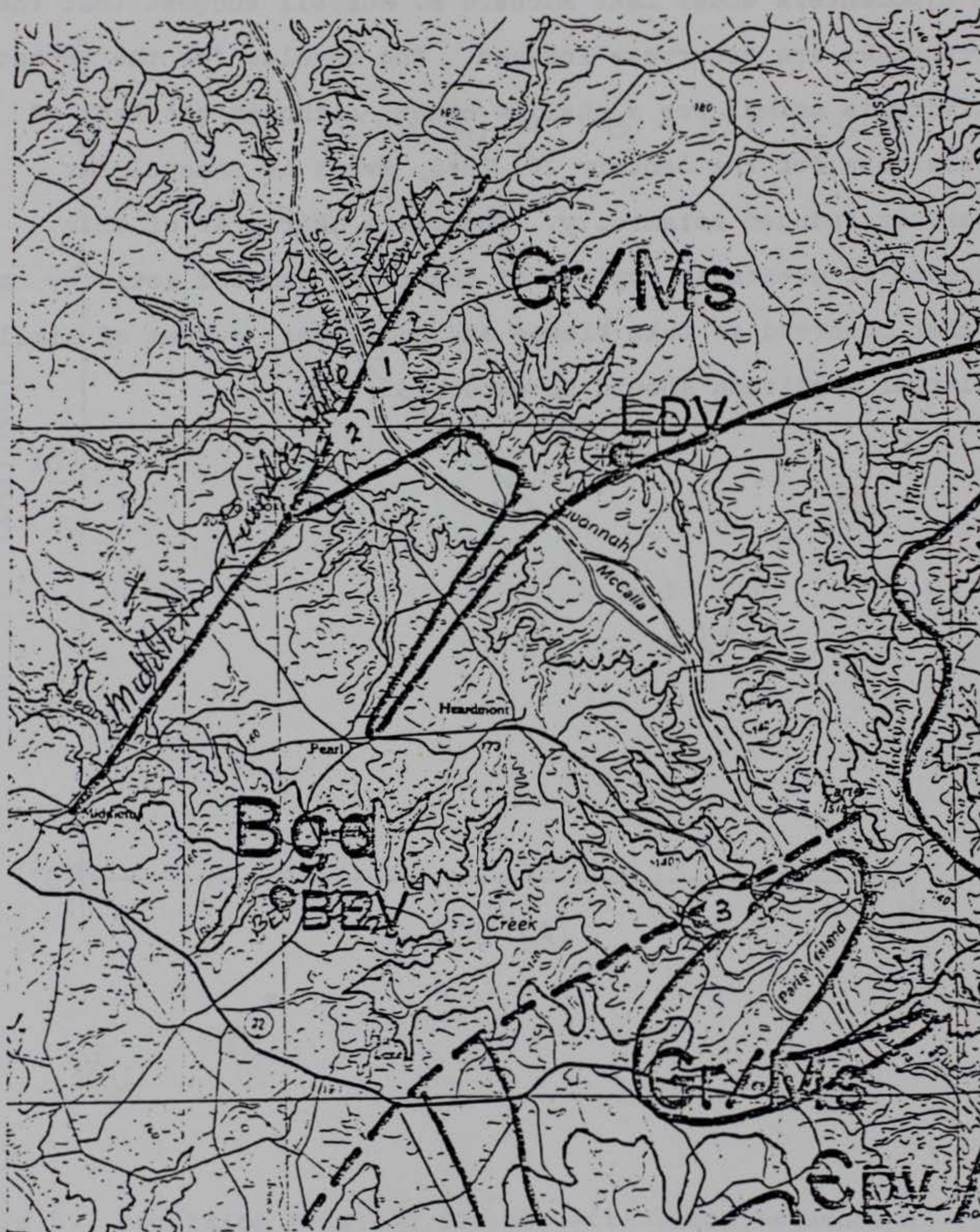


Figure 5. Recursion relation for the aftershock sequence of type 1 events.

Conclusion

The history of induced seismicity at nearby reservoirs and the hypocenters under Lake Richard B. Russell suggest that these earthquakes are reservoir induced. The b-value for the recent activity is normal for a shallow event, although the lack of aftershocks for the January 26, 1988, event is unusual for reservoir induced seismicity. The swarm character of this sequence of events is typical of reservoir induced activity, such as that observed at Lake Kiowee and additional swarms of similar or larger magnitude should be expected.



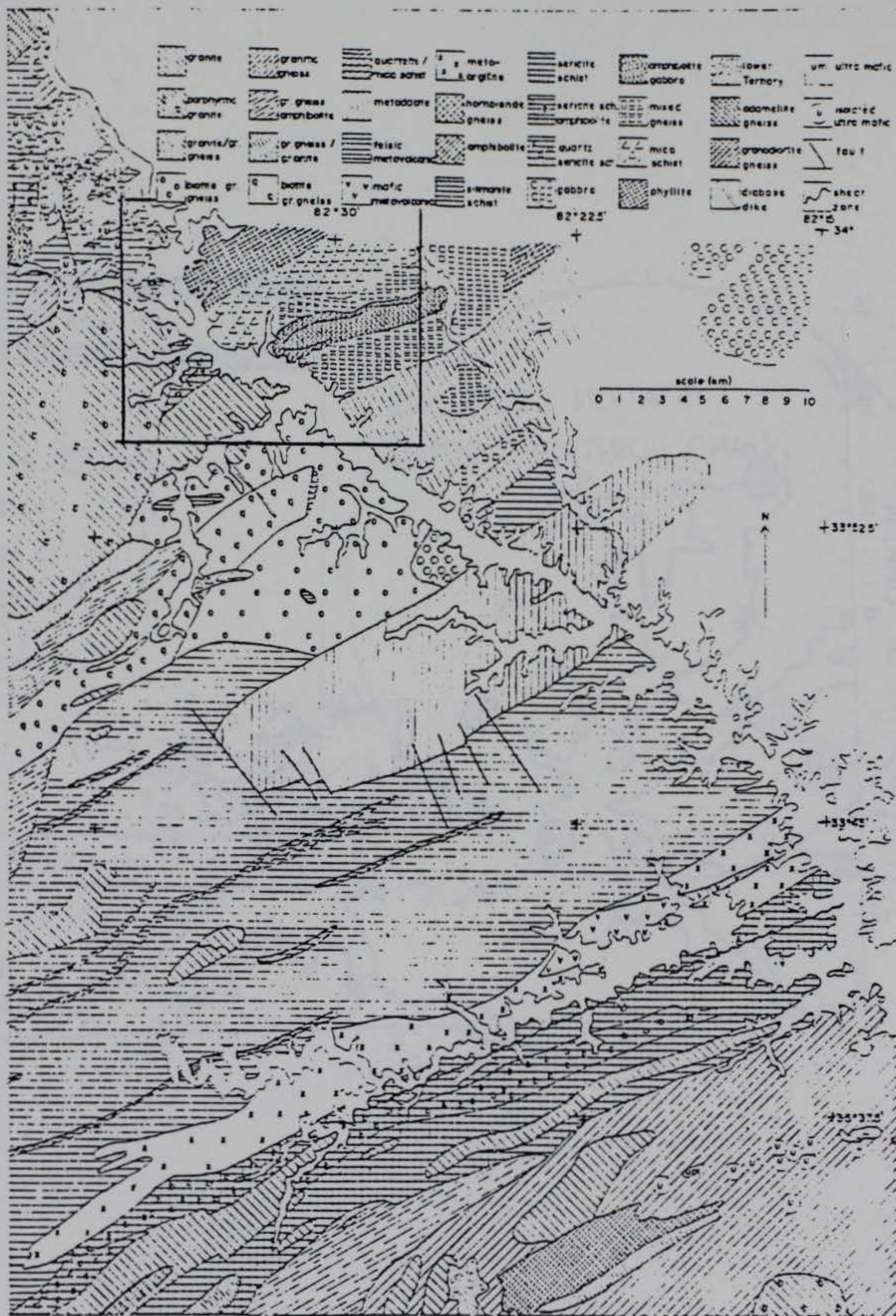


Figure 1. Location map for area of joint measurements in the Clarks Hill Reservoir. Geology abstracted from Griffin (1973) Geologic Map of Georgia, Georgia Geological Survey, 1976.

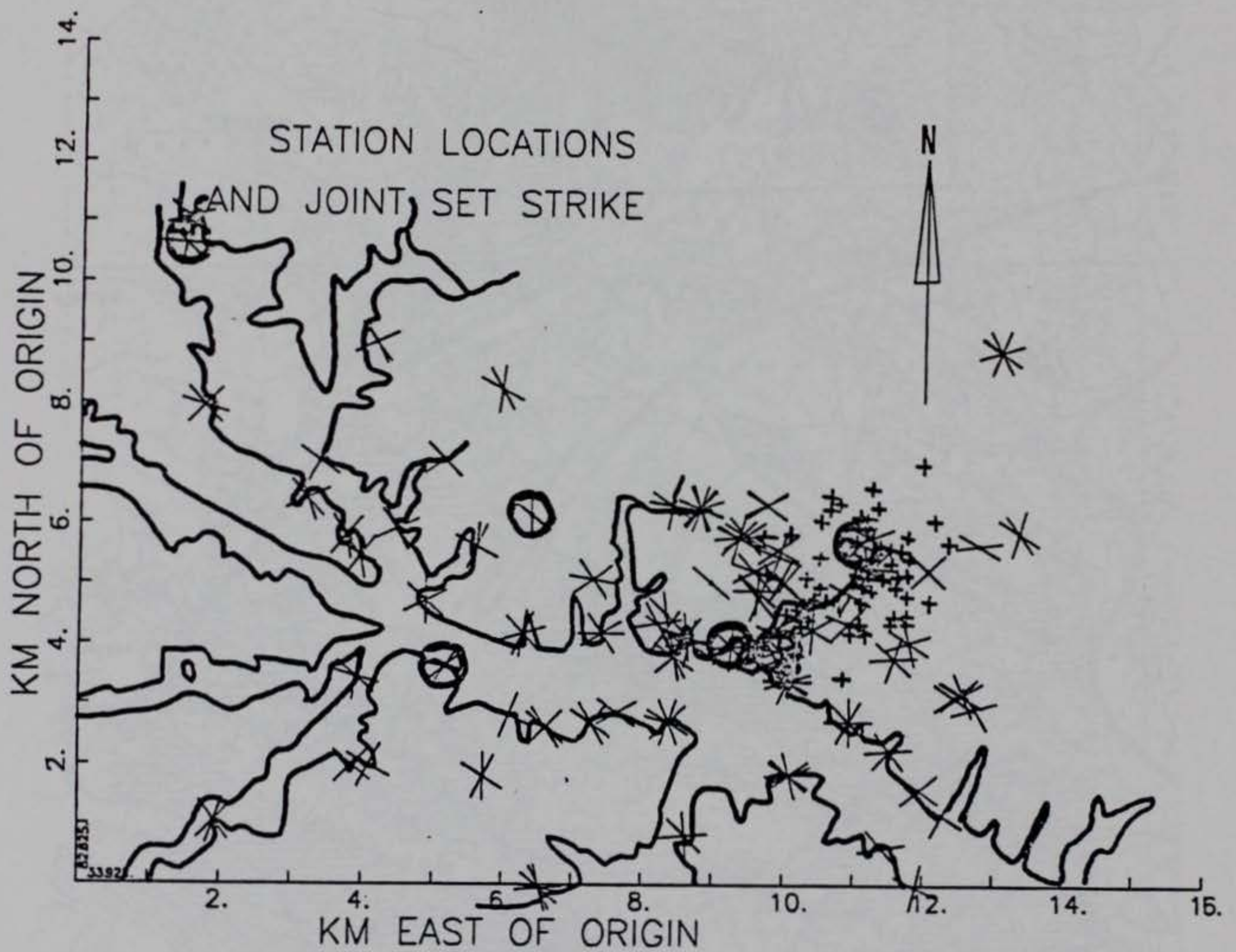


Figure 2. Outline of the study area showing station locations and joint directions. Small crosses are the epicenters of earthquakes from Dunbar (1977). Origin is 33.925 N, 82.625 W.

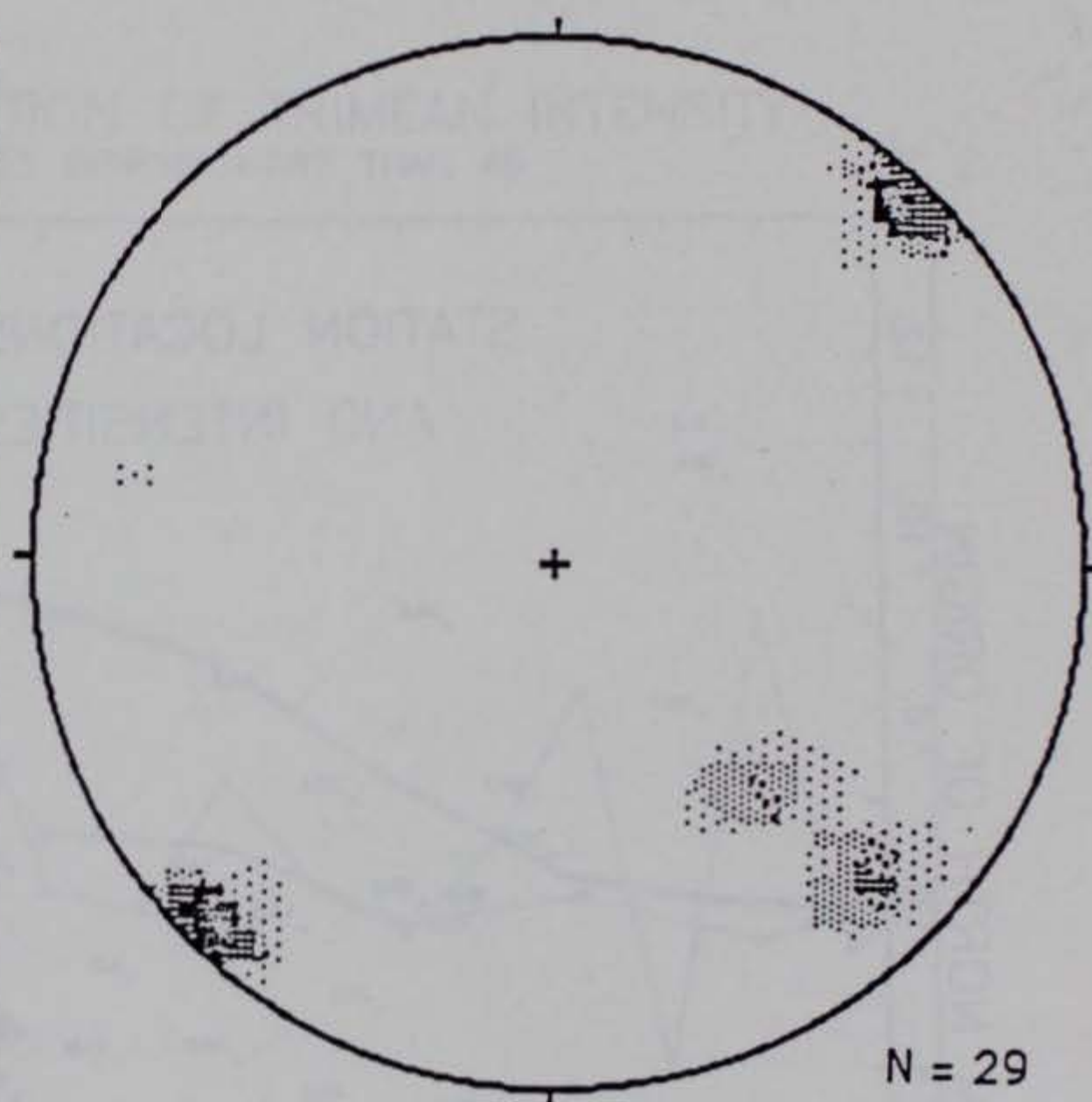
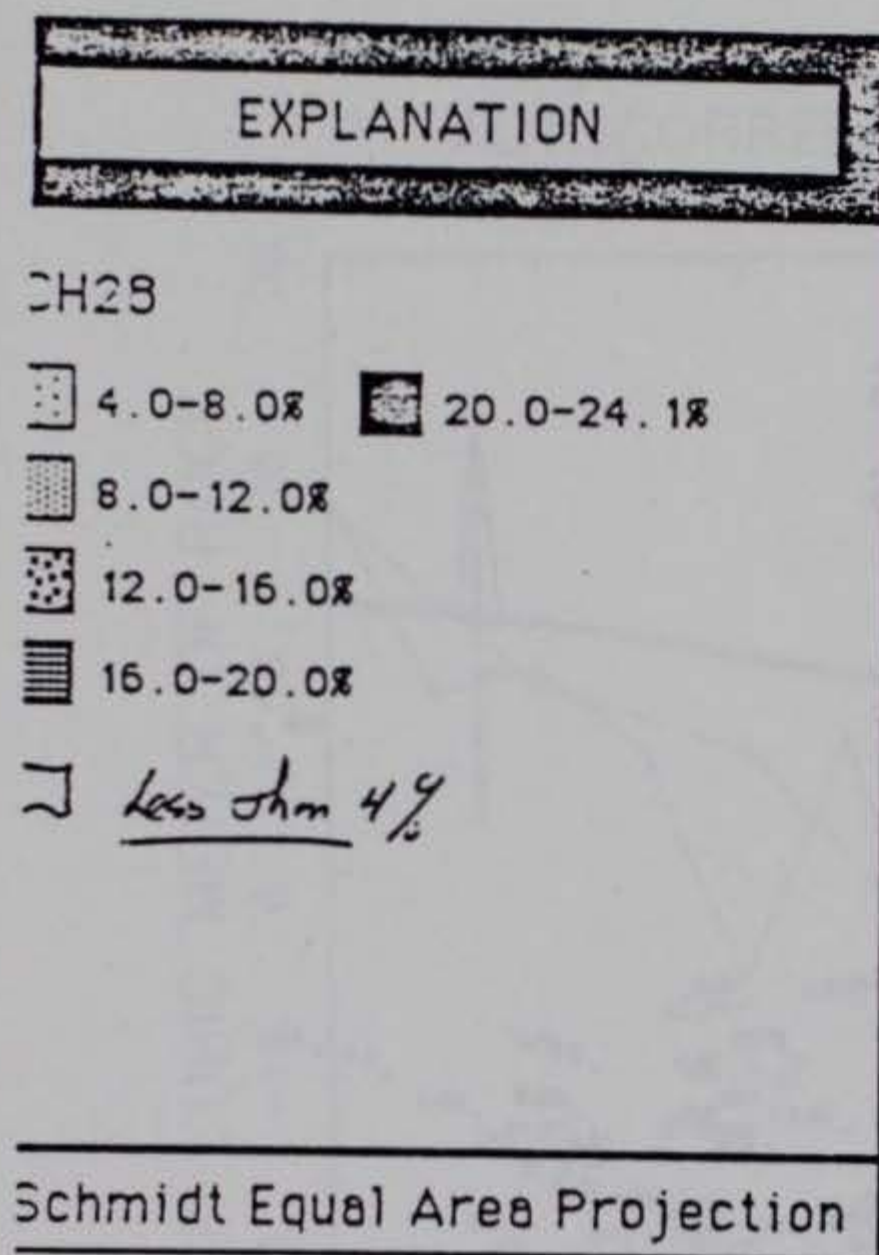


Figure 3. Joint pole plot for station ch28 showing dominant joint set for the Clarks Hill Reservoir

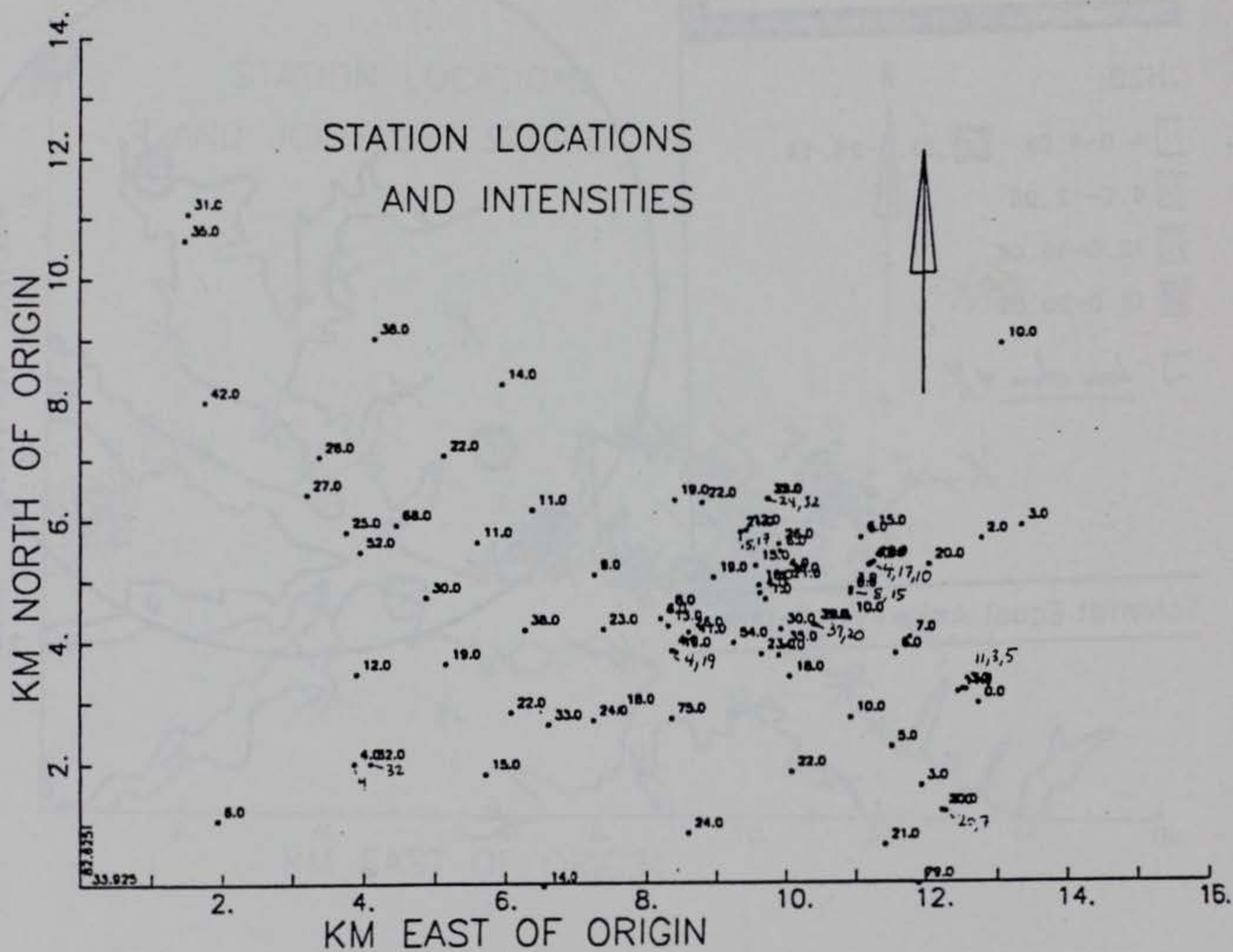


Figure 4. Average fracture intensity plot of observation points

AUTOCORRELATION OF TRIMEAN INTENSITY SETS DIPPING MORE THAN 45

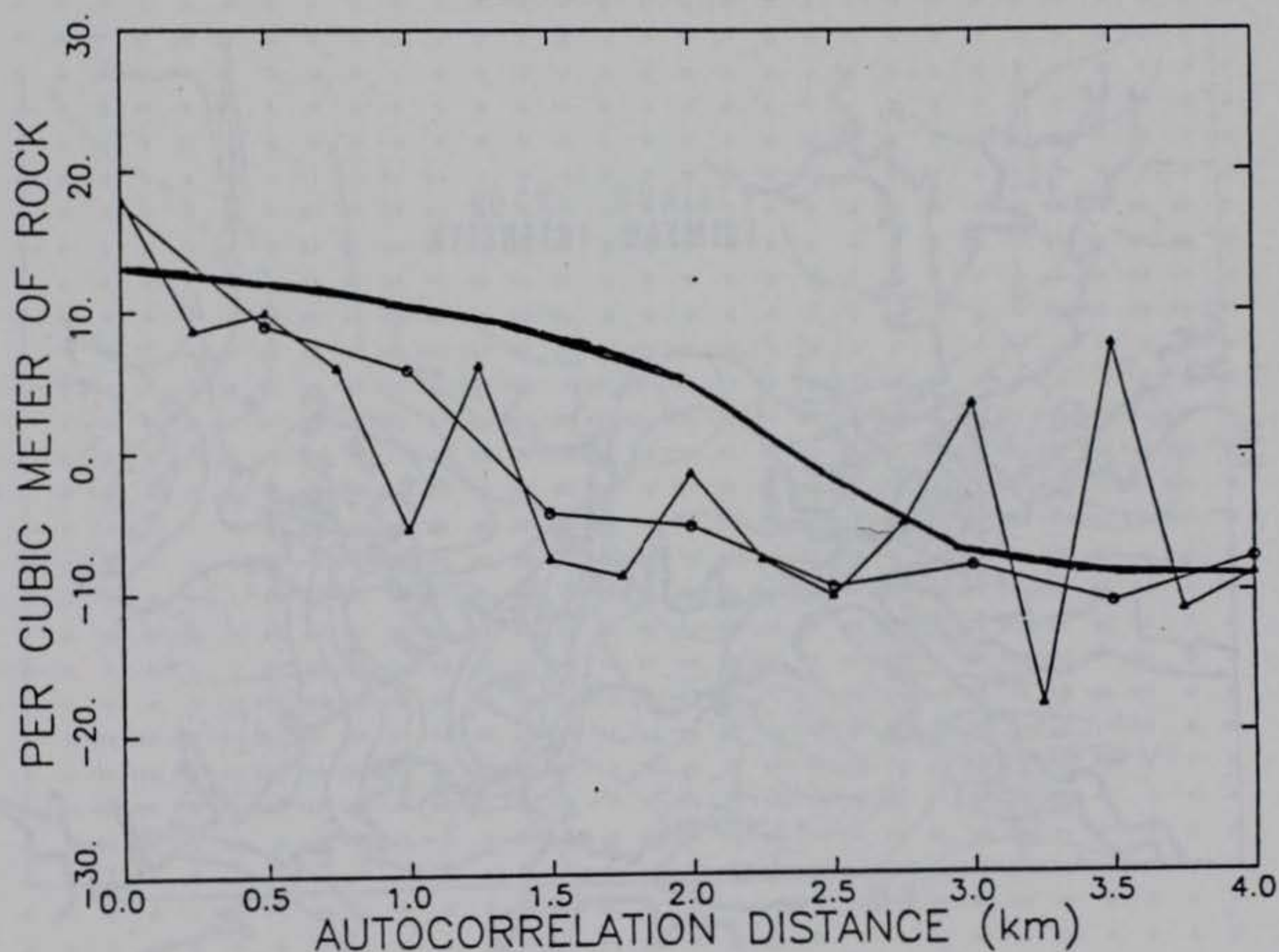


Figure 5. Autocorrelation of the trimean intensity data at separation distances of 0.5 and 0.25 km. Heavy line is autocorrelation function for the gridded data.

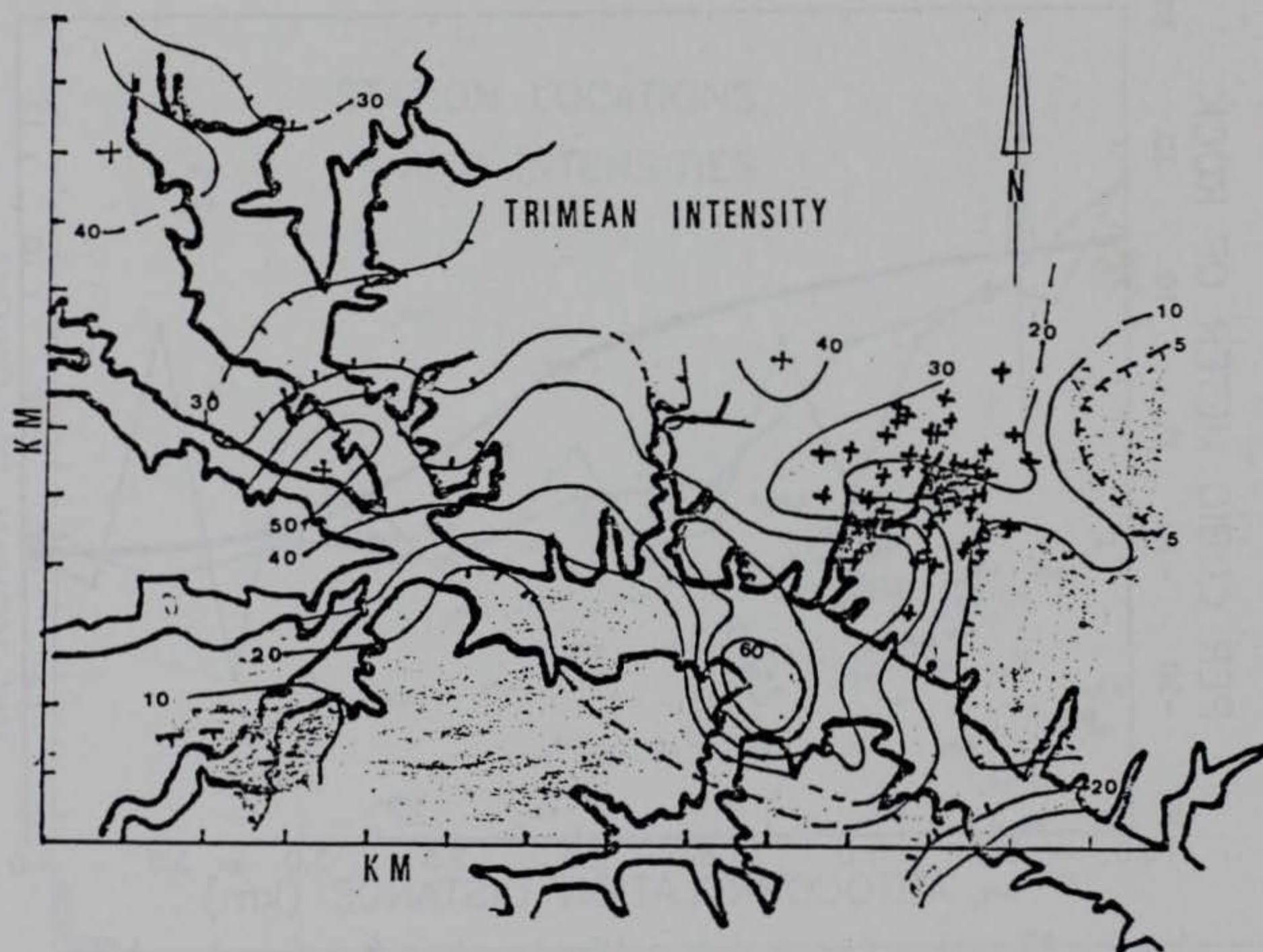


Figure 6. Contoured map of the trimean fracture intensity. The crosses indicate locations of epicenters.

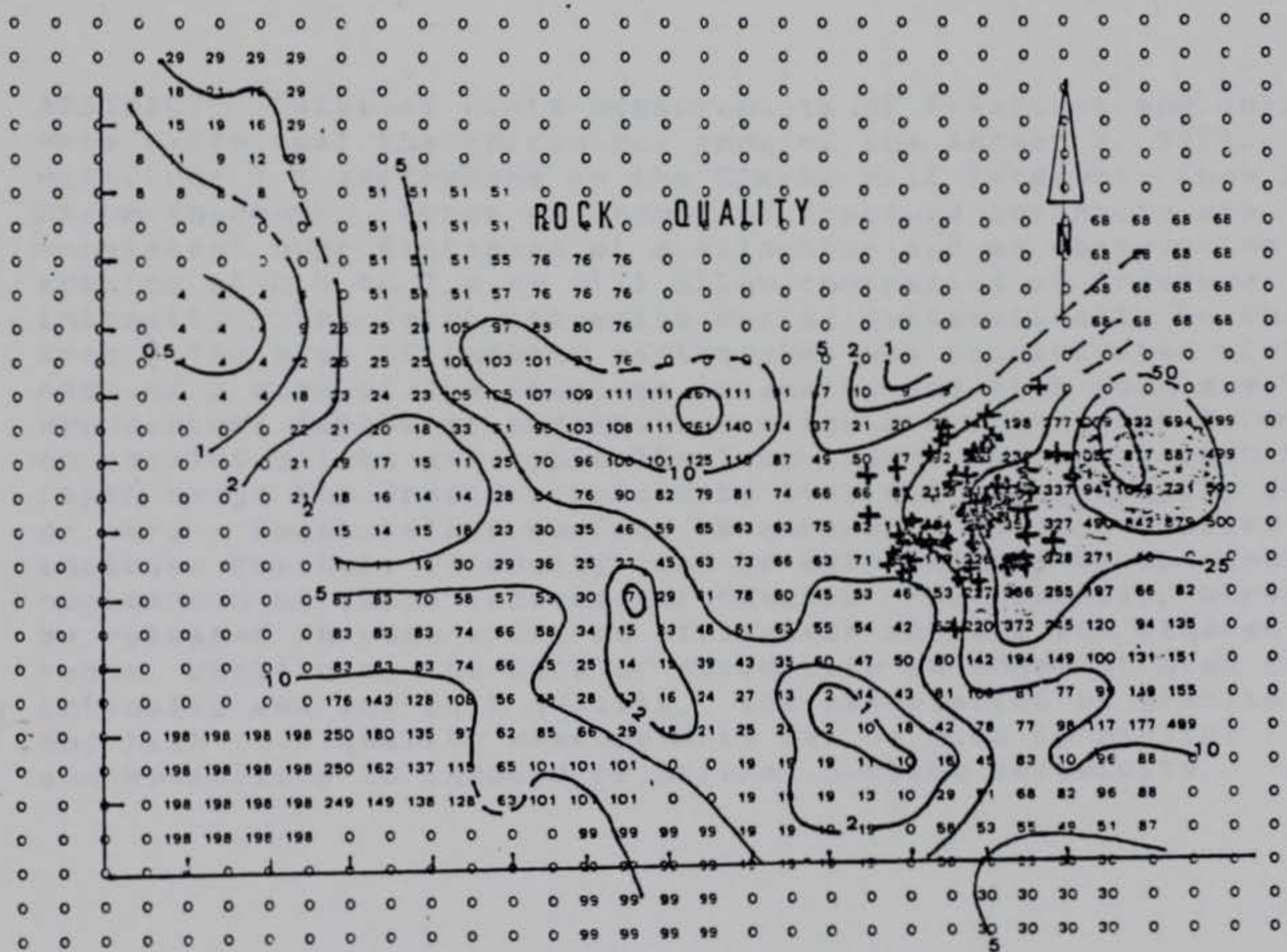


Figure 7. Contoured map of Rock Quality. The crosses indicate locations of epicenters.

FRACTURE INTENSITY AND RESERVOIR INDUCED SEISMICITY

by

Leland Timothy Long¹
Christopher C. Sorlien²
and Thomas J. Schmitt³

¹ School of Geophysical Sciences, Georgia Institute of Technology, Atlanta, Georgia 30332.

² now at Department of Geology, University of California at Santa Barbara, Santa Barbara, California.

³ Georgia Geologic Survey, 19 Dr. Martin Luther Dr., Atlanta, GA 30334.

ABSTRACT: Detailed field measurements of fractures and joints were taken near the epicentral zone of the August 2, 1974, magnitude 4.3 earthquake in the Clarks Hill Reservoir (now Lake Strom Thurmon). Zones of anomalous fracture intensity are consistent over distances of a kilometer and an observation spacing of 0.5 to 1.0 km will allow contouring of fracture intensity. The joint intensity varied systematically in the study area. The area of induced earthquakes was concentrated along the edge of a zone of low fracture intensity and high rock quality. Hypocentral depths of earthquakes which are attributed to movement on shallow joints are typically less than 1 km, and within this depth range the fracture intensity does not significantly decrease or vary. Quantitative surface measurements of rock quality (which includes fracture intensity) can be extrapolated to the depths of nucleation of these induced earthquakes. In contrast, stress may be released through creep on (foliated) schists and altered mafic rocks, explaining the lack of seismicity in zones of high fracture intensity and low rock quality. The association of granite gneiss and high rock quality measurements can be used to predict susceptibility to induced or natural shallow seismicity.

Introduction

Earthquakes in the Piedmont Province of Georgia and South Carolina have unique properties that distinguish them from events in many other seismic areas of the continental interior. These properties are their near surface to 2.0 km depth of focus (Dunbar, 1977; Fogle et al., 1976; Talwani, 1977;), their swarm-type occurrence and associated high b values (Long, 1974; Talwani et al., 1979; Johnson, 1984), their cubic high-frequency spectral decay (Marion and Long, 1980), their association with reservoirs and water loading (Talwani, 1976; Costain et al 1987; Jones et al, 1986), and the similarity between joint directions and focal mechanism solutions (Guinn, 1980). Taken singly or in concert, these properties of Piedmont earthquakes have been interpreted as supporting an association between Piedmont seismicity and shallow joints or fractures.

In a study of the geology of the area of induced seismicity around Monticello Reservoir, Secor, et al. (1982) observed numerous diversely oriented small fractures and lithological inhomogeneities in the Winnsboro complex, and speculated that these control the diffuse induced seismicity. Although the association between seismicity and jointing or small fractures has been established on the basis of depths of focus, source spectral properties, and a comparison of focal mechanisms with joint plane patterns in the Southern Piedmont, the details of the style of jointing and its correlation with seismicity have not previously been investigated. This study was undertaken to discover how joints and fractures are related to induced seismicity and, hopefully, to suggest ways in which rock quality may be used to asses a potential for induced seismicity. The objective of this paper is to present our systematic examination of joints and fractures in an area of induced seismicity.

The Study Area

The study area is a rectangle of 6 by 12 km which covers the epicentral zone of the August 2, 1974, M_L 4.3 earthquake (Fogle et al, 1974). Portable seismographs were deployed immediately following the 1974 event (Talwani et al., 1975) in an aftershock survey. Additional intermittent monitoring in the aftershock zone (Bridges, 1975; Guinn, 1977) and continuous monitoring by a regional network (Long et al., 1976) has defined the distribution of epicenters. The aftershocks and study area are located in the upper reaches of the Storm Thurmond Reservoir (figure 1). The aftershocks were not restricted to a single fault plane, but instead were scattered over 7 km² area centered 1.5 km northeast of the Savannah River channel. The depth-of-focus of aftershocks to the 1974 earthquake were computed by Talwani (1976) to range from 0.5 to 2.5 km. A relocation using a revised velocity model on an independent set of 81 aftershocks showed that most are above 1 km (Dunbar, 1977). The relocated events had a hypocentral precision of better than 200 meters both horizontally and vertically. The 1974 event and its aftershock sequence was not the

first occurrence of seismicity in the Strom Thurmond Reservoir area, with notable events in 1969 (Long 1971) and an intensity VI earthquake felt near Lincolnton, Georgia, in 1875 (Long, 1984)

The geology of the study area is complex, (Griffin, 1973; Hatcher, 1987) consisting of metamorphic lithologies which have been migmatized and intruded by granite. The major contacts strike northeast parallel to the Charlotte belt structures in which they reside. An advantage of the study area is the availability of rock exposures along the shoreline of the Strom Thurmond Reservoir and in adjacent streams. The rocks in these exposures were sufficiently intact to allow joint spacing measurements and most were easily accessible from the reservoir or roads.

Analysis and Field Methods

Well defined cracks or fractures pervade the near-surface crystalline rocks of the Piedmont province. We refer to these cracks or fractures as joints if the slippage of one block against the other can not be determined or is very slight. The average separation of joints in a joint set may be difficult to quantify because the joint spacing and distribution may display great variety which (among other factors) depends on rock type. The trimean joint intensity was proposed (Wheeler and Dixon, 1980) as a means of quantifying rock strength properties based on field measurements and as a means of minimizing the effects of extreme values of joint spacing. The intensity of a joint set has the dimensions of surface area of joints per cubic meter with units of inverse meters. The trimean estimator of joint spacing was used in this study to compute the trimean intensity, and effectively minimize the effects of extreme values in the separation of joints. The trimean spacing is calculated for each joint set by adding the first and third quartiles to twice the median spacing and dividing by 4 (Wheeler and Dixon, 1980). Trimean intensity then uses trimean spacing in the same way as average spacing is used in average intensity calculations, and is considered a statistically robust estimator of joint intensity.

A proper choice of statistical measures for joint spacing is not well established. The use of average spacing or trimean spacing assumes a distribution of spacings about some mean or median value. In field observations, the distribution of joint spacings can be highly irregular, with variations from almost uniformly spaced joints to highly bunched joints with many small spacings and a few large spacings.

An alternate statistical technique for quantifying joints is to find their fractal dimension. Many related natural systems, such as rock permeability (Wong, 1988) or the roughness of joint and fault surfaces (Scholz and Aviles, 1986), satisfy self similar (fractal) models. In this evaluation we considered that the distribution of joint spacings would satisfy the relation,

$$N = A \left[\frac{L}{r} \right]^{dr} \quad (1)$$

where N is the number of joints spacings of length greater than or equal to r in a total length (outcrop length) L. The A is a constant of approximate value one that represents the difference between the measured L and its statistical estimate. The fractal dimension is dr and is computed from a least squares estimate of the slope of Log(N) versus Log(L) - Log(r). For those sites that satisfied a self similar distribution, the fractal dimension has the advantage of being the most robust statistical parameter. A disadvantage is that the relation between fractal dimension and rock quality is unknown.

Fracture intensity and fractal dimension determinations require measurements of the attitudes of joint sets and spacings between individual joints. A study of the spatial variation of joint intensity requires a relatively uniform distribution of rock exposures. The shoreline and tributaries of the reservoir provided nearly continuous rock exposure except where limited by the area covered by the lake and by deeply weathered saprolite in the higher elevations northeast of the epicentral zone. Where possible in the study area, rock outcrops were examined at a separation of no more than 2 km. More dense observations were taken along the shore line and where possible in the epicentral zone. Along the lake shore, a minimum of 1 km spacing was maintained, and for 20 stations in the epicentral area, separations of 100 to 500 m were achieved. In the northeast sector, saprolite and rock exposures were limited to stream beds where the saprolite was fresh enough to preserve exposed joint surfaces. The shores of the reservoir provide nearly continuous saprolite or unweathered rock outcrops. Most stream outcrops were from 1 to 5 square meters, and had to be reached on foot. The precision of map coordinate measurement was 0.01 minute or approximately 20 m. Hence, stations located on distinct physiographic features such as points of land by the lake were located to within 20 meters. Those few stations on streams or unmapped roads, which were devoid of easily identified landmarks, allowed a precision that was about 50 meters. No corrections were made for magnetic deviation in location or in fracture attitude measurements, since the magnetic deviation of the study area was less than 1 degree, which is less than the precision of the measurements.

The primary goal of the field study was to obtain fracture spacing measurements distributed uniformly over the study area for the major joint sets. The criteria for the degree of variation of attitude within one set was dependent on ability to accurately measure the perpendicular spacing measurement. Joints that intersect might be separated into two sets, while the same range of attitudes might fit in one set if attitudes vary smoothly across an outcrop. Usually a variation of 20 degrees about a mean is permitted within one set for both strike and dip, unless there are two distinct sets of parallel joints within that range. The

average strike and dip of each joint set was divided into six groups based on azimuth and dip. The classification allowed independent examination of distinct joint sets and a comparison of them with rock quality, average intensity, trimean intensity, and fractil dimension.

Where attitude measurements were limited, usually a few attitudes could be measured to allow correction of joint spacings to the perpendicular. For 75 percent of the measuring locations, the outcrop allowed spacing to be measured perpendicular to the joint surface for each joint set. The resulting data set includes over 4000 spacing measurements. In vertical outcrops, usually only a few spacings of horizontal joints could be measured. Few sub-horizontal joints could be found in the horizontal outcrops.

Fracture and Rock Quality Measurements

The fracture or joint intensity for a rock volume was determined by adding the intensities of each joint set. To minimize the effects of extreme values, the trimean measure of intensity was adopted. Trimean fracture intensity was computed directly from the inverse of the trimean spacing, where trimean spacing is the weighted average of the first quartile, the third quartile, and the median (Wheeler and Dixon, 1980) according to the equation:

$$I = \sum_{i=1}^n I(i)$$

where $I(i) = 4/(S_1 + S_3 + 2S_2)$

for the i th joint set and,

S_1 = first quartile,

S_2 = median spacing

and S_3 = third quartile.

Fracture intensity can be used directly in the calculation of rock quality by using the system described by Barton et al. (1974). This system uses six parameters to describe the rock mass quality, Q . The parameters used in this study include; the number of joint sets (J_{sn}), the roughness, flatness, and continuity of the joint surface (J_{rn}), alterations of the joint surface (J_{an}), and the rock quality designation (RQD) computed from the fracture intensity. The ratio of the joint water reduction factor to the stress reduction factor in this study was taken as one to be compatible with near-surface conditions. Hence, in this study,

rock mass quality Q was computed from,

$$Q = (RQD/Jsn)(Jrn/Jan)$$

where $RQD = 115 - 3.3I$, and where Jsn, Jrn, and Jan were estimated according to the scales presented in Barton et al. (1974). In this study, all subplanar open cracks were measured. Because Barton et al. (1974) considers only systematic through-going joints, the data needed to be adjusted. This was accomplished by use of high (1.5 to 2.5) joint roughness numbers for discontinuous, uneven, or extremely fine cracks. Since the surface rocks measured in this study varied from fine, discontinuous cracks to open, mineralized systematic joints, these four parameters serve as a correction for the variability in importance of the fractures in different types of rock. In this study of the variation in rock quality, Q should be a better measure of rock strength than fracture intensity.

Because the size and quality of the outcrops varied widely, a supplemental weighting for the data based on outcrop size and degree of weathering was developed. Although most features were evident in the unweighted data (figure 4), the weighting of the data helped identify the erratic data of poor quality.

Rock types within five kilometers of inlet A (Figure 2) were in order of predominance, coarse grain granite, coarse and fine grain gray granite gneiss, layered and folded or contorted gneiss, and red clay saprolite derived from mica schist. Mafic dikes with an average thickness of one meter intrude these rocks. Ten stations had more than 25 percent of the measurements in pegmatite dikes or quartz veins, and two stations were entirely in quartzite. Three stations and three stream substations were in unweathered rock. Generally, joints would cut across granite, granite-gneiss, and gneiss equally when present in the same outcrop, but weathering of the gneiss or very coarse grain granite can form a surface crust that obscures fine fractures. These rocks dominate the immediate epicentral region, as well as the area across the lake to the southwest. Therefore, in this study area variations in joint intensity should be determined by factors other than rock type. Outcrops of highly decomposed mica schist that might be expected to fracture with a different intensity under identical conditions are found outside the study area. At stations where mica-schist was found in the study area, systematic joints cross both rock types, but are much less noticeable in the mica schist. Stations where a red clay saprolite was found were not used in the trimean data and are given very low weights. The preferential appearance of unfractured rock in outcrops due to its resistance to weathering was considered as a potential source of bias. Although this could influence isolated outcrops, the continuous exposure of rocks along the reservoir shoreline provided data independent of rock hardness. In contrast, thin quartz veins or pegmatite dikes have either more fracturing or more easily recognizable fracturing than the country rock. Outcrops with thin quartz veins or pegmatite dikes generally have lower joint intensities. Although no adjustment for rock type was made, the

spatial weighting of the large numbers of stations tend to smooth out local effects.

Observations of Joint Sets

The SE and NE striking near-vertical joints occur systematically throughout the Clarks Hill study area (Figure 2). Stream courses near inlet A are controlled by the SE and NE joint sets. The most planar and parallel joint set strikes SE between 110 and 140 degrees azimuth and the less important strikes NE between 40 and 60 degrees azimuth (Figure 3). Bell (1973) has also shown NE and SE lineaments in the topography in the southern part of the study area, and the same trends in joint orientations. Bevis and Gilbert (1984) describe pervasive NE and SE striking conjugate joint sets in the southeastern United States. The regional nature of the major joint sets make it improbable that they are purely a near surface phenomena. The SE joint set is probably the oldest, as other sets abut against them and dikes are intruded parallel to the SE set in some outcrops. Generally, the SE set terminates against the NE set. The SE striking set is easily recognized because the joints that make up the set are very continuous, planar, and parallel. At CH37 this set has a 5 mm mineral coating, implying that they were more under tension than other orientations at the time of mineralization. In some cases subhorizontal micro-faults offset vertical joints, while in others the subhorizontal surfaces of joints terminate against other joints. In both cases the subhorizontal joint surfaces are more recent, and may be related to unloading. Observations immediately after the 1974 event in this area revealed flaking or chipping of a crust that forms during weathering of some granitoid outcrops. This effect was not noticed during the 1987 study. Chipping is taken to represent surface movement on joints during the 1974-1975 activity.

RESULTS

For purposes of contouring the data, the value at each point in an evenly spaced distribution of points was estimated by a normalized weighted average determined from the product of the size and quality weight with the inverse of the square of the distance from measured outcrops. A 0.5 km spacing was used in this study and only outcrops within a radius of 1 km were considered in the weighted average. The weighted average smoothes the local variations in fracturing and suppresses spurious values associated with smaller outcrops and lower quality rocks.

The raw data show scatter (Figure 4) and to evaluate the appropriateness of the data for contouring we computed its autocorrelation function (figure 5). The variance of the trimean intensities is 18, but the non-random or correlated portion of this is about 12 suggesting an uncertainty of ± 2.3 and a spatial variance of 3.4. The autocorrelation distance is about 1.5 km. An autocorrelation distance of 1.5 km suggests that a data separa-

tion of 0.5 to 1.0 km would be sufficient to define the anomalies in this study area. The uncertainty of 2.3 suggests that a contour interval of 5 would be appropriate for this data. The gridded data have the same spatial variance of 12; however, the process of gridding has extended the autocorrelation distance to 2.0 to 2.5 km. The extension of the autocorrelation distance was influenced by the smoothing effects of areas of sparse data on the fringes of the study area, whereas the gridding process would retain the details of the densely sampled central area.

The trimean fracture intensity (Figure 6) shows areas of high and low intensity which generally follow the reservoir. Some of the low fracture intensities adjacent to high fracture intensity are related to the condition or size of the outcrops. The assigned weights for these stations were effective in suppressing the influence of the low quality and smaller outcrops in generating the concurred versions of the data. Some of the variability on a scale of less than 500 m is real and related to lithology or small scale fracture zones or areas where different fracture sets cross. Examination of the data in its gridded format assumes that the variations on a scale of 10's of meters are not as important to the stress level that can be supported by the rock as are the variations on a scale of kilometers. We consider bulk strength on a scale of kilometers more important than local rock strength.

The contoured values of rock quality (Figure 7) show a large area to the east of the aftershock zone where fracture intensity is very low and rock quality high. A belt of more highly fractured rock extends to the west-northwest. The aftershocks of the August 2, 1974, earthquake occurred along the steep gradient in joint intensity separating the low intensity zone from the high-intensity zone. Low fracture intensities are also found to the southeast, but are based on sparse (two) data points with low weights. These two sites were also more highly weathered and the crusted boulders could have obscured some fractures. Outcrop condition was not a problem in half of the 14 outcrops that showed low fracture intensity near the epicentral zone. The contours of high fracture intensity tended to be elongated parallel to the SE striking fracture set. With the rock quality, (figure 7) a SE striking zone of low rock quality determination values follows the channel of the Savannah River in the reservoir. Rock quality, which uses average intensity, has slightly different contours than the trimean intensity. Where outcrops permit evaluation of Jrn and Jan, and if these evaluations are consistent, rock quality is a better indicator of rock strength. An example of the effect on rock quality occurs at stations CH47 and CH65, where intense but fine and sometimes discontinuous joints were measured. A Jrn of 2.0 caused the rock quality to be double what it would have been if the joints had been open, through, and systematic.

The trimean data (Figure 6) excluded the near-horizontal joint systems, because they are difficult to measure in many of the horizontal and flat outcrops. Since the data requirements were more severe for the trimean computation, these measures should be less dependent of outcrop quality. Generally, trimean

intensities were about 25 percent higher than average intensities. This is explained by the suppression of a few large joint spacings by the trimean computation method. Station 4.1 was an example of the influence of widely varying joint spacing on joint intensity estimates. The trimean joint intensity will emphasize the weakest zones of the rock.

Discussion

A key element in associating joint patterns with induced seismicity is verifying that the surface expression of joints extends to the focal depth of the earthquakes. Seeberger and Zoback (1982) showed that in 8 wells near the San Andreas fault in California, the fracture intensity is not dependent on depth in the upper 250 meters. Zoback and Hickman (1982) showed that intensity is only slightly dependent on depth for the upper 1100 meters near Monticello reservoir in the Piedmont of South Carolina. The geology of the Monticello area and the Strom Thurmond Reservoir area are similar and hence the joint intensity likewise in the study area would not be expected to vary significantly with depth. In contrast, the joint intensity of the subhorizontal joints may vary significantly with depth since the subhorizontal joints may have formed relatively recently in a compressive near-surface stress field. Schaeffer (1988) has reviewed evidence for joint intensity variations with depth in the vicinity of the Bad Creek project, South Carolina, and found little variations in intensity to the 1000 m depths comparable to the hypocentral depths of the induced seismicity.

Although the lithology is variable in the study area, the discontinuities tend to strike NE and dip steeply, and much of the variation is between granitoid rocks of assumed similar rheology. The fact that the major trend in rock quality contours (figure 7) trends SE, while the strike of most lithologic units is NE, suggests that regional fracture sets, and not lithology, most affects fracturing.

State of Stress

Focal mechanisms of the aftershocks of the McCormick earthquake were not consistent, with individual aftershocks often showing focal mechanisms that differed from previous events (Guinn, 1980). These include a low angle thrust for the main quake; EW striking sinistral faults, SE striking normal and dextral faulting, and low angle thrusting for aftershocks. A mixture of focal mechanism solutions and stress directions have been observed at other reservoirs in the S. Carolina Piedmont (Zoback and Hickman, 1982; Haimson and Zoback, 1984). Talwani (1977) reports that focal mechanism solutions favor a maximum horizontal compressive stress axis oriented NW at Lake Jocassee, while nearby hydraulic fracturing (Haimson, 1975) show it to be NE. The horizontal stress levels are typically high in the crystalline Piedmont rocks. Stress inferred in wells in Virginia (Rundle et al, 1985), and at Monticello Reservoir in South

Carolina (Zoback and Hickman, 1982), show that the rock is near failure.

Reservoir induced seismicity is generally hypothesized to be related to the release of elastic stress due to loading, and to the increase in pore pressure reducing effective stress (Simpson and Narasimhan, 1986). Marion and Long (1978) suggest a process of pressure solution and mineral alteration weakening joints until failure occurs. Near the surface, the residual stress may be related to the formation of tension joints. These release residual horizontal stress (Price, 1966). The release of horizontal stress would contribute to a variable stress field related to fracture intensity. Highly fractured areas would be under a lower stress field, one more favorable to normal faulting than adjacent unfractured regions of low intensity or high rock quality. Hence, as suggested in this paper, rock quality may control the availability of stress for reservoir induced earthquake.

CONCLUSIONS

Aftershocks of the 1974 McCormick South Carolina earthquake near Clarks Hill Reservoir are spatially related to the border between relatively unfractured rock to the southeast and intensely fractured rock to the northwest. Seismicity occurred in areas of gneiss and granite, and not in mica schist, which is assumed not rigid enough to accumulate high stresses. The region of lightly fractured high quality rock will not deform at the same rate as intensely fractured rock, and so higher than average stresses were concentrated along the margin. Rock strength is lower in highly fractured areas, and so with a homogeneous stress field failure will occur there. Thus the largest shallow earthquakes should take place on pre-existing fractures in otherwise high quality rock.

Pressure solution along joints, or alteration of feldspars will weaken the strength of a fracture and accelerate the time of failure. Major through-going faults are not required in this model, although ancient faulting may influence fracture intensity. The dominant orthogonal joints are continuous enough to form fracture zones that could transmit hydraulic pressure pulses or be permeable, especially if in an orientation under tension in the current stress field, or if they were rebroken in the main quake. A combination of long term alteration in joints, yearly spring rises in lake level, rapid rise after heavy rainfall, and possibly infiltration of rain directly into joints could affect the timing of aftershocks here. The low recent level of seismicity means that most of the excess stress along the unfractured rock margin was released.

We conclude that induced earthquakes are unlikely to occur in unfractured crystalline rock, and unlikely to occur in the middle of a large area of low rock quality or otherwise weak rock. Therefore areas of intense fracturing in rigid rock adjacent to

unfractured rock should be avoided in the siting of facilities that might be damaged by shallow focus local magnitude 4 to 5 earthquakes.

List of Figures

Figure 1. Location map for area of joint measurements in the Clarks Hill Reservoir. Geology abstracted from Griffin (1973)

Figure 2. Outline of the study area showing station locations and joint directions. Small crosses are the epicenters of earthquakes from Dunbar (1977). Origin is 33.925 N, 82.625 W.

Figure 3. Joint pole plot for station ch28 showing dominant joint set for the Clarks Hill Reservoir

Figure 4. Average fracture intensity plot of observation points

Figure 5. Autocorrelation of the trimean intensity data at separation distances of 0.5 and 0.25 km. Heavy line is autocorrelation function for the gridded data.

Figure 6. Contoured map of the trimean fracture intensity. The crosses indicate locations of epicenters.

Figure 7. Contoured map of Rock Quality. The crosses indicate locations of epicenters.

For appendix references, see Bibliography

Appendix V, List of Piedmont Earthquakes

YEAR	MO	DA	TIME	UT		LAT	LONG	INT	MAG	E.	MAG
1774	2	21	0	-0	-.0	3610	8020	3.0	0.0		3.0
1776	11	5	0	-0	-.0	3520	8300	4.0	0.0		3.6
1787	11	9	0	-0	-.0	3610	8020	3.0	0.0		3.0
1792	8	11	0	-0	-.0	3610	8020	3.0	0.0		3.0
1808	12	13	9	30	-.0	3580	7860	3.0	0.0		3.0
1811	11	27	8	-0	-.0	3610	8020	4.0	0.0		3.6
1817	1	8	4	-0	-.0	3600	8020	5.0	0.0		5.0
1823	8	23	-0	-0	-.0	3610	8020	3.0	0.0		3.0
1826	11	11	-0	-0	-.0	3610	8020	3.0	0.0		3.0
1827	5	11	-0	-0	-.0	3610	8120	4.0	0.0		3.6
1833	8	27	11	0	-.0	3770	7800	6.0	0.0		5.0
1844	6	-0	-0	-0	-.0	3530	8320	3.0	0.0		3.0
1848	-0	-0	-0	-0	-.0	3560	8200	3.0	0.0		3.0
1850	3	30	15	-0	-.0	3540	7800	3.0	0.0		3.0
1850	10	17	0	0	-.0	3730	7840	4.0	0.0		3.6
1851	8	11	1	55	-.0	3560	8260	5.0	0.0		4.2
1852	11	2	23	35	-.0	3760	7860	6.0	0.0		4.3
1853	5	20	0	0	-.0	3400	8120	6.0	0.0		4.8
1855	2	2	8	0	-.0	3700	7860	5.0	0.0		4.0
1861	8	31	10	22	-.0	3620	8120	6.0	0.0		5.1
1872	6	5	3	0	-.0	3770	7800	4.0	0.0		3.6
1872	6	17	20	0	-.0	3310	8330	5.0	0.0		4.2
1873	10	3	12	45	-.0	3720	7820	4.0	0.0		3.6
1874	2	10	0	0	-.0	3570	8210	5.0	0.0		4.2
1875	7	28	23	5	-.0	3310	8330	3.0	0.0		3.0
1875	11	2	2	55	-.0	3380	8250	6.0	0.0		4.8
1875	12	23	4	45	-.0	3760	7850	7.0	0.0		4.5
1876	1	23	-0	-0	-.0	3560	8200	3.0	0.0		3.0
1877	4	26	22	-0	-.0	3610	7830	3.0	0.0		3.0
1877	10	9	1	-0	-.0	3530	8240	3.0	0.0		3.0
1879	12	13	7	0	-.0	3520	8080	4.0	0.0		3.6
1880	1	28	-0	-0	-.0	3560	8200	3.0	0.0		3.0
1880	2	10	-0	-0	-.0	3560	8200	3.0	0.0		3.0
1883	9	21	11	45	-.0	3610	7980	5.0	0.0		4.2
1884	1	-0	-0	-0	-.0	3560	8200	3.0	0.0		3.0
1884	3	31	10	0	-.0	3330	8300	4.0	0.0		3.6
1885	8	6	13	-0	-.0	3620	8160	5.0	0.0		4.2
1885	10	17	22	20	-.0	3300	8300	4.0	0.0		3.6
1895	10	7	4	30	-.0	3590	7750	3.0	0.0		3.0
1896	2	11	1	45	-.0	3630	7860	4.0	0.0		3.6
1897	11	27	20	56	-.0	3770	7750	4.0	0.0		3.6
1897	12	18	23	45	-.0	3770	7750	5.0	0.0		4.0
1898	2	11	4	30	-.0	3580	7860	3.0	0.0		3.0
1907	2	11	00	30	-.0	3780	7850	3.0	0.0		3.0
1907	2	11	13	22	-.0	3770	7830	6.0	0.0		4.8
1908	8	23	9	30	-.0	3750	7790	5.0	0.0		4.2
1911	2	10	10	22	-.0	3660	7940	4.0	0.0		3.6
1911	4	20	22	-0	-.0	3510	8270	5.0	0.0		4.2
1912	8	8	1	-0	-.0	3770	7840	4.0	0.0		3.6
1912	10	23	1	15	-.0	3260	8300	5.0	3.6		3.6
1912	12	7	19	10	-.0	3470	8170	4.0	0.0		3.6
1913	1	1	18	28	-.0	3470	8170	7.5	0.0		5.1

Appendix V, Continued

YEAR	MO	DA	TIME	UT		LAT	LONG	INT	MAG	E.	MAG
1914	3	5	20	5	- . 0	3360	8370	7. 0	0. 0		4. 8
1916	2	21	22	39	- . 0	3550	8250	7. 0	0. 0		5. 4
1916	3	2	5	2	- . 0	3450	8270	4. 0	0. 0		3. 6
1916	8	26	19	36	- . 0	3600	8100	5. 0	0. 0		4. 2
1921	8	7	6	30	- . 0	3780	7840	6. 0	0. 0		4. 8
1923	12	31	20	6	- . 0	3480	8250	4. 0	0. 0		3. 6
1924	1	1	1	6	- . 0	3480	8250	4. 0	0. 0		3. 6
1924	10	20	8	30	- . 0	3500	8260	5. 0	0. 0		4. 2
1926	7	8	9	50	- . 0	3590	8210	7. 0	0. 0		5. 4
1928	12	23	2	30	- . 0	3530	8030	4. 0	0. 0		3. 6
1929	10	28	2	15	- . 0	3430	8240	4. 0	0. 0		3. 6
1929	12	26	2	56	- . 0	3810	7850	6. 0	0. 0		4. 8
1930	12	10	0	2	- . 0	3430	8240	4. 0	0. 0		3. 6
1930	12	26	3	0	- . 0	3450	8030	4. 0	0. 0		3. 6
1931	5	6	12	18	- . 0	3430	8240	4. 0	0. 0		3. 6
1932	1	5	4	5	- . 0	3760	7840	4. 0	0. 0		3. 6
1933	6	9	11	30	- . 0	3330	8330	4. 0	0. 0		3. 6
1941	5	10	11	12	- . 0	3560	8260	4. 0	0. 0		3. 6
1942	10	7	2	15	- . 0	3760	7840	4. 0	0. 0		3. 6
1945	10	12	19	-0	- . 0	3750	7850	4. 0	0. 0		3. 6
1945	10	30	1	29	- . 0	3750	7850	4. 0	0. 0		3. 6
1946	5	24	19	40	- . 0	3800	7860	3. 0	0. 0		3. 0
1948	1	4	23	-0	- . 0	3760	7860	4. 0	0. 0		3. 6
1948	1	5	2	45	- . 0	3770	7830	4. 0	0. 0		3. 6
1948	1	5	3	20	- . 0	3750	7850	5. 0	0. 0		4. 2
1949	5	8	11	1	- . 0	3760	7760	5. 0	0. 0		4. 2
1950	11	26	7	45	- . 0	3770	7830	5. 0	0. 0		4. 2
1951	3	9	7	-0	- . 0	3760	7760	5. 0	0. 0		4. 2
1955	1	17	12	37	- . 0	3730	7840	4. 0	0. 0		3. 6
1956	1	5	8	-0	- . 0	3430	8240	4. 0	0. 0		3. 6
1956	1	5	8	30	- . 0	3430	8240	4. 0	0. 0		3. 6
1956	5	19	19	-0	- . 0	3430	8240	4. 0	0. 0		3. 6
1956	5	27	23	25	- . 0	3430	8240	4. 0	0. 0		3. 6
1957	5	13	14	24	51. 1	3580	8214	6. 0	4. 1		4. 1
1958	10	20	6	16	- . 0	3450	8170	5. 0	0. 0		4. 2
1959	10	27	2	7	28. 0	3450	8020	6. 0	0. 0		4. 8
1963	4	11	17	45	- . 0	3490	8240	4. 0	0. 0		3. 6
1964	3	13	1	20	16. 7	3314	8336	5. 0	3. 9		4. 4
1965	7	22	23	55	32. 0	3324	8336	0. 0	0. 0		2. 5
1965	9	9	14	42	20. 0	3470	8120	0. 0	3. 9		4. 1
1965	11	8	12	58	1. 0	3314	8336	0. 0	0. 0		2. 5
1965	11	8	13	4	11. 0	3314	8336	0. 0	0. 0		3. 3
1966	5	31	6	18	59. 5	3766	7813	5. 0	3. 5		3. 7
1966	6	27	17	29	- . 0	3310	8350	0. 0	0. 0		2. 8
1968	3	18	23	58	- . 0	3320	8330	0. 0	0. 0		2. 0
1968	9	22	21	41	18. 2	3411	8148	4. 0	3. 5		3. 7
1969	5	18	0	-0	- . 0	3395	8258	0. 0	3. 5		3. 8
1969	11	4	18	58	23. 0	3320	8330	0. 0	0. 0		2. 4
1969	12	11	23	44	37. 4	3784	7767	5. 0	3. 4		3. 4
1969	12	13	10	19	29. 7	3504	8285	5. 0	3. 7		3. 7
1970	9	10	1	41	5. 2	3602	8142	5. 0	3. 1		4. 2
1971	7	13	11	42	26. 0	3480	8300	5. 0	3. 8		3. 8

Appendix V, Continued

YEAR	MO	DA	TIME	UT	LAT	LONG	INT	MAG	E.	MAG
1971	9	12	0	6	27.6	3815	7759	5.0	3.6	3.4
1971	9	12	0	9	22.6	3810	7740	4.0	3.2	3.2
1972	9	5	16	-0	-.0	3760	7770	4.0	3.3	3.4
1974	8	2	8	52	11.1	3391	8253	6.0	4.1	4.3
1974	10	8	9	17	-.0	3320	8330	0.0	0.0	2.2
1974	10	28	11	33	-.0	3379	8192	4.0	3.0	3.0
1974	11	5	3	-0	-.0	3373	8222	3.0	3.7	3.7
1974	11	7	21	31	4.5	3775	7820	4.0	2.4	2.4
1975	4	1	21	9	39.7	3338	8313	0.0	3.9	3.0
1975	10	18	4	31	-.0	3490	8300	4.0	0.0	3.6
1975	11	25	15	17	34.8	3493	8290	4.0	3.2	3.2
1976	8	8	3	28	00.2	3323	8333	0.0	0.0	2.5
1976	8	9	1	56	-.0	3320	8330	0.0	0.0	1.5
1977	2	27	20	5	34.6	3790	7863	5.0	2.4	2.4
1978	2	25	3	53	27.2	3615	7932	4.0	2.2	2.2
1978	10	7	0	24	57.7	3322	8342	0.0	0.0	2.3
1978	10	29	12	22	42.9	3803	7811	0.0	1.1	1.1
1980	4	22	3	14	4.6	3640	8061	4.0	2.8	2.8
1980	5	18	22	33	55.5	3797	7807	0.0	0.0	0.0
1981	1	19	21	54	19.3	3773	7844	0.0	0.6	0.6
1981	1	21	16	29	58.1	3777	7842	0.0	0.3	0.3
1981	2	11	13	44	16.4	3772	7844	4.0	3.4	3.4
1981	2	11	13	50	31.4	3775	7841	4.0	3.2	3.2
1981	2	11	13	51	38.6	3772	7845	3.0	2.9	2.9
1981	2	12	10	41	59.0	3773	7842	0.0	-.6	-.6
1981	3	4	20	44	43.8	3581	7974	4.0	2.8	2.8
1981	4	9	7	10	31.2	3551	8205	5.0	3.0	3.0
1981	4	16	13	49	20.5	3761	7821	0.0	0.1	0.1
1981	5	5	21	21	56.7	3533	8242	5.0	3.5	3.5
1981	7	30	11	59	48.5	3819	7809	3.0	3.1	3.1
1982	1	13	13	16	25.0	3775	7807	0.0	1.5	1.5
1982	4	11	20	01	14.6	3773	7842	0.0	0.9	0.9
1982	10	31	3	7	36.7	3267	8487	5.0	2.9	2.9
1983	3	25	2	47	11.1	3533	8246	5.0	3.2	3.2
1983	7	3	16	29	24.9	3764	7837	0.0	1.2	1.2
1983	8	10	12	29	34.1	3777	7842	0.0	1.8	1.8
1984	4	12	23	46	30.6	3794	7802	0.0	-.8	-.8
1987	1	13	5	45	51.8	3434	8132	0.0	1.9	1.9
1987	1	29	9	40	18.8	3320	8318	0.0	2.0	2.0
1987	2	19	4	43	20.7	3322	8316	0.0	2.1	2.1
1987	2	24	5	25	33.9	3322	8322	1.0	1.8	1.8
1987	6	1	2	20	9.9	3479	8291	0.0	1.8	1.8
1987	7	9	1	3	54.1	3478	8295	0.0	2.0	2.0
1987	7	9	3	51	40.7	3318	8322	2.0	2.0	2.0
1987	11	21	1	3	21.0	3676	8071	0.0	2.1	2.1
1987	12	18	23	20	17.5	3511	8297	0.0	2.7	2.7

APPENDIX F:

RECOMMENDED ACCELEROGRAMS AND RESPONSE SPECTRA

From California Institute of Technology Strong Motion Data Base

11B032 65.001.0 OLYMPIA, WASHINGTON HWY TEST LAB COMP 586W

STEADY STATE VALUES: ACCEL = -194.5 CM/SEC/SEC VELOCITY = 12.7 CM/SEC DISPL = -3.6 CM

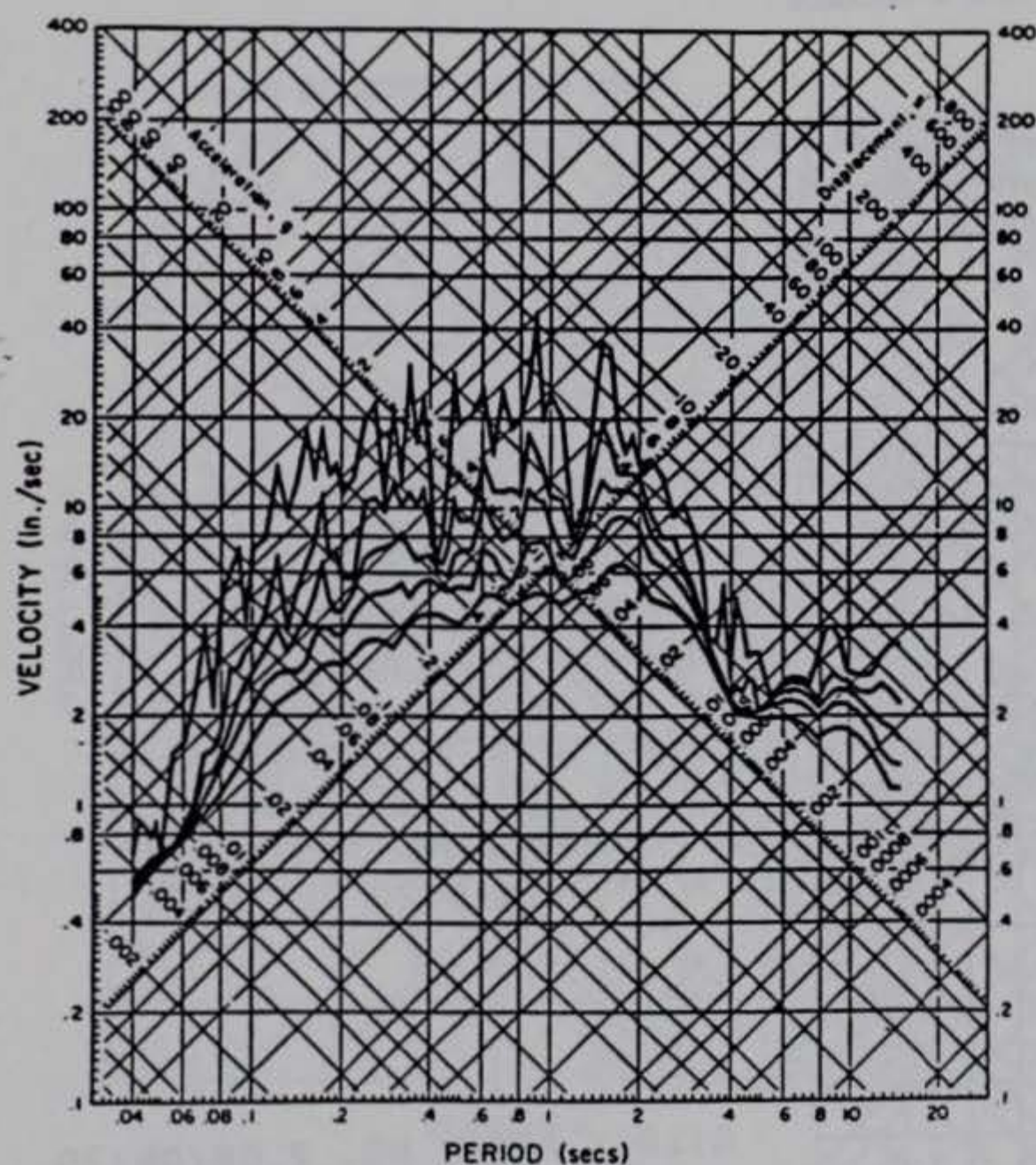
ACCELERATION
CM/SEC/SEC

VELOCITY
CM/SEC

DISPLACEMENT
CM

TIME - SECONDS

CIT EERL 72-50



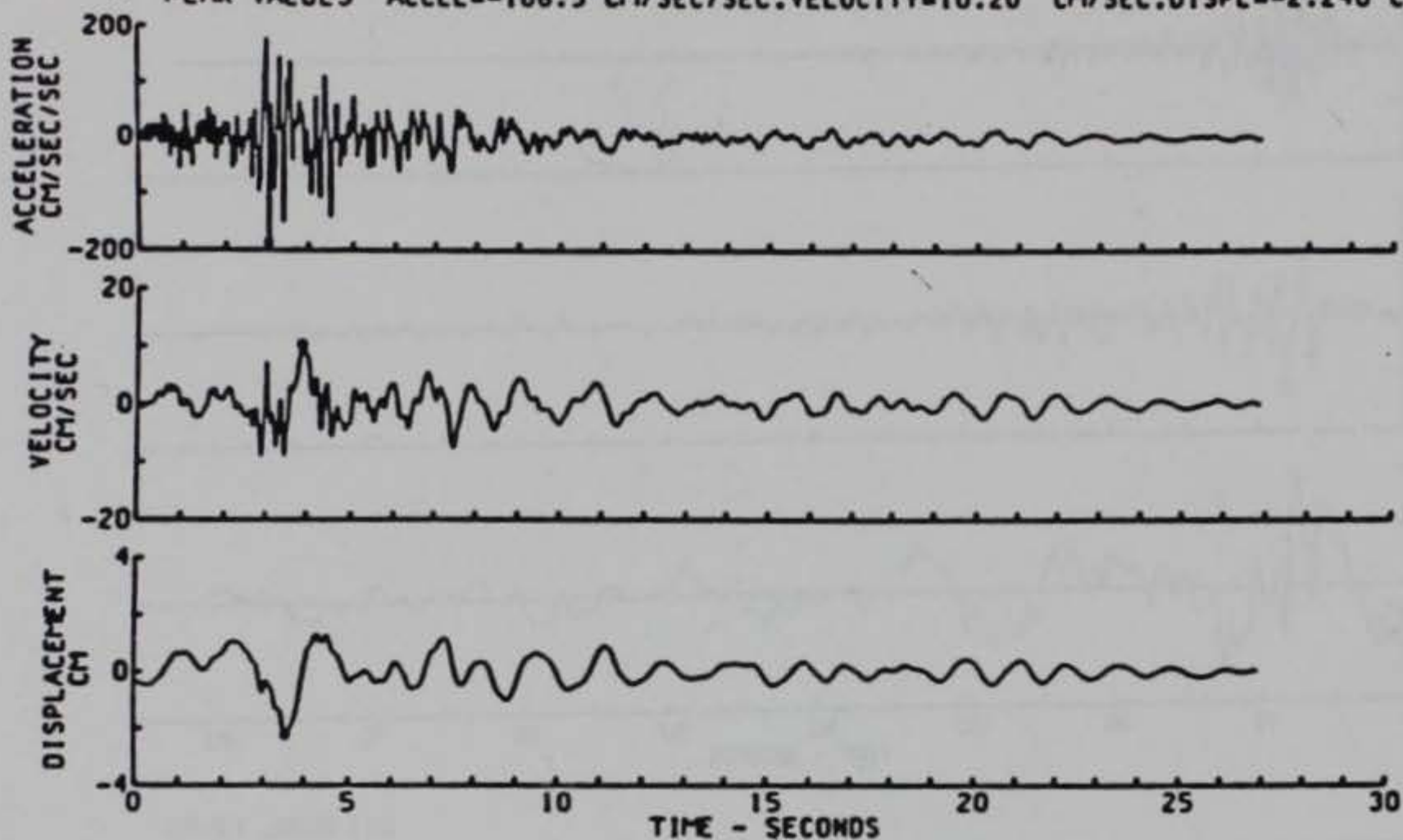
CIT EERL 73-80

IIIB032 65.001.0 OLYMPIA, WASHINGTON
HWT TEST LAB COMP 5864
DAMPING VALUES ARE
0. 2. 5. 10 AND 20 PERCENT OF CRITICAL

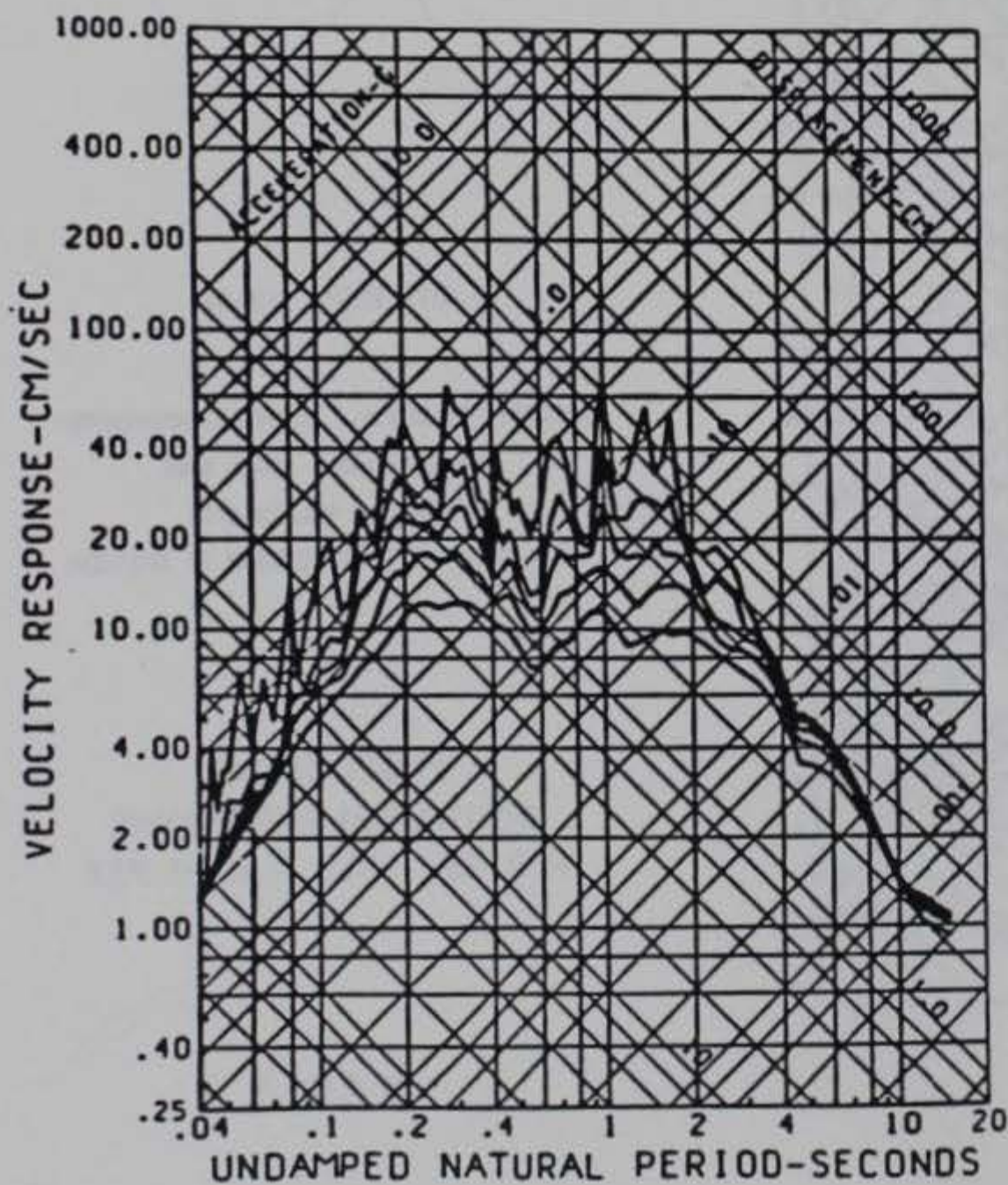
PUGET SOUND
 WASHINGTON EARTHQUAKE
 APR 29, 1965 - 0728 PST

WAS 5

CORRECTED ACCELERATION, VELOCITY, DISPLACEMENT
 COYOTE LAKE, CA EARTHQUAKE OF AUGUST 6, 1979-1705
 GILROY ARRAY NO. 2, MISSION TRAILS MOTEL, 050 DEGREES
 DATA IS PLOTTED AT EQUAL TIME INCREMENTS OF .01000 SEC
 ACCELEROGRAM IS BAND PASSED, WITH RAMPS OF .050 - .250 AND 23.00 - 25.00 CYC/SEC
 * PEAK VALUES ACCEL=-186.5 CM/SEC/SEC, VELOCITY=10.20 CM/SEC, DISPL=-2.240 CM



CDMG PR 24 USGS OF 81-42



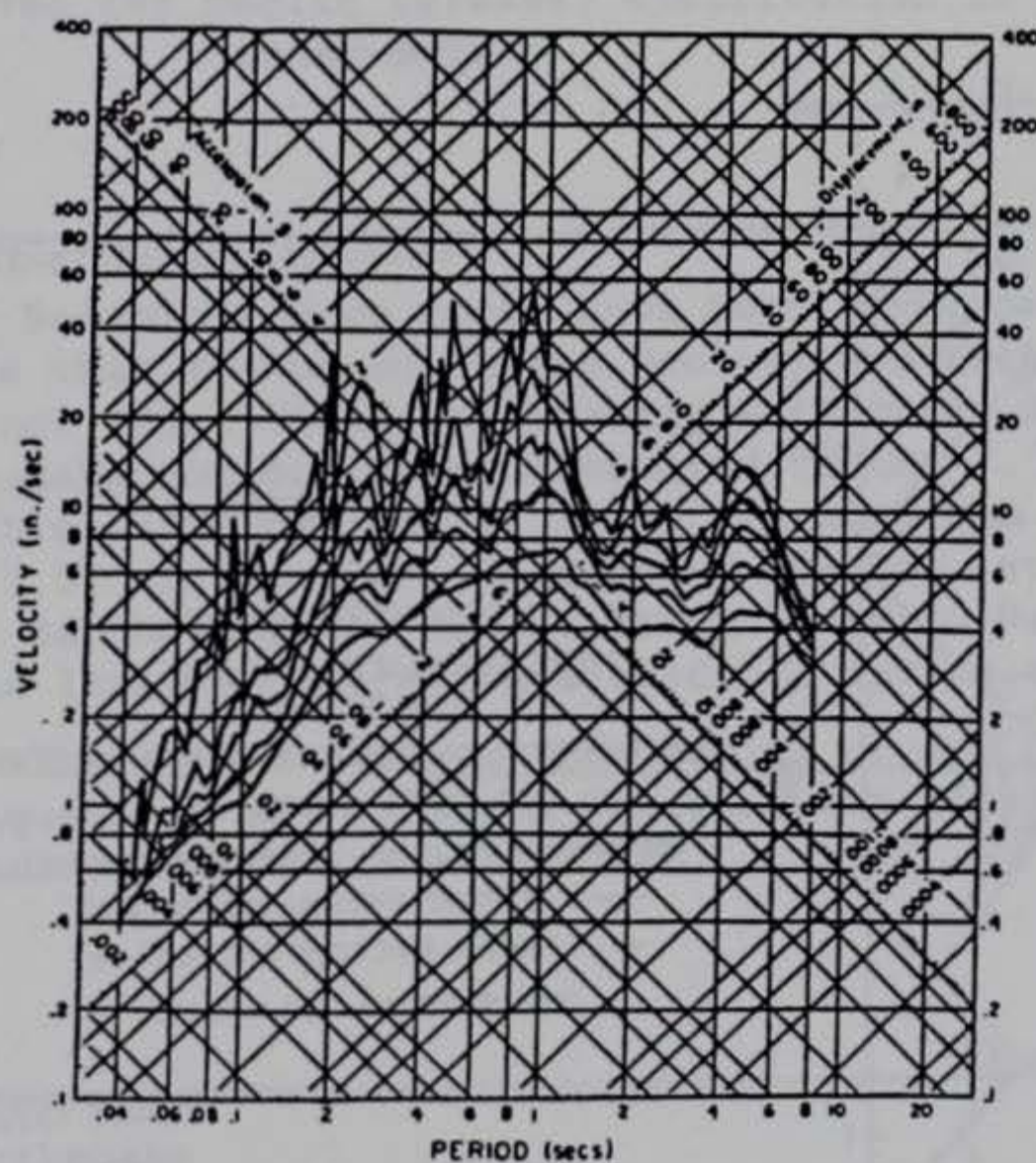
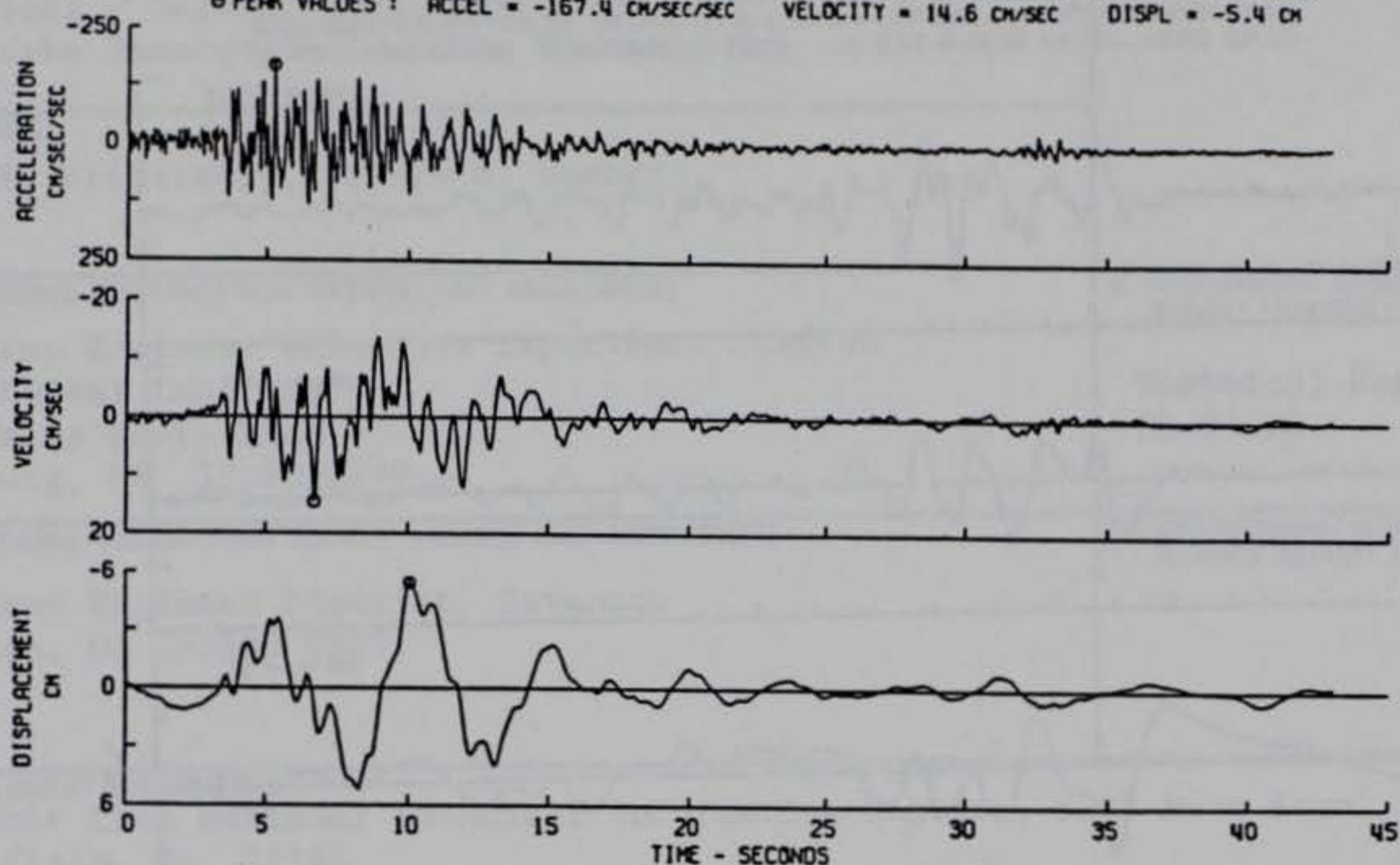
CDMG PR 24 USGS OF 81-42

SEISMIC ENGINEERING
 BRANCH/USGS
 BAND PASSED FROM
 .050- .250 TO 23.00-25.00 HZ
 050 DEGREES
 CRITICAL DAMPING
 0.2.5.10.20 PERCENT

GILROY ARRAY NO. 2.08/06/79

CAL 107

SAN FERNANDO EARTHQUAKE FEB 9, 1971 - 0600 PST
 110198 71.069.0 GRIFFITH PARK OBSERVATORY, MOON ROOM, LOS ANGELES, CAL. COMP 5904
 ○ PEAK VALUES : ACCEL = -167.4 CM/SEC/SEC VELOCITY = 14.6 CM/SEC DISPL = -5.4 CM

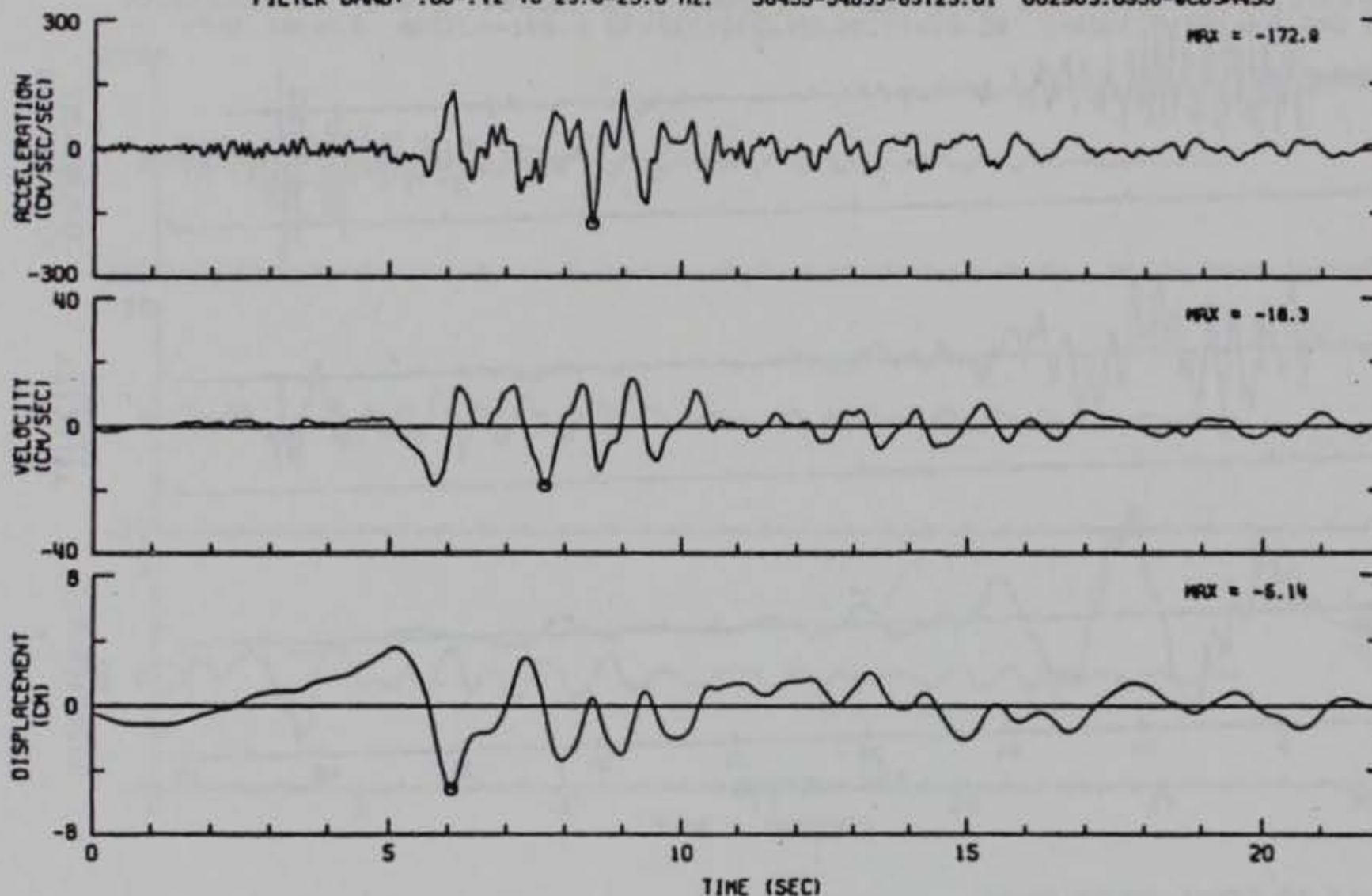


1110198 71.069.0 GRIFFITH PARK OBSERVATORY
 MOON ROOM, LOS ANGELES, CAL. COMP 5904
 DAMPING VALUES ARE
 0. 2. 5. 10 AND 20 PERCENT OF CRITICAL

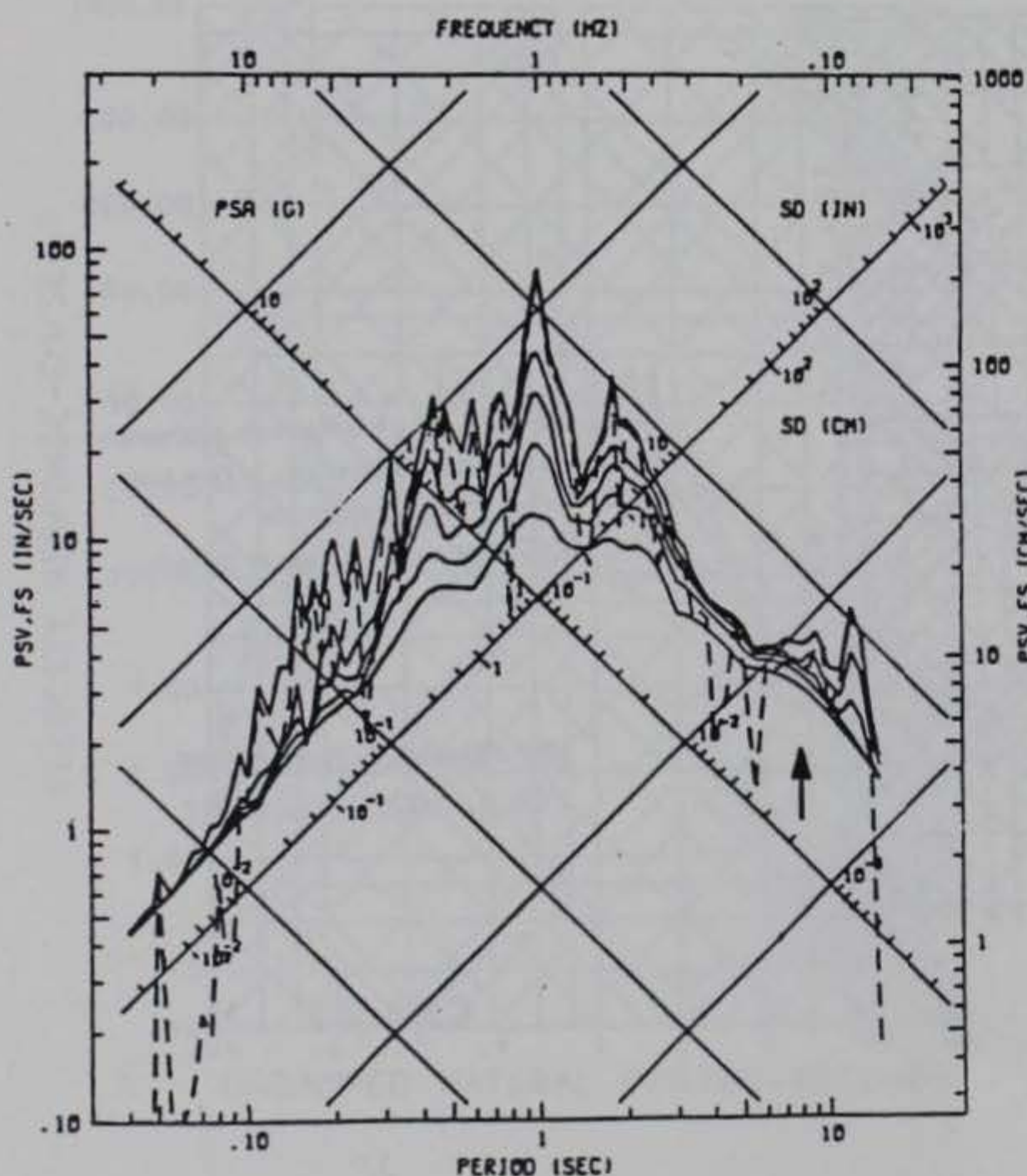
SAN FERNANDO EARTHQUAKE
 FEB 9, 1971 - 0600 PST

CAL 47

COALINGA EARTHQUAKE MAY 2, 1983 16:42 PDT
 PARKFIELD VINEYARD CANTON 1 E CHN 3: 0 DEG
 INSTRUMENT-CORRECTED AND BANDPASS-FILTERED ACCELERATION, VELOCITY AND DISPLACEMENT
 FILTER BAND: .05-.12 TO 23.0-25.0 HZ. 36455-54833-83123.01 062983.0956-0C83A455



CDM6 PRINTOUT



CDM6 PRINTOUT

COALINGA EARTHQUAKE
 PARKFIELD VINEYARD CANTON 1 E
 CHN 3: 0 DEG
 ACCELEROGRAM BANDPASS-FILTERED WITH RAMPS AT
 .05-.07 TO 23.0-25.0 HZ.
 36455-54833-83123.01 062883.1344-0C83A455
 — RESPONSE SPECTRA: PSV, PSA & SD
 - - FOURIER AMPLITUDE SPECTRUM: FS
 DAMPING VALUES: 0.2, 5, 10, 20%

MAY 2, 1983 16:42 PDT

CAL 192

REPORT DOCUMENTATION PAGE

Form Approved
OMB No. 0704-0188

Public reporting burden for this collection of information is estimated to average 1 hour per response, including the time for reviewing instructions, searching existing data sources, gathering and maintaining the data needed, and completing and reviewing the collection of information. Send comments regarding this burden estimate or any other aspect of this collection of information, including suggestions for reducing this burden, to Washington Headquarters Services, Directorate for Information Operations and Reports, 1215 Jefferson Davis Highway, Suite 1204, Arlington, VA 22202-4302, and to the Office of Management and Budget, Paperwork Reduction Project (0704-0188), Washington, DC 20503.

1. AGENCY USE ONLY (Leave blank)		2. REPORT DATE August 1993	3. REPORT TYPE AND DATES COVERED Final Report	
4. TITLE AND SUBTITLE Geological - Seismological Evaluation of Earthquake Hazards at J. Strom Thurmond Dam			5. FUNDING NUMBERS	
6. AUTHOR(S) Ellis L. Krinitzsky, Joseph B. Dunbar				
7. PERFORMING ORGANIZATION NAME(S) AND ADDRESS(ES) U.S. Army Engineer Waterways Experiment Station Geotechnical Laboratory 3909 Halls Ferry Road Vicksburg, MS 39180-6199			8. PERFORMING ORGANIZATION REPORT NUMBER Technical Report GL-93-18	
9. SPONSORING / MONITORING AGENCY NAME(S) AND ADDRESS(ES) U.S. Army Engineer District, Savannah Savannah, GA 31402-0889			10. SPONSORING / MONITORING AGENCY REPORT NUMBER	
11. SUPPLEMENTARY NOTES Available from National Technical Information Service, 5285 Port Royal Road, Springfield, VA 22161				
12a. DISTRIBUTION / AVAILABILITY STATEMENT Approved for public release; distribution is unlimited.			12b. DISTRIBUTION CODE	
13. ABSTRACT (Maximum 200 words) <p>Seismic source zones have been developed for the Southeastern United States that are based on the geology and historic seismicity as active faults have not identified. A floating earthquake was assigned to each source zone and earthquake motions were attenuated to the J. Strom Thurmond Dam. The maximum credible earthquake at J. Strom Thurmond Dam is a far field intensity MM VII (M = 5.5) earthquake. Because of the low level of seismicity, an operating basis earthquake for the J. Strom Thurmond Dam is not specified but may be taken at the level of the maximum credible earthquake.</p> <p>The values for <u>peak horizontal ground motions</u> for a maximum credible earthquake at the J. Strom Thurmond Dam based on the Krinitzsky and Chang (1987) intensity curves are as follows:</p> <p style="text-align: right;">(Continued)</p>				
14. SUBJECT TERMS Earthquake Geological-Seismological J. Strom Thurmond Dam			15. NUMBER OF PAGES 356	
			16. PRICE CODE	
17. SECURITY CLASSIFICATION OF REPORT UNCLASSIFIED	18. SECURITY CLASSIFICATION OF THIS PAGE UNCLASSIFIED	19. SECURITY CLASSIFICATION OF ABSTRACT	20. LIMITATION OF ABSTRACT	

13. (Continued).

South Carolina Seismic Zone

Hard Site, Far Field, MMI - VII

	<u>Acceleration</u> <u>(cm/sec²)</u>	<u>Velocity</u> <u>(cm/sec)</u>	<u>Duration</u> <u>Sec. \geq 0.05 g</u>
Mean	130	9	5
Mean + S. D.	190	14	11

Accelerograms and response spectra are included as representative of appropriate ground motions. Where vertical motions are considered, they may be taken at 2/3 of the horizontal.